

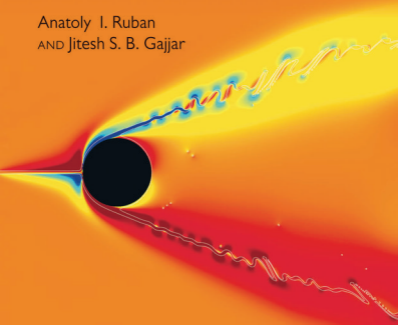
OXFORD

PART I

Fluid Dynamics

CLASSICAL FLUID DYNAMICS

Anatoly I. Ruban
AND Jitesh S. B. Gajjar



Fluid Dynamics

Fluid Dynamics

Part 1: Classical Fluid Dynamics

Anatoly I. Ruban

*Department of Mathematics
Imperial College London*

Jitesh S. B. Gajjar

*School of Mathematics
University of Manchester*

OXFORD
UNIVERSITY PRESS

OXFORD
UNIVERSITY PRESS

Great Clarendon Street, Oxford, OX2 6DP,
United Kingdom

Oxford University Press is a department of the University of Oxford.
It furthers the University's objective of excellence in research, scholarship,
and education by publishing worldwide. Oxford is a registered trade mark of
Oxford University Press in the UK and in certain other countries

© Anatoly I. Ruban and Jitesh S. B. Gajjar 2014

The moral rights of the authors have been asserted

First Edition published in 2014

Impression: 1

All rights reserved. No part of this publication may be reproduced, stored in
a retrieval system, or transmitted, in any form or by any means, without the
prior permission in writing of Oxford University Press, or as expressly permitted
by law, by licence or under terms agreed with the appropriate reprographics
rights organization. Enquiries concerning reproduction outside the scope of the
above should be sent to the Rights Department, Oxford University Press, at the
address above

You must not circulate this work in any other form
and you must impose this same condition on any acquirer

Published in the United States of America by Oxford University Press
198 Madison Avenue, New York, NY 10016, United States of America

British Library Cataloguing in Publication Data

Data available

Library of Congress Control Number: 2013953774

ISBN 978-0-19-968173-0

Printed in Great Britain by
Clays Ltd, St Ives plc

Preface

This book is the first of a series on fluid dynamics that will comprise the following four parts:

Part 1. Classical Fluid Dynamics

Part 2. Asymptotic Problems of Fluid Dynamics

Part 3. Boundary Layers

Part 4. Hydrodynamic Stability Theory

The series is designed to give a comprehensive and coherent description of fluid dynamics, starting with chapters on classical theory suitable for an introductory undergraduate lecture course, and then progressing through more advanced material up to the level of modern research in the field. Our main attention will be on high-Reynolds-number flows, both incompressible and compressible. Correspondingly, the target reader groups are undergraduate and MSc students reading mathematics, aeronautical engineering, or physics, as well as PhD students and established researchers working in the field.

Over the last 50 years, there have been major advances in various aspects of fluid dynamics. In particular, significant progress has been achieved in understanding the behaviour of compressible fluid flows, including the *supersonic*, *transonic*, and *hypersonic* flow regimes. Also during these years, two fundamental fluid-dynamic phenomena, namely *boundary-layer separation* and *laminar-turbulent transition*, have received significant attention from researchers.

Success in studying these and other phenomena has been facilitated by the development of modern *asymptotic methods*. These are now an inherent part of applied mathematics, but it was fluid dynamics where various asymptotic techniques, including the *method of matched asymptotic expansions*, were first formulated and used. Keeping this in mind, we start Part 2 of this series with a discussion of the mathematical aspects of the asymptotic theory. This is followed by an exposition of the results of inviscid flow theory, starting with *thin aerofoil theory* for incompressible and subsonic flows, steady and unsteady. Then we turn our attention to the properties of supersonic flows, where the linear Ackeret theory is followed by second-order Buzemann analysis. Both the flow near the aerofoil surface and in the far field are discussed. Part 2 also includes a discussion of the properties of *transonic* and *hypersonic* inviscid flows. We will conclude Part 2 with a brief discussion of viscous low-Reynolds-number flows.

Part 3 is devoted to the theory of high-Reynolds-number fluid flows. We first consider a class of flows that can be described in the framework of classical boundary-layer theory. These include the Blasius flow past a flat plate and the Falkner–Skan solutions for the flow over a wedge surface. We also discuss the Chapman shear-layer flow and Schlichting's solution for the laminar jet. Among other examples are Tollmien's solution for the viscous wake behind a rigid body and the periodic boundary layer on the

surface of a rapidly rotating cylinder. This is followed by a discussion of the properties of compressible boundary layers, including hypersonic boundary layers, which are known to involve extremely strong heating of the gas near the body surface. We then turn our attention to the phenomenon of flow separation from a rigid-body surface, which cannot be described in the framework of classical boundary-layer theory. Instead, one has to use the *viscous–inviscid interaction* concept, also known under the name of the *triple-deck model*. We first formulate the triple-deck theory in application to self-induced boundary-layer separation in supersonic flow, and then use it to describe the incompressible flow near the trailing edge of a flat plate. This is followed by an exposition of other applications, including incompressible flow separation from a smooth body surface and *marginal separation theory*, which describes flow separation at the leading edge of a thin aerofoil.

Part 4 of the series is devoted to *hydrodynamic stability theory*, which serves to predict the onset of *laminar–turbulent transition* in fluid flows. Similar to Part 3, we start with the classical results. We introduce the concept of linear instability of fluid flows, and formulate the Orr–Sommerfeld equation, which describes the stability properties of *parallel* and *quasi-parallel* flows, such as boundary layers. We also discuss the stability properties of ‘inviscid flows’ governed by the Rayleigh equation. This is followed by an exposition of the results of the application of the theory to various flows. Then we turn our attention to more recent developments, including *receptivity theory* and *nonlinear stability theory*. Receptivity theory is now an integral part of the theoretical predictions of laminar–turbulent transition in aerodynamic flows. It deals with the process of excitation of instability modes in the boundary layer, namely, the generation of Tollmien–Schlichting waves, cross-flow vortices, and Görtler vortices, resulting from the interaction of the boundary layer with external perturbations, for example acoustic noise, free-stream turbulence, or wall roughness. Finally, the nonlinear stability of fluid flows will be discussed, including the Landau–Stuart weakly nonlinear theory, and the derivation of the Ginzburg–Landau equation. We conclude Part 4 with a discussion of linear and nonlinear critical layers.

The present Part 1 is aimed at giving an introduction to fluid dynamics, and to prepare the reader for the more advanced material in Parts 2, 3, and 4. The book series is based on courses given by the authors over a number of years at the Moscow Institute of Physics and Technology, the University of Manchester, and Imperial College London. In fact, the majority of the material follows closely the actual lecture notes, and is supplemented with Exercises that have been used in problem classes.

Our observation is that the students find it helpful when the results of the theoretical analysis of fluid motion are compared with experiments. We make such comparisons, where appropriate, throughout the book series. Every effort has been made to contact the holders of copyright in materials reproduced in the book. Any omissions will be rectified in future printings if notice is given to the publisher.

Contents

Introduction	1
1 Fundamentals of Fluid Dynamics	4
1.1 The Continuum Hypothesis	4
1.2 Forces Acting on a Fluid	7
1.2.1 Surface forces	8
1.2.2 The concept of a fluid	13
1.3 Thermodynamic Relations	14
1.3.1 The First Law of Thermodynamics	19
1.3.2 Enthalpy and entropy	23
Exercises 1	25
1.4 Kinematics of the Flow Field	26
1.4.1 Eulerian approach	27
1.4.2 Streamlines and pathlines	29
1.4.3 Vorticity	31
1.4.4 Circulation	33
Exercises 2	34
1.4.5 Rate-of-strain tensor	36
1.5 Constitutive Equation	41
Exercises 3	50
1.6 Equations of Motion	51
1.6.1 Continuity equation in Eulerian variables	51
1.6.2 Momentum equation	53
1.6.3 The energy equation	58
1.7 The Navier–Stokes Equations	61
1.7.1 Incompressible fluid flows	61
1.7.2 Compressible fluid flows	62
1.7.3 Integral momentum equation	67
1.7.4 Similarity rules in fluid dynamics	69
Exercises 4	72
1.8 Curvilinear Coordinates	73
Exercises 5	93
2 Solutions of the Navier–Stokes Equations	95
2.1 Exact Solutions	95
2.1.1 Couette flow	95
2.1.2 Poiseuille flow	98
2.1.3 Hagen–Poiseuille flow	100
2.1.4 Flow between two coaxial cylinders	103
2.1.5 Impulsively started flat plate	105

viii Contents

2.1.6	Dissipation of the potential vortex	110
2.1.7	Kármán flow	113
	Exercises 6	118
2.2	Numerical Solutions	123
2.2.1	Viscous flow past a circular cylinder	123
2.2.2	Lid-driven cavity flow	126
3	Inviscid Incompressible Flows	129
3.1	Integrals of Motion	129
3.1.1	Bernoulli integral	130
3.1.2	Kelvin's Circulation Theorem	130
3.1.3	Cauchy–Lagrange integral	134
	Exercises 7	135
3.2	Potential Flows	139
3.2.1	Potential flow past a sphere	145
3.2.2	Virtual mass	148
3.3	Two-Dimensional Flows	152
3.3.1	Stream function	155
	Exercises 8	157
3.4	Complex Potential	160
3.4.1	Boundary-value problem for the complex potential	164
3.4.2	Flow past a circular cylinder	165
3.4.3	Force on a cylinder	170
	Exercises 9	174
3.5	The Method of Conformal Mapping	181
3.5.1	Mapping with a linear function	181
3.5.2	Conformal mapping	184
3.5.3	Mapping with the power function	185
3.5.4	Linear fractional transformation	186
3.5.5	Application to fluid dynamics	189
3.5.6	Circular cylinder with an angle of attack	191
	Exercises 10	191
3.5.7	Joukovskii transformation	194
3.6	Flat Plate at an Incidence	197
3.7	Joukovskii Aerofoils	201
	Exercises 11	205
3.8	Free Streamline Theory	210
3.8.1	Kirchhoff model	210
3.8.2	Two-dimensional inviscid jets	223
	Exercises 12	229
4	Elements of Gasdynamics	233
4.1	General Properties of Compressible Flows	233
4.1.1	Euler equations for gas flows	234
4.1.2	Piston theory	235
4.2	Integrals of Motion	239

4.2.1	Bernoulli's integral	239
4.2.2	Entropy conservation law	241
4.2.3	Kelvin's Circulation Theorem	242
4.2.4	Crocco's formula	244
4.2.5	D'Alembert's paradox	245
	Exercises 13	247
4.3	Steady Potential Flows	250
4.3.1	Two-dimensional flows	251
4.4	The Theory of Characteristics	252
4.4.1	The method of characteristics	256
4.4.2	Supersonic flows	257
4.4.3	Prandtl–Meyer flow	263
	Exercises 14	266
4.5	Shock Waves	272
4.5.1	The shock relations	273
4.5.2	Normal shock	276
4.5.3	Oblique shocks	279
4.6	Supersonic Flows past a Wedge and a Cone	285
4.6.1	Flow past a wedge	285
4.6.2	Flow past a circular cone	286
	Exercises 15	291
4.7	One-Dimensional Unsteady Flows	292
4.7.1	Expansion wave	293
4.7.2	Compression flow	296
4.7.3	Shock-tube theory	299
	Exercises 16	301
4.8	Blast-Wave Theory	305
	References	313
	Index	315

Introduction

The history of theoretical fluid dynamics dates back over 250 years, originating in 1755, when Euler derived the differential equations describing the ‘frictionless’ motion of an incompressible fluid. Euler was the first to recognise the importance of the pressure forces acting inside the moving fluid, but he disregarded the forces of internal viscosity. The ‘viscous’ fluid dynamic equations, known as the Navier–Stokes equations, were later deduced by Navier (1827), Poisson (1831), Saint-Venant (1843), and Stokes (1845).

As with any other branch of physics, it was through a combination of experimental observations and theoretical reasoning that the principal concepts of fluid dynamics (such as the continuum description of a moving fluid) were introduced, and the equations of fluid motion were derived. One might presume that once the governing equations became known, the analysis of various fluid flows could be conducted mathematically by solving these equations. This, of course, did not happen, since a direct solution of the Navier–Stokes equations proved to be very difficult except for a limited number of cases for which *exact solutions* were possible; see Chapter 2. This difficulty is a reflection of the fact that fluid flows are rather complex and also rich in their diversity. Consequently, to achieve progress in understanding fluid flow behaviour, appropriate simplification in the mathematical formulation of the problem reflecting the physical nature of the flow being considered is required.

In order to demonstrate how this works, let us consider, as an example, the jet that forms when a fluid such as water escapes from a large container through an orifice equipped with a mouthpiece as shown in Figure I.1(a). We shall assume that the mouthpiece is symmetric and composed of two flat plates, AB and $A'B'$, with the container being on the left of A and A' . This flow was first studied by Helmholtz (1868) with the aim of comparing it with the electrostatic field between two charged plates; see Figure I.1(b). The electric field potential φ is known to satisfy the Laplace equation

$$\nabla^2\varphi = 0 \tag{I.1}$$

everywhere outside the plates AB and $A'B'$. If the plates are good electrical conductors (such as a metal), then the potential will be constant along each plate, which means that equation (I.1) should be solved with the boundary conditions

$$\varphi = \begin{cases} 0 & \text{on } AB, \\ Q & \text{on } A'B'. \end{cases} \tag{I.2}$$

Here the potential has arbitrarily been taken equal to zero on AB , and the difference Q in the potential between AB and $A'B'$ depends on the electrical charge distribution on the plates. The solution of the boundary-value problem (I.1), (I.2) is shown in Figure I.1(b) in the form of equipotential lines.

2 Introduction

Let us now turn our attention to the fluid flow in Figure I.1(a). It is known that in many flows the internal viscosity of the flow is very small. For example, in the jet created with a teapot spout, the viscous forces are thousands of times smaller than the pressure forces. We shall show in Chapter 3 that if the viscosity of the fluid is disregarded, then one can investigate the flow by solving the Laplace equation

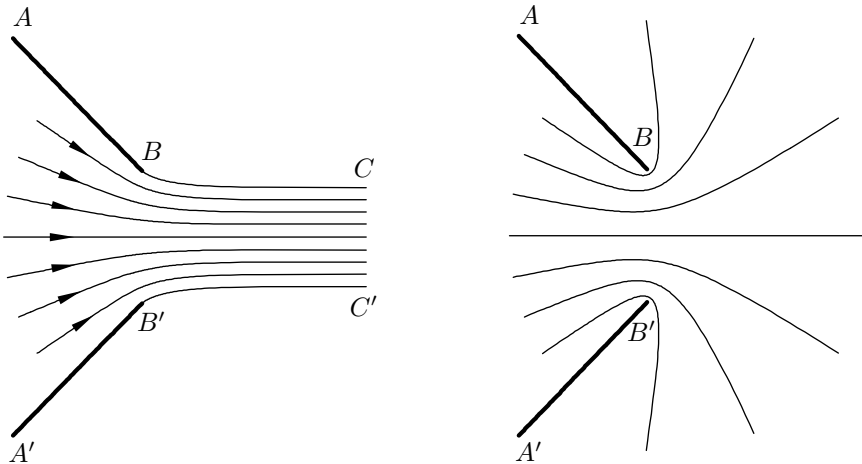
$$\nabla^2\psi = 0 \tag{I.3}$$

for the stream function ψ . The main property of the stream function is that the lines of constant ψ represent the trajectories of the fluid particles. Therefore, keeping in mind that the fluid moves along the plates AB and $A'B'$, one can write the boundary conditions for (I.3) as

$$\psi = \begin{cases} 0 & \text{on } AB, \\ Q & \text{on } A'B', \end{cases} \tag{I.4}$$

with Q now representing the rate of fluid flux through the mouthpiece.

The two mathematical problems (I.1), (I.2) and (I.3), (I.4) are absolutely equivalent. The solution of (I.1), (I.2) shown in Figure I.1(b) correctly models the physical situation for an electric field between the two plates. A ‘mathematician’ could expect the trajectories of the fluid particles in the jet (Figure I.1a) to coincide with the equipotential lines in Figure I.1(b). However, an ‘experimentalist’ and, in fact, anyone who has observed how tea is served, would disagree. The observations clearly show that the flow through a mouthpiece does not exhibit the pattern shown in Figure I.1(b). The fluid is never observed to turn around the edges of the flat plates at B and B' ,



(a) Streamlines in the incompressible fluid flow through a mouthpiece composed of two flat plates AB and $A'B'$.

(b) Equipotential lines in the electrostatic field between two flat plates AB and $A'B'$.

Fig. I.1: Comparison of the electrostatic field between two semi-infinite flat plates with the corresponding fluid flow.

and flow back over the external surfaces AB and $A'B'$. Instead, the flow separates at points B and B' to form a confined jet surrounded by the ambient air.

This dilemma led Helmholtz to a conjecture that, in addition to the smooth solution shown in Figure I.1(b), the Laplace equation also allows for a solution where the fluid velocity has a jump across the boundaries of the jet, BC and $B'C'$ (see Figure I.1a). We shall discuss these types of solutions in Section 3.8. Helmholtz further argued that it is the fluid viscosity that, despite being very small, is responsible for global changes in the fluid motion.

In the history of fluid dynamics, there have been many episodes like these, when the alliance of theory and experiment has led to novel concepts and ideas. About fifty years ago, a new member of the alliance emerged, computational fluid dynamics (CFD). It relies on numerical solution of the Navier–Stokes equations as a means of studying the behaviour of fluid flows. At the beginning, some researchers called this approach ‘numerical experimentation’, and speculated that it could become a substitute for real experiments; the latter were known to be very expensive, especially when large-scale wind tunnels were involved. There were others who believed that with the development of CFD the role of theory would diminish. It is, of course, true that over the years CFD has become a powerful tool. However, both experiments and theory retain their importance. In particular, theory remains, and always will, an ideal instrument for uncovering the fundamental physical processes behind observed fluid flow behaviour. It also remains the preferred way of presenting the subject of fluid dynamics to students.

In this book series we shall mainly rely on theoretical fluid dynamics, although some elements of CFD will be introduced where this is useful for the presentation of the material.

1

Fundamentals of Fluid Dynamics

1.1 The Continuum Hypothesis

Theoretical fluid dynamics is a subdivision of continuum mechanics and as such does not attempt to describe either the molecular structure of a medium or the motion of individual molecules.¹ The continuum models matter that is sufficiently dense such that averaging over a very large number of molecules permits a meaningful definition of macroscopic quantities. Of course, this approach has certain inherent restrictions, and these may be expressed in terms of the *Knudsen number*.

Let us consider fluid flow past a rigid body, say a sphere as sketched in Figure 1.1, and try to determine the *density* of the flowing matter. The density ρ is defined as the ratio of the mass $m_{\mathcal{D}}$ to the volume $\tau_{\mathcal{D}}$ contained in a region \mathcal{D} inside the flow. If there were no variation of density throughout the flow field then the region \mathcal{D} could be chosen arbitrarily. However, many fluids of practical interest are compressible and undergo density changes as they move. For example, for the situation shown in

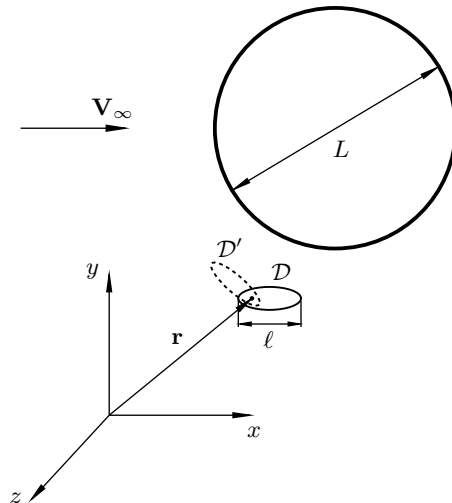


Fig. 1.1: Calculation of density $\rho(\mathbf{r}, t)$ at point \mathbf{r} and time t in a fluid flow.

¹It should be noted the Navier–Stokes equations governing fluid motion may be derived not only using the continuum mechanics approach as described in this book, but also based on the *Boltzmann equation* of the kinetic theory of gases, which treats fluid flow as the motion of an assemblage of molecules.

Figure 1.1, the fluid experiences deceleration near the front part of the sphere as it approaches from upstream, resulting in a process of compression. As the fluid subsequently moves around the sphere, it undergoes acceleration and a process of expansion. This is followed by a second compression occurring as the fluid decelerates near the rear portion of the sphere. The characteristic length scale associated with these variations coincides with the diameter L of the sphere. Therefore, in order to define the density, it is necessary to first choose an observation point in the flow. In Figure 1.1 this is denoted by the radius vector \mathbf{r} . This point must then be surrounded by region \mathcal{D} , whose characteristic length scale ℓ is small compared with L . The density at point \mathbf{r} and time t is then evaluated as

$$\rho(\mathbf{r}, t) \approx \frac{m_{\mathcal{D}}}{\tau_{\mathcal{D}}}. \quad (1.1.1)$$

Formula (1.1.1) becomes progressively more accurate as the region \mathcal{D} is made smaller, and a more precise definition of *density* should be written in the form

$$\rho(\mathbf{r}, t) = \lim_{\ell \rightarrow 0} \frac{m_{\mathcal{D}}}{\tau_{\mathcal{D}}}. \quad (1.1.2)$$

Thus the question of whether the concept of a continuum is useful in a particular flow becomes a question of whether the limit in equation (1.1.2) exists.

In general, the variations of $m_{\mathcal{D}}/\tau_{\mathcal{D}}$ with decreasing ℓ are quite complex, as shown schematically in Figure 1.2. When ℓ is comparable to the body scale L , then $m_{\mathcal{D}}/\tau_{\mathcal{D}}$ is found to be dependent not only on the volume $\tau_{\mathcal{D}}$, but also on the shape of region \mathcal{D} . If this region is stretched to the front of the cylinder (like region \mathcal{D}' shown by the dashed line in Figure 1.1) then formula (1.1.1) will obviously overestimate the real density at point \mathbf{r} ; if, on the other hand, it is stretched towards a region where the fluid experiences an expansion (solid line in Figure 1.1) then (1.1.1) will underestimate the density. This is illustrated in Figure 1.2, where the solid curve corresponds to region \mathcal{D} in Figure 1.1 while the dashed line corresponds to region \mathcal{D}' .

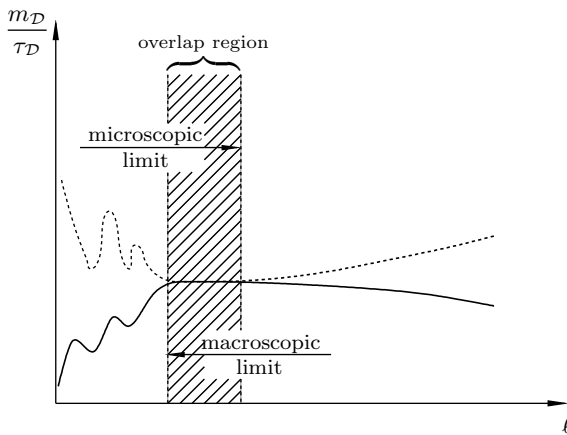


Fig. 1.2: Variations of $m_{\mathcal{D}}/\tau_{\mathcal{D}}$ for different possible shapes of region \mathcal{D} . Here the solid and dashed lines represent the solid and dashed shapes of region \mathcal{D} in Figure 1.1.

6 Chapter 1. Fundamentals of Fluid Dynamics

For a fluid medium that is sufficiently dense, the apparent density as measured with various shapes of region \mathcal{D} converge to the same value as $\tau_{\mathcal{D}}$ shrinks to the observation point \mathbf{r} , thereby indicating the existence of the limit in equation (1.1.2). However, this limit is only an intermediate *macroscopic limit* since a further decrease in region \mathcal{D} eventually reveals complex fluctuations in the apparent density, which are associated with chaotic motions at the molecular level; by this stage $\tau_{\mathcal{D}}$ is so small that any measurement of $m_{\mathcal{D}}$ is strongly dependent on the number of molecules that happen to be in \mathcal{D} at instant t , and therefore the fluctuations are also time-dependent. Oscillations, such as those depicted in Figure 1.2, would be recorded when ℓ becomes small enough that it is comparable to the *molecular mean free path*, λ . Here λ is defined as the average distance an individual molecule travels in a gas before colliding with another molecule. Thus the macroscopic intermediate limit (see Figure 1.2) exists only if ℓ is small with respect to L , but at the same time large with respect to λ , namely

$$\lambda \ll \ell \ll L. \quad (1.1.3)$$

The density $\rho(\mathbf{r}, t)$ may also be defined from a *microscopic point of view* as follows. If $N_{\mathcal{D}}$ denotes the number of molecules contained at time t within region \mathcal{D} and m_0 is the average mass of an individual molecule then

$$\rho(\mathbf{r}, t) = \frac{m_0 N_{\mathcal{D}}}{\tau_{\mathcal{D}}}. \quad (1.1.4)$$

It is known from statistical thermodynamics that chaotic fluctuations in the apparent value of ρ that can occur as molecules pass in and out of the measuring region \mathcal{D} do not influence the values of macroscopic quantities provided that the system of molecules being considered is large enough. Thus formula (1.1.4) should be more precisely written as

$$\rho(\mathbf{r}, t) = \lim_{N_{\mathcal{D}} \rightarrow \infty} \frac{m_0 N_{\mathcal{D}}}{\tau_{\mathcal{D}}}. \quad (1.1.5)$$

The process indicated in equation (1.1.5) is called the *microscopic limit* and again must be interpreted as an intermediate one. It should be noted here that the notation ' $N_{\mathcal{D}} \rightarrow \infty$ ' does not actually imply that $N_{\mathcal{D}}$, and therefore the region \mathcal{D} , must become indefinitely large. To avoid performing an average for the density over a region whose size ℓ is comparable to the body scale L , the restriction $\ell \ll L$ must still be observed.

Formulae (1.1.2) and (1.1.5) give the same result in the so-called *overlap region* (see Figure 1.2) where both restrictions in (1.1.3) are observed.² The *Knudsen number* is defined by

$$Kn = \frac{\lambda}{L},$$

and it immediately follows from (1.1.3) that Kn must be small compared with unity. Alternatively, if $Kn \ll 1$ then any point in the flow may be surrounded by a small region whose characteristic length scale ℓ satisfies the conditions (1.1.3). Being considered as a material fragment of the moving medium, such a region represents the

²For a detailed discussion of the notion of overlap region, the reader is referred to Part 2 of this book series.

basic notion of the continuum description of fluid flows, the notion of a *fluid particle*.

Definition 1.1 *The **fluid particle** is an elementary part of the moving fluid that possesses all the macroscopic properties of the fluid; it should be regarded as small enough that variations of macroscopic quantities over its volume may be neglected but, at the same time, large enough that microscopic variations are not important.*

In the continuum mechanical description of fluid motion, the entire flow field is envisaged as being continuously filled with fluid particles; in addition all quantities describing the dynamic and thermodynamic characteristics of the fluid particles, such as the velocity vector $\mathbf{V}(\mathbf{r}, t)$, pressure $p(\mathbf{r}, t)$, density $\rho(\mathbf{r}, t)$, temperature $T(\mathbf{r}, t)$, etc., are considered to be continuous and smooth functions of the spatial coordinates $\mathbf{r} = (x, y, z)$.

1.2 Forces Acting on a Fluid

All the forces acting on a moving fluid may be subdivided into two classes: *body forces* and *surface forces*. A typical representative of a body force is the force due to gravity. Recall that any material body of mass m placed in the Earth's gravitational field experiences a force

$$\mathbf{F} = m\mathbf{g},$$

where \mathbf{g} is the gravitational acceleration vector directed vertically downwards. Near the Earth's surface, $|\mathbf{g}| = 9.8 \text{ m s}^{-2}$.

In fluid dynamics, one deals with a mass continuously distributed in space, and so it is convenient to express the body force \mathbf{F} through its density distribution vector $\mathbf{f}(\mathbf{r}, t)$. The latter is defined as a body force per unit mass and may be calculated via the limit

$$\mathbf{f}(\mathbf{r}, t) = \lim_{\ell \rightarrow 0} \frac{\mathbf{F}_{\mathcal{D}}}{m_{\mathcal{D}}}, \quad (1.2.1)$$

where $\mathbf{F}_{\mathcal{D}}$ is the force acting on the fluid contained in a small region \mathcal{D} whose characteristic length scale is denoted, as before, by ℓ , with the mass of the fluid inside \mathcal{D} being $m_{\mathcal{D}}$. Since $m_{\mathcal{D}} = \rho\tau_{\mathcal{D}}$, we can also write

$$\mathbf{f}(\mathbf{r}, t) = \lim_{\ell \rightarrow 0} \frac{\mathbf{F}_{\mathcal{D}}}{\rho\tau_{\mathcal{D}}} = \frac{1}{\rho} \lim_{\tau_{\mathcal{D}} \rightarrow 0} \frac{\mathbf{F}_{\mathcal{D}}}{\tau_{\mathcal{D}}}. \quad (1.2.2)$$

As the body forces act on volume elements of a fluid, they are also referred to as *volume forces*. For the gravitational force, the vector $\mathbf{f}(\mathbf{r}, t)$ is simply

$$\mathbf{f}(\mathbf{r}, t) = \mathbf{g}.$$

Other volume forces of interest in fluid dynamics are *inertial forces* and *electromagnetic forces*. An example of an inertial force is the Coriolis force. This should be taken into account when a fluid motion is considered in a rotating coordinate system, which is convenient, for example, for flow analysis through compressor and turbine blades inside a jet engine. For a fluid motion considered in a coordinate system *Oxyz*

that rotates with constant angular velocity $\boldsymbol{\Omega}$ around axis OO' passing through the coordinate origin O , the inertial force is calculated as

$$\mathbf{f} = (\boldsymbol{\Omega} \times \mathbf{r}) \times \boldsymbol{\Omega} + 2(\mathbf{V} \times \boldsymbol{\Omega}).$$

Electromagnetic forces need to be considered when an electrically conducting fluid is moving in a magnetic field. The branch of fluid dynamics that deals with such flows is called *magnetohydrodynamics*. The interaction of an electric current in a fluid flow with a magnetic field results in a volume force known as the Lorentz force,

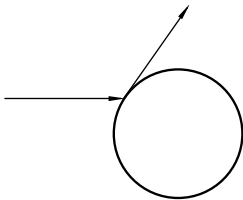
$$\mathbf{f} = \frac{1}{\rho} (\mathbf{j} \times \mathbf{B}).$$

Here the vectors \mathbf{j} and \mathbf{B} are the electric current density and the magnetic field, respectively.

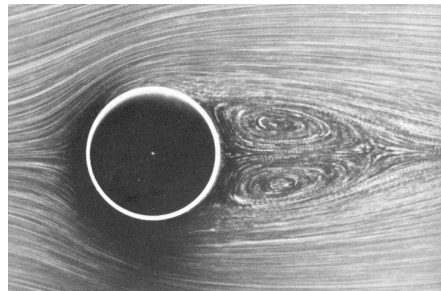
1.2.1 Surface forces

In the other group are the surface forces, such as the *pressure* and *internal viscosity*. They play a most important role in fluid flows, representing the means by which the fluid particles ‘communicate’ with one another. The importance of the pressure forces in a moving fluid was first recognised by Euler (1755), who not only derived the differential equations for inviscid fluid motion, known as the Euler equations, but also put forward a new *non-collision* concept of flow over a rigid body. In the earlier so-called ‘Newtonian model’, it was supposed that all fluid particles move towards a body along straight trajectories and exert a force on the body by simple collision with the body surface (see Figure 1.3a). Meanwhile, in reality, the interaction of a fluid flow with a rigid body always leads to a pressure increase in front of the body, making the fluid particles deviate from straight-line motion and adjust their trajectories in such a way that they smoothly flow around the body surface as shown in Figure 1.3(b).

The surface forces have a direct molecular origin and are produced by the interaction of molecules with each other via the mutual forces of attraction and repulsion. Most simply, the process of the interaction may be accounted for in gases. Gas



(a) Interaction of fluid particles with a rigid body surface according to the ‘Newtonian model’.



(b) Visualization of cylinder flow at $Re = 26$ by S. Taneda (see Van Dyke, 1982, p. 28).

Fig. 1.3: Comparison of the ‘Newtonian model’ with a real flow past a circular cylinder.

molecules spend most of their life flying freely in intermolecular space. They interact with each other via collisions, in the course of which they change their velocities and directions of flight. Since the characteristic time of the collision is much smaller than the mean flight time between collisions, we do not need to describe the collision process in detail. To determine the surface forces in gases, it is sufficient to know only the result of the collision—more precisely, the transport of momentum from gas molecules to rigid bodies if the force on the rigid body surface is to be found, or the transport of momentum from one molecule to another if the force in the bulk of the gas is to be found.

Figure 1.4(a) illustrates what happens when molecule a crosses an imaginary surface SS' in a gas medium and after colliding with molecule b on the other side of the surface is reflected back into the region above SS' . Of course, the force exerted on molecule b is very small, but in normal circumstances there are so many molecules crossing SS' that the integral effect is substantial. If the gas is at rest then averaging over a large number of molecules results in the pressure force acting perpendicular to surface SS' . If the gas is moving, then, in addition to the pressure, there is also a tangential force acting along SS' . It is known as the shear force and is attributed to the internal viscosity of the fluid. Figure 1.4(b) illustrates how this force is produced. Suppose that the average velocity of molecules in region 1 above the surface SS' is larger than that in region 2 below SS' , as shown by arrows in Figure 1.4(b). Suppose further that a set of molecules from region 1 migrate in their Brownian motion into region 2. In region 2 they have to adjust their average velocity to that of the surrounding medium; this is achieved through collisions of molecules. As a result a certain amount of momentum is transmitted to the gas in region 2. This action is equivalent to a tangential force between regions 1 and 2.

Molecules in liquids are ‘packed’ much closer to each other—in fact, so close that each of them appears to be under the permanent influence of a number of surrounding molecules. Consequently, the surface forces in liquid media are dependent not only on the mean velocity of molecules in their thermal motion, but also on the manner by which they are composed in a liquid and the way in which the intermolecular forces depend on the distance between molecules.

In both cases (gases or liquids) the surface forces are created by ‘short-range’ processes taking place in a very thin layer near the surface of a body placed in a flow or an imaginary surface drawn through the bulk of the fluid. The thickness of the layer is of the order of the molecular mean free path λ . Therefore, as $Kn = \lambda/L \rightarrow 0$,

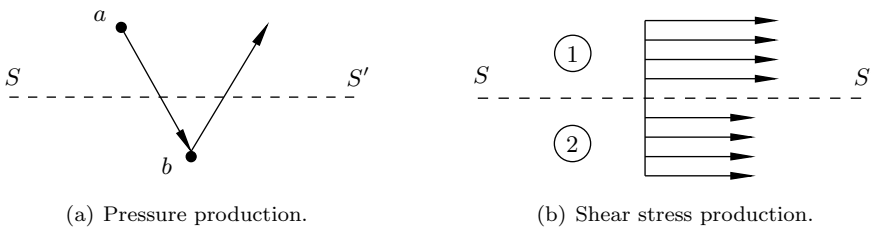


Fig. 1.4: The origin of surface forces.

this layer degenerates into a surface, and the intermolecular interaction forces, being considered from the macroscopic point of view, turn into true surface forces.

Again, instead of a surface force, we shall be dealing with its density, which is called the *stress*. The formal definition of the stress applicable for any motion of a fluid may be introduced as follows. Let M be a point where the stress is to be found. The position of this point is defined by the position vector \mathbf{r} , as shown in Figure 1.5. We draw a surface S through M and choose one side of S to be its front side; correspondingly, the other side of S will be called its rear side. The unit vector \mathbf{n} normal to S is introduced in such a way that it points into the fluid on the front side of S , and serves here to define the orientation of surface S .

Let us consider a small element of surface S whose area is ΔS (it is shown in Figure 1.5 as the region with the grid of squares), and denote by $\Delta \mathbf{P}_n$ the surface force that the fluid on the front side of S exerts through ΔS on the fluid on the rear side of S . Let us now assume that the element ΔS shrinks to point M . The *stress* is a vector quantity defined by the limit

$$\mathbf{p}_n = \lim_{\Delta S \rightarrow 0} \frac{\Delta \mathbf{P}_n}{\Delta S}. \quad (1.2.3)$$

Notice that by Newton's Third Law the force acting through ΔS on the fluid on the front side of S has the same magnitude but opposite direction, i.e. is equal to $-\Delta \mathbf{P}_n$.

The suffix n in (1.2.3) is used to indicate that the stress vector \mathbf{p}_n is dependent not only on the location of the point M , but also on the orientation of the surface S drawn through M . We shall now demonstrate that the stress \mathbf{p}_n can always be found if nine components of the so-called *stress tensor* are known.

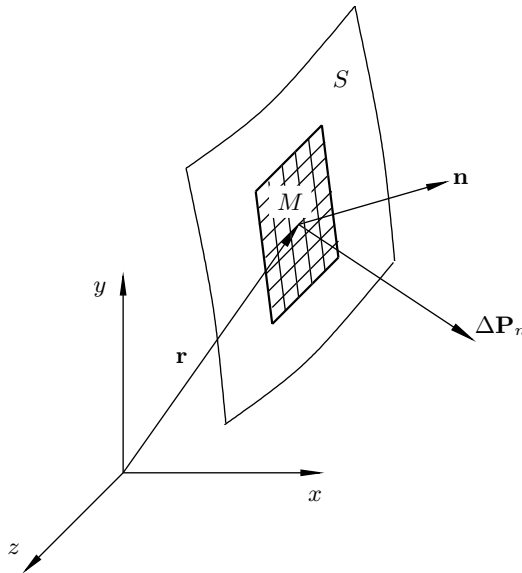
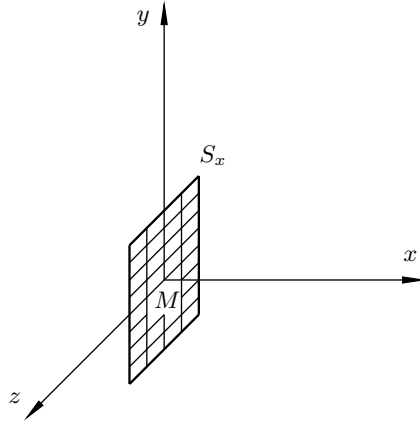


Fig. 1.5: The surface element used in equation (1.2.3) to define the stress \mathbf{p}_n .

Fig. 1.6: The surface element for defining \mathbf{p}_x .

In order to introduce the notion of the stress tensor, let us place the origin of Cartesian coordinate system (x, y, z) into point M as shown in Figure 1.6, and draw through M a plane surface S_x perpendicular to the x -axis. We shall choose the side of S_x facing the positive direction of the x -axis as its front side. The stress on S_x is denoted by \mathbf{p}_x . Like any other vector quantity, it may be represented in the coordinate decomposition form

$$\mathbf{p}_x = p_{xx}\mathbf{i} + p_{xy}\mathbf{j} + p_{xz}\mathbf{k}, \quad (1.2.4)$$

where \mathbf{i} , \mathbf{j} , and \mathbf{k} are the unit coordinate vectors.

Similarly one can consider surface S_y perpendicular to the y -axis and surface S_z perpendicular to the z -axis, with the corresponding stresses being \mathbf{p}_y and \mathbf{p}_z , respectively. Their coordinate decompositions are written as

$$\begin{aligned} \mathbf{p}_y &= p_{yx}\mathbf{i} + p_{yy}\mathbf{j} + p_{yz}\mathbf{k}, \\ \mathbf{p}_z &= p_{zx}\mathbf{i} + p_{zy}\mathbf{j} + p_{zz}\mathbf{k}. \end{aligned} \quad (1.2.5)$$

Combined together, the components of \mathbf{p}_x , \mathbf{p}_y , and \mathbf{p}_z form the stress tensor

$$\mathcal{P} = \begin{pmatrix} p_{xx} & p_{xy} & p_{xz} \\ p_{yx} & p_{yy} & p_{yz} \\ p_{zx} & p_{zy} & p_{zz} \end{pmatrix}. \quad (1.2.6)$$

The diagonal components of the stress tensor are called the *normal stresses*. For example, p_{xx} represents the x -component of the stress (1.2.4) acting on a surface perpendicular to the x -axis. The two other terms in (1.2.4) and correspondingly all the non-diagonal components of the stress tensor (1.2.6) are the *tangential* or *shear stresses*.

We shall now deduce a formula that expresses the stress \mathbf{p}_n on an arbitrarily oriented surface via the components of the stress tensor \mathcal{P} . For this purpose, we apply Newton's Second Law to the fluid contained inside a small tetrahedron $MABC$ (see Figure 1.7) with apex M placed at the point where the stress \mathbf{p}_n is to be calculated. Let the area of the front face ABC be ΔS_n . The three other faces that are perpendicular

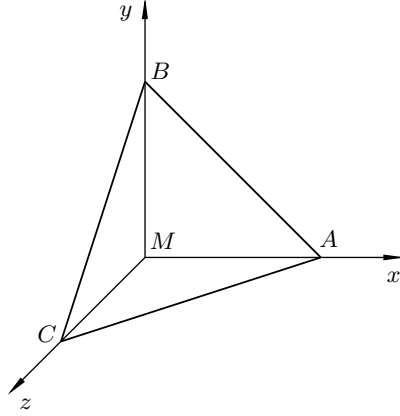


Fig. 1.7: A fluid element in the shape of tetrahedron.

to the x -, y -, and z -axes have areas ΔS_x , ΔS_y , and ΔS_z respectively. With \mathbf{n} being the unit vector normal to the front face ABC , we have

$$\Delta S_x = n_x \Delta S_n, \quad \Delta S_y = n_y \Delta S_n, \quad \Delta S_z = n_z \Delta S_n. \quad (1.2.7)$$

Let us now apply Newton's Second Law to the fluid element contained inside the tetrahedron $MABC$. If \mathbf{V} is the velocity of the fluid element and ρ the density then

$$\rho \tau_{\mathcal{D}} \frac{d\mathbf{V}}{dt} = \rho \tau_{\mathcal{D}} \mathbf{f} + \mathbf{p}_n \Delta S_n - \mathbf{p}_x \Delta S_x - \mathbf{p}_y \Delta S_y - \mathbf{p}_z \Delta S_z. \quad (1.2.8)$$

Here $\tau_{\mathcal{D}}$ denotes, as before, the volume of the fluid element considered. When calculating the force acting on the fluid element through face ABM , it has been taken into account that the fluid element is situated in front of ΔS_x . Meanwhile, \mathbf{p}_x was introduced as the stress by which the fluid on the front side of S_x (see Figure 1.6) acts upon the fluid behind S_x . Since we need to consider the surface force that acts precisely in the opposite direction, the corresponding term $\mathbf{p}_x \Delta S_x$ in (1.2.8) is taken with the minus sign. The same arguments apply equally to the following terms, $\mathbf{p}_y \Delta S_y$ and $\mathbf{p}_z \Delta S_z$.

It is easily seen that with ℓ denoting the characteristic linear size of the tetrahedron $MABC$, the left-hand side of equation (1.2.8) as well as the first term on the right-hand side may be estimated as $O(\ell^3)$. The rest of the terms are proportional to ℓ^2 . Therefore, in the limit $\ell \rightarrow 0$, when the tetrahedron $MABC$ shrinks to point M , equation (1.2.8) reduces to a balance of the surface forces

$$\mathbf{p}_n \Delta S_n - \mathbf{p}_x \Delta S_x - \mathbf{p}_y \Delta S_y - \mathbf{p}_z \Delta S_z = 0. \quad (1.2.9)$$

Substitution of (1.2.7) into (1.2.9) yields

$$\mathbf{p}_n = n_x \mathbf{p}_x + n_y \mathbf{p}_y + n_z \mathbf{p}_z. \quad (1.2.10)$$

The coordinate decomposition of (1.2.10) reads

$$\left. \begin{aligned} p_{nx} &= n_x p_{xx} + n_y p_{yx} + n_z p_{zx}, \\ p_{ny} &= n_x p_{xy} + n_y p_{yy} + n_z p_{zy}, \\ p_{nz} &= n_x p_{xz} + n_y p_{yz} + n_z p_{zz}, \end{aligned} \right\} \quad (1.2.11)$$

which shows that we really need to know the *nine* components of the stress tensor \mathcal{P} at point M to calculate the stress on an arbitrary surface S drawn through M .

Equation (1.2.10) may also be expressed in tensor form

$$\mathbf{p}_n = \mathbf{n}\mathcal{P}. \quad (1.2.12)$$

Notice that vector \mathbf{n} is written here in front of the tensor \mathcal{P} to show that the column-by-column multiplication rule has to be applied to find the components of the stress vector \mathbf{p}_n .

1.2.2 The concept of a fluid

The term *fluid* is generally used to describe either a liquid or a gas since both have a common feature that makes it possible to construct a unified dynamical theory for liquids and gases simultaneously. This common property is referred to as *fluidity*, which is broadly defined as a tendency of either medium to flow under action of any external force,³ no matter how small; in other words, a fluid moves and deforms continuously as long as an external force is applied. This behaviour may be contrasted with that of a solid, which when exposed to external forces will undergo a certain deformation, but then internal stresses will develop in the solid that will resist further deformation. As a result, the solid will assume a new state as shown in Figure 1.8.

In a fluid, shear stresses are not possible when the material is at rest. They can only exist if portions of the fluid are moving relative to one another. Such stresses are associated with the internal viscosity of fluids and are called *viscous forces*.

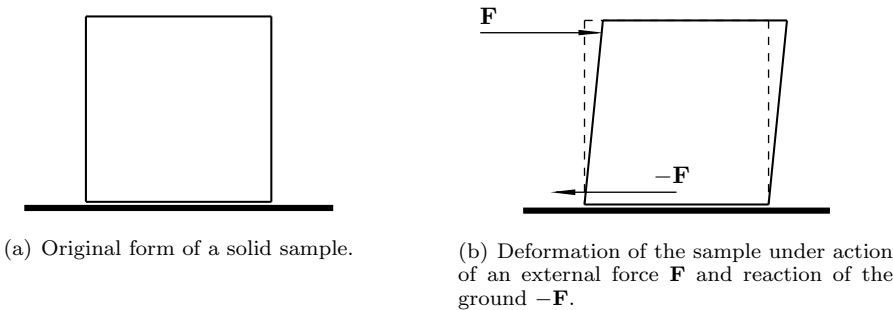


Fig. 1.8: Deformation of a solid body with rectangular cross-section placed on a flat surface.

³The only exception is the pressure; when it is distributed evenly in space it does not cause a fluid to move.

14 Chapter 1. Fundamentals of Fluid Dynamics

The only surface force possible in a fluid at rest is the pressure p . It acts equally in all directions and therefore the stress tensor may be written as

$$\mathcal{P} = \begin{pmatrix} -p & 0 & 0 \\ 0 & -p & 0 \\ 0 & 0 & -p \end{pmatrix}. \quad (1.2.13)$$

Indeed, the pressure force acting upon the fluid behind the surface S_x of Figure 1.6 is perpendicular to this surface and directed opposite to the x -axis. This suggests that the components of vector \mathbf{p}_x as given by (1.2.4) may be written as

$$p_{xx} = -p, \quad p_{xy} = 0, \quad p_{xz} = 0.$$

Similarly the components of vectors \mathbf{p}_y and \mathbf{p}_z may be written for a fluid at rest as

$$\begin{aligned} p_{yx} = 0, & \quad p_{yy} = -p, & \quad p_{yz} = 0, \\ p_{zx} = 0, & \quad p_{zy} = 0, & \quad p_{zz} = -p. \end{aligned}$$

With (1.2.13), equation (1.2.12) reduces to

$$\mathbf{p}_n = -p\mathbf{n}. \quad (1.2.14)$$

We need now to generalise the notion of the pressure for a moving fluid, where, in addition to the pressure, the forces of internal viscosity act through any surface S drawn through the fluid. Since only the total stress can be measured, it is up to us to decide which part of the stress has to be assigned to the pressure. Intuitively, the pressure is associated with the normal stresses. However, in a moving fluid the diagonal elements of the stress tensor (1.2.6) do not coincide with one another. Keeping this in mind, we shall define the pressure as the mean normal stress with sign reversed:

$$p = -\frac{1}{3}(p_{xx} + p_{yy} + p_{zz}). \quad (1.2.15)$$

The reason for this is twofold. Firstly, it is known from tensor theory that the sum of the diagonal elements is an invariant under rotation of the coordinate system, which ensures that the pressure defined by (1.2.15) is a scalar quantity. Secondly, for a fluid at rest when the stress tensor has the form of (1.2.13), formula (1.2.15) reduces to the conventional static pressure.

1.3 Thermodynamic Relations

Although the equations of motion may be derived, as we shall see, in a general form that is applicable for both liquids and gases, it is important to appreciate that the motion of these media may be quite different. The reason for this lies, first and foremost, in the effect of *compressibility*. In general, liquids exhibit very high resistance to compression, and, in normal circumstances, the pressure variations that are produced as a result of fluid acceleration or deceleration in a flow past a rigid body are well below the level

necessary to make even slight changes in the volume of a fluid particle. For this reason, the density in a liquid flow is essentially constant throughout the flow field

$$\rho = \text{const}, \quad (1.3.1)$$

and is therefore considered to be a known quantity. Such flows are termed *incompressible*.

In contrast, in the analysis of gas flows the density distribution must be evaluated as a part of the solution of the governing fluid-dynamic equations.⁴ The addition of the density to the parameters defining the motion of a fluid requires its relation to other thermodynamic functions to be specified. When describing gas flows we will be dealing with density ρ , pressure p , temperature T , internal energy e , enthalpy h , and entropy S . It is known that for a gas in the state of thermodynamic equilibrium only two of these quantities are independent. If, say, the temperature and density are known then the pressure is determined by the so-called *equation of state*

$$p = p(\rho, T).$$

Intuitively, this may be understood by considering a gas contained in a vessel. This gas is composed of many molecules moving in random paths at very high speeds and colliding at intervals with each other and the vessel walls. The force they exert through these collisions against any solid surface is observed as the pressure of the gas. The frequency of the collisions depends on the gas density, and the force produced by an individual collision grows with mean kinetic energy of a molecule, which is known to be proportional to the temperature.

The main focus in this book series is on gases that obey the *ideal gas law* given by the *Clapeyron equation*

$$p = \rho RT. \quad (1.3.2)$$

Here T is the *absolute temperature* measured in kelvin (K), and R is the gas constant. It is related to the universal gas constant $R_u = 8310 \text{ m}^2 \text{ s}^{-2} \text{ K}^{-1}$ by $R = R_u/\mu_g$, where μ_g is the molecular weight of the gas measured in relative non-dimensional units. For air, which is of particular interest in aerodynamic applications, $\mu_g = 28.97$. A fluid that conforms to equation (1.3.2) is referred to as a *perfect gas*.

Equation (1.3.2) was originally deduced from experimental observations. It may be also derived on the basis of the *kinetic theory of gases*, a short account of which will be now presented. Let us consider a fluid that is composed of \mathcal{N} molecules. Let us assume, to begin with, that all the molecules are identical and monatomic. The discussion that follows will be also valid for more complicated molecules with ‘frozen’ internal degrees of freedom, rotation of molecules, and oscillation of atoms in molecules. Under this assumption, the dynamical behaviour of each molecule, say molecule with number i , is fully defined by its position \mathbf{r}_i in space and velocity vector $\boldsymbol{\xi}_i$. In order to describe the assemblage of \mathcal{N} molecules, $6\mathcal{N}$ -dimensional Γ -space is introduced. A point

$$(\mathbf{r}_1, \dots, \mathbf{r}_{\mathcal{N}}, \boldsymbol{\xi}_1, \dots, \boldsymbol{\xi}_{\mathcal{N}}) \quad (1.3.3)$$

in this space defines a state of the assemblage.

⁴Interestingly enough, it follows from these equations that gas flows may be treated as incompressible as long as the Mach number is small (see Problem 4 in Exercises 4).

16 Chapter 1. Fundamentals of Fluid Dynamics

Although the molecules obey dynamical laws, there are so many of them as to make statistical description of their motion appropriate. This may be done by introducing the distribution function

$$F_N(\mathbf{r}_1, \dots, \mathbf{r}_N, \boldsymbol{\xi}_1, \dots, \boldsymbol{\xi}_N, t),$$

which, when multiplied by the volume element

$$\delta\tau_N = \delta\mathbf{r}_1 \cdot \dots \cdot \delta\mathbf{r}_N \cdot \delta\boldsymbol{\xi}_1 \cdot \dots \cdot \delta\boldsymbol{\xi}_N$$

of the Γ -space centred at point (1.3.3), gives the probability of the assemblage to be in this volume element at instant t .

The forces acting between molecules depend on their distribution in physical space. This is accounted for by the position vectors $\mathbf{r}_1, \dots, \mathbf{r}_N$ in the assemblage state vector (1.3.3). Since the interaction between molecules that are not close to one another may be neglected, one is normally interested in a cluster of a small number, say s , neighbouring molecules. The state of the cluster is considered in the γ_s -space

$$(\mathbf{r}_1, \dots, \mathbf{r}_s, \boldsymbol{\xi}_1, \dots, \boldsymbol{\xi}_s). \quad (1.3.4)$$

The function

$$F_s(\mathbf{r}_1, \dots, \mathbf{r}_s, \boldsymbol{\xi}_1, \dots, \boldsymbol{\xi}_s, t) = \int \dots \int F_N d\mathbf{r}_{s+1} \cdot \dots \cdot d\mathbf{r}_N \cdot d\boldsymbol{\xi}_{s+1} \cdot \dots \cdot d\boldsymbol{\xi}_N$$

gives the probability of the s molecules in the cluster to be at instant t in a unit volume of the γ_s -space centred at point (1.3.4) independent of the positions of the rest of the molecules.

The feature of a gas to which most of its distinctive properties are attributed is the wide separation of the molecules and the dynamical isolation of each molecule during most of its life. Gas molecules exert no force on each other except at collisions. A collision is a process in which one molecule comes so close to another that the mutual repulsive force becomes large enough to change their trajectories. The separation of the molecules at a collision d_0 is termed the diameter of a molecule, and in normal conditions d_0 is much smaller as compared with the molecular mean free path, i.e.

$$\epsilon = \frac{d_0}{\lambda} \ll 1. \quad (1.3.5)$$

This suggests that the statistical description of a perfect gas may be based on the function $F_1(\mathbf{r}_1, \boldsymbol{\xi}_1, t)$, which gives the probability of the first molecule of the assemblage to find itself in a unit volume of the γ_1 -space independent of the locations of the rest of the molecules. Correspondingly, the function

$$f(\mathbf{r}, \boldsymbol{\xi}, t) = \mathcal{N}F_1(\mathbf{r}, \boldsymbol{\xi}, t),$$

when multiplied by $\delta\mathbf{r} \delta\boldsymbol{\xi}$, gives the *number of molecules* expected at instant t in a volume element $\delta\mathbf{r} = \delta x \delta y \delta z$ of the physical space, and a volume element $\delta\boldsymbol{\xi} = \delta\xi_x \delta\xi_y \delta\xi_z$ of the velocity space. In particular, $f(\mathbf{r}, \boldsymbol{\xi}, t) \delta\boldsymbol{\xi}$ gives the expected number

of molecules in a unit volume of the physical space that have velocity components in the range $\delta\xi_x, \delta\xi_y, \delta\xi_z$ about ξ_x, ξ_y, ξ_z , respectively. Thus the number of molecules in a unit volume (independent of their velocities) is calculated as

$$n(\mathbf{r}, t) = \iiint_{-\infty}^{\infty} f(\mathbf{r}, \boldsymbol{\xi}, t) d\boldsymbol{\xi}, \quad (1.3.6)$$

and, with m_0 being the mass of a molecule, the fluid density

$$\rho(\mathbf{r}, t) = m_0 \iiint_{-\infty}^{\infty} f(\mathbf{r}, \boldsymbol{\xi}, t) d\boldsymbol{\xi}.$$

An average molecular velocity is given by the integral

$$\mathbf{V}(\mathbf{r}, t) = \frac{1}{n} \iiint_{-\infty}^{\infty} \boldsymbol{\xi} f(\mathbf{r}, \boldsymbol{\xi}, t) d\boldsymbol{\xi},$$

and this coincides with the macroscopic velocity of a fluid particle that happens to be at point \mathbf{r} at instant t .

The thermal velocity of molecules in the coordinate system moving with the fluid particle is defined as

$$\mathbf{c} = \boldsymbol{\xi} - \mathbf{V}.$$

The average kinetic energy of molecules in their translational thermal motion is

$$\frac{1}{n} \iiint_{-\infty}^{\infty} \frac{m_0 c^2}{2} f(\mathbf{r}, \boldsymbol{\xi}, t) d\boldsymbol{\xi},$$

using which we shall define the gas temperature $T(\mathbf{r}, t)$ as

$$\frac{3}{2} kT(\mathbf{r}, t) = \frac{1}{n} \frac{m_0}{2} \iiint_{-\infty}^{\infty} c^2 f(\mathbf{r}, \boldsymbol{\xi}, t) d\boldsymbol{\xi}, \quad (1.3.7)$$

where k is an absolute constant known as *Boltzmann's constant*:

$$k = 1.3806488 \times 10^{-23} \text{ kg m}^2 \text{ s}^{-2} \text{ K}^{-1}.$$

Let us consider a small surface element ΔS moving with the fluid, and calculate the flux of momentum across ΔS due to the chaotic molecular motion. The orientation of the surface element is given as before by the unit normal vector \mathbf{n} (see Figure 1.9), and a flux in the direction of \mathbf{n} will be reckoned as positive. The surface element ΔS is crossed by molecules with different values of the velocity vector $\boldsymbol{\xi}$. Let us consider molecules with velocity in the range $\delta\boldsymbol{\xi}$ about $\boldsymbol{\xi}$. To cross ΔS , they have to come from the cylindrical region \mathcal{D} whose base coincides with ΔS while the sides are parallel to

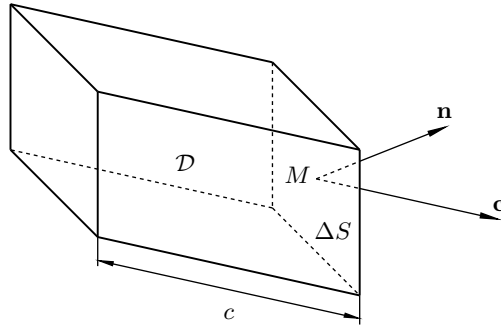


Fig. 1.9: Calculation of the momentum flux through surface element ΔS .

the relative velocity vector \mathbf{c} . If we want to know the number of molecules crossing ΔS per unit time then we have to choose the sides of region \mathcal{D} to have the length $c = |\mathbf{c}|$ as shown in Figure 1.9. All the molecules inside \mathcal{D} will cross ΔS , while those further away will not be able to reach this surface.

The height of region \mathcal{D} is given by the scalar product $\mathbf{c} \cdot \mathbf{n}$, and its volume equals $(\mathbf{c} \cdot \mathbf{n}) \Delta S$. Therefore the number of molecules crossing ΔS per unit time with velocity in the range $\delta \boldsymbol{\xi}$ about $\boldsymbol{\xi}$ is

$$(\mathbf{c} \cdot \mathbf{n}) \Delta S f(\mathbf{r}, \boldsymbol{\xi}, t) \delta \boldsymbol{\xi}.$$

Each of the molecules carries momentum $m_0 \mathbf{c}$. Thus the total flux of momentum is

$$m_0 \Delta S \iiint_{-\infty}^{\infty} \mathbf{c} (\mathbf{c} \cdot \mathbf{n}) f(\mathbf{r}, \boldsymbol{\xi}, t) d\boldsymbol{\xi}.$$

It coincides with the surface force $\Delta \mathbf{P}_n$ acting on the fluid on the front side of the surface element. Hence, using formula (1.2.3) and relying on Newton's Third Law, we find that the stress \mathbf{p}_n may be calculated as

$$\mathbf{p}_n = -m_0 \iiint_{-\infty}^{\infty} \mathbf{c} (\mathbf{c} \cdot \mathbf{n}) f(\mathbf{r}, \boldsymbol{\xi}, t) d\boldsymbol{\xi}.$$

In particular, choosing \mathbf{n} to be along the x -axis, we can write

$$\mathbf{p}_x = -m_0 \iiint_{-\infty}^{\infty} \mathbf{c} c_x f(\mathbf{r}, \boldsymbol{\xi}, t) d\boldsymbol{\xi}.$$

Being projected, say, on the y -axis, this formula gives

$$p_{xy} = -m_0 \iiint_{-\infty}^{\infty} c_y c_x f(\mathbf{r}, \boldsymbol{\xi}, t) d\boldsymbol{\xi}. \quad (1.3.8)$$

Formulae like (1.3.8) are more conveniently expressed using the index notation where x, y, z are denoted as x_1, x_2, x_3 , respectively. Then any element p_{ij} of the stress tensor (1.2.6) may be written as

$$p_{ij} = -m_0 \iiint_{-\infty}^{\infty} c_i c_j f(\mathbf{r}, \boldsymbol{\xi}, t) d\boldsymbol{\xi}. \quad (1.3.9)$$

Substituting (1.3.9) into (1.2.15), we find

$$p = -\frac{1}{3}(p_{11} + p_{22} + p_{33}) = \frac{m_0}{3} \iiint_{-\infty}^{\infty} (c_1^2 + c_2^2 + c_3^2) f(\mathbf{r}, \boldsymbol{\xi}, t) d\boldsymbol{\xi},$$

which, when compared with (1.3.7), yields

$$p = nkT. \quad (1.3.10)$$

It remains to note that the density $\rho = m_0 n$, and (1.3.10) reduces to (1.3.2) with the gas constant

$$R = k/m_0.$$

It is interesting that the above analysis does not rely on the assumption that the gas is in a state of thermodynamic equilibrium. Therefore, the following statement is valid. *With the pressure defined by (1.2.15), the Clapeyron equation is valid for a perfect gas no matter how far from equilibrium.*

1.3.1 The First Law of Thermodynamics

The First Law of Thermodynamics is essentially a statement of the law of conservation of energy. It states that *heat energy and mechanical energy are equivalent and interchangeable*. In fact, formula (1.3.7) indicates that heat energy is really mechanical energy on a molecular scale.

According to the First Law of Thermodynamics, if a quantity of heat is introduced into a closed system (say, a gas) it must either be accumulated by the system as internal energy or reappear externally as work done by the gas on its surroundings. This is written as

$$dQ = dE + dW, \quad (1.3.11)$$

where dQ is the heat, E is the internal energy of the gas, and dW is the work done by the gas.

For simplicity, we shall consider a cylinder with a movable piston of area A containing a gas of volume V at pressure p (see Figure 1.10). We shall suppose that the piston is balanced by a force F so that

$$F = pA.$$

Let us assume that the piston moves to the right through a distance dx . Then the gas

20 Chapter 1. Fundamentals of Fluid Dynamics

performs a work against the force F of amount⁵

$$dW = F dx = pA dx = p dV,$$

where dV is the change in volume of the gas. The First Law (1.3.11) may now be written as

$$dQ = dE + p dV. \tag{1.3.12}$$

When referred to a unit mass of a gas, equation (1.3.12) reads

$$dQ = de + p dv, \tag{1.3.13}$$

where the volume v occupied by a unit mass of the gas is related to the density via the equation

$$v = \frac{1}{\rho}. \tag{1.3.14}$$

If the volume is kept constant then (1.3.13) takes the form

$$dQ = de.$$

The specific heat at constant volume c_v with units $\text{kJ kg}^{-1} \text{K}^{-1}$ is defined as the rate of heat addition per one degree of temperature rise per unit mass, dQ/dT . It may be calculated as

$$c_v = \left(\frac{dQ}{dT} \right)_v = \left(\frac{de}{dT} \right)_v. \tag{1.3.15}$$

The internal energy e is made up of the following contributions that occur at the microscopic level: (i) the total kinetic energy of the translational motion of molecules in their thermal motion, (ii) the total rotational energy of the molecules, and (iii) the total vibrational energy of individual atoms comprising a gas molecule as they oscillate with respect to each other inside the molecule. The potential energy associated with intermolecular interactions is very small for a perfect gas in which condition (1.3.5) holds.

The specific heat c_v depends on the structure of the gas molecules and, principally, on the number of atoms in each molecule. For monatomic molecules (such as the dissociated gases H, N, O, etc.), internal energy is stored entirely in their translational

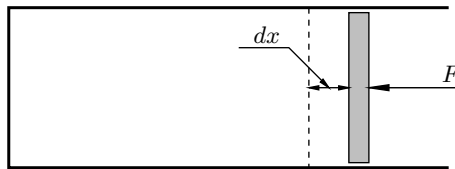


Fig. 1.10: The work performed by a gas contained in a cylinder with the piston moving against force F through a distance dx .

⁵This formula may be easily generalised for arbitrary deformation of the region occupied by the gas.

motion. Taking into account that the average kinetic energy of molecules in the thermal motion is given by the right-hand side of formula (1.3.7), the internal energy per unit mass for a monatomic gas may be found by dividing the left-hand side of (1.3.7) by the mass of a molecule m_0 :

$$e = \frac{3}{2} \frac{k}{m_0} T = \frac{3}{2} RT. \quad (1.3.16)$$

Using (1.3.16) in (1.3.15), we can easily find that for a monatomic gas

$$c_v = \frac{3}{2} R. \quad (1.3.17)$$

In order to deduce the corresponding formulae for the energy e and specific heat c_v for diatomic molecules, we have to restrict our analysis to a gas in a state of thermodynamic equilibrium. In this case function $f(\mathbf{r}, \boldsymbol{\xi}, t)$ is known to be represented by the *Boltzmann distribution*

$$f = A e^{-\epsilon/kT}. \quad (1.3.18)$$

Here A is a factor to be found and ϵ is the energy of an individual molecule. If we return for a moment to monatomic molecules (or molecules where all other degrees of freedom except translational motion are frozen), then

$$\epsilon = \frac{1}{2} m_0 c^2 = \frac{1}{2} m_0 (c_x^2 + c_y^2 + c_z^2),$$

which when substituted into (1.3.18) and then into (1.3.6) yields

$$A = n \left(\frac{m_0}{2\pi kT} \right)^{2/3}.$$

As a result, (1.3.18) turns into the classical *Maxwell distribution of molecular velocities*

$$f(\mathbf{r}, \boldsymbol{\xi}, t) = n(\mathbf{r}, t) \left(\frac{m_0}{2\pi kT(\mathbf{r}, t)} \right)^{3/2} e^{-m_0 c^2 / 2kT(\mathbf{r}, t)},$$

where $\mathbf{c} = \boldsymbol{\xi} - \mathbf{V}(\mathbf{r}, t)$.

The energy of a diatomic gas molecule is composed of the kinetic energy of translational motion, the energy of rotation of the molecule, and the energy of oscillations of atoms with respect to one another inside the molecule. At normal temperatures the oscillation mode is 'frozen', and therefore molecules may be considered as rigid bodies. This allows us to express the energy of an individual molecule in the form

$$\epsilon = \frac{1}{2} m_0 c_x^2 + \frac{1}{2} m_0 c_y^2 + \frac{1}{2} m_0 c_z^2 + \frac{1}{2} I_1 \Omega_1^2 + \frac{1}{2} I_2 \Omega_2^2. \quad (1.3.19)$$

Here I_1, I_2 are the moments of inertia of the molecule with respect to the principal axes and Ω_1, Ω_2 are the angular velocities of rotation around these axes.

22 Chapter 1. Fundamentals of Fluid Dynamics

To calculate the factor A in the Boltzmann distribution (1.3.18), we shall again use the density integral. Now, instead of (1.3.6), we have to write

$$n = \int_{-\infty}^{\infty} \cdots \int_{-\infty}^{\infty} f \, dc_x \, dc_y \, dc_z \, d\Omega_1 \, d\Omega_2. \quad (1.3.20)$$

Substitution of (1.3.19) into (1.3.18) and then into (1.3.20) yields

$$A = n \frac{(m_0 I_1 I_2)^{1/2}}{(2\pi kT)^{5/2}}.$$

The gas *energy per unit volume* is calculated as

$$\int_{-\infty}^{\infty} \cdots \int_{-\infty}^{\infty} \left(\frac{m_0 c_x^2}{2} + \frac{m_0 c_y^2}{2} + \frac{m_0 c_z^2}{2} + \frac{I_1 \Omega_1^2}{2} + \frac{I_2 \Omega_2^2}{2} \right) f \, dc_x \, dc_y \, dc_z \, d\Omega_1 \, d\Omega_2, \quad (1.3.21)$$

which gives⁶

$$\frac{5}{2} n k T. \quad (1.3.22)$$

The gas mass per unit volume equals

$$n m_0. \quad (1.3.23)$$

Dividing (1.3.22) by (1.3.23), we find that the energy per unit mass is

$$e = \frac{5}{2} \frac{k}{m_0} T = \frac{5}{2} R T.$$

Using (1.3.15), we see that for a gas with diatomic molecules

$$c_v = \frac{5}{2} R. \quad (1.3.24)$$

The increase in c_v over monatomic gases (1.3.17) is due to the additional energy associated with rotational degrees of freedom of the diatomic gas molecules. It is interesting to notice that each quadratic term in the parentheses in the energy integral (1.3.21) gives the same contribution $\frac{1}{2} n k T$ to the result of the integration. Being referred to unit mass, this translates into $\frac{1}{2} R T$ contribution of each degree of freedom of a molecule to the total gas energy e . This result is known as the *principle of equipartition of energy*.

In aerodynamic flows the fluid, air, is a mixture of gases, most of which have diatomic molecules (N_2 , O_2 , H_2 , etc.). At normal temperatures, very little energy is partitioned into the vibrational modes of these molecules, and therefore the formula (1.3.24) is normally used for the specific heat c_v . It becomes invalid for very low temperatures that may be observed, for example, in a supersonic wind tunnel, and

⁶See Problem 2(c) in Exercises 1.

at very high temperatures typical of hypersonic flows. A wind tunnel is a device that serves to convert the internal energy of air into its kinetic energy. If a wind tunnel is designed for high-Mach-number experiments, the temperature in the test section may be so low that the rotational degrees of freedom become frozen and instead of (1.3.24) one has to use for c_v the monatomic formula (1.3.17).

On the other hand, with increasing temperature, excitation of atomic oscillation in molecules is ultimately activated. The two atoms composing a molecule perform oscillations along an imaginary line connecting them. To account for this motion, two additional quadratic terms should be written in (1.3.19), the first one representing the kinetic energy of the oscillational motion and the second the potential energy of the attraction/repulsion force acting between the atoms in a molecule. As a result, the specific heat increases to

$$c_v = \frac{7}{2}R. \quad (1.3.25)$$

In most circumstances the flow conditions do not reach these extremes, and the specific heat c_v may be treated as constant. In particular, for air it is given by (1.3.24). The internal energy of a perfect gas is then expressed by the equation

$$e = c_v T. \quad (1.3.26)$$

1.3.2 Enthalpy and entropy

The *enthalpy* per unit mass in units of kJ kg^{-1} is defined by

$$h = e + \frac{p}{\rho}, \quad (1.3.27)$$

and it follows from (1.3.26) and the state equation (1.3.2) that

$$h = c_p T, \quad (1.3.28)$$

where c_p is the specific heat at constant pressure given by

$$c_p = c_v + R. \quad (1.3.29)$$

Indeed, equation (1.3.13) may be rearranged as

$$dQ = de + p dv = de + d(pv) - v dp = d(e + pv) - v dp,$$

and using (1.3.14) we find

$$dQ = d\left(e + \frac{p}{\rho}\right) - \frac{dp}{\rho} = dh - \frac{dp}{\rho}. \quad (1.3.30)$$

Thus, if the pressure is kept constant then $dQ = dh$ and

$$c_p = \left(\frac{dQ}{dT}\right)_p = \left(\frac{dh}{dT}\right)_p.$$

The ratio of specific heats

$$\gamma = \frac{c_p}{c_v} \quad (1.3.31)$$

is an important non-dimensional parameter that is characteristic of compressible gas flows. For air, c_p and c_v are given by equations (1.3.24) and (1.3.29), whence $\gamma_{\text{air}} = 1.4$.

24 Chapter 1. Fundamentals of Fluid Dynamics

With (1.3.31), equation (1.3.29) may be rewritten as

$$c_p = \frac{c_p}{\gamma} + R,$$

and it follows that

$$c_p = \frac{\gamma}{\gamma - 1} R.$$

This formula when substituted into (1.3.28) yields

$$h = \frac{\gamma}{\gamma - 1} RT. \quad (1.3.32)$$

It remains to make use of the state equation (1.3.2), and we will have the following expression for the enthalpy:

$$h = \frac{\gamma}{\gamma - 1} \frac{p}{\rho}. \quad (1.3.33)$$

One more function that we will be dealing with in gas flows is called the *entropy* S . It is defined by the equation

$$dS = \frac{dQ}{T}. \quad (1.3.34)$$

Substitution of (1.3.32) into (1.3.30) and then into (1.3.34) yields

$$dS = \frac{\gamma}{\gamma - 1} R \frac{dT}{T} - \frac{dp}{\rho T}. \quad (1.3.35)$$

It follows from the state equation (1.3.2) that $\rho T = p/R$, which, being used in the second term on the right-hand side of equation (1.3.35), results in

$$dS = \frac{\gamma}{\gamma - 1} R \frac{dT}{T} - R \frac{dp}{p} = \frac{R}{\gamma - 1} \left[\gamma \frac{dT}{T} - (\gamma - 1) \frac{dp}{p} \right].$$

Integrating this equation, we have

$$S = C + \frac{R}{\gamma - 1} \ln \frac{T^\gamma}{p^{\gamma-1}}. \quad (1.3.36)$$

Let us now write the state equation (1.3.2) as

$$T = \frac{p}{\rho R},$$

and use it to eliminate T from (1.3.36). This results in the following equation:

$$S = \tilde{C} + \frac{R}{\gamma - 1} \ln \frac{p}{\rho^\gamma}, \quad (1.3.37)$$

which expresses the entropy per unit mass in terms of pressure p and density ρ . For our purposes the constant $\tilde{C} = C - [\gamma/(\gamma - 1)] R \ln R$ can remain arbitrary.

Exercises 1

1. Thermodynamic relations, including equations (1.3.26), (1.3.33), and (1.3.37) for the internal energy, enthalpy, and entropy, may be used provided that the medium is in the state of thermodynamic equilibrium. From the microscopic point of view, the equilibrium is represented by specific form of the distribution function f , which for a perfect gas is given by the Boltzmann distribution (1.3.18). This distribution is set up through mutual collisions of the molecules, and it is known that a molecule should undergo just a few collisions for the equilibrium to be established. In a moving gas the surrounding conditions for each fluid particle are constantly changing, and we can only speak about a quasi-equilibrium state.

Consider a perfect gas flowing past a rigid body as shown, for example, in Figure 1.1. With V_∞ and \bar{c} denoting the free-stream flow velocity and mean molecular velocity, respectively, show that the quasi-equilibrium is achieved for each fluid particle provided that

$$Kn \frac{V_\infty}{\bar{c}} \ll 1.$$

Hint: Compare the average time a molecule spends in flight between two collisions with the characteristic time a fluid particle experiences a changing environment in its motion past the rigid body.

2. Consider the Boltzmann distribution (1.3.18) for a diatomic gas, when the energy ϵ is given by equation (1.3.19).
- (a) Verify that the factor A in (1.3.18) can indeed be calculated using the equation

$$A = n \frac{(m_0 I_1 I_2)^{1/2}}{(2\pi kT)^{5/2}}.$$

- (b) Confirm that equation (1.3.7), used to define the gas temperature T in terms of average kinetic energy of *translational* motion of molecules, still holds.
- (c) Demonstrate that each quadratic term in parentheses in the energy integral (1.3.21) gives the same contribution $\frac{1}{2}nkT$ to the result of the integration.

Suggestion: You may use without proof the fact that for any positive α ,

$$\int_{-\infty}^{\infty} e^{-\alpha x^2} dx = \sqrt{\frac{\pi}{\alpha}}, \quad \int_{-\infty}^{\infty} x^2 e^{-\alpha x^2} dx = \frac{\sqrt{\pi}}{2} \alpha^{-3/2}.$$

3. A thermodynamic process is termed *adiabatic* if there is no exchange of heat between the system considered and the environment ($dQ = 0$). Using the definition of entropy (1.3.34) and equation (1.3.37), argue that for a perfect gas in an adiabatic process the pressure p and density ρ are related as

$$\frac{p}{\rho^\gamma} = \text{const.}$$

Using further the Clapeyron equation (1.3.2), find the corresponding relationship between the temperature T and density ρ .

1.4 Kinematics of the Flow Field

Two distinct ways to describe the motion of continuous media are utilised in fluid dynamics, namely, the Lagrangian and Eulerian descriptions. The *Lagrangian approach* is similar to that of classical mechanics when one considers a set of material particles moving in space. In this problem, a number i is ascribed to each particle, and its position with respect to a suitably chosen coordinate system (x, y, z) is given at time t by the position vector $\mathbf{r}_i(t)$ with coordinates $x_i(t)$, $y_i(t)$ and $z_i(t)$.

The continuum model assumes that fluid particles are continuously distributed throughout the flow field in a population that is indefinitely large and cannot be enumerated. In the Lagrangian approach, one particle is distinguished from another by specifying its location in the field at some initial instant $t = t_0$. This is done in the following way. Let \mathcal{D}_0 be a region fixed in the coordinate system (x, y, z) with fluid continually passing through it (see Figure 1.11). We shall consider a set composed of all fluid particles that happen to be inside \mathcal{D}_0 at the initial instant $t = t_0$. In an experiment one could mark the fluid particles with different colour dyes; in the theoretical description the initial position vector, \mathbf{r}_0 , which points at a fluid particle inside \mathcal{D}_0 serves this purpose.

As time increases, a fluid particle moves in space and its location may be expressed in the form

$$\mathbf{r} = \mathbf{r}(t, \mathbf{r}_0), \quad (1.4.1)$$

signifying that \mathbf{r} is a function of two independent variables, time t and initial position vector \mathbf{r}_0 . If the second argument \mathbf{r}_0 in (1.4.1) is fixed and time t increases, then an observer will record the trajectory of the particle as indicated by the dotted line in Figure 1.11. A transition from one fluid particle to another is accomplished by a change of \mathbf{r}_0 .

In the Lagrangian approach, not only the position vector (1.4.1) but all other fluid quantities are considered as functions of t and \mathbf{r}_0 . For example, density ρ and fluid

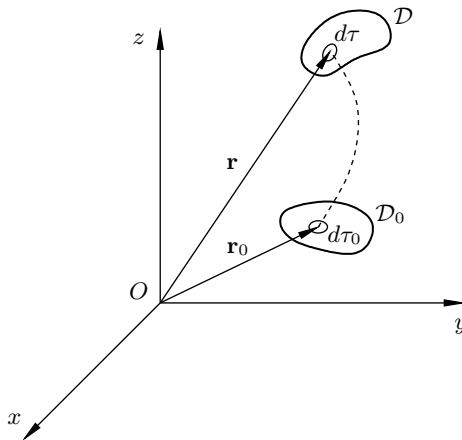


Fig. 1.11: Lagrangian description of the flow field.

temperature T are written as

$$\rho = \rho(t, \mathbf{r}_0), \quad T = T(t, \mathbf{r}_0). \quad (1.4.2)$$

If the functions $\mathbf{r}(t, \mathbf{r}_0)$, $\rho(t, \mathbf{r}_0)$, and $T(t, \mathbf{r}_0)$ were known, then all other fluid-dynamic quantities could be easily obtained from well-known thermodynamic and kinematic relations. For instance, the velocity and acceleration of a fluid particle may be determined by differentiating (1.4.1) with respect to time:

$$\mathbf{V} = \frac{\partial \mathbf{r}}{\partial t}, \quad \mathbf{a} = \frac{\partial^2 \mathbf{r}}{\partial t^2}. \quad (1.4.3)$$

In order to determine the functions (1.4.1) and (1.4.2), one has to use the conservation laws of mass, momentum, and energy. We shall show here how the mass conservation law may be formulated in the Lagrangian variables. Let \mathcal{D} be a region occupied by fluid particles from \mathcal{D}_0 at a later instant, $t > t_0$. Consider a small element of volume $d\tau$ in \mathcal{D} that originates in its counterpart in region \mathcal{D}_0 of volume $d\tau_0$; see Figure 1.11. As we are dealing with the same fluid particle, the law of conservation of mass states

$$\rho_0 d\tau_0 = \rho d\tau. \quad (1.4.4)$$

Here ρ_0 and ρ denote the density of the fluid particle at times t_0 and t respectively.

In order to establish a relationship between the volumes $d\tau_0$ and $d\tau$, let us return to equation (1.4.1). It may be interpreted as a transformation of coordinates from (x_0, y_0, z_0) to (x, y, z) . For any such transformation, the volume elements are known to be related via

$$d\tau = \left| \frac{\partial(x, y, z)}{\partial(x_0, y_0, z_0)} \right| d\tau_0. \quad (1.4.5)$$

Substitution of (1.4.5) into (1.4.4) yields

$$\left| \frac{\partial(x, y, z)}{\partial(x_0, y_0, z_0)} \right| = \frac{\rho_0}{\rho}, \quad (1.4.6)$$

which is the *continuity equation* in Lagrangian variables.

1.4.1 Eulerian approach

In the *Eulerian description* of the motion, the viewpoint is entirely different, and rather than following individual fluid particles, the main interest is in the state and development of the flow field. The functions of interest include the velocity vector, density, and temperature,

$$\mathbf{V} = \mathbf{V}(t, \mathbf{r}), \quad \rho = \rho(t, \mathbf{r}), \quad T = T(t, \mathbf{r}), \quad (1.4.7)$$

with time t and the position vector $\mathbf{r} = (x, y, z)$ being independent variables. To explain how these functions must be interpreted, let us consider, for example, the function $\mathbf{V}(t, \mathbf{r})$. This function represents the flow velocity at point (x, y, z) at time t , or, more precisely, gives the velocity of the fluid particle that happens to be at point (x, y, z) at time t .

Since a new fluid particle passes through a given point at each instant, the acceleration \mathbf{a} of a particle cannot be determined as the partial derivative of $\mathbf{V}(t, \mathbf{r})$ with respect to t . In order to determine the acceleration \mathbf{a} , the Lagrangian representation (1.4.1) for the fluid particle location must be substituted into the Eulerian representation (1.4.7) of the velocity. This gives the velocity of a fluid particle

$$\mathbf{V}_p(t) = \mathbf{V}[t, \mathbf{r}(t, \mathbf{r}_0)] = \mathbf{V}[t, x(t, \mathbf{r}_0), y(t, \mathbf{r}_0), z(t, \mathbf{r}_0)]. \quad (1.4.8)$$

Formula (1.4.8) is then differentiated with respect to t using the chain rule:

$$\mathbf{a} = \frac{d\mathbf{V}_p}{dt} = \frac{\partial \mathbf{V}}{\partial t} + \frac{\partial \mathbf{V}}{\partial x} \frac{\partial x}{\partial t} \Big|_p + \frac{\partial \mathbf{V}}{\partial y} \frac{\partial y}{\partial t} \Big|_p + \frac{\partial \mathbf{V}}{\partial z} \frac{\partial z}{\partial t} \Big|_p, \quad (1.4.9)$$

where the suffix p is used to indicate that the differentiation is carried out for the fluid particle that passes point \mathbf{r} at time t . Writing the first of equations (1.4.3) in the coordinate decomposition form, we have⁷

$$u = \frac{\partial x}{\partial t} \Big|_p, \quad v = \frac{\partial y}{\partial t} \Big|_p, \quad w = \frac{\partial z}{\partial t} \Big|_p.$$

Hence, equation (1.4.9) may be written as

$$\mathbf{a} = \frac{\partial \mathbf{V}}{\partial t} + u \frac{\partial \mathbf{V}}{\partial x} + v \frac{\partial \mathbf{V}}{\partial y} + w \frac{\partial \mathbf{V}}{\partial z}$$

or

$$\mathbf{a} = \frac{D\mathbf{V}}{Dt} = \frac{\partial \mathbf{V}}{\partial t} + (\mathbf{V} \cdot \nabla)\mathbf{V}. \quad (1.4.10)$$

Here the differential operator

$$\frac{D}{Dt} = \frac{\partial}{\partial t} + (\mathbf{V} \cdot \nabla)$$

is called the *material* or *full derivative* and gives rise to two terms in equation (1.4.10). The first term, $\partial \mathbf{V} / \partial t$, is called the *local acceleration*. It represents an acceleration due to temporal changes in the velocity field as the fluid particle arrives at the point in question. The second term, $(\mathbf{V} \cdot \nabla)\mathbf{V}$, is called the *convective acceleration* and is an acceleration due to the fact that the fluid particle is being convected into a point with different velocity. The convective derivative is the scalar product of the velocity vector and the gradient operator defined by

$$\mathbf{V} = \mathbf{i}u + \mathbf{j}v + \mathbf{k}w, \quad \nabla = \mathbf{i} \frac{\partial}{\partial x} + \mathbf{j} \frac{\partial}{\partial y} + \mathbf{k} \frac{\partial}{\partial z},$$

with $\mathbf{i}, \mathbf{j}, \mathbf{k}$ being the unit basis vector triad of the Cartesian coordinate system.

⁷In fluid dynamics, the components of the velocity vector \mathbf{V} are usually denoted by u, v , and w .

1.4.2 Streamlines and pathlines

The *streamline* and *pathline* patterns are extremely useful when ‘visualising’ the results of fluid flow analysis. Suppose that the velocity vector field is known in terms of Eulerian variables:

$$\mathbf{V} = \mathbf{V}(t, \mathbf{r}).$$

To determine the streamline pattern, one first has to choose the time of observation t and, keeping it fixed, make use of the following definition.

Definition 1.2 *Line \mathcal{L} is called a **streamline** if at each point M on this line the velocity vector \mathbf{V} is tangent to \mathcal{L} ; see Figure 1.12.*

If \mathbf{r} is the position vector of point M and $d\mathbf{r}$ is its increment along the streamline \mathcal{L} connecting point M with a neighbouring point M' , then $d\mathbf{r}$ should be parallel to \mathbf{V} for small enough $|d\mathbf{r}|$. Therefore, the vector product of $d\mathbf{r}$ and \mathbf{V} should be zero,

$$d\mathbf{r} \times \mathbf{V} = 0. \quad (1.4.11)$$

More explicitly, equation (1.4.11) may be written as

$$\begin{aligned} d\mathbf{r} \times \mathbf{V} &= \begin{vmatrix} \mathbf{i} & \mathbf{j} & \mathbf{k} \\ dx & dy & dz \\ u & v & w \end{vmatrix} \\ &= \mathbf{i}(w \, dy - v \, dz) + \mathbf{j}(u \, dz - w \, dx) + \mathbf{k}(v \, dx - u \, dy) = 0. \end{aligned} \quad (1.4.12)$$

Since each component in (1.4.12) must be zero, the differentials dx , dy , and dz are related to each other by

$$\frac{dx}{u(t, x, y, z)} = \frac{dy}{v(t, x, y, z)} = \frac{dz}{w(t, x, y, z)}, \quad (1.4.13)$$

where the coordinate arguments x, y, z of the velocity components u, v, w are varying along the streamline considered, while time t is fixed, implying that at each instant the streamline pattern may be different.

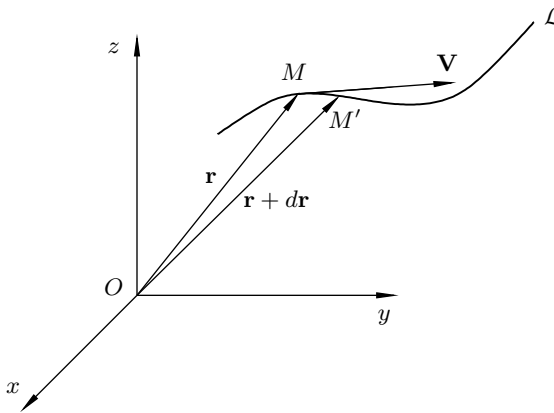


Fig. 1.12: A streamline.

Definition 1.3 Pathlines are the trajectories of fluid particles.

With known velocity field $\mathbf{V}(t, \mathbf{r})$, the equation for pathlines is

$$\frac{d\mathbf{r}}{dt} = \mathbf{V}(t, \mathbf{r}).$$

It consists of three components

$$\frac{dx}{dt} = u(t, x, y, z), \quad \frac{dy}{dt} = v(t, x, y, z), \quad \frac{dz}{dt} = w(t, x, y, z)$$

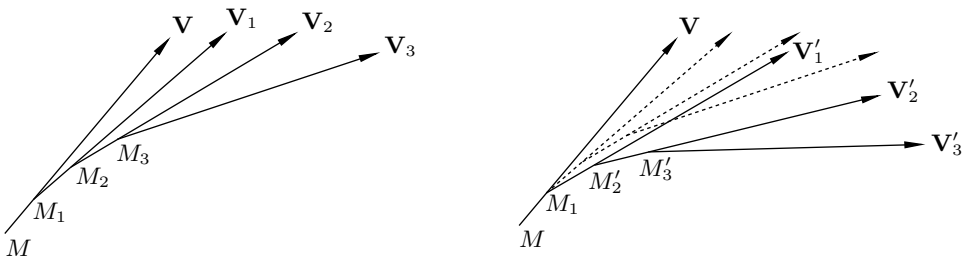
and may be expressed in a form similar to (1.4.13),

$$\frac{dx}{u(t, x, y, z)} = \frac{dy}{v(t, x, y, z)} = \frac{dz}{w(t, x, y, z)} = dt, \quad (1.4.14)$$

but now time t varies while a fluid particle is travelling along a pathline.

In order to demonstrate the difference between streamlines and pathlines, let us choose a point in the flow field (in Figure 1.13, it is shown as point M) and draw the streamline and pathline originating from M . In accordance with their definitions, both the streamline and pathline must follow the direction of the velocity vector. So we take the velocity \mathbf{V} at point M and place point M_1 a small distance from M in the direction of \mathbf{V} . It will be a common point for both the streamline and pathline. Now, if the streamline is to be plotted, the velocity vector \mathbf{V}_1 at point M_1 must be taken at the same time t as at point M . The next point on the streamline will be M_2 ; see Figure 1.13(a). This procedure being repeated many times results in a broken line $MM_1M_2 \dots$, which tends to the actual streamline as the distances between points M , M_1 , M_2 , etc. tend to zero.

If the pathline is to be constructed, one has to take into account that while the fluid particle is travelling from M to M_1 , the velocity vector, being dependent on time, changes to become \mathbf{V}'_1 ; see Figure 1.13(b). So the next point on the pathline will be M'_2 , not M_2 . The more steps that are made along the pathline, the more significant



(a) Construction of a streamline.

(b) Pathline; the 'dashed' vectors reproduce vectors $\mathbf{V}_1, \mathbf{V}_2$, etc. from the previous sketch.

Fig. 1.13: Comparison of a streamline with the corresponding pathline.

is expected to be its deviation from the streamline. However, if the velocity field is independent of time,

$$\mathbf{V} = \mathbf{V}(x, y, z),$$

then the streamline and the pathline obviously coincide with each other. Flows of this kind are called *steady flows*. They have an important role in fluid dynamics. Because of the time independence of fluid-dynamic functions, steady flows are easier to analyse theoretically and experimentally. They are, at the same time, of great importance from an applied engineering point of view. Steady flows may be observed, for example, in wind tunnel experiments when in the laboratory coordinate frame the velocity at each point of the flow does not change with time t . The flow over an aircraft in cruise flight is also steady for the passengers on board, but is unsteady for an observer on the Earth's surface.

The notion of a steady flow, obviously, makes sense only in Eulerian variables. Time dependence in the Lagrangian trajectory function $\mathbf{r} = \mathbf{r}(t, \mathbf{r}_0)$ may disappear only if there is no fluid motion at all. Even in a flow that is steady from the Eulerian point of view, fluid particles experience acceleration and deceleration in the vicinity of a solid body, making the analysis in Lagrangian variables as difficult as it is for non-steady flows. For that reason, Eulerian variables are normally more convenient to use.

1.4.3 Vorticity

With known velocity $\mathbf{V} = \mathbf{V}(t, \mathbf{r})$, the vorticity field $\boldsymbol{\omega}$ may be defined as

$$\boldsymbol{\omega} = \text{curl } \mathbf{V}.$$

Here 'curl' is a differential operator defined as the vector product of the gradient operator

$$\nabla = \mathbf{i} \frac{\partial}{\partial x} + \mathbf{j} \frac{\partial}{\partial y} + \mathbf{k} \frac{\partial}{\partial z}$$

and the velocity vector

$$\mathbf{V} = \mathbf{i}u + \mathbf{j}v + \mathbf{k}w.$$

In the coordinate decomposition form, it may be written as

$$\begin{aligned} \boldsymbol{\omega} = \text{curl } \mathbf{V} = \nabla \times \mathbf{V} &= \begin{vmatrix} \mathbf{i} & \mathbf{j} & \mathbf{k} \\ \frac{\partial}{\partial x} & \frac{\partial}{\partial y} & \frac{\partial}{\partial z} \\ u & v & w \end{vmatrix} \\ &= \mathbf{i} \left(\frac{\partial w}{\partial y} - \frac{\partial v}{\partial z} \right) + \mathbf{j} \left(\frac{\partial u}{\partial z} - \frac{\partial w}{\partial x} \right) + \mathbf{k} \left(\frac{\partial v}{\partial x} - \frac{\partial u}{\partial y} \right). \end{aligned} \quad (1.4.15)$$

The vorticity $\boldsymbol{\omega}$ serves to describe local rotation of fluid particles about their 'centres'. If, in particular, we consider a special form of fluid flow, when the fluid moves as if it was a rigid body,⁸ then the velocity field can be written as

$$\mathbf{V} = \mathbf{V}_0 + \boldsymbol{\Omega} \times (\mathbf{r} - \mathbf{r}_0). \quad (1.4.16)$$

⁸The term 'rigid body' is used in situations when a solid body may be treated as undeformable.

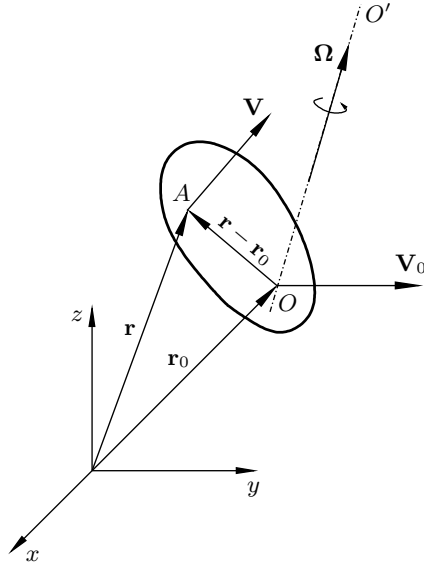


Fig. 1.14: Graphical illustration of formula (1.4.16).

Indeed, it is known from classical mechanics that any rigid-body motion may be represented as a *superposition of (i) translational motion of arbitrary chosen ‘centre’ O inside the body (see Figure 1.14) and (ii) rotation around the axis OO’ that is drawn through the centre O parallel to the angular velocity vector Ω .*

The meaning of different terms in formula (1.4.16) is demonstrated by Figure 1.14. The vector \mathbf{V} on the left-hand side of (1.4.16) is the velocity of an arbitrary chosen point A whose position vector is \mathbf{r} . The first term on the right-hand side is the translational velocity \mathbf{V}_0 of the centre O and the second term, $\Omega \times (\mathbf{r} - \mathbf{r}_0)$, is the circumferential velocity of the body in rotation around the axis OO' ; the latter is drawn through the centre O in the direction of the angular velocity vector Ω . Notice that in a rigid-body motion, Ω is independent of a choice of the centre O and remains the same for any point A situated inside the body.

The coordinate decomposition of equation (1.4.16) is written as

$$\begin{aligned} u &= u_0 + \Omega_y(z - z_0) - \Omega_z(y - y_0), \\ v &= v_0 + \Omega_z(x - x_0) - \Omega_x(z - z_0), \\ w &= w_0 + \Omega_x(y - y_0) - \Omega_y(x - x_0), \end{aligned} \tag{1.4.17}$$

where Ω_x , Ω_y , and Ω_z are the projections of the angular velocity vector Ω on the x -, y -, and z -axes, respectively.

Substitution of (1.4.17) into (1.4.15) yields

$$\boldsymbol{\omega} = \mathbf{i} 2\Omega_x + \mathbf{j} 2\Omega_y + \mathbf{k} 2\Omega_z = 2\Omega.$$

Thus, for a fluid in rigid-body motion, the vorticity $\boldsymbol{\omega}$ is simply twice the angular velocity, Ω .

1.4.4 Circulation

If C is a closed contour inside a moving fluid, then the circulation Γ of the velocity vector \mathbf{V} along C is defined as

$$\Gamma = \oint_C \mathbf{V} \cdot d\mathbf{r}. \tag{1.4.18}$$

We also need to give here the definition of a *vortex line*.

Definition 1.4 Line \mathcal{L} is called a **vortex line** if at each point M on \mathcal{L} the vorticity vector $\boldsymbol{\omega}$ is tangent to \mathcal{L} .

Let us consider a closed contour C , and use it to form a *vortex tube*. The latter is made of the vortex lines originating from contour C . In Figure 1.15, the vortex tube is shown as surface Σ . Let us now draw another contour C' on Σ and ‘close’ the tube from both sides using surface σ that rests on C and surface σ' that rests on C' . We shall call the region bounded by Σ , σ , and σ' region \mathcal{D} . Using Gauss’s divergence theorem, we can write

$$\iiint_{\mathcal{D}} \operatorname{div} \boldsymbol{\omega} \, d\tau = \iint_S (\boldsymbol{\omega} \cdot \mathbf{n}) \, ds, \tag{1.4.19}$$

where S is the surface surrounding \mathcal{D} and \mathbf{n} is the external unit vector normal to S .

The divergence of $\boldsymbol{\omega}$ is given by the formula

$$\operatorname{div} \boldsymbol{\omega} = \frac{\partial \omega_x}{\partial x} + \frac{\partial \omega_y}{\partial y} + \frac{\partial \omega_z}{\partial z}. \tag{1.4.20}$$

Using (1.4.15) in (1.4.20), it is easy to find that for any velocity field

$$\operatorname{div} \boldsymbol{\omega} = 0.$$

Taking further into account that on Σ the vorticity vector $\boldsymbol{\omega}$ is perpendicular to \mathbf{n} , we can see that (1.4.19) reduces to

$$\iint_{\sigma} (\boldsymbol{\omega} \cdot \mathbf{n}) \, ds + \iint_{\sigma'} (\boldsymbol{\omega} \cdot \mathbf{n}) \, ds = 0.$$

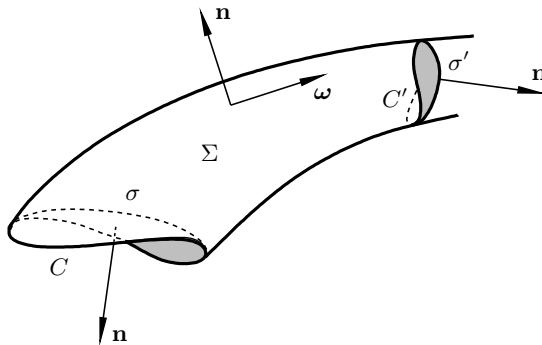


Fig. 1.15: Vortex tube.

34 Chapter 1. Fundamentals of Fluid Dynamics

If we change the direction of the normal vector \mathbf{n} on σ' to the opposite one, making it the same as on σ , then we will have

$$\iint_{\sigma'} (\boldsymbol{\omega} \cdot \mathbf{n}) \, ds = \iint_{\sigma} (\boldsymbol{\omega} \cdot \mathbf{n}) \, ds.$$

We have proved that the flux of the vorticity through a cross-section of a vortex tube does not depend either on the form of the cross-section or on its position along the tube.

In accordance with Stokes's theorem,

$$\iint_{\sigma} (\boldsymbol{\omega} \cdot \mathbf{n}) \, ds = \oint_C \mathbf{V} \cdot d\mathbf{x},$$

which means that the following result, known as the *First Helmholtz Theorem*, is valid.

Theorem 1.1 *The circulation of the velocity vector along a closed contour embracing a vortex tube is an invariant quantity. It is called the **intensity** of the vortex tube.*

Exercises 2

1. The motion of a fluid is described by the following Lagrangian coordinate functions:

$$x = x_0 \left(1 + \frac{t}{\tau}\right), \quad y = y_0 \left(1 + 2\frac{t}{\tau}\right), \quad z = z_0 \left(1 + \frac{t^2}{\tau^2}\right),$$

where τ is a constant.

- (a) Find the velocity field.
 - (b) Consider the fluid particle that was at the point (a, b, c) at time $t = \tau$, and find its position at $t = 3\tau$.
2. Consider the motion of a fluid with velocity field defines in Eulerian variables by the following equations:

$$u = kx, \quad v = -ky, \quad w = 0,$$

where k is a constant. Also assume that the density is given by

$$\rho = \rho_0 + Aye^{kt}.$$

What is the rate of density change for each individual fluid particle (ρ_0 and A are constants)?

3. Find Lagrangian coordinate functions

$$x = x(t, x_0, y_0, z_0), \quad y = (t, x_0, y_0, z_0), \quad z = z(t, x_0, y_0, z_0)$$

corresponding to the following Eulerian velocity field:

$$u = -Ax, \quad v = By, \quad w = 0,$$

where A and B are positive constants.

4. Find the streamlines and pathlines for a flow in which the velocity components are

$$u = u_0, \quad v = v_0 \sin \Omega t, \quad w = w_0,$$

where u_0 , v_0 , w_0 , and Ω are constants.

5. Taking into account that the vorticity $\boldsymbol{\omega}$ in a three-dimensional flow is calculated using equation (1.4.15), show that in a two-dimensional flow, where $w = 0$, and u and v are independent of z , the vector $\boldsymbol{\omega}$ has only one non-zero component ω_z . Give an expression for ω_z .
6. In the Couette flow between two flat plates, one of which is stationary, and another is moving parallel it with constant velocity (see Figure 1.16), the velocity components are known to be (see Section 2.1.1)

$$u = ay, \quad v = 0, \quad w = 0.$$

Determine the pathlines (streamlines) and the vorticity of the flow. Explain how with the straight trajectories of fluid particles, the vorticity may be non-zero.

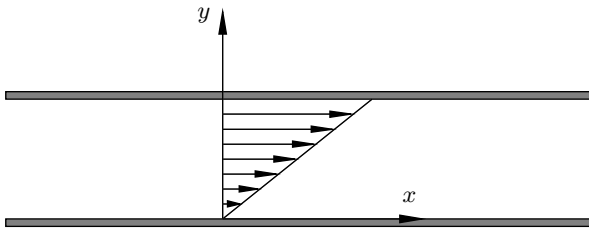


Fig. 1.16: Couette flow.

7. The ‘potential vortex’ is a two-dimensional flow with streamlines having the form of concentric circles (Figure 1.17). In Section 3.4, we will see that in the potential vortex the radial velocity component V_r is zero everywhere in the flow field, and the circumferential velocity V_ϕ is inversely proportional to the distance r from the

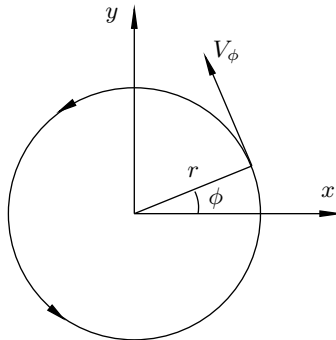


Fig. 1.17: The potential vortex.

vortex centre:

$$V_\phi = \frac{\Gamma}{2\pi r}.$$

Determine the vorticity distribution in this flow.

Hint: You may use without proof the fact that in cylindrical polar coordinates (r, ϕ) , the vorticity ω_z may be calculated using the equation⁹

$$\omega_z = \frac{1}{r} \frac{\partial(rV_\phi)}{\partial r} - \frac{1}{r} \frac{\partial V_r}{\partial \phi}.$$

1.4.5 Rate-of-strain tensor

In addition to translation and rotation, fluid particles are also subject to deformation. In order to understand what the *deformational motion* of a fluid is, let us compare the velocity field of an undeformable rigid body with that of an arbitrarily moving fluid. Recall that any motion of a rigid body may be represented as a superposition of the translational motion of an arbitrarily chosen ‘centre’ O and rotation around the axis OO' passing through the centre (see Figure 1.14). This statement is expressed by equation (1.4.16) with coordinate decomposition given by (1.4.17).

Taking into account that the vorticity $\boldsymbol{\omega}$ is twice the angular velocity $\boldsymbol{\Omega}$, we can write (1.4.17) in the form

$$\left. \begin{aligned} u &= u_0 + \frac{1}{2}\omega_y(z - z_0) - \frac{1}{2}\omega_z(y - y_0), \\ v &= v_0 + \frac{1}{2}\omega_z(x - x_0) - \frac{1}{2}\omega_x(z - z_0), \\ w &= w_0 + \frac{1}{2}\omega_x(y - y_0) - \frac{1}{2}\omega_y(x - x_0). \end{aligned} \right\} \quad (1.4.21)$$

Equation (1.4.15) shows that the components of the vorticity vector $\boldsymbol{\omega}$ are calculated as

$$\omega_x = \frac{\partial w}{\partial y} - \frac{\partial v}{\partial z}, \quad \omega_y = \frac{\partial u}{\partial z} - \frac{\partial w}{\partial x}, \quad \omega_z = \frac{\partial v}{\partial x} - \frac{\partial u}{\partial y}. \quad (1.4.22)$$

Substitution of (1.4.22) into (1.4.21) yields

$$\left. \begin{aligned} u &= u_0 + \frac{1}{2} \left(\frac{\partial u}{\partial z} - \frac{\partial w}{\partial x} \right) (z - z_0) - \frac{1}{2} \left(\frac{\partial v}{\partial x} - \frac{\partial u}{\partial y} \right) (y - y_0), \\ v &= v_0 + \frac{1}{2} \left(\frac{\partial v}{\partial x} - \frac{\partial u}{\partial y} \right) (x - x_0) - \frac{1}{2} \left(\frac{\partial w}{\partial y} - \frac{\partial v}{\partial z} \right) (z - z_0), \\ w &= w_0 + \frac{1}{2} \left(\frac{\partial w}{\partial y} - \frac{\partial v}{\partial z} \right) (y - y_0) - \frac{1}{2} \left(\frac{\partial u}{\partial z} - \frac{\partial w}{\partial x} \right) (x - x_0). \end{aligned} \right\} \quad (1.4.23)$$

For a flow of a deformable medium, the formula (1.4.16) is not applicable, nor can the notion of angular velocity $\boldsymbol{\Omega}$, being constant over a finite fluid volume, even be introduced. However, assuming that the velocity field is smooth, we can study the *local* behaviour of the flow field as follows. Let us consider a small fluid element (see Figure 1.18) in the flow with the velocity $\mathbf{V} = \mathbf{V}(t, \mathbf{r})$ defined in the Euler variables.

⁹See equation (1.8.38c) on page 82.

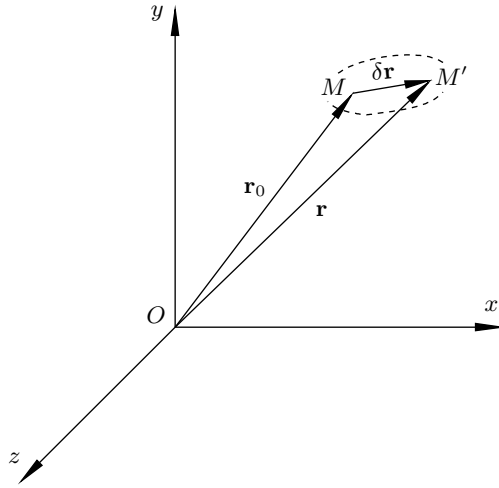


Fig. 1.18: Deformation of a fluid element.

We choose a point M inside the element as its ‘centre’. The position of this point at instant t is defined by the position vector \mathbf{r}_0 . We then consider (at the same instant) a neighbouring point M' whose position vector is $\mathbf{r} = \mathbf{r}_0 + \delta\mathbf{r}$. Here the symbol δ is used to signify that the variation of coordinates is taken at the same instant t .

Taking into account that the viscous forces always act to smooth out possible discontinuities in flow functions, we shall suppose that the velocity components are differentiable, and therefore may be represented by the Taylor expansions

$$\begin{aligned} u(t, \mathbf{r}) &= u(t, \mathbf{r}_0 + \delta\mathbf{r}) = u(t, \mathbf{r}_0) + \frac{\partial u}{\partial x} \delta x + \frac{\partial u}{\partial y} \delta y + \frac{\partial u}{\partial z} \delta z, \\ v(t, \mathbf{r}) &= v(t, \mathbf{r}_0 + \delta\mathbf{r}) = v(t, \mathbf{r}_0) + \frac{\partial v}{\partial x} \delta x + \frac{\partial v}{\partial y} \delta y + \frac{\partial v}{\partial z} \delta z, \\ w(t, \mathbf{r}) &= w(t, \mathbf{r}_0 + \delta\mathbf{r}) = w(t, \mathbf{r}_0) + \frac{\partial w}{\partial x} \delta x + \frac{\partial w}{\partial y} \delta y + \frac{\partial w}{\partial z} \delta z. \end{aligned}$$

or, after regrouping,

$$\begin{aligned} u(t, \mathbf{r}) &= u(t, \mathbf{r}_0) + \frac{1}{2} \left(\frac{\partial u}{\partial z} - \frac{\partial w}{\partial x} \right) \delta z - \frac{1}{2} \left(\frac{\partial v}{\partial x} - \frac{\partial u}{\partial y} \right) \delta y \\ &\quad + \frac{\partial u}{\partial x} \delta x + \frac{1}{2} \left(\frac{\partial u}{\partial y} + \frac{\partial v}{\partial x} \right) \delta y + \frac{1}{2} \left(\frac{\partial u}{\partial z} + \frac{\partial w}{\partial x} \right) \delta z, \end{aligned} \quad (1.4.24a)$$

$$\begin{aligned} v(t, \mathbf{r}) &= v(t, \mathbf{r}_0) + \frac{1}{2} \left(\frac{\partial v}{\partial x} - \frac{\partial u}{\partial y} \right) \delta x - \frac{1}{2} \left(\frac{\partial w}{\partial y} - \frac{\partial v}{\partial z} \right) \delta z \\ &\quad + \frac{1}{2} \left(\frac{\partial v}{\partial x} + \frac{\partial u}{\partial y} \right) \delta x + \frac{\partial v}{\partial y} \delta y + \frac{1}{2} \left(\frac{\partial v}{\partial z} + \frac{\partial w}{\partial y} \right) \delta z, \end{aligned} \quad (1.4.24b)$$

$$\begin{aligned}
 w(t, \mathbf{r}) = w(t, \mathbf{r}_0) &+ \frac{1}{2} \left(\frac{\partial w}{\partial y} - \frac{\partial v}{\partial z} \right) \delta y - \frac{1}{2} \left(\frac{\partial u}{\partial z} - \frac{\partial w}{\partial x} \right) \delta x \\
 &+ \frac{1}{2} \left(\frac{\partial w}{\partial x} + \frac{\partial u}{\partial z} \right) \delta x + \frac{1}{2} \left(\frac{\partial w}{\partial y} + \frac{\partial v}{\partial z} \right) \delta y + \frac{\partial w}{\partial z} \delta z. \quad (1.4.24c)
 \end{aligned}$$

The first lines in the expressions (1.4.24a), (1.4.24b) and (1.4.24c) are easily seen to coincide with the formulae (1.4.23). They describe the ‘quasi-rigid’ motion of the fluid element, which would be its only motion if the fluid element suddenly solidified. Consequently, the second lines in (1.4.23) should be attributed to the *deformational motion* of the fluid:

$$\left. \begin{aligned}
 u_{\text{def}} &= \frac{\partial u}{\partial x} \delta x + \frac{1}{2} \left(\frac{\partial u}{\partial y} + \frac{\partial v}{\partial x} \right) \delta y + \frac{1}{2} \left(\frac{\partial u}{\partial z} + \frac{\partial w}{\partial x} \right) \delta z, \\
 v_{\text{def}} &= \frac{1}{2} \left(\frac{\partial v}{\partial x} + \frac{\partial u}{\partial y} \right) \delta x + \frac{\partial v}{\partial y} \delta y + \frac{1}{2} \left(\frac{\partial v}{\partial z} + \frac{\partial w}{\partial y} \right) \delta z, \\
 w_{\text{def}} &= \frac{1}{2} \left(\frac{\partial w}{\partial x} + \frac{\partial u}{\partial z} \right) \delta x + \frac{1}{2} \left(\frac{\partial w}{\partial y} + \frac{\partial v}{\partial z} \right) \delta y + \frac{\partial w}{\partial z} \delta z.
 \end{aligned} \right\} \quad (1.4.25)$$

The tensor composed of the coefficients of δx , δy , and δz in (1.4.25)

$$\mathcal{E} = \begin{pmatrix} \varepsilon_{xx} & \varepsilon_{xy} & \varepsilon_{xz} \\ \varepsilon_{yx} & \varepsilon_{yy} & \varepsilon_{yz} \\ \varepsilon_{zx} & \varepsilon_{zy} & \varepsilon_{zz} \end{pmatrix} = \begin{pmatrix} \frac{\partial u}{\partial x} & \frac{1}{2} \left(\frac{\partial u}{\partial y} + \frac{\partial v}{\partial x} \right) & \frac{1}{2} \left(\frac{\partial u}{\partial z} + \frac{\partial w}{\partial x} \right) \\ \frac{1}{2} \left(\frac{\partial v}{\partial x} + \frac{\partial u}{\partial y} \right) & \frac{\partial v}{\partial y} & \frac{1}{2} \left(\frac{\partial v}{\partial z} + \frac{\partial w}{\partial y} \right) \\ \frac{1}{2} \left(\frac{\partial w}{\partial x} + \frac{\partial u}{\partial z} \right) & \frac{1}{2} \left(\frac{\partial w}{\partial y} + \frac{\partial v}{\partial z} \right) & \frac{\partial w}{\partial z} \end{pmatrix}, \quad (1.4.26)$$

is called the *rate-of-strain tensor*.

Using this tensor, equations (1.4.24) may be expressed in the form

$$\mathbf{V}(t, \mathbf{r}) = \mathbf{V}(t, \mathbf{r}_0) + \boldsymbol{\Omega} \times \delta \mathbf{r} + \mathcal{E} \delta \mathbf{r} \quad (1.4.27)$$

which proves the *Second Helmholtz Theorem*.

Theorem 1.2 *Any motion of a small fluid element is a superposition of (i) quasi-rigid motion represented by the first two terms in (1.4.27) and (ii) deformational motion with the velocity $\mathbf{V}_{\text{def}} = \mathcal{E} \delta \mathbf{r}$.*

Notice that the rate-of-strain tensor (1.4.26) is symmetric with respect to the principal diagonal, since

$$\varepsilon_{yx} = \varepsilon_{xy}, \quad \varepsilon_{zx} = \varepsilon_{xz}, \quad \varepsilon_{zy} = \varepsilon_{yz}.$$

The six unequal elements of the tensor represent six possible modes of the deformation of a fluid particle. To reveal their physical content, it is convenient to use a moving Cartesian coordinate system $Oxyz$ with the origin O being in the fluid element ‘centre’ at all times and the coordinate axes x , y , z rotating together with angular velocity $\boldsymbol{\Omega} = \frac{1}{2} \text{curl } \mathbf{V}$. The only fluid motion that may be observed in this coordinate system is the deformation of the fluid element with respect to the centre. At any point inside the fluid particle, the deformation velocity is calculated as

$$\mathbf{V} = \mathcal{E} \delta \mathbf{r},$$

where $\delta \mathbf{r}$ is the position vector of the point of interest.

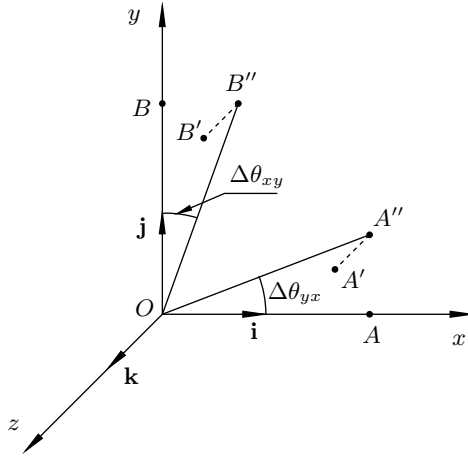


Fig. 1.19: Deformation of a fluid element.

Let us, for example, consider point A situated on the x -axis as shown in Figure 1.19. The position vector of this point may be written as $\delta \mathbf{r} = \mathbf{i} \delta x$, where \mathbf{i} is the unit vector along the x -axis. The fluid velocity at point A is

$$\mathbf{V} = \mathcal{E} \delta \mathbf{r} = \begin{pmatrix} \varepsilon_{xx} & \varepsilon_{xy} & \varepsilon_{xz} \\ \varepsilon_{yx} & \varepsilon_{yy} & \varepsilon_{yz} \\ \varepsilon_{zx} & \varepsilon_{zy} & \varepsilon_{zz} \end{pmatrix} \begin{pmatrix} \delta x \\ 0 \\ 0 \end{pmatrix} = \begin{pmatrix} \varepsilon_{xx} \delta x \\ \varepsilon_{yx} \delta x \\ \varepsilon_{zx} \delta x \end{pmatrix},$$

which is written in coordinate-decomposition form as

$$u = \varepsilon_{xx} \delta x, \quad v = \varepsilon_{yx} \delta x, \quad w = \varepsilon_{zx} \delta x.$$

Consequently, the fluid particle that was at point A at initial instant t translates shortly afterwards to a new position A' (see Figure 1.19) with the coordinates

$$x = \delta x + \varepsilon_{xx} \delta x \Delta t, \quad y = \varepsilon_{yx} \delta x \Delta t, \quad z = \varepsilon_{zx} \delta x \Delta t. \quad (1.4.28)$$

Here Δt denotes the time spent by the fluid particle when travelling between points A and A' .

The distance between the new location A' of the fluid particle and the coordinate origin O is

$$\begin{aligned} l_{OA'} &= \delta x \sqrt{(1 + \varepsilon_{xx} \Delta t)^2 + (\varepsilon_{yx} \Delta t)^2 + (\varepsilon_{zx} \Delta t)^2} \\ &= \delta x \sqrt{1 + 2\varepsilon_{xx} \Delta t + O[(\Delta t)^2]} = \delta x (1 + \varepsilon_{xx} \Delta t) + O[\delta x (\Delta t)^2]. \end{aligned}$$

It differs from the distance $l_{OA} = \delta x$ between the original location A and the coordinate origin O by the value

$$\Delta l = l_{OA'} - l_{OA} = \varepsilon_{xx} \delta x \Delta t. \quad (1.4.29)$$

Formula (1.4.29), obviously, holds for any fluid particle situated on the x -axis in the vicinity of the centre O . Therefore, if we consider a material line composed of the fluid particles occupying the interval (O, A) of the x -axis, then we can see that the material line experiences uniform extension at a relative rate

$$\frac{1}{\delta x} \lim_{\Delta t \rightarrow 0} \frac{\Delta l}{\Delta t} = \varepsilon_{xx}.$$

In addition to the extension, the material line deviates from the x -axis. According to (1.4.28), its projection (O, A'') upon the (x, y) -plane (see Figure 1.19) makes an angle

$$\Delta\theta_{yx} = \arctan \frac{y}{x} \tag{1.4.30}$$

with the x -axis. Substituting (1.4.28) into (1.4.30), we have

$$\Delta\theta_{yx} = \arctan \frac{\varepsilon_{yx} \Delta t}{1 + \varepsilon_{xx} \Delta t},$$

which for small Δt reduces to

$$\Delta\theta_{yx} = \arctan (\varepsilon_{yx} \Delta t) = \varepsilon_{yx} \Delta t.$$

In the same way, it may be shown that the material line composed of the fluid particles from the interval (O, B) of the y -axis experiences extension with the rate ε_{yy} and deviates from the y -axis such that its projection (O, B'') upon the (x, y) -plane makes an angle

$$\Delta\theta_{xy} = \varepsilon_{xy} \Delta t$$

with the y -axis (see Figure 1.19). Consequently, the original right angle between the material lines (O, A) and (O, B) decreases by an amount

$$\Delta\theta_{yx} + \Delta\theta_{xy} = (\varepsilon_{yx} + \varepsilon_{xy}) \Delta t.$$

Taking into account that $\varepsilon_{yx} = \varepsilon_{xy}$, we can conclude that the angle between the x - and y -axes decreases with the rate

$$\lim_{\Delta t \rightarrow 0} \frac{\Delta\theta_{yx} + \Delta\theta_{xy}}{\Delta t} = \varepsilon_{yx} + \varepsilon_{xy} = 2\varepsilon_{xy}.$$

The same arguments may be, of course, applied to a material line on the z -axis, leading to the conclusion that the three diagonal elements ε_{xx} , ε_{yy} , ε_{zz} of the rate-of-strain tensor (1.4.30) describe linear expansion of a small fluid element in the x -, y -, and z -directions, respectively. The non-diagonal elements ε_{xy} , ε_{xz} , ε_{yz} and their symmetric counterparts ε_{yx} , ε_{zx} , ε_{zy} serve to describe angular compression of the fluid element in the (x, y) -, (x, z) -, and (y, z) -planes.

1.5 Constitutive Equation

Returning to the question of the origin of the surface forces acting in fluids (see Section 1.2), one has to remember that these are the short-range forces produced by the interaction of molecules via mutual forces of attraction and repulsion. In particular, in gases, the dominant mechanism is transport of momentum from one fluid layer to another due to collisions of molecules in their thermal motion. In a fluid at rest, the only surface force possible is the pressure p acting equally in all directions, with the stress tensor assuming the form (1.2.13):

$$\mathcal{P} = \begin{pmatrix} -p & 0 & 0 \\ 0 & -p & 0 \\ 0 & 0 & -p \end{pmatrix} = -pI, \quad (1.5.1)$$

where

$$I = \begin{pmatrix} 1 & 0 & 0 \\ 0 & 1 & 0 \\ 0 & 0 & 1 \end{pmatrix}$$

is the unit tensor.

If a fluid moves like a rigid body (translation and rotation), then the interaction between the molecules will remain the same as they would be in this fluid at rest. Consequently, the stress tensor will remain unchanged, i.e. it could be represented by equation (1.5.1). Keeping this in mind, we shall write the stress tensor (1.2.6) for an arbitrarily moving fluid as

$$\mathcal{P} = -pI + \mathcal{T}, \quad (1.5.2)$$

where the tensor

$$\mathcal{T} = \begin{pmatrix} \tau_{xx} & \tau_{xy} & \tau_{xz} \\ \tau_{yx} & \tau_{yy} & \tau_{yz} \\ \tau_{zx} & \tau_{zy} & \tau_{zz} \end{pmatrix}$$

is called the *deviatoric stress tensor*. Its existence is entirely attributable to the deformational motion of a fluid.

The purpose of the following analysis will be to find an explicit form of the relationship between \mathcal{T} and the rate-of-strain tensor \mathcal{E} . Such a relationship is termed the *constitutive equation*. Since the rate-of-strain tensor (1.4.26) is symmetrical, there exists a privileged Cartesian coordinate system $(\hat{x}, \hat{y}, \hat{z})$ where \mathcal{E} assumes a diagonal form

$$\begin{pmatrix} \varepsilon_{\hat{x}\hat{x}} & 0 & 0 \\ 0 & \varepsilon_{\hat{y}\hat{y}} & 0 \\ 0 & 0 & \varepsilon_{\hat{z}\hat{z}} \end{pmatrix}. \quad (1.5.3)$$

These coordinates are called the *principal axes* of the rate-of-strain tensor.

Our strategy will be to deduce the constitutive equation in the principal axes $(\hat{x}, \hat{y}, \hat{z})$ and then we will return to the original Cartesian coordinates (x, y, z) . If we write the deviatoric stress tensor in the principal $(\hat{x}, \hat{y}, \hat{z})$ -axes,

$$\mathcal{T} = \begin{pmatrix} \tau_{\hat{x}\hat{x}} & \tau_{\hat{x}\hat{y}} & \tau_{\hat{x}\hat{z}} \\ \tau_{\hat{y}\hat{x}} & \tau_{\hat{y}\hat{y}} & \tau_{\hat{y}\hat{z}} \\ \tau_{\hat{z}\hat{x}} & \tau_{\hat{z}\hat{y}} & \tau_{\hat{z}\hat{z}} \end{pmatrix}, \quad (1.5.4)$$

then each element in (1.5.4) has to be a function of the three elements of the tensor (1.5.3).

In this presentation, we restrict our attention to fluids that satisfy the following two postulates.

1. **Linearity postulate.** All the elements of the deviatoric stress tensor (1.5.4) are linear functions of the three elements of the rate-of-strain tensor (1.5.3). For example, the first diagonal element may be written as

$$\tau_{\hat{x}\hat{x}} = a_1\varepsilon_{\hat{x}\hat{x}} + a_2\varepsilon_{\hat{y}\hat{y}} + a_3\varepsilon_{\hat{z}\hat{z}}. \tag{1.5.5}$$

Here the coefficients a_1 , a_2 , and a_3 are assumed to be independent on the velocity field, but might depend on the local thermodynamic state of the fluid.

2. **Isotropy postulate.** The form of the equations, such as (1.5.5), relating the elements of the deviatoric stress tensor (1.5.4) to the elements of the rate-of-strain tensor (1.5.3) should be independent on the choice of Cartesian coordinates aligned with the principal axes.

Applying the first postulate to the second diagonal element of the tensor (1.5.4), we can write

$$\tau_{\hat{y}\hat{y}} = b_1\varepsilon_{\hat{x}\hat{x}} + b_2\varepsilon_{\hat{y}\hat{y}} + b_3\varepsilon_{\hat{z}\hat{z}}. \tag{1.5.6}$$

We shall now prove that the coefficients b_1 , b_2 , b_3 in (1.5.6) are not independent of the coefficients a_1 , a_2 , a_3 in (1.5.5). For this purpose, we rotate the coordinate system as shown in Figure 1.20. According to the second postulate, equation (1.5.6) is invariant with respect to the rotation, and in the ‘new coordinates’ $(\hat{x}', \hat{y}', \hat{z}')$, it should be written as

$$\tau_{\hat{y}'\hat{y}'} = b_1\varepsilon_{\hat{x}'\hat{x}'} + b_2\varepsilon_{\hat{y}'\hat{y}'} + b_3\varepsilon_{\hat{z}'\hat{z}'}.$$

It is obvious that $\tau_{\hat{y}'\hat{y}'}$ and $\tau_{\hat{x}\hat{x}}$ represent the same physical quantity, the projection on the \hat{x} -axis of the stress acting on a surface element drawn perpendicular to the \hat{x} -axis (with the pressure subtracted). Hence, we can write

$$\tau_{\hat{x}\hat{x}} = \tau_{\hat{y}'\hat{y}'} = b_1\varepsilon_{\hat{x}'\hat{x}'} + b_2\varepsilon_{\hat{y}'\hat{y}'} + b_3\varepsilon_{\hat{z}'\hat{z}'} . \tag{1.5.7}$$

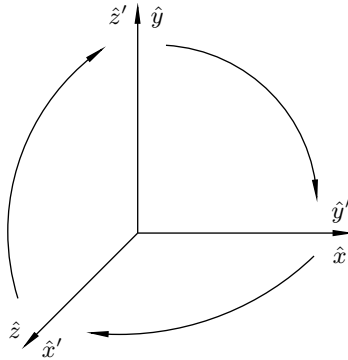


Fig. 1.20: Rotation of the principal axes.

It further easily seen from Figure 1.20 that

$$\begin{aligned}\hat{x}' &= \hat{z}, & \hat{y}' &= \hat{x}, & \hat{z}' &= \hat{y}, \\ \hat{u}' &= \hat{w}, & \hat{v}' &= \hat{u}, & \hat{w}' &= \hat{v}.\end{aligned}$$

Consequently, using the formula for the first diagonal element of \mathcal{E} in (1.4.26), we find

$$\varepsilon_{\hat{x}'\hat{x}'} = \frac{\partial \hat{u}'}{\partial \hat{x}'} = \frac{\partial \hat{w}}{\partial \hat{z}} = \varepsilon_{\hat{z}\hat{z}}. \quad (1.5.8)$$

Similarly, it can be deduced that

$$\varepsilon_{\hat{y}'\hat{y}'} = \varepsilon_{\hat{x}\hat{x}}, \quad \varepsilon_{\hat{z}'\hat{z}'} = \varepsilon_{\hat{y}\hat{y}}. \quad (1.5.9)$$

Substitution of (1.5.8) and (1.5.9) into (1.5.7) results in

$$\tau_{\hat{x}\hat{x}} = b_1 \varepsilon_{\hat{z}\hat{z}} + b_2 \varepsilon_{\hat{x}\hat{x}} + b_3 \varepsilon_{\hat{y}\hat{y}}. \quad (1.5.10)$$

It remains to compare (1.5.10) with (1.5.5), and we can conclude that $b_1 = a_3$, $b_2 = a_1$, and $b_3 = a_2$, which allows us to write (1.5.6) as

$$\tau_{\hat{y}\hat{y}} = a_1 \varepsilon_{\hat{y}\hat{y}} + a_2 \varepsilon_{\hat{z}\hat{z}} + a_3 \varepsilon_{\hat{x}\hat{x}}. \quad (1.5.11)$$

Similarly, it may be shown that

$$\tau_{\hat{z}\hat{z}} = a_1 \varepsilon_{\hat{z}\hat{z}} + a_2 \varepsilon_{\hat{x}\hat{x}} + a_3 \varepsilon_{\hat{y}\hat{y}}. \quad (1.5.12)$$

Let us now show that $a_2 = a_3$. For this purpose, we rotate the coordinate system around the \hat{x} -axis through a right angle as shown in Figure 1.21. The new axes \hat{x}' , \hat{y}' ,

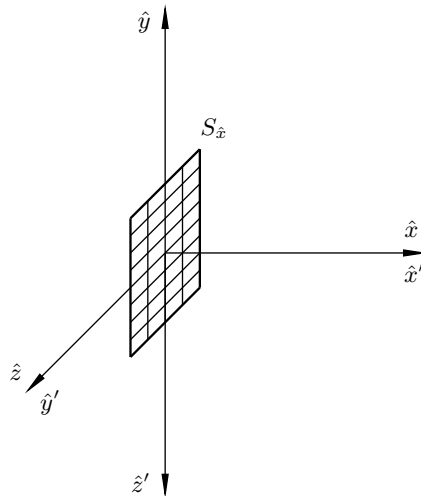


Fig. 1.21: Rotation of the principal axes around the \hat{x} -axis through an angle $\pi/2$.

and \hat{z}' lie along the principal axes of the rate-of-strain tensor \mathcal{E} , and therefore, according to the second postulate, we can still use equation (1.5.5). In the new coordinates, it is written as

$$\tau_{\hat{x}'\hat{x}'} = a_1 \varepsilon_{\hat{x}'\hat{x}'} + a_2 \varepsilon_{\hat{y}'\hat{y}'} + a_3 \varepsilon_{\hat{z}'\hat{z}'} . \quad (1.5.13)$$

The new and old coordinates and the components of the velocity vector are related to one another as

$$\begin{aligned} \hat{x}' &= \hat{x}, & \hat{y}' &= \hat{z}, & \hat{z}' &= -\hat{y}, \\ \hat{u}' &= \hat{u}, & \hat{v}' &= \hat{w}, & \hat{w}' &= -\hat{v}. \end{aligned}$$

Consequently,

$$\begin{aligned} \varepsilon_{\hat{x}'\hat{x}'} &= \frac{\partial \hat{u}'}{\partial \hat{x}'} = \frac{\partial \hat{u}}{\partial \hat{x}} = \varepsilon_{\hat{x}\hat{x}}, & \varepsilon_{\hat{y}'\hat{y}'} &= \frac{\partial \hat{v}'}{\partial \hat{y}'} = \frac{\partial \hat{w}}{\partial \hat{z}} = \varepsilon_{\hat{z}\hat{z}}, \\ \varepsilon_{\hat{z}'\hat{z}'} &= \frac{\partial \hat{w}'}{\partial \hat{z}'} = \frac{\partial \hat{v}}{\partial \hat{y}} = \varepsilon_{\hat{y}\hat{y}} . \end{aligned}$$

Using these in (1.5.13), we find

$$\tau_{\hat{x}'\hat{x}'} = a_1 \varepsilon_{\hat{x}\hat{x}} + a_3 \varepsilon_{\hat{y}\hat{y}} + a_2 \varepsilon_{\hat{z}\hat{z}} . \quad (1.5.14)$$

It remains to compare (1.5.14) with (1.5.5) and take into account that $\tau_{\hat{x}'\hat{x}'}$ and $\tau_{\hat{x}\hat{x}}$ represent the same physical quantity, namely, the normal component of the stress acting upon surface $S_{\hat{x}}$ drawn perpendicular to the \hat{x} -axis, with the pressure subtracted. We see that a_2 and a_3 are really equal to one another.

Two factors a_1 and a_2 in (1.5.5), (1.5.11), and (1.5.12) remain independent of one another. If instead we introduce parameters λ and μ such that

$$a_1 = \lambda + 2\mu, \quad a_2 = a_3 = \lambda,$$

then equations (1.5.5), (1.5.11), and (1.5.12) assume the forms

$$\left. \begin{aligned} \tau_{\hat{x}\hat{x}} &= \lambda(\varepsilon_{\hat{x}\hat{x}} + \varepsilon_{\hat{y}\hat{y}} + \varepsilon_{\hat{z}\hat{z}}) + 2\mu\varepsilon_{\hat{x}\hat{x}}, \\ \tau_{\hat{y}\hat{y}} &= \lambda(\varepsilon_{\hat{x}\hat{x}} + \varepsilon_{\hat{y}\hat{y}} + \varepsilon_{\hat{z}\hat{z}}) + 2\mu\varepsilon_{\hat{y}\hat{y}}, \\ \tau_{\hat{z}\hat{z}} &= \lambda(\varepsilon_{\hat{x}\hat{x}} + \varepsilon_{\hat{y}\hat{y}} + \varepsilon_{\hat{z}\hat{z}}) + 2\mu\varepsilon_{\hat{z}\hat{z}}. \end{aligned} \right\} \quad (1.5.15)$$

The parameter μ is called the *first viscosity coefficient* and the parameter λ the *second viscosity coefficient*. Since

$$\varepsilon_{\hat{x}\hat{x}} + \varepsilon_{\hat{y}\hat{y}} + \varepsilon_{\hat{z}\hat{z}} = \frac{\partial \hat{u}}{\partial \hat{x}} + \frac{\partial \hat{v}}{\partial \hat{y}} + \frac{\partial \hat{w}}{\partial \hat{z}} = \operatorname{div} \mathbf{V},$$

equations (1.5.15) may be written as

$$\left. \begin{aligned} \tau_{\hat{x}\hat{x}} &= \lambda \operatorname{div} \mathbf{V} + 2\mu\varepsilon_{\hat{x}\hat{x}}, \\ \tau_{\hat{y}\hat{y}} &= \lambda \operatorname{div} \mathbf{V} + 2\mu\varepsilon_{\hat{y}\hat{y}}, \\ \tau_{\hat{z}\hat{z}} &= \lambda \operatorname{div} \mathbf{V} + 2\mu\varepsilon_{\hat{z}\hat{z}}. \end{aligned} \right\} \quad (1.5.16)$$

We shall now show that all the non-diagonal elements of the deviatoric stress tensor (1.5.4) vanish when \mathcal{T} is written in the principal axes \hat{x} , \hat{y} , \hat{z} of the rate-of-strain tensor \mathcal{E} . It is sufficient to prove that $\tau_{\hat{x}\hat{y}} = 0$. According to the first postulate, we can write

$$\tau_{\hat{x}\hat{y}} = c_1 \varepsilon_{\hat{x}\hat{x}} + c_2 \varepsilon_{\hat{y}\hat{y}} + c_3 \varepsilon_{\hat{z}\hat{z}}. \quad (1.5.17)$$

If we rotate the coordinate system around the \hat{x} -axis through an angle π , as shown in Figure 1.22, then, using postulate 2, we can also write

$$\tau_{\hat{x}'\hat{y}'} = c_1 \varepsilon_{\hat{x}'\hat{x}'} + c_2 \varepsilon_{\hat{y}'\hat{y}'} + c_3 \varepsilon_{\hat{z}'\hat{z}'}. \quad (1.5.18)$$

The new and old coordinates, and the corresponding velocity components, are related as

$$\begin{aligned} \hat{x}' &= \hat{x}, & \hat{y}' &= -\hat{y}, & \hat{z}' &= -\hat{z}, \\ \hat{u}' &= \hat{u}, & \hat{v}' &= -\hat{v}, & \hat{w}' &= -\hat{w}. \end{aligned}$$

Consequently,

$$\begin{aligned} \varepsilon_{\hat{x}'\hat{x}'} &= \frac{\partial \hat{u}'}{\partial \hat{x}'} = \frac{\partial \hat{u}}{\partial \hat{x}} = \varepsilon_{\hat{x}\hat{x}}, & \varepsilon_{\hat{y}'\hat{y}'} &= \frac{\partial \hat{v}'}{\partial \hat{y}'} = \frac{\partial \hat{v}}{\partial \hat{y}} = \varepsilon_{\hat{y}\hat{y}}, \\ \varepsilon_{\hat{z}'\hat{z}'} &= \frac{\partial \hat{w}'}{\partial \hat{z}'} = \frac{\partial \hat{w}}{\partial \hat{z}} = \varepsilon_{\hat{z}\hat{z}}, \end{aligned}$$

which, when substituted into equation (1.5.18), render it in the form

$$\tau_{\hat{x}'\hat{y}'} = c_1 \varepsilon_{\hat{x}\hat{x}} + c_2 \varepsilon_{\hat{y}\hat{y}} + c_3 \varepsilon_{\hat{z}\hat{z}}. \quad (1.5.19)$$

Since the right-hand sides in (1.5.19) and (1.5.17) coincide with one another, we can conclude that

$$\tau_{\hat{x}'\hat{y}'} = \tau_{\hat{x}\hat{y}}. \quad (1.5.20)$$

The second equation relating these quantities may be deduced by simply recalling the physical content of $\tau_{\hat{x}\hat{y}}$ and $\tau_{\hat{x}'\hat{y}'}$: the former is the \hat{y} -projection of the stress acting

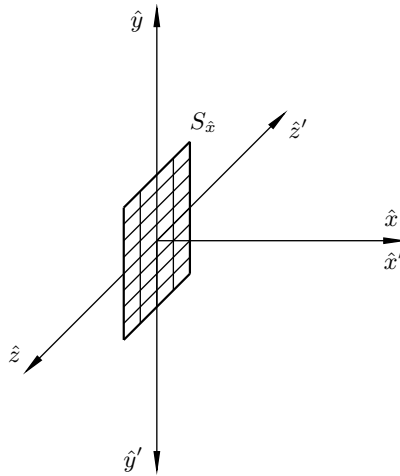


Fig. 1.22: Rotation of the coordinate system around the \hat{x} -axis through an angle π .

upon the surface $S_{\hat{x}}$ drawn perpendicular to the \hat{x} -axis (see Figure 1.22), while the latter is the projection of the same stress on the \hat{y}' -axis. Since the \hat{y} - and \hat{y}' -axes are directed opposite to one another,

$$\tau_{\hat{x}'\hat{y}'} = -\tau_{\hat{x}\hat{y}}. \tag{1.5.21}$$

It follows from (1.5.20) and (1.5.21) that $\tau_{\hat{x}\hat{y}}$ is, indeed, zero, and we can conclude that the deviatoric stress tensor (1.5.4) assumes a diagonal form

$$\mathcal{T} = \begin{pmatrix} \tau_{\hat{x}\hat{x}} & 0 & 0 \\ 0 & \tau_{\hat{y}\hat{y}} & 0 \\ 0 & 0 & \tau_{\hat{z}\hat{z}} \end{pmatrix}. \tag{1.5.22}$$

Using (1.5.16) in (1.5.22), we find that the sought constitutive equation has the form

$$\mathcal{T} = \lambda \operatorname{div} \mathbf{V} \begin{pmatrix} 1 & 0 & 0 \\ 0 & 1 & 0 \\ 0 & 0 & 1 \end{pmatrix} + 2\mu \begin{pmatrix} \varepsilon_{\hat{x}\hat{x}} & 0 & 0 \\ 0 & \varepsilon_{\hat{y}\hat{y}} & 0 \\ 0 & 0 & \varepsilon_{\hat{z}\hat{z}} \end{pmatrix},$$

or, equivalently,

$$\mathcal{T} = \lambda \operatorname{div} \mathbf{V} I + 2\mu \mathcal{E}. \tag{1.5.23}$$

Tensor equations, such as (1.5.23), do not depend on a choice of the coordinate system. Therefore, we can now return from the principal axes $(\hat{x}, \hat{y}, \hat{z})$ to arbitrarily oriented Cartesian coordinates (x, y, z) ; equation (1.5.23) will remain valid. Substituting (1.5.23) into (1.5.2), we find that the *constitutive equation* relating the stress tensor \mathcal{P} to the rate-of-strain tensor \mathcal{E} has the form

$$\mathcal{P} = (-p + \lambda \operatorname{div} \mathbf{V}) I + 2\mu \mathcal{E}, \tag{1.5.24}$$

or, equivalently,

$$\begin{pmatrix} p_{xx} & p_{xy} & p_{xz} \\ p_{yx} & p_{yy} & p_{yz} \\ p_{zx} & p_{zy} & p_{zz} \end{pmatrix} = (-p + \lambda \operatorname{div} \mathbf{V}) \begin{pmatrix} 1 & 0 & 0 \\ 0 & 1 & 0 \\ 0 & 0 & 1 \end{pmatrix} + 2\mu \begin{pmatrix} \varepsilon_{xx} & \varepsilon_{xy} & \varepsilon_{xz} \\ \varepsilon_{yx} & \varepsilon_{yy} & \varepsilon_{yz} \\ \varepsilon_{zx} & \varepsilon_{zy} & \varepsilon_{zz} \end{pmatrix}.$$

It remains to make use of equation (1.4.26) that expresses the elements of the rate-of-strain tensor in terms of the velocity components, and we can conclude that

$$p_{ij} = (-p + \lambda \operatorname{div} \mathbf{V}) \delta_{ij} + \mu \left(\frac{\partial V_i}{\partial x_j} + \frac{\partial V_j}{\partial x_i} \right), \quad i, j = 1, 2, 3. \tag{1.5.25}$$

Here we use index notation, with coordinates (x, y, z) denoted by (x_1, x_2, x_3) and the velocity components (u, v, w) by (V_1, V_2, V_3) respectively; δ_{ij} is the Kronecker delta,

$$\delta_{ij} = \begin{cases} 1 & \text{if } i = j \\ 0 & \text{if } i \neq j \end{cases}.$$

The following experiment may be used to reveal the physical significance of the coefficient μ in the constitutive equation (1.5.25). Let us consider two coaxial cylinders

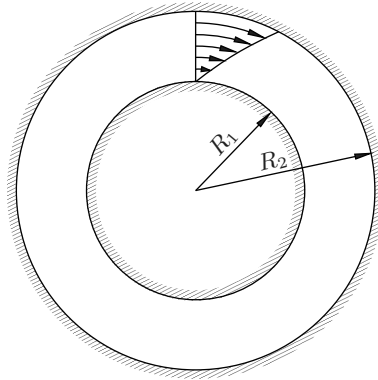


Fig. 1.23: Flow between two coaxial cylinders.

of radii R_1 and R_2 respectively and suppose that the annular space between them is filled with a fluid (see Figure 1.23). Suppose further that the internal cylinder is held at rest, while the external cylinder is rotated around its axis. Owing to the viscosity of the fluid, a certain torque has to be applied to the external cylinder to keep it moving. This torque may easily be recorded and then used to determine the viscosity characteristics of the fluid. For more details, see Section 2.1.4 and Problem 6 in Exercises 6.

If the distance $h = R_2 - R_1$ between the cylinders is small compared with the average radius $R = \frac{1}{2}(R_1 + R_2)$, then the problem reduces to a simple Couette flow between two parallel plates, as shown in Figure 1.24. In this flow, the fluid moves in layers parallel to the plates with a velocity that grows linearly with distance y from the lower flat plate (see Section 2.1.1):

$$u = \frac{U}{h}y.$$

Here U denotes the velocity of the upper plate.

Taking into account that in Couette flow the velocity component normal to the plates $v = 0$, we can easily deduce from (1.5.25) that the shear stress acting between the fluid layers

$$\tau_{yx} = \mu \frac{\partial u}{\partial y}. \quad (1.5.26)$$

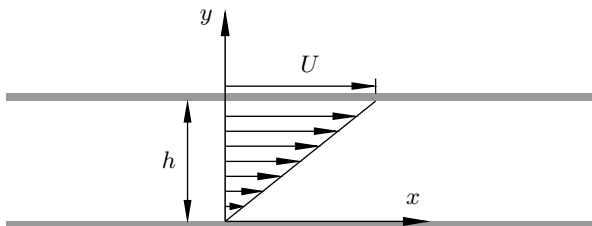


Fig. 1.24: Couette flow.

For Couette flow, equation (1.5.26) takes the form

$$\tau_{yx} = \mu \frac{U}{h}.$$

Therefore, with S being the surface area of the upper plate, the force that should be applied to this plate to keep it in a steady motion may be calculated as

$$F = \mu \frac{U}{h} S.$$

Formula (1.5.26) is known as the *Newtonian law*. The coefficient μ depends on the fluid considered and is called the *viscosity coefficient* or, more precisely, the *dynamic viscosity coefficient* in contrast to the *kinematic viscosity coefficient*, which is defined as

$$\nu = \frac{\mu}{\rho}.$$

Experimental measurements show that for most fluids the viscosity μ is a function of temperature only; under normal conditions, μ does not depend on pressure. It appears to behave differently for liquids and gases. For liquids, μ normally decays as the temperature rises. In contrast, for gases, μ grows with temperature. Tables 1.1 and 1.2 show the viscosity coefficients for water and air.

It should be noted that liquid flows, as well as slow gas flows (with speed small compared with the speed of sound), are incapable of producing a noticeable variation of temperature. Therefore, unless the moving fluid is heated or cooled by an external source, the viscosity coefficient μ may be assumed constant throughout the flow field. For high-speed subsonic and supersonic gas flows, the temperature variations become significant, and in order to study such flows one needs to specify the dependence of μ on the temperature T . A good approximation of the experimental data is given by the Sutherland law:

$$\frac{\mu}{\mu_0} = \left(\frac{T}{T_0} \right)^{3/2} \frac{T_0 + S}{T + S}.$$

Here the temperature T is measured on the Kelvin scale; for air $S = 110.4$ K, $T_0 = 273.1$ K, and μ_0 is the value of the viscosity coefficient at 0°C (see Table 1.2).

Table 1.1: The viscosity coefficient of water as a function of temperature

Temperature ($^\circ\text{C}$)	$\mu \times 10^3$ (kg m $^{-1}$ s $^{-1}$)	Temperature ($^\circ\text{C}$)	$\mu \times 10^3$ (kg m $^{-1}$ s $^{-1}$)
0	1.792	40	0.656
5	1.519	45	0.599
10	1.308	50	0.549
15	1.140	60	0.469
20	1.005	70	0.406
25	0.894	80	0.357
30	0.801	90	0.317
35	0.723	100	0.284

Table 1.2: The viscosity coefficient of air as a function of temperature

Temperature (°C)	$\mu \times 10^5$ (kg m ⁻¹ s ⁻¹)	Temperature (°C)	$\mu \times 10^5$ (kg m ⁻¹ s ⁻¹)
0	1.709	260	2.806
20	1.808	280	2.877
40	1.904	300	2.946
60	1.997	320	3.014
80	2.088	340	3.080
100	2.175	360	3.146
120	2.260	380	3.212
140	2.344	400	3.277
160	2.425	420	3.340
180	2.505	440	3.402
200	2.582	460	3.463
220	2.658	480	3.523
240	2.733	500	3.583

For theoretical studies of viscous gas flows, the power law

$$\frac{\mu}{\mu_*} = \left(\frac{T}{T_*} \right)^n$$

is often used. The choice of reference values of viscosity μ_* and temperature T_* depends on the particular problem considered. For example, in a uniform flow past a rigid body, μ_* and T_* may be chosen to coincide with the values of the viscosity μ_∞ and temperature T_∞ in the oncoming flow. As far as the parameter n is concerned, we shall see in Part 3 of this book series that the theoretical analysis of high-speed boundary-layer flows may be significantly simplified by choosing $n = 1$; however, experimental data are better represented with $n = 0.76$.

Let us now turn our attention to the *second viscosity coefficient* λ . With the pressure defined by equation (1.2.15), it may easily be deduced that

$$\lambda = -\frac{2}{3}\mu. \quad (1.5.27)$$

Indeed, using (1.5.25) in (1.2.15), we find

$$p = -\frac{1}{3}(p_{11} + p_{11} + p_{11}) = p - \left(\lambda + \frac{2}{3}\mu \right) \operatorname{div} \mathbf{V}. \quad (1.5.28)$$

If $\operatorname{div} \mathbf{V} = 0$, then the second viscosity has no significance, since the term $\lambda \operatorname{div} \mathbf{V}$ simply disappears in the constitutive equation (1.5.25). If, on the other hand, $\operatorname{div} \mathbf{V} \neq 0$, then to satisfy equation (1.5.28) we have to set $\lambda + \frac{2}{3}\mu = 0$. Substituting (1.5.27) back into (1.5.25), we can finally express the constitutive equation in the form

$$p_{ij} = -\left(p + \frac{2}{3}\mu \operatorname{div} \mathbf{V} \right) \delta_{ij} + \mu \left(\frac{\partial V_i}{\partial x_j} + \frac{\partial V_j}{\partial x_i} \right). \quad (1.5.29)$$

To conclude this discussion, we shall make the following comments on the two postulates that were used in the above analysis leading to the constitutive equation (1.5.29). The isotropy postulate represents one of the fundamental physical principles any isotropic fluid should obey. The linearity postulate is an approximation valid for fluid motions with not too strong velocity gradients, when the leading-order linear term of the Taylor expansion may be used to approximate an ‘exact’ relationship between the stress and rate-of-strain tensors. A large body of experimental evidence shows that under normal conditions many common liquids and all gases satisfy this restriction, and their motion may be described quite accurately based on the constitutive equation (1.5.29). Such fluids are termed *Newtonian*, in recognition of the fact that the simple relationship (1.5.26) was proposed by Newton.

In the other category are liquids with unusual molecular structure, for example those with long molecular chains, such as synthetic paints, plastic materials, rubber-like liquids, and some emulsions and suspensions, for which the constitutive equation (1.5.29) becomes inaccurate in normal flow conditions. Such liquids are termed *non-Newtonian*, and they will not be considered further in these books.

Exercises 3

1. When deducing the constitutive equation (1.5.25), rotation of coordinates was used: first they were rotated from general Cartesian coordinates to the principle axes of the rate-of-strain tensor, and then, after the form of the constitutive equation (1.5.23) has been established in the principle axes, they were rotated back to the original coordinates. At this stage, it was implicitly assumed that the constitutive equation (1.5.23) remained invariant with respect to the rotation. However, this is only true if both the stress and rate-of-strain tensors are real tensors (more precisely, affine orthogonal tensors of second rank), i.e. they satisfy conventional rules of tensor transformation with transformation of coordinates. These rules are formulated as follows.

Suppose that Cartesian coordinate systems $(Ox_1x_2x_3)$ and $(Ox'_1x'_2x'_3)$ have common origin O , and may be obtained from one another by rotation around O . Let $(\mathbf{e}_1, \mathbf{e}_2, \mathbf{e}_3)$ be the coordinate unit vectors in the $(Ox_1x_2x_3)$ coordinate system and $(\mathbf{e}'_1, \mathbf{e}'_2, \mathbf{e}'_3)$ the coordinate unit vectors in the $(Ox'_1x'_2x'_3)$ coordinate system. Then the transformations of coordinates from x_1, x_2, x_3 to x'_1, x'_2, x'_3 and backwards are performed by means of the equations

$$x'_i = \alpha_{ij}x_j, \quad x_i = \alpha_{ji}x'_j,$$

where α_{ij} are the cosines of the angles between the corresponding axes, which may be expressed as

$$\alpha_{ij} = \cos(x'_i, x_j) = \mathbf{e}'_i \cdot \mathbf{e}_j.$$

For

$$\mathcal{Q} = \begin{pmatrix} q_{11} & q_{12} & q_{13} \\ q_{21} & q_{22} & q_{23} \\ q_{31} & q_{32} & q_{33} \end{pmatrix}$$

to be a tensor, its elements should satisfy the following transformation rule:

$$q'_{ij} = \alpha_{ik}\alpha_{jl}q_{kl}.$$

Using this information and

- (a) applying equation (1.2.10) for a direction $\mathbf{n} = \mathbf{e}'_i$ along the x'_i -axis, prove that the stress tensor (1.2.6) is a real tensor;
- (b) taking into account that the velocity components transform as

$$V'_i = \alpha_{ij}V_j, \quad V_i = \alpha_{ji}V'_j,$$

prove that the rate-of-strain tensor (1.4.26) is also a real tensor.

1.6 Equations of Motion

The differential equations describing fluid motion may be deduced from conservation of mass, momentum, and energy. The mass conservation law has been already used to formulate the Lagrangian continuity equation (1.4.6). We shall now do it using Eulerian variables.

1.6.1 Continuity equation in Eulerian variables

In order to formulate the mass conservation law in Eulerian variables, we shall consider an arbitrary region \mathcal{D} fixed in space (see Figure 1.25a) with fluid passing through \mathcal{D} as time t increases. We denote the surface surrounding region \mathcal{D} by S and the external unit normal to S by \mathbf{n} . The fluid mass contained in region \mathcal{D} at instant t is given by the integral

$$m(t) = \iiint_{\mathcal{D}} \rho(t, \mathbf{r}) d\tau, \quad (1.6.1)$$

where $d\tau$ is a volume element in \mathcal{D} .

Notice that time t plays the role of a parameter in the integral (1.6.1). Since region \mathcal{D} does not change with time, the differentiation of (1.6.1) involves variation of the integrand only. We have

$$\frac{dm}{dt} = \iiint_{\mathcal{D}} \frac{\partial \rho}{\partial t} d\tau, \quad (1.6.2)$$

which represents the rate of change of mass inside region \mathcal{D} .

Provided that there are no sources or sinks of fluid inside \mathcal{D} , this mass variation can be due only to the influx of fluid through the surface S . The mass flux through a small element ds of the surface S is given by

$$\rho(\mathbf{V} \cdot \mathbf{n}) ds.$$

It equals the local density ρ multiplied by the volume of the slanted parallelepiped (see Figure 1.25b) swept by the fluid passing through ds per unit time. The area of the base of the parallelepiped is ds and its ribs are $|\mathbf{V}|$ long and have the same direction as the velocity vector \mathbf{V} .

52 Chapter 1. Fundamentals of Fluid Dynamics

The total mass flux through the entire surface S is

$$\iint_S (\rho \mathbf{V} \cdot \mathbf{n}) \, ds. \tag{1.6.3}$$

Since \mathbf{n} is the external normal, the integral (1.6.3) represents the outflow from region \mathcal{D} . So the mass conservation law, applied to \mathcal{D} , can be written as

$$\iint_S (\rho \mathbf{V} \cdot \mathbf{n}) \, ds = -\frac{dm}{dt}.$$

Applying Gauss's divergence theorem to the left-hand side of this equation, we have

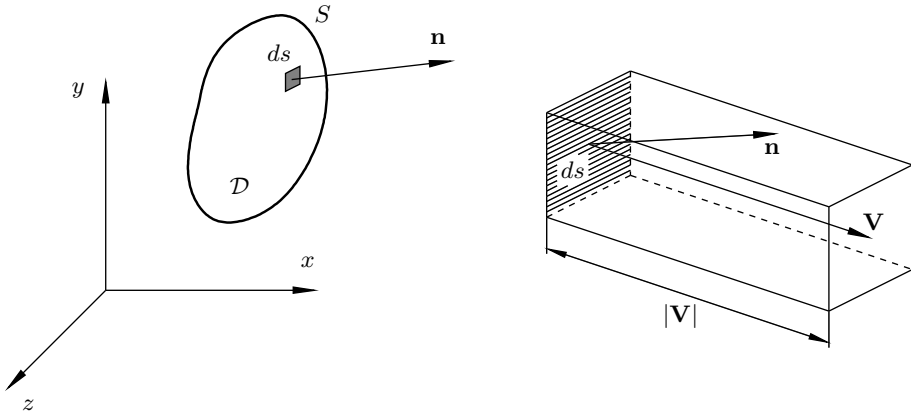
$$\iiint_{\mathcal{D}} \operatorname{div}(\rho \mathbf{V}) \, d\tau = -\frac{dm}{dt}. \tag{1.6.4}$$

Combining (1.6.2) with (1.6.4) results in

$$\iiint_{\mathcal{D}} \left[\frac{\partial \rho}{\partial t} + \operatorname{div}(\rho \mathbf{V}) \right] d\tau = 0. \tag{1.6.5}$$

Let us suppose that both ρ and \mathbf{V} have continuous derivatives. Then, by virtue of the arbitrariness of region \mathcal{D} , the integrand in (1.6.5) should be zero everywhere in the flow field, and so

$$\frac{\partial \rho}{\partial t} + \operatorname{div}(\rho \mathbf{V}) = 0. \tag{1.6.6}$$



(a) Region \mathcal{D} used in derivation of the mass conservation law.

(b) Zoomed surface element ds and cylindrical region filled by the fluid passing through ds per unit time.

Fig. 1.25: Geometrical layout used in the derivation of the mass conservation law.

Indeed, if the function

$$\Phi = \frac{\partial \rho}{\partial t} + \operatorname{div}(\rho \mathbf{V})$$

did not vanish (say, it was positive) at least at one point in the flow, then, because Φ is continuous, it would be positive in a small vicinity of this point. Hence the integral (1.6.5) taken over such a vicinity would also be positive.

Equation (1.6.6) is the *continuity equation* in Eulerian variables. In Chapters 2 and 3, we will be dealing with so-called *incompressible fluid flows*. These are flows where the fluid density ρ remains constant, and the continuity equation (1.6.6) reduces to

$$\operatorname{div} \mathbf{V} = 0. \quad (1.6.7)$$

1.6.2 Momentum equation

We shall now formulate the fluid-dynamic version of Newton's Second Law. When applied to a solid body, Newton's Second Law is written as

$$m \mathbf{a} = \mathbf{F}. \quad (1.6.8)$$

Here m is the mass of the body, \mathbf{a} its acceleration, and \mathbf{F} the force applied to the body.

The following three remarks should be made concerning equation (1.6.8). First, this equation is valid if a body's motion is analysed in the framework of an *inertial coordinate system*. Second, if more than one force is applied to the body, then the vector \mathbf{F} in (1.6.8) must be interpreted as the resultant force that is equal to the vector sum of all forces acting on the body. Third, if the body is not 'small' and its different parts experience different accelerations, then equation (1.6.8) serves to determine the acceleration \mathbf{a} of the *mass centre*. A convenient idealisation is based on the assumption that the body size is small compared with the characteristic path traced by the body during the time of observation, in which case the body may be thought as a *material point*. In fluid dynamics, the role of material points is played by the fluid particles.

Let us consider an assemblage of N material points. Each element obeys Newton's Second Law

$$m_i \frac{d\mathbf{V}_i}{dt} = \mathbf{F}_i. \quad (1.6.9)$$

Here suffix i is used to enumerate the elements in the assemblage, and the acceleration \mathbf{a}_i of the i th element is written via the velocity derivative $d\mathbf{V}_i/dt$. Since the mass m_i does not vary with time, equation (1.6.9) may also be written as

$$\frac{d\mathbf{K}_i}{dt} = \mathbf{F}_i, \quad (1.6.10)$$

with $\mathbf{K}_i = m_i \mathbf{V}_i$ being the momentum of the i th material point.

The force \mathbf{F}_i is represented as a superposition of internal and external forces:

$$\mathbf{F}_i = \sum_{j=1}^N \mathbf{F}_{ij} + \mathbf{F}_{ie}, \quad (1.6.11)$$

where \mathbf{F}_{ij} is the force exerted by the element with number j upon the element with number i , and \mathbf{F}_{ie} is the external force produced by any physical agents outside the system under consideration.

54 Chapter 1. Fundamentals of Fluid Dynamics

Substitution of (1.6.11) into (1.6.10) and summation over all the elements in the assemblage yields the momentum equation

$$\frac{d\mathbf{K}}{dt} = \mathbf{R}, \tag{1.6.12}$$

where \mathbf{K} is the momentum of the entire material system,

$$\mathbf{K} = \sum_{i=1}^N m_i \mathbf{V}_i, \tag{1.6.13}$$

and \mathbf{R} is the resultant external force,

$$\mathbf{R} = \sum_{i=1}^N \mathbf{F}_{ie}.$$

Internal forces obviously cancel in the course of summation owing to Newton's Third Law, which states that an action and reaction are equal and opposite: $\mathbf{F}_{ij} = -\mathbf{F}_{ji}$.

Now we shall apply equation (1.6.12) to a moving fluid. To express the derivative $d\mathbf{K}/dt$ on the left-hand side of (1.6.12) in terms of the fluid-dynamic variables, we have to keep in mind that the momentum equation (1.6.12) is valid for a material system consisting of the same elements; no exchange of matter between the system under consideration and the surrounding medium is allowed.

Let \mathcal{D} be again an arbitrary region in an inertial coordinate system. The surface surrounding \mathcal{D} we will denote as before by S and the external unit normal to S by \mathbf{n} (see Figure 1.26). However, now we shall treat this region differently. We choose an arbitrary instant t and 'mark' all the fluid particles that happen to be inside \mathcal{D} at this instant. Then we follow these fluid particles as time increases; considered together,

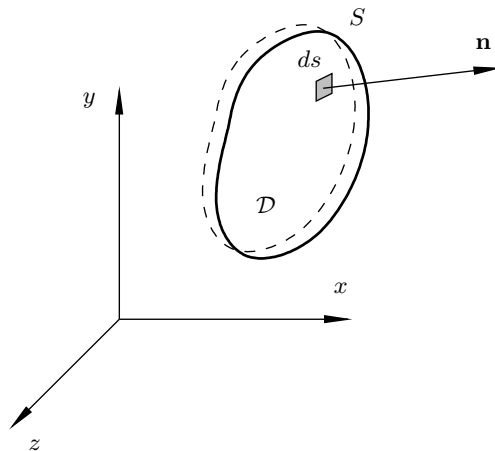


Fig. 1.26: Fluid body deforming with time.

they form a *fluid body*, to which we shall apply the momentum equation (1.6.12). The momentum (1.6.13) of the body is expressed by the integral

$$\mathbf{K}(t) = \iiint_{\mathcal{D}} \rho(t, \mathbf{r}) \mathbf{V}(t, \mathbf{r}) d\tau. \quad (1.6.14)$$

Direct differentiation of (1.6.14) with respect to t involves differentiation of the integrand $\rho \mathbf{V}$ as well as analysis of the fluid body deformation,¹⁰ which is significantly more intricate. This may be avoided if, before differentiating $\mathbf{K}(t)$, a transformation of integration variables is performed in (1.6.14) with new variables chosen in such a way that the region of integration ceases to depend on time t . A proper choice is obviously provided by the Lagrangian position vector function

$$\mathbf{r} = \mathbf{r}(t, \mathbf{r}_0), \quad (1.6.15)$$

which relates the ‘initial location’ \mathbf{r}_0 of a fluid particle at time t_0 to its current location \mathbf{r} at time t . Formula (1.6.15) may obviously be considered as a transformation of variables from (x, y, z) to (x_0, y_0, z_0) and vice versa. Using (1.6.15) in (1.6.14) results in

$$\mathbf{K}(t) = \iiint_{\mathcal{D}_0} \rho[t, \mathbf{r}(t, \mathbf{r}_0)] \mathbf{V}[t, \mathbf{r}(t, \mathbf{r}_0)] \left| \frac{\partial(x, y, z)}{\partial(x_0, y_0, z_0)} \right| d\tau_0, \quad (1.6.16)$$

where \mathcal{D}_0 is the region occupied by the fluid body at the initial time t_0 and $d\tau_0$ is a volume element from \mathcal{D}_0 .

It follows from the continuity equation in Lagrangian variables (1.4.6) that

$$\left| \frac{\partial(x, y, z)}{\partial(x_0, y_0, z_0)} \right| = \frac{\rho_0}{\rho}.$$

Hence, (1.6.16) may be rewritten as

$$\mathbf{K}(t) = \iiint_{\mathcal{D}_0} \rho_0 \mathbf{V}[t, \mathbf{r}(t, \mathbf{r}_0)] d\tau_0. \quad (1.6.17)$$

Here both the initial density ρ_0 and initial region \mathcal{D}_0 are independent of t . Therefore differentiation of (1.6.17) yields

$$\frac{d\mathbf{K}}{dt} = \iiint_{\mathcal{D}_0} \rho_0 \left[\frac{\partial \mathbf{V}}{\partial t} + \frac{\partial \mathbf{V}}{\partial x} \frac{\partial x(t, \mathbf{r}_0)}{\partial t} + \frac{\partial \mathbf{V}}{\partial y} \frac{\partial y(t, \mathbf{r}_0)}{\partial t} + \frac{\partial \mathbf{V}}{\partial z} \frac{\partial z(t, \mathbf{r}_0)}{\partial t} \right] d\tau_0.$$

Taking into account that the expression in the square brackets is the acceleration of a fluid particle (1.4.10), we can further write

$$\frac{d\mathbf{K}}{dt} = \iiint_{\mathcal{D}_0} \rho_0 \frac{D\mathbf{V}}{Dt} d\tau_0.$$

¹⁰The shape of the body at the next instant $t + dt$ is depicted in Figure 1.26 by the dashed line.

It remains to return to the original integration variables (x, y, z) , and we will have

$$\frac{d\mathbf{K}}{dt} = \iiint_{\mathcal{D}} \rho \frac{D\mathbf{V}}{Dt} d\tau. \quad (1.6.18)$$

We shall now calculate the resultant force \mathbf{R} acting on the fluid inside region \mathcal{D} . As we know, all the forces acting on a moving fluid may be subdivided into two classes: body forces and surface forces. With $\mathbf{f}(\mathbf{r}, t)$ denoting the body force upon a unit mass, the force acting on a volume element $d\tau$ inside \mathcal{D} is calculated as

$$\rho(\mathbf{r}, t)\mathbf{f}(\mathbf{r}, t) d\tau,$$

and the entire body force acting upon the fluid contained in region \mathcal{D} proves to be

$$\iiint_{\mathcal{D}} \rho(\mathbf{r}, t)\mathbf{f}(\mathbf{r}, t) d\tau. \quad (1.6.19)$$

Let us now turn to the surface forces. According to (1.2.3), an element ds of the surface S surrounding region \mathcal{D} experiences a force (see Figure 1.27)

$$d\mathbf{P}_n = \mathbf{p}_n ds. \quad (1.6.20)$$

The total force acting upon the fluid in \mathcal{D} through S is calculated as

$$\mathbf{R}_s = \iint_S \mathbf{p}_n ds. \quad (1.6.21)$$

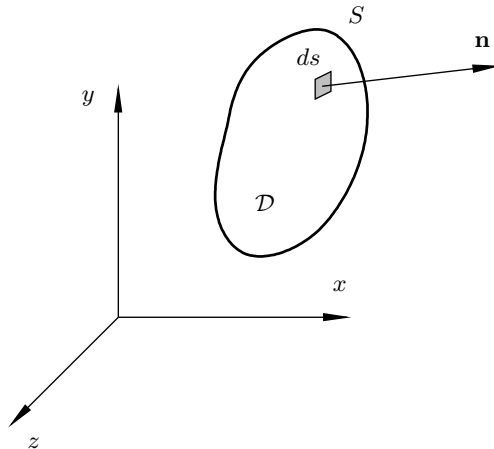


Fig. 1.27: Calculation of the surface force.

Adding (1.6.21) to (1.6.19), we obtain the resultant force \mathbf{R} that should be used on the right-hand side of equation (1.6.12). Using for the left-hand side the formula (1.6.18), we arrive at the following integral form of the momentum equation:

$$\iiint_{\mathcal{D}} \rho \frac{D\mathbf{V}}{Dt} d\tau = \iiint_{\mathcal{D}} \rho \mathbf{f} d\tau + \iint_S \mathbf{p}_n ds. \quad (1.6.22)$$

In order to express this equation in a differential form, we need to convert the integral (1.6.21) for the surface force \mathbf{R}_s into a volume integral. When performing this task, it is convenient to use index notation, with (x, y, z) denoted as (x_1, x_2, x_3) . Taking into account that, according to (1.2.10),¹¹

$$\mathbf{p}_n = n_i \mathbf{p}_i,$$

the projection of the vector equation (1.6.21) on the x_α -axis may be written as

$$\mathbf{R}_s \Big|_\alpha = \iint_S n_i p_{i\alpha} ds, \quad \alpha = 1, 2, 3. \quad (1.6.23)$$

If we introduce the vector $\mathbf{A} = (A_1, A_2, A_3)$ such that

$$A_i = p_{i\alpha}, \quad i = 1, 2, 3,$$

then the right-hand side of (1.6.23) may be expressed via the scalar product of \mathbf{A} and the normal unit vector \mathbf{n} . We have

$$\mathbf{R}_s \Big|_\alpha = \iint_S (\mathbf{A} \cdot \mathbf{n}) ds.$$

Now Gauss's divergence theorem may be used, leading to

$$\mathbf{R}_s \Big|_\alpha = \iiint_{\mathcal{D}} \operatorname{div} \mathbf{A} d\tau.$$

Here

$$\operatorname{div} \mathbf{A} = \frac{\partial A_i}{\partial x_i} = \frac{\partial p_{i\alpha}}{\partial x_i},$$

and therefore

$$\mathbf{R}_s \Big|_\alpha = \iiint_{\mathcal{D}} \frac{\partial p_{i\alpha}}{\partial x_i} d\tau. \quad (1.6.24)$$

¹¹Here we again use the well-known summation convention according to which terms containing a repeated suffix are to be regarded as summed over all three possible values of the suffix, i.e.

$$n_i \mathbf{p}_i = \sum_{i=1}^3 n_i \mathbf{p}_i.$$

Since equation (1.6.24) is valid for all $\alpha = 1, 2, 3$, it may be written in vector form as

$$\mathbf{R}_s = \iiint_{\mathcal{D}} \operatorname{div} \mathcal{P} \, d\tau. \quad (1.6.25)$$

The vector $\operatorname{div} \mathcal{P}$ is referred to as the divergence of the stress tensor (1.2.6); its components are written as

$$\left. \begin{aligned} (\operatorname{div} \mathcal{P})_x &= \frac{\partial p_{xx}}{\partial x} + \frac{\partial p_{yx}}{\partial y} + \frac{\partial p_{zx}}{\partial z}, \\ (\operatorname{div} \mathcal{P})_y &= \frac{\partial p_{xy}}{\partial x} + \frac{\partial p_{yy}}{\partial y} + \frac{\partial p_{zy}}{\partial z}, \\ (\operatorname{div} \mathcal{P})_z &= \frac{\partial p_{xz}}{\partial x} + \frac{\partial p_{yz}}{\partial y} + \frac{\partial p_{zz}}{\partial z}. \end{aligned} \right\} \quad (1.6.26)$$

Substitution of (1.6.25) into (1.6.22) yields

$$\iiint_{\mathcal{D}} \left(\rho \frac{D\mathbf{V}}{Dt} - \rho \mathbf{f} - \operatorname{div} \mathcal{P} \right) d\tau = 0,$$

and we can conclude that in a region of smooth variation of the fluid-dynamic functions ρ , p , and \mathbf{V} , the following equation holds:

$$\rho \frac{D\mathbf{V}}{Dt} = \rho \mathbf{f} + \operatorname{div} \mathcal{P}, \quad (1.6.27)$$

which represents the sought differential form of the *momentum equation*.

1.6.3 The energy equation

To derive the energy equation we shall return to the First Law of Thermodynamics (1.3.11) and apply it to the fluid body contained at time t inside region \mathcal{D} as shown in Figure 1.26. Instead of the work performed by the body, we will consider an opposite quantity, the work performed by the forces acting upon the body. Correspondingly, we shall write equation (1.3.11) in the form

$$\frac{dE}{dt} = W + Q, \quad (1.6.28)$$

where E is the energy of the fluid body, W the work performed per unit time by the forces acting on the body, and Q the rate of heat transfer to the body.

In a fluid in motion, the energy E consists of the internal energy of fluid particles and their kinetic energy. The internal energy per unit mass is e . Hence the internal energy of a fluid particle occupying a volume element $d\tau$ is $e\rho d\tau$. The kinetic energy of the fluid particle is $\frac{1}{2}V^2\rho d\tau$. This means that the entire energy E of the fluid body occupying region \mathcal{D} at time t may be written as

$$E(t) = \iiint_{\mathcal{D}} \rho \left(e + \frac{V^2}{2} \right) d\tau.$$

The derivative of this function is calculated in the same way as the derivative of the momentum $\mathbf{K}(t)$ given by (1.6.18). We have

$$\frac{dE}{dt} = \iiint_{\mathcal{D}} \rho \frac{D}{Dt} \left(e + \frac{V^2}{2} \right) d\tau. \quad (1.6.29)$$

Let us now calculate the work W on the right-hand side of (1.6.28). It is known that the work is given by the scalar product $\mathbf{F} \cdot \delta\mathbf{r}$ of the force \mathbf{F} acting on a body, and the distance $\delta\mathbf{r}$ travelled by the body. Thus the work per unit time will be $\mathbf{F} \cdot \mathbf{V}$. The work performed by the body force acting on a fluid particle is $\rho(\mathbf{f} \cdot \mathbf{V})d\tau$, and therefore the entire work of the body forces acting upon region \mathcal{D} is

$$W_b = \iiint_{\mathcal{D}} \rho(\mathbf{f} \cdot \mathbf{V}) d\tau. \quad (1.6.30)$$

The surface force acting on an element ds of surface S (see Figure 1.27) is given by equation (1.6.20). The work performed by this force is $(\mathbf{p}_n ds \cdot \mathbf{V})$. Integrating over the entire surface S surrounding the fluid body in region \mathcal{D} yields

$$W_s = \iint_S (\mathbf{p}_n \cdot \mathbf{V}) ds. \quad (1.6.31)$$

The second term on the right-hand side of equation (1.6.28) represents the heat rate Q . We shall assume that the only physical process that leads to heat transfer is the heat conduction due to the temperature variation in the flow field.¹² The heat conduction vector \mathbf{q} is known to be proportional to the temperature gradient, i.e.

$$\mathbf{q} = -\kappa \nabla T,$$

where κ is a positive constant called the *heat conductivity coefficient*. It depends on the temperature only, and is related to the dynamic viscosity coefficient, μ , such that the quantity

$$Pr = \frac{\mu c_p}{\kappa}, \quad (1.6.32)$$

called the *Prandtl number*, can be treated as a constant for a given fluid. In particular, for air at ‘room temperature’ and atmospheric pressure, $Pr \approx 0.713$.

With \mathbf{n} being the external normal to the surface S (see Figure 1.27), the heat transfer towards the fluid body contained in region \mathcal{D} is calculated as

$$Q = - \iint_S (\mathbf{q} \cdot \mathbf{n}) ds = \iint_S (\kappa \nabla T \cdot \mathbf{n}) ds. \quad (1.6.33)$$

Substituting (1.6.29), (1.6.30), (1.6.31), and (1.6.33) into (1.6.28), we arrive at the

¹²In hypersonic flows, the gas temperature might become sufficiently high to provoke an additional process, namely radiation of heat.

following integral form of the energy equation:

$$\iiint_{\mathcal{D}} \rho \frac{D}{Dt} \left(e + \frac{V^2}{2} \right) d\tau = \iiint_{\mathcal{D}} \rho \mathbf{f} \cdot \mathbf{V} d\tau + \iint_S \mathbf{p}_n \cdot \mathbf{V} ds + \iint_S \kappa \nabla T \cdot \mathbf{n} ds. \quad (1.6.34)$$

In order to convert the surface work integral (1.6.31) into a volume integral, we again use formula (1.2.10). We have

$$\mathbf{p}_n \cdot \mathbf{V} = (n_i \mathbf{p}_i) \cdot \mathbf{V} = n_i (\mathbf{p}_i \cdot \mathbf{V}) = n_i p_{ij} V_j.$$

Hence, if we introduce a vector $\mathbf{A} = (A_1, A_2, A_3)$ such that

$$A_i = p_{ij} V_j, \quad i = 1, 2, 3, \quad (1.6.35)$$

then the integral (1.6.31) may be written as

$$W_s = \iint_S \mathbf{p}_n \cdot \mathbf{V} ds = \iint_S (\mathbf{A} \cdot \mathbf{n}) ds.$$

Now we can use Gauss's divergence theorem. We have

$$\iint_S \mathbf{p}_n \cdot \mathbf{V} ds = \iiint_{\mathcal{D}} \operatorname{div} \mathbf{A} d\tau = \iiint_{\mathcal{D}} \operatorname{div}(\mathcal{P}\mathbf{V}) d\tau. \quad (1.6.36)$$

Here it is taken into account that the vector \mathbf{A} , whose components are defined by equation (1.6.35), is equal to the product of the stress tensor (1.2.6) and the velocity vector \mathbf{V} .

Applying Gauss's divergence theorem also to the heat transfer integral on the right-hand side of equation (1.6.34), we can express this equation in the form

$$\iiint_{\mathcal{D}} \left[\rho \frac{D}{Dt} \left(e + \frac{V^2}{2} \right) - \rho \mathbf{f} \cdot \mathbf{V} - \operatorname{div}(\mathcal{P}\mathbf{V}) - \operatorname{div}(\kappa \nabla T) \right] d\tau = 0.$$

Taking into account that the region \mathcal{D} is arbitrary, we deduce that the integrand must be zero. We have

$$\rho \frac{D}{Dt} \left(e + \frac{V^2}{2} \right) = \rho \mathbf{f} \cdot \mathbf{V} + \operatorname{div}(\mathcal{P}\mathbf{V}) + \operatorname{div}(\kappa \nabla T) = 0. \quad (1.6.37)$$

The kinetic energy term on the left-hand side of (1.6.37) may be calculated using the momentum equation (1.6.27). Indeed, scalar multiplication of (1.6.27) with the velocity vector \mathbf{V} yields

$$\rho \frac{D}{Dt} \left(\frac{V^2}{2} \right) = \rho \mathbf{f} \cdot \mathbf{V} + \mathbf{V} \cdot \operatorname{div} \mathcal{P},$$

which, when subtracted from (1.6.37), results in the following form of the *energy equation*:

$$\rho \frac{De}{Dt} = \operatorname{div}(\mathcal{P}\mathbf{V}) - \mathbf{V} \cdot \operatorname{div} \mathcal{P} + \operatorname{div}(\kappa \nabla T). \quad (1.6.38)$$

1.7 The Navier–Stokes Equations

The Navier–Stokes equations are obtained by using the constitutive equation (1.5.25) in the momentum (1.6.27) and energy (1.6.38) equations. At this stage, it is convenient to consider incompressible and compressible fluid flows separately.

1.7.1 Incompressible fluid flows

In an incompressible flow, the fluid density ρ is a constant quantity, which means that the continuity equation (1.6.6) may be written as

$$\operatorname{div} \mathbf{V} = 0. \quad (1.7.1)$$

Consequently, the constitutive equation (1.5.25) reduces to

$$p_{ij} = -p\delta_{ij} + \mu \left(\frac{\partial V_i}{\partial x_j} + \frac{\partial V_j}{\partial x_i} \right). \quad (1.7.2)$$

As has already been mentioned in Section 1.5, liquid flows, as well as slow gas flows, are incapable of producing a noticeable variation of temperature. Therefore, the viscosity coefficient μ may be assumed constant in (1.7.2).

Now, we need to write equations (1.6.26) using index notations. We see that, with i playing the role of the summations index, the projection of $\operatorname{div} \mathcal{P}$ upon the x_j -axis is

$$(\operatorname{div} \mathcal{P})_j = \frac{\partial p_{ij}}{\partial x_i}, \quad j = 1, 2, 3. \quad (1.7.3)$$

Substitution of (1.7.2) into (1.7.3) yields

$$(\operatorname{div} \mathcal{P})_j = -\frac{\partial p}{\partial x_j} + \mu \frac{\partial}{\partial x_i} \left(\frac{\partial V_i}{\partial x_j} \right) + \mu \frac{\partial^2 V_j}{\partial x_i \partial x_i}.$$

Changing the order of differentiation in the second term,

$$\frac{\partial}{\partial x_i} \left(\frac{\partial V_i}{\partial x_j} \right) = \frac{\partial}{\partial x_j} \left(\frac{\partial V_i}{\partial x_i} \right) = \frac{\partial}{\partial x_j} (\operatorname{div} \mathbf{V}),$$

and using the continuity equation (1.7.1), we arrive at the conclusion that this term is zero. Hence,

$$(\operatorname{div} \mathcal{P})_j = -\frac{\partial p}{\partial x_j} + \mu \frac{\partial^2 V_j}{\partial x_i \partial x_i}, \quad j = 1, 2, 3.$$

In vector form, this equation is written as

$$\operatorname{div} \mathcal{P} = -\nabla p + \mu \nabla^2 \mathbf{V}, \quad (1.7.4)$$

where the symbol $\nabla^2 \mathbf{V}$ denotes a vector whose components are $(\nabla^2 u, \nabla^2 v, \nabla^2 w)$.

With (1.7.4), the momentum equation (1.6.27) becomes¹³

$$\frac{D\mathbf{V}}{Dt} = \mathbf{f} - \frac{1}{\rho}\nabla p + \nu\nabla^2\mathbf{V}. \quad (1.7.5a)$$

This should be supplemented with the continuity equation

$$\operatorname{div}\mathbf{V} = 0 \quad (1.7.5b)$$

to form a closed set of *Navier–Stokes equations* that govern the motion of incompressible fluids. In coordinate decomposition form, they are written as

$$\frac{\partial u}{\partial t} + u\frac{\partial u}{\partial x} + v\frac{\partial u}{\partial y} + w\frac{\partial u}{\partial z} = f_x - \frac{1}{\rho}\frac{\partial p}{\partial x} + \nu\left(\frac{\partial^2 u}{\partial x^2} + \frac{\partial^2 u}{\partial y^2} + \frac{\partial^2 u}{\partial z^2}\right), \quad (1.7.6a)$$

$$\frac{\partial v}{\partial t} + u\frac{\partial v}{\partial x} + v\frac{\partial v}{\partial y} + w\frac{\partial v}{\partial z} = f_y - \frac{1}{\rho}\frac{\partial p}{\partial y} + \nu\left(\frac{\partial^2 v}{\partial x^2} + \frac{\partial^2 v}{\partial y^2} + \frac{\partial^2 v}{\partial z^2}\right), \quad (1.7.6b)$$

$$\frac{\partial w}{\partial t} + u\frac{\partial w}{\partial x} + v\frac{\partial w}{\partial y} + w\frac{\partial w}{\partial z} = f_z - \frac{1}{\rho}\frac{\partial p}{\partial z} + \nu\left(\frac{\partial^2 w}{\partial x^2} + \frac{\partial^2 w}{\partial y^2} + \frac{\partial^2 w}{\partial z^2}\right), \quad (1.7.6c)$$

$$\frac{\partial u}{\partial x} + \frac{\partial v}{\partial y} + \frac{\partial w}{\partial z} = 0. \quad (1.7.6d)$$

These four equations involve four unknown functions: the velocity components u , v , w and the pressure p . It should be noted here that when calculating the velocity and pressure fields in an incompressible flow, we do not need the energy equation.

1.7.2 Compressible fluid flows

We start again with the momentum equation (1.6.27). This may be projected on the three coordinate axes. The x -component of the momentum equation is written, using the first of equations (1.6.26), as

$$\rho\frac{Du}{Dt} = \rho f_x + \frac{\partial p_{xx}}{\partial x} + \frac{\partial p_{yx}}{\partial y} + \frac{\partial p_{zx}}{\partial z}. \quad (1.7.7)$$

From the constitutive equation (1.5.25), it is easily found that

$$p_{xx} = -p + \mu\left[\frac{4}{3}\frac{\partial u}{\partial x} - \frac{2}{3}\left(\frac{\partial v}{\partial y} + \frac{\partial w}{\partial z}\right)\right],$$

$$p_{yx} = \mu\left(\frac{\partial v}{\partial x} + \frac{\partial u}{\partial y}\right),$$

$$p_{zx} = \mu\left(\frac{\partial w}{\partial x} + \frac{\partial u}{\partial z}\right),$$

¹³Recall that the kinetic viscosity $\nu = \mu/\rho$.

which, after substitution into (1.7.7), yields

$$\begin{aligned} & \rho \left(\frac{\partial u}{\partial t} + u \frac{\partial u}{\partial x} + v \frac{\partial u}{\partial y} + w \frac{\partial u}{\partial z} \right) \\ &= \rho f_x - \frac{\partial p}{\partial x} + \frac{\partial}{\partial x} \left\{ \mu \left[\frac{4}{3} \frac{\partial u}{\partial x} - \frac{2}{3} \left(\frac{\partial v}{\partial y} + \frac{\partial w}{\partial z} \right) \right] \right\} \\ & \quad + \frac{\partial}{\partial y} \left[\mu \left(\frac{\partial u}{\partial y} + \frac{\partial v}{\partial x} \right) \right] + \frac{\partial}{\partial z} \left[\mu \left(\frac{\partial u}{\partial z} + \frac{\partial w}{\partial x} \right) \right]. \end{aligned} \quad (1.7.8)$$

Similarly, the y -component of the momentum equation may be shown to be

$$\begin{aligned} & \rho \left(\frac{\partial v}{\partial t} + u \frac{\partial v}{\partial x} + v \frac{\partial v}{\partial y} + w \frac{\partial v}{\partial z} \right) \\ &= \rho f_y - \frac{\partial p}{\partial y} + \frac{\partial}{\partial y} \left\{ \mu \left[\frac{4}{3} \frac{\partial v}{\partial y} - \frac{2}{3} \left(\frac{\partial u}{\partial x} + \frac{\partial w}{\partial z} \right) \right] \right\} \\ & \quad + \frac{\partial}{\partial x} \left[\mu \left(\frac{\partial u}{\partial y} + \frac{\partial v}{\partial x} \right) \right] + \frac{\partial}{\partial z} \left[\mu \left(\frac{\partial v}{\partial z} + \frac{\partial w}{\partial y} \right) \right], \end{aligned} \quad (1.7.9)$$

and the z -component is written as

$$\begin{aligned} & \rho \left(\frac{\partial w}{\partial t} + u \frac{\partial w}{\partial x} + v \frac{\partial w}{\partial y} + w \frac{\partial w}{\partial z} \right) \\ &= \rho f_z - \frac{\partial p}{\partial z} + \frac{\partial}{\partial z} \left\{ \mu \left[\frac{4}{3} \frac{\partial w}{\partial z} - \frac{2}{3} \left(\frac{\partial v}{\partial y} + \frac{\partial u}{\partial x} \right) \right] \right\} \\ & \quad + \frac{\partial}{\partial x} \left[\mu \left(\frac{\partial u}{\partial z} + \frac{\partial w}{\partial x} \right) \right] + \frac{\partial}{\partial y} \left[\mu \left(\frac{\partial v}{\partial z} + \frac{\partial w}{\partial y} \right) \right]. \end{aligned} \quad (1.7.10)$$

Let us now turn to the energy equation (1.6.38),

$$\rho \frac{De}{Dt} = \operatorname{div}(\mathcal{P}\mathbf{V}) - \mathbf{V} \cdot \operatorname{div} \mathcal{P} + \operatorname{div}(\kappa \nabla T). \quad (1.7.11)$$

Remember that $\mathcal{P}\mathbf{V}$ coincides with the vector \mathbf{A} whose components are given by equation (1.6.35). Consequently,

$$\operatorname{div}(\mathcal{P}\mathbf{V}) = \frac{\partial A_i}{\partial x_i} = \frac{\partial}{\partial x_i} (p_{ij} V_j) = p_{ij} \frac{\partial V_j}{\partial x_i} + V_j \frac{\partial p_{ij}}{\partial x_i}. \quad (1.7.12)$$

Taking into account that the components of the vector $\operatorname{div} \mathcal{P}$ are given by (1.7.3), we can easily see that

$$V_j \frac{\partial p_{ij}}{\partial x_i} = \mathbf{V} \cdot \operatorname{div} \mathcal{P}. \quad (1.7.13)$$

Substituting (1.7.13) into (1.7.12) and then into (1.7.11) renders the energy equation in the form

$$\rho \frac{De}{Dt} = p_{ij} \frac{\partial V_j}{\partial x_i} + \operatorname{div}(\kappa \nabla T). \quad (1.7.14)$$

Using the constitutive equation (1.5.29), we can express the first term on the right-hand side of (1.7.14) as

$$p_{ij} \frac{\partial V_j}{\partial x_i} = -\left(p + \frac{2}{3}\mu \operatorname{div} \mathbf{V}\right) \operatorname{div} \mathbf{V} + \mu \frac{\partial V_j}{\partial x_i} \left(\frac{\partial V_i}{\partial x_j} + \frac{\partial V_j}{\partial x_i}\right).$$

Direct summation with respect to indices $i, j = 1, 2, 3$ yields

$$\begin{aligned} \frac{\partial V_j}{\partial x_i} \left(\frac{\partial V_i}{\partial x_j} + \frac{\partial V_j}{\partial x_i}\right) &= 2 \left[\left(\frac{\partial u}{\partial x}\right)^2 + \left(\frac{\partial v}{\partial y}\right)^2 + \left(\frac{\partial w}{\partial z}\right)^2 \right] \\ &\quad + \left(\frac{\partial u}{\partial y} + \frac{\partial v}{\partial x}\right)^2 + \left(\frac{\partial u}{\partial z} + \frac{\partial w}{\partial x}\right)^2 + \left(\frac{\partial v}{\partial z} + \frac{\partial w}{\partial y}\right)^2, \end{aligned}$$

and we can conclude that the energy equation (1.7.14) may be written in the form

$$\begin{aligned} \rho \frac{De}{Dt} &= -p \operatorname{div} \mathbf{V} - \frac{2}{3}\mu (\operatorname{div} \mathbf{V})^2 + 2\mu \left[\left(\frac{\partial u}{\partial x}\right)^2 + \left(\frac{\partial v}{\partial y}\right)^2 + \left(\frac{\partial w}{\partial z}\right)^2 \right] \\ &\quad + \mu \left[\left(\frac{\partial u}{\partial y} + \frac{\partial v}{\partial x}\right)^2 + \left(\frac{\partial u}{\partial z} + \frac{\partial w}{\partial x}\right)^2 + \left(\frac{\partial v}{\partial z} + \frac{\partial w}{\partial y}\right)^2 \right] + \operatorname{div}(\kappa \nabla T). \end{aligned} \quad (1.7.15)$$

For an incompressible fluid flow, equation (1.7.15) turns into the following equation for the temperature T :

$$\begin{aligned} \rho c_v \left(\frac{\partial T}{\partial t} + u \frac{\partial T}{\partial x} + v \frac{\partial T}{\partial y} + w \frac{\partial T}{\partial z} \right) &- \kappa \left(\frac{\partial^2 T}{\partial x^2} + \frac{\partial^2 T}{\partial y^2} + \frac{\partial^2 T}{\partial z^2} \right) \\ &= 2\mu \left[\left(\frac{\partial u}{\partial x}\right)^2 + \left(\frac{\partial v}{\partial y}\right)^2 + \left(\frac{\partial w}{\partial z}\right)^2 \right] \\ &\quad + \mu \left[\left(\frac{\partial u}{\partial y} + \frac{\partial v}{\partial x}\right)^2 + \left(\frac{\partial u}{\partial z} + \frac{\partial w}{\partial x}\right)^2 + \left(\frac{\partial v}{\partial z} + \frac{\partial w}{\partial y}\right)^2 \right]. \end{aligned} \quad (1.7.16)$$

Indeed, the first and second terms on the right-hand side of (1.7.15) disappear in view of the fact that in incompressible flows $\operatorname{div} \mathbf{V} = 0$. When dealing with the internal energy e on the left-hand side of (1.7.15), equation (1.3.26) has been used. Also, we have used the fact that in incompressible flows, the heat transfer coefficient κ and the viscosity coefficient μ are constant throughout the flow field. Equation (1.7.16) allows us to calculate the temperature variations over the flow field after the velocity field has been found by solving equations (1.7.6).

Now, returning to compressible flows, it is convenient to express the energy equation (1.7.15) as an equation for the enthalpy h . In order to perform this task, we start with the continuity equation (1.6.6):

$$\frac{\partial \rho}{\partial t} + \operatorname{div}(\rho \mathbf{V}) = 0. \quad (1.7.17)$$

We note that

$$\operatorname{div}(\rho\mathbf{V}) = \frac{\partial(\rho V_i)}{\partial x_i} = \rho \frac{\partial V_i}{\partial x_i} + V_i \frac{\partial \rho}{\partial x_i} = \rho \operatorname{div}\mathbf{V} + \mathbf{V} \cdot \nabla \rho.$$

Hence, the continuity equation (1.7.17) may be written as

$$\frac{D\rho}{Dt} + \rho \operatorname{div}\mathbf{V} = 0,$$

and therefore, the first term on the right-hand side of (1.7.15) can be substituted by

$$-p \operatorname{div}\mathbf{V} = \frac{p}{\rho} \frac{D\rho}{Dt}.$$

Using further the identity

$$\frac{p}{\rho} \frac{D\rho}{Dt} = \frac{Dp}{Dt} - \rho \frac{D}{Dt} \left(\frac{p}{\rho} \right),$$

and taking into account that the enthalpy is defined as $h = e + p/\rho$, we see that the energy equation (1.7.15) may be written in the form

$$\begin{aligned} \rho \frac{Dh}{Dt} = \frac{Dp}{Dt} - \frac{2}{3} \mu (\operatorname{div}\mathbf{V})^2 + 2\mu \left[\left(\frac{\partial u}{\partial x} \right)^2 + \left(\frac{\partial v}{\partial y} \right)^2 + \left(\frac{\partial w}{\partial z} \right)^2 \right] \\ + \mu \left[\left(\frac{\partial u}{\partial y} + \frac{\partial v}{\partial x} \right)^2 + \left(\frac{\partial u}{\partial z} + \frac{\partial w}{\partial x} \right)^2 + \left(\frac{\partial v}{\partial z} + \frac{\partial w}{\partial y} \right)^2 \right] + \operatorname{div}(\kappa \nabla T). \end{aligned} \quad (1.7.18)$$

In this book series, our main attention will be on perfect gas flows, in which case the enthalpy h is given by equation (1.3.28),

$$h = c_p T.$$

Therefore, assuming c_p constant, we have

$$\nabla T = \frac{1}{c_p} \nabla h.$$

This equation can be rearranged, using (1.6.32), as

$$\kappa \nabla T = \frac{\mu}{Pr} \nabla h. \quad (1.7.19)$$

It remains to substitute (1.7.19) into (1.7.18), and we have the *energy equation for a perfect gas flow* in the form

$$\begin{aligned} \rho \frac{Dh}{Dt} = \frac{Dp}{Dt} - \frac{2}{3} \mu (\operatorname{div}\mathbf{V})^2 + 2\mu \left[\left(\frac{\partial u}{\partial x} \right)^2 + \left(\frac{\partial v}{\partial y} \right)^2 + \left(\frac{\partial w}{\partial z} \right)^2 \right] \\ + \mu \left[\left(\frac{\partial u}{\partial y} + \frac{\partial v}{\partial x} \right)^2 + \left(\frac{\partial u}{\partial z} + \frac{\partial w}{\partial x} \right)^2 + \left(\frac{\partial v}{\partial z} + \frac{\partial w}{\partial y} \right)^2 \right] + \frac{1}{Pr} \operatorname{div}(\mu \nabla h). \end{aligned} \quad (1.7.20)$$

Collecting together the momentum equations (1.7.8), (1.7.9), (1.7.10), the energy equation (1.7.20), the continuity equation (1.6.6), and the perfect gas state equation (1.3.33), we can write the *Navier–Stokes equations governing the motion of a perfect gas* as

$$\begin{aligned} \rho \left(\frac{\partial u}{\partial t} + u \frac{\partial u}{\partial x} + v \frac{\partial u}{\partial y} + w \frac{\partial u}{\partial z} \right) \\ = \rho f_x - \frac{\partial p}{\partial x} + \frac{\partial}{\partial x} \left\{ \mu \left[\frac{4}{3} \frac{\partial u}{\partial x} - \frac{2}{3} \left(\frac{\partial v}{\partial y} + \frac{\partial w}{\partial z} \right) \right] \right\} \\ + \frac{\partial}{\partial y} \left[\mu \left(\frac{\partial u}{\partial y} + \frac{\partial v}{\partial x} \right) \right] + \frac{\partial}{\partial z} \left[\mu \left(\frac{\partial u}{\partial z} + \frac{\partial w}{\partial x} \right) \right], \end{aligned} \quad (1.7.21a)$$

$$\begin{aligned} \rho \left(\frac{\partial v}{\partial t} + u \frac{\partial v}{\partial x} + v \frac{\partial v}{\partial y} + w \frac{\partial v}{\partial z} \right) \\ = \rho f_y - \frac{\partial p}{\partial y} + \frac{\partial}{\partial y} \left\{ \mu \left[\frac{4}{3} \frac{\partial v}{\partial y} - \frac{2}{3} \left(\frac{\partial u}{\partial x} + \frac{\partial w}{\partial z} \right) \right] \right\} \\ + \frac{\partial}{\partial x} \left[\mu \left(\frac{\partial u}{\partial y} + \frac{\partial v}{\partial x} \right) \right] + \frac{\partial}{\partial z} \left[\mu \left(\frac{\partial v}{\partial z} + \frac{\partial w}{\partial y} \right) \right], \end{aligned} \quad (1.7.21b)$$

$$\begin{aligned} \rho \left(\frac{\partial w}{\partial t} + u \frac{\partial w}{\partial x} + v \frac{\partial w}{\partial y} + w \frac{\partial w}{\partial z} \right) \\ = \rho f_z - \frac{\partial p}{\partial z} + \frac{\partial}{\partial z} \left\{ \mu \left[\frac{4}{3} \frac{\partial w}{\partial z} - \frac{2}{3} \left(\frac{\partial v}{\partial y} + \frac{\partial u}{\partial x} \right) \right] \right\} \\ + \frac{\partial}{\partial x} \left[\mu \left(\frac{\partial u}{\partial z} + \frac{\partial w}{\partial x} \right) \right] + \frac{\partial}{\partial y} \left[\mu \left(\frac{\partial v}{\partial z} + \frac{\partial w}{\partial y} \right) \right], \end{aligned} \quad (1.7.21c)$$

$$\begin{aligned} \rho \left(\frac{\partial h}{\partial t} + u \frac{\partial h}{\partial x} + v \frac{\partial h}{\partial y} + w \frac{\partial h}{\partial z} \right) &= \frac{\partial p}{\partial t} + u \frac{\partial p}{\partial x} + v \frac{\partial p}{\partial y} + w \frac{\partial p}{\partial z} \\ &+ \frac{1}{Pr} \left[\frac{\partial}{\partial x} \left(\mu \frac{\partial h}{\partial x} \right) + \frac{\partial}{\partial y} \left(\mu \frac{\partial h}{\partial y} \right) + \frac{\partial}{\partial z} \left(\mu \frac{\partial h}{\partial z} \right) \right] \\ &+ \mu \left(\frac{\partial u}{\partial y} + \frac{\partial v}{\partial x} \right)^2 + \mu \left(\frac{\partial u}{\partial z} + \frac{\partial w}{\partial x} \right)^2 + \mu \left(\frac{\partial v}{\partial z} + \frac{\partial w}{\partial y} \right)^2 \\ &+ \frac{4}{3} \mu \left[\left(\frac{\partial u}{\partial x} - \frac{\partial v}{\partial y} \right) \frac{\partial u}{\partial x} + \left(\frac{\partial v}{\partial y} - \frac{\partial w}{\partial z} \right) \frac{\partial v}{\partial y} + \left(\frac{\partial w}{\partial z} - \frac{\partial u}{\partial x} \right) \frac{\partial w}{\partial z} \right], \end{aligned} \quad (1.7.21d)$$

$$\frac{\partial \rho}{\partial t} + \frac{\partial \rho u}{\partial x} + \frac{\partial \rho v}{\partial y} + \frac{\partial \rho w}{\partial z} = 0, \quad (1.7.21e)$$

$$h = \frac{\gamma}{\gamma - 1} \frac{p}{\rho}. \quad (1.7.21f)$$

1.7.3 Integral momentum equation

If the solution of the Navier–Stokes equations is found for a particular flow, say, for a flow past a rigid body, then the total force experienced by the body may be calculated through integration of the stress \mathbf{p}_n produced by the moving fluid on the body surface. However, it often happens that only partial information about the flow field is available. For example, an experimentalist might want to avoid disturbing the flow in the immediate vicinity of the body surface, and choose to perform the measurements at some distance from the body. A theoretician might be able to find the behaviour of the solution in the ‘far field’, but not close to the body. The force experienced by the body may still be calculated, for which purpose the integral momentum equation is used.

When deducing this equation, we shall assume that the flow considered is steady ($\partial\mathbf{V}/\partial t = 0$) and the body force is negligibly small ($\mathbf{f} = 0$). Then the momentum equation (1.6.27) takes the form

$$\rho(\mathbf{V} \cdot \nabla)\mathbf{V} = \operatorname{div} \mathcal{P}.$$

Projecting this equation upon the x_α -axis, we have

$$\rho V_i \frac{\partial V_\alpha}{\partial x_i} = \frac{\partial p_{i\alpha}}{\partial x_i}, \quad \alpha = 1, 2, 3. \quad (1.7.22)$$

Here the x_α -component of $\operatorname{div} \mathcal{P}$ is calculated according to the rule given by equations (1.6.26).

For a steady flow, compressible or incompressible, the continuity equation (1.6.6) is written as

$$\operatorname{div}(\rho\mathbf{V}) = 0,$$

or, equivalently,

$$\frac{\partial}{\partial x_i}(\rho V_i) = 0. \quad (1.7.23)$$

Multiplying (1.7.23) by V_α and adding the result to (1.7.22) yields

$$\frac{\partial}{\partial x_i}(\rho V_i V_\alpha) = \frac{\partial p_{i\alpha}}{\partial x_i}. \quad (1.7.24)$$

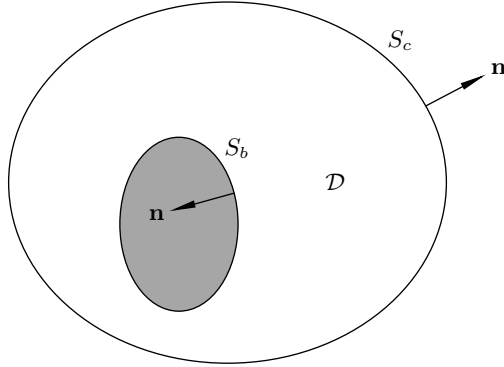
Hence, if we introduce a vector \mathbf{A} whose components are defined as

$$A_i = \rho V_i V_\alpha - p_{i\alpha}, \quad i = 1, 2, 3, \quad (1.7.25)$$

then we can write equation (1.7.24) as

$$\operatorname{div} \mathbf{A} = 0.$$

Let us integrate this equation over the region \mathcal{D} , termed *control volume*, that lies between the body surface S_b and an arbitrarily chosen surface S_c embracing the body

Fig. 1.28: Control volume \mathcal{D} .

as shown in Figure 1.28; both the body and control surface are assumed to be fixed with respect to an inertial coordinate system (x_1, x_2, x_3) . We have

$$\iiint_{\mathcal{D}} \operatorname{div} \mathbf{A} \, d\tau = 0.$$

Then using Gauss's divergence theorem, we can write

$$\iint_{S_c} (\mathbf{A} \cdot \mathbf{n}) \, ds + \iint_{S_b} (\mathbf{A} \cdot \mathbf{n}) \, ds = 0, \quad (1.7.26)$$

where \mathbf{n} is the unit normal vector external to \mathcal{D} .

It follows from (1.7.25) and (1.2.11) that

$$\mathbf{A} \cdot \mathbf{n} = A_i n_i = \rho V_\alpha (V_i n_i) - p_{i\alpha} n_i = \rho V_\alpha (\mathbf{V} \cdot \mathbf{n}) - p_{n\alpha},$$

which, when substituted into (1.7.26), yields

$$\iint_{S_c} [\rho V_\alpha (\mathbf{V} \cdot \mathbf{n}) - p_{n\alpha}] \, ds + \iint_{S_b} [\rho V_\alpha (\mathbf{V} \cdot \mathbf{n}) - p_{n\alpha}] \, ds = 0.$$

Since this equation is valid for $\alpha = 1, 2, 3$, it may be written in a vector form

$$\iint_{S_c} [\rho (\mathbf{V} \cdot \mathbf{n}) \mathbf{V} - \mathbf{p}_n] \, ds + \iint_{S_b} [\rho (\mathbf{V} \cdot \mathbf{n}) \mathbf{V} - \mathbf{p}_n] \, ds = 0. \quad (1.7.27)$$

Let us examine the second integral in (1.7.27). We note, first, that the surface of a rigid body is impenetrable by a fluid. This means that the normal velocity component $V_n = \mathbf{V} \cdot \mathbf{n}$ is zero everywhere on S_b . Second, returning to (1.2.3), we recall that $\mathbf{p}_n \, ds$ is the force acting through ds on the fluid situated on the rear side of S_b . With

the direction of \mathbf{n} as shown in Figure 1.28, this is the force experienced by the fluid surrounding the body. Hence, the force acting upon the body is given by

$$\mathbf{F} = - \iint_{S_b} \mathbf{p}_n ds. \quad (1.7.28)$$

Combining (1.7.27) and (1.7.28), we have

$$\mathbf{F} = \iint_{S_c} \mathbf{p}_n ds - \iint_{S_c} \rho(\mathbf{V} \cdot \mathbf{n}) \mathbf{V} ds. \quad (1.7.29)$$

This shows that *the force exerted by the flow on a rigid body equals the force acting on the control surface S_c minus the momentum flux through this surface.*

Of course, if there is no rigid body inside the control surface S_c and the entire region \mathcal{D} is filled with moving fluid, then equation (1.7.29) reduces to

$$\iint_{S_c} \rho(\mathbf{V} \cdot \mathbf{n}) \mathbf{V} ds = \iint_{S_c} \mathbf{p}_n ds, \quad (1.7.30)$$

stating that *the momentum flux through a control surface equals the total surface force acting on this surface.*

1.7.4 Similarity rules in fluid dynamics

When solving the Navier–Stokes equations (1.7.21), one needs to use an appropriate set of boundary conditions. The form of the latter depends on the particular problem considered. Here we shall assume that we are dealing with a rigid body, say, an aircraft wing, placed in a uniform flow of a perfect gas. We shall denote the gas velocity far from the body (termed the *free-stream velocity*) as V_∞ , the free-stream pressure as p_∞ , the gas density in the free stream as ρ_∞ , and the dynamic viscosity coefficient as μ_∞ . The coordinate system can always be rotated to make the x -axis parallel to the free-stream velocity vector, and then we will have

$$u = V_\infty, \quad v = w = 0, \quad p = p_\infty, \quad \rho = \rho_\infty \quad \text{at} \quad x^2 + y^2 + z^2 = \infty. \quad (1.7.31)$$

Let us further assume that the body force \mathbf{f} is that due to gravity. For an aircraft in cruise, this is directed vertically downwards, i.e.

$$f_x = f_z = 0, \quad f_y = -g, \quad (1.7.32)$$

where g is the acceleration of free fall.

Finally, the boundary conditions on the wing surface S have to be formulated. We shall assume that the wing surface equation may be written in the form

$$\Phi\left(\frac{x}{L}, \frac{y - y_0(t)}{L}, \frac{z}{L}\right) = 0. \quad (1.7.33)$$

Here the arguments of the function Φ are made dimensionless using the wing chord L . This allows us to consider a family of wings that are geometrically similar to one another but have different size L .

Equation (1.7.33) also allows for wing oscillations to be included in the discussion, as we want to model phenomena such as wing flutter.¹⁴ For our purposes, it is sufficient to assume that the wing moves as a whole along the y -axis, being described by the equation

$$y_0(t) = L\bar{y}_0\left(\frac{t}{T}\right),$$

with the period T of the oscillation used to make the argument of the function \bar{y}_0 dimensionless.

The fluid velocity has to satisfy the following conditions on the body surface S :

$$u = w = 0, \quad v = \frac{dy_0}{dt} \quad \text{on } S. \quad (1.7.34)$$

These conditions represent a fundamental property of fluid motion, which consists in the following observation. When a fluid particle comes in contact with a solid body, it always assumes the same velocity as the corresponding element of the body surface. This is attributed to the molecular forces acting between fluids and solids. They prevent the fluid from ‘sliding’ along the body surface. The resulting restriction on the fluid velocity field is called the *no-slip condition*. Theoretical justification of this result is still to be found for a general fluid flow, and therefore one has to rely on the available experimental evidence. The latter is ample and supports the view that the no-slip condition is a universal law of fluid dynamics.

In addition to (1.7.34), one has to formulate a boundary condition for the enthalpy h . If we assume that the body surface S is thermally isolated, i.e. there is no heat transfer through S , then

$$\nabla h \cdot \mathbf{n} = 0 \quad \text{on } S. \quad (1.7.35)$$

This closes the formulation of the boundary-value problem for the Navier-Stokes equations (1.7.21).

We shall now cast the equations (1.7.21) and the boundary conditions (1.7.31), (1.7.34), (1.7.35) in non-dimensional form. We introduce the non-dimensional variables (denoted by the ‘bar’) using the following transformations

$$\left. \begin{aligned} t &= T\bar{t}, & x &= L\bar{x}, & y &= L\bar{y}, & z &= L\bar{z}, \\ u &= V_\infty\bar{u}, & v &= V_\infty\bar{v}, & w &= V_\infty\bar{w}, \\ p &= p_\infty + \rho_\infty V_\infty^2\bar{p}, & \rho &= \rho_\infty\bar{\rho}, & h &= V_\infty^2\bar{h}, & \mu &= \mu_\infty\bar{\mu}. \end{aligned} \right\} \quad (1.7.36)$$

Substitution of (1.7.36) into (1.7.21) results in

¹⁴Flutter is observed when an aircraft’s speed exceeds a critical value, and then violent oscillations of the wing take place, which can result in destruction of the wing frame.

$$\begin{aligned}
& \bar{\rho} \left(St \frac{\partial \bar{u}}{\partial \bar{t}} + \bar{u} \frac{\partial \bar{u}}{\partial \bar{x}} + \bar{v} \frac{\partial \bar{u}}{\partial \bar{y}} + \bar{w} \frac{\partial \bar{u}}{\partial \bar{z}} \right) \\
&= -\frac{\partial \bar{p}}{\partial \bar{x}} + \frac{1}{Re} \frac{\partial}{\partial \bar{x}} \left\{ \bar{\mu} \left[\frac{4}{3} \frac{\partial \bar{u}}{\partial \bar{x}} - \frac{2}{3} \left(\frac{\partial \bar{v}}{\partial \bar{y}} + \frac{\partial \bar{w}}{\partial \bar{z}} \right) \right] \right\} \\
&\quad + \frac{1}{Re} \frac{\partial}{\partial \bar{y}} \left[\bar{\mu} \left(\frac{\partial \bar{u}}{\partial \bar{y}} + \frac{\partial \bar{v}}{\partial \bar{x}} \right) \right] + \frac{1}{Re} \frac{\partial}{\partial \bar{z}} \left[\bar{\mu} \left(\frac{\partial \bar{u}}{\partial \bar{z}} + \frac{\partial \bar{w}}{\partial \bar{x}} \right) \right], \quad (1.7.37a)
\end{aligned}$$

$$\begin{aligned}
& \bar{\rho} \left(St \frac{\partial \bar{v}}{\partial \bar{t}} + \bar{u} \frac{\partial \bar{v}}{\partial \bar{x}} + \bar{v} \frac{\partial \bar{v}}{\partial \bar{y}} + \bar{w} \frac{\partial \bar{v}}{\partial \bar{z}} \right) \\
&= -\frac{1}{Fr^2} \bar{\rho} - \frac{\partial \bar{p}}{\partial \bar{y}} + \frac{1}{Re} \frac{\partial}{\partial \bar{y}} \left\{ \bar{\mu} \left[\frac{4}{3} \frac{\partial \bar{v}}{\partial \bar{y}} - \frac{2}{3} \left(\frac{\partial \bar{u}}{\partial \bar{x}} + \frac{\partial \bar{w}}{\partial \bar{z}} \right) \right] \right\} \\
&\quad + \frac{1}{Re} \frac{\partial}{\partial \bar{x}} \left[\bar{\mu} \left(\frac{\partial \bar{u}}{\partial \bar{y}} + \frac{\partial \bar{v}}{\partial \bar{x}} \right) \right] + \frac{1}{Re} \frac{\partial}{\partial \bar{z}} \left[\bar{\mu} \left(\frac{\partial \bar{v}}{\partial \bar{z}} + \frac{\partial \bar{w}}{\partial \bar{y}} \right) \right], \quad (1.7.37b)
\end{aligned}$$

$$\begin{aligned}
& \bar{\rho} \left(St \frac{\partial \bar{w}}{\partial \bar{t}} + \bar{u} \frac{\partial \bar{w}}{\partial \bar{x}} + \bar{v} \frac{\partial \bar{w}}{\partial \bar{y}} + \bar{w} \frac{\partial \bar{w}}{\partial \bar{z}} \right) \\
&= -\frac{\partial \bar{p}}{\partial \bar{z}} + \frac{1}{Re} \frac{\partial}{\partial \bar{z}} \left\{ \bar{\mu} \left[\frac{4}{3} \frac{\partial \bar{w}}{\partial \bar{z}} - \frac{2}{3} \left(\frac{\partial \bar{v}}{\partial \bar{y}} + \frac{\partial \bar{u}}{\partial \bar{x}} \right) \right] \right\} \\
&\quad + \frac{1}{Re} \frac{\partial}{\partial \bar{x}} \left[\bar{\mu} \left(\frac{\partial \bar{u}}{\partial \bar{z}} + \frac{\partial \bar{w}}{\partial \bar{x}} \right) \right] + \frac{1}{Re} \frac{\partial}{\partial \bar{y}} \left[\bar{\mu} \left(\frac{\partial \bar{v}}{\partial \bar{z}} + \frac{\partial \bar{w}}{\partial \bar{y}} \right) \right], \quad (1.7.37c)
\end{aligned}$$

$$\begin{aligned}
& \bar{\rho} \left(St \frac{\partial \bar{h}}{\partial \bar{t}} + \bar{u} \frac{\partial \bar{h}}{\partial \bar{x}} + \bar{v} \frac{\partial \bar{h}}{\partial \bar{y}} + \bar{w} \frac{\partial \bar{h}}{\partial \bar{z}} \right) = St \frac{\partial \bar{p}}{\partial \bar{t}} + \bar{u} \frac{\partial \bar{p}}{\partial \bar{x}} + \bar{v} \frac{\partial \bar{p}}{\partial \bar{y}} + \bar{w} \frac{\partial \bar{p}}{\partial \bar{z}} \\
&\quad + \frac{1}{RePr} \left[\frac{\partial}{\partial \bar{x}} \left(\bar{\mu} \frac{\partial \bar{h}}{\partial \bar{x}} \right) + \frac{\partial}{\partial \bar{y}} \left(\bar{\mu} \frac{\partial \bar{h}}{\partial \bar{y}} \right) + \frac{\partial}{\partial \bar{z}} \left(\bar{\mu} \frac{\partial \bar{h}}{\partial \bar{z}} \right) \right] \\
&\quad + \frac{1}{Re} \left\{ \bar{\mu} \left(\frac{\partial \bar{u}}{\partial \bar{y}} + \frac{\partial \bar{v}}{\partial \bar{x}} \right)^2 + \bar{\mu} \left(\frac{\partial \bar{u}}{\partial \bar{z}} + \frac{\partial \bar{w}}{\partial \bar{x}} \right)^2 + \bar{\mu} \left(\frac{\partial \bar{v}}{\partial \bar{z}} + \frac{\partial \bar{w}}{\partial \bar{y}} \right)^2 \right. \\
&\quad \left. + \frac{4}{3} \bar{\mu} \left[\left(\frac{\partial \bar{u}}{\partial \bar{x}} - \frac{\partial \bar{v}}{\partial \bar{y}} \right) \frac{\partial \bar{u}}{\partial \bar{x}} + \left(\frac{\partial \bar{v}}{\partial \bar{y}} - \frac{\partial \bar{w}}{\partial \bar{z}} \right) \frac{\partial \bar{v}}{\partial \bar{y}} + \left(\frac{\partial \bar{w}}{\partial \bar{z}} - \frac{\partial \bar{u}}{\partial \bar{x}} \right) \frac{\partial \bar{w}}{\partial \bar{z}} \right] \right\}, \quad (1.7.37d)
\end{aligned}$$

$$St \frac{\partial \bar{\rho}}{\partial \bar{t}} + \frac{\partial \bar{\rho} \bar{u}}{\partial \bar{x}} + \frac{\partial \bar{\rho} \bar{v}}{\partial \bar{y}} + \frac{\partial \bar{\rho} \bar{w}}{\partial \bar{z}} = 0, \quad (1.7.37e)$$

$$\bar{h} = \frac{1}{(\gamma - 1) M_\infty^2} \frac{1}{\bar{\rho}} + \frac{\gamma}{\gamma - 1} \frac{\bar{p}}{\bar{\rho}}. \quad (1.7.37f)$$

The free-stream boundary conditions (1.7.31) are written in the non-dimensional variables as

$$\bar{u} = \bar{\rho} = 1, \quad \bar{v} = \bar{w} = \bar{p} = 0 \quad \text{at} \quad \bar{x}^2 + \bar{y}^2 + \bar{z}^2 = \infty, \quad (1.7.38a)$$

and the conditions on the wing surface, (1.7.34) and (1.7.35), assume the form

$$\bar{u} = \bar{w} = 0, \quad \bar{v} = St \frac{d\bar{y}_0}{d\bar{t}}, \quad \nabla \bar{h} \cdot \mathbf{n} = 0 \quad \text{on} \quad S. \quad (1.7.38b)$$

72 Chapter 1. Fundamentals of Fluid Dynamics

The equations (1.7.37) and boundary conditions (1.7.38) involve six non-dimensional parameters. Two of these, the ratio of specific heats γ and the Prandtl number Pr , were introduced in Sections 1.3.2 and 1.6.3, respectively. The four ‘new’ parameters are

$$\begin{aligned} \text{Reynolds number} \quad Re &= \frac{\rho_\infty V_\infty L}{\mu_\infty}, \\ \text{Mach number} \quad M_\infty &= \frac{V_\infty}{\sqrt{\gamma p_\infty / \rho_\infty}}, \\ \text{Strouhal number} \quad St &= \frac{L}{V_\infty T}, \\ \text{Froude number} \quad Fr &= \frac{V_\infty}{\sqrt{gL}}. \end{aligned}$$

Provided that the solution of the boundary-value problem (1.7.37), (1.7.38) exists and is unique, the following statement is valid. If two wings with different chords L and different periods of oscillations T are placed into two flows with different V_∞ , p_∞ , and ρ_∞ , but (i) the functions Φ and \bar{y}_0 representing the wings’ geometry and motion are the same and (ii) the similarity parameters Re , M_∞ , St , Fr , Pr , and γ are also the same in the two flows, then these flows will appear identical in the non-dimensional variables. The first of the above conditions is known as *geometric similarity* and the second as *dynamic similarity*.

The similarity properties of fluid flows are widely used by experimentalists. In particular, an essential part of the aircraft design process is wind tunnel testing. These tests are performed on scaled-down models of the entire aircraft or its elements. To achieve dynamic similarity of the flow in a wind tunnel with that in real flight, one needs to reproduce the Mach number M_∞ and the Reynolds number Re as closely as possible,¹⁵ and then the velocity, density and pressure fields are expected to be the same in the non-dimensional variables. The dimensional quantities are recalculated in an obvious way, keeping in mind that

$$\frac{u}{V_\infty}, \quad \frac{v}{V_\infty}, \quad \frac{w}{V_\infty}, \quad \frac{\rho}{\rho_\infty}, \quad \frac{p - p_\infty}{\rho_\infty V_\infty^2}$$

remain the same at the corresponding points in the flow field.

Exercises 4

1. Does the continuity equation

$$\frac{\partial \rho}{\partial t} + \text{div}(\rho \mathbf{V}) = 0$$

admit a simplification in the case when ρ remains unchanged for each fluid particle but is different for different fluid particles? An example of such a fluid is sea water. It has different salt concentration, depending on the water depth.

¹⁵In aerodynamic flows, one does not need to think of the Froude number, since gravitational effects are too small. Also, when dealing with a steady flow, typical of cruise flight, the Strouhal number becomes unimportant.

2. Verify the identity

$$(\mathbf{V} \cdot \nabla)\mathbf{V} = \boldsymbol{\omega} \times \mathbf{V} + \nabla\left(\frac{V^2}{2}\right),$$

known as the *Lamb formula*. Here V is the modulus of the velocity vector \mathbf{V} .

Hint: It is sufficient to consider, say, the x -component of the identity.

3. Prove that $\nabla^2\mathbf{V}$, representing the viscous term on the right-hand side of the incompressible Navier–Stokes equation (1.7.5a), may be written as

$$\nabla^2\mathbf{V} = -\text{curl}\boldsymbol{\omega}.$$

Suggestion: As with the previous problem, you only need to consider the x -component of the identity.

4. The role of the Mach number in compressible flow behaviour is discussed in detail in Chapter 4; see, in particular, Section 4.1. Here your task is to show that for small values of the Mach number, the gas flows may be described by the incompressible Navier–Stokes equations (1.7.6).

When performing your analysis, assume that gravitational effects may be disregarded ($Fr = \infty$). Assume further that the Reynolds number Re and the Strouhal number St are finite. Finally, assume that the Mach number M_∞ is small, and represent the solution of the compressible Navier–Stokes equations (1.7.37) in the form

$$\begin{aligned}\bar{u} &= u_0 + M_\infty^2 u_1 + \cdots, & \bar{v} &= v_0 + M_\infty^2 v_1 + \cdots, & \bar{w} &= w_0 + M_\infty^2 w_1 + \cdots, \\ \bar{p} &= p_0 + M_\infty^2 p_1 + \cdots, & \bar{\rho} &= 1 + M_\infty^2 \rho_1 + \cdots, & \bar{h} &= \frac{1}{(\gamma - 1)M_\infty^2} + h_1 + \cdots, \\ \bar{\mu} &= 1 + M_\infty^2 \mu_1 + \cdots,\end{aligned}$$

and, working with the leading-order terms, show that the velocity components u_0, v_0, w_0 and the pressure p_0 satisfy the incompressible Navier–Stokes equations (1.7.6).

Suggestion: Start your analysis with the continuity equation (1.7.37e).

1.8 Curvilinear Coordinates

There are many situations where, instead of Cartesian coordinates, it is more convenient to write the Navier–Stokes equations in curvilinear coordinates. For example, to take advantage of simplifications that arise when dealing with an axisymmetric flow, one needs to use cylindrical coordinates; see Figure 1.30 on page 80.

Any coordinate system serves the following purposes. First of all, it should specify the position of a point in space. In the Cartesian coordinate system, this is achieved by ascribing particular values to x, y, z . For each point, these are found as the projections on the three coordinate axes. Inversely, given three coordinates x, y, z , the position of the corresponding point in space is uniquely defined. Any other coordinate system (q_1, q_2, q_3) should perform the same task; namely, it should provide a one-to-one correspondence between the points and their coordinates q_1, q_2, q_3 .

A curvilinear coordinate system (q_1, q_2, q_3) may be introduced by specifying the three functions on the right-hand sides of the equations

$$x = x(q_1, q_2, q_3), \quad y = y(q_1, q_2, q_3), \quad z = z(q_1, q_2, q_3). \quad (1.8.1)$$

With (1.8.1) given, the task of determining the position of a point in space through its curvilinear coordinates q_1, q_2, q_3 reduces to the conventional task of identifying this point in the Cartesian coordinates x, y, z .

Let M be a point whose curvilinear coordinates are q_1, q_2, q_3 . Three coordinate lines may be drawn through this point; see Figure 1.29(a). The q_1 -coordinate line is produced by increasing q_1 from its value at M and keeping q_2 and q_3 unchanged. The q_2 - and q_3 -coordinate lines are produced by increasing q_2 and q_3 , respectively, and keeping the two other coordinates unchanged.

The second purpose for which coordinate systems are used is the presentation of vectors by their components. In Cartesian coordinates any vector \mathbf{A} may be decomposed as

$$\mathbf{A} = A_x \mathbf{i} + A_y \mathbf{j} + A_z \mathbf{k}.$$

with \mathbf{i}, \mathbf{j} and \mathbf{k} being the unit vectors along the x -, y - and z -axes. When dealing with a curvilinear coordinate system, the unit vectors $\mathbf{e}_1, \mathbf{e}_2$, and \mathbf{e}_3 are drawn tangentially to the q_1 -, q_2 -, and q_3 -axes, respectively. Using vector triad $(\mathbf{e}_1, \mathbf{e}_2, \mathbf{e}_3)$, we can represent vector \mathbf{A} as

$$\mathbf{A} = A_1 \mathbf{e}_1 + A_2 \mathbf{e}_2 + A_3 \mathbf{e}_3, \quad (1.8.2)$$

where (A_1, A_2, A_3) are the components of \mathbf{A} in the curvilinear coordinates (q_1, q_2, q_3) . Notice that, unlike Cartesian unit vectors $(\mathbf{i}, \mathbf{j}, \mathbf{k})$, the curvilinear coordinate triad $(\mathbf{e}_1, \mathbf{e}_2, \mathbf{e}_3)$ changes its orientation when the point of observation M moves in the space. In other words, the vectors $\mathbf{e}_1, \mathbf{e}_2$, and \mathbf{e}_3 are functions of q_1, q_2 , and q_3 . In what follows, we shall assume that the unit vectors $(\mathbf{e}_1, \mathbf{e}_2, \mathbf{e}_3)$ remain perpendicular to one another. Coordinate systems that satisfy this restriction are termed *orthogonal*.

Let us now place point M_1 on the q_1 -axis close to point M ; the coordinates of point M_1 are $q_1 + dq_1, q_2, q_3$. Similarly, we place point $M_2(q_1, q_2 + dq_2, q_3)$ on the q_2 -axis and point $M_3(q_1, q_2, q_3 + dq_3)$ on the q_3 -axis. We then build a small coordinate

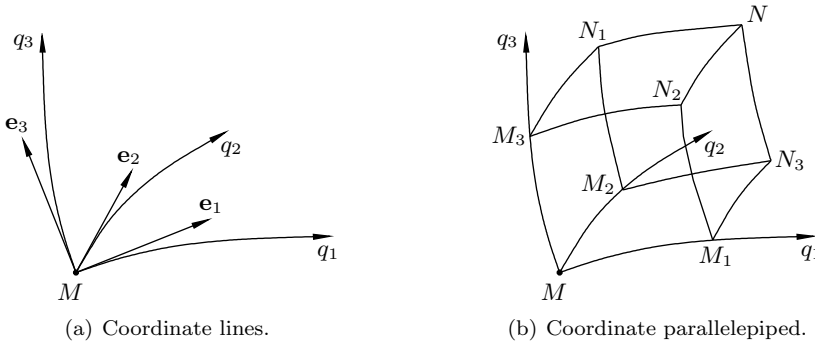


Fig. 1.29: Curvilinear coordinates.

parallelepiped as shown in Figure 1.29(b). Its faces are made of the coordinate surfaces. Two of them, $MM_2N_1M_3$ and $M_1N_3NN_2$, are drawn through points M and M_1 orthogonal to the q_1 -axis. The orthogonality condition is the requirement that on these surfaces the first coordinate remains constant; it equals q_1 on $MM_2N_1M_3$ and $q_1 + dq_1$ on $M_1N_3NN_2$. The other four faces of the coordinate parallelepiped are constructed in an obvious way.

Let us now discuss the geometrical properties of the coordinate parallelepiped. The length of edge MM_1 may be calculated as

$$dl_1 = \sqrt{(dx)^2 + (dy)^2 + (dz)^2}.$$

Since the coordinates of points M and M_1 are (q_1, q_2, q_3) and $(q_1 + dq_1, q_2, q_3)$, respectively, it follows from (1.8.1) that

$$dx = \frac{\partial x}{\partial q_1} dq_1, \quad dy = \frac{\partial y}{\partial q_1} dq_1, \quad dz = \frac{\partial z}{\partial q_1} dq_1,$$

and therefore

$$dl_1 = \sqrt{\left(\frac{\partial x}{\partial q_1}\right)^2 + \left(\frac{\partial y}{\partial q_1}\right)^2 + \left(\frac{\partial z}{\partial q_1}\right)^2} dq_1. \quad (1.8.3a)$$

Similarly, the length of edge MM_2 is calculated as

$$dl_2 = \sqrt{\left(\frac{\partial x}{\partial q_2}\right)^2 + \left(\frac{\partial y}{\partial q_2}\right)^2 + \left(\frac{\partial z}{\partial q_2}\right)^2} dq_2, \quad (1.8.3b)$$

and for MM_3 we have

$$dl_3 = \sqrt{\left(\frac{\partial x}{\partial q_3}\right)^2 + \left(\frac{\partial y}{\partial q_3}\right)^2 + \left(\frac{\partial z}{\partial q_3}\right)^2} dq_3. \quad (1.8.3c)$$

The quantities

$$\left. \begin{aligned} H_1 &= \sqrt{\left(\frac{\partial x}{\partial q_1}\right)^2 + \left(\frac{\partial y}{\partial q_1}\right)^2 + \left(\frac{\partial z}{\partial q_1}\right)^2}, \\ H_2 &= \sqrt{\left(\frac{\partial x}{\partial q_2}\right)^2 + \left(\frac{\partial y}{\partial q_2}\right)^2 + \left(\frac{\partial z}{\partial q_2}\right)^2}, \\ H_3 &= \sqrt{\left(\frac{\partial x}{\partial q_3}\right)^2 + \left(\frac{\partial y}{\partial q_3}\right)^2 + \left(\frac{\partial z}{\partial q_3}\right)^2} \end{aligned} \right\} \quad (1.8.4)$$

are known as the *Lamé coefficients* or *scale factors*. They serve to convert the increments dq_1, dq_2, dq_3 of the curvilinear coordinates q_1, q_2, q_3 to the actual distances

measured along the coordinate axes. Using (1.8.4), equations (1.8.3) can be written in a more compact form

$$dl_1 = H_1 dq_1, \quad dl_2 = H_2 dq_2, \quad dl_3 = H_3 dq_3. \quad (1.8.5)$$

Since the coordinate system (q_1, q_2, q_3) is orthogonal, the task of calculating the area of any of the six faces of the coordinate parallelepiped (Figure 1.29b) reduces to a simple multiplication of two length elements from (1.8.5). For example, the area of the left-hand side face is

$$\sigma_1 = dl_2 dl_3 = H_2 H_3 dq_2 dq_3.$$

Similarly, the areas of the front and bottom faces are

$$\sigma_2 = H_1 H_3 dq_1 dq_3, \quad \sigma_3 = H_1 H_2 dq_1 dq_2.$$

The volume of the coordinate parallelepiped is

$$\tau = dl_1 dl_2 dl_3 = H_1 H_2 H_3 dq_1 dq_2 dq_3.$$

We are now ready to consider differential operators such as the *gradient*, *divergence*, and *curl*. Our task will be to express them in the curvilinear coordinates (q_1, q_2, q_3) . We start with the gradient. Recall that the gradient of a scalar function ϕ is defined in Cartesian coordinates as

$$\nabla\phi = \mathbf{i}\frac{\partial\phi}{\partial x} + \mathbf{j}\frac{\partial\phi}{\partial y} + \mathbf{k}\frac{\partial\phi}{\partial z}.$$

This definition, however, is not suitable for our purpose. We need a definition that does not depend on a particular choice of coordinate system. We shall use the following one.

Definition 1.5 Let P and P' be two points situated close to one another, and let $d\mathbf{r}$ be the vector connecting P with P' . Then we shall call the vector \mathbf{A} the **gradient** of the scalar function ϕ if

$$\mathbf{A} \cdot d\mathbf{r} = \phi(P') - \phi(P) + \alpha(d\mathbf{r}), \quad (1.8.6)$$

where the remainder term $\alpha(d\mathbf{r})$ is such that

$$\lim_{|d\mathbf{r}| \rightarrow 0} \frac{\alpha(d\mathbf{r})}{|d\mathbf{r}|} = 0.$$

Suppose that function ϕ is given in curvilinear coordinates (q_1, q_2, q_3) . Let us choose point P to coincide with point M of Figure 1.29(b) and point P' with point M_1 . Then the vector connecting these points is

$$d\mathbf{r} = dl_1 \mathbf{e}_1 = H_1 \mathbf{e}_1 dq_1.$$

Using for the vector \mathbf{A} its coordinate decomposition (1.8.2), we can see that the left-hand side of equation (1.8.6) is

$$\mathbf{A} \cdot d\mathbf{r} = A_1 H_1 dq_1. \quad (1.8.7)$$

The increment of the function ϕ on the right-hand side of (1.8.6) may be represented as

$$\phi(P') - \phi(P) = \phi(q_1 + dq_1, q_2, q_3) - \phi(q_1, q_2, q_3) = \frac{\partial \phi}{\partial q_1} dq_1 + \beta(dq_1), \quad (1.8.8)$$

with the remainder term satisfying the condition

$$\lim_{dq_1 \rightarrow 0} \frac{\beta(dq_1)}{dq_1} = 0.$$

Substituting (1.8.7) and (1.8.8) into (1.8.6) and taking $dq_1 \rightarrow 0$, we find that

$$A_1 = \frac{1}{H_1} \frac{\partial \phi}{\partial q_1}.$$

Similarly, the other two components may be shown to be

$$A_2 = \frac{1}{H_2} \frac{\partial \phi}{\partial q_2}, \quad A_3 = \frac{1}{H_3} \frac{\partial \phi}{\partial q_3}.$$

Consequently, we can conclude that the gradient of the function ϕ is written in orthogonal curvilinear coordinates (q_1, q_2, q_3) as

$$\nabla \phi = \frac{1}{H_1} \frac{\partial \phi}{\partial q_1} \mathbf{e}_1 + \frac{1}{H_2} \frac{\partial \phi}{\partial q_2} \mathbf{e}_2 + \frac{1}{H_3} \frac{\partial \phi}{\partial q_3} \mathbf{e}_3. \quad (1.8.9)$$

Let us now calculate the divergence of a vector field $\mathbf{A}(q_1, q_2, q_3)$. We shall use for this purpose Gauss's divergence theorem

$$\iiint_{\mathcal{D}} \operatorname{div} \mathbf{A} \, d\tau = \iint_S (\mathbf{A} \cdot \mathbf{n}) \, d\sigma. \quad (1.8.10)$$

Here \mathcal{D} is an arbitrary region; the surface around \mathcal{D} we denote by S , with \mathbf{n} being the unit external normal to S , and $d\sigma$ the area of a small element of the surface S . We shall apply equation (1.8.10) to the coordinate parallelepiped of Figure 1.29(b). Since the region confined by this parallelepiped is small, $\operatorname{div} \mathbf{A}$ remains almost constant over \mathcal{D} , and therefore the volume integral on the left-hand side of (1.8.10) may be calculated as

$$\iiint_{\mathcal{D}} \operatorname{div} \mathbf{A} \, d\tau = \operatorname{div} \mathbf{A} \, \tau = \operatorname{div} \mathbf{A} \, H_1 H_2 H_3 \, dq_1 \, dq_2 \, dq_3. \quad (1.8.11)$$

In order to evaluate the surface integral on the right-hand side of equation (1.8.10), we need to calculate the flux of the vector \mathbf{A} through the six faces of the coordinate parallelepiped. We start with the pair of faces orthogonal to the q_1 -axis. On $MM_2N_1M_3$,

the normal vector $\mathbf{n} = -\mathbf{e}_1$. Hence,

$$\mathbf{A} \cdot \mathbf{n} = -A_1,$$

and the flux of the vector \mathbf{A} through $MM_2N_1M_3$ is

$$-A_1\sigma_1 = -A_1H_2H_3 dq_2 dq_3. \quad (1.8.12)$$

On the opposite face $M_1N_3NN_2$, the normal vector $\mathbf{n} = \mathbf{e}_1$, which means that we have to change the sign in (1.8.12). We also have to take into account that on $M_1N_3NN_2$ the first coordinate is $q_1 + dq_1$, not q_1 . Therefore the flux of the vector \mathbf{A} through $M_1N_3NN_2$ is expressed as

$$\left(A_1H_2H_3 + \frac{\partial(A_1H_2H_3)}{\partial q_1} dq_1 \right) dq_2 dq_3. \quad (1.8.13)$$

Adding (1.8.12) and (1.8.13) together, we can conclude that the flux of the vector \mathbf{A} through the two faces orthogonal to the q_1 -axis equals

$$\frac{\partial(A_1H_2H_3)}{\partial q_1} dq_1 dq_2 dq_3. \quad (1.8.14)$$

Similarly, the flux of the vector \mathbf{A} through the two faces orthogonal to the q_2 -axis may be shown to be

$$\frac{\partial(A_2H_3H_1)}{\partial q_2} dq_1 dq_2 dq_3, \quad (1.8.15)$$

and, finally, the flux through the two faces that are orthogonal to the q_3 -axis is expressed as

$$\frac{\partial(A_3H_1H_2)}{\partial q_3} dq_1 dq_2 dq_3. \quad (1.8.16)$$

Combining (1.8.14), (1.8.15), and (1.8.16), we have

$$\iint_S (\mathbf{A} \cdot \mathbf{n}) d\sigma = \left[\frac{\partial(A_1H_2H_3)}{\partial q_1} + \frac{\partial(A_2H_3H_1)}{\partial q_2} + \frac{\partial(A_3H_1H_2)}{\partial q_3} \right] dq_1 dq_2 dq_3. \quad (1.8.17)$$

It remains to substitute (1.8.11) and (1.8.17) into (1.8.10), and we find that

$$\operatorname{div} \mathbf{A} = \frac{1}{H_1H_2H_3} \left[\frac{\partial(A_1H_2H_3)}{\partial q_1} + \frac{\partial(A_2H_3H_1)}{\partial q_2} + \frac{\partial(A_3H_1H_2)}{\partial q_3} \right]. \quad (1.8.18)$$

Finally, we shall consider the curl of a vector field $\mathbf{A}(q_1, q_2, q_3)$. In order to deduce an expression for $\operatorname{curl} \mathbf{A}$ in the curvilinear coordinates, we will make use of Stokes's theorem

$$\iint_S (\operatorname{curl} \mathbf{A} \cdot \mathbf{n}) d\sigma = \oint_C \mathbf{A} \cdot d\mathbf{r}. \quad (1.8.19)$$

Here C is a closed contour, S an open surface based on this contour, and \mathbf{n} the unit vector normal to S . The integration along the contour C on the right-hand side of

(1.8.19) should be performed in the counter-clockwise direction when the contour C is observed from the tip of the vector \mathbf{n} .

We start by choosing S to coincide with the left-hand side face $MM_2N_1M_3$ of the coordinate parallelepiped; see Figure 1.29. Let us further choose the normal vector \mathbf{n} to be in the positive direction of the q_1 -coordinate, i.e.

$$\mathbf{n} = \mathbf{e}_1.$$

Representing $\text{curl } \mathbf{A}$ through its components in the curvilinear coordinates,

$$\text{curl } \mathbf{A} = (\text{curl } \mathbf{A})_1 \mathbf{e}_1 + (\text{curl } \mathbf{A})_2 \mathbf{e}_2 + (\text{curl } \mathbf{A})_3 \mathbf{e}_3,$$

we find that

$$\text{curl } \mathbf{A} \cdot \mathbf{n} = (\text{curl } \mathbf{A})_1.$$

Therefore, the integral on the left-hand side of (1.8.19) appears to be

$$\iint_S (\text{curl } \mathbf{A} \cdot \mathbf{n}) d\sigma = (\text{curl } \mathbf{A})_1 \sigma_1 = (\text{curl } \mathbf{A})_1 H_2 H_3 dq_2 dq_3. \quad (1.8.20)$$

Now we turn to the contour integral on the right-hand side of (1.8.19). It may be calculated by considering the contributions from the four edges that bound the left-hand side face of the coordinate parallelepiped. When integrating from M to M_2 , we have to take

$$d\mathbf{r} = \mathbf{e}_2 dl_2 = \mathbf{e}_2 H_2 dq_2,$$

and therefore

$$\int_{MM_2} \mathbf{A} \cdot d\mathbf{r} = A_2 H_2 dq_2. \quad (1.8.21)$$

On the opposite edge N_1M_3 , the integration is performed from N_1 to M_3 , which means that we have to change the sign in (1.8.21). Besides, on N_1M_3 , the third coordinate is $q_3 + dq_3$, not q_3 as on MM_2 . Consequently,

$$\int_{N_1M_3} \mathbf{A} \cdot d\mathbf{r} = - \left[A_2 H_2 + \frac{\partial(A_2 H_2)}{\partial q_3} dq_3 \right] dq_2. \quad (1.8.22)$$

The integrals along M_2N_1 and M_3M are calculated in a similar way, leading to

$$\int_{M_2N_1} \mathbf{A} \cdot d\mathbf{r} = \left[A_3 H_3 + \frac{\partial(A_3 H_3)}{\partial q_2} dq_2 \right] dq_3, \quad (1.8.23)$$

$$\int_{M_3M} \mathbf{A} \cdot d\mathbf{r} = -A_3 H_3 dq_3. \quad (1.8.24)$$

Adding (1.8.21), (1.8.22), (1.8.23), and (1.8.24) together, we find that the contour

integral on the right-hand side of equation (1.8.19) is

$$\oint_C \mathbf{A} \cdot d\mathbf{r} = \left[\frac{\partial(A_3 H_3)}{\partial q_2} - \frac{\partial(A_2 H_2)}{\partial q_3} \right] dq_2 dq_3.$$

Comparing this with the surface integral (1.8.20) on the left-hand side of (1.8.19), leads to the conclusion that

$$(\text{curl } \mathbf{A})_1 = \frac{1}{H_2 H_3} \left[\frac{\partial(A_3 H_3)}{\partial q_2} - \frac{\partial(A_2 H_2)}{\partial q_3} \right]. \quad (1.8.25)$$

The other two components of $\text{curl } \mathbf{A}$ may be found by applying Stokes's theorem (1.8.19) to the front and bottom faces of the coordinate parallelepiped of Figure 1.29. Alternatively, one can exploit the freedom in choosing the notations for the coordinates used, namely, coordinate q_1 may be always re-denoted as q_2 , coordinate q_2 as q_3 , and coordinate q_3 as q_1 . Making the correspondent alterations in (1.8.25), we have

$$(\text{curl } \mathbf{A})_2 = \frac{1}{H_3 H_1} \left[\frac{\partial(A_1 H_1)}{\partial q_3} - \frac{\partial(A_3 H_3)}{\partial q_1} \right], \quad (1.8.26)$$

$$(\text{curl } \mathbf{A})_3 = \frac{1}{H_1 H_2} \left[\frac{\partial(A_2 H_2)}{\partial q_1} - \frac{\partial(A_1 H_1)}{\partial q_2} \right]. \quad (1.8.27)$$

Cylindrical polar coordinates

In cylindrical coordinates (see Figure 1.30), the position of point M is given by the distance r from the z -axis, the angle ϕ between the x -axis and the straight line connecting the projection of M upon the (x, y) -plane with the coordinate origin, and the

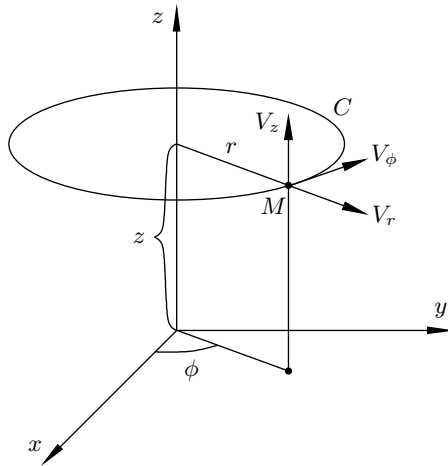


Fig. 1.30: Cylindrical coordinates.

altitude z of point M above the (x, y) -plane. We have

$$q_1 = r, \quad q_2 = \phi, \quad q_3 = z.$$

The cylindrical coordinates are related to Cartesian coordinates by

$$x = r \cos \phi, \quad y = r \sin \phi, \quad z = z. \quad (1.8.28)$$

Substitution of (1.8.28) into (1.8.4) yields, after simple manipulations, that

$$H_1 = 1, \quad H_2 = r, \quad H_3 = 1. \quad (1.8.29)$$

Alternatively, one can take advantage of the fact that the Lamé coefficients have a clear geometrical meaning, and deduce formulae (1.8.29) directly from (1.8.5). Indeed, if we increase r by dr and keep ϕ and z unchanged, then point M in Figure 1.30 will travel through a distance

$$dl_1 = dr.$$

Repeating this procedure for the other two coordinates, ϕ and z , we find

$$dl_2 = r d\phi, \quad dl_3 = dz.$$

Comparing these equations with (1.8.5), we can see the Lamé coefficients are really given by (1.8.29).

We are now ready to consider the Navier–Stokes equations. For simplicity, we shall restrict our attention here to incompressible fluid flows, when the Navier–Stokes equations (1.7.5) are written as

$$\frac{\partial \mathbf{V}}{\partial t} + (\mathbf{V} \cdot \nabla) \mathbf{V} = \mathbf{f} - \frac{1}{\rho} \nabla p + \nu \nabla^2 \mathbf{V}, \quad (1.8.30a)$$

$$\operatorname{div} \mathbf{V} = 0. \quad (1.8.30b)$$

The convective term on the left-hand side of the momentum equation (1.8.30a) may be expressed in terms of conventional differential operators using the *Lamb formula*¹⁶

$$(\mathbf{V} \cdot \nabla) \mathbf{V} = \boldsymbol{\omega} \times \mathbf{V} + \nabla \left(\frac{V^2}{2} \right), \quad (1.8.31)$$

Here $\boldsymbol{\omega} = \operatorname{curl} \mathbf{V}$ and V is the modulus of the velocity vector \mathbf{V} . For the viscous terms on the right-hand side of (1.8.30a), we shall use the following identity (see Problem 3 in Exercises 4)

$$\nabla^2 \mathbf{V} = \nabla(\operatorname{div} \mathbf{V}) - \operatorname{curl} \boldsymbol{\omega}.$$

The continuity equation (1.8.30b) reduces it to

$$\nabla^2 \mathbf{V} = -\operatorname{curl} \boldsymbol{\omega}. \quad (1.8.32)$$

¹⁶see Problem 2 in Exercises 4

After making use of (1.8.31) and (1.8.32), the momentum equation (1.8.30a) takes the form

$$\frac{\partial \mathbf{V}}{\partial t} + \boldsymbol{\omega} \times \mathbf{V} + \nabla \left(\frac{V^2}{2} \right) = \mathbf{f} - \frac{1}{\rho} \nabla p - \nu \operatorname{curl} \boldsymbol{\omega}. \quad (1.8.33)$$

The velocity vector \mathbf{V} is decomposed in cylindrical polar coordinates as

$$\mathbf{V} = V_r \mathbf{e}_1 + V_\phi \mathbf{e}_2 + V_z \mathbf{e}_3. \quad (1.8.34)$$

Here the unit vector triad $(\mathbf{e}_1, \mathbf{e}_2, \mathbf{e}_3)$ is built at the point M (see Figure 1.30) in the following way. The vector \mathbf{e}_1 points in the radial direction, the vector \mathbf{e}_2 is tangent to the circle C that lies in the plane drawn through point M perpendicular to the z -axis and has its centre on the z -axis, and, finally, the vector \mathbf{e}_3 is parallel to the z -axis. Corresponding to this, V_r is called the radial velocity component, V_ϕ the circumferential component, and V_z the axial component.

Applying the divergence operator (1.8.18) to the velocity vector (1.8.34), we find that the continuity equation (1.8.30b) is written in cylindrical coordinates as

$$\frac{\partial V_r}{\partial r} + \frac{1}{r} \frac{\partial V_\phi}{\partial \phi} + \frac{\partial V_z}{\partial z} + \frac{V_r}{r} = 0. \quad (1.8.35)$$

Now we turn to the momentum equation (1.8.33). In (1.8.34), the unit vectors \mathbf{e}_1 , \mathbf{e}_2 , and \mathbf{e}_3 depend on the position of point M but not on time. Therefore,

$$\frac{\partial \mathbf{V}}{\partial t} = \frac{\partial V_r}{\partial t} \mathbf{e}_1 + \frac{\partial V_\phi}{\partial t} \mathbf{e}_2 + \frac{\partial V_z}{\partial t} \mathbf{e}_3. \quad (1.8.36)$$

The second term on the left-hand side of (1.8.33) is calculated as

$$\begin{aligned} \boldsymbol{\omega} \times \mathbf{V} &= \begin{vmatrix} \mathbf{e}_1 & \mathbf{e}_2 & \mathbf{e}_3 \\ \omega_r & \omega_\phi & \omega_z \\ V_r & V_\phi & V_z \end{vmatrix} \\ &= \mathbf{e}_1(\omega_\phi V_z - \omega_z V_\phi) + \mathbf{e}_2(\omega_z V_r - \omega_r V_z) + \mathbf{e}_3(\omega_r V_\phi - \omega_\phi V_r), \end{aligned} \quad (1.8.37)$$

where, according to (1.8.25)–(1.8.27),

$$\omega_r = \frac{1}{r} \left[\frac{\partial V_z}{\partial \phi} - \frac{\partial(rV_\phi)}{\partial z} \right] = \frac{1}{r} \frac{\partial V_z}{\partial \phi} - \frac{\partial V_\phi}{\partial z}, \quad (1.8.38a)$$

$$\omega_\phi = \frac{\partial V_r}{\partial z} - \frac{\partial V_z}{\partial r}, \quad (1.8.38b)$$

$$\omega_z = \frac{1}{r} \left[\frac{\partial(rV_\phi)}{\partial r} - \frac{\partial V_r}{\partial \phi} \right] = \frac{\partial V_\phi}{\partial r} - \frac{1}{r} \frac{\partial V_r}{\partial \phi} + \frac{V_\phi}{r}. \quad (1.8.38c)$$

Finally, for the third term on the left-hand side of (1.8.33), formula (1.8.9) should be

used. Taking into account that $V^2 = V_r^2 + V_\phi^2 + V_z^2$, we have

$$\begin{aligned} \nabla\left(\frac{V^2}{2}\right) &= \nabla\left(\frac{V_r^2 + V_\phi^2 + V_z^2}{2}\right) = \left(V_r \frac{\partial V_r}{\partial r} + V_\phi \frac{\partial V_\phi}{\partial r} + V_z \frac{\partial V_z}{\partial r}\right) \mathbf{e}_1 \\ &\quad + \frac{1}{r} \left(V_r \frac{\partial V_r}{\partial \phi} + V_\phi \frac{\partial V_\phi}{\partial \phi} + V_z \frac{\partial V_z}{\partial \phi}\right) \mathbf{e}_2 \\ &\quad + \left(V_r \frac{\partial V_r}{\partial z} + V_\phi \frac{\partial V_\phi}{\partial z} + V_z \frac{\partial V_z}{\partial z}\right) \mathbf{e}_3. \end{aligned} \quad (1.8.39)$$

At this stage, it is convenient to deal with the three components of the momentum equation (1.8.33) separately. If we consider, for example, the radial component, then, collecting the corresponding terms in (1.8.36), (1.8.37), and (1.8.39), we find

$$\left[\frac{\partial \mathbf{V}}{\partial t} + \boldsymbol{\omega} \times \mathbf{V} + \nabla\left(\frac{V^2}{2}\right)\right]_r = \frac{\partial V_r}{\partial t} + \omega_\phi V_z - \omega_z V_\phi + V_r \frac{\partial V_r}{\partial r} + V_\phi \frac{\partial V_\phi}{\partial r} + V_z \frac{\partial V_z}{\partial r}.$$

It remains to make use of formulae (1.8.38b) and (1.8.38c), and we find that the radial component of the left-hand side of the momentum equation (1.8.33) is

$$\left[\frac{\partial \mathbf{V}}{\partial t} + \boldsymbol{\omega} \times \mathbf{V} + \nabla\left(\frac{V^2}{2}\right)\right]_r = \frac{\partial V_r}{\partial t} + V_r \frac{\partial V_r}{\partial r} + \frac{V_\phi}{r} \frac{\partial V_r}{\partial \phi} + V_z \frac{\partial V_r}{\partial z} - \frac{V_\phi^2}{2}. \quad (1.8.40)$$

Now we turn to the right-hand side of (1.8.33). The first two terms, being projected on the radial direction, are written as

$$\left[\mathbf{f} - \frac{1}{\rho} \nabla p\right]_r = f_r - \frac{1}{\rho} \frac{\partial p}{\partial r}. \quad (1.8.41)$$

Here f_r denotes the radial component of the body force \mathbf{f} .

In order to calculate the viscous term, we use formula (1.8.25). We have

$$(\text{curl } \boldsymbol{\omega})_r = \frac{1}{r} \frac{\partial \omega_z}{\partial \phi} - \frac{\partial \omega_\phi}{\partial z}. \quad (1.8.42)$$

Substitution of (1.8.38b) and (1.8.38c) into (1.8.42) leads to

$$(\text{curl } \boldsymbol{\omega})_r = \frac{1}{r} \frac{\partial^2 V_\phi}{\partial r \partial \phi} - \frac{1}{r^2} \frac{\partial^2 V_r}{\partial \phi^2} + \frac{1}{r^2} \frac{\partial V_\phi}{\partial \phi} - \frac{\partial^2 V_r}{\partial z^2} + \frac{\partial^2 V_z}{\partial r \partial z}. \quad (1.8.43)$$

Finally, we combine (1.8.43) with (1.8.41) on the right-hand side of equation (1.8.33) and use formula (1.8.40) for the left-hand side. As a result, we have the radial momentum equation in the form

$$\begin{aligned} \frac{\partial V_r}{\partial t} + V_r \frac{\partial V_r}{\partial r} + \frac{V_\phi}{r} \frac{\partial V_r}{\partial \phi} + V_z \frac{\partial V_r}{\partial z} - \frac{V_\phi^2}{2} &= f_r - \frac{1}{\rho} \frac{\partial p}{\partial r} \\ &+ \nu \left[-\frac{1}{r} \frac{\partial^2 V_\phi}{\partial r \partial \phi} + \frac{1}{r^2} \frac{\partial^2 V_r}{\partial \phi^2} - \frac{1}{r^2} \frac{\partial V_\phi}{\partial \phi} + \frac{\partial^2 V_r}{\partial z^2} - \frac{\partial}{\partial r} \left(\frac{\partial V_z}{\partial z} \right) \right]. \end{aligned} \quad (1.8.44)$$

The canonical form of the radial momentum equation is obtained by solving the continuity equation (1.8.35) for $\partial V_z / \partial z$ and substituting into the last term in (1.8.44).

The resulting equation is written below together with the circumferential and axial momentum equations which are deduced using a similar procedure. For completeness, we also include the continuity equation (1.8.35). We have

$$\begin{aligned} \frac{\partial V_r}{\partial t} + V_r \frac{\partial V_r}{\partial r} + \frac{V_\phi}{r} \frac{\partial V_r}{\partial \phi} + V_z \frac{\partial V_r}{\partial z} - \frac{V_\phi^2}{r} = f_r - \frac{1}{\rho} \frac{\partial p}{\partial r} \\ + \nu \left(\frac{\partial^2 V_r}{\partial z^2} + \frac{1}{r^2} \frac{\partial^2 V_r}{\partial \phi^2} - \frac{2}{r^2} \frac{\partial V_\phi}{\partial \phi} + \frac{\partial^2 V_r}{\partial r^2} + \frac{1}{r} \frac{\partial V_r}{\partial r} - \frac{V_r}{r^2} \right), \end{aligned} \quad (1.8.45a)$$

$$\begin{aligned} \frac{\partial V_\phi}{\partial t} + V_r \frac{\partial V_\phi}{\partial r} + \frac{V_\phi}{r} \frac{\partial V_\phi}{\partial \phi} + V_z \frac{\partial V_\phi}{\partial z} + \frac{V_r V_\phi}{r} = f_\phi - \frac{1}{\rho r} \frac{\partial p}{\partial \phi} \\ + \nu \left(\frac{\partial^2 V_\phi}{\partial z^2} + \frac{1}{r^2} \frac{\partial^2 V_\phi}{\partial \phi^2} + \frac{2}{r^2} \frac{\partial V_r}{\partial \phi} + \frac{\partial^2 V_\phi}{\partial r^2} + \frac{1}{r} \frac{\partial V_\phi}{\partial r} - \frac{V_\phi}{r^2} \right), \end{aligned} \quad (1.8.45b)$$

$$\begin{aligned} \frac{\partial V_z}{\partial t} + V_r \frac{\partial V_z}{\partial r} + \frac{V_\phi}{r} \frac{\partial V_z}{\partial \phi} + V_z \frac{\partial V_z}{\partial z} = f_z - \frac{1}{\rho} \frac{\partial p}{\partial z} \\ + \nu \left(\frac{\partial^2 V_z}{\partial z^2} + \frac{1}{r^2} \frac{\partial^2 V_z}{\partial \phi^2} + \frac{\partial^2 V_z}{\partial r^2} + \frac{1}{r} \frac{\partial V_z}{\partial r} \right), \end{aligned} \quad (1.8.45c)$$

$$\frac{\partial V_r}{\partial r} + \frac{1}{r} \frac{\partial V_\phi}{\partial \phi} + \frac{\partial V_z}{\partial z} + \frac{V_r}{r} = 0. \quad (1.8.45d)$$

Spherical polar coordinates

In spherical polar coordinates (see Figure 1.31), the position of point M is defined by the distance r from M to the coordinate origin O , the angle ϑ made by the position vector \mathbf{r} with the x -axis, and the angle ϕ between the (x, y) -plane and the plane S drawn through point M and the x -axis. Correspondingly, the velocity vector \mathbf{V} is represented by three components V_r , V_ϕ , and V_ϑ . The radial component V_r is parallel

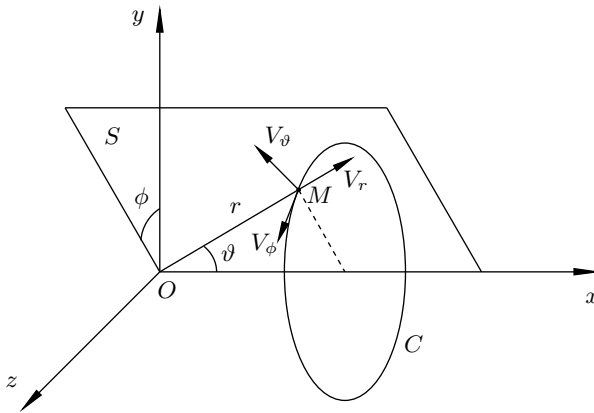


Fig. 1.31: Spherical polar coordinates.

to the radius r . The azimuthal component V_ϕ is tangent to circle C that lies in the plane drawn through point M perpendicular to the x -axis and has its centre on the x -axis. Finally, the meridional velocity component V_ϑ lies in plane S and is perpendicular to the radius OM .

It is easily seen from Figure 1.31 that the spherical polar coordinates are related to the Cartesian coordinates by

$$x = r \cos \vartheta, \quad y = r \sin \vartheta \cos \phi, \quad z = r \sin \vartheta \sin \phi. \quad (1.8.46)$$

Therefore, choosing $q_1 = r$, $q_2 = \vartheta$, and $q_3 = \phi$ and substituting (1.8.46) into (1.8.4), leads to the conclusion that in spherical polar coordinates the Lámé coefficients are

$$H_1 = 1, \quad H_2 = r, \quad H_3 = r \sin \vartheta. \quad (1.8.47)$$

We can now employ the same routine as the one used in the previous section for cylindrical polar coordinates. We find that the Navier–Stokes equations are written in spherical polar coordinates as

$$\begin{aligned} \frac{\partial V_r}{\partial t} + V_r \frac{\partial V_r}{\partial r} + \frac{V_\vartheta}{r} \frac{\partial V_r}{\partial \vartheta} + \frac{V_\phi}{r \sin \vartheta} \frac{\partial V_r}{\partial \phi} - \frac{V_\vartheta^2 + V_\phi^2}{r} &= f_r - \frac{1}{\rho} \frac{\partial p}{\partial r} \\ + \nu \left(\frac{\partial^2 V_r}{\partial r^2} + \frac{1}{r^2} \frac{\partial^2 V_r}{\partial \vartheta^2} + \frac{1}{r^2 \sin^2 \vartheta} \frac{\partial^2 V_r}{\partial \phi^2} + \frac{2}{r} \frac{\partial V_r}{\partial r} \right. \\ \left. + \frac{1}{r^2 \tan \vartheta} \frac{\partial V_r}{\partial \vartheta} - \frac{2}{r^2} \frac{\partial V_\vartheta}{\partial \vartheta} - \frac{2}{r^2 \sin \vartheta} \frac{\partial V_\phi}{\partial \phi} - \frac{2V_r}{r^2} - \frac{2V_\vartheta}{r^2 \tan \vartheta} \right), \end{aligned} \quad (1.8.48a)$$

$$\begin{aligned} \frac{\partial V_\vartheta}{\partial t} + V_r \frac{\partial V_\vartheta}{\partial r} + \frac{V_\vartheta}{r} \frac{\partial V_\vartheta}{\partial \vartheta} + \frac{V_\phi}{r \sin \vartheta} \frac{\partial V_\vartheta}{\partial \phi} + \frac{V_r V_\vartheta}{r} - \frac{V_\phi^2}{r \tan \vartheta} &= f_\vartheta - \frac{1}{\rho r} \frac{\partial p}{\partial \vartheta} \\ + \nu \left(\frac{\partial^2 V_\vartheta}{\partial r^2} + \frac{1}{r^2} \frac{\partial^2 V_\vartheta}{\partial \vartheta^2} + \frac{1}{r^2 \sin^2 \vartheta} \frac{\partial^2 V_\vartheta}{\partial \phi^2} + \frac{2}{r} \frac{\partial V_\vartheta}{\partial r} \right. \\ \left. + \frac{1}{r^2 \tan \vartheta} \frac{\partial V_\vartheta}{\partial \vartheta} - \frac{2 \cos \vartheta}{r^2 \sin^2 \vartheta} \frac{\partial V_\phi}{\partial \phi} + \frac{2}{r^2} \frac{\partial V_r}{\partial r} - \frac{V_\vartheta}{r^2 \sin^2 \vartheta} \right), \end{aligned} \quad (1.8.48b)$$

$$\begin{aligned} \frac{\partial V_\phi}{\partial t} + V_r \frac{\partial V_\phi}{\partial r} + \frac{V_\vartheta}{r} \frac{\partial V_\phi}{\partial \vartheta} + \frac{V_\phi}{r \sin \vartheta} \frac{\partial V_\phi}{\partial \phi} + \frac{V_r V_\phi}{r} + \frac{V_\vartheta V_\phi}{r \tan \vartheta} &= f_\phi - \frac{1}{\rho r \sin \vartheta} \frac{\partial p}{\partial \phi} \\ + \nu \left(\frac{\partial^2 V_\phi}{\partial r^2} + \frac{1}{r^2} \frac{\partial^2 V_\phi}{\partial \vartheta^2} + \frac{1}{r^2 \sin^2 \vartheta} \frac{\partial^2 V_\phi}{\partial \phi^2} + \frac{2}{r} \frac{\partial V_\phi}{\partial r} \right. \\ \left. + \frac{1}{r^2 \tan \vartheta} \frac{\partial V_\phi}{\partial \vartheta} + \frac{2}{r^2 \sin \vartheta} \frac{\partial V_r}{\partial r} + \frac{2 \cos \vartheta}{r^2 \sin^2 \vartheta} \frac{\partial V_\vartheta}{\partial \vartheta} - \frac{V_\phi}{r^2 \sin^2 \vartheta} \right), \end{aligned} \quad (1.8.48c)$$

$$\frac{\partial V_r}{\partial r} + \frac{1}{r} \frac{\partial V_\vartheta}{\partial \vartheta} + \frac{1}{r \sin \vartheta} \frac{\partial V_\phi}{\partial \phi} + \frac{2V_r}{r} + \frac{V_\vartheta}{r \tan \vartheta} = 0. \quad (1.8.48d)$$

Body-fitted coordinates

When analysing fluid motion in close proximity to the surface of a rigid body, the body-fitted coordinate system

$$q_1 = s, \quad q_2 = n, \quad q_3 = z$$

is often used. We shall assume that the body in question has a cylindrical surface. Figure 1.32 shows the cross-section of the body in a plane drawn perpendicular to the surface generatrix. When dealing with body-fitted coordinates, one starts by choosing a point on the body contour to be the coordinate origin O . The position of any point M in the flow field is then defined by the distance s measured along the body contour from O to point N , which is obtained by dropping the perpendicular from M to the body surface; the second coordinate n is the distance between M and the body surface. Finally, the spanwise coordinate z is measured along the surface generatrix, i.e. perpendicular to the plane of the sketch in Figure 1.32.

The unit vector triad $(\mathbf{e}_1, \mathbf{e}_2, \mathbf{e}_3)$ is oriented at point M such that \mathbf{e}_1 is parallel to the tangent to the body contour drawn through point N ; \mathbf{e}_2 is directed along the n -axis and \mathbf{e}_3 along the body generatrix. Corresponding to this, the velocity vector is decomposed as

$$\mathbf{V} = V_\tau \mathbf{e}_1 + V_n \mathbf{e}_2 + V_z \mathbf{e}_3,$$

with V_τ termed the tangential velocity, V_n the normal velocity, and V_z the spanwise velocity.

In order to calculate the Lamé coefficients, the following simple geometrical arguments may be used. If we give the first coordinate s a small increment ds and keep n and z fixed, then point M will travel to a new position M_1 . The distance between M and M_1 is denoted, as usual, by dl_1 . It may be related to ds through the equation

$$\frac{dl_1}{R + n} = \frac{ds}{R},$$

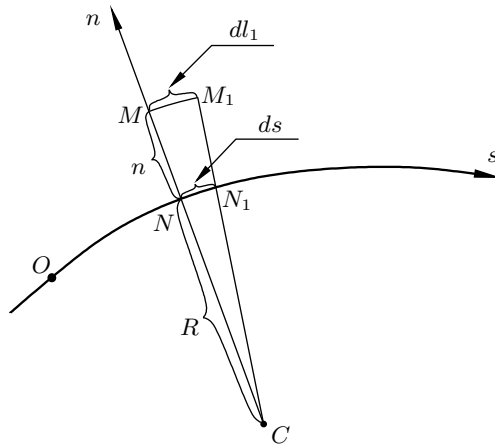


Fig. 1.32: Body-fitted coordinates.

where R is the local radius of the body contour. Taking further into account that the curvature of the body contour $\kappa(s) = 1/R$, we find¹⁷

$$H_1 = \frac{dl_1}{ds} = 1 + \kappa(s)n.$$

The length elements dl_2 and dl_3 in the other two directions coincide with dn and dz , respectively, and therefore $H_2 = H_3 = 1$. We have

$$H_1 = 1 + \kappa n, \quad H_2 = 1, \quad H_3 = 1.$$

Now the routine of recasting of the Navier–Stokes equations in curvilinear coordinates may be undertaken, leading to

$$\begin{aligned} \frac{\partial V_\tau}{\partial t} + \frac{V_\tau}{H_1} \frac{\partial V_\tau}{\partial s} + V_n \frac{\partial V_\tau}{\partial n} + V_z \frac{\partial V_\tau}{\partial z} + \frac{\kappa V_\tau V_n}{H_1} = f_\tau - \frac{1}{\rho H_1} \frac{\partial p}{\partial s} \\ + \nu \left[\frac{1}{H_1} \frac{\partial}{\partial s} \left(\frac{1}{H_1} \frac{\partial V_\tau}{\partial s} \right) + \frac{\partial^2 V_\tau}{\partial n^2} + \frac{\partial^2 V_\tau}{\partial z^2} \right. \\ \left. + \kappa \frac{\partial}{\partial n} \left(\frac{V_\tau}{H_1} \right) + \frac{\kappa}{H_1^2} \frac{\partial V_n}{\partial s} + \frac{1}{H_1} \frac{\partial}{\partial s} \left(\frac{\kappa V_n}{H_1} \right) \right], \quad (1.8.49a) \end{aligned}$$

$$\begin{aligned} \frac{\partial V_n}{\partial t} + \frac{V_\tau}{H_1} \frac{\partial V_n}{\partial s} + V_n \frac{\partial V_n}{\partial n} + V_z \frac{\partial V_n}{\partial z} - \frac{\kappa V_\tau^2}{H_1} = f_n - \frac{1}{\rho} \frac{\partial p}{\partial n} \\ + \nu \left[\frac{1}{H_1} \frac{\partial}{\partial s} \left(\frac{1}{H_1} \frac{\partial V_n}{\partial s} \right) + \frac{\partial^2 V_n}{\partial n^2} + \frac{\partial^2 V_n}{\partial z^2} \right. \\ \left. + \kappa \frac{\partial}{\partial n} \left(\frac{V_n}{H_1} \right) - \frac{\kappa}{H_1^2} \frac{\partial V_\tau}{\partial s} - \frac{1}{H_1} \frac{\partial}{\partial s} \left(\frac{\kappa V_\tau}{H_1} \right) \right], \quad (1.8.49b) \end{aligned}$$

$$\begin{aligned} \frac{\partial V_z}{\partial t} + \frac{V_\tau}{H_1} \frac{\partial V_z}{\partial s} + V_n \frac{\partial V_z}{\partial n} + V_z \frac{\partial V_z}{\partial z} = f_z - \frac{1}{\rho} \frac{\partial p}{\partial z} \\ + \nu \left[\frac{1}{H_1} \frac{\partial}{\partial s} \left(\frac{1}{H_1} \frac{\partial V_z}{\partial s} \right) + \frac{\partial^2 V_z}{\partial n^2} + \frac{\partial^2 V_z}{\partial z^2} + \frac{\kappa}{H_1} \frac{\partial V_z}{\partial n} \right], \quad (1.8.49c) \end{aligned}$$

$$\frac{1}{H_1} \frac{\partial V_\tau}{\partial s} + \frac{\partial V_n}{\partial n} + \frac{\partial V_z}{\partial z} + \frac{\kappa V_n}{H_1} = 0. \quad (1.8.49d)$$

Stress tensor

Once the solution of the Navier–Stokes equations has been found for a particular flow, it is often required to determine the forces acting in the interior of the fluid and on the body surface washed by the flow. Here we shall show how to express the stress tensor in curvilinear coordinates. In Section 1.2.1, we introduced the stress tensor

$$\mathcal{P} = \begin{pmatrix} p_{xx} & p_{xy} & p_{xz} \\ p_{yx} & p_{yy} & p_{yz} \\ p_{zx} & p_{zy} & p_{zz} \end{pmatrix}$$

¹⁷Notice that κ is positive for a convex wall and negative for a concave wall.

using Cartesian coordinates. For this purpose, we considered a plane surface S_x perpendicular to the x -axis (see Figure 1.6 on page 11) and denoted the stress on S_x by \mathbf{p}_x . We then represented \mathbf{p}_x in the coordinate decomposition form (1.2.4)

$$\mathbf{p}_x = p_{xx}\mathbf{i} + p_{xy}\mathbf{j} + p_{xz}\mathbf{k}.$$

The three components p_{xx} , p_{xy} , and p_{xz} of the stress \mathbf{p}_x form the first row in the stress tensor \mathcal{P} . The second and third rows are obtained in a similar way by considering the stresses \mathbf{p}_y and \mathbf{p}_z on surfaces S_y and S_z perpendicular to the y - and z -axes, respectively.

In order to write the stress tensor \mathcal{P} in a curvilinear coordinate system, one needs to consider, first of all, the stress \mathbf{p}_1 on a surface element S_1 perpendicular to the unit vector \mathbf{e}_1 ; see Figure 1.29(a) on page 74. The coordinate decomposition of \mathbf{p}_1 is

$$\mathbf{p}_1 = p_{11}\mathbf{e}_1 + p_{12}\mathbf{e}_2 + p_{13}\mathbf{e}_3.$$

Similarly, the stresses \mathbf{p}_2 and \mathbf{p}_3 on the surfaces S_2 and S_3 perpendicular to the unit vectors \mathbf{e}_2 and \mathbf{e}_3 are decomposed as

$$\begin{aligned}\mathbf{p}_2 &= p_{21}\mathbf{e}_1 + p_{22}\mathbf{e}_2 + p_{23}\mathbf{e}_3, \\ \mathbf{p}_3 &= p_{31}\mathbf{e}_1 + p_{32}\mathbf{e}_2 + p_{33}\mathbf{e}_3.\end{aligned}$$

Correspondingly, in the coordinate system considered, the stress tensor is written as

$$\mathcal{P} = \begin{pmatrix} p_{11} & p_{12} & p_{13} \\ p_{21} & p_{22} & p_{23} \\ p_{31} & p_{32} & p_{33} \end{pmatrix}. \quad (1.8.50)$$

In order to express the elements p_{ij} of the stress tensor (1.8.50) in terms of the components of the velocity vector $\mathbf{V} = (V_1, V_2, V_3)$, the constitutive equation (1.5.24) will be used. In the coordinate system considered, it is written as

$$\begin{pmatrix} p_{11} & p_{12} & p_{13} \\ p_{21} & p_{22} & p_{23} \\ p_{31} & p_{32} & p_{33} \end{pmatrix} = (-p + \lambda \operatorname{div} \mathbf{V}) \begin{pmatrix} 1 & 0 & 0 \\ 0 & 1 & 0 \\ 0 & 0 & 1 \end{pmatrix} + 2\mu \begin{pmatrix} \varepsilon_{11} & \varepsilon_{12} & \varepsilon_{13} \\ \varepsilon_{21} & \varepsilon_{22} & \varepsilon_{23} \\ \varepsilon_{31} & \varepsilon_{32} & \varepsilon_{33} \end{pmatrix}. \quad (1.8.51)$$

The elements ε_{ij} of the rate-of-strain tensor

$$\mathcal{E} = \begin{pmatrix} \varepsilon_{11} & \varepsilon_{12} & \varepsilon_{13} \\ \varepsilon_{21} & \varepsilon_{22} & \varepsilon_{23} \\ \varepsilon_{31} & \varepsilon_{32} & \varepsilon_{33} \end{pmatrix} \quad (1.8.52)$$

may be calculated in the same way as was done in Section 1.4.5, where the motion of a fluid particle was analysed. Now the analysis has to be repeated using curvilinear coordinates. Alternatively, one can start with the Second Helmholtz Theorem. It is expressed by equation (1.4.27), which holds in any coordinate system.

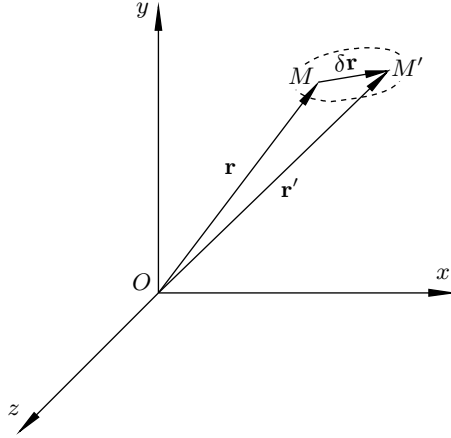


Fig. 1.33: Deformation of a fluid element.

Remember that the vector $\mathbf{V}(t, \mathbf{r})$ on the left-hand side of (1.4.27) is the fluid velocity at point M' in Figure 1.18, while the first term $\mathbf{V}(t, \mathbf{r}_0)$ on the right-hand side is the fluid velocity at point M . Consequently,

$$\mathbf{V}(t, \mathbf{r}) - \mathbf{V}(t, \mathbf{r}_0) = \frac{d\mathbf{r}}{dt} - \frac{d\mathbf{r}_0}{dt} = \frac{d}{dt}(\delta\mathbf{r}),$$

which allows to write equation (1.4.27) as

$$\frac{d}{dt}(\delta\mathbf{r}) = \boldsymbol{\Omega} \times \delta\mathbf{r} + \mathcal{E}\delta\mathbf{r}. \quad (1.8.53)$$

Since $\boldsymbol{\Omega} \times \delta\mathbf{r}$ is perpendicular to $\delta\mathbf{r}$, the rotational motion may be excluded from this equation through scalar multiplication of both sides of (1.8.53) with the vector $\delta\mathbf{r}$. We have

$$\frac{1}{2} \frac{d}{dt}(|\delta\mathbf{r}|^2) = (\delta\mathbf{r} \cdot \mathcal{E}\delta\mathbf{r}). \quad (1.8.54)$$

Let us return to Figure 1.18 and change the notations slightly. For our purposes, it is convenient to denote the position vector of the fluid particle point M as \mathbf{r} and the position vector of the fluid particle at point M' as \mathbf{r}' ; see Figure 1.33. We shall assign to the fluid particle at point M coordinates (q_1, q_2, q_3) ; the coordinates of the fluid particle at point M' will be (q'_1, q'_2, q'_3) . Then, in view of (1.8.5),

$$|\delta\mathbf{r}|^2 = |\mathbf{r} - \mathbf{r}'|^2 = \sum_{i=1}^3 H_i^2 (q'_i - q_i)^2. \quad (1.8.55)$$

With time, the two fluid particles move in space, changing their coordinates. Differentiation of (1.8.55) gives

$$\frac{1}{2} \frac{d}{dt}(|\delta\mathbf{r}|^2) = \sum_{i=1}^3 \sum_{j=1}^3 H_i \frac{\partial H_i}{\partial q_j} \frac{dq_j}{dt} (q'_i - q_i)^2 + \sum_{i=1}^3 H_i^2 (q'_i - q_i) \left(\frac{dq'_i}{dt} - \frac{dq_i}{dt} \right). \quad (1.8.56)$$

Here it has been taken into account that the Lamé coefficients do not depend on time explicitly but only through the coordinates q_1 , q_2 , and q_3 .

When the fluid particle at point M moves in space along q_i -axis, changing its coordinate q_i by a small value dq_i , the actual distance travelled is $H_i dq_i$. Consequently, the corresponding velocity component is given by

$$V_i = H_i \frac{dq_i}{dt}. \quad (1.8.57)$$

Solving (1.8.57) for dq_i/dt , we have

$$\frac{dq_i}{dt} = \frac{V_i(q_1, q_2, q_3)}{H_i(q_1, q_2, q_3)}. \quad (1.8.58)$$

Similarly, for the fluid particle at point M' ,

$$\frac{dq'_i}{dt} = \frac{V_i(q'_1, q'_2, q'_3)}{H_i(q'_1, q'_2, q'_3)}.$$

Therefore, taking into account that points M and M' are situated close to one another, we can write

$$\frac{dq'_i}{dt} - \frac{dq_i}{dt} = \sum_{j=1}^3 \frac{\partial}{\partial q_j} \left(\frac{V_i}{H_i} \right) (q'_j - q_j). \quad (1.8.59)$$

Substitution of (1.8.58) and (1.8.59) into (1.8.56) yields

$$\frac{1}{2} \frac{d}{dt} (|\delta \mathbf{r}|^2) = \sum_{i=1}^3 \sum_{j=1}^3 \frac{\partial H_i}{\partial q_j} \frac{H_i}{H_j} V_j (\delta q_i)^2 + \sum_{i=1}^3 \sum_{j=1}^3 H_i^2 \frac{\partial}{\partial q_j} \left(\frac{V_i}{H_i} \right) \delta q_i \delta q_j,$$

where $\delta q_i = q'_i - q_i$. It remains to express the increments δq_i of the curvilinear coordinates q_i through the corresponding length elements $dl_i = H_i \delta q_i$, and we will have the left-hand side of equation (1.8.54) in the form

$$\frac{1}{2} \frac{d}{dt} (|\delta \mathbf{r}|^2) = \sum_{i=1}^3 \sum_{j=1}^3 \left[\frac{V_j}{H_i H_j} \frac{\partial H_i}{\partial q_j} (dl_i)^2 + \frac{H_i}{H_j} \frac{\partial}{\partial q_j} \left(\frac{V_i}{H_i} \right) dl_i dl_j \right].$$

Consequently,

$$(\delta \mathbf{r} \cdot \mathcal{E} \delta \mathbf{r}) = \sum_{i=1}^3 \sum_{j=1}^3 \left[\frac{V_j}{H_i H_j} \frac{\partial H_i}{\partial q_j} (dl_i)^2 + \frac{H_i}{H_j} \frac{\partial}{\partial q_j} \left(\frac{V_i}{H_i} \right) dl_i dl_j \right]. \quad (1.8.60)$$

We shall now use equation (1.8.60) to determine the elements of the stress tensor (1.8.52). If we choose the vector $\delta \mathbf{r}$ to be aligned with the q_1 -axis (see Figure 1.29 on page 74), namely,

$$\delta \mathbf{r} = (dl_1, 0, 0), \quad (1.8.61)$$

then the rate-of-strain tensor (1.8.52), being multiplied by $\delta \mathbf{r}$, will produce a vector

with components

$$\mathcal{E}\delta\mathbf{r} = (\varepsilon_{11}dl_1, \varepsilon_{21}dl_1, \varepsilon_{31}dl_1).$$

The scalar product of this vector with $\delta\mathbf{r}$ is easily seen to be

$$(\delta\mathbf{r} \cdot \mathcal{E}\delta\mathbf{r}) = \varepsilon_{11}(dl_1)^2,$$

With (1.8.61), the right-hand side of equation (1.8.60) reduces to

$$\sum_{j=1}^3 \frac{V_j}{H_1 H_j} \frac{\partial H_1}{\partial q_j} (dl_1)^2 + \frac{\partial}{\partial q_1} \left(\frac{V_1}{H_1} \right) (dl_1)^2,$$

and we can conclude that

$$\varepsilon_{11} = \frac{1}{H_1} \frac{\partial V_1}{\partial q_1} + \frac{V_2}{H_1 H_2} \frac{\partial H_1}{\partial q_2} + \frac{V_3}{H_1 H_3} \frac{\partial H_1}{\partial q_3}. \quad (1.8.62a)$$

The other two diagonal elements, ε_{22} and ε_{33} of the rate-of-strain tensor (1.8.52) are calculated by choosing $\delta\mathbf{r} = (0, dl_2, 0)$ and $\delta\mathbf{r} = (0, 0, dl_3)$, respectively. We find

$$\varepsilon_{22} = \frac{1}{H_2} \frac{\partial V_2}{\partial q_2} + \frac{V_3}{H_2 H_3} \frac{\partial H_2}{\partial q_3} + \frac{V_1}{H_2 H_1} \frac{\partial H_2}{\partial q_1}, \quad (1.8.62b)$$

$$\varepsilon_{33} = \frac{1}{H_3} \frac{\partial V_3}{\partial q_3} + \frac{V_1}{H_3 H_1} \frac{\partial H_3}{\partial q_1} + \frac{V_2}{H_3 H_2} \frac{\partial H_3}{\partial q_2}. \quad (1.8.62c)$$

If we now choose the vector $\delta\mathbf{r}$ to be $(dl_1, dl_2, 0)$, then the left-hand side of equation (1.8.60) assumes the form

$$(\delta\mathbf{r} \cdot \mathcal{E}\delta\mathbf{r}) = \varepsilon_{11}(dl_1)^2 + 2\varepsilon_{12}dl_1dl_2 + \varepsilon_{22}(dl_2)^2. \quad (1.8.63)$$

Using (1.8.62a) and (1.8.62b) for ε_{11} and ε_{22} in (1.8.63), and calculating the right-hand side of (1.8.60) with $\delta\mathbf{r} = (dl_1, dl_2, 0)$, we find that

$$\varepsilon_{12} = \varepsilon_{21} = \frac{1}{2} \left[\frac{H_1}{H_2} \frac{\partial}{\partial q_2} \left(\frac{V_1}{H_1} \right) + \frac{H_2}{H_1} \frac{\partial}{\partial q_1} \left(\frac{V_2}{H_2} \right) \right]. \quad (1.8.64a)$$

The four remaining elements of the rate-of-strain tensor,

$$\varepsilon_{13} = \varepsilon_{31} = \frac{1}{2} \left[\frac{H_1}{H_3} \frac{\partial}{\partial q_3} \left(\frac{V_1}{H_1} \right) + \frac{H_3}{H_1} \frac{\partial}{\partial q_1} \left(\frac{V_3}{H_3} \right) \right], \quad (1.8.64b)$$

$$\varepsilon_{23} = \varepsilon_{32} = \frac{1}{2} \left[\frac{H_2}{H_3} \frac{\partial}{\partial q_3} \left(\frac{V_2}{H_2} \right) + \frac{H_3}{H_2} \frac{\partial}{\partial q_2} \left(\frac{V_3}{H_3} \right) \right], \quad (1.8.64c)$$

are calculated in a similar way.

Now we can return to the constitutive equation (1.8.51) and use equations (1.8.62) and (1.8.64) to determine the elements of the stress tensor \mathcal{P} . We find that for an

incompressible flow, when $\text{div}\mathbf{V} = 0$, the diagonal elements of the stress tensor are given by¹⁸

$$p_{ii} = -p + 2\mu \left(\frac{1}{H_i} \frac{\partial V_i}{\partial q_i} + \frac{V_{i+1}}{H_i H_{i+1}} \frac{\partial H_i}{\partial q_{i+1}} + \frac{V_{i+2}}{H_i H_{i+2}} \frac{\partial H_i}{\partial q_{i+2}} \right),$$

The non-diagonal elements are calculated as

$$p_{ij} = \mu \left[\frac{H_i}{H_j} \frac{\partial}{\partial q_j} \left(\frac{V_i}{H_i} \right) + \frac{H_j}{H_i} \frac{\partial}{\partial q_i} \left(\frac{V_j}{H_j} \right) \right].$$

In particular, in cylindrical coordinates,

$$\left. \begin{aligned} p_{rr} &= -p + 2\mu \frac{\partial V_r}{\partial r}, & p_{r\phi} &= \mu \left(\frac{1}{r} \frac{\partial V_r}{\partial \phi} + \frac{\partial V_\phi}{\partial r} - \frac{V_\phi}{r} \right), \\ p_{\phi\phi} &= -p + 2\mu \left(\frac{1}{r} \frac{\partial V_\phi}{\partial \phi} + \frac{V_r}{r} \right), & p_{rz} &= \mu \left(\frac{\partial V_r}{\partial z} + \frac{\partial V_z}{\partial r} \right), \\ p_{zz} &= -p + 2\mu \frac{\partial V_z}{\partial z}, & p_{\phi z} &= \mu \left(\frac{\partial V_\phi}{\partial z} + \frac{1}{r} \frac{\partial V_z}{\partial \phi} \right). \end{aligned} \right\} \quad (1.8.65)$$

In spherical polar coordinates

$$\begin{aligned} p_{rr} &= -p + 2\mu \frac{\partial V_r}{\partial r}, & p_{r\vartheta} &= \mu \left(\frac{1}{r} \frac{\partial V_r}{\partial \vartheta} + \frac{\partial V_\vartheta}{\partial r} - \frac{V_\vartheta}{r} \right), \\ p_{\vartheta\vartheta} &= -p + 2\mu \left(\frac{1}{r} \frac{\partial V_\vartheta}{\partial \vartheta} + \frac{V_r}{r} \right), & p_{r\phi} &= \mu \left(\frac{\partial V_\phi}{\partial r} + \frac{1}{r \sin \vartheta} \frac{\partial V_r}{\partial \phi} - \frac{V_\phi}{r} \right), \\ p_{\phi\phi} &= -p + 2\mu \left(\frac{1}{r \sin \vartheta} \frac{\partial V_\phi}{\partial \phi} + \frac{V_r}{r} + \frac{V_\vartheta}{r \tan \vartheta} \right), \\ p_{\vartheta\phi} &= \mu \left(\frac{1}{r \sin \vartheta} \frac{\partial V_\vartheta}{\partial \phi} + \frac{1}{r} \frac{\partial V_\phi}{\partial \vartheta} - \frac{V_\phi}{r \tan \vartheta} \right), \end{aligned}$$

and, finally, in body-fitted coordinates

$$\left. \begin{aligned} p_{\tau\tau} &= -p + \frac{2\mu}{1 + \kappa n} \left(\frac{\partial V_\tau}{\partial s} + \kappa V_n \right), & p_{\tau n} &= \mu \left(\frac{\partial V_\tau}{\partial n} + \frac{\partial V_n / \partial s - \kappa V_\tau}{1 + \kappa n} \right), \\ p_{nn} &= -p + 2\mu \frac{\partial V_n}{\partial n}, & p_{\tau z} &= \mu \left(\frac{\partial V_\tau}{\partial z} + \frac{1}{1 + \kappa n} \frac{\partial V_z}{\partial s} \right), \\ p_{zz} &= -p + 2\mu \frac{\partial V_z}{\partial z}, & p_{nz} &= \mu \left(\frac{\partial V_n}{\partial z} + \frac{\partial V_z}{\partial n} \right). \end{aligned} \right\} \quad (1.8.66)$$

¹⁸Here the conventional index cycling rules are used, with 2 + 2 and 3 + 1 meaning 1, and 3 + 2 meaning 2.

Exercises 5

1. Show that for a two-dimensional flow, considered in body-fitted coordinates, the streamlines are given by the equation

$$\frac{dn}{ds} = [1 + \kappa(s)n] \frac{V_n}{V_\tau}. \quad (1.8.67)$$

Suggestion: Notice that in body-fitted coordinates

$$d\mathbf{r} = \mathbf{e}_1 H_1 ds + \mathbf{e}_2 dn,$$

and therefore, equation (1.4.12) becomes

$$d\mathbf{r} \times \mathbf{V} = \begin{vmatrix} \mathbf{e}_1 & \mathbf{e}_2 & \mathbf{e}_3 \\ (H_1 ds) & dn & dz \\ V_\tau & V_n & 0 \end{vmatrix} = 0.$$

2. A circular cylinder container of radius R is filled with water and placed on a horizontal disk such that the axis of symmetry of the container passes through the disk centre (see Figure 1.34). The disk is then brought to steady rotation with angular velocity Ω .

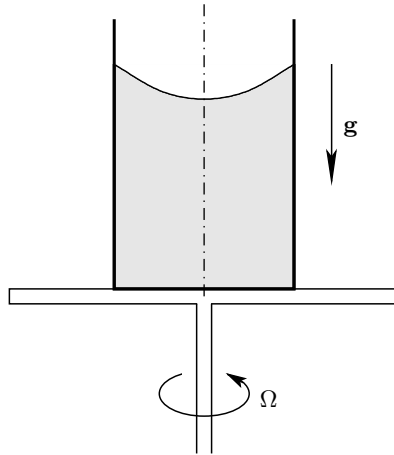


Fig. 1.34: Rotating cylinder.

- (a) Assume that after an initial ‘relaxation’ period, the water inside the cylinder assumes steady rotation as a rigid body. Taking into account the presence of the Earth’s gravitational field ($f_z = -g$), show that the height z of the water surface depends on the distance r from the axis of rotation as

$$z = \frac{\Omega^2}{2g} r^2 + \frac{C - p_a}{\rho g},$$

where p_a is the atmospheric pressure, ρ is the density of the water, and C is a constant whose value depends on the amount of water in the container.

- (b) Taking into account that the mass M of water in the container may be calculated as

$$M = \rho \int_0^R z 2\pi r dr,$$

find the critical value Ω_c of the angular velocity Ω above which a dry patch forms at the bottom of the container.

Suggestion: When dealing with this flow it is convenient to use cylindrical polar coordinates (see Figure 1.30) with z -axis aligned with the axis of rotation of the fluid. Simplify the Navier–Stokes equations (1.8.45) assuming that the water in the cylinder rotates like a rigid body, i.e.

$$V_\phi = \Omega r, \quad V_r = V_z = 0. \tag{1.8.68}$$

Determine the pressure distribution inside the water and on its surface.

3. It is known that the Earth is not a perfect sphere. It is also known that the pressure in the ocean increases with depth much faster than it decreases in the atmosphere. Keeping this in mind, find the shape of the Earth by assuming that it may be thought of as a rotating volume of fluid surrounded by vacuum. The fluid is kept together through the action of the gravitational force. Assume that this force has only a radial component, which is proportional to the distance from the Earth’s centre, namely

$$f_r = -\alpha r.$$

Given that the angular velocity of the Earth’s rotation is Ω , and the Earth’s radius at the North Pole is R_0 , show that at any other meridional angle ϑ (measured from the North Pole), the distance R from the Earth’s surface to the centre is given by

$$R = \frac{R_0}{\sqrt{1 - \frac{\Omega^2}{\alpha} \sin^2 \vartheta}}. \tag{1.8.69}$$

Suggestion: Thanks to the fact that the fluid motion is symmetric with respect to the Earth’s axis, it is convenient to use spherical polar coordinates (see Figure 1.31), where the Navier–Stokes equations are given by (1.8.48). Take into account that

$$V_\phi = \Omega r \sin \vartheta, \quad V_r = 0, \quad V_\vartheta = 0,$$

and, using (1.8.48), show that the pressure is zero on the surface given by (1.8.69).

2

Solutions of the Navier–Stokes Equations

Having now established the governing Navier–Stokes equations, one can expect to be able to study various fluid flows by constructing the corresponding solutions to these equations. However, this strategy has proven to be difficult to implement. The reason lies in the complexity of the Navier–Stokes equations, which, of course, reflects the complexity of fluid motion itself. As a result, the development of fluid dynamics has always been based on various simplifications of the Navier–Stokes equations. We will rely on this approach throughout this book series. However, to start with, we shall consider a number of cases when direct solution of the Navier–Stokes equations is possible. An exposition of such cases is presented in Section 2.1. Then in Section 2.2, to illustrate various properties of fluid motion, we will give some examples of numerical solutions of the Navier–Stokes equations.

2.1 Exact Solutions

The term *exact solution* is used in situations where the governing fluid-dynamic equations may be solved in an analytical form or where they may be reduced to ordinary differential equations.

2.1.1 Couette flow

Let us consider a layer of incompressible fluid of thickness h confined between two parallel flat plates as shown in Figure 2.1. The lower plate is kept motionless in the laboratory frame, while the upper moves parallel to itself with a constant velocity U . In order to study the fluid motion between the plates, we shall use Cartesian coordinates with the x -axis drawn along the surface of the lower plate in the direction of motion of

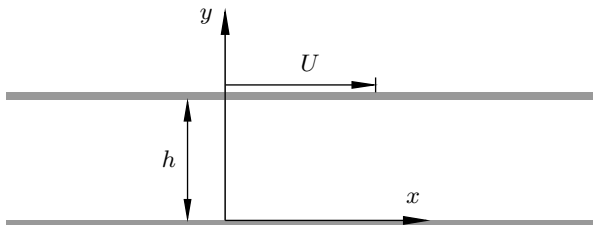


Fig. 2.1: The problem layout.

the upper plate, the y -axis perpendicular to the plates, and the z -axis perpendicular to the sketch plane in Figure 2.1.

When studying this flow, we can make the following simplifications in the Navier–Stokes equations (1.7.6):

1. We shall assume that the body forces are negligible compared with the viscous forces acting in the fluid, which allows us to set

$$f_x = f_y = f_z = 0. \tag{2.1.1}$$

2. We shall further assume that the velocity of the upper plate has been kept constant for long enough for the flow to become steady, i.e.

$$\frac{\partial u}{\partial t} = \frac{\partial v}{\partial t} = \frac{\partial w}{\partial t} = 0. \tag{2.1.2}$$

3. If the distance h between the plates is small compared with the characteristic longitudinal and spanwise lengths of the plates, then the plates may be viewed as infinite. In this case, the solution should be invariant with respect to an arbitrary shift in the x - or z -direction, which means that the fluid-dynamic functions are independent of x and z , i.e.

$$\frac{\partial}{\partial x} = \frac{\partial}{\partial z} = 0. \tag{2.1.3}$$

We shall start our analysis with the continuity equation (1.7.6d). In view of (2.1.3), the first and third terms in this equation should be disregarded, and we are left with

$$\frac{\partial v}{\partial y} = 0. \tag{2.1.4}$$

When integrating this equation, we will take into account that the fluid particles are not allowed to cross the surface of either of the plates. This requirement is written as

$$v \Big|_{y=0} = v \Big|_{y=h} = 0, \tag{2.1.5}$$

and is known as the *impermeability condition*. It holds on any rigid-body surface, except in special cases when, for example, the surface is artificially perforated for the purpose of flow control by means of suction or blowing through the perforation. Solving (2.1.4) with (2.1.5), we see that

$$v = 0 \tag{2.1.6}$$

everywhere in the flow field.

Let us now consider the x -momentum equation (1.7.6a). Term-by-term analysis of this equation shows that it may be simplified significantly. In fact, all the under-braced terms

$$\underbrace{\frac{\partial u}{\partial t}}_{(2.1.2)} + \underbrace{u \frac{\partial u}{\partial x}}_{(2.1.3)} + \underbrace{v \frac{\partial u}{\partial y}}_{(2.1.6)} + \underbrace{w \frac{\partial u}{\partial z}}_{(2.1.3)} = \underbrace{f_x}_{(2.1.1)} - \underbrace{\frac{1}{\rho} \frac{\partial p}{\partial x}}_{(2.1.3)} + \underbrace{\nu \frac{\partial^2 u}{\partial x^2}}_{(2.1.3)} + \nu \frac{\partial^2 u}{\partial y^2} + \underbrace{\nu \frac{\partial^2 u}{\partial z^2}}_{(2.1.3)}$$

appear to vanish; the reason for this is indicated by the equation number below the corresponding term. We have

$$\frac{\partial^2 u}{\partial y^2} = 0.$$

This equation has to be solved with the no-slip conditions on the two plates¹

$$u \Big|_{y=0} = 0, \quad u \Big|_{y=h} = U.$$

We find that

$$u = \frac{U}{h}y. \quad (2.1.7)$$

Thus the fluid velocity grows linearly from zero on the lower plate to U on the upper plate, as shown in Figure 2.2.

We shall conclude the analysis of Couette flow by demonstrating that w , the projection of the velocity vector on the z -axis² is zero. In view of (2.1.1)–(2.1.3) and (2.1.6), the z -momentum equation (1.7.6c) reduces to

$$\frac{\partial^2 w}{\partial y^2} = 0.$$

In order to solve this equation, we need to formulate the no-slip condition on the two plates. Thanks to the fact that the x -axis is chosen to point in the direction of motion of the upper plate, we have

$$w \Big|_{y=0} = w \Big|_{y=h} = 0.$$

Consequently, the solution for w is, indeed, $w = 0$.

We see that in Couette flow, all the fluid particles are travelling along straight lines parallel to the x -axis with velocity given by (2.1.7).

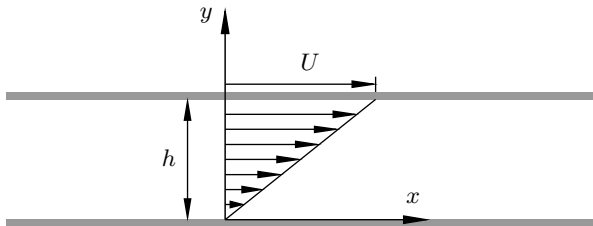


Fig. 2.2: Couette flow.

¹In a more general case, the no-slip condition is expressed by equations (1.7.34).

²In what follows, we shall often call this velocity component the *spanwise velocity*.

2.1.2 Poiseuille flow

Let us now assume that both plates in Figure 2.1 are motionless, and form a channel through which the fluid is driven by the pressure difference $\Delta p = p_1 - p_2$ between the two channel ends. Here p_1 and p_2 are the values of the pressure in cross-sections 1 and 2, respectively; see Figure 2.3. As an example, one might think of a pipeline used for transporting oil or natural gas. In order to maintain the flow through the pipeline, suitably spaced pump stations are built to create a pressure difference along the corresponding segments of the line. If we denote the length of the channel by L , then an average pressure gradient along the channel may be calculated as

$$\left. \frac{dp}{dx} \right|_{\text{average}} = \frac{\Delta p}{L}. \quad (2.1.8)$$

Note that for the fluid to flow from left to right, Δp should be negative.

If the channel is long enough, then, after initial adjustment near the channel intake (cross-section 2), the longitudinal velocity profile establishes itself and for the rest of the flow appears to be independent of x , i.e.

$$\frac{\partial u}{\partial x} = 0. \quad (2.1.9)$$

Since the problem considered is invariant with respect to an arbitrary shift in the spanwise direction, we can also claim that the derivative of any function with respect to z is zero:

$$\frac{\partial}{\partial z} = 0. \quad (2.1.10)$$

With (2.1.9) and (2.1.10), the continuity equation (1.7.6d) reduces again to

$$\frac{\partial v}{\partial y} = 0,$$

which, being integrated with the impermeability condition (2.1.5), leads to the conclusion that

$$v = 0 \quad (2.1.11)$$

everywhere in the flow field.

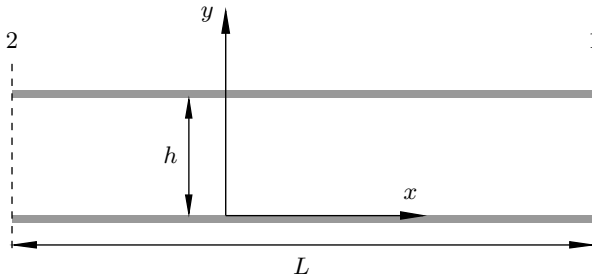


Fig. 2.3: Poiseuille flow.

Using (2.1.1), (2.1.2) and (2.1.9)–(2.1.11) in the x -momentum equation (1.7.6a), we have

$$\frac{\partial^2 u}{\partial y^2} = \frac{1}{\mu} \frac{\partial p}{\partial x}. \quad (2.1.12)$$

Since the flow considered is incompressible, we can assume that the dynamic viscosity coefficient μ is constant. Substituting (2.1.11) into the y -momentum equation (1.7.6b), we find that

$$\frac{\partial p}{\partial y} = 0, \quad (2.1.13)$$

which means that the pressure does not change across the channel. Differentiation of (2.1.12) with respect to x yields

$$\frac{\partial}{\partial x} \left(\frac{\partial p}{\partial x} \right) = \mu \frac{\partial^2}{\partial y^2} \left(\frac{\partial u}{\partial x} \right). \quad (2.1.14)$$

Using (2.1.9) on the right-hand side of (2.1.14), we see that

$$\frac{\partial}{\partial x} \left(\frac{\partial p}{\partial x} \right) = 0. \quad (2.1.15)$$

It follows from (2.1.13) and (2.1.15) that the pressure gradient $\partial p/\partial x$ remains constant all over the flow field, which makes formula (2.1.8) applicable for calculating not only an average but also the actual pressure gradient.

Integrating (2.1.12) with the no-slip conditions on the two plates,

$$u \Big|_{y=0} = u \Big|_{y=h} = 0,$$

we find that in the flow considered the velocity profile is parabolic (see Figure 2.4):

$$u = \frac{1}{2\mu} \frac{dp}{dx} (y - h)y.$$

The maximum velocity is reached at the middle of the channel, $y = \frac{1}{2}h$, and is given by

$$u_{\max} = \frac{h^2}{8\mu} \left| \frac{dp}{dx} \right| = \frac{h^2 |\Delta p|}{8\mu L}.$$

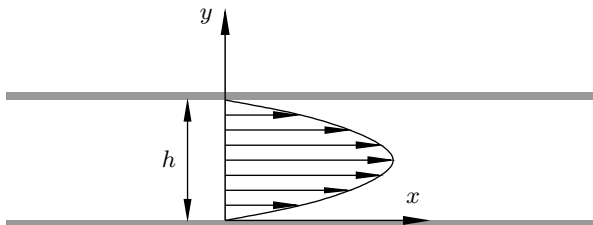


Fig. 2.4: Velocity profile in Poiseuille flow.

2.1.3 Hagen–Poiseuille flow

Now we shall consider an axisymmetric analogue of the channel Poiseuille flow discussed in Section 2.1.2. We shall assume now that an incompressible fluid flows through a tube of circular cross-section, being driven by a pressure difference Δp between the tube ends. This flow received its name in honour of Hagen (1839) and Poiseuille (1840, 1841) for their contribution to studying the flows of this type.

When dealing with Hagen–Poiseuille flow, it is convenient to use cylindrical polar coordinates. In order to preserve the notation introduced in Figure 1.30, we shall place the z -axis of the cylindrical coordinate system (Figure 1.30) along the centre-line of the tube (Figure 2.5). Similar to the previous examples, we shall assume that the tube is long enough for the longitudinal velocity V_z to be independent of the position along the tube, i.e.

$$\frac{\partial V_z}{\partial z} = 0. \quad (2.1.16)$$

We can simplify the problem further by taking into account that the flow is axisymmetric, and therefore all the fluid dynamic functions are independent of the circumferential coordinate ϕ :

$$\frac{\partial}{\partial \phi} = 0. \quad (2.1.17)$$

Using (2.1.16) and (2.1.17) in the continuity equation (1.8.45d), we find

$$\frac{\partial V_r}{\partial r} + \frac{V_r}{r} = 0,$$

or, equivalently,

$$\frac{\partial}{\partial r}(rV_r) = 0.$$

We see that rV_r is a function of ϕ and z only, say, $F(\phi, z)$. Consequently, the radial velocity component

$$V_r = \frac{F(\phi, z)}{r}. \quad (2.1.18)$$

The function $F(\phi, z)$ may be found from the impermeability condition on the tube wall. Denoting the radius of the tube by R , we have

$$V_r \Big|_{r=R} = 0. \quad (2.1.19)$$

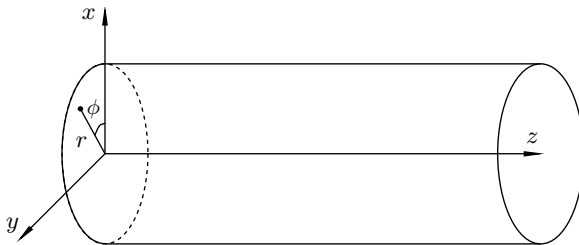


Fig. 2.5: Hagen–Poiseuille flow.

Substitution of (2.1.18) into (2.1.19) shows that $F(z, \phi) = 0$, and therefore

$$V_r = 0 \quad (2.1.20)$$

throughout the flow field.

Let us now turn to the circumferential momentum equation (1.8.45b). We assume that the flow is steady, i.e. $\partial V_\phi / \partial t = 0$, and the body force f_ϕ is negligible. We further assume that, similar to V_z , the circumferential velocity component V_ϕ is independent of the longitudinal coordinate z , and both V_ϕ and the pressure p are independent of ϕ . Then equation (1.8.45b) reduces to

$$\frac{\partial^2 V_\phi}{\partial r^2} + \frac{1}{r} \frac{\partial V_\phi}{\partial r} - \frac{V_\phi}{r^2} = 0. \quad (2.1.21)$$

This is a partial differential equation, but it involves only derivatives with respect to r , and therefore may be treated as an ordinary differential equation. We shall seek the two complementary solutions of (2.1.21) in the form

$$V_\phi = r^\lambda. \quad (2.1.22)$$

Substitution of (2.1.22) into (2.1.21) leads to the quadratic equation

$$\lambda^2 - 1 = 0,$$

with the two solutions being

$$\lambda_1 = 1, \quad \lambda_2 = -1.$$

Consequently, the general solution to (2.1.21) is written as

$$V_\phi = F(\phi, z) r + G(\phi, z) \frac{1}{r}.$$

We see that with $G(\phi, z) \neq 0$ the circumferential velocity V_ϕ develops a singularity at $r = 0$. This sort of behaviour could only be possible if there was a fast rotating cylinder of infinitely small radius inserted in the flow along the axis of symmetry.³ Since our flow is free of such devices, we have to set $G(\phi, z) = 0$.

Using further the no-slip condition on the tube wall,

$$V_\phi \Big|_{r=R} = 0,$$

we find that $F(\phi, z)$ is also zero. Thus, in the flow considered, the circumferential velocity component

$$V_\phi = 0. \quad (2.1.23)$$

³When using a cylindrical coordinate system, one has to keep in mind that this coordinate system does not provide a one-to-one correspondence between the position of a point in space and coordinates (r, ϕ, z) . Indeed, for any point situated on the axis of symmetry, the angle ϕ appears to be undetermined. This is why a singularity in the solution at $r = 0$ is to be expected.

Now it is easily found from the radial momentum equation (1.8.45a) that the pressure does not change with r :

$$\frac{\partial p}{\partial r} = 0.$$

Finally, it remains to consider the axial momentum equation (1.8.45c). Under the conditions stated above, it reduces to

$$\frac{\partial^2 V_z}{\partial r^2} + \frac{1}{r} \frac{\partial V_z}{\partial r} = \frac{1}{\mu} \frac{\partial p}{\partial z}. \quad (2.1.24)$$

Notice that the pressure gradient $\partial p/\partial z$ on the right-hand side of (2.1.24) represents the force that drives the fluid through the tube. In view of (2.1.16), the left-hand side of equation (2.1.24) is independent of z , and therefore so should the right-hand side. This means that the pressure gradient $\partial p/\partial z$ is constant throughout the flow field, and may be calculated as

$$\frac{\partial p}{\partial z} = \frac{\Delta p}{L}.$$

Here we use the same notation as in the channel Poiseuille problem (see Section 2.1.2), with $\Delta p = p_2 - p_1 < 0$ being the pressure difference between the tube ends and L the length of the tube.

Since V_z is a function of r only, we shall write equation (2.1.24) using ordinary derivatives:

$$\frac{d^2 V_z}{dr^2} + \frac{1}{r} \frac{dV_z}{dr} = \frac{1}{\mu} \frac{\Delta p}{L}.$$

Multiplying both sides of this equation by r , we have

$$\frac{d}{dr} \left(r \frac{dV_z}{dr} \right) = \frac{1}{\mu} \frac{\Delta p}{L} r.$$

This equation is easily integrated to yield

$$\frac{dV_z}{dr} = \frac{1}{2\mu} \frac{\Delta p}{L} r + \frac{C_1}{r}. \quad (2.1.25)$$

Integration of (2.1.25) results in

$$V_z = \frac{1}{4\mu} \frac{\Delta p}{L} r^2 + C_1 \ln r + C_2. \quad (2.1.26)$$

It remains to find the constants of integration C_1 and C_2 . In order for the velocity V_z to remain finite, the first of these, C_1 , should be set to zero. The second constant, C_2 , may be found from the no-slip condition

$$V_z \Big|_{r=R} = 0.$$

We have

$$C_2 = -\frac{1}{4\mu} \frac{\Delta p}{L} R^2,$$

which, being substituted back into (2.1.26), yields

$$V_z = \frac{1}{4\mu} \frac{\Delta p}{L} (r^2 - R^2). \quad (2.1.27)$$

With the velocity profile known, we can calculate the volumetric flow rate, called the *flux*, through any cross-section of the tube as follows. If we consider an annular element of the cross-section of radius r and width dr , then the area of this element will be $2\pi r dr$, and the flux⁴

$$dQ = V_z 2\pi r dr. \quad (2.1.28)$$

Substituting (2.1.27) into (2.1.28) and performing the integration, we find that the entire flux

$$Q = \frac{\pi}{2\mu} \frac{\Delta p}{L} \int_0^R (r^2 - R^2) r dr = -\frac{\pi}{8\mu} \frac{\Delta p}{L} R^4. \quad (2.1.29)$$

An average velocity \bar{V}_z may be defined as the ratio of the fluid flux Q and the cross-sectional area of the tube πR^2 . We have

$$\bar{V}_z = \frac{|\Delta p|}{8\mu L} R^2.$$

Referring the axial velocity V_z to its average value \bar{V}_z , we can express the velocity profile (2.1.27) in the following non-dimensional form:

$$\frac{V_z}{\bar{V}_z} = 2 \left(1 - \frac{r^2}{R^2} \right).$$

We see that the maximum velocity appears to be twice the average velocity.

2.1.4 Flow between two coaxial cylinders

Here we consider two coaxial cylinders of radii R_1 and R_2 rotating with angular velocities Ω_1 and Ω_2 , respectively; see Figure 2.6. The space between the cylinders is filled with an incompressible fluid of density ρ and dynamic viscosity coefficient μ . Our task is to determine the velocity and pressure distributions between the cylinders.

When dealing with this problem, it is convenient again to use cylindrical polar coordinates (Figure 1.30) with the z -axis now aligned with the common axis of the cylinders. In the flow considered, the Navier–Stokes equations (1.8.45) allow for the following simplifications. First, the flow is two-dimensional, which means that the derivatives of all the functions with respect to z are zero. Also, the axial velocity is zero:

$$\frac{\partial}{\partial z} = 0, \quad V_z = 0. \quad (2.1.30)$$

Second, none of the functions depend on the circumferential angle ϕ , i.e.

$$\frac{\partial}{\partial \phi} = 0. \quad (2.1.31)$$

⁴Notice that the mass flux is obtained by multiplying the volumetric flux by the fluid density ρ .

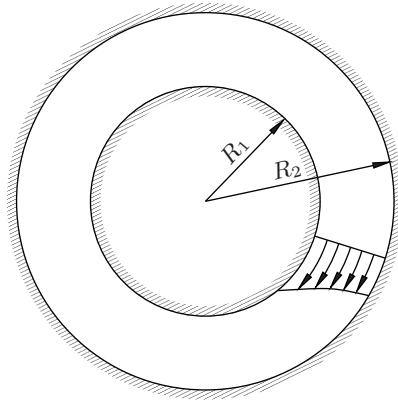


Fig. 2.6: Flow between two coaxial cylinders.

We start with the continuity equation (1.8.45d). In view of (2.1.30) and (2.1.31), it reduces to

$$\frac{\partial V_r}{\partial r} + \frac{V_r}{r} = 0,$$

with the general solution given by (2.1.18):

$$V_r = \frac{F(\phi, z)}{r}.$$

The impermeability condition on the two cylinders,

$$V_r \Big|_{r=R_1} = V_r \Big|_{r=R_2} = 0,$$

is satisfied by setting $F(\phi, z) = 0$. We can conclude that

$$V_r = 0 \tag{2.1.32}$$

throughout the flow field.

With (2.1.30)–(2.1.32), the radial (1.8.45a) and circumferential (1.8.45b) momentum equations reduce to

$$\frac{1}{\rho} \frac{\partial p}{\partial r} = \frac{V_\phi^2}{r}, \tag{2.1.33a}$$

$$\frac{\partial^2 V_\phi}{\partial r^2} + \frac{1}{r} \frac{\partial V_\phi}{\partial r} - \frac{V_\phi}{r^2} = 0. \tag{2.1.33b}$$

Equation (2.1.33b) may be solved independently of (2.1.33a). It coincides with equation (2.1.21), which has been shown to have two complementary solutions, r and $1/r$. Therefore, the general solution of equation (2.1.33b) is written as

$$V_\phi = C_1 r + \frac{C_2}{r}. \tag{2.1.34}$$

The constants C_1 and C_2 may be found using the no-slip conditions on the two cylinders:

$$V_\phi \Big|_{r=R_1} = V_1, \quad V_\phi \Big|_{r=R_2} = V_2. \quad (2.1.35)$$

Here $V_1 = \Omega_1 R_1$ and $V_2 = \Omega_2 R_2$. Substituting (2.1.34) into (2.1.35) and solving the resulting equations for C_1 and C_2 , we find

$$C_1 = \frac{V_1 R_1 - V_2 R_2}{R_1^2 - R_2^2}, \quad C_2 = R_1 R_2 \frac{V_1 R_2 - V_2 R_1}{R_2^2 - R_1^2}. \quad (2.1.36)$$

It remains to substitute (2.1.36) back into (2.1.34) and we will have the distribution of the velocity V_ϕ between the cylinders.

In order to determine the pressure distribution, we substitute (2.1.34) into the radial momentum equation (2.1.33a). We find that

$$\frac{dp}{dr} = \rho C_1^2 r + \frac{2\rho C_1 C_2}{r} + \frac{\rho C_2^2}{r^3}. \quad (2.1.37)$$

Integration of (2.1.37) yields

$$p = p_0 + \frac{1}{2}\rho C_1^2 r^2 + 2\rho C_1 C_2 \ln r - \frac{\rho C_2^2}{2r^2},$$

where the constant of integration p_0 remains arbitrary. Notice that in the case of incompressible flows the Navier–Stokes equations (1.7.6) involve the pressure gradient only, not the pressure itself. Therefore, adding a constant to the pressure does not affect these equations.

2.1.5 Impulsively started flat plate

Let us assume that an incompressible viscous fluid occupies a semi-infinite region that is bounded on one side by a flat surface. The latter may be thought of as the surface of an infinitely large flat plate. Let us further assume that initially both the fluid and the plate were kept at rest. Then, at time $t = 0$, the plate is suddenly brought into motion parallel itself with a velocity U that remains constant for all $t > 0$.

Through the action of the viscous forces, the fluid close to the plate and then further in the field will be brought in motion, and our task is to describe how it happens. We

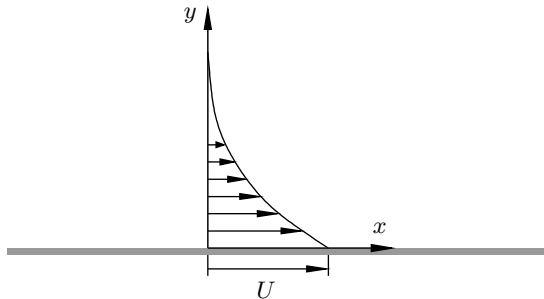


Fig. 2.7: The flow above an impulsively started flat plate.

shall use Cartesian coordinates with x measured along the plate in the direction of its motion and y perpendicular to the plate surface (see Figure 2.7). The governing Navier–Stokes equations (1.7.6) allow for the following simplifications.

First of all, the problem considered is invariant with respect to an arbitrary shift in the x - and z -directions. Therefore, the derivatives of all the fluid-dynamic functions with respect to x and z are zero, i.e.

$$\frac{\partial}{\partial x} = \frac{\partial}{\partial z} = 0. \quad (2.1.38)$$

This reduces the continuity equation (1.7.6d) to

$$\frac{\partial v}{\partial y} = 0.$$

Integration of this equation with the impermeability condition at the plate surface,

$$v \Big|_{y=0} = 0,$$

leads to the conclusion that

$$v = 0 \quad (2.1.39)$$

everywhere in the flow field.

If the x -component f_x of the body force \mathbf{f} is negligible, then, in view of (2.1.38) and (2.1.39), the x -momentum equation (1.7.6a) will reduce to

$$\frac{\partial u}{\partial t} = \nu \frac{\partial^2 u}{\partial y^2}. \quad (2.1.40)$$

When formulating the boundary conditions for this equation, one needs to keep in mind that a set of boundary conditions compatible with a particular partial differential equation depends on its type. Equation (2.1.40) is *parabolic* as it has a second-order derivative with respect to y and only a first-order derivative with respect to t . A classical example of a parabolic equation is the heat transfer equation. When applied, say, to a heat-conducting rod, it may be written as

$$\frac{\partial T}{\partial t} = a \frac{\partial^2 T}{\partial x^2}, \quad (2.1.41)$$

where a is a positive constant, representing the thermal conductivity of the material of which the rod is made, T is the temperature to be found, t is time, and x is the coordinate measured along the rod. The latter is assumed to occupy the interval $x \in [0, d]$ of the x -axis, as shown in Figure 2.8. In order to determine the temperature T at a point $y = y_0$ inside the rod, at time $t = t_0$, it is necessary to specify the temperature distribution along the rod at initial instant $t = 0$ and also to formulate the thermal conditions at the rod ends for $t \in [0, t_0]$. These boundaries are shown by braces in Figure 2.8. The solution at point (t_0, x_0) , obviously, does not depend on the boundary conditions at the rod ends at later times $t > t_0$.

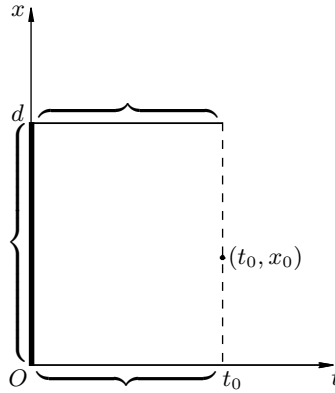


Fig. 2.8: The boundary conditions for the heat transfer equation (2.1.41).

Similarly, when dealing with equation (2.1.40), one needs, first of all, to formulate an initial condition. Since, for all $t < 0$, the fluid remained at rest, we can write

$$u = 0 \quad \text{at} \quad t = 0, \quad y \in (0, \infty). \quad (2.1.42)$$

In addition to this, equation (2.1.40) requires two boundary conditions. The first is the no-slip condition on the plate surface:

$$u = U \quad \text{at} \quad y = 0, \quad t > 0. \quad (2.1.43)$$

The second boundary condition should be formulated at large values of y , where the fluid is expected to remain motionless for all finite values of t :

$$u = 0 \quad \text{at} \quad y = \infty, \quad t > 0. \quad (2.1.44)$$

Now our task will be to find the solution to the problem (2.1.40)–(2.1.44). We start by noting that no characteristic length or time scales can be assigned to the problem, which suggests that the solution may be expected to have a *self-similar* form. This means that if the distribution of the velocity u in the direction perpendicular to the plate is known at some time t , then at any other time it may be found by means of ‘zooming’. Mathematically, this zooming is performed via affine transformations.

Let

$$u = F(t, y). \quad (2.1.45)$$

be the solution of (2.1.40)–(2.1.44). We shall seek the affine transformation in the form

$$u = A\bar{u}, \quad t = B\bar{t}, \quad y = C\bar{y}, \quad (2.1.46)$$

where A , B , and C are constants. Substitution of (2.1.46) into equation (2.1.40) yields

$$\frac{1}{B} \frac{\partial \bar{u}}{\partial \bar{t}} = \frac{\nu}{C^2} \frac{\partial^2 \bar{u}}{\partial \bar{y}^2},$$

while the boundary conditions (2.1.42)–(2.1.44) become

$$\begin{aligned}\bar{u} &= 0 & \text{at } \bar{t} &= 0, \\ A\bar{u} &= U & \text{at } \bar{y} &= 0, \\ \bar{u} &= 0 & \text{at } \bar{y} &= \infty.\end{aligned}$$

If we choose

$$A = 1, \quad B = C^2, \quad (2.1.47)$$

then the transformed problem will be identical to the original one. It therefore admits the solution (2.1.45), which should now be written as

$$\bar{u} = F(\bar{t}, \bar{y}). \quad (2.1.48)$$

Returning in (2.1.48) to the original variables (2.1.46), we have

$$\frac{u}{A} = F\left(\frac{t}{B}, \frac{y}{C}\right)$$

which, in view of (2.1.47), may also be written as

$$u(t, y) = F\left(\frac{t}{C^2}, \frac{y}{C}\right). \quad (2.1.49)$$

The parameter C in (2.1.49) may assume an arbitrary value, and therefore it may be treated as an additional independent variable. Still, it has been introduced artificially; the solution does not really depend on it. To ‘hide’ this parameter, we can choose, for example, $C = \sqrt{t}$, which leads to

$$u = F\left(1, \frac{y}{\sqrt{t}}\right).$$

This shows that the solution of the problem (2.1.40)–(2.1.44) has the form

$$u(t, y) = f(\eta), \quad (2.1.50)$$

where the independent variable

$$\eta = \frac{y}{\sqrt{t}} \quad (2.1.51)$$

is referred to as the *similarity variable*.

In order to deduce a differential equation for the function $f(\eta)$ we need to substitute (2.1.50) and (2.1.51) into the governing equation (2.1.40). It is easily seen that

$$\frac{\partial \eta}{\partial t} = -\frac{1}{2} \frac{y}{t^{3/2}} = -\frac{1}{2} \frac{\eta}{t}, \quad \frac{\partial \eta}{\partial y} = \frac{1}{\sqrt{t}}.$$

Therefore,

$$\frac{\partial u}{\partial t} = f'(\eta) \frac{\partial \eta}{\partial t} = -\frac{1}{2} \frac{\eta}{t} f'(\eta), \quad \frac{\partial u}{\partial y} = f'(\eta) \frac{\partial \eta}{\partial y} = \frac{1}{\sqrt{t}} f'(\eta), \quad \frac{\partial^2 u}{\partial y^2} = \frac{1}{t} f''(\eta),$$

which reduces (2.1.40) to

$$\nu f'' + \frac{1}{2}\eta f' = 0. \quad (2.1.52)$$

The boundary conditions for this equation are formulated by substituting (2.1.50) and (2.1.51) into (2.1.42)–(2.1.44). Taking into account that $\eta = \infty$ at $t = 0$, we find from (2.1.42) that

$$f(\infty) = 0. \quad (2.1.53)$$

Condition (2.1.43) is imposed at $y = 0$, where $\eta = 0$. We have

$$f(0) = U. \quad (2.1.54)$$

Finally, we need to use condition (2.1.44), but it is easily seen to lead again to (2.1.53). Thus, our task now will be to solve equation (2.1.52) subject to the boundary conditions (2.1.53) and (2.1.54).

Equation (2.1.52) may be integrated once by making use of separation of variables:

$$\frac{f''}{f'} = -\frac{\eta}{2\nu}.$$

We find that

$$f' = C_1 e^{-\eta^2/4\nu}.$$

A second integration yields

$$f(\eta) = C_1 \int_0^\eta e^{-s^2/4\nu} ds + C_2.$$

The integration constants C_1 and C_2 may be found from the boundary conditions (2.1.53) and (2.1.54) to be⁵

$$C_1 = -\frac{U}{\sqrt{\pi\nu}}, \quad C_2 = U.$$

Consequently,

$$f(\eta) = U - \frac{U}{\sqrt{\pi\nu}} \int_0^\eta e^{-s^2/4\nu} ds. \quad (2.1.55)$$

Introducing a new integration variable $\zeta = s/\sqrt{4\nu}$ in (2.1.55) and returning to (2.1.50)

⁵When applying condition (2.1.54), the following formula is used:

$$\int_0^\infty e^{-\alpha s^2} ds = \frac{1}{2} \sqrt{\frac{\pi}{\alpha}}.$$

and (2.1.51), we finally have the solution in the form

$$u(t, y) = U \operatorname{erfc}\left(\frac{y}{2\sqrt{\nu t}}\right), \quad (2.1.56)$$

where

$$\operatorname{erfc} x = 1 - \frac{2}{\sqrt{\pi}} \int_0^x e^{-\zeta^2} d\zeta$$

is referred to as the complementary error function. It follows from (2.1.56) that the thickness of the layer of fluid involved in motion by the viscous forces may be estimated as

$$y \sim \sqrt{\nu t}. \quad (2.1.57)$$

The above solution was first produced by Stokes (1851); hence the layer of the fluid put in motion by the plate is termed the *Stokes layer*.

2.1.6 Dissipation of the potential vortex

Let us assume that an incompressible fluid is involved in rotational motion with the velocity field represented by the potential vortex solution, which is written in cylindrical polar coordinates as

$$V_r = 0, \quad V_\phi = \frac{\Gamma}{2\pi r}, \quad V_z = 0. \quad (2.1.58)$$

Physically, this motion may be produced with a help of a circular cylinder of small radius placed inside the fluid and brought in rotation around its axis with a large angular velocity (see Problem 5 in Exercises 6).

Suppose that at time $t = 0$ the cylinder suddenly ‘vanishes’, and the fluid particles on the opposite sides of its surface come in contact with each other, generating extremely large shear stress at the centre of rotation. This will make the singularity that the initial velocity (2.1.58) has at $r = 0$ disappear immediately. We then expect the action of the viscous forces to lead to a gradual deceleration of the fluid rotation, and our task is to describe how this happens.

We start, as usual, with the continuity equation (1.8.45d). Taking into account that the flow is axisymmetric and two-dimensional, we can disregard the derivatives with respect to ϕ and z , which yields

$$\frac{\partial V_r}{\partial r} + \frac{V_r}{r} = 0.$$

The solution of this equation is written as

$$V_r = \frac{F(t)}{r}.$$

The function $F(t)$ defines the volumetric fluid flux through a circle centred at the axis of rotation:

$$Q = 2\pi r V_r = 2\pi F(t).$$

Therefore, assuming that there are no sources or sinks situated at $r = 0$, we have to set $F(t) = 0$, and we arrive at the conclusion that

$$V_r = 0 \quad \text{for all } t > 0.$$

We then see that the circumferential momentum equation (1.8.45b) takes the form

$$\frac{\partial V_\phi}{\partial t} = \nu \left(\frac{\partial^2 V_\phi}{\partial r^2} + \frac{1}{r} \frac{\partial V_\phi}{\partial r} - \frac{V_\phi}{r^2} \right). \quad (2.1.59)$$

Again, the choice of the boundary conditions for equation (2.1.59) depends on its type. The latter is determined by the higher-order derivatives. Equation (2.1.59) has only one derivative with respect to time, which is $\partial V_\phi / \partial t$, and the second-order derivative with respect to r is $\partial^2 V_\phi / \partial r^2$. Hence, the equation is parabolic, and requires one initial condition and two boundary conditions.

The initial condition follows directly from (2.1.58), and is written as

$$V_\phi = \frac{\Gamma}{2\pi r} \quad \text{at } t = 0, \quad r > 0. \quad (2.1.60)$$

The far field is expected to remain undisturbed as long as time t is finite, which gives the first boundary condition:

$$V_\phi = \frac{\Gamma}{2\pi r} \quad \text{as } r \rightarrow \infty, \quad t > 0. \quad (2.1.61)$$

In order to formulate the second boundary condition, we shall assume that, owing to the action of viscous forces, the singularity at the centre of rotation will vanish momentarily, and there exists a positive constant M such that

$$|V_\phi| < M \quad \text{at } r = 0, \quad t > 0. \quad (2.1.62)$$

The problem (2.1.59)–(2.1.62) does not involve any characteristic length or time scales. This suggests that the solution may be expected to have a self-similar form. To verify this possibility, we use the affine transformations

$$V_\phi = A\bar{V}_\phi, \quad t = B\bar{t}, \quad r = C\bar{r}. \quad (2.1.63)$$

Substituting (2.1.63) into the analysed equation (2.1.59), we find

$$\frac{A}{B} \frac{\partial \bar{V}_\phi}{\partial \bar{t}} = \frac{A}{C^2} \nu \left(\frac{\partial^2 \bar{V}_\phi}{\partial \bar{r}^2} + \frac{1}{\bar{r}} \frac{\partial \bar{V}_\phi}{\partial \bar{r}} - \frac{\bar{V}_\phi}{\bar{r}^2} \right).$$

The boundary conditions (2.1.60)–(2.1.62), written in the new variables, take the form

$$\begin{aligned} A\bar{V}_\phi &= \frac{1}{C} \frac{\Gamma}{2\pi\bar{r}} \quad \text{at } \bar{t} = 0, \\ A\bar{V}_\phi &= \frac{1}{C} \frac{\Gamma}{2\pi\bar{r}} \quad \text{at } \bar{r} = \infty, \\ |\bar{V}_\phi| &< \bar{M} \quad \text{at } \bar{r} = 0. \end{aligned}$$

In order for the transformed problem to be identical to the original one, we have to set

$$B = C^2, \quad A = \frac{1}{C},$$

where C remains arbitrary.

If $V_\phi = F(t, r)$ is the solution of the original problem, then the solution of the transformed problem is written as

$$\bar{V}_\phi = F(\bar{t}, \bar{r}). \quad (2.1.64)$$

Returning in (2.1.64) to the original variables (2.1.63), we have

$$V_\phi = AF\left(\frac{t}{B}, \frac{r}{C}\right) = \frac{1}{C}F\left(\frac{t}{C^2}, \frac{r}{C}\right).$$

As C is arbitrary, we can choose $C = r$, which leads to

$$V_\phi = \frac{1}{r}F\left(\frac{t}{r^2}, 1\right).$$

This suggests that the sought solution may be written in the form

$$V_\phi = \frac{1}{r}f(\eta), \quad \eta = \frac{r^2}{t}. \quad (2.1.65)$$

Substitution of (2.1.65) into (2.1.59) leads to the following equation for the function $f(\eta)$:

$$f'' + \frac{1}{4\nu}f' = 0. \quad (2.1.66)$$

The boundary conditions for this equation are deduced by substituting (2.1.65) into (2.1.60)–(2.1.62). We have

$$f(0) = 0, \quad f(\infty) = \frac{\Gamma}{2\pi}. \quad (2.1.67)$$

The general solution of equation (2.1.66) is written as

$$f(\eta) = C_1 + C_2e^{-\eta/4\nu}, \quad (2.1.68)$$

where the constants C_1 and C_2 may be found from (2.1.67) to be

$$C_1 = \frac{\Gamma}{2\pi}, \quad C_2 = -\frac{\Gamma}{2\pi}. \quad (2.1.69)$$

It remains to substitute (2.1.69) back into (2.1.68) and then into (2.1.65). We see that the circumferential velocity is given by the equation

$$V_\phi = \frac{\Gamma}{2\pi r} \left[1 - \exp\left(-\frac{r^2}{4\nu t}\right) \right], \quad (2.1.70)$$

first deduced by Hamel (1916).

It follows from (2.1.70) that the vortex has a viscous core of radius $r \sim \sqrt{\nu t}$. If $r \gg \sqrt{\nu t}$, then the velocity field is represented by the potential vortex solution

$$V_\phi = \frac{\Gamma}{2\pi r} \quad \text{for} \quad \frac{r^2}{\nu t} \gg 1,$$

If, on the other hand, $r \ll \sqrt{\nu t}$, then, using the Taylor expansion for the exponential function,⁶ we can find

$$V_\phi = \frac{\Gamma r}{8\pi\nu t} \quad \text{for} \quad \frac{r^2}{\nu t} \ll 1,$$

which shows that, near the centre of the vortex core, the circumferential velocity grows linearly with the radius r .

2.1.7 Kármán flow

Whereas the examples of the exact solutions we have met in the earlier sections deal with two-dimensional flows, planar or axisymmetric, the flow over an infinite rotating disk considered here gives rise to a fully three-dimensional solution of the Navier–Stokes equations. It was first put forward by Kármán (1921)—hence the name *Kármán flow*.

We shall formulate the problem as follows. Let us assume that a plane disk is placed in an infinite reservoir filled with a stagnant incompressible fluid. The disk is brought in rotation in its plane around the centre O ; see Figure 2.9. Owing to the action of viscous forces, the fluid particles adjacent to the disk will start to move following the disk, but their trajectories will not be circular. Because of inertia, the fluid particles will also tend to move away from the axis of rotation.

If the angular velocity of the disk rotation Ω is kept constant for a long enough time, then the flow eventually becomes steady. As the flow is expected to be symmetric

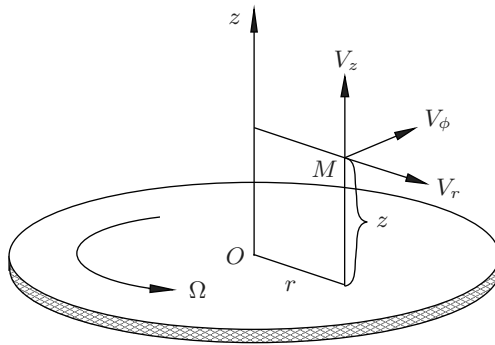


Fig. 2.9: Kármán flow.

⁶Recall that

$$e^x = 1 + x + \dots \quad \text{as} \quad x \rightarrow 0.$$

with respect to the axis of rotation, we shall use cylindrical polar coordinates (see Figure 1.30 on page 80), choosing the z -axis to coincide with the axis of rotation of the disk as shown in Figure 2.9. Disregarding the body force \mathbf{f} and taking into account that the derivatives with respect to time t and the circumferential angle ϕ are zero, we have the Navier–Stokes equations (1.8.45) in the form

$$V_r \frac{\partial V_r}{\partial r} + V_z \frac{\partial V_r}{\partial z} - \frac{V_\phi^2}{r} = -\frac{1}{\rho} \frac{\partial p}{\partial r} + \nu \left(\frac{\partial^2 V_r}{\partial z^2} + \frac{\partial^2 V_r}{\partial r^2} + \frac{1}{r} \frac{\partial V_r}{\partial r} - \frac{V_r}{r^2} \right), \quad (2.1.71a)$$

$$V_r \frac{\partial V_\phi}{\partial r} + V_z \frac{\partial V_\phi}{\partial z} + \frac{V_r V_\phi}{r} = \nu \left(\frac{\partial^2 V_\phi}{\partial z^2} + \frac{\partial^2 V_\phi}{\partial r^2} + \frac{1}{r} \frac{\partial V_\phi}{\partial r} - \frac{V_\phi}{r^2} \right), \quad (2.1.71b)$$

$$V_r \frac{\partial V_z}{\partial r} + V_z \frac{\partial V_z}{\partial z} = -\frac{1}{\rho} \frac{\partial p}{\partial z} + \nu \left(\frac{\partial^2 V_z}{\partial z^2} + \frac{\partial^2 V_z}{\partial r^2} + \frac{1}{r} \frac{\partial V_z}{\partial r} \right), \quad (2.1.71c)$$

$$\frac{\partial V_r}{\partial r} + \frac{\partial V_z}{\partial z} + \frac{V_r}{r} = 0. \quad (2.1.71d)$$

In order to formulate the boundary conditions for these equations and predict the form of the solution, we shall discuss the physical processes involved in more detail. As has been already mentioned, owing to the action of the viscous forces, it is expected that a layer of the fluid will form above the disk, where the fluid particles will perform circumferential motion following the rotation of the disk. The circumferential velocity component V_ϕ has to satisfy the no-slip condition on the disk surface:

$$V_\phi = \Omega r \quad \text{at} \quad z = 0, \quad (2.1.72)$$

which states that the fluid particles adjacent to the disk have to move with the same velocity as the corresponding elements of the disk surface. Of course, further away from the disk, the fluid in the reservoir is motionless. Therefore, the second boundary condition for V_ϕ is

$$V_\phi = 0 \quad \text{at} \quad z = \infty. \quad (2.1.73)$$

Inside the rotating fluid layer, the circumferential velocity varies between (2.1.72) and (2.1.73), which suggests that V_ϕ may be estimated as

$$V_\phi \sim \Omega r. \quad (2.1.74)$$

Let us now consider the radial velocity component V_r . The motion of the fluid in the radial direction is caused by the centrifugal force, which is represented by the third term, V_ϕ^2/r , on the left-hand side of the radial momentum equation (2.1.71a). The acceleration of the fluid particles in the radial direction is represented by the first term, $V_r \partial V_r / \partial r$, in equation (2.1.71a). Clearly, they have to be in ‘balance’ with one another, i.e.

$$V_r \frac{\partial V_r}{\partial r} \sim \frac{V_\phi^2}{r}. \quad (2.1.75)$$

Using (2.1.74), we can estimate the centrifugal term as

$$\frac{V_\phi^2}{r} \sim \Omega^2 r,$$

which, being substituted into (2.1.75), yields

$$V_r \frac{\partial V_r}{\partial r} \sim \Omega^2 r.$$

Solving this equation for V_r , we arrive at the conclusion that

$$V_r \sim \Omega r. \quad (2.1.76)$$

Of course, V_r also depends on z , and is expected to have a maximum somewhere in the middle of the rotating fluid layer. Still, on the disk surface, it has to satisfy the no-slip condition

$$V_r = 0 \quad \text{at} \quad z = 0. \quad (2.1.77)$$

As an observation point moves upwards towards the ‘outer edge’ of the rotating fluid layer, the centrifugal force, V_ϕ^2/r , vanishes, which suggests the second boundary condition for V_r to be

$$V_r = 0 \quad \text{at} \quad z = \infty. \quad (2.1.78)$$

The circumferential motion of the fluid is governed by equation (2.1.71b). The tangential viscous stress, which brings the fluid in rotation, is represented by the first term on the right-hand side of (2.1.71b). In order to estimate the thickness of the layer of fluid involved in rotation above the disk, we need to compare it with a convective term on the left-hand side of (2.1.71b). Using, for example, the first convective term, we can write

$$V_r \frac{\partial V_\phi}{\partial r} \sim \nu \frac{\partial^2 V_\phi}{\partial z^2}.$$

It follows from (2.1.74) and (2.1.76) that

$$V_r \frac{\partial V_\phi}{\partial r} \sim \Omega^2 r,$$

and therefore

$$\frac{\partial^2 V_\phi}{\partial z^2} \sim \frac{\Omega^2}{\nu} r. \quad (2.1.79)$$

Keeping in mind that $V_\phi \sim \Omega r$, we can see that the balance (2.1.79) can only hold if the thickness of the rotating fluid layer is independent of r , being estimated as

$$z \sim \sqrt{\frac{\nu}{\Omega}}. \quad (2.1.80)$$

We are prepared now to find an estimate for the axial velocity component V_z . We shall use for this purpose the mass conservation law with the control volume in the form of a circular cylinder installed on the disk surface as shown in Figure 2.10. We

know that the fluid is moving from this cylinder through its side surface. As the area of this surface is $2\pi rz$, the corresponding fluid mass flux is calculated as

$$Q \sim \rho V_r 2\pi rz.$$

It has to be ‘resupplied’ through the top surface of the cylinder. The fluid flux through this surface is estimated as

$$Q \sim \rho V_z \pi r^2.$$

Consequently, the mass conservation law states

$$\rho V_r 2\pi rz \sim \rho V_z \pi r^2. \tag{2.1.81}$$

Using (2.1.76) and (2.1.80) on the left-hand side of (2.1.81), and solving the resulting equation for V_z , we find that⁷

$$V_z \sim \sqrt{\Omega\nu}. \tag{2.1.82}$$

When formulating boundary conditions for V_z , one has to keep in mind that the mass conservation law is represented by the continuity equation (2.1.71d), which is a first-order differential equation. It allows for just one boundary condition for V_z . We shall require that

$$V_z = 0 \quad \text{at} \quad z = 0. \tag{2.1.83}$$

It remains to see what happens with the pressure p . If the disk radius is infinite, then, outside the rotating fluid layer, the fluid velocity V_z will stay independent of r , as equation (2.1.82) suggests. The pressure is also expected to remain constant. We shall denote its value as p_0 , and then the boundary condition for the pressure is written as

$$p = p_0 \quad \text{at} \quad z = \infty. \tag{2.1.84}$$

The variation of the pressure across the rotating fluid layer is governed by equation (2.1.71c). It is convenient to compare the pressure gradient in this equation with the

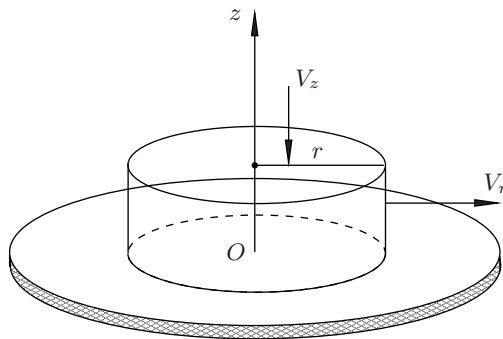


Fig. 2.10: Application of the mass conservation law.

⁷As we are conducting an order-of-magnitude analysis, we can disregard the factor 2 on the left-hand side of equation (2.1.81).

second convective term, i.e.

$$V_z \frac{\partial V_z}{\partial z} \sim \frac{1}{\rho} \frac{\partial p}{\partial z},$$

and we see that

$$p - p_0 \sim \rho \Omega \nu. \quad (2.1.85)$$

We shall now return from the physical arguments to the mathematical analysis of equations (2.1.71). Being guided by (2.1.74), (2.1.76), (2.1.80), (2.1.82), and (2.1.85), we shall seek the solution for the velocity components and the pressure in the form

$$V_r = \Omega r F(\zeta), \quad V_\phi = \Omega r G(\zeta), \quad V_z = \sqrt{\Omega \nu} H(\zeta), \quad p = p_0 + \rho \Omega \nu P(\zeta), \quad (2.1.86)$$

where

$$\zeta = \sqrt{\frac{\Omega}{\nu}} z.$$

Substitution of (2.1.86) into the Navier–Stokes equations (2.1.71) reduces these equations to a set of ordinary differential equations

$$F^2 + HF - G^2 = F'', \quad (2.1.87a)$$

$$2FG + HG' = G'', \quad (2.1.87b)$$

$$HH' = -P' + H'', \quad (2.1.87c)$$

$$2F + H' = 0. \quad (2.1.87d)$$

One can see that equations (2.1.87a,b,d) do not involve the pressure $P(\zeta)$, and may be solved separately from equation (2.1.87c). Considered together, they constitute a set of ordinary differential equations of fifth order, and require five boundary conditions. These may be obtained by substituting (2.1.86) into (2.1.72), (2.1.73), (2.1.77), (2.1.78), and (2.1.83). We have

$$\left. \begin{array}{llll} F = 0, & G = 1, & H = 0 & \text{at } \zeta = 0, \\ F = 0, & G = 0 & & \text{at } \zeta = \infty. \end{array} \right\} \quad (2.1.88)$$

The results of numerical solution of equations (2.1.87a,b,d) with the boundary conditions (2.1.88) are displayed in Figure 2.11. We see that the circumferential velocity component $V_\phi = \Omega r G(\zeta)$ decays monotonically from $V_\phi = \Omega r$ on the disk surface to zero at the outer edge of the rotating fluid layer ($\zeta = \infty$). The radial velocity component $V_r = \Omega r F(\zeta)$ is positive everywhere inside the rotating fluid layer, which confirms that, owing to the action of centrifugal forces, the fluid moves away from the axis of rotation with a speed that grows linearly with the radius r . We also see that the axial velocity component $\sqrt{\Omega \nu} H(\zeta)$ is negative. The absolute value of the function $H(\zeta)$ grows from zero on the disk surface to $|H(\infty)| = 0.883$ at the outer edge of the rotating fluid layer. Correspondingly, the fluid ‘resupply’ velocity appears to be

$$V_z = -0.883 \sqrt{\Omega \nu}.$$

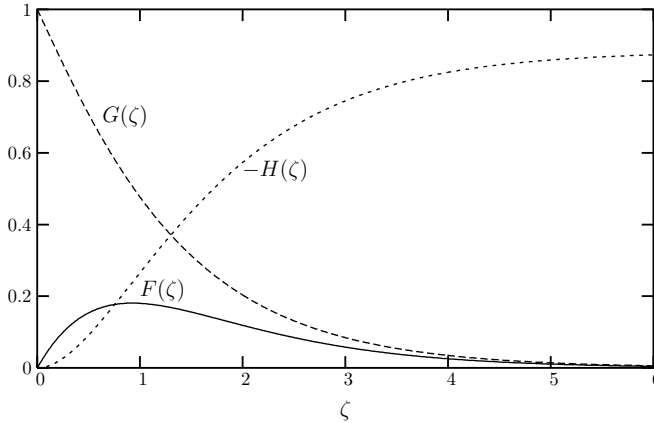


Fig. 2.11: Radial, $F(\zeta)$, circumferential, $G(\zeta)$, and axial, $H(\zeta)$, velocity profiles for rotating-disk flow.

With known velocity field, the pressure is easily found by integrating equation (2.1.87c). We have

$$P = H' - \frac{1}{2}H^2 + C.$$

In order to determine the constant of integration C , one needs to use the boundary condition (2.1.84). Substitution of the equation for p from (2.1.86) into (2.1.84) yields

$$P(\infty) = 0,$$

and we can conclude that $C = \frac{1}{2}[H(\infty)]^2$.

Exercises 6

1. Consider Hagen–Poiseuille flow in a circular pipe of radius R and, instead of using the Navier–Stokes equations (1.8.45), deduce equation (2.1.25) by balancing the forces that act on a control volume \mathcal{D} (see Figure 2.12). This volume has the form of a circular cylinder of radius $r < R$, whose axis coincides with the axis z of the pipe. The surface S_c surrounding the control volume \mathcal{D} is composed of the cylindrical side surface Σ and two circular end disks S_1 and S_2 .

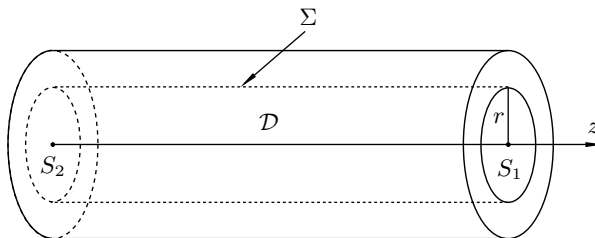


Fig. 2.12: Hagen–Poiseuille flow.

Suggestion: Start with the z -component of the integral momentum equation (1.7.30), and notice that, for the flow considered, the momentum flux on the left-hand side of (1.7.30) becomes zero automatically. This means that the momentum equation reduces to the balance of forces acting on the control surface S_c :

$$\iint_{S_c} \mathbf{p}_n ds = 0.$$

Project the above equation on the z -axis and observe that it represents the balance between the pressure forces acting on the end surfaces S_2 and S_1 and the shear stress acting on the side surface Σ . In order to calculate the corresponding integrals, recall that in cylindrical coordinates the components of the stress tensor are given by (1.8.65). In particular,

$$p_{zz} = -p + 2\mu \frac{\partial V_z}{\partial z}, \quad p_{rz} = \mu \left(\frac{\partial V_r}{\partial z} + \frac{\partial V_z}{\partial r} \right).$$

- Find the velocity profile in *Couette–Poiseuille flow*, i.e. the flow between two parallel plates (see Figure 2.13), one of which is kept motionless while the other moves parallel to it with constant velocity U . The distance between the plates is h . Unlike in Couette flow, there is a non-zero pressure difference Δp between the channel ends. The length of the channel is L .

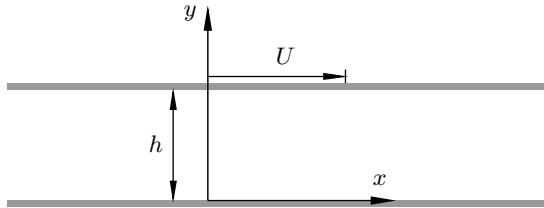


Fig. 2.13: Couette–Poiseuille flow.

- Consider the motion of an incompressible viscous fluid through a tube of elliptic cross-section given by the equation

$$\frac{y^2}{a^2} + \frac{z^2}{b^2} = 1.$$

The pressure difference between the tube ends is Δp . Assuming that the tube length L is large, find the velocity distribution in the tube.

Suggestion: Use Cartesian coordinates with the x -axis directed along the centre-line of the tube. You may assume without proof that the y - and z -components of the velocity are zero. Seek the solution of the x -momentum equation

$$u \frac{\partial u}{\partial x} + v \frac{\partial u}{\partial y} + w \frac{\partial u}{\partial z} = -\frac{1}{\rho} \frac{\partial p}{\partial x} + \nu \left(\frac{\partial^2 u}{\partial x^2} + \frac{\partial^2 u}{\partial y^2} + \frac{\partial^2 u}{\partial z^2} \right)$$

in the form

$$u = C_1 + C_2 y^2 + C_3 z^2,$$

where C_1 , C_2 , and C_3 are constants to be found.

4. Consider viscous fluid flow down an infinite flat slope under the action of the gravitational field \mathbf{g} . The angle between the slope and horizon is α ; see Figure 2.14. Assume that the fluid forms a layer of constant thickness h . Assume also that the flow is steady and none of the fluid-dynamic functions depends on the coordinate x measured along the slope. Your task is to find the velocity distribution across the layer.

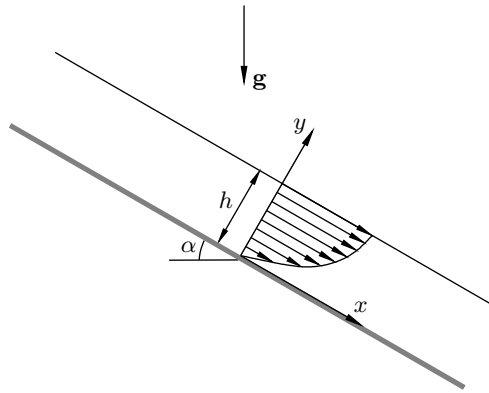


Fig. 2.14: Fluid layer on the downslope.

Hint: Use the Navier–Stokes equations written in Cartesian coordinates, and notice that the tangential stress

$$\tau_{yx} = \mu \left(\frac{\partial v}{\partial x} + \frac{\partial u}{\partial y} \right)$$

is zero at the upper edge of the fluid layer.

5. Consider a circular cylinder of radius R surrounded by viscous fluid of density ρ and dynamic viscosity μ . The cylinder rotates around its axis with angular velocity Ω . Assuming that the fluid remains at rest far from the cylinder ($r \rightarrow \infty$), prove that the velocity field and pressure are given by the ‘potential vortex’ solution

$$V_r = 0, \quad V_\phi = \frac{\Gamma}{2\pi r}, \quad V_z = 0, \quad p = p_\infty - \frac{\rho\Gamma^2}{8\pi^2 r^2}. \quad (2.1.89)$$

How does the circulation Γ depend on the cylinder radius R and angular velocity Ω ?

Hint: This may be done through direct substitution of (2.1.89) into the Navier–Stokes equations (1.8.45).

6. Consider again flow between two coaxial circular cylinders of radii R_1 and R_2 (see Figure 2.6), but now assume that the inner cylinder kept at rest as shown in Figure 2.15. What torque (per unit length in the axial direction) has to be applied to the outer cylinder to rotate it steadily with angular velocity Ω_2 ?

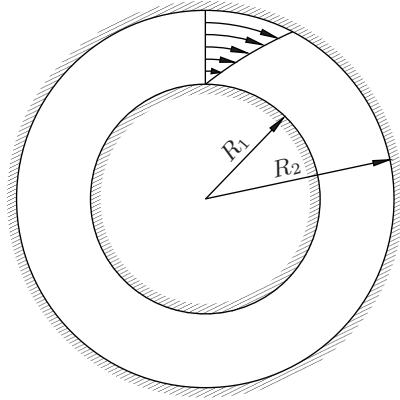


Fig. 2.15: The flow between two coaxial cylinders.

Hint: According to (1.8.65) the tangential stress on the surface of the outer cylinder is calculated as

$$p_{r\phi} = \mu \left(\frac{1}{r} \frac{\partial V_r}{\partial \phi} + \frac{\partial V_\phi}{\partial r} - \frac{V_\phi}{r} \right).$$

7. Generalise the solution (2.1.34), (2.1.36) for flow between two coaxial cylinders (Figure 2.6) by assuming that they are made permeable, allowing the fluid to flow across the gap between the cylinders. Let the amount of fluid supplied (per unit time and unit length in the axial direction) into the gap through the inner cylinder by Q , with an equal amount removed through the outer cylinder.

Show that in this flow the circumferential velocity is given by

$$V_\phi = \frac{C_1}{r} + C_2 r^{1+q/\nu}, \tag{2.1.90}$$

where $q = Q/2\pi$ and

$$C_1 = \frac{V_1 - V_2 (R_1/R_2)^{1+q/\nu}}{1 - (R_1/R_2)^{2+q/\nu}} R_1, \quad C_2 = \frac{V_2 - V_1 (R_1/R_2)}{1 - (R_1/R_2)^{2+q/\nu}} \frac{1}{R_2^{1+q/\nu}}. \tag{2.1.91}$$

8. Consider an incompressible viscous fluid that occupies a semi-infinite region on one side of an infinite flat plate (as shown in Figure 2.16). The plate performs oscillatory motion in its plane with velocity given by

$$u = U \cos(\omega t). \tag{2.1.92}$$

Here U is the amplitude of the oscillations and ω is the frequency. Find the velocity distribution in the fluid above the surface.

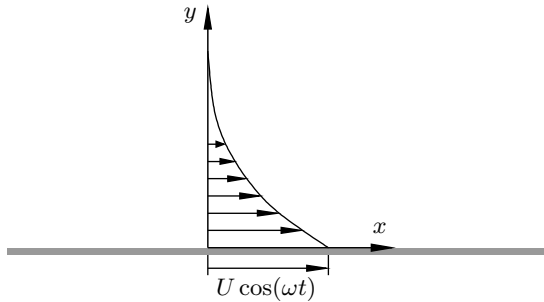


Fig. 2.16: Flow above an oscillating plate.

Suggestion: Argue that in the flow considered the fluid velocity satisfies equation (2.1.40). Notice that equation (2.1.92) may be written as

$$u = \frac{1}{2}Ue^{i\omega t} + \frac{1}{2}Ue^{-i\omega t},$$

and try to find the solution of (2.1.40) in the form

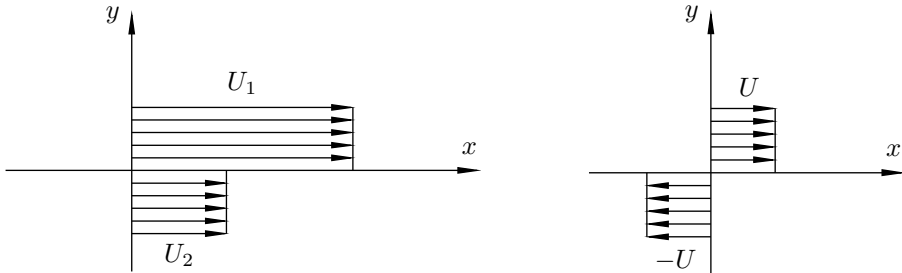
$$u = f(y)e^{i\omega t} + \bar{f}(y)e^{-i\omega t},$$

where $f(y)$ is a complex-valued function, and $\bar{f}(y)$ is the complex conjugate of $f(y)$.

9. Consider two-dimensional flow with the initial velocity field represented by two adjacent uniform streams, namely

$$u = \begin{cases} U_1 & \text{if } y > 0, \\ U_2 & \text{if } y < 0, \end{cases} \quad \text{for all } x,$$

with $v = 0$ for all x and y . This field has a tangential discontinuity along the x -axis, as shown in Figure 2.17(a), which can only make sense in the framework of inviscid flow theory (see Chapter 3).



(a) Velocity field in the ‘laboratory’ frame.

(b) Velocity field in the frame moving with velocity $\frac{1}{2}(U_1 + U_2)$.

Fig. 2.17: Initial velocity profiles in the ‘laboratory’ and moving frames.

Assume that at time $t = 0$, the viscosity is ‘switched on’, and the discontinuity starts to smooth out, creating a transitional layer between the two streams. Find the velocity distribution in the layer.

Hint: If this problem is considered in the coordinate frame that moves steadily along the x -axis with speed $u_{\text{frame}} = \frac{1}{2}(U_1 + U_2)$, then the flow becomes symmetric with respect to the x -axis. The initial velocity profile in this frame is shown in Figure 2.17(b), where $U = \frac{1}{2}(U_1 - U_2)$.

2.2 Numerical Solutions

Exact solutions of the Navier–Stokes equations have an important role in revealing the physical nature of fluid motion. However, the situations where the Navier–Stokes equations allow for exact solutions are limited to rather simple cases. In all the examples considered in Section 2.1, with the exception of the Kármán flow, the nonlinear convective terms in the Navier–Stokes equations happen to vanish. In the Kármán flow, they do not disappear, but the flow displays a monotonic acceleration as the fluid particles move in the radial direction. In the general case, things are much more complicated. The problem of uniform flow past a rigid body may be regarded as one of the fundamental flow configurations in fluid dynamics. In Section 2.2.1 and then, in more detail, in Chapter 3 we shall study flow past a circular cylinder. We shall see that the fluid acceleration over the front part of the cylinder surface is followed by a deceleration near its rear part. The deceleration causes the flow to separate from the cylinder surface, which leads to the formation of a recirculating eddy behind the cylinder. The theory of flow separation will be presented in Part 3 of this book series. Here we shall restrict ourselves to showing the results of the numerical solution of the Navier–Stokes equations; no discussion of the numerical technique will be given. Our goal is to show how the flow past a circular cylinder changes with Reynolds number. Then, in Section 2.2.2, we consider another classical fluid-dynamic problem, recirculating flow in a rectangular cavity driven by a flat lid that moves parallel to itself. We use this example to demonstrate that the flow in the recirculation region becomes more and more complicated as the eddies in the recirculation region multiply with increasing Reynolds number.

2.2.1 Viscous flow past a circular cylinder

Let a circular cylinder of radius a be placed in a uniform flow of an incompressible viscous fluid; see Figure 2.18. We denote the free-stream velocity of the fluid far from the cylinder as V_∞ and the free-stream pressure as p_∞ . The fluid density ρ and the kinematic viscosity coefficient ν are assumed known constants. In order to describe the flow, we introduce a Cartesian coordinate system with its origin at the centre of the cylinder, the x -axis parallel to the free-stream velocity vector, the z -axis along the axis of the cylinder, and the y -axis in the perpendicular direction.

We shall assume that the free-stream velocity vector is perpendicular to the generatrix of the cylinder. In this case, one can expect the flow past the cylinder to be two-dimensional; that is, the ‘spanwise’ velocity component w is zero and none of the fluid-dynamic functions depends on z . We shall further assume that the flow is

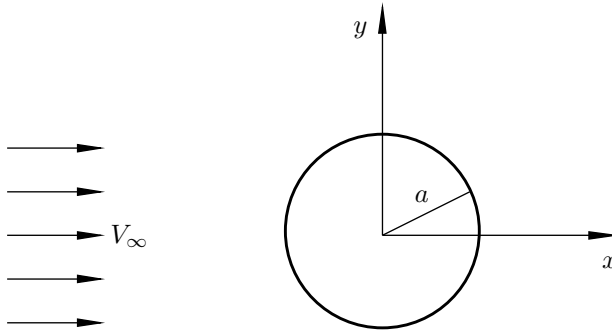


Fig. 2.18: Steady uniform flow past a circular cylinder.

steady and the body force \mathbf{f} is negligibly small. In these conditions, the Navier–Stokes equations (1.7.6) assume the form

$$u \frac{\partial u}{\partial x} + v \frac{\partial u}{\partial y} = -\frac{1}{\rho} \frac{\partial p}{\partial x} + \nu \left(\frac{\partial^2 u}{\partial x^2} + \frac{\partial^2 u}{\partial y^2} \right), \quad (2.2.1a)$$

$$u \frac{\partial v}{\partial x} + v \frac{\partial v}{\partial y} = -\frac{1}{\rho} \frac{\partial p}{\partial y} + \nu \left(\frac{\partial^2 v}{\partial x^2} + \frac{\partial^2 v}{\partial y^2} \right), \quad (2.2.1b)$$

$$\frac{\partial u}{\partial x} + \frac{\partial v}{\partial y} = 0. \quad (2.2.1c)$$

They have to be solved with the free-stream conditions,

$$u = V_\infty, \quad v = 0, \quad p = p_\infty \quad \text{at} \quad x^2 + y^2 = \infty, \quad (2.2.2)$$

and the no-slip conditions on the cylinder surface,

$$u = v = 0 \quad \text{if} \quad x^2 + y^2 = a^2. \quad (2.2.3)$$

When performing the calculations, it is convenient to use non-dimensional variables. These are introduced by means of the transformations

$$\begin{aligned} x &= a\bar{x}, & y &= a\bar{y}, \\ u &= V_\infty \bar{u}, & v &= V_\infty \bar{v}, & \hat{p} &= p_\infty + \rho V_\infty^2 \bar{p}. \end{aligned}$$

As a result, the Navier–Stokes equations (2.2.1) take the form

$$\bar{u} \frac{\partial \bar{u}}{\partial \bar{x}} + \bar{v} \frac{\partial \bar{u}}{\partial \bar{y}} = -\frac{\partial \bar{p}}{\partial \bar{x}} + \frac{1}{Re} \left(\frac{\partial^2 \bar{u}}{\partial \bar{x}^2} + \frac{\partial^2 \bar{u}}{\partial \bar{y}^2} \right), \quad (2.2.4a)$$

$$\bar{u} \frac{\partial \bar{v}}{\partial \bar{x}} + \bar{v} \frac{\partial \bar{v}}{\partial \bar{y}} = -\frac{\partial \bar{p}}{\partial \bar{y}} + \frac{1}{Re} \left(\frac{\partial^2 \bar{v}}{\partial \bar{x}^2} + \frac{\partial^2 \bar{v}}{\partial \bar{y}^2} \right), \quad (2.2.4b)$$

$$\frac{\partial \bar{u}}{\partial \bar{x}} + \frac{\partial \bar{v}}{\partial \bar{y}} = 0, \quad (2.2.4c)$$

where the Reynolds number Re is given by

$$Re = \frac{V_\infty a}{\nu}.$$

The free-stream conditions (2.2.2) are written in the non-dimensional variables as

$$\bar{u} = 1, \quad \bar{v} = \bar{p} = 0 \quad \text{at} \quad \bar{x}^2 + \bar{y}^2 = \infty, \quad (2.2.5)$$

and the no-slip conditions (2.2.3) become

$$\bar{u} = \bar{v} = 0 \quad \text{if} \quad \bar{x}^2 + \bar{y}^2 = 1. \quad (2.2.6)$$

For very small or very large values of the Reynolds number, analytical methods may be used to study the flow. However, when the Reynolds number is of order unity, the boundary-value problem (2.2.4)–(2.2.6) has to be solved numerically. The results of the calculations are shown in Figures 2.19 and 2.20 in the form of streamline plots.

At zero Reynolds number (see Figure 2.19a), the flow appears to be symmetric not only with respect to the \bar{x} -axis but also with respect to the \bar{y} -axis. When the Reynolds number increases to $Re = 2.5$, the flow loses its symmetry with respect to the \bar{y} -axis, but remains attached to the cylinder surface (see Figure 2.19b). Further increase of the Reynolds number leads to flow separation from the cylinder surface. As a result, two eddies form behind the cylinder. When the eddies first appear, they occupy a small vicinity of the rear stagnation point (see Figure 2.20). Then, as the Reynolds number increases, the separation point moves upstream along the cylinder surface, and by $Re = 200$ reaches its limiting position. The length of the eddies continues to grow as the Reynolds number increases beyond $Re = 200$. However, the flow in the vicinity of the cylinder stays almost unchanged.

It should be emphasised that the calculations were performed under the steady flow assumption. In reality, this assumption holds for $Re < 24$. As the Reynolds number exceeds $Re = 24$, laboratory observations as well as numerical simulations show that the flow becomes oscillatory, with vortices periodically shedding from the upper and lower sides of the cylinder. This vortex system is known as the *Kármán vortex street*.

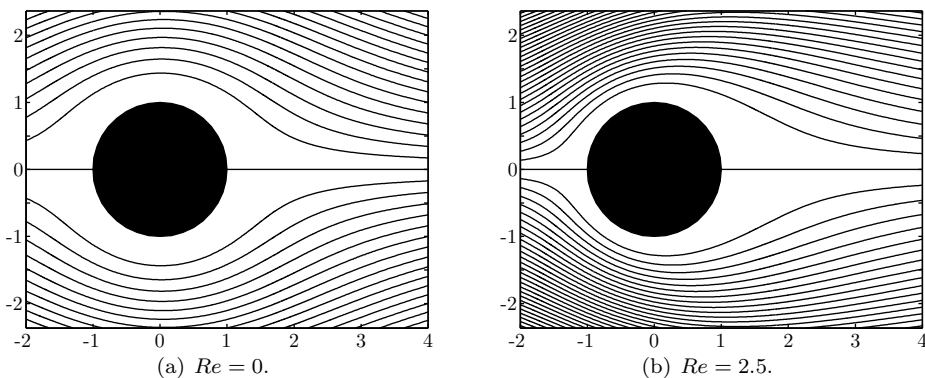


Fig. 2.19: Steady flow past a circular cylinder for Reynolds numbers $Re = 0$ and $Re = 2.5$.

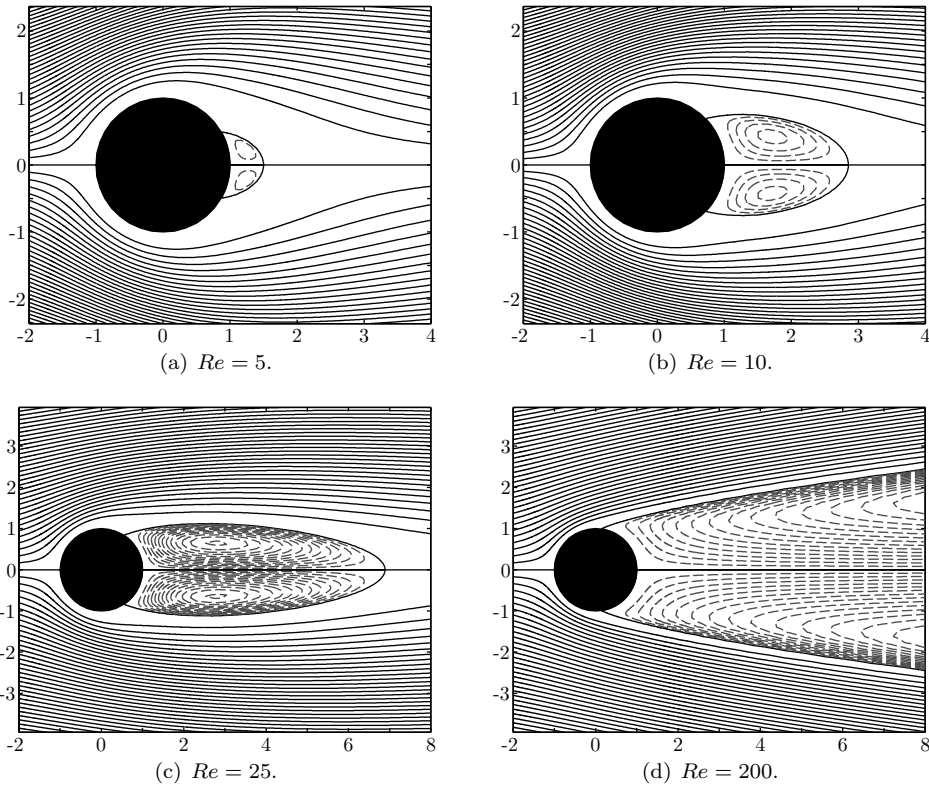


Fig. 2.20: Steady flow past a circular cylinder for Reynolds numbers $Re = 5, 10, 25,$ and 200 . The dashed lines show the streamlines in the recirculation eddies.

2.2.2 Lid-driven cavity flow

Another example that demonstrates the complexity of recirculation eddies is flow inside a cylinder with a square cross-section (see Figure 2.21). Here we assume that the two side walls AB and CD and the bottom wall AD are motionless, while the upper wall BC , termed the ‘lid’, moves parallel to itself with constant velocity V_0 . It is expected that the tangential stress produced by the lid motion will bring the fluid inside the ‘cavity’ into a recirculatory motion.

We shall study this motion assuming that the flow is steady and two-dimensional. We shall also assume that the body force \mathbf{f} is negligible. Under these conditions, the Navier–Stokes equations assume the form given by (2.2.1). They have to be solved with the no-slip conditions on the three motionless walls of the cavity,

$$u = v = 0 \quad \text{at} \quad \begin{cases} x = 0, & y \in [0, L], \\ y = 0, & x \in [0, L], \\ x = L, & y \in [0, L]. \end{cases} \quad (2.2.7a)$$

and, on the surface of the lid,

$$u = V_0, \quad v = 0 \quad \text{at} \quad y = L, \quad x \in [0, L], \quad (2.2.7b)$$

Here L denotes the width of the cavity, and we shall consider, as an example, the case when the height of the cavity coincides with its width; see Figure 2.21.

The non-dimensional variables are introduced by means of the equations⁸

$$\left. \begin{aligned} x &= L\bar{x}, & y &= L\bar{y}, \\ u &= V_0\bar{u}, & v &= V_0\bar{v}, & \hat{p} &= p_0 + \rho V_0^2\bar{p}. \end{aligned} \right\} \quad (2.2.8)$$

These turn the Navier–Stokes equations into

$$\bar{u} \frac{\partial \bar{u}}{\partial \bar{x}} + \bar{v} \frac{\partial \bar{u}}{\partial \bar{y}} = -\frac{\partial \bar{p}}{\partial \bar{x}} + \frac{1}{Re} \left(\frac{\partial^2 \bar{u}}{\partial \bar{x}^2} + \frac{\partial^2 \bar{u}}{\partial \bar{y}^2} \right), \quad (2.2.9a)$$

$$\bar{u} \frac{\partial \bar{v}}{\partial \bar{x}} + \bar{v} \frac{\partial \bar{v}}{\partial \bar{y}} = -\frac{\partial \bar{p}}{\partial \bar{y}} + \frac{1}{Re} \left(\frac{\partial^2 \bar{v}}{\partial \bar{x}^2} + \frac{\partial^2 \bar{v}}{\partial \bar{y}^2} \right), \quad (2.2.9b)$$

$$\frac{\partial \bar{u}}{\partial \bar{x}} + \frac{\partial \bar{v}}{\partial \bar{y}} = 0, \quad (2.2.9c)$$

which are identical to the equations (2.2.4) that we used in the circular cylinder problem. The only difference is that the Reynolds number is now defined as

$$Re = \frac{LV_0}{\nu}.$$

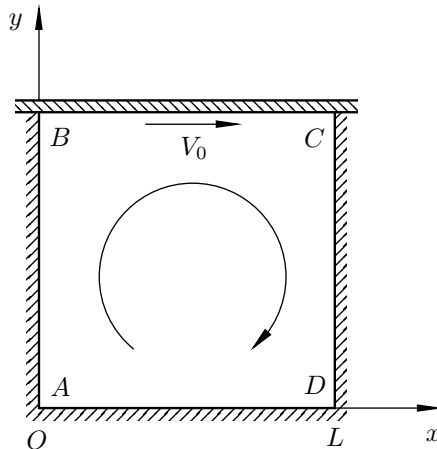


Fig. 2.21: Lid-driven cavity flow.

⁸Clearly, the choice of the ‘background’ pressure p_0 does not influence the velocity field.

The boundary conditions (2.2.7) are written in the non-dimensional variables as

$$\bar{u} = \bar{v} = 0 \quad \text{at} \quad \begin{cases} \bar{x} = 0, & \bar{y} \in [0, 1], \\ \bar{y} = 0, & \bar{x} \in [0, 1], \\ \bar{x} = 1, & \bar{y} \in [0, 1]. \end{cases} \quad (2.2.10a)$$

$$\bar{u} = 1, \quad v = 0 \quad \text{at} \quad \bar{y} = 1, \quad \bar{x} \in [0, 1], \quad (2.2.10b)$$

The results of the numerical solution of the boundary-value problem (2.2.9), (2.2.10) are displayed in Figure 2.22, where the streamlines are shown at different values of the Reynolds number. We see that when $Re = 0$ almost the entire flow region is occupied by a single primary eddy. Still, two small counter-rotating secondary eddies are observed near the lower corners of the cavity. The latter grow as the Reynolds number increases, and then additional eddies form inside the secondary eddies (see Figure 2.22d). Notice that flow separation is also observed on the left-hand side wall before the moving lid.

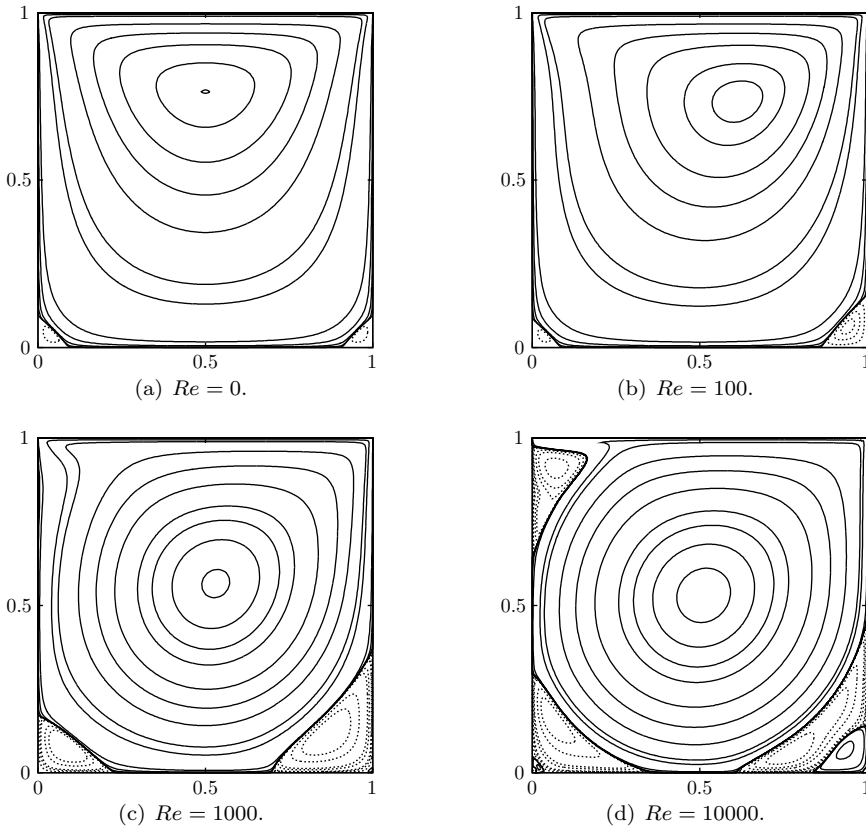


Fig. 2.22: Steady flow in a lid-driven cavity. The dashed lines show the eddies rotating in the anticlockwise direction.

3

Inviscid Incompressible Flows

3.1 Integrals of Motion

The motion of inviscid incompressible fluid flows is governed by the *Euler equations*

$$\frac{\partial \mathbf{V}}{\partial t} + (\mathbf{V} \cdot \nabla) \mathbf{V} = \mathbf{f} - \frac{1}{\rho} \nabla p \quad (\text{momentum equation}), \quad (3.1.1a)$$

$$\operatorname{div} \mathbf{V} = 0 \quad (\text{continuity equation}), \quad (3.1.1b)$$

which are obtained from the Navier–Stokes equations (1.7.5) by setting the viscosity coefficient ν to zero.¹

An alternative form of writing the momentum equation arises from using the Lamb formula (see Problem 2 in Exercises 4)

$$(\mathbf{V} \cdot \nabla) \mathbf{V} = \boldsymbol{\omega} \times \mathbf{V} + \nabla \left(\frac{V^2}{2} \right). \quad (3.1.2)$$

Here $\boldsymbol{\omega} = \operatorname{curl} \mathbf{V}$ and V is the modulus of the velocity vector \mathbf{V} . Substitution of (3.1.2) into (3.1.1) leads to the so-called *Gromeko–Lamb* form of the momentum equation:

$$\frac{\partial \mathbf{V}}{\partial t} + \boldsymbol{\omega} \times \mathbf{V} + \nabla \left(\frac{V^2}{2} \right) = \mathbf{f} - \frac{1}{\rho} \nabla p. \quad (3.1.3)$$

In further analysis, we will often use simplifications arising from the assumption that the body force \mathbf{f} is potential.

Definition 3.1 A body force field \mathbf{f} is termed *potential (or conservative)* if there exists a scalar function U such that

$$\mathbf{f} = -\nabla U. \quad (3.1.4)$$

The gravitational force clearly belongs to this class. If we introduce a Cartesian coordinate system with x and y lying in the horizontal plane and z directed vertically upwards, then equation (3.1.4) may be written in coordinate-decomposition form as

$$0 = -\frac{\partial U}{\partial x}, \quad 0 = -\frac{\partial U}{\partial y}, \quad -g = -\frac{\partial U}{\partial z},$$

¹Of course, the Euler equations were deduced significantly earlier than the Navier–Stokes equations. In fact, this was done by Euler as early as in 1755.

leading to

$$U = gz + C, \quad (3.1.5)$$

where C is an arbitrary constant.

We shall start our analysis of inviscid incompressible fluid motion by introducing a number of important integrals of the momentum equation. The first of these is the *Bernoulli integral*, which allows one to find the pressure distribution over a flow field with known velocity distribution.

3.1.1 Bernoulli integral

Theorem 3.1 *Let the fluid flow be steady and the body force potential. Then along any streamline, the Bernoulli integral*

$$\frac{V^2}{2} + \frac{p}{\rho} + U = H, \quad (3.1.6)$$

holds, where H remains constant along each streamline but might be different for different streamlines.

Proof Since the flow is steady ($\partial \mathbf{V} / \partial t = 0$) and the body force is potential ($\mathbf{f} = -\nabla U$), we can write the momentum equation (3.1.3) as

$$\boldsymbol{\omega} \times \mathbf{V} + \nabla \left(\frac{V^2}{2} + \frac{p}{\rho} + U \right) = 0. \quad (3.1.7)$$

Let line \mathcal{L} be a streamline. The unit vector $\boldsymbol{\tau}$ tangent to \mathcal{L} is parallel to the velocity vector \mathbf{V} , and therefore is perpendicular to $\boldsymbol{\omega} \times \mathbf{V}$, which ensures that the scalar product of $\boldsymbol{\tau}$ and $\boldsymbol{\omega} \times \mathbf{V}$ is zero. Hence, multiplying equation (3.1.7) by $\boldsymbol{\tau}$, we have

$$\boldsymbol{\tau} \cdot \nabla \left(\frac{V^2}{2} + \frac{p}{\rho} + U \right) = 0.$$

This proves that the expression in parentheses really stays constant along \mathcal{L} . □

3.1.2 Kelvin's Circulation Theorem

Kelvin's (1869) Circulation Theorem concerns the circulation of the velocity vector along a *fluid contour*. To introduce the notion of a fluid contour, let us consider a closed contour C_0 that is fixed with respect to the coordinate system $Oxyz$ as shown in Figure 3.1. Let us then 'mark' all the fluid particles that happen to be on the contour C_0 at an initial instant t_0 . We shall follow these particles as they move in space with increasing time t . Considered together, they constitute a fluid contour C that, owing to the continuity of the flow field, will remain closed for $t > t_0$.

The circulation along this contour is given by the integral (1.4.18):

$$\Gamma(t) = \oint_C \mathbf{V} \cdot d\mathbf{r}. \quad (3.1.8)$$

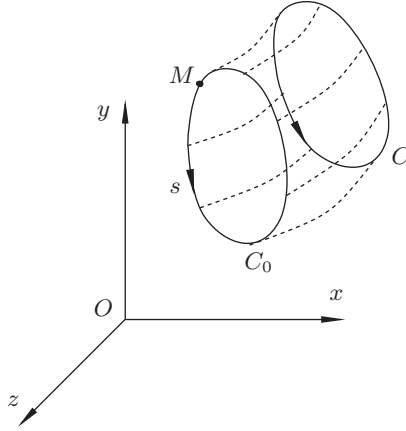


Fig. 3.1: Fluid contour.

Let us differentiate this integral with respect to time t . To perform the differentiation, it is convenient to introduce the Lagrangian position vector

$$\mathbf{r} = \mathbf{r}(t, \mathbf{r}_0). \quad (3.1.9)$$

Taking into account that, at $t = t_0$, all the fluid particles in which we are interested lie on C_0 , we can ‘mark’ them using the distance s measured along C_0 from, say, point M (see Figure 3.1). Correspondingly, we will write (3.1.9) as

$$\mathbf{r} = \mathbf{r}(t, s).$$

At each instant t , the variation of the position vector along C is given by

$$d\mathbf{r} = \frac{\partial \mathbf{r}}{\partial s} ds. \quad (3.1.10)$$

Using (3.1.10) in (3.1.8) yields

$$\Gamma(t) = \int_0^L \left(\mathbf{V} \cdot \frac{\partial \mathbf{r}}{\partial s} \right) ds, \quad (3.1.11)$$

where $\mathbf{V} = \mathbf{V}[t, \mathbf{r}(t, s)]$ and L is the entire length of the initial contour C_0 . Differentiation of (3.1.11) results in

$$\frac{d\Gamma}{dt} = \int_0^L \left(\frac{D\mathbf{V}}{Dt} \cdot \frac{\partial \mathbf{r}}{\partial s} \right) ds + \int_0^L \left(\mathbf{V} \cdot \frac{\partial^2 \mathbf{r}}{\partial s \partial t} \right) ds. \quad (3.1.12)$$

Taking into account that

$$\mathbf{V} = \frac{\partial \mathbf{r}}{\partial t},$$

we can calculate the second integral in (3.1.12) as

$$\int_0^L \left(\mathbf{V} \cdot \frac{\partial^2 \mathbf{r}}{\partial s \partial t} \right) ds = \int_0^L \left(\mathbf{V} \cdot \frac{\partial \mathbf{V}}{\partial s} \right) ds = \int_0^L \frac{\partial}{\partial s} \left(\frac{V^2}{2} \right) ds = \frac{V^2}{2} \Big|_{s=L} - \frac{V^2}{2} \Big|_{s=0}, \quad (3.1.13)$$

and, since $s = L$ and $s = 0$ represent the same point on contour C , we can conclude that this integral is zero.

Turning to the first integral in (3.1.12), we shall assume that the body force \mathbf{f} is potential. In this case, using (3.1.4) in (3.1.1a) yields

$$\frac{D\mathbf{V}}{Dt} = -\nabla \left(U + \frac{p}{\rho} \right),$$

and we have

$$\int_0^L \left(\frac{D\mathbf{V}}{Dt} \cdot \frac{\partial \mathbf{r}}{\partial s} \right) ds = - \oint_C \nabla \left(U + \frac{p}{\rho} \right) \cdot d\mathbf{r} = - \oint_C d \left(U + \frac{p}{\rho} \right). \quad (3.1.14)$$

Observing that the point of integration, after making a full circle along C , returns to its original position, we can conclude that the integral (3.1.14) is also zero.

This proves the following statement, known as *Kelvin's Circulation Theorem*.

Theorem 3.2 *In an inviscid incompressible fluid flow, the circulation Γ along any closed fluid contour does not change with time; i.e.*

$$\frac{d\Gamma}{dt} = 0,$$

*provided that the body force is potential.*²

This theorem plays an important role in fluid dynamics; it lays a foundation for potential flow theory. As we shall see, many inviscid flows may be treated as potential, in which case the Euler equations (3.1.1) reduce to the simpler Laplace equation. In fact, it is primarily because of this simplification that significant progress in inviscid flow theory has been achieved.

Before turning to a description of potential flow theory, we shall give here two examples that demonstrate how the Kelvin theorem may be used. The first concerns fluid flows that start from rest. If at an initial instant t_0 the flow velocity $\mathbf{V} = 0$, then the circulation along any closed contour C_0 is zero. According to Kelvin's Circulation Theorem, it will remain zero after the fluid is put into motion, and at any time $t > t_0$,

$$\oint_C \mathbf{V} \cdot d\mathbf{r} = 0, \quad (3.1.15)$$

where C is the fluid contour originating from C_0 .

²In particular, this theorem may be used when there is no body force at all.

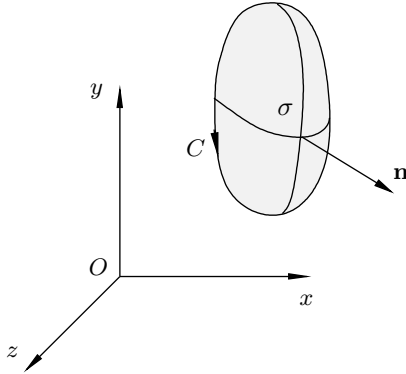


Fig. 3.2: Surface σ to which Stokes's theorem is applied.

Let us now consider a surface σ based on C as shown in Figure 3.2. We denote the unit vector normal to σ by \mathbf{n} and the area of a small element of σ by ds . Then, using Stokes's theorem, we have

$$\oint_C (\mathbf{V} \cdot d\mathbf{r}) = \iint_{\sigma} (\text{curl } \mathbf{V} \cdot \mathbf{n}) ds = \iint_{\sigma} (\boldsymbol{\omega} \cdot \mathbf{n}) ds,$$

and it follows that

$$\iint_{\sigma} (\boldsymbol{\omega} \cdot \mathbf{n}) ds = 0.$$

Taking into account the arbitrariness of C , we can conclude that any flow of this kind is *irrotational*, i.e. free of vorticity:

$$\boldsymbol{\omega} = \text{curl } \mathbf{V} = 0. \quad (3.1.16)$$

In the second example, we consider a rigid body placed into a uniform stream with free-stream velocity V_{∞} , as sketched in Figure 3.3. Assuming that there are no

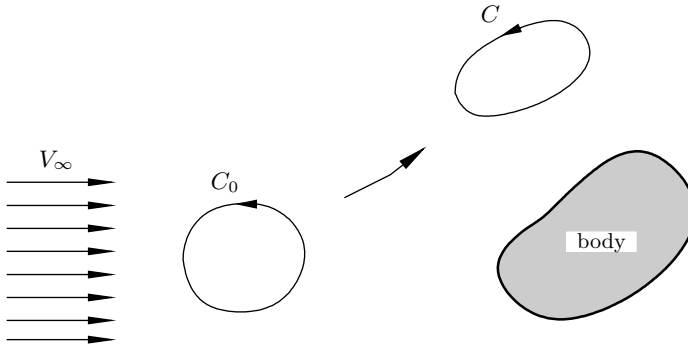


Fig. 3.3: Fluid contour motion in flow past a rigid body.

recirculating regions (these may form if the flow separates from the body surface), one can claim that any closed contour C in the flow field ‘originates’ from the corresponding contour C_0 in the oncoming flow. Since on C_0 the fluid velocity is constant, $\mathbf{V} = \mathbf{V}_\infty$, the circulation along C_0 is zero. According to Kelvin’s Circulation Theorem, it will remain zero as C_0 deforms into C . Hence, equation (3.1.15) holds again, and using Stokes’s theorem, we can prove that the flow is irrotational.

3.1.3 Cauchy–Lagrange integral

It will be shown in Section 3.2 that, for any irrotational flow satisfying equation (3.1.16), there exists a scalar function $\varphi(t, \mathbf{r})$, called the *velocity potential*, such that

$$\mathbf{V} = \nabla\varphi. \quad (3.1.17)$$

Hence, irrotational flows are also termed *potential flows*. In order to relate the pressure p to the velocity $V = |\mathbf{V}|$ in a potential flow, steady or unsteady, the *Cauchy–Lagrange theorem* may be used.

Theorem 3.3 *Suppose that the flow of an inviscid incompressible fluid is potential, $\mathbf{V} = \nabla\varphi$. Suppose further that the body force has potential U , such that $\mathbf{f} = -\nabla U$. Then the Cauchy–Lagrange integral holds:*

$$\frac{\partial\varphi}{\partial t} + \frac{V^2}{2} + \frac{p}{\rho} + U = \mathcal{F}(t) \quad (3.1.18)$$

with the function $\mathcal{F}(t)$ being independent of position in the flow field.

Proof Under the conditions of the theorem, we can write the momentum equation (3.1.3) as

$$\nabla\left(\frac{\partial\varphi}{\partial t}\right) + \boldsymbol{\omega} \times \mathbf{V} + \nabla\left(\frac{V^2}{2}\right) = -\nabla U - \nabla\left(\frac{p}{\rho}\right). \quad (3.1.19)$$

Substitution of (3.1.17) into (1.4.15) shows that any potential flow is irrotational, i.e. $\boldsymbol{\omega} = 0$. Thus, equation (3.1.19) may be written as

$$\nabla\left(\frac{\partial\varphi}{\partial t} + \frac{V^2}{2} + U + \frac{p}{\rho}\right) = 0,$$

which immediately proves that (3.1.18) is valid. \square

If the conditions of both Theorem 3.1 and Theorem 3.3 hold simultaneously, namely,

- the flow considered is steady,
- the body force is potential,
- and the flow is irrotational,

then the function H in (3.1.6) becomes independent of the streamline considered and the function $\mathcal{F}(t)$ is independent of time. Hence, we can write

$$\frac{V^2}{2} + \frac{p}{\rho} + U = C, \quad (3.1.20)$$

where C is a true constant.

Exercises 7

1. Consider a pipe with cross-sectional area A placed vertically into the Earth's gravitational field \mathbf{g} and connected to a horizontal pipe whose cross-sectional area is $A' = kA$, as shown in Figure 3.4. The vertical pipe is filled with water to height h_0 ; shutters FF' and GG' are used to prevent the water flowing into the horizontal pipe. Find the time that is required to discharge the vertical pipe after the shutters are opened. Both vertical and horizontal pipes are open to the atmosphere.

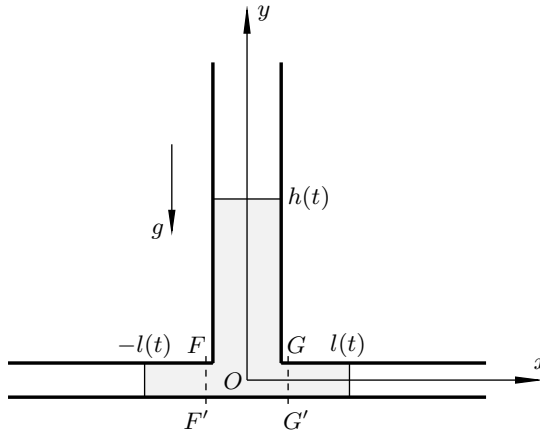


Fig. 3.4: Geometrical layout of the problem.

To solve this problem, denote the height of the water column in the vertical pipe at time t by $h(t)$, and use the Euler equations (3.1.1) to determine the pressure distribution in this pipe between $y = 0$ and $y = h(t)$.

Repeat the analysis for the horizontal pipe, and find the pressure distribution between $x = 0$ and $x = l(t)$.

Taking into account that at point O the pressure should be the same for the horizontal and vertical pipes, show that the function $h(t)$ satisfies the differential equation

$$\left(1 - \frac{1}{4k^2}\right)hh'' + \frac{h_0}{4k^2}h'' + gh = 0.$$

Solve this equation assuming that $k = A'/A = 0.5$.

Hint: You may assume that the water motion in both pipes is one-dimensional.

2. Prove that the Bernoulli integral (3.1.6) holds not only along streamlines but also along vortex lines.
3. An open barrel has a small orifice in the wall just above the base. It is filled with water to height h and placed into the Earth's gravitational field as shown in Figure 3.5. Using Bernoulli's equation, show that the velocity V in the jet that

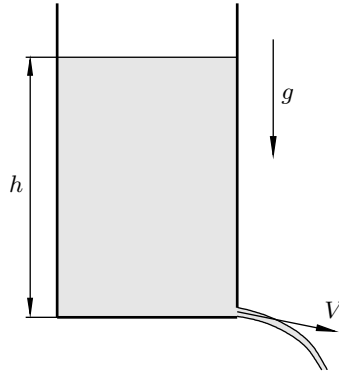


Fig. 3.5: Water escaping through a hole in a barrel.

forms as the water flows through the orifice may be calculated using the *Torricelli formula*

$$V = \sqrt{2gh}.$$

4. A thin spherical shell of radius R_0 is filled with water vapour and placed in deep water. At initial instant $t = 0$, the shell is destroyed and the vapour comes in contact with the water (see Figure 3.6).

Show that the time t_c that it takes for the bubble to collapse to a point may be calculated as

$$t_c = \int_0^{R_0} \frac{dR}{\sqrt{\frac{2\Delta p}{3\rho} \left(\frac{R_0^3}{R^3} - 1 \right)}}, \quad (3.1.21)$$

Here $\Delta p = p_\infty - p_0$, with p_∞ denoting the pressure far from the centre of the sphere and p_0 the vapour pressure.

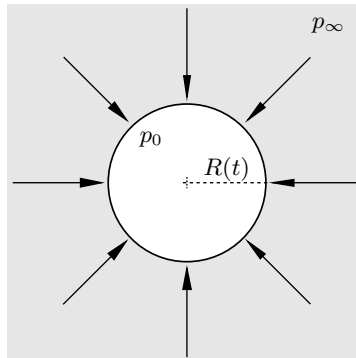


Fig. 3.6: Vapour bubble in deep water.

You may assume that the flow may be treated as inviscid. You may also assume that the flow is symmetrical with respect to the bubble centre and that gravitational effects are too small to affect the collapse process. You may finally assume that the pressure p_∞ far from the bubble and the vapour pressure p_0 inside the bubble remain constant during the collapse process. The governing Euler equations may be obtained by setting $\nu = 0$ in the Navier–Stokes equations (1.8.48).

- (a) Start your analysis with the continuity equation, and deduce that $r^2 V_r$ is a function of time only, say $f(t)$:

$$r^2 V_r = f(t). \quad (3.1.22)$$

Then, using the impermeability condition on the bubble surface, $r = R(t)$, show that

$$R^2 \frac{dR}{dt} = f(t). \quad (3.1.23)$$

- (b) Now, solve (3.1.22) for V_r , and using it in the radial momentum equation, deduce that

$$-\frac{f'(t)}{r} + \frac{1}{2} \frac{[f(t)]^2}{r^4} = -\frac{p}{\rho} + F(t). \quad (3.1.24)$$

Taking into account that the pressure far from the bubble centre is p_∞ and the pressure on the bubble surface is p_0 , deduce that

$$-\frac{f'(t)}{R(t)} + \frac{1}{2} \frac{[f(t)]^2}{[R(t)]^4} = \frac{p_\infty - p_0}{\rho}. \quad (3.1.25)$$

- (c) Equations (3.1.23) and (3.1.25) involve two unknown function, $f(t)$ and $R(t)$. In order to solve these equations, represent the function $f(t)$ in the form

$$f(t) = \Phi[R(t)],$$

and deduce that

$$\Phi = \pm \sqrt{R \left(C - \frac{2\Delta p}{3\rho} R^3 \right)},$$

where C is a constant. Then return to equation (3.1.23) and show that the time that it takes for the bubble to collapse to a point is given by (3.1.21).

5. Consider inviscid incompressible fluid flow through a symmetrical diffuser as shown in Figure 3.7. The diffuser expands from cross-section AA' , whose area is S_1 , to cross-section BB' with area S_2 . The fluid velocity at BB' is V .

Owing to the symmetry of the diffuser geometry, the total pressure force acting upon the inner surface of the diffuser (called the *thrust*) is directed along the diffuser axis. Using the integral momentum equation (1.7.30), find the value of the thrust

$$T = - \iint_{S_c} p n_x ds,$$

where n_x is the projection of \mathbf{n} on the x -axis drawn along the axis of the diffuser.

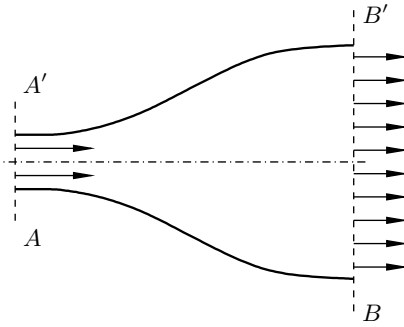


Fig. 3.7: Flow through a diffuser.

Suggestion: In the inviscid flow, the surface stress \mathbf{p}_n is represented by the pressure only, and is given by (1.2.14):

$$\mathbf{p}_n = -p\mathbf{n}, \quad (3.1.26)$$

where \mathbf{n} is the unit vector normal to the control surface S_c . With (3.1.26), the integral momentum equation (1.7.30) assumes the form

$$\iint_{S_c} [\rho(\mathbf{V} \cdot \mathbf{n})\mathbf{V} + p\mathbf{n}] ds = 0. \quad (3.1.27)$$

Choose the control surface S_c to be composed of the two walls of the diffuser, AB and $A'B'$, and the cross-sections AA' and BB' shown by the dashed lines in Figure 3.7, and consider the projection of the momentum equation (3.1.27) on the x -axis.

6. A jet of width d impinges upon a flat wall at an angle α as shown in Figure 3.8.

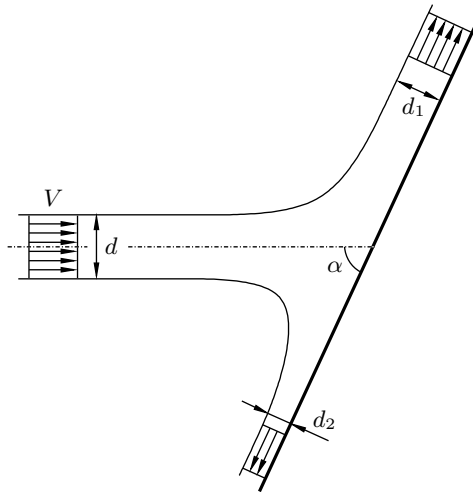


Fig. 3.8: Interaction of a jet with a flat wall.

The fluid velocity is uniform across the jet and equals V . Assuming that the flow is two-dimensional, i.e. the velocity vector $\mathbf{V} = (u, v, 0)$, find the total pressure force (per unit depth normal to the plane of the figure)

$$F = \int_{-\infty}^{\infty} (p - p_a) dx,$$

exerted on the wall. Here x is measured along the wall and p_a denotes the atmospheric pressure. What are the thicknesses d_1 and d_2 of the two streams propagating up and down the wall from the point of impact?

Suggestion: Consider two projections of equation (3.1.27), parallel to the wall and in the perpendicular direction. Use the Bernoulli equation to find the fluid velocity in the two streams propagating up and down the wall.

3.2 Potential Flows

We shall now prove that for any irrotational flow, i.e. a flow satisfying the equation

$$\boldsymbol{\omega} = \text{curl } \mathbf{V} = 0, \quad (3.2.1)$$

there exists a scalar function $\varphi(t, \mathbf{r})$, called the *velocity potential*, such that

$$\nabla\varphi = \mathbf{V}.$$

We start by choosing a reference point M_0 whose position vector is \mathbf{r}_0 ; see Figure 3.9. For any other point M in the flow field, we define a function $\varphi(t, \mathbf{r})$ as

$$\varphi(t, \mathbf{r}) = \int_C \mathbf{V} \cdot d\mathbf{r}, \quad (3.2.2)$$

where C is a contour connecting points M_0 and M .

It may easily be shown that $\varphi(t, \mathbf{r})$ is a scalar function, i.e. it depends on the position vector \mathbf{r} of point M but not on the choice of contour C . Indeed, if we choose another contour C' and write

$$\varphi'(t, \mathbf{r}) = \int_{C'} \mathbf{V} \cdot d\mathbf{r},$$

then the difference between $\varphi(t, \mathbf{r})$ and $\varphi'(t, \mathbf{r})$ may be expressed as

$$\varphi(t, \mathbf{r}) - \varphi'(t, \mathbf{r}) = \int_C \mathbf{V} \cdot d\mathbf{r} - \int_{C'} \mathbf{V} \cdot d\mathbf{r} = \oint_{\tilde{C}} \mathbf{V} \cdot d\mathbf{r},$$

where \tilde{C} is the closed contour composed of C and C' , the latter being traced in the negative direction, i.e. from M to M_0 . If an open surface σ lying entirely in the flow

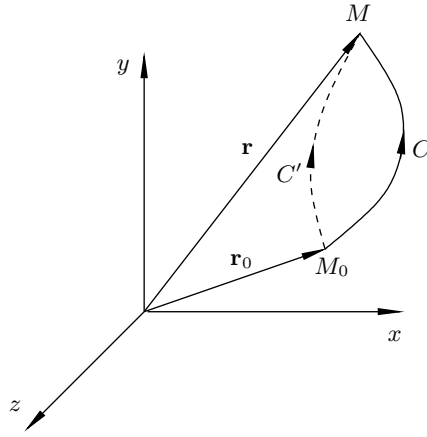


Fig. 3.9: Calculation of the velocity potential.

field may be built on contour \tilde{C} (as in Figure 3.2), then, using Stokes's theorem, we can write

$$\oint_{\tilde{C}} \mathbf{V} \cdot d\mathbf{r} = \iint_{\sigma} (\text{curl } \mathbf{V} \cdot \mathbf{n}) ds, \quad (3.2.3)$$

and it follows from (3.2.1) that $\varphi(t, \mathbf{r}) = \varphi'(t, \mathbf{r})$.

As the result of integration in (3.2.2) does not depend on the choice of contour C , it is more appropriate to write

$$\varphi(t, \mathbf{r}) = \int_{\mathbf{r}_0}^{\mathbf{r}} \mathbf{V} \cdot d\mathbf{r}. \quad (3.2.4)$$

A small variation $\delta\mathbf{r}$ of the position vector \mathbf{r} leads to

$$\varphi(t, \mathbf{r} + \delta\mathbf{r}) = \int_{\mathbf{r}_0}^{\mathbf{r} + \delta\mathbf{r}} \mathbf{V} \cdot d\mathbf{r},$$

whence

$$\varphi(t, \mathbf{r} + \delta\mathbf{r}) - \varphi(t, \mathbf{r}) = \int_{\mathbf{r}}^{\mathbf{r} + \delta\mathbf{r}} \mathbf{V} \cdot d\mathbf{r}. \quad (3.2.5)$$

If \mathbf{V} is a continuous function of \mathbf{r} , then, owing to the smallness of $\delta\mathbf{r}$, the integral on the right-hand side of (3.2.5) may be approximated by $\mathbf{V}(t, \mathbf{r}) \cdot \delta\mathbf{r}$, and we have

$$\varphi(t, \mathbf{r} + \delta\mathbf{r}) - \varphi(t, \mathbf{r}) = \mathbf{V}(t, \mathbf{r}) \cdot \delta\mathbf{r}.$$

This proves that $\mathbf{V}(t, \mathbf{r})$ is indeed equal to the gradient of the function $\varphi(t, \mathbf{r})$:

$$\mathbf{V} = \nabla\varphi. \quad (3.2.6)$$

It should be noted that equation (3.2.2) defines the velocity potential φ to within an arbitrary function of time t , which depends on the choice of the reference point \mathbf{r}_0 .

However, the difference between the values of $\varphi(t, \mathbf{r})$ corresponding to two different choices of \mathbf{r}_0 is independent of \mathbf{r} , and therefore has no effect on the velocity field calculated with the help of (3.2.6).

Substitution of (3.2.6) into the continuity equation (3.1.1b) leads to Laplace's equation

$$\nabla^2 \varphi = 0. \quad (3.2.7)$$

The boundary conditions for this equation depend on the particular problem under consideration. Let us suppose, for example, that flow past a rigid body is being studied. If the flow were viscous, then the no-slip conditions would have to be used on the body surface. However, unlike the Navier–Stokes equation (1.7.5a), the Euler equation (3.1.1a) does not contain the second-order derivative on the right-hand side. Therefore, the no-slip condition has to be relaxed, and one has to use instead the *impermeability condition*. This condition implies that the surface of a rigid body is impenetrable,³ which means that the fluid particles that come in contact with the body's surface will remain on this surface for some time, moving along it downstream.

If the body's surface is represented by the equation

$$\Phi(t, \mathbf{r}) = \text{const},$$

then, using the Lagrangian position function $\mathbf{r} = \mathbf{r}(t, \mathbf{r}_0)$, we can claim that, for all fluid particles that happen to be on this surface,

$$\Phi[t, \mathbf{r}(t, \mathbf{r}_0)] = \text{const}. \quad (3.2.8)$$

Differentiation of (3.2.8) with respect to t yields

$$\frac{\partial \Phi}{\partial t} + \nabla \Phi \cdot \frac{\partial \mathbf{r}}{\partial t} = 0,$$

and, since the derivative of the position vector $\partial \mathbf{r} / \partial t$ gives the fluid velocity \mathbf{V} , we can write

$$\left(\frac{1}{|\nabla \Phi|} \frac{\partial \Phi}{\partial t} + \mathbf{V} \cdot \mathbf{n} \right) \Big|_S = 0. \quad (3.2.9)$$

Here the subscript S is used to indicate that this equation holds on the body's surface and \mathbf{n} denotes the unit vector normal to this surface,

$$\mathbf{n} = \frac{1}{|\nabla \Phi|} \nabla \Phi.$$

When the body remains motionless in the coordinate frame used, the impermeability condition (3.2.9) reduces to

$$(\mathbf{V} \cdot \mathbf{n}) \Big|_S = 0, \quad (3.2.10)$$

which means that the velocity vector should be tangent to the surface of a rigid body.

³This, of course, is not true if, say, flow over a perforated wall is studied.

Condition (3.2.10) may be rewritten for the velocity potential φ as follows:

$$(\nabla\varphi \cdot \mathbf{n})\Big|_S = \frac{\partial\varphi}{\partial n}\Big|_S = 0.$$

One can intuitively expect the flow past a rigid body to depend on the body's shape as well as on the characteristics of the oncoming flow. Information about the body's shape is given by the impermeability condition. A second boundary condition, termed the *free-stream condition*, is needed to specify the oncoming flow. If, far from the body, the flow is uniform, with velocity \mathbf{V}_∞ , then we can write

$$\mathbf{V} \rightarrow \mathbf{V}_\infty \quad \text{as} \quad |\mathbf{r}| \rightarrow \infty. \quad (3.2.11)$$

This may be reformulated for the potential function φ as

$$\varphi = \mathbf{V}_\infty \cdot \mathbf{r} + \cdots \quad \text{as} \quad |\mathbf{r}| \rightarrow \infty.$$

Hence, to describe potential flow past a motionless body, one needs to solve the following problem.

Problem 3.1 Find the velocity potential φ that satisfies Laplace's equation

$$\nabla^2\varphi = 0 \quad (3.2.12a)$$

everywhere inside the flow field. It should also satisfy the impermeability condition

$$\frac{\partial\varphi}{\partial n}\Big|_S = 0 \quad (3.2.12b)$$

on the body's surface and the free-stream condition

$$\varphi = \mathbf{V}_\infty \cdot \mathbf{r} + \cdots \quad \text{as} \quad |\mathbf{r}| \rightarrow \infty \quad (3.2.12c)$$

in the far field.

We shall now discuss various ways in which Laplace's equation (3.2.12a) can be solved. We shall start with the *principle of superposition*, which is applicable to any linear equation. It is easily seen that if the functions φ_1 and φ_2 satisfy Laplace's equation, then their linear combination $\varphi = c_1\varphi_1 + c_2\varphi_2$, with arbitrary coefficients c_1 and c_2 , is also a solution of Laplace's equation. Keeping this in mind, we shall introduce some simple examples of potential flows that may be used as building blocks for more complicated solutions.

Flow from a source

Let us start with flow from a point source in otherwise stagnant fluid. We shall define the intensity of the source, q , as a quantity that, when multiplied by the fluid density ρ , gives the mass of fluid produced by the source per unit time. Taking into account the spherical symmetry of the flow, we use spherical polar coordinates; see Figure 3.10.

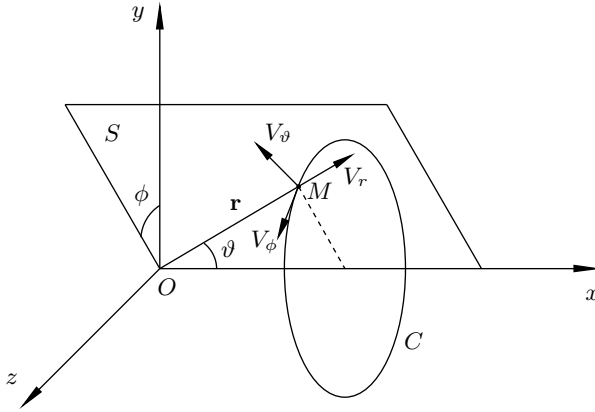


Fig. 3.10: Spherical polar coordinates.

We place the source at the coordinate origin O , and we expect that at any point M , with position vector \mathbf{r} , the velocity is directed from the source, i.e. along \mathbf{r} . This means that in the flow considered here, only the radial velocity V_r is non-zero, and it does not depend on the angles ϕ and ϑ . Therefore, if we draw a sphere of radius r with centre at the source, then, using the mass conservation law, we can write

$$4\pi r^2 V_r = q, \quad (3.2.13)$$

where $4\pi r^2$ stands for the area of the sphere surface. Solving (3.2.13) for V_r , we have

$$V_r = \frac{q}{4\pi r^2}. \quad (3.2.14)$$

In order to find the velocity potential φ for this flow, equation (3.2.6) should be used. Inserting (1.8.47) into (1.8.9), we see that the gradient of φ is written in spherical polar coordinates as

$$\nabla\varphi = \frac{\partial\varphi}{\partial r}\mathbf{e}_r + \frac{1}{r}\frac{\partial\varphi}{\partial\vartheta}\mathbf{e}_\vartheta + \frac{1}{r\sin\vartheta}\frac{\partial\varphi}{\partial\phi}\mathbf{e}_\phi.$$

Consequently, equation (3.2.6) is written in coordinate-decomposition form as

$$V_r = \frac{\partial\varphi}{\partial r}, \quad V_\vartheta = \frac{1}{r}\frac{\partial\varphi}{\partial\vartheta}, \quad V_\phi = \frac{1}{r\sin\vartheta}\frac{\partial\varphi}{\partial\phi}. \quad (3.2.15)$$

Combining the first of equations (3.2.15) with (3.2.14) yields

$$\frac{\partial\varphi}{\partial r} = \frac{q}{4\pi r^2}, \quad (3.2.16)$$

while from the second and third equations in (3.2.15) we see that φ is independent of ϑ and ϕ .

Integration of (3.2.16) results in⁴

$$\varphi = -\frac{q}{4\pi r}, \quad (3.2.17)$$

which is the sought potential of a source (sink for $q < 0$) situated at the origin. If a source is placed at point \mathbf{r}_0 , then (3.2.17) should be rewritten as

$$\varphi = -\frac{q}{4\pi|\mathbf{r} - \mathbf{r}_0|}.$$

Dipole

Let us now consider a source and a sink of the same intensity placed close to one another. We shall assume that the source is situated at the coordinate origin and the sink at the point with position vector $\delta\mathbf{r}_0$. Then, using the principle of superposition, we have

$$\varphi = \underbrace{-\frac{q}{4\pi|\mathbf{r}|}}_{\text{source}} + \underbrace{\frac{q}{4\pi|\mathbf{r} - \delta\mathbf{r}_0|}}_{\text{sink}}. \quad (3.2.18)$$

If $|\delta\mathbf{r}_0|$ is small, then, neglecting squares of perturbations, we can write

$$\begin{aligned} |\mathbf{r} - \delta\mathbf{r}_0| &= \sqrt{(x - \delta x_0)^2 + (y - \delta y_0)^2 + (z - \delta z_0)^2} \\ &= \sqrt{x^2 + y^2 + z^2 - 2x\delta x_0 - 2y\delta y_0 + 2z\delta z_0 + \dots}, \end{aligned}$$

or, equivalently,

$$|\mathbf{r} - \delta\mathbf{r}_0| = \sqrt{r^2 - 2(\mathbf{r} \cdot \delta\mathbf{r}_0) + \dots} = r \left(1 - 2 \frac{\mathbf{r} \cdot \delta\mathbf{r}_0}{r^2} + \dots \right)^{1/2}. \quad (3.2.19)$$

Formula (3.2.19) may be simplified further using the well-known Taylor expansion

$$(1 + \varepsilon)^\alpha = 1 + \alpha\varepsilon + O(\varepsilon^2). \quad (3.2.20)$$

Choosing $\alpha = \frac{1}{2}$ in (3.2.20), we can see that (3.2.19) may be written as

$$|\mathbf{r} - \delta\mathbf{r}_0| = r \left(1 - \frac{\mathbf{r} \cdot \delta\mathbf{r}_0}{r^2} \right) + O(|\delta\mathbf{r}_0|^2). \quad (3.2.21)$$

It remains to substitute (3.2.21) into (3.2.18),

$$\varphi = -\frac{q}{4\pi r} + \frac{q}{4\pi r} \frac{1}{1 - (\mathbf{r} \cdot \delta\mathbf{r}_0)/r^2},$$

and use (3.2.20) again, now with $\alpha = -1$. We find

⁴An arbitrary constant may always be added to (3.2.17) since the velocity potential is defined to within an arbitrary choice of the reference position vector \mathbf{r}_0 .

$$\begin{aligned}\varphi &= -\frac{q}{4\pi r} + \frac{q}{4\pi r} \left(1 + \frac{\mathbf{r} \cdot \delta\mathbf{r}_0}{r^2}\right) + O(|\delta\mathbf{r}_0|^2) \\ &= \frac{q}{4\pi} \frac{\mathbf{r} \cdot \delta\mathbf{r}_0}{r^3} + O(|\delta\mathbf{r}_0|^2).\end{aligned}\tag{3.2.22}$$

Finally, we assume that $|\delta\mathbf{r}_0|$ tends to zero and q tends to infinity such that their product remains finite. This leads to the following expression for the dipole potential:

$$\varphi = \frac{\mathbf{m} \cdot \mathbf{r}}{4\pi r^3}.\tag{3.2.23}$$

Here the vector $\mathbf{m} = q \delta\mathbf{r}_0$ is referred to as the *dipole moment*.

The dipole flow (3.2.23) is symmetric with respect to an axis drawn along the vector \mathbf{m} . In particular, if $\mathbf{m} = (m, 0, 0)$, then the axis of symmetry coincides with the x -axis, and the streamline pattern in the S -plane of Figure 3.10 is independent of the azimuthal angle ϕ . It is shown in Figure 3.11.

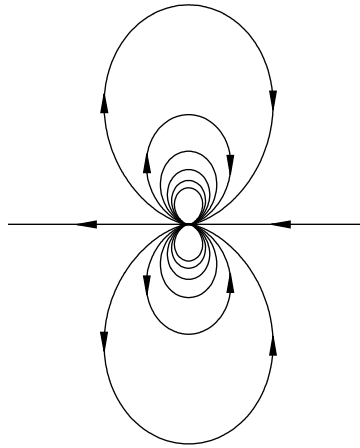


Fig. 3.11: Dipole streamline pattern.

3.2.1 Potential flow past a sphere

We shall now show that a superposition of a uniform flow and a dipole gives a solution of Problem 3.1 (see page 142) that describes flow past a rigid motionless sphere. For any direction of the oncoming flow, one can always rotate the coordinate system to make the x -axis aligned with the free-stream velocity (see Figure 3.12). Then the potential (3.2.12c) of the uniform flow becomes

$$\varphi = V_\infty x.\tag{3.2.24}$$

Let us place the dipole into the sphere's centre and assume that it is also aligned with

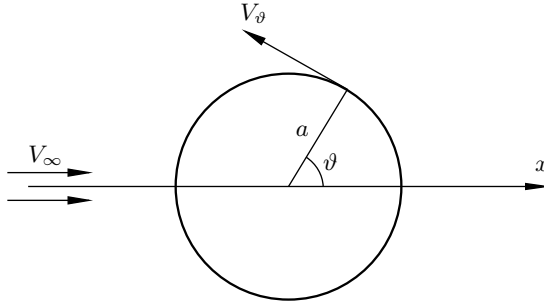


Fig. 3.12: The flow view in the plane S of Figure 3.10.

the x -axis, i.e. its moment $\mathbf{m} = (m, 0, 0)$. In this case, (3.2.23) reduces to

$$\varphi = \frac{mx}{4\pi r^3}. \tag{3.2.25}$$

Superposing (3.2.24) with (3.2.25), we have

$$\varphi = V_\infty x + \frac{mx}{4\pi r^3}. \tag{3.2.26}$$

Let us now examine the boundary conditions (3.2.12b,c). As $r \rightarrow \infty$, the second term in (3.2.26) tends to zero, reducing (3.2.26) to (3.2.24), which proves that the free-stream boundary condition is satisfied. Turning to the impermeability condition (3.2.12b), we note that at any point situated outside the sphere, $x = r \cos \vartheta$, and equation (3.2.26) may be written as

$$\varphi = V_\infty r \cos \vartheta + \frac{m \cos \vartheta}{4\pi r^2}. \tag{3.2.27}$$

With a being the radius of the sphere, we have

$$\left. \frac{\partial \varphi}{\partial n} \right|_S = \left. \frac{\partial \varphi}{\partial r} \right|_{r=a} = \left(V_\infty - \frac{m}{2\pi a^3} \right) \cos \vartheta.$$

Therefore, by choosing

$$m = 2\pi a^3 V_\infty, \tag{3.2.28}$$

we can satisfy the impermeability condition (3.2.12b) for all values of ϑ , i.e. on the entire surface of the sphere. This proves that formula (3.2.27) really represents the solution for the flow past the sphere. Substituting (3.2.28) back into (3.2.27) results in

$$\varphi = V_\infty \left(r + \frac{a^3}{2r^2} \right) \cos \vartheta. \tag{3.2.29}$$

In this flow, the azimuthal velocity V_ϕ is, obviously, zero. The radial and meridional velocities may be calculated using formulae (3.2.15):

$$V_r = \frac{\partial \varphi}{\partial r} = V_\infty \left(1 - \frac{a^3}{r^3} \right) \cos \vartheta, \quad V_\vartheta = \frac{1}{r} \frac{\partial \varphi}{\partial \vartheta} = -V_\infty \left(1 + \frac{a^3}{2r^3} \right) \sin \vartheta. \tag{3.2.30}$$

On the sphere's surface ($r = a$), the radial velocity component disappears, as it should in view of the impermeability condition. Hence, the velocity vector is tangent to the sphere's surface and given by

$$V_\vartheta \Big|_{r=a} = -\frac{3}{2}V_\infty \sin \vartheta. \quad (3.2.31)$$

The minus sign in this formula implies that the velocity is directed against increasing ϑ ; see Figure 3.12. It turns zero at the front ($\vartheta = \pi$) and rear ($\vartheta = 0$) stagnation points, and reaches its maximum at the equator ($\vartheta = \pi/2$), where $|V_\vartheta| = \frac{3}{2}V_\infty$.

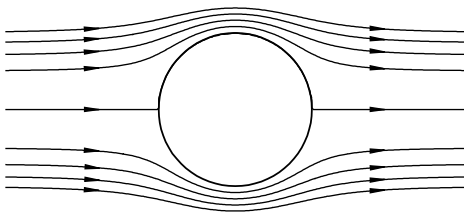
It is interesting to note that the velocity (3.2.31) is symmetric with respect to the equator ($\vartheta = \frac{1}{2}\pi$). Let us now find the pressure distribution. Since the flow considered is steady and potential, one can use the Bernoulli equation in the form given by (3.1.20). Disregarding the body force and using the free-stream conditions to calculate the constant C on the right-hand side of (3.1.20), we have

$$\frac{V^2}{2} + \frac{p}{\rho} = \frac{V_\infty^2}{2} + \frac{p_\infty}{\rho}. \quad (3.2.32)$$

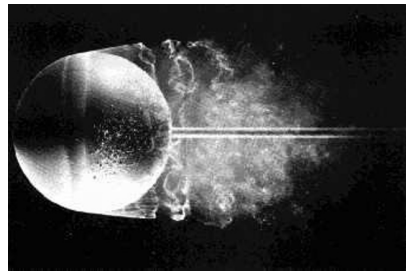
Substituting (3.2.31) into (3.2.32) and solving the resulting equation for p , we find that on the surface of the sphere

$$p = p_\infty + \frac{1}{2}\rho V_\infty^2 \left(1 - \frac{9}{4}\sin^2 \vartheta\right).$$

Since the pressure is symmetric with respect to the equator, the integral pressure force acting upon the front hemisphere is entirely balanced by the pressure force acting upon the rear hemisphere, which suggests that the sphere should experience no resistance when moving through a fluid with constant velocity. This result is known as the *d'Alembert paradox*. As unrealistic as it appears to be, zero-drag prediction is not a unique property of the sphere flow, but rather a common feature of inviscid flow theory.



(a) Theoretical streamline pattern.



(b) Visualization of sphere flow at $Re = 15,000$ by H. Werlé; (see Figure 55 in Van Dyke, 1982, p. 34).

Fig. 3.13: Comparison of potential flow theory with experimental observations.

In Figure 3.13, the streamline pattern, drawn using solution (3.2.29), is compared with an experimental visualisation of the flow. As can be seen, in reality, the flow does not remain attached to the sphere's surface. Instead, it separates near the equator, leading to a distortion in the flow field. The flow loses its symmetry and, as a result, a non-zero drag is produced. Experimental observations also show that, once separated, the flow normally develops unsteadiness, which leads to an additional drag.

3.2.2 Virtual mass

Unlike the steady flow past a sphere, an unsteady flow can remain attached for a period of time. Here we shall consider the flow around a sphere that is produced in the following way. Suppose that the sphere is initially kept at rest and is surrounded by a fluid that is also motionless. Then the sphere is brought in motion, causing the fluid around it to yield. Numerous experiments show that the resulting fluid flow remains fully attached for some time. During this time, the solution (3.2.29) remains valid.

We shall now generalise the above analysis for a sphere that moves through a fluid with variable velocity. In this case, the coordinate system attached to the sphere appears to be non-inertial, and we shall use instead the 'laboratory coordinate system' $O'x'y'z'$, in which the fluid far from the moving sphere remains at rest.

If we assume, to begin with, that the velocity of the sphere is constant, then the solution in the laboratory frame may be obtained from (3.2.29) by means of a Galilean transformation (see Figure 3.14):

$$\begin{aligned} x &= x' + V_\infty t, & y &= y', & z &= z', \\ u &= u' + V_\infty, & v &= v', & w &= w', \\ \varphi &= \varphi' + V_\infty x. \end{aligned} \tag{3.2.33}$$

Taking into account that $r \cos \vartheta = x$ (see Figure 3.10) and using (3.2.29) in (3.2.33), we find

$$\varphi' = V_\infty \frac{a^3}{2r^2} \cos \vartheta, \tag{3.2.34}$$

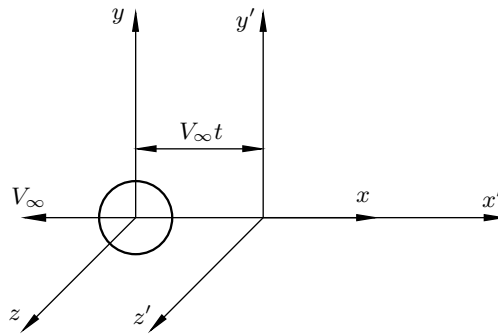


Fig. 3.14: Laboratory frame (x', y', z') and coordinate frame (x, y, z) moving with the sphere.

where

$$\cos \vartheta = \frac{x}{r} = \frac{x' + V_\infty t}{r}, \quad r = \sqrt{x^2 + y^2 + z^2} = \sqrt{(x' + V_\infty t)^2 + y'^2 + z'^2}.$$

We shall now generalise this solution for a sphere moving along the x' -axis with variable velocity $V_0(t)$; it will be assumed that positive V_0 corresponds to motion in the positive x' -direction. Taking into account that formula (3.2.34) represents the solution for a sphere that moves in the laboratory frame in the negative x' -direction with velocity V_∞ , we have to replace V_∞ in (3.2.34) by $-V_0(t)$, which yields

$$\varphi' = -V_0(t) \frac{a^3}{2r^2} \cos \vartheta. \quad (3.2.35)$$

Here

$$\cos \vartheta = \frac{x' - x_0(t)}{r}, \quad r^2 = [x' - x_0(t)]^2 + y'^2 + z'^2,$$

with $x_0(t)$ being the position of the sphere's centre at instant t , such that

$$\frac{dx_0}{dt} = V_0(t).$$

In order to demonstrate that the heuristic approach employed to deduce formula (3.2.35) really gives the sought solution for the velocity potential, we need to return to Problem 3.1 (see page 142). First of all, the velocity potential φ has to satisfy Laplace's equation (3.2.12a). This requirement may be verified by direct differentiation of (3.2.35). Alternatively, one can notice that (3.2.35) represents a particular form of the dipole (3.2.23); the latter was introduced as an elementary solution of Laplace's equation.

Turning to the impermeability condition (3.2.12b), we have to write it in the form (3.2.9) suitable for unsteady flows. With the velocity component normal to the sphere expressed as

$$(\mathbf{V} \cdot \mathbf{n}) \Big|_S = \frac{\partial \varphi'}{\partial r} \Big|_{r=a},$$

the impermeability condition (3.2.9) assumes the form

$$\left(\frac{1}{|\nabla \Phi|} \frac{\partial \Phi}{\partial t} + \frac{\partial \varphi'}{\partial r} \right) \Big|_{r=a} = 0. \quad (3.2.36)$$

Here the function $\Phi(t, x', y', z')$ represents the body's surface. For the sphere of radius a ,

$$\Phi(t, x', y', z') = [x' - x_0(t)]^2 + y'^2 + z'^2 - a^2.$$

We see that

$$\frac{\partial \Phi}{\partial t} = -2[x' - x_0(t)] \frac{dx_0}{dt} = -2[x' - x_0(t)] V_0(t) = -2r \cos \vartheta V_0(t).$$

The modulus of the gradient of the function Φ is calculated as

$$|\nabla\Phi| = \sqrt{\left(\frac{\partial\Phi}{\partial x'}\right)^2 + \left(\frac{\partial\Phi}{\partial y'}\right)^2 + \left(\frac{\partial\Phi}{\partial z'}\right)^2} = \sqrt{4[x' - x_0(t)]^2 + 4y'^2 + 4z'^2} = 2r.$$

Consequently, the first term in (3.2.36) is

$$\frac{1}{|\nabla\Phi|} \frac{\partial\Phi}{\partial t} = -V_0(t) \cos \vartheta.$$

The second term is obtained by differentiating (3.2.35) with respect to r :

$$\left. \frac{\partial\varphi'}{\partial r} \right|_{r=a} = V_0(t) \cos \vartheta.$$

This proves that the function (3.2.35) satisfies the impermeability condition (3.2.36).

Finally, we need to check if the far-field boundary condition (3.2.12c) is satisfied. In the laboratory frame, it is written as

$$\varphi' \rightarrow 0 \quad \text{as} \quad r \rightarrow \infty,$$

which is certainly true for (3.2.35)

Having established the validity of the solution (3.2.35), we shall now turn to calculation of the resultant force acting on the sphere. As the flow around the sphere is axisymmetric, only the projection of the force on the x' -axis needs to be calculated. If ds is the area of a small element of the sphere's surface, then the pressure force acting on this element

$$dF = p ds.$$

Its projection on the x' -axis is (see Figure 3.15)

$$dF_x = p ds \cos \vartheta. \tag{3.2.37}$$

Let us consider an annular element of width b on the sphere's surface, shown in Figure 3.15 by dashed lines. Its area is calculated as

$$ds = b 2\pi h.$$

Here h is the radius of the annular element; it may be expressed via the sphere radius a as $h = a \sin \vartheta$. Taking further into account that $b = a d\vartheta$, we can write (3.2.37) in the form⁵

$$dF_x = 2\pi a^2 p \cos \vartheta \sin \vartheta d\vartheta. \tag{3.2.38}$$

Integration of (3.2.38) gives the resultant force

$$F_x = 2\pi a^2 \int_0^\pi p \cos \vartheta \sin \vartheta d\vartheta. \tag{3.2.39}$$

⁵Notice that positive dF_x corresponds to a force directed opposite to the x' -axis.

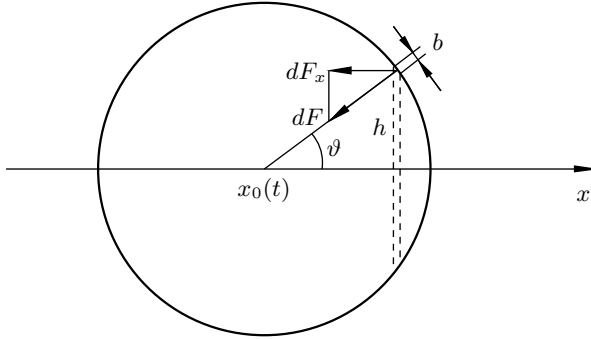


Fig. 3.15: Calculation of the drag of accelerating sphere.

To calculate the integral in (3.2.39), we need to know the pressure distribution along the sphere surface. It may be calculated using the Cauchy–Lagrange integral (3.1.18). Assuming that the body force \mathbf{f} is negligible, we can write

$$\frac{\partial \varphi}{\partial t} + \frac{V^2}{2} + \frac{p}{\rho} = \mathcal{F}(t). \quad (3.2.40)$$

Differentiation of (3.2.35) with respect to time t yields

$$\frac{\partial \varphi'}{\partial t} = -\frac{dV_0}{dt} \frac{a^3}{2r^2} \cos \vartheta + \frac{1}{2} a^3 [V_0(t)]^2 \left\{ \frac{1}{r^3} - 3 \frac{[x' - x_0(t)]^2}{r^5} \right\}. \quad (3.2.41)$$

The squared velocity term in (3.2.40) may be obtained using (3.2.15). We have

$$V^2 = V_r^2 + V_\vartheta^2 = \left(\frac{\partial \varphi'}{\partial r} \right)^2 + \frac{1}{r^2} \left(\frac{\partial \varphi'}{\partial \vartheta} \right)^2 = \frac{a^6}{r^6} [V_0(t)]^2 \left(\cos^2 \vartheta + \frac{1}{4} \sin^2 \vartheta \right).$$

We see that V^2 is symmetric with respect to the equator ($\vartheta = \frac{1}{2}\pi$) of the sphere. It may therefore be disregarded in (3.2.40) since it does not contribute to the result of the integration in (3.2.39). The same is true for the second term on the right-hand side of equation (3.2.41). Consequently, setting $r = a$ in (3.2.41) and using the Cauchy–Lagrange integral (3.2.40), we find that on the sphere

$$p \Big|_{r=a} = \frac{1}{2} \frac{dV_0}{dt} \rho a \cos \vartheta + \{\text{symmetric part}\}. \quad (3.2.42)$$

It remains to substitute (3.2.42) into (3.2.39), and we arrive at the conclusion that the drag of the sphere

$$F_x = \pi a^3 \rho \frac{dV_0}{dt} \int_0^\pi \cos^2 \vartheta \sin \vartheta \, d\vartheta = \frac{2}{3} \pi a^3 \rho \frac{dV_0}{dt}. \quad (3.2.43)$$

If a sphere of mass m accelerates in vacuum then, according to Newton's Second

Law, the force exerted on the sphere

$$F = m \frac{dV_0}{dt}.$$

If the same sphere accelerates in a fluid medium then, taking into account the drag force (3.2.43), we have to write instead

$$F = \left(m + \frac{2}{3} \pi a^3 \rho \right) \frac{dV_0}{dt}.$$

This explains why the factor $\frac{2}{3} \pi a^3 \rho$ in (3.2.43) is termed the *virtual mass* of the sphere.

3.3 Two-Dimensional Flows

Let us consider inviscid flow of an incompressible fluid past a rigid body of cylindrical shape whose cross-section is sketched in Figure 3.16; the generator of the body's surface is a straight line perpendicular to the sketch plane. We shall assume that the cylinder is infinite in the spanwise direction.⁶ We shall further assume that the velocity vector of the oncoming flow is perpendicular to the body's generator. In this case, none of the fluid-dynamic functions is expected to be dependent on the spanwise coordinate z measured along the body's generator, namely

$$\frac{\partial}{\partial z} = 0. \tag{3.3.1}$$

Also, the spanwise velocity component w is expected to be zero, so that the velocity vector

$$\mathbf{V} = (u, v, 0). \tag{3.3.2}$$

Fluid flows that satisfy conditions (3.3.1) and (3.3.2) are termed *two-dimensional*.

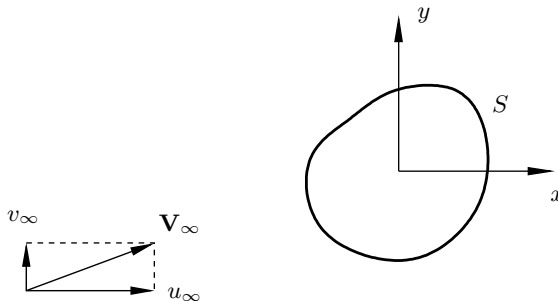


Fig. 3.16: A two-dimensional flow.

⁶In practice it is sufficient for the spanwise length of a cylinder to be much larger than the characteristic dimension of its cross-section.

In a two-dimensional flow, the vorticity vector $\boldsymbol{\omega}$ has just one component, ω_z , perpendicular to the plane of fluid motion. Indeed, using (3.3.1) and (3.3.2) in (1.4.15), we have

$$\boldsymbol{\omega} = \mathbf{k} \left(\frac{\partial v}{\partial x} - \frac{\partial u}{\partial y} \right).$$

If the flow considered is irrotational, i.e.

$$\omega_z = \frac{\partial v}{\partial x} - \frac{\partial u}{\partial y} = 0, \quad (3.3.3)$$

then there exists a velocity potential φ . It is related to the velocity field through the integral (3.2.2). In a two-dimensional flow, this integral assumes the form

$$\varphi(t, \mathbf{r}) = \int_{\mathbf{r}_0}^{\mathbf{r}} \mathbf{V} \cdot d\mathbf{r} = \int_{\mathbf{r}_0}^{\mathbf{r}} (u dx + v dy). \quad (3.3.4)$$

When dealing with three-dimensional flow (see Figure 3.9 on page 140), we demonstrated that the integral for $\varphi(t, \mathbf{r})$ does not depend on a choice of contour C connecting points \mathbf{r}_0 and \mathbf{r} . We shall now look at this result more closely. We took two contours C and C' connecting \mathbf{r}_0 and \mathbf{r} , and denoted the results of the integration along C and C' by $\varphi(t, \mathbf{r})$ and $\varphi'(t, \mathbf{r})$, respectively. Then the difference between $\varphi(t, \mathbf{r})$ and $\varphi'(t, \mathbf{r})$ was calculated using Stokes's theorem:

$$\varphi(t, \mathbf{r}) - \varphi'(t, \mathbf{r}) = \int_C \mathbf{V} \cdot d\mathbf{r} - \int_{C'} \mathbf{V} \cdot d\mathbf{r} = \oint_{\tilde{C}} \mathbf{V} \cdot d\mathbf{r} = \iint_{\sigma} (\boldsymbol{\omega} \cdot \mathbf{n}) ds.$$

Here \tilde{C} is a closed contour composed of C and C' , and σ is an open surface built on \tilde{C} as shown in Figure 3.2 on page 133.

We see that if $\boldsymbol{\omega} = 0$ everywhere on σ , then $\varphi(t, \mathbf{r}) = \varphi'(t, \mathbf{r})$. This conclusion, however, relies on the assumption that the region occupied by the moving fluid is *singly connected*, i.e., for any closed contour \tilde{C} , there exists a surface σ , resting on \tilde{C} , that lies entirely inside the flow field. Two-dimensional flows past cylindrical bodies clearly do not belong to this category: one path connecting points \mathbf{r}_0 and \mathbf{r} might go around one side of the body and the other might go around the other side, and the result of the integration in (3.3.4) cannot be proven to be the same.

Corresponding to this, we can subdivide all closed contours into two classes. In the first class are contours like C_1 in Figure 3.17 that may be reduced to a point by a continuous deformation (shrinking). When the position vector \mathbf{r} in the integral (3.3.4) makes a circle around such a contour, the potential $\varphi(t, \mathbf{r})$ returns to its initial value. In the second category are contours like C_2 . When travelling around such a contour, the potential increases by a value

$$\Delta\varphi = \oint_{C_2} \mathbf{V} \cdot d\mathbf{r} = \Gamma, \quad (3.3.5)$$

which coincides with the velocity circulation in the flow past a rigid body.

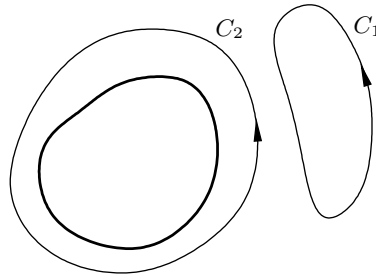


Fig. 3.17: Classification of closed contours in two-dimensional flows.

It is easily shown that the circulation Γ is a universal constant for a given two-dimensional flow, independent of the choice of a contour embracing the body. Indeed, let us consider two contours C_2 and C'_2 as shown in Figure 3.18, and write

$$\Gamma = \oint_{C_2} \mathbf{V} \cdot d\mathbf{r}, \quad \Gamma' = \oint_{C'_2} \mathbf{V} \cdot d\mathbf{r}.$$

Then, using Stokes's theorem, we will have

$$\oint_{C_2} \mathbf{V} \cdot d\mathbf{r} - \oint_{C'_2} \mathbf{V} \cdot d\mathbf{r} = \iint_{\sigma} \omega_z ds, \tag{3.3.6}$$

with σ now denoting the region between C_2 and C'_2 . Since in this region equation (3.3.3) holds, we can conclude that the two integrals on the left-hand side of (3.3.6) coincide with one another.

Thus, when dealing with two-dimensional irrotational flows past solid bodies, one can still introduce the velocity potential φ with the help of the integral (3.3.4). However, in the general case, φ will not be a single-valued function, although the non-uniqueness in φ is rather simple. Each time an observer goes around the body, the value of φ at a given point \mathbf{r} increases by the circulation Γ . In what follows, Γ will be assumed positive when the integral in (3.3.5) is calculated in the counter-clockwise direction.

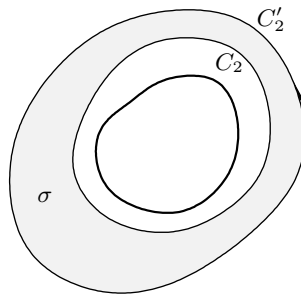


Fig. 3.18: Two closed contours C_2 and C'_2 and the surface σ exploited in equation (3.3.6).

Of course, each single-valued branch of the velocity potential φ still satisfies Laplace's equation (3.2.7), which is written in two dimensions as

$$\frac{\partial^2 \varphi}{\partial x^2} + \frac{\partial^2 \varphi}{\partial y^2} = 0.$$

3.3.1 Stream function

Similar to the velocity potential $\varphi(t, \mathbf{r})$, which has been introduced based on the zero-vorticity equation (3.3.3), we can use the continuity equation (3.1.1b), written in two dimensions as

$$\frac{\partial u}{\partial x} + \frac{\partial v}{\partial y} = 0, \quad (3.3.7)$$

to introduce another scalar function $\psi(t, \mathbf{r})$, termed the *stream function*, such that

$$\frac{\partial \psi}{\partial x} = -v, \quad \frac{\partial \psi}{\partial y} = u. \quad (3.3.8)$$

For this purpose, we consider a vector field

$$\mathbf{A} = (A_x, A_y, A_z)$$

such that

$$A_x = -v, \quad A_y = u, \quad A_z = 0, \quad (3.3.9)$$

Since neither u nor v depends on z ,

$$\text{curl } \mathbf{A} = \begin{vmatrix} \mathbf{i} & \mathbf{j} & \mathbf{k} \\ \frac{\partial}{\partial x} & \frac{\partial}{\partial y} & 0 \\ -v & u & 0 \end{vmatrix} = \mathbf{k} \left(\frac{\partial u}{\partial x} + \frac{\partial v}{\partial y} \right) = 0.$$

Hence, the vector field \mathbf{A} is irrotational, and there exists a scalar function $\psi(t, \mathbf{r})$ that, similar to (3.3.4), may be introduced using the integral

$$\psi(t, \mathbf{r}) = \int_{\mathbf{r}_0}^{\mathbf{r}} \mathbf{A} \cdot d\mathbf{r} = \int_{\mathbf{r}_0}^{\mathbf{r}} (-v dx + u dy). \quad (3.3.10)$$

Variation of the upper limit of integration in (3.3.10) results in

$$\nabla \psi = \mathbf{A} = (-v, u). \quad (3.3.11)$$

Writing (3.3.11) in the coordinate-decomposition form

$$\frac{\partial \psi}{\partial x} = A_x = -v, \quad \frac{\partial \psi}{\partial y} = A_y = u$$

proves the validity of equations (3.3.8).

The existence of the stream function relies solely on the continuity equation or, more precisely, on the form (3.3.7) it assumes in two-dimensional incompressible flows.

It does not matter if the flow is steady or unsteady, inviscid or viscous, irrotational or with non-zero vorticity, one can still introduce the stream function. In the case of irrotational flow, the stream function is easily seen to satisfy Laplace's equation

$$\nabla^2\psi = \frac{\partial^2\psi}{\partial x^2} + \frac{\partial^2\psi}{\partial y^2} = 0,$$

which is obtained by substituting (3.3.8) into (3.3.3).

In order to clarify the physical content of the stream function, let us consider two points M and M' in the (x, y) -plane (see Figure 3.19) and calculate the fluid volume flux across a curve \mathcal{L} joining M and M' or, more precisely, the flux across an open surface swept out by translating curve \mathcal{L} through unit distance in the z -direction. Reckoning the flux positive when it is in the direction shown by the arrow in Figure 3.19, we write

$$Q = - \int_{\mathcal{L}} \mathbf{V} \cdot \mathbf{n} dl = - \int_{\mathcal{L}} (un_x + vn_y) dl. \tag{3.3.12}$$

Here $\mathbf{n} = (n_x, n_y)$ is a unit vector normal to \mathcal{L} and dl is the length of a small element of \mathcal{L} . Notice that, unlike for the mass flux (1.6.3), the volume flux integral (3.3.12) does not involve the fluid density ρ .

Let us now introduce a unit vector $\boldsymbol{\tau} = (\tau_x, \tau_y)$ tangent to \mathcal{L} . It may be easily seen that

$$n_x = -\tau_y, \quad n_y = \tau_x.$$

Hence, using (3.3.8), we can express the integral in (3.3.12) as

$$Q = \int_{\mathcal{L}} \left(\frac{\partial\psi}{\partial x} \tau_x + \frac{\partial\psi}{\partial y} \tau_y \right) dl = \int_{\mathcal{L}} (\nabla\psi \cdot \boldsymbol{\tau}) dl = \int_{\mathcal{L}} \nabla\psi \cdot d\mathbf{r},$$

with $d\mathbf{r}$ being an increment of the position vector \mathbf{r} along \mathcal{L} . We see that the volume flux across any curve joining two points in the flow field equals the difference between the values of ψ at these points:

$$Q = \psi(M') - \psi(M). \tag{3.3.13}$$

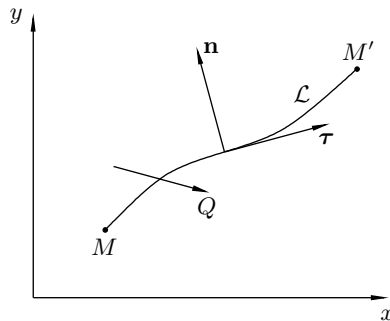


Fig. 3.19: Calculation of volume flux Q through curve \mathcal{L} between points M and M' .

We can now prove the following theorem.

Theorem 3.4 *The stream function is constant along any streamline, and any line defined by the equation*

$$\psi = \text{const} \quad (3.3.14)$$

is a streamline.

Proof If line \mathcal{L} in Figure 3.19 is a streamline, then, according to Definition 1.2 on page 29, the velocity vector is tangent to \mathcal{L} , and therefore there is no fluid flux across \mathcal{L} . Hence, $Q = 0$, and, using (3.3.13), we can conclude that for any two points M and M' which belong to the same streamline, $\psi(M') = \psi(M)$. This proves the first part of the theorem.

To prove that any line defined by equation (3.3.14) is a streamline, we note that for a line represented by equation (3.3.14), the unit vector normal to this line, \mathbf{n} , may be calculated as

$$\mathbf{n} = \frac{\nabla\psi}{|\nabla\psi|} = \frac{1}{|\nabla\psi|} \left(\frac{\partial\psi}{\partial x}, \frac{\partial\psi}{\partial y} \right).$$

Let us consider the scalar product of the velocity vector \mathbf{V} and the normal vector \mathbf{n} :

$$\mathbf{V} \cdot \mathbf{n} = \frac{1}{|\nabla\psi|} \left(u \frac{\partial\psi}{\partial x} + v \frac{\partial\psi}{\partial y} \right). \quad (3.3.15)$$

Using (3.3.8) in (3.3.15), we see that $\mathbf{V} \cdot \mathbf{n} = 0$, which proves that the velocity vector \mathbf{V} is perpendicular to \mathbf{n} , and therefore is tangent to the line considered. \square

Exercises 8

1. Consider a building in the form of a hemisphere that has an open ventilation window at the top of the roof. The entrance door, which is situated at point O on the ground level, is initially sealed and does not allow air to penetrate through it. The building is exposed to wind, which is directed such that the entrance door finds itself at the front stagnation point; see Figure 3.20.

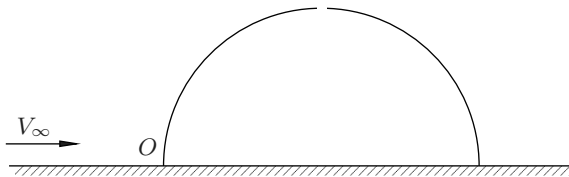


Fig. 3.20: Problem layout.

Show that the force that has to be applied to the door to open it outwards is

$$F = \frac{9}{8} \rho V_\infty^2 A,$$

where ρ is the air density, V_∞ the wind speed, and A the area of the door surface.

Suggestion: You may assume that the ventilation window is small compared with the radius of the dome, and so is the door.

2. For a two-dimensional flow, the Euler equations are written as

$$\begin{aligned} \frac{\partial u}{\partial t} + u \frac{\partial u}{\partial x} + v \frac{\partial u}{\partial y} &= f_x - \frac{1}{\rho} \frac{\partial p}{\partial x}, \\ \frac{\partial v}{\partial t} + u \frac{\partial v}{\partial x} + v \frac{\partial v}{\partial y} &= f_y - \frac{1}{\rho} \frac{\partial p}{\partial y}, \\ \frac{\partial u}{\partial x} + \frac{\partial v}{\partial y} &= 0. \end{aligned}$$

Performing cross-differentiation of the x - and y -momentum equations, deduce a condition that should be imposed upon the body force \mathbf{f} to ensure that the vorticity remains constant for each fluid particle as it travels through the flow field.

3. Prove that in a two-dimensional flow past a rigid cylindrical body the stream function ψ is a single-valued function, i.e., after making a circle around the closed contour C_2 of Figure 3.17, ψ returns to its original value.
4. Assume that a flow of an incompressible fluid is steady and may be treated as inviscid. Assume further that the body force \mathbf{f} is potential, i.e. there exists a scalar function U such that $\mathbf{f} = \nabla U$. Show that under these conditions the gradient of the function H in the Bernoulli function (3.1.6) is related to the vorticity $\boldsymbol{\omega}$ by the equation

$$\nabla H = \mathbf{V} \times \boldsymbol{\omega}. \tag{3.3.16}$$

Suggestion: Use the Gromeko–Lamb form (3.1.3) of the Euler equations.

5. The streamline pattern in a two-dimensional flow is defined by equation (3.3.14), with different values of the stream function ψ corresponding to different streamlines. Therefore, function H on the right-hand side of the Bernoulli equation (3.1.6) may be treated as a function of ψ . Starting with equation (3.3.16), prove that

$$\frac{dH}{d\psi} = -\omega_z.$$

Hence, deduce that H is constant in an irrotational flow.

6. Suppose that a two-dimensional flow is irrotational and has velocity potential φ given by

$$\varphi = ax(x^2 - 3y^2),$$

where a is a positive constant. Find the fluid volume flux across a curve connecting points $M = (0, 0)$ and $M' = (1, 1)$ in the (x, y) -plane.

7. The continuity equation for an incompressible fluid is written in spherical polar coordinates as

$$\frac{\partial V_r}{\partial r} + \frac{1}{r} \frac{\partial V_\vartheta}{\partial \vartheta} + \frac{1}{r \sin \vartheta} \frac{\partial V_\phi}{\partial \phi} + \frac{2V_r}{r} + \frac{V_\vartheta}{r \tan \vartheta} = 0. \tag{3.3.17}$$

Assume that the flow considered is axisymmetric with respect to the x -axis (see Figure 1.31 on page 84), and show that in this case equation (3.3.17) assumes the

form

$$\frac{\partial}{\partial r}(r^2 \sin \vartheta V_r) + \frac{\partial}{\partial \vartheta}(r \sin \vartheta V_\vartheta) = 0.$$

Based on this equation, introduce a scalar function $\psi(r, \vartheta)$, known as the *Stokes stream function*, such that

$$\frac{\partial \psi}{\partial r} = -r \sin \vartheta V_\vartheta, \quad \frac{\partial \psi}{\partial \vartheta} = r^2 \sin \vartheta V_r, \quad (3.3.18)$$

and prove that the equation

$$\psi = \text{const}$$

defines the streamlines in the flow.

Hint: You may use without proof the fact that gradient of ψ is written in spherical polar coordinates as

$$\nabla \psi = \frac{\partial \psi}{\partial r} \mathbf{e}_r + \frac{1}{r \sin \vartheta} \frac{\partial \psi}{\partial \phi} \mathbf{e}_\phi + \frac{1}{r} \frac{\partial \psi}{\partial \vartheta} \mathbf{e}_\vartheta,$$

with \mathbf{e}_r , \mathbf{e}_ϑ , and \mathbf{e}_ϕ denoting the unit vectors in the radial, azimuthal, and meridional directions, respectively.

8. Combine (3.3.18) with the solution (3.2.30) for V_r and V_ϑ in the flow past a sphere, and show that in this flow

$$\psi = \frac{V_\infty}{2} \left(r^2 - \frac{a^3}{r} \right) \sin^2 \vartheta.$$

9. Consider the steady inviscid flow of an incompressible fluid past a swept wing shown in Figure 3.21. The wing has an infinite span, and its profile at each cross-section OO' remains the same, i.e. is independent of the spanwise coordinate z . Write the Euler equations (3.1.1) and the impermeability (3.2.10) and free-stream (3.2.11) conditions in coordinate-decomposition form using Cartesian coordinates x , y , z with z -axis parallel to the wing generatrix.

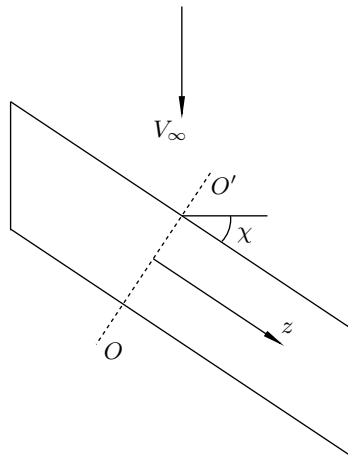


Fig. 3.21: Swept wing.

Prove that the flow in the (x, y) -plane perpendicular to the generatrix may be treated as two-dimensional.

3.4 Complex Potential

If a two-dimensional flow is irrotational and the fluid is incompressible, then equations (3.3.3) and (3.3.7) hold:

$$\frac{\partial v}{\partial x} - \frac{\partial u}{\partial y} = 0, \quad \frac{\partial u}{\partial x} + \frac{\partial v}{\partial y} = 0. \quad (3.4.1)$$

It follows from the first of these that there exists a velocity potential φ related to the velocity vector by means of equation (3.2.6). In a two-dimensional flow, it is written as

$$u = \frac{\partial \varphi}{\partial x}, \quad v = \frac{\partial \varphi}{\partial y}. \quad (3.4.2)$$

The second of equations (3.4.1) guarantees the existence of the stream function ψ , and we can use equations (3.3.8):

$$u = \frac{\partial \psi}{\partial y}, \quad v = -\frac{\partial \psi}{\partial x}. \quad (3.4.3)$$

Comparing (3.4.2) with (3.4.3), we see that

$$\frac{\partial \varphi}{\partial x} = \frac{\partial \psi}{\partial y}, \quad \frac{\partial \varphi}{\partial y} = -\frac{\partial \psi}{\partial x}. \quad (3.4.4)$$

These are the Cauchy–Riemann equations representing the necessary and sufficient conditions for the function

$$w(z) = \varphi + i\psi \quad (3.4.5)$$

to be an analytical function of the complex variable $z = x + iy$. This function is called the *complex potential*.

If $w(z)$ were known, then the velocity component u and v could be obtained by means of differentiating $w(z)$. We have

$$\frac{dw}{dz} = \frac{\partial \varphi}{\partial x} + i \frac{\partial \psi}{\partial x},$$

which, using (3.4.2) and (3.4.3), may be written as

$$\frac{dw}{dz} = u - iv = \bar{V}(z). \quad (3.4.6)$$

The function $\bar{V}(z) = u - iv$ is called the *complex conjugate velocity*. Being the derivative of an analytic function, the complex conjugate velocity $\bar{V}(z)$ is also an analytic function. The latter is confirmed by equations (3.4.1), which are the Cauchy–Riemann conditions for $\bar{V}(z) = u - iv$.

We shall now consider a number of elementary two-dimensional flows and deduce the corresponding expressions for the complex potential.

Uniform flow

Let the velocity vector \mathbf{V} be constant over the entire flow field. In what follows, we shall often use the complex potential of the uniform flow for the purpose of representing the unperturbed free stream approaching a rigid body. Keeping this in mind, we shall denote the modulus of the velocity \mathbf{V} by V_∞ . If the angle that the velocity vector makes with the x -axis is α (see Figure 3.22), then the two velocity components are

$$u = V_\infty \cos \alpha, \quad v = V_\infty \sin \alpha,$$

and the complex conjugate velocity may be written as⁷

$$\bar{V}(z) = u - iv = V_\infty(\cos \alpha - i \sin \alpha) = V_\infty e^{-i\alpha}. \quad (3.4.7)$$

Substituting (3.4.7) into (3.4.6), we have

$$\frac{dw}{dz} = V_\infty e^{-i\alpha},$$

which is easily integrated to yield

$$w(z) = e^{-i\alpha} V_\infty z + C.$$

Here the constant of integration $C = C_r + iC_i$ may be disregarded without loss of generality since both the velocity potential φ and the stream function ψ are defined to within arbitrary constants. Keeping this in mind, we shall write the complex potential for a uniform flow as

$$w(z) = e^{-i\alpha} V_\infty z. \quad (3.4.8)$$

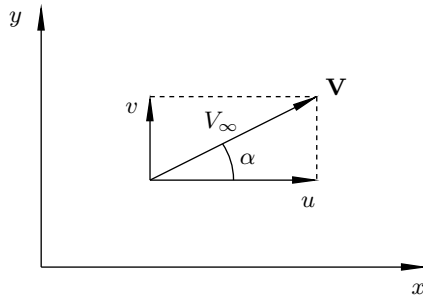


Fig. 3.22: Uniform flow.

Two-dimensional source

Let us suppose that a straight line \mathcal{L} is drawn perpendicular to the (x, y) -plane. Let us further suppose that three-dimensional sources are continuously distributed along \mathcal{L} . We shall define the strength q of the two-dimensional source as the volume of the

⁷Here the well-known Euler formula, $e^{i\alpha} = \cos \alpha + i \sin \alpha$, is used.

fluid produced (per unit time) by a segment of \mathcal{L} of unit length. If the line \mathcal{L} is infinite, and q remains constant along \mathcal{L} , then the integral effect will be a two-dimensional flow in planes perpendicular \mathcal{L} . In Figure 3.23, we show one of these planes, with the line \mathcal{L} passing through the coordinate origin. In this plane, the fluid moves in the radial direction, and at a point M , situated at distance r from the source, the velocity V_r is given by

$$V_r = \frac{q}{2\pi r}. \tag{3.4.9}$$

Indeed, the circumference of the circle C drawn through M is $2\pi r$, and therefore the mass conservation law states

$$2\pi r V_r = q.$$

Here it is taken into account that, owing to the symmetry of the flow, the velocity vector has only a radial component V_r , which is the same at all points on C . An alternative way of deducing equation (3.4.9) is discussed in Problem 1 in Exercises 9.

Denoting by ϑ the angle made by the velocity vector with the x -axis, we can write

$$u = V_r \cos \vartheta = \frac{q}{2\pi} \frac{\cos \vartheta}{r}, \quad v = V_r \sin \vartheta = \frac{q}{2\pi} \frac{\sin \vartheta}{r},$$

and therefore

$$\bar{V}(z) = u - iv = \frac{q}{2\pi} \frac{\cos \vartheta - i \sin \vartheta}{r}. \tag{3.4.10}$$

Multiplying the numerator and denominator in (3.4.10) by $\cos \vartheta + i \sin \vartheta$, we have

$$\bar{V}(z) = \frac{q}{2\pi} \frac{1}{r(\cos \vartheta + i \sin \vartheta)} = \frac{q}{2\pi z}. \tag{3.4.11}$$

Integration of (3.4.11) leads to

$$w(z) = \frac{q}{2\pi} \ln z, \tag{3.4.12}$$

which is the sought complex potential of a two-dimensional point source centred at $z = 0$.

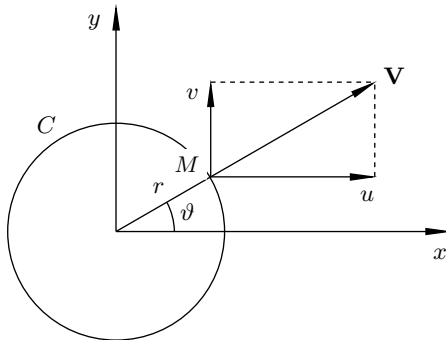


Fig. 3.23: Two-dimensional source.

Dipole

Similar to the three-dimensional dipole, we shall introduce its two-dimensional counterpart as a superposition of a source and a sink. If a source is situated at $z = 0$ and a sink of equal strength is situated at $z = \delta z_0$, then we can write

$$\begin{aligned} w(z) &= \frac{q}{2\pi} \ln z - \frac{q}{2\pi} \ln(z - \delta z_0) \\ &= \frac{q}{2\pi} \ln z - \frac{q}{2\pi} \ln \left[z \left(1 - \frac{\delta z_0}{z} \right) \right] = -\frac{q}{2\pi} \ln \left(1 - \frac{\delta z_0}{z} \right). \end{aligned} \quad (3.4.13)$$

We shall now suppose that $|\delta z_0|$ is small compared with $|z|$. In this case, the Taylor expansion for the logarithm, $\ln(1 + \varepsilon) = \varepsilon + \dots$, may be used. We have

$$\ln \left(1 - \frac{\delta z_0}{z} \right) = -\frac{\delta z_0}{z} + \dots,$$

which reduces (3.4.13) to

$$w(z) = \frac{m e^{i\alpha}}{2\pi z}. \quad (3.4.14)$$

Here $m = q|\delta z_0|$ is the moment of the dipole and $\alpha = \arg \{\delta z_0\}$ defines the orientation of the dipole in the (x, y) -plane.

Potential vortex

Here we shall use a different strategy. Instead of trying to find the form of the complex potential for a given flow field, we shall start with a formula for $w(z)$ and then our task will be to determine the flow it represents. The complex potential of the source (3.4.12) is given by the logarithmic function $\ln z$ with real factor $q/2\pi$. Let us now assume that the factor is imaginary, i.e.

$$w(z) = \frac{\kappa}{2\pi i} \ln z, \quad (3.4.15)$$

with κ being a real constant.

In order to determine the form of the streamlines in this flow, we shall rely on Theorem 3.4 (see page 157). We first need to separate the real and imaginary parts of the complex potential (3.4.15). Expressing z in the exponential form $z = r e^{i\vartheta}$, we have

$$w(z) = \varphi + i\psi = \frac{\kappa}{2\pi i} (\ln r + i\vartheta) = \frac{\kappa}{2\pi} \vartheta - i \frac{\kappa}{2\pi} \ln r.$$

Hence, the velocity potential and stream function are given by

$$\varphi = \frac{\kappa}{2\pi} \vartheta, \quad \psi = -\frac{\kappa}{2\pi} \ln r.$$

It is easily seen that the potential φ increases by a value of κ each time a point in the complex z -plane makes a full circle around the vortex centre. Therefore, according

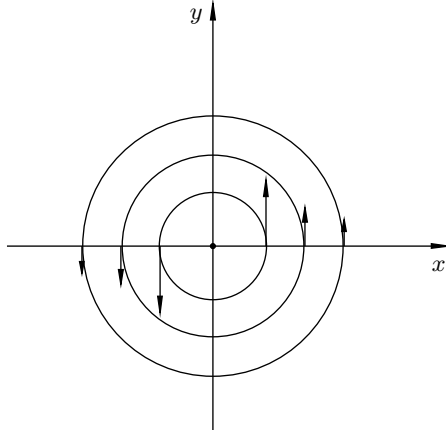


Fig. 3.24: Streamline pattern for the vortex flow (3.4.15).

to (3.3.5), κ is the circulation Γ and we can write (3.4.15) as

$$w(z) = \frac{\Gamma}{2\pi i} \ln z. \tag{3.4.16}$$

Correspondingly, the stream function takes the form

$$\psi = -\frac{\Gamma}{2\pi} \ln r.$$

It should remain constant along each streamline, which can only happen if the radius r is constant. This means that the streamlines have the form of concentric circles with centre situated at $z = 0$ (see Figure 3.24).

In order to find the velocity, we differentiate (3.4.16) with respect to z :

$$\bar{V}(z) = \frac{dw}{dz} = \frac{\Gamma}{2\pi iz}. \tag{3.4.17}$$

As the velocity vector is tangent to the streamlines, the shape of which is already known, we only need to find the modulus of the velocity

$$|\mathbf{V}| = |\bar{V}(z)| = \frac{\Gamma}{2\pi|z|} = \frac{\Gamma}{2\pi r}. \tag{3.4.18}$$

Thus, $|\mathbf{V}|$ is inversely proportional to the distance from the vortex centre.

3.4.1 Boundary-value problem for the complex potential

When dealing with more complicated flows, it is important to have the corresponding boundary-value problem properly formulated. Such a formulation provides a strict mathematical basis for the fluid-dynamic analysis. In three dimensions, the behaviour of potential flow past a motionless body is governed by Problem 3.1 (see page 142). For two-dimensional flows, this problem may be more conveniently re-formulated in terms of the complex potential $w(z)$.

Problem 3.2 Find the complex potential $w(z) = \varphi + i\psi$ such that

1. $w(z)$ is an analytic function of the complex variable $z = x + iy$ everywhere outside the body contour S ;
2. it satisfies the impermeability condition on the body contour

$$\Im\{w(z)\}\Big|_S = \text{const}, \quad (3.4.19)$$

3. and it satisfies the free-stream condition

$$\frac{dw}{dz} = u_\infty - iv_\infty \quad \text{at } z = \infty, \quad (3.4.20)$$

where u_∞, v_∞ are the components of the velocity vector \mathbf{V}_∞ in the oncoming flow.

Condition 1 is equivalent to the requirement that the velocity potential φ satisfy Laplace's equation. Indeed, any analytical function $w(z) = \varphi(x, y) + i\psi(x, y)$ has to satisfy the Cauchy–Riemann conditions

$$\frac{\partial\varphi}{\partial x} = \frac{\partial\psi}{\partial y}, \quad \frac{\partial\varphi}{\partial y} = -\frac{\partial\psi}{\partial x}. \quad (3.4.21)$$

Cross-differentiation of (3.4.21) leads to the Laplace equation for φ .

Condition 2 states that the stream function ψ should be constant along the body surface. According to Theorem 3.4 (see page 157), this means that the body surface has to coincide with one of the streamlines. Since the velocity vector is always tangent to a streamline, condition 2 represents the impermeability condition on the surface of a motionless body, which may be expressed in the form of equation (3.2.10) or, equivalently, by equation (3.2.12b) in the formulation of Problem 3.1.

Finally, equation (3.4.20) simply casts the free-stream condition (3.2.12c) in terms of the complex conjugate velocity, \overline{V} .

3.4.2 Flow past a circular cylinder

Here we shall demonstrate that the solution of Problem 3.2 for the two-dimensional flow past a circular cylinder may be constructed as a superposition of the uniform flow (3.4.8) and the dipole (3.4.14). Without loss of generality, one can always choose the x -axis to be parallel to the oncoming flow; see Figure 3.25. With this choice, the angle of attack α in (3.4.8) has to be set to zero, and we have the complex potential of the uniform flow in the form

$$w(z) = V_\infty z. \quad (3.4.22)$$

We then place the dipole at the coordinate origin and assume that it is also aligned with the x -axis. We therefore choose $\alpha = 0$ in (3.4.14), leading to

$$w(z) = \frac{m}{2\pi z}. \quad (3.4.23)$$

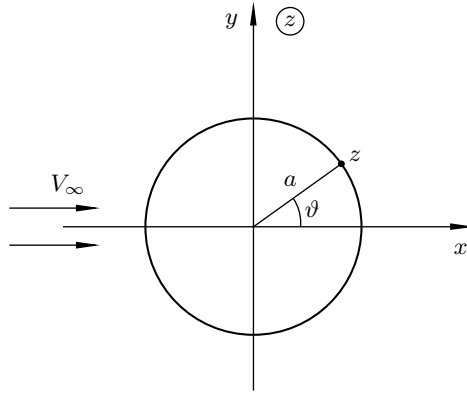


Fig. 3.25: Flow past a circular cylinder.

Adding (3.4.22) and (3.4.23) together yields

$$w(z) = V_\infty z + \frac{m}{2\pi z}. \tag{3.4.24}$$

The function (3.4.24) obviously satisfies condition 1 of Problem 3.2, since $w(z)$ is analytic everywhere except at the point $z = 0$. This point lies inside the body contour; meanwhile analyticity of $w(z)$ should be ensured in the flow field. Turning to condition 2, we shall assume that the cylinder has its centre at $z = 0$, with the radius being a . Then, for any point on the cylinder's surface,

$$z = ae^{i\vartheta}, \tag{3.4.25}$$

where ϑ is the position angle measured from the real positive semi-axis, as shown in Figure 3.25. Substitution of (3.4.25) into (3.4.24) results in

$$w(z) = V_\infty ae^{i\vartheta} + \frac{m}{2\pi a} e^{-i\vartheta}. \tag{3.4.26}$$

The stream function on the cylinder's surface is given by the imaginary part of (3.4.26):

$$\psi \Big|_{r=a} = \Im\{w(z)\} = \left(V_\infty a - \frac{m}{2\pi a} \right) \sin \vartheta.$$

It may be made zero for all values of ϑ by choosing

$$m = 2\pi V_\infty a^2. \tag{3.4.27}$$

Substituting (3.4.27) back into (3.4.24), we have

$$w(z) = V_\infty \left(z + \frac{a^2}{z} \right). \tag{3.4.28}$$

It remains to observe that the function (3.4.28) also satisfies condition 3 of Problem 3.2. Indeed, as $z \rightarrow \infty$, the second term in the parentheses tends to zero, and (3.4.28) reduces to $w(z) = V_\infty z$, which represents a uniform flow parallel to the x -axis.

Differentiating (3.4.28), we find that at any point z in the flow field, the complex conjugate velocity

$$\bar{V}(z) = \frac{dw}{dz} = V_\infty \left(1 - \frac{a^2}{z^2} \right). \quad (3.4.29)$$

In particular, on the cylinder's surface, where z is given by (3.4.25), we have

$$\bar{V} \Big|_{r=a} = u - iv = V_\infty (1 - e^{-2i\vartheta}),$$

which may be rearranged as

$$\bar{V} \Big|_{r=a} = V_\infty e^{-i\vartheta} (e^{i\vartheta} - e^{-i\vartheta}) = 2V_\infty i e^{-i\vartheta} \frac{e^{i\vartheta} - e^{-i\vartheta}}{2i} = 2V_\infty e^{i(\pi/2 - \vartheta)} \sin \vartheta.$$

The modulus of the velocity vector \mathbf{V} is calculated as $|\mathbf{V}| = \sqrt{u^2 + v^2}$, and obviously coincides with the modulus of the complex conjugate velocity $\bar{V} = u - iv$. Consequently, we can conclude that on the cylinder's surface

$$|\mathbf{V}| = 2V_\infty \sin \vartheta. \quad (3.4.30)$$

We see that there are two points where $|\mathbf{V}| = 0$: the front stagnation point ($\vartheta = \pi$) and the rear stagnation point ($\vartheta = 0$). Between them, the fluid velocity (3.4.30) appears to be symmetric with respect to the middle point ($\vartheta = \pi/2$), where it reaches the maximum value of

$$|\mathbf{V}|_{\max} = 2V_\infty.$$

In order to determine the pressure distribution, we shall use the Bernoulli equation (3.2.32):

$$\frac{V^2}{2} + \frac{p}{\rho} = \frac{V_\infty^2}{2} + \frac{p_\infty}{\rho}. \quad (3.4.31)$$

Substituting (3.4.30) into (3.4.31), it is easily deduced that on the cylinder's surface

$$p = p_\infty + \frac{1}{2} \rho V_\infty^2 (1 - 4 \sin^2 \vartheta).$$

Similar to the flow past a sphere, the solution for a circular cylinder appears to be symmetric with respect to the y -axis (see Figure 3.25), which implies again a zero drag force. In reality, though, the flow separates from the cylinder's surface, as the flow visualisation in Figure 3.26(a) clearly shows. The separation leads to a redistribution of the pressure on the cylinder surface. As a result a non-zero drag is produced.

Interestingly enough, experiments also show that the separation may be suppressed by rotating the cylinder around its centre. A non-dimensional parameter that governs the flow past a rotating cylinder is

$$\frac{a\Omega}{V_\infty}.$$

Here Ω denotes the angular velocity with which the cylinder rotates. Figure 3.26 shows that with increasing Ω , the separation region becomes smaller, and disappears altogether when $a\Omega/V_\infty$ reaches a critical value slightly above 4; see Figure 3.26(d).

In order to model theoretically the effect of the cylinder's rotation on the flow, we add the potential vortex (3.4.16) to the solution (3.4.28):

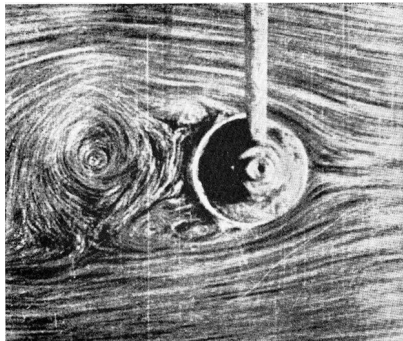
$$w(z) = V_\infty \left(z + \frac{a^2}{z} \right) + \frac{\Gamma}{2\pi i} \ln z. \tag{3.4.32}$$

Now we need to prove that (3.4.32) is a true solution to Problem 3.2. We first note that the function $w(z)$ as defined by (3.4.32) is analytic everywhere in the flow field ($|z| > a$). Second, on the cylinder surface, where $z = ae^{i\vartheta}$, we have

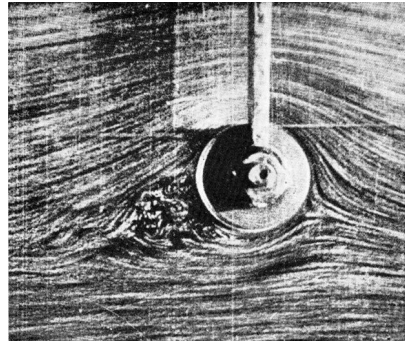
$$w(z) = V_\infty (ae^{i\vartheta} + ae^{-i\vartheta}) - i \frac{\Gamma}{2\pi} (\ln a + i\vartheta) = 2V_\infty a \cos \vartheta + \frac{\Gamma\vartheta}{2\pi} - i \frac{\Gamma}{2\pi} \ln a,$$

which shows that the imaginary part of $w(z)$ is indeed constant on the cylinder's surface:

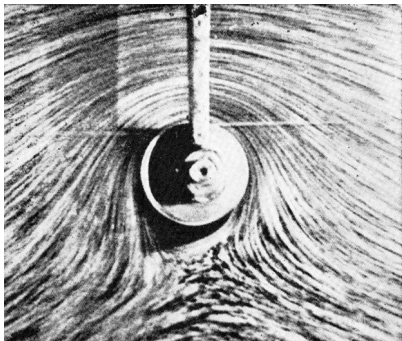
$$\Im\{w(z)\} \Big|_{|z|=a} = -\frac{\Gamma}{2\pi} \ln a.$$



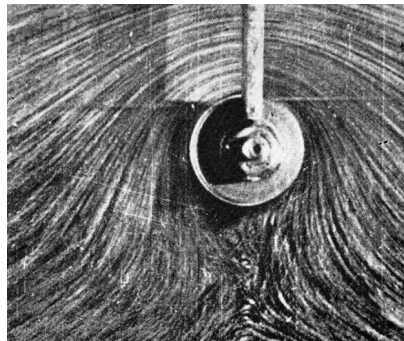
(a) $a\Omega/V_\infty = 0$.



(b) $a\Omega/V_\infty = 2$.



(c) $a\Omega/V_\infty = 4$.



(d) $a\Omega/V_\infty = 6$.

Fig. 3.26: Visualisation of the flow past a rotating cylinder (Prandtl and Tietjens, 1934); the flow is from right to left.

Third, the complex conjugate velocity is calculated as

$$\bar{V}(z) = \frac{dw}{dz} = V_\infty \left(1 - \frac{a^2}{z^2} \right) + \frac{\Gamma}{2\pi iz}, \quad (3.4.33)$$

and obviously satisfies the free-stream condition (3.4.20).

The following two comments are appropriate here. First, while it is clear that the circulation Γ in (3.4.32) is somehow linked to the speed of rotation of the cylinder, the inviscid flow formulation does not allow for such a link to be established. Indeed, the impermeability condition on the cylinder surface, (3.4.19), does not change if instead of being motionless, a rotating cylinder is considered. Second, the boundary-value problem of two-dimensional inviscid flow theory, namely, Problem 3.2 (see page 165), is not a well-posed problem in the classical sense, since it does not define a unique solution. Instead, it admits a family of solutions, with the circulation Γ being a free parameter.

In order to see how changing Γ influences the flow past a circular cylinder, let us consider the velocity distribution along the cylinder's surface. Substituting (3.4.25) into (3.4.33), we have

$$\bar{V}(z) = u - iv = V_\infty (1 - e^{-2i\vartheta}) - \frac{i\Gamma}{2\pi a} e^{-i\vartheta} = ie^{-i\vartheta} \left(2V_\infty \sin \vartheta - \frac{\Gamma}{2\pi a} \right). \quad (3.4.34)$$

It follows from (3.4.34) that a point on the cylinder's surface whose position angle ϑ satisfies the equation

$$\sin \vartheta = \frac{\Gamma}{4\pi a V_\infty} \quad (3.4.35)$$

is a stagnation point where both velocity components u and v simultaneously vanish.

In the case of zero circulation, $\Gamma = 0$, the flow is symmetric with respect to the x -axis, and the stagnation points are located at $\vartheta = 0$ and $\vartheta = \pi$. The corresponding streamline pattern is shown in Figure 3.27(a). In order to reproduce the visualisation results of Figure 3.26, where the stagnation points lie on the lower side of the cylinder, we have to assume that the circulation Γ is negative. If $-4\pi a V_\infty < \Gamma < 0$, then equation (3.4.35) has two solutions, which represent two stagnation points situated symmetrically on the lower surface of the cylinder as shown in Figure 3.27(b). When $\Gamma = -4\pi a V_\infty$, these points come together and the streamline pattern takes the form shown in Figure 3.27(c). Finally, for $\Gamma < -4\pi a V_\infty$, no solutions of (3.4.35) can be found, which suggests that the stagnation point moves from the cylinder surface into the interior of the flow field; see Figure 3.27(d). Notice that at this stage the theoretical streamline pattern starts to show a good agreement with the experimental observations (see Figure 3.26d), and so does the pressure distribution on the cylinder's surface.

We have seen that with $\Gamma \neq 0$ the flow past the cylinder loses its symmetry with respect to the x -axis. As a result, the pressure below the cylinder appears to be larger than the pressure above it, and a side force acting perpendicular to the direction of the oncoming flow is created. Its value is given by the *Joukovskii formula*

$$L = -\rho V_\infty \Gamma,$$

which will be deduced in Section 3.4.3 (see also Problem 6 in Exercises 9).

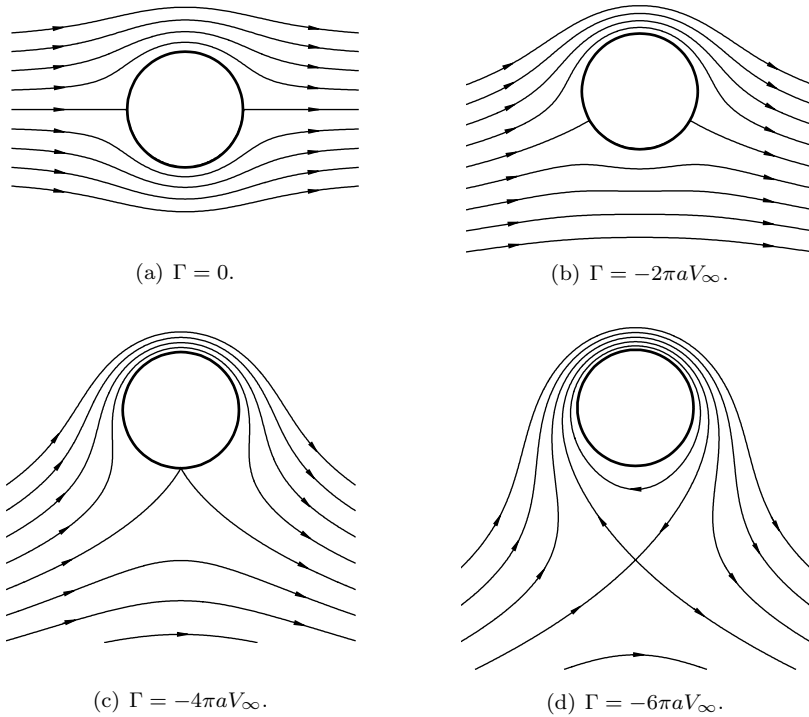


Fig. 3.27: Flow past a circular cylinder for different values of the circulation Γ .

The formation of the side force on a rotating cylinder is known as the *Magnus effect*, named after the scientist who first performed a detailed experimental study of the flow around a rotating cylinder (see Magnus, 1852). In everyday life, the Magnus effect may be observed in a variety of situations. In particular, it represents an integral part of various sports, ranging from football to table tennis. It would perhaps be too optimistic to suggest that sportsmen understand the theory behind the phenomenon, but they certainly know how by spinning a ball they can influence its behaviour in flight.

3.4.3 Force on a cylinder

Let us consider a steady two-dimensional flow past a cylindrical body as shown in Figure 3.28(a). If we assume that the body force \mathbf{f} acting on the moving fluid is negligibly small, then the pressure at any point in the flow field may be found using the Bernoulli equation (3.1.6):

$$\frac{p}{\rho} + \frac{V^2}{2} = H. \tag{3.4.36}$$

Provided that the oncoming flow is uniform, Bernoulli's function H is a constant that does not depend on the streamline considered. Indeed, using the free-stream conditions,

one can find that

$$H = \frac{p_\infty}{\rho} + \frac{V_\infty^2}{2}.$$

In order to calculate the resultant force acting on the cylinder, we consider a small element dl of the cylinder contour C ; see Figure 3.28(a). The integration along this contour will be performed in the counter-clockwise direction. The pressure force acting on the contour element dl (per unit length in the spanwise direction) is

$$F = p dl. \tag{3.4.37}$$

The projections of this force upon the x - and y -axes are (see Figure 3.28b)

$$dX = -F \sin \vartheta, \quad dY = F \cos \vartheta, \tag{3.4.38}$$

where ϑ is the angle between the tangent to the body contour and the x -axis.

Substitution of (3.4.37) into (3.4.38) yields

$$dX = -p \sin \vartheta dl, \quad dY = p \cos \vartheta dl.$$

Since

$$dx = dl \cos \vartheta, \quad dy = dl \sin \vartheta,$$

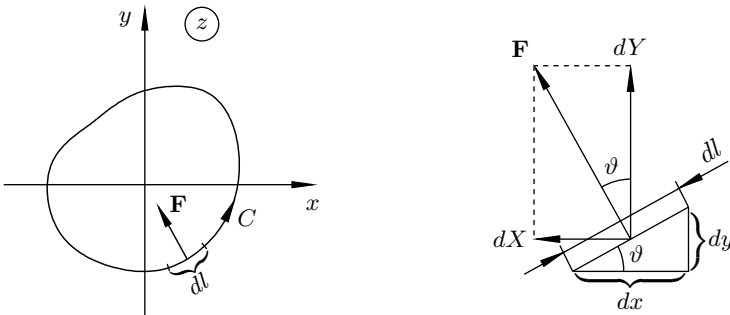
we can conclude that

$$dX = -p dy, \quad dY = p dx. \tag{3.4.39}$$

Integrating (3.4.39) around the cylinder surface, we have the following formulae for the components of the resultant force:

$$X = -\oint_C p dy, \quad Y = \oint_C p dx.$$

It is convenient to combine them into the so-called ‘complex-conjugate force’:



(a) Pressure force \mathbf{F} on an element dl of the cylinder's surface.

(b) Coordinate decomposition of the pressure force acting on an element dl of the cylinder's surface.

Fig. 3.28: Calculation of the pressure force on the cylinder's surface.

$$X - iY = - \oint_C p(dy + i dx) = -i \oint_C p(dx - i dy) = -i \oint_C p d\bar{z}. \quad (3.4.40)$$

It follows from the Bernoulli equation (3.4.36) that

$$p = \rho H - \frac{\rho}{2} V^2,$$

which, when substituted into (3.4.40), gives⁸

$$X - iY = i \frac{\rho}{2} \oint_C V^2 d\bar{z}. \quad (3.4.41)$$

Let dz be a small element of the integration contour C and ϑ the angle made by dz with the x -axis (see Figure 3.29). Then

$$dz = |dz|e^{i\vartheta} \quad \text{and} \quad d\bar{z} = |dz|e^{-i\vartheta}. \quad (3.4.42)$$

Since the velocity vector is tangent to the surface, we can write

$$\bar{V}(z) = V e^{-i\vartheta}.$$

Solving this equation for V , we have

$$V = \bar{V} e^{i\vartheta}. \quad (3.4.43)$$

Substitution of (3.4.42) and (3.4.43) into (3.4.41) yields

$$X - iY = i \frac{\rho}{2} \oint_C \bar{V}^2 e^{i2\vartheta} |dz| e^{-i\vartheta} = i \frac{\rho}{2} \oint_C \bar{V}^2 |dz| e^{i\vartheta} = i \frac{\rho}{2} \oint_C \left(\frac{dw}{dz} \right)^2 dz. \quad (3.4.44)$$

This equation is called the *Blasius–Chaplygin formula* in recognition of the fact that Blasius (1910) and Chaplygin (1910) were the first to derive it.

Taking into account that the integrand in (3.4.44) is an analytic function, we can change the integration path and use instead of the body contour C any other closed contour embracing the body. In particular, the integration may be performed along a

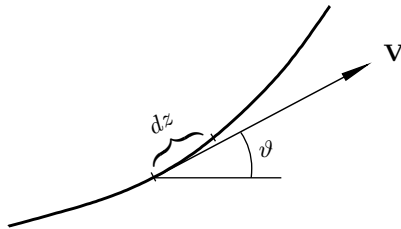


Fig. 3.29: An element of the body surface.

⁸Here it is taken into account that the integral of a constant along a closed contour is always zero.

circle C_R of large enough radius, and then $\bar{V}(z)$ may be represented by its far-field asymptotic expansion. The latter is obtained as follows.

Assuming that there are no discontinuities of the velocity in the flow field, we can treat $\bar{V}(z)$ as a single-valued analytical function. According to the free-stream boundary condition (3.4.20), $\bar{V}(z)$ is finite at $z = \infty$, and therefore the Laurent series for $\bar{V}(z)$ is written as

$$\bar{V}(z) = \frac{dw}{dz} = a_0 + \frac{a_1}{z} + \frac{a_2}{z^2} + \cdots \quad \text{as } z \rightarrow \infty. \quad (3.4.45)$$

The leading-order term is easily seen to be

$$a_0 = u_\infty - iv_\infty = V_\infty e^{-i\alpha}.$$

In order to clarify the physical meaning of the factor a_1 in the second term, we integrate (3.4.45), which gives

$$w(z) = V_\infty e^{-i\alpha} z + a_1 \ln z + O\left(\frac{1}{z}\right).$$

Let us assume that the point of observation z makes a full circle around the body. This results in an increment of the complex potential,

$$\Delta w = \Delta\varphi + i\Delta\psi = a_1 2\pi i. \quad (3.4.46)$$

According to (3.3.5), $\Delta\varphi$ coincides with the circulation Γ . For a body with an impenetrable surface, $\Delta\psi = 0$ (see Problem 3 in Exercises 8). Consequently, it follows from (3.4.46) that

$$a_1 = \frac{\Gamma}{2\pi i},$$

and (3.4.45) may be written as

$$\frac{dw}{dz} = V_\infty e^{-i\alpha} + \frac{\Gamma}{2\pi iz} + O\left(\frac{1}{z^2}\right). \quad (3.4.47)$$

Substituting (3.4.47) into (3.4.44), we have

$$\begin{aligned} X - iY &= i \frac{\rho}{2} \oint_C \left(V_\infty^2 e^{-i2\alpha} + \frac{V_\infty e^{-i\alpha} \Gamma}{\pi iz} + \cdots \right) dz \\ &= i \frac{\rho}{2} \frac{V_\infty e^{-i\alpha} \Gamma}{\pi i} 2\pi i = i\rho V_\infty e^{-i\alpha} \Gamma. \end{aligned}$$

Separation of the real and imaginary parts yields

$$X = \rho V_\infty \Gamma \sin \alpha, \quad Y = -\rho V_\infty \Gamma \cos \alpha. \quad (3.4.48)$$

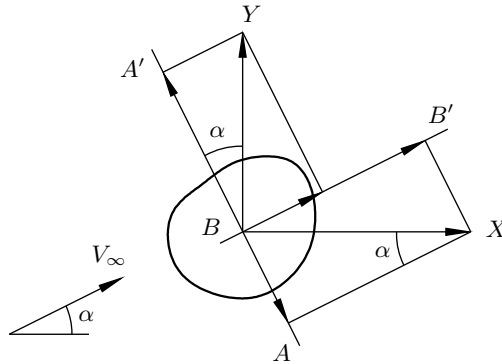


Fig. 3.30: Calculation of the lift and drag forces.

The *lift force* L is defined as the projection of the resultant force upon the direction perpendicular to the free stream. It is calculated by projecting Y and X upon line AA' in Figure 3.30:

$$L = Y \cos \alpha - X \sin \alpha. \tag{3.4.49}$$

Substituting (3.4.48) into (3.4.49), we find that

$$L = -\rho V_\infty \Gamma. \tag{3.4.50}$$

The *drag force* D is the projection of the resultant force upon line BB' parallel to the direction of the free stream. It is calculated as

$$D = Y \sin \alpha + X \cos \alpha.$$

Using (3.4.48), we can see that $D = 0$, which proves that d'Alembert's paradox holds for an arbitrary two-dimensional body.

Formula (3.4.50), which gives a surprisingly simple relationship between the lift force L and the circulation Γ , is known as the *Joukovskii formula*. Interestingly, in the original paper by Joukovskii (1906), the derivation of this formula was much more involved.

Exercises 9

1. Consider a straight line \mathcal{L} drawn perpendicular to the (x, y) -plane, and suppose that three-dimensional sources are continuously and uniformly distributed along \mathcal{L} with density q . The latter is defined as the volume of the fluid produced (per unit time) by a segment of \mathcal{L} of unit length. In particular, if we consider a small segment of length dz of the line \mathcal{L} near point S , then the volume of fluid produced by this segment per unit time will be $q dz$. According to (3.2.14), the velocity produced by this segment at point M (see Figure 3.31) will be

$$\bar{V}_r = \frac{q dz}{4\pi(z^2 + r^2)}.$$

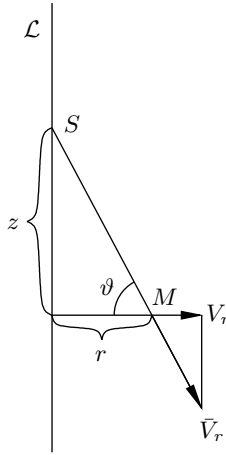


Fig. 3.31: Calculation of the velocity V_r produced by the two-dimensional source.

Project this velocity on the direction perpendicular to the line \mathcal{L} and integrate along the line \mathcal{L} and compare your result with equation (3.4.9).

2. Consider a flow given by the complex potential

$$w(z) = (1 - i) \ln \frac{z - 1}{z + 1},$$

and find the circulation of the velocity vector along a circle C that has unit radius and is centred at $z = -1$ (see Figure 3.32).

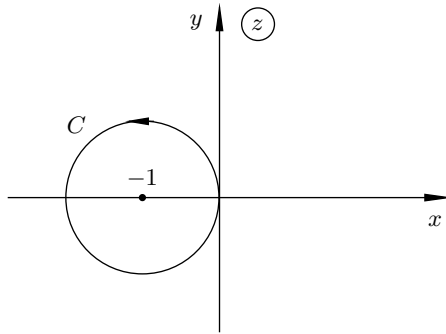


Fig. 3.32: Contour C along which the circulation is to be found.

3. Consider the two-dimensional inviscid flow of incompressible fluid inside a quarter-plane bounded by two plane walls placed along the positive x - and y -semi-axes as shown in Figure 3.33. The flow is produced by a source of strength q situated at the point $z = 1 + i$.

Calculate the fluid volume flux Q through a line that connects the source with the point $z = i$.

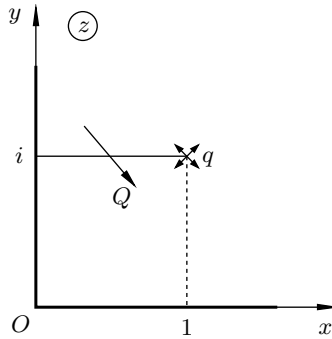


Fig. 3.33: Flow within a quarter-plane produces by a source.

Hint: Note that neither the source at $z = 1 + i$ nor its reflection in the y -axis contribute to the fluid flux.

4. Find the form of streamlines in the two-dimensional flow given by the complex potential

$$w(z) = bz^2, \tag{3.4.51}$$

where b is a real constant.

5. Study the flow in a small vicinity of the front stagnation point on the surface of a circular cylinder (Figure 3.25). Consider, for simplicity, the case where the circulation $\Gamma = 0$.
 - (a) Try to find the complex potential behaviour near the stagnation point by setting $z = -a + z'$ in (3.4.28) and assuming that $|z'|$ is much smaller than the cylinder radius a . Compare your result with (3.4.51).
 - (b) Show that on the cylinder's surface the fluid velocity grows linearly with distance from the stagnation point:

$$V = \frac{2}{a} V_\infty |z'|. \tag{3.4.52}$$

Hint: You may use without proof the Taylor expansion

$$\frac{1}{1+x} = 1 - x + x^2 + \dots,$$

valid for small x , real or complex.

6. By direct integration of the pressure distribution on the surface of a circular cylinder (see Figure 3.25), confirm that the lift force is given by the Joukovskii formula, $L = -\rho V_\infty \Gamma$. You can use without derivation the fact that on the cylinder surface the complex conjugate velocity is given by equation (3.4.34):

$$\bar{V}(z) = ie^{-i\vartheta} \left(2V_\infty \sin \vartheta - \frac{\Gamma}{2\pi a} \right).$$

7. A log of semicircular cross-section is placed on the ground as shown in Figure 3.34. Given that the radius of the log is a and the mass per unit length in the spanwise direction is m , find the critical wind speed V_∞ capable of lifting the log.

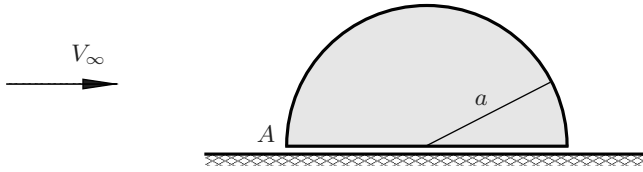


Fig. 3.34: Log on the ground.

When solving this problem, start with analysis of the pressure force acting on a small element of the contour of the upper surface of the body. Project the force on the vertical axis, and show that the integral force

$$L = \int_{-a}^a (p_0 - p) dx,$$

where x is measured along the ground and p_0 is the pressure in the gap between the log and the ground. You may assume that p_0 is constant and coincides with the pressure at the front stagnation point A .

Using the Bernoulli equation, determine the pressure distribution on the upper surface of the log and the pressure in the gap between the log and the ground.

Finally, balancing the lift force with the log weight, find the critical value of the free-stream velocity.

8. A two-dimensional point source of strength q is placed at distance h from an infinite flat plate (see Figure 3.35). Assuming that there is no fluid motion far from the source centre and the impermeability condition holds on plate surface, find the velocity distribution along the plate and calculate the integral pressure force acting upon the plate,

$$F = \int_{-\infty}^{\infty} (p - p_{\infty}) dx,$$

where p_{∞} is the unperturbed pressure far from the vortex.

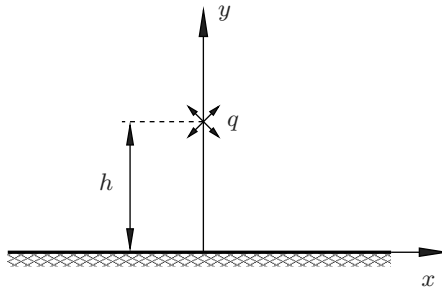


Fig. 3.35: Source above a flat surface.

Substitute the source by a vortex with circulation Γ , and repeat the calculations.

Suggestion: In order to satisfy the impermeability condition on the plate surface, the source should be reflected in the x -axis with the same sign, and the vortex with the opposite sign.

9. Consider a two-dimensional flow produced by a superposition of a uniform flow along the x -axis with velocity V_∞ and the flow from a source of strength q situated at the origin $z = 0$, where $z = x + iy$. Write down the complex potential $w = \varphi + i\psi$ for this flow. Consider a semi-infinite rigid body whose contour coincides with the streamline originating from the front stagnation point A (see Figure 3.36); it is known as a Rankine body. Show that the body contour is given by the equation

$$y = \frac{q}{2V_\infty} \left(1 - \frac{\vartheta}{\pi} \right),$$

and determine the width $2d$ in the limit as $x \rightarrow \infty$.

Calculate the drag

$$D = \int_{-d}^d (p - p_\infty) dy$$

of the Rankine body.

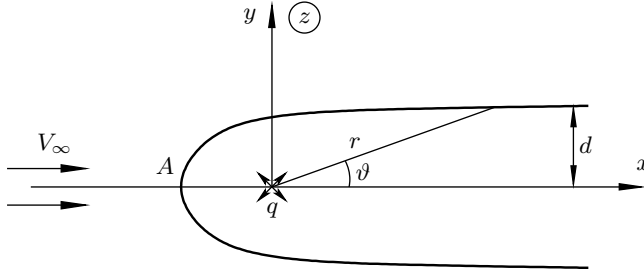


Fig. 3.36: Rankine body.

Hint: When performing this task, note that on the body's surface

$$r = \frac{y}{\sin \vartheta},$$

and express the integral for D via the angle ϑ made by the position vector with the x -axis (see Figure 3.36).

10. If the velocity field \mathbf{V} in a fluid flow is known, then the vorticity $\boldsymbol{\omega}$ may be calculated through formula (1.4.15). If, on the other hand, the vorticity field is known and the fluid is incompressible, then the velocity field may be determined through solving the equations

$$\operatorname{div} \mathbf{V} = 0, \quad \operatorname{curl} \mathbf{V} = \boldsymbol{\omega}. \tag{3.4.53}$$

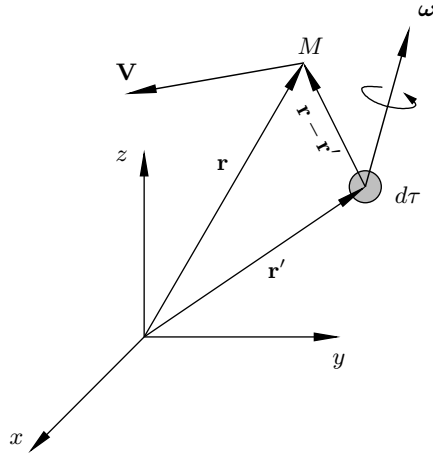


Fig. 3.37: Graphical illustration of the Biot–Savart formula (3.4.54).

Assuming that the vorticity is distributed over region \mathcal{D} and the fluid is at rest in the far field, the solution to the set of equations (3.4.53) may be expressed by the *Biot–Savart formula*,

$$\mathbf{V}(\mathbf{r}) = \iiint_{\mathcal{D}} \frac{\boldsymbol{\omega}(\mathbf{r}') \times (\mathbf{r} - \mathbf{r}')}{4\pi|\mathbf{r} - \mathbf{r}'|^3} d\tau. \quad (3.4.54)$$

Here \mathbf{r} is the position vector of the point M where the velocity \mathbf{V} is to be found, \mathbf{r}' denotes the vector that scans region \mathcal{D} in the course of integration, and $d\tau$ is a volume element of \mathcal{D} ; see Figure 3.37.

Suppose that the vorticity is confined within a cylinder that has infinite length and a small radius. Suppose further that as the cross-sectional area S of the vortex region tends to zero, the vorticity $|\boldsymbol{\omega}|$ tends to infinity, such that the circulation $\Gamma = |\boldsymbol{\omega}|S$ remains finite. This leads to an idealisation known as a line vortex.

Using (3.4.54), show that in the flow field induced by the line vortex, all fluid particles go around the vortex with velocity

$$V = \frac{\Gamma}{2\pi r},$$

where r is the distance from the vortex axis (see Figure 3.38).

Suggestion: Assume that the axis of the vortex coincides with the z -axis as shown in Figure 3.38, and consider a circle C lying in the (x, y) -plane. When calculating the velocity V at point M on the circle, take into account that the volume element $d\tau$ may be calculated as $d\tau = S dz'$. When performing the integration, it is convenient to change the integration variable and use instead of z' the angle θ between $\boldsymbol{\omega}$ and the position vector $\mathbf{r} - \mathbf{r}'$.

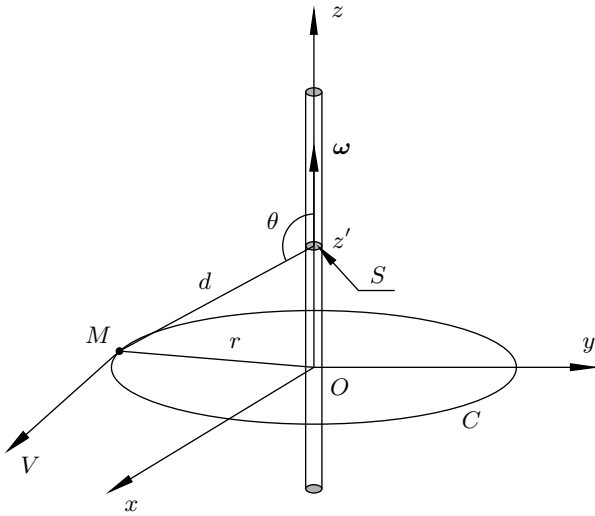


Fig. 3.38: Line vortex.

11. Consider a pair of vortices that are set free to travel in an inviscid fluid that remains motionless at infinity (see Figure 3.39). Notice that Kelvin's circulation theorem ensures that the circulations Γ_1 and Γ_2 of the vortices remain constant. When analysing the motion of vortices, take into account that a vortex cannot act on itself; i.e. it would remain at rest if placed alone into a otherwise stagnant fluid.

Denoting the coordinates of the vortices by z_1 and z_2 , deduce that the equations of motion for the vortex pair are written as

$$\frac{d\bar{z}_1}{dt} = \frac{\Gamma_2}{2\pi i} \frac{1}{z_1 - z_2}, \quad \frac{d\bar{z}_2}{dt} = \frac{\Gamma_1}{2\pi i} \frac{1}{z_2 - z_1}.$$

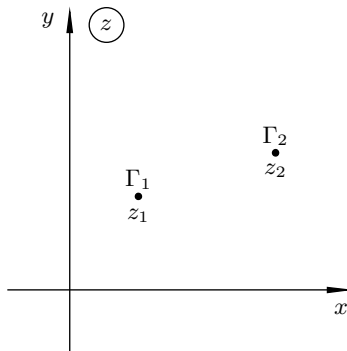


Fig. 3.39: Vortex pair.

Separating the real and imaginary parts in these equations, show that the ‘mass centre’ of the pair, whose coordinates are defined as

$$x_c = \frac{\Gamma_1 x_1 + \Gamma_2 x_2}{\Gamma_1 + \Gamma_2}, \quad y_c = \frac{\Gamma_1 y_1 + \Gamma_2 y_2}{\Gamma_1 + \Gamma_2},$$

remains at the same position at all times. Show further that the distance between the vortices remains constant. Hence, conclude that the vortices travel around one other along concentric circular trajectories.

12. What is the trajectory and speed of a single vortex placed at height h above a flat surface as shown in Figure 3.40.

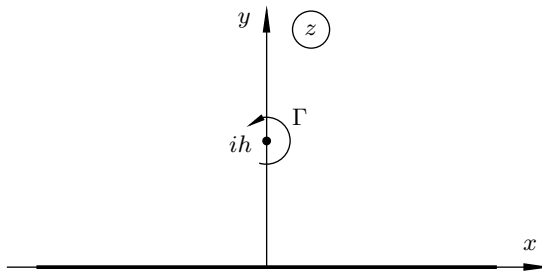


Fig. 3.40: Vortex above a flat surface.

3.5 The Method of Conformal Mapping

One of the most powerful tools in the theory of two-dimensional inviscid flows is the method of conformal mapping. Before turning to fluid-dynamic applications of the method, we shall discuss basic mathematical aspects of the theory of conformal mapping.

Any complex function $\zeta = f(z)$ serves the purpose of defining the value of $\zeta = \xi + i\eta$ for a given value of the argument $z = x + iy$. It may therefore be thought of as a mapping of points in the z -plane into the corresponding points in the ζ -plane.

3.5.1 Mapping with a linear function

To start with, we shall consider the mapping with a linear function

$$\zeta = az + b, \tag{3.5.1}$$

where a and b are complex numbers. If, in particular, $a = 1$, then, denoting the real and imaginary parts of b by b_r and b_i , respectively, we have

$$\xi = x + b_r, \quad \eta = y + b_i.$$

This shows that mapping with the function $\zeta = z + b$ represents parallel translation of all the points in the complex plane.

Let us now consider the case where b in (3.5.1) is zero and a is an arbitrary complex number different from zero and infinity. It may then be represented in the exponential form

$$a = \kappa e^{i\delta}, \tag{3.5.2}$$

where κ is the modulus of a and δ its argument. With a given by (3.5.2) and $b = 0$, the mapping (3.5.1) takes the form

$$\zeta = \kappa e^{i\delta} z.$$

Since z may also be written in the exponential form (see Figure 3.41a)

$$z = r e^{i\vartheta},$$

we have

$$\zeta = \kappa e^{i\delta} r e^{i\vartheta} = (\kappa r) e^{i(\delta+\vartheta)}.$$

Thus, the mapping $\zeta = az$ leads to magnification of $|z|$ by a factor $\kappa = |a|$ and rotation through an angle $\delta = \arg a$ (see Figure 3.41b).

Let us now return to the general linear function (3.5.1) and consider two points z' and z'' in the z -plane. Their images in the ζ -plane are

$$\zeta' = az' + b, \quad \zeta'' = az'' + b,$$

and we see that

$$\zeta'' - \zeta' = a(z'' - z'). \tag{3.5.3}$$

If we again use the exponential form (3.5.2) for a and represent $z'' - z'$ as

$$z'' - z' = |z'' - z'| e^{i\vartheta},$$

then (3.5.3) becomes

$$\zeta'' - \zeta' = \kappa e^{i\delta} |z'' - z'| e^{i\vartheta} = \kappa |z'' - z'| e^{i(\delta+\vartheta)}.$$

This shows that mapping with the linear function (3.5.1) rotates a segment of a straight line through an angle δ and stretches it κ times (compresses, if $\kappa < 1$).

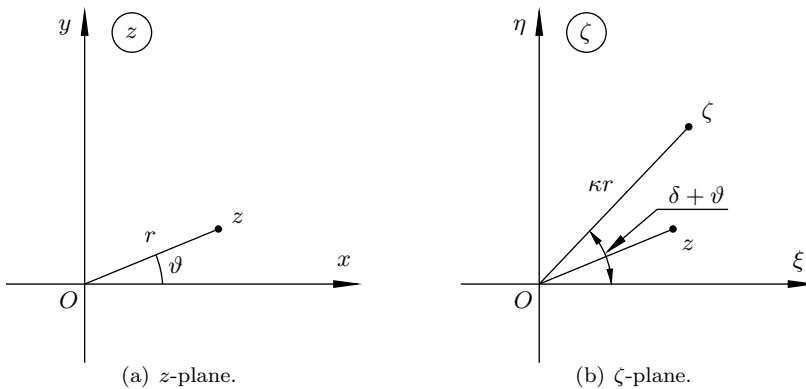


Fig. 3.41: Mapping with the function $\zeta = az$.

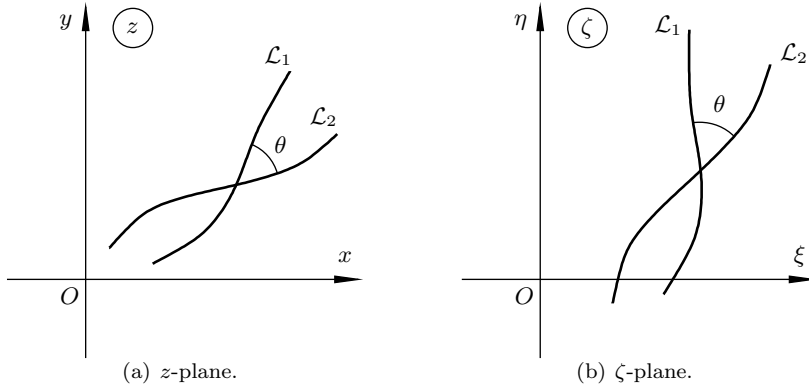


Fig. 3.42: Preservation of the angle θ between intersecting lines \mathcal{L}_1 and \mathcal{L}_2 when mapping with the linear function (3.5.1).

Since the angle of rotation does not depend on the initial orientation of the segment in the z -plane or on its length, the following two statements are valid: (i) a straight line in the z -plane is mapped by the linear function (3.5.1) onto a straight line in the ζ -plane; (ii) if two lines in the z -plane make an angle θ at the point of their intersection, then this angle is preserved in the course of the mapping with a linear function; see Figure 3.42.

We can further prove the following theorem.

Theorem 3.5 *The linear function*

$$\zeta = az + b,$$

where $a \neq 0$, transforms any circle on the z -plane into a circle on the ζ -plane.

Proof Let us consider a circle C_z of radius r centred at point z_0 in the z -plane (see Figure 3.43). We denote its image in the ζ -plane by C_ζ . For any point z lying on C_z , the following equation is valid:

$$|z - z_0| = r.$$

Using z_0 instead of z' and z instead of z'' in (3.5.3), we have

$$\zeta - \zeta_0 = a(z - z_0). \tag{3.5.4}$$

Here ζ_0 is the image of the centre z_0 and ζ lies on the image C_ζ of the circle C_z .

It follows from (3.5.4) that

$$|\zeta - \zeta_0| = |a| |z - z_0| = kr,$$

which proves that C_ζ is indeed a circle. □

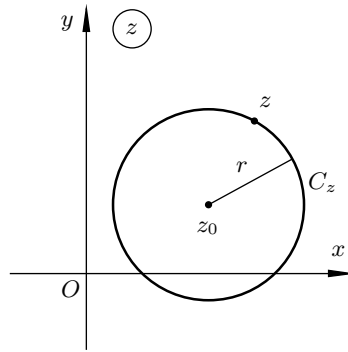


Fig. 3.43: Mapping of a circle.

3.5.2 Conformal mapping

We shall use the following definition of conformal mapping.

Definition 3.2 The mapping $\zeta = f(z)$ is said to be **conformal** at a point z_0 if the function $f(z)$ is analytic at z_0 and $f'(z_0) \neq 0$.

Remember that a function $f(z)$ is called analytic at a point z_0 if it is differentiable at this point, i.e. there exists the limit

$$f'(z_0) = \lim_{\Delta z \rightarrow 0} \frac{f(z_0 + \Delta z) - f(z_0)}{\Delta z},$$

which is independent of the orientation of Δz in the complex plane. This means that in a small neighbourhood of z_0 ,

$$f(z_0 + \Delta z) - f(z_0) = f'(z_0) \Delta z + \alpha(z_0, \Delta z) \Delta z,$$

where the function $\alpha(z_0, \Delta z)$ is such that

$$\lim_{\Delta z \rightarrow 0} \alpha(z_0, \Delta z) = 0.$$

Therefore, if we restrict our attention to a small neighbourhood of z_0 , then we can write

$$f(z_0 + \Delta z) - f(z_0) = f'(z_0) \Delta z.$$

Finally, denoting $z = z_0 + \Delta z$ and taking into account that $\zeta = f(z)$ and $\zeta_0 = f(z_0)$, we have

$$\zeta - \zeta_0 = f'(z_0) (z - z_0),$$

or, equivalently,

$$\zeta = az + b,$$

where

$$a = f'(z_0), \quad b = \zeta_0 - f'(z_0) z_0. \tag{3.5.5}$$

We can conclude that any conformal mapping behaves locally as a linear mapping. In particular, it maps small circles onto small circles and preserves the angles between

intersecting lines. It further follows from (3.5.2) and the first of equations (3.5.5) that $|f'(z)|$ is the magnification factor κ of the mapping $\zeta = f(z)$, while the angle of rotation δ is given by

$$\delta = \arg \left(\frac{df}{dz} \right). \tag{3.5.6}$$

3.5.3 Mapping with the power function

The power function is given by

$$\zeta = z^\alpha, \tag{3.5.7}$$

with α being a real constant. The function (3.5.7) is analytic in the whole complex plane except at $z = 0$ and $z = \infty$. Therefore if one wants to deal with a single-valued analytic branch of the power function, a branch cut should be made in the z -plane connecting points $z = 0$ and $z = \infty$.

The derivative of (3.5.7)

$$\frac{d\zeta}{dz} = \alpha z^{\alpha-1}$$

remains finite at all finite z . As $z \rightarrow 0$, it tends to zero for all $\alpha > 1$. If, on the other hand, $\alpha < 1$, then $d\zeta/dz$ becomes infinite at $z = 0$. This suggests that the mapping performed by (3.5.7) preserves angles at all points of the complex plane, except $z = 0$.

As an example let us consider the corner made of two rays OA and OB emerging from point O at an angle $\pi - \theta$ to one another; see Figure 3.44(a). For our purposes, it is convenient to place the coordinate origin at the point O and draw the real axis along one of the rays, say, OA .

Representing z in the exponential form

$$z = r e^{i\vartheta} \tag{3.5.8}$$

and substituting (3.5.8) into (3.5.7) yields

$$\zeta = r^\alpha e^{i\alpha\vartheta}.$$

This shows that the mapping with the power function (3.5.7) increases all the angles by a factor α . It obviously leaves the first ray OA at the original place. The second ray OB is rotated around point O , changing its angle from $\pi - \theta$ to $\alpha(\pi - \theta)$. We see

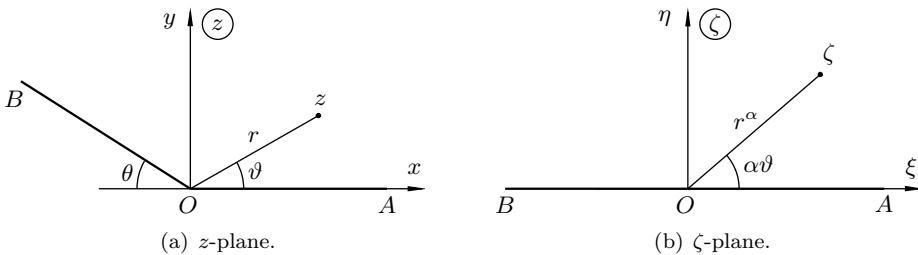


Fig. 3.44: Mapping with the power function (3.5.7).

that if, for example, we need to map the region above the corner in the z -plane onto the upper half of the ζ -plane, then we have to set

$$\alpha(\pi - \theta) = \pi.$$

We can conclude that the power function (3.5.7) performs the desired mapping, provided that

$$\alpha = \frac{\pi}{\pi - \theta}.$$

3.5.4 Linear fractional transformation

The mapping

$$\zeta = \frac{az + b}{cz + d}, \quad (3.5.9)$$

where a , b , c , and d are complex constants such that $ad - bc \neq 0$, is called a *linear fractional transformation*.

If $c = 0$, then (3.5.9) reduces to the linear transformation (3.5.1). If, on the other hand, $c \neq 0$, then (3.5.9) may be written in the form

$$\zeta = \frac{a}{c} + \frac{bc - ad}{c} \frac{1}{cz + d}, \quad (3.5.10)$$

which shows that the condition $ad - bc \neq 0$ is necessary to ensure that the linear fractional transformation (3.5.9) is not a constant function mapping all the points in the z -plane into just one point in the ζ -plane.

When cleared of fractions, equation (3.5.9) takes the form

$$c\zeta z + d\zeta - az - b = 0, \quad (3.5.11)$$

which is linear in z and linear in ζ ; i.e. it is bilinear in z and ζ . Hence, another name for the linear fractional transformation (3.5.9) is a *bilinear transformation*.

Solving equation (3.5.11) for z , we find

$$z = \frac{-d\zeta + b}{c\zeta - a}. \quad (3.5.12)$$

It follows from (3.5.9) and (3.5.12) that each point in the z -plane (except possibly $z = -d/c$) has one and only one image point in the ζ -plane. Conversely, each point in the ζ -plane (except possibly $\zeta = a/c$) has one and only one image point in the z -plane. In order to include the points $z = -d/c$ and $\zeta = a/c$ in our considerations, we adopt the following conventions for the *complex number* ∞ :

1. If a is a finite number, then

$$\frac{a}{\infty} = 0.$$

2. If $a \neq 0$, then

$$\frac{a}{0} = \infty.$$

It is easily seen that for large but finite z , equation (3.5.9) may be written as

$$\zeta = \frac{a + b/z}{c + d/z}.$$

For this reason, we will say that

$$\zeta = \frac{a}{c} \quad \text{at} \quad z = \infty. \quad (3.5.13)$$

If z approaches $-d/c$, then (3.5.9) gives

$$\zeta = \frac{b - ad/c}{0},$$

and we will say that

$$\zeta = \infty \quad \text{at} \quad z = -\frac{d}{c}. \quad (3.5.14)$$

With the extensions (3.5.13) and (3.5.14) the linear fractional function (3.5.9) performs a one-to-one mapping of the *extended* z -plane onto the *extended* ζ -plane.

Definition 3.3 *The complex z -plane with included infinite number $z = \infty$ is called the **extended z -plane**.*

Let us now return to formula (3.5.10). It shows that the linear fractional mapping (3.5.9) can be obtained by the superposition of the following three mappings:

$$z_1 = cz + d, \quad (3.5.15a)$$

$$\zeta_1 = \frac{1}{z_1}, \quad (3.5.15b)$$

$$\zeta = \frac{a}{c} + \frac{bc - ad}{c} \zeta_1. \quad (3.5.15c)$$

The first and third are linear mappings, the properties of which we already know. Hence, we only need to clarify the properties of the second mapping, (3.5.15b). Changing notation slightly, we write

$$\zeta = \frac{1}{z}. \quad (3.5.16)$$

If we use the exponential form for z , namely $z = |z|e^{i\vartheta}$, then (3.5.16) gives

$$\zeta = \frac{1}{|z|} e^{-i\vartheta}.$$

We see that the transformation (3.5.16) consists of (i) reflection of point z in the circle of unit radius (in this reflection, the image of z stays on the same radius but its modulus changes to $1/|z|$) and (ii) reflection in the real axis; see Figure 3.45.

An important property of the linear fractional transformation is the *circle property*, which is expressed by the following theorem.

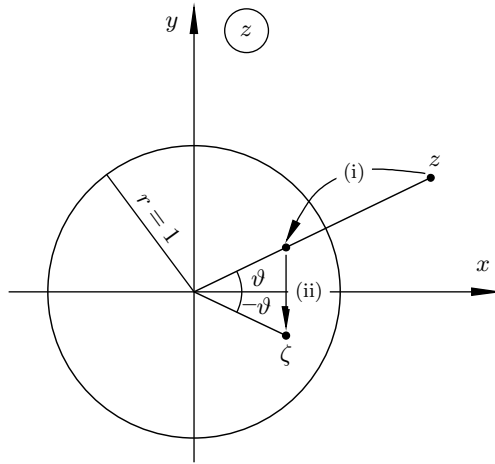


Fig. 3.45: Two steps of the transformation (3.5.16).

Theorem 3.6 *The linear fractional transformation*

$$\zeta = \frac{az + b}{cz + d}$$

maps any circle on the extended z -plane into a circle on the extended ζ -plane.

Proof Consider, first, the mapping with the function (3.5.16). The inverse to (3.5.16) is written as

$$z = \frac{1}{\zeta}.$$

Expressing z and ζ via their real and imaginary parts

$$z = x + iy, \quad \zeta = \xi + i\eta,$$

we have

$$x + iy = \frac{1}{\xi + i\eta} = \frac{\xi - i\eta}{\xi^2 + \eta^2}.$$

Hence,

$$x = \frac{\xi}{\xi^2 + \eta^2}, \quad y = -\frac{\eta}{\xi^2 + \eta^2}. \tag{3.5.17}$$

Any circle in the z -plane may be written as

$$A(x^2 + y^2) + Bx + Cy + D = 0, \tag{3.5.18}$$

where $A, B, C,$ and D are real numbers. Substitution of (3.5.17) into (3.5.18) leads to

$$D(\xi^2 + \eta^2) + B\xi - C\eta + A = 0, \tag{3.5.19}$$

which represents a circle in the ζ -plane.

Notice that with $D = 0$ the circle (3.5.18) in the z -plane passes through the origin ($x = y = 0$). Its image (3.5.19) in the ζ -plane appears to be a straight line. If, on the other hand, $A = 0$, then the circle (3.5.19) in the ζ -plane passes through the origin ($\xi = \eta = 0$), while the circle (3.5.18) in the z -plane degenerates into a straight line. Taking this into account, we will identify straight lines on the extended complex plane as circles of infinite radius.

This completes the proof of the circle property for the transformation (3.5.16). It remains to recall that the linear fractional transformation (3.5.9) may be performed in three steps (3.5.15): linear mapping (3.5.15a), mapping with the function (3.5.15b), and then the linear mapping (3.5.15c). All of these transformations assume the circle property, and therefore, so does their superposition, the linear fractional transformation (3.5.9). \square

3.5.5 Application to fluid dynamics

Let us consider the two-dimensional inviscid flow of an incompressible fluid under conditions where the fluid motion may be treated as irrotational. In this case, the flow analysis may be conducted in the complex plane z , where the body contour is denoted by S_z ; see Figure 3.46(a). In what follows, we shall refer to this plane as the physical plane.

Let us further suppose that, corresponding to the flow in the physical plane z , we can introduce an auxiliary complex plane ζ with a body contour S_ζ that is simple enough, say, a circle (see Figure 3.46b), such that the complex potential $W(\zeta)$ for the flow in the ζ -plane is known. If the conformal mapping $\zeta = f(z)$ of the exterior of the body contour S_z in the z -plane onto the exterior of the body contour S_ζ in the auxiliary plane ζ is also known, then the composite function

$$w(z) = W[f(z)] \quad (3.5.20)$$

represents the sought complex potential of the flow in the physical z -plane.

Indeed, since the function $W(\zeta)$ represents the complex potential of a fluid flow, it

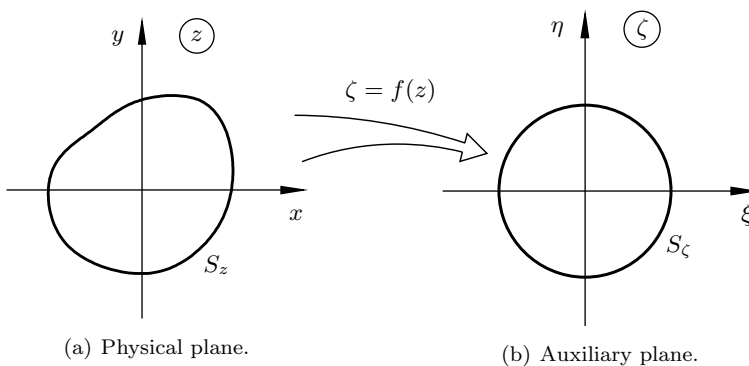


Fig. 3.46: Conformal mapping.

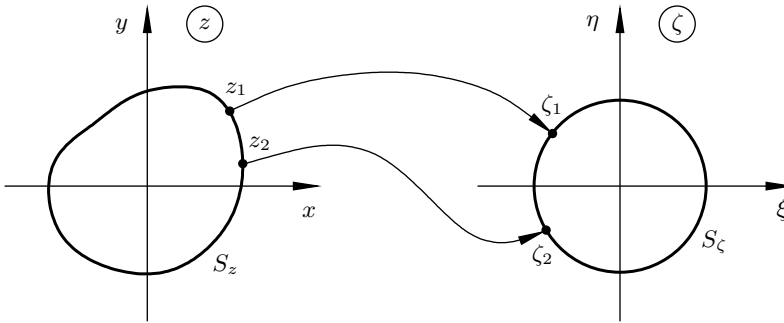


Fig. 3.47: Correspondence of the boundary points.

should be an analytic function, as condition 1 of Problem 3.2 (see page 165) requires. The function $f(z)$ performing the conformal mapping of the z -plane onto ζ -plane is also an analytic function. Therefore, we can claim that the function $w(z)$, being a superposition of $W(\zeta)$ and $f(z)$, is an analytic function everywhere outside S_z .

Turning to condition 2 of Problem 3.2, we note that, since $W(\zeta)$ represents a fluid flow, the imaginary part of $W(\zeta)$ should be constant along the body contour S_ζ in the ζ -plane, i.e.

$$\Im\{W(\zeta)\}\Big|_{S_\zeta} = \text{const.} \tag{3.5.21}$$

The principle of the correspondence of boundaries in a conformal mapping states that any two points ζ_1 and ζ_2 that lie on the boundary S_ζ in the ζ -plane are images of points z_1 and z_2 that lie on the boundary S_z in the z -plane (see Figure 3.47), i.e.

$$\zeta_1 = f(z_1), \quad \zeta_2 = f(z_2). \tag{3.5.22}$$

It follows from (3.5.21) that

$$\Im\{W(\zeta_1)\} = \Im\{W(\zeta_2)\}.$$

Therefore, combining (3.5.20) and (3.5.22), we see that

$$\Im\{w(z_1)\} = \Im\{w(z_2)\},$$

which, owing to the arbitrariness of z_1 and z_2 on S_z , proves that

$$\Im\{w(z)\}\Big|_{S_z} = \text{const.}$$

Unfortunately, conformal mapping does not guarantee that condition 3 of Problem 3.2 is satisfied automatically. For this reason, the flow behaviour in the free stream should be verified each time when the method of conformal mapping is employed.

3.5.6 Circular cylinder with an angle of attack

We shall start with a simple example that demonstrates how the method of conformal mapping may be used to generalise the solution for the flow past a circular cylinder (3.4.32) to include an angle of attack. Suppose that in the physical z -plane we have a circular cylinder of radius a centred at the coordinate origin $z = 0$. The oncoming flow is such that the free-stream velocity vector has modulus V_∞ and makes an angle α with the x -axis; see Figure 3.48.

To reduce this problem to the one considered in Section 3.4.2, we introduce an auxiliary plane ζ , which is obtained by rotating the z -plane through an angle α in the clockwise direction:

$$\zeta = e^{-i\alpha} z. \quad (3.5.23)$$

This rotation aligns the oncoming flow with the real ξ -axis in the auxiliary plane, making the equation (3.4.32) for the complex potential applicable. Expressing this equation in terms of the auxiliary plane variables, we have

$$W(\zeta) = V_\infty \left(\zeta + \frac{a^2}{\zeta} \right) + \frac{\Gamma}{2\pi i} \ln \zeta. \quad (3.5.24)$$

Substituting (3.5.23) into (3.5.24), we find that in the z -plane

$$w(z) = V_\infty \left(ze^{-i\alpha} + \frac{a^2}{ze^{-i\alpha}} \right) + \frac{\Gamma}{2\pi i} \ln z. \quad (3.5.25)$$

The additive constant $-\alpha\Gamma/2\pi$ has been disregarded.

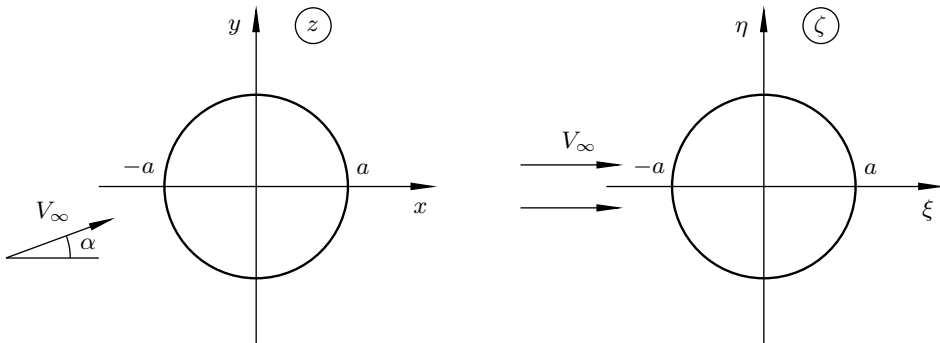


Fig. 3.48: Rotation of the cylinder through an angle α .

Exercises 10

1. Consider two-dimensional irrotational inviscid flow of an incompressible fluid past a body whose contour has a corner point (see Figure 3.49) with positive or negative angle θ . Making use of the method of conformal mapping, find the complex potential of the flow near the corner point. Determine the behaviour of the velocity V in the flow field as a function of the distance $r = |z|$ from the apex of

the corner, and discuss the theoretical predictions for pressure distribution on the body surface for concave ($\theta > 0$) and convex ($\theta < 0$) corners.

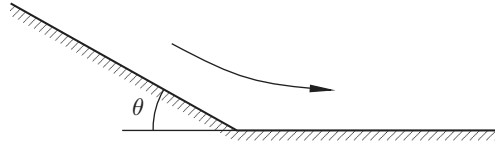


Fig. 3.49: Zoomed view of a corner point on a body contour.

Suggestion: Use the conformal mapping shown in Figure 3.44. Assume that in the auxiliary plane ζ the flow above the flat surface BOA is unidirectional and parallel to this surface.

2. Consider the flow in Figure 3.49 again, but this time analyse the flow field by solving Laplace's equation $\nabla^2\varphi = 0$ for the velocity potential φ .

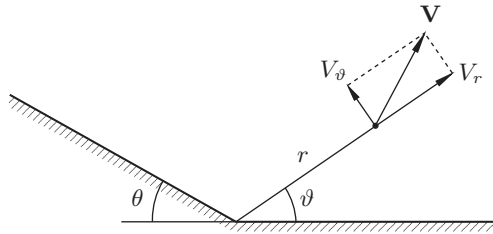


Fig. 3.50: Polar coordinates.

Introduce the polar coordinates (see Figure 3.50) and show, using (1.8.9), (1.8.18), and (1.8.29), that Laplace's equation is written in these coordinates as

$$\nabla^2\varphi = \frac{1}{r} \frac{\partial}{\partial r} \left(r \frac{\partial\varphi}{\partial r} \right) + \frac{1}{r^2} \frac{\partial^2\varphi}{\partial\vartheta^2} = 0.$$

Try to find the solution of this equation in the form

$$\varphi = \varphi_0 + r^\lambda f(\vartheta),$$

where φ_0 is the value of the velocity potential at the corner point and λ is a constant to be found; restrict your attention to positive values of λ .

Remember that the radial and circumferential velocity components are calculated in polar coordinates as

$$V_r = \frac{\partial\varphi}{\partial r}, \quad V_\vartheta = \frac{1}{r} \frac{\partial\varphi}{\partial\vartheta}, \tag{3.5.26}$$

and, using the impermeability condition on the two walls, deduce that a non-trivial solution exists if

$$\lambda = \lambda_k = \frac{\pi k}{\pi - \theta}, \quad k = 1, 2, 3, \dots \tag{3.5.27}$$

Show that, corresponding to (3.5.27),

$$f_k(\vartheta) = C_k \cos(\lambda_k \vartheta),$$

and conclude that the solution can be written as

$$\varphi = \varphi_0 + \sum_{k=1}^{\infty} C_k r^{\lambda_k} \cos(\lambda_k \vartheta). \tag{3.5.28}$$

Assume that r is small and disregard all the terms in the sum in (3.5.28) except the first one. Deduce that the tangential velocity on the corner walls

$$\left. \begin{aligned} V_r \Big|_{\vartheta=0} &= C_1 \lambda_1 r^{\theta/(\pi-\theta)} + \dots, \\ V_r \Big|_{\vartheta=\pi-\theta} &= -C_1 \lambda_1 r^{\theta/(\pi-\theta)} + \dots \end{aligned} \right\} \text{ as } r \rightarrow 0. \tag{3.5.29}$$

3. Study the flow round the tip of a semi-infinite flat plate as shown in Figure 3.51, for which purpose you may use the solution of Problem 1 (see Figure 3.49) with $\theta = -\pi$.

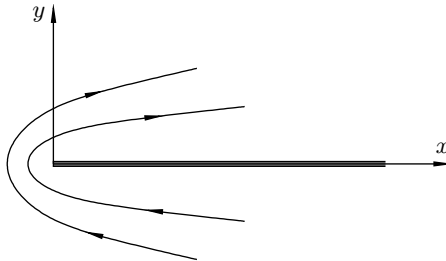


Fig. 3.51: Flow around a plate tip.

Show that each streamline in this flow has a parabolic shape. Choose one of the streamlines and, treating it as the surface of a solid body, calculate the integral pressure force

$$F_x = 2 \int_0^{\infty} (p - p_{\infty}) dy$$

acting upon the body parallel to the plate surface. Observe that the force F_x does not depend on the streamline considered, which is why this force may be thought of as a ‘suction force’ acting on the tip of the plate.

Hint: When using the Bernoulli equation, take into account that, far from the plate tip ($x^2 + y^2 \rightarrow \infty$), the flow velocity $|\mathbf{V}|$ tends to zero. Denote the value of the pressure in the ‘far field’ by p_{∞} .

4. Consider an inviscid incompressible fluid flow above flat ground on which a thin fence of height h is installed; in Figure 3.52, the ground coincides with the x -axis and the fence occupies an interval $[0, h]$ of the y -axis. The flow velocity far upstream of the fence is V_{∞} .

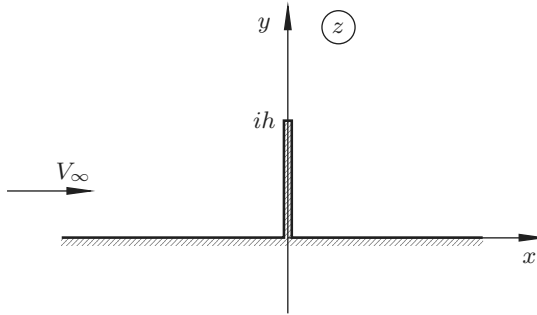


Fig. 3.52: Flow over a fence.

Deduce that the conformal mapping of the physical z -plane shown in Figure 3.52 onto the upper half-plane in the auxiliary ζ -plane is given by

$$\zeta = \sqrt{z^2 + h^2}.$$

Assume that in the auxiliary plane the complex potential may be written as

$$W(\zeta) = \tilde{V}_\infty \zeta,$$

and find the value of the real constant \tilde{V}_∞ , taking into account that in the physical plane the free-stream velocity is V_∞ .

Find the pressure distribution along the ground ($z = x$). Use of the Bernoulli equation for this purpose.

Calculate the integral pressure force

$$F = \int_{-\infty}^{\infty} (p - p_\infty) dx$$

acting upon the ground; here p_∞ is the unperturbed pressure in the oncoming flow.

3.5.7 Joukovskii transformation

Many fluid flows may be studied using the Joukovskii transformation. In order to introduce this transformation, let us find the conformal mapping of a circular arc onto a full circle. More precisely, we shall consider a region that consists of the whole z -plane with the exception of a branch cut along a circular arc of depth h , with the interval $[-a, a]$ of the real axis serving as the arc chord; see Figure 3.53(a). This region is to be mapped onto the exterior of a circle that is centered at $\zeta = ih$ and intersects the real axis at points $-a$ and a as shown in Figure 3.53(b).

We shall denote the angle between the tangent to the arc at point B and the real axis in the z -plane by β ; see Figure 3.53(a). It is well known that a straight line connecting the top point of the arc, $z = ih$, with the right-hand edge of the arc B

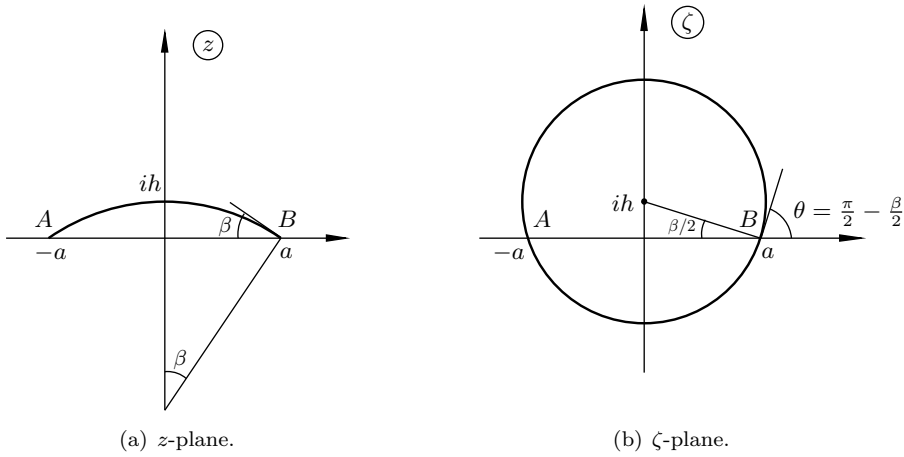


Fig. 3.53: Joukovskii transformation.

bisects the angle β . This means that a straight line, connecting the centre of the circle and point B in the ζ -plane, makes an angle $\frac{1}{2}\beta$ with the real axis (Figure 3.53a).

Let us start with the z -plane, to which the following linear fractional transformation will first be applied:

$$z_1 = \frac{z - a}{z + a}. \tag{3.5.30}$$

The transformation (3.5.30) assumes the circle property, i.e. it maps a circle (or circular arc) in the z -plane onto a circle (or a straight line) in the z_1 -plane.

It is easily seen that the function (3.5.30) maps point B , situated at the right-hand end of the arc in the z -plane into the origin $z_1 = 0$ in the z_1 -plane. The image of the left-hand end A of the arc, where $z = -a$, is easily seen to be $z_1 = \infty$. Thus, the arc is transformed into a ray emerging from the origin and extending to infinity as shown in Figure 3.54(a).

The orientation of the ray may be found using formula (3.5.6), which gives the angle δ of rotation of any line (more precisely, a small segment of a line) in the z -plane when it is mapped onto the z_1 -plane. Differentiating (3.5.30), we have

$$\frac{dz_1}{dz} = \frac{2a}{(z + a)^2}.$$

At point B , $z = a$ and the derivative is real and positive:

$$\left. \frac{dz_1}{dz} \right|_{z=a} = \frac{1}{2a}.$$

This means that a small segment of the arc in Figure 3.53(a) near point B does not experience any rotation, $\delta = 0$. Hence, the angle between the ray and the negative real semi-axis in the z_1 -plane (see Figure 3.54a) has to be equal to the angle β between the arc and the real axis at point B in the z -plane (Figure 3.53a).

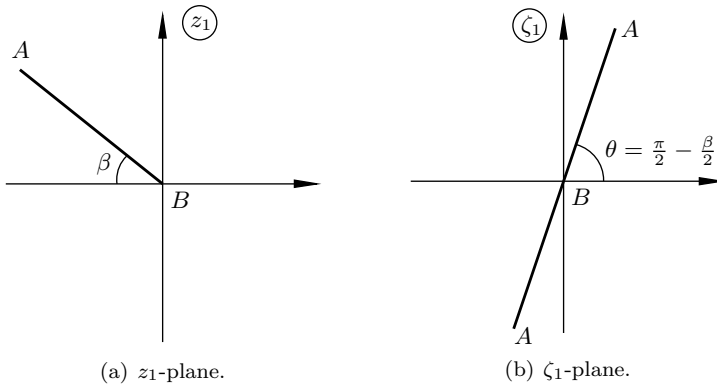


Fig. 3.54: Auxiliary planes z_1 and ζ_1 .

We now apply the same transformation to the circle in the ζ -plane (Figure 3.53b):

$$\zeta_1 = \frac{\zeta - a}{\zeta + a}. \tag{3.5.31}$$

As a result, point B is mapped into $\zeta_1 = 0$ and point A into an infinite point $\zeta_1 = \infty$. The derivative of the function (3.5.31) at $\zeta = a$ is real and positive, which means again that a small segment of the circle in Figure 3.53(b) near $\zeta = a$ does not experience any rotation. Its image in the ζ_1 -plane is a straight line that makes an angle $\theta = \pi/2 - \beta/2$ with the real positive axis; see Figure 3.54(b). The exterior of the circle is mapped onto the half-plane to the right of this line.

It is easily seen that the mapping between the z_1 - and ζ_1 -planes is performed by the function

$$z_1 = \zeta_1^2. \tag{3.5.32}$$

Substitution of (3.5.30) and (3.5.31) into (3.5.32) gives

$$\frac{z - a}{z + a} = \left(\frac{\zeta - a}{\zeta + a} \right)^2. \tag{3.5.33}$$

The simple manipulations

$$\begin{aligned} \frac{z + a - 2a}{z + a} &= \left(\frac{\zeta + a - 2a}{\zeta + a} \right)^2, \\ 1 - \frac{2a}{z + a} &= \left(1 - \frac{2a}{\zeta + a} \right)^2 = 1 - \frac{4a}{\zeta + a} + \frac{4a^2}{(\zeta + a)^2}, \\ \frac{1}{z + a} &= \frac{2}{\zeta + a} - \frac{2a}{(\zeta + a)^2} = \frac{2\zeta}{(\zeta + a)^2}, \\ z + a &= \frac{(\zeta + a)^2}{2\zeta} = a + \frac{\zeta^2 + a^2}{2\zeta} \end{aligned}$$

show that

$$z = \frac{1}{2} \left(\zeta + \frac{a^2}{\zeta} \right), \quad (3.5.34)$$

which is the sought function performing the conformal mapping of the exterior of the circle in the ζ -plane (see Figure 3.53) onto the exterior of the arc in the z -plane. It is called the *Joukovskii transformation*.

Multiplying both sides of (3.5.34) by 2ζ ,

$$\zeta^2 - 2z\zeta + a^2 = 0, \quad (3.5.35)$$

and solving the quadratic equation (3.5.35) for ζ , we find that the inverse transformation is given by

$$\zeta = z \pm \sqrt{z^2 - a^2}.$$

Notice that while the Joukovskii transformation (3.5.34) is a single-valued function; its inverse is double-valued. For each point in the z -plane, it produces two points in the ζ -plane. One of them is situated outside the circle (see Figure 3.53b), while the other finds itself inside the circle. If we take, for instance, $z = 2a$, then

$$\zeta_{1,2} = (2 \pm \sqrt{3}) a.$$

We see that in order to deal with the exterior of the circle in the auxiliary plane ζ , we have to write the inverse transformation as

$$\zeta = z + \sqrt{z^2 - a^2}. \quad (3.5.36)$$

3.6 Flat Plate at an Incidence

To describe the flow past a flat plate, we return to Figure 3.53 and notice that the camber of the arc in the physical plane z depends on the parameter h . If h is chosen to be zero, then the arc becomes a segment of a straight line connecting points A and B . At the same time, with $h = 0$, the centre of the circle in the auxiliary ζ -plane moves into the coordinate origin. The radius of the circle becomes a , since it still has to be drawn through points A and B . We see that the Joukovskii transformation (3.5.36) performs a conformal mapping of the whole z -plane except for a branch cut along a segment $[-a, a]$ of the real axis onto the exterior of a circle that has radius a and is centred at $\zeta = 0$ in the auxiliary plane; see Figure 3.55.

According to (3.5.25), the complex potential in the auxiliary plane is written as

$$W(\zeta) = \tilde{V}_\infty \left(\zeta e^{-i\alpha} + \frac{a^2}{\zeta e^{-i\alpha}} \right) + \frac{\Gamma}{2\pi i} \ln \zeta. \quad (3.6.1)$$

Here \tilde{V}_∞ denotes the free-stream velocity in the auxiliary plane, which does not necessarily coincide with the free-stream velocity in the physical z -plane. In order to obtain the complex potential $w(z)$ in the physical plane, we have to combine (3.6.1) with the Joukovskii transformation (3.5.36), namely $w(z) = W[\zeta(z)]$.

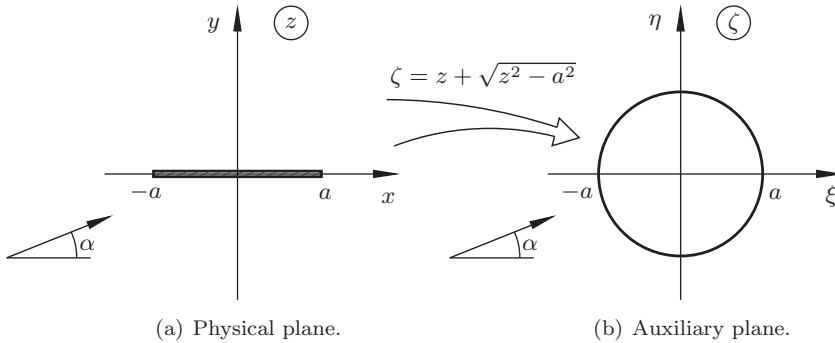


Fig. 3.55: Transformation of a flat plate onto a circle.

The complex conjugate velocity in the z -plane may be calculated as

$$\bar{V}(z) = \frac{dw}{dz} = \frac{dW}{d\zeta} \frac{d\zeta}{dz} = \frac{dW}{d\zeta} \frac{1}{dz/d\zeta}. \quad (3.6.2)$$

It follows from (3.6.1) that

$$\frac{dW}{d\zeta} = \tilde{V}_\infty \left(e^{-i\alpha} - \frac{a^2}{\zeta^2 e^{-i\alpha}} \right) + \frac{\Gamma}{2\pi i \zeta}. \quad (3.6.3)$$

Differentiating (3.5.34), we find

$$\frac{dz}{d\zeta} = \frac{1}{2} \left(1 - \frac{a^2}{\zeta^2} \right). \quad (3.6.4)$$

In the far field ($z \rightarrow \infty, \zeta \rightarrow \infty$), formulae (3.6.3) and (3.6.4) reduce to

$$\frac{dW}{d\zeta} = \tilde{V}_\infty e^{-i\alpha}, \quad \frac{dz}{d\zeta} = \frac{1}{2}.$$

Therefore

$$\bar{V}(z) \rightarrow 2\tilde{V}_\infty e^{-i\alpha} \quad \text{as } z \rightarrow \infty,$$

and if the modulus of the velocity in the oncoming flow in the physical plane is V_∞ , then in the auxiliary plane we have to take

$$\tilde{V}_\infty = \frac{1}{2} V_\infty. \quad (3.6.5)$$

The solution still involves one unknown parameter, the circulation Γ , and our task now will be to study its influence on the flow behaviour. If, for example, we set $\Gamma = 0$, then the streamline pattern will have the form shown in Figure 3.56.⁹ We see that the

⁹These streamlines were drawn using the following procedure. We introduced a uniform mesh in the z -plane and calculated ζ for each node point z using (3.5.36). Then the value of ζ for the node considered was used in formula (3.6.4) to calculate the complex potential. Its imaginary part gives the stream function at the node points. As soon as the distribution of the stream function over the mesh is known, the contour plot may drawn using a standard plotting package.

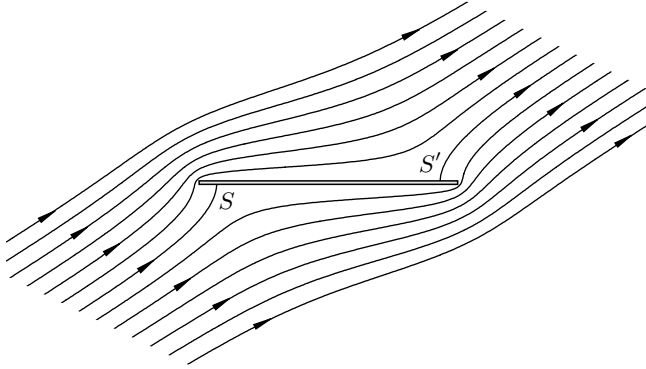


Fig. 3.56: The streamline pattern for the flow past a flat plate with $\Gamma = 0$ and incidence $\alpha = 30^\circ$.

flow goes round the leading and trailing edges of the plate, where the velocity should become infinite.¹⁰ Indeed, according to (3.6.4) the derivative $dz/d\zeta$ becomes zero at $\zeta = -a$ and $\zeta = a$, which is translated into singularities in the velocity (3.6.2) at $z = -a$ and $z = a$.

We further see that with $\Gamma = 0$ there are two stagnation points on the plate surface, S and S' . Their positions may be found by setting $dW/d\zeta$ as given by (3.6.3) to zero. We have

$$e^{-i\alpha} - \frac{a^2}{\zeta^2 e^{-i\alpha}} = 0,$$

which, being solved for ζ , gives

$$\zeta = \pm a e^{i\alpha}.$$

Their loci in the z -plane may be found using (3.5.34):

$$z = \pm \frac{1}{2} \left(a e^{i\alpha} + \frac{a^2}{a e^{i\alpha}} \right) = \pm a \cos \alpha.$$

Experimental observations show that the flow normally leaves the trailing edge in a smooth fashion. The reason for this is that, near the trailing edge, the boundary layer is well developed, and it is known to be unable to sustain violent variations of the pressure that would happen if the flow were really going round the trailing edge as shown in Figure 3.56.¹¹ Meanwhile, it may easily be seen that the flow can be made smooth near the trailing edge by a proper choice of the circulation Γ . Indeed, the singularity in (3.6.2) can be avoided if we set $dW/d\zeta$ as given by (3.6.3) equal to zero at the point $\zeta = a$, which represents the trailing edge of the plate in the auxiliary ζ -plane. Substituting (3.6.5) into (3.6.3) and setting $\zeta = a$, we write

$$\frac{V_\infty}{2} (e^{-i\alpha} - e^{i\alpha}) + \frac{\Gamma}{2\pi i a} = 0.$$

¹⁰See Problem 3 in Exercises 10.

¹¹The properties of the viscous boundary layer will be discussed in Part 3 of this book series. In particular, the trailing-edge flow will be studied in detail.

Solving this equation for Γ , we find that the circulation

$$\Gamma = -2\pi a V_\infty \sin \alpha. \tag{3.6.6}$$

The streamline pattern for the flow field with the circulation given by (3.6.6) is shown in Figure 3.57.

Let us now calculate the velocity field for this flow. Substitution of (3.6.5) and (3.6.6) into (3.6.3) yields

$$\begin{aligned} \frac{dW}{d\zeta} &= \frac{V_\infty}{2} \left(e^{-i\alpha} - \frac{a^2}{\zeta^2 e^{-i\alpha}} \right) - V_\infty \frac{a \sin \alpha}{i\zeta} \\ &= \frac{V_\infty}{2} \cos \alpha - i \frac{V_\infty}{2} \sin \alpha - \frac{V_\infty a^2}{2 \zeta^2} \cos \alpha - i \frac{V_\infty a^2}{2 \zeta^2} \sin \alpha + i V_\infty \frac{a}{\zeta} \sin \alpha \\ &= \frac{V_\infty}{2} \left(1 - \frac{a^2}{\zeta^2} \right) \cos \alpha - i \frac{V_\infty}{2} \left(1 - \frac{a}{\zeta} \right)^2 \sin \alpha. \end{aligned} \tag{3.6.7}$$

Now we substitute (3.6.7) and (3.6.4) into (3.6.2). We have

$$\bar{V} = \frac{dW}{d\zeta} \frac{1}{dz/d\zeta} = V_\infty \cos \alpha - i V_\infty \sin \alpha \frac{\zeta - a}{\zeta + a}.$$

Finally, using (3.5.36), we find that

$$\frac{\zeta - a}{\zeta + a} = \frac{z - a + \sqrt{z^2 - a^2}}{z + a + \sqrt{z^2 - a^2}} = \frac{\sqrt{z - a}(\sqrt{z - a} + \sqrt{z + a})}{\sqrt{z + a}(\sqrt{z + a} + \sqrt{z - a})} = \sqrt{\frac{z - a}{z + a}},$$

and therefore

$$\bar{V}(z) = V_\infty \cos \alpha - i V_\infty \sin \alpha \sqrt{\frac{z - a}{z + a}}.$$

Notice that at the trailing edge ($z = a$) the velocity is directed parallel to the plate surface and has finite modulus $|\bar{V}| = V_\infty \cos \alpha$.

The condition that the velocity at the trailing edge should be finite was first introduced by Joukovskii (1910) and Kutta (1910), and since then has been referred to as the *Joukovskii-Kutta hypothesis*.

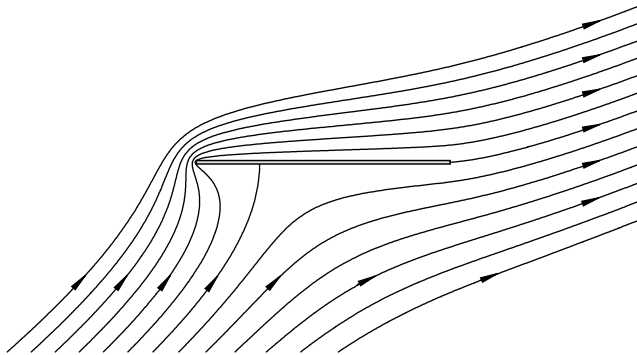


Fig. 3.57: The streamline pattern for $\alpha = 30^\circ$ and the circulation given by (3.6.6).

3.7 Joukovskii Aerofoils

In Section 3.5.7, it was demonstrated that the Joukovskii transformation

$$\zeta = z + \sqrt{z^2 - a^2} \tag{3.7.1}$$

gives a conformal mapping of a circular arc in the z -plane onto a circle in the ζ -plane (see Figure 3.53). The arc connects points $-a$ and a on the real axis in the z -plane and crosses the imaginary axis at the point $z = ih$. Its image in the ζ -plane is a circle that has its centre at $\zeta = ih$ and intersects the real axis at the points $-a$ and a .

We shall now use this mapping to introduce a family of aerofoil shapes known as *Joukovskii aerofoils*. These are obtained in the following way. We extend the segment of a straight line connecting the points $\zeta = ih$ and $\zeta = a$ in the ζ -plane beyond the point $\zeta = ih$ as shown in Figure 3.58(b), and place the point ζ_0 on the extension a distance d from the point ih . We then use ζ_0 as the centre of a new circle, and choose its radius to be

$$R = d + \sqrt{a^2 + h^2},$$

which ensures that the circle passes through point B , where $\zeta = a$. In Figure 3.58(b), this new circle is shown by the solid line; we also reproduce here the ‘old circle’ of Figure 3.53(b) with the dashed line. In what follows, we shall refer to these as ‘large’ and ‘small’ circles, respectively.

The inverse Joukovskii transformation

$$z = \frac{1}{2} \left(\zeta + \frac{a^2}{\zeta} \right) \tag{3.7.2}$$

maps the small circle onto a circular arc in the z -plane, shown in Figure 3.58(a) by the dashed line. The image of the large circle represents a *Joukovskii aerofoil*. Since at point B in the ζ -plane, the two circles are tangent to one another, their images

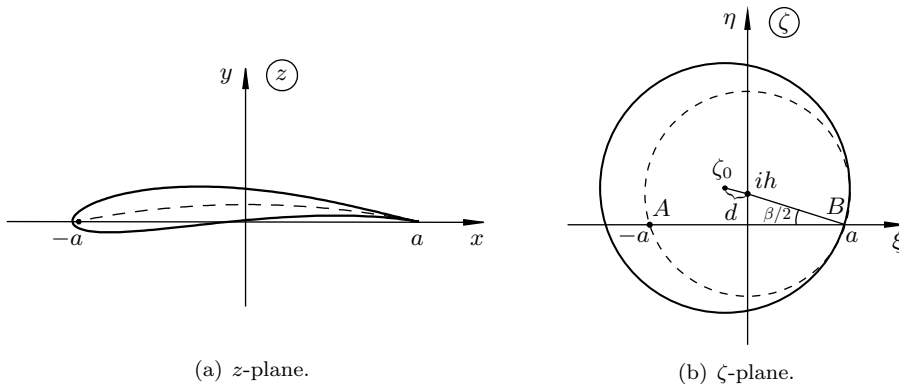


Fig. 3.58: Mapping of a circle in the auxiliary plane onto a Joukovskii aerofoil in the physical plane. The particular shape of the aerofoil shown in the z -plane has been calculated for $h/a = 0.1$ and $d/a = 0.1$.

in the z -plane should also be tangent. This means that at the trailing edge both the upper and lower surfaces of the aerofoil (see Figure 3.58a) are tangent to the arc, and therefore the aerofoil contour forms a cusp at the trailing edge. Moving away from point B in the auxiliary ζ -plane results in wider separation of the two circles. Correspondingly, in the z -plane, the distance between the arc and the upper and lower surfaces of the aerofoil contour grows larger. Since point A in the ζ -plane is situated inside the large circle, the leading edge of the aerofoil appears to be rounded.

Apart from the parameter a , which may be used to change the aerofoil chord, there are two more parameters controlling the aerofoil shape, namely the camber parameter h and the thickness parameter d . The particular shape shown in Figure 3.58 was drawn for $h/a = 0.1$ and $d/a = 0.1$. This was done numerically by placing a sufficiently large number of points distributed uniformly round the circle in the ζ -plane and using the Joukovskii transformation (3.7.2) to calculate their coordinates in the z -plane.

Now we need to adjust the complex potential (3.5.25) that describes the flow past a circular cylinder shown on the left-hand side of Figure 3.48 (see page 191) to the flow past the ‘large circle’ in the auxiliary ζ -plane (Figure 3.58b). Taking into account that the radius of the circle now equals R and its centre is shifted to the point ζ_0 , we write

$$W(\zeta) = \tilde{V}_\infty \left[(\zeta - \zeta_0)e^{-i\alpha} + \frac{R^2}{(\zeta - \zeta_0)e^{-i\alpha}} \right] + \frac{\Gamma}{2\pi i} \ln(\zeta - \zeta_0). \quad (3.7.3)$$

Remember that with the method of conformal mapping conditions 1 and 2 in the formulation of Problem 3.2 (see page 165) are satisfied automatically, but the free-stream condition 3 requires special attention.

The complex conjugate velocity in the physical plane (Figure 3.58a) is calculated as

$$\bar{V}(z) = \frac{dW}{d\zeta} \frac{d\zeta}{dz}, \quad (3.7.4)$$

where

$$\frac{dW}{d\zeta} = \tilde{V}_\infty \left[e^{-i\alpha} - \frac{R^2}{(\zeta - \zeta_0)^2 e^{-i\alpha}} \right] + \frac{\Gamma}{2\pi i} \frac{1}{\zeta - \zeta_0} \quad (3.7.5)$$

and

$$\frac{d\zeta}{dz} = 1 + \frac{z}{\sqrt{z^2 - a^2}}. \quad (3.7.6)$$

At large values of z and ζ ,

$$\frac{dW}{d\zeta} = \tilde{V}_\infty e^{-i\alpha}, \quad \frac{d\zeta}{dz} = 2,$$

which on substitution into (3.7.4) yield

$$\bar{V}(z) = 2\tilde{V}_\infty e^{-i\alpha} + \dots \quad \text{as } z \rightarrow \infty.$$

We see that the free-stream condition is satisfied with

$$\tilde{V}_\infty = \frac{1}{2} V_\infty. \quad (3.7.7)$$

Let us now study the flow near the aerofoil. It follows from (3.7.6) that there are two singular points: $z = -a$ and $z = a$. However, in the flow past the Joukovskii

aerofoil (Figure 3.58a), the first of these points, $z = -a$, is situated inside the aerofoil, and we only need to consider the point $z = a$, which lies at the trailing edge of the aerofoil. Its image in the auxiliary plane is the point B where $\zeta = a$; see Figure 3.58(b). According to the Joukovskii–Kutta condition, the complex conjugate velocity $\bar{V}(z)$ has to be finite at the trailing edge, which is only possible if

$$\left. \frac{dW}{d\zeta} \right|_B = 0. \quad (3.7.8)$$

It may easily be seen from Figure 3.58(b) that, at point B ,

$$\zeta - \zeta_0 = a - \zeta_0 = Re^{-i\beta/2}. \quad (3.7.9)$$

Using (3.7.9) and (3.7.7) in (3.7.5) allows us to express equation (3.7.8) in the form

$$\frac{V_\infty}{2} \left(e^{-i\alpha} - \frac{1}{e^{-i(\alpha+\beta)}} \right) - i \frac{\Gamma}{2\pi} \frac{1}{Re^{-i\beta/2}} = 0,$$

which, being solved for Γ , yields

$$\Gamma = -2\pi RV_\infty \frac{e^{i(\alpha+\beta/2)} - e^{-i(\alpha+\beta/2)}}{2i} = -2\pi RV_\infty \sin(\alpha + \beta/2). \quad (3.7.10)$$

This completes the task of finding the complex potential of the flow past a Joukovskii aerofoil. Now any fluid-dynamic function may easily be determined. In particular, in Figure 3.59, we show the streamline pattern for a Joukovskii aerofoil with $h/a = 0.1$ and $d/a = 0.1$ at incidence $\alpha = 20^\circ$. This was obtained numerically by distributing the mesh points on a set of concentric circles surrounding the large circle in Figure 3.58(b). For each such point, the location of its image in the physical z -plane is calculated using the Joukovskii transformation (3.7.2). The value of the complex potential at this point is found using equation (3.7.3) with (3.7.7) and (3.7.10). Separating the imaginary part of W yields the stream function, ψ . The contours of constant ψ produce the streamline pattern.

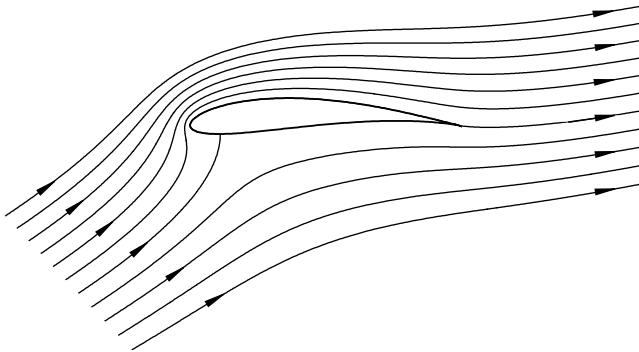


Fig. 3.59: Streamline pattern for the aerofoil in Figure 3.58(a); incidence $\alpha = 20^\circ$.

If one wants to find the fluid velocity at a given point z in the physical plane, then the position ζ of the image of this point in the auxiliary plane should first be found, using equation (3.7.1). Then, equation (3.7.4) together with (3.7.5) and (3.7.6) can be used to determine the velocity components, u and v . Once the velocity is known, the pressure at any point in the flow field and on the aerofoil surface can be found using the Bernoulli equation

$$\frac{V^2}{2} + \frac{p}{\rho} = \frac{V_\infty^2}{2} + \frac{p_\infty}{\rho}.$$

Of course, one does not need to integrate the pressure over the aerofoil surface to determine the lift force. This can be done with the help of the Joukovskii formula:

$$L = -\rho V_\infty \Gamma = \rho V_\infty^2 2\pi R \sin(\alpha + \beta/2). \quad (3.7.11)$$

The theoretical predictions for the lift force are in good agreement with the experimental data, but only for angles of attack below some critical value that depends on the aerofoil shape. The reason is that the Joukovskii–Kutta condition presumes that the flow remains attached to the aerofoil surface. While aerofoils are specially designed to maintain attached flow, in reality separation can be avoided only within a narrow range of angles of attack. As an example, in Figure 3.60 the flow past a NACA 4412 aerofoil is shown. We see that at an angle of attack $\alpha = 5^\circ$ the flow is attached to the aerofoil surface, but at $\alpha = 10^\circ$ separation develops near the trailing edge. This leads to a reduction of the circulation Γ produced by an aerofoil, and hence to a loss in the lift force.

Despite the fact that inviscid flow theory completely fails to predict the drag force, it has been used extensively in aerofoil design. The analysis of Joukovskii aerofoils presented above takes advantage of the fact that the function performing the conformal mapping of the aerofoil on a circle in the auxiliary plane can be expressed in the analytic form (3.7.1). In the more general case, the mapping function should be found

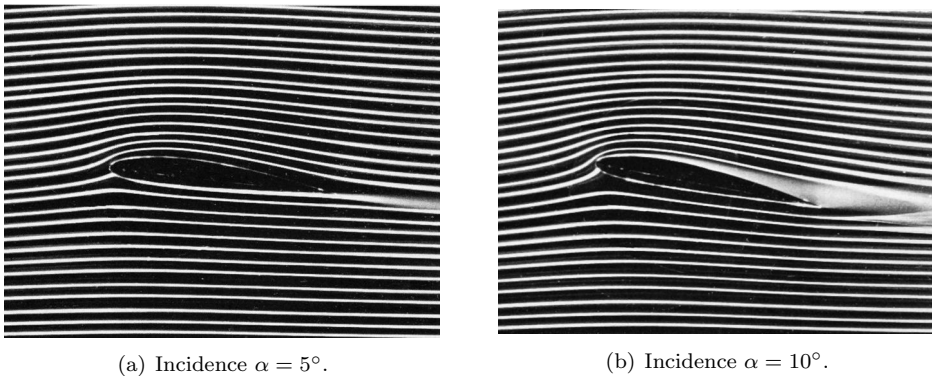


Fig. 3.60: Visualisation of the flow past a NACA 4412 aerofoil by Akira Ito. Reprinted from *Visualized Flow: Fluid motion in basic and engineering situations revealed by flow visualization*, Pergamon Press. Figures 123 and 124, page 77. Copyright 1988.

numerically. As this task is quite complicated, the flow behaviour past an aerofoil is normally predicted through direct numerical solution of Problem 3.1; see page 142.

Exercises 11

1. Consider an incompressible inviscid flow past a circular arc at zero angle of attack; see Figure 3.61.

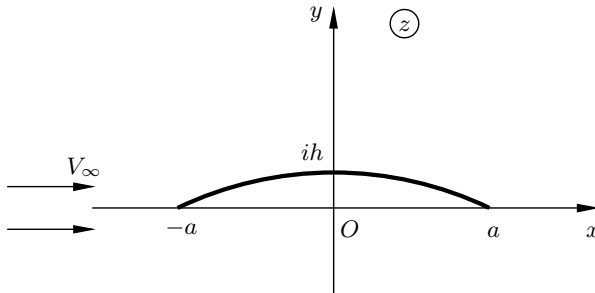


Fig. 3.61: Flow past a circular arc.

Show that the lift force produced by the arc is

$$L = \rho V_\infty^2 2\pi h.$$

Suggestion: You may use without proof formula (3.7.11) for the lift force of a Joukovskii aerofoil.

2. An incompressible inviscid fluid flows past an ellipse whose large axis is aligned with the free-stream velocity vector; see Figure 3.62(a).

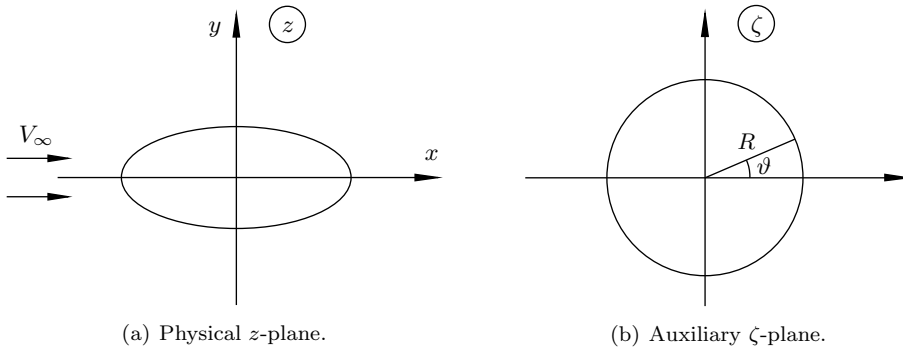


Fig. 3.62: Flow past an ellipse.

- (a) Verify that the Joukovskii transformation

$$z = \frac{1}{2} \left(\zeta + \frac{a^2}{\zeta} \right) \tag{3.7.12}$$

performs a conformal mapping of a circle of radius $R > a$ in the ζ -plane (Figure 3.62b) onto an ellipse in the z -plane (Figure 3.62a). For this purpose, express the equation of the circle in the auxiliary ζ -plane in the form

$$\zeta = Re^{i\vartheta}. \tag{3.7.13}$$

Substitute (3.7.13) into (3.7.12) and separate the real and imaginary parts. Then eliminate ϑ , and show that

$$\frac{x^2}{\alpha^2} + \frac{y^2}{\beta^2} = 1, \tag{3.7.14}$$

where

$$\alpha = \frac{1}{2} \left(R + \frac{a^2}{R} \right), \quad \beta = \frac{1}{2} \left(R - \frac{a^2}{R} \right).$$

- (b) Denote the free-stream velocity in the auxiliary plane by \tilde{V}_∞ and, assuming that the circulation $\Gamma = 0$, write the complex potential as

$$W(\zeta) = \tilde{V}_\infty \left(\zeta + \frac{R^2}{\zeta} \right).$$

Given that the free-stream velocity in the physical plane is V_∞ , find the free-stream velocity \tilde{V}_∞ in the auxiliary plane.

- (c) Deduce that the maximum value of the velocity on the surface of the ellipse is given by

$$V_{\max} = \frac{2V_\infty}{1 + a^2/R^2},$$

and determine the pressure difference between the front stagnation point and the point of maximum velocity.

3. Return to the flow past a flat plate at an incidence (Figure 3.55a). According to the general theory of two-dimensional potential flows, the resultant pressure force acting on the plate should be directed perpendicular to the free-stream velocity vector (see Section 3.4.3). On the other hand, the pressure on the lower and upper sides of the plate produces a force directed perpendicular to the plate surface. Therefore, common sense suggests that resultant force should also be directed perpendicular to the plate, not to the free-stream velocity. How can this dilemma be resolved?

Hint: You might find Problem 3 in Exercises 10 useful.

4. Consider a two-dimensional source of strength q placed at a point $z = b$ outside a circular cylinder as shown in Figure 3.63. The cylinder is centred at the coordinate origin and has radius a .

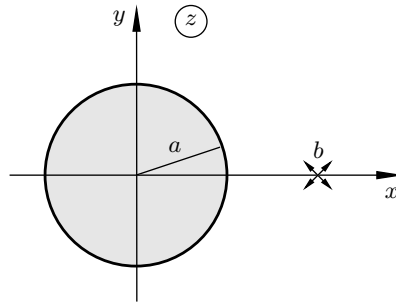


Fig. 3.63: Flow over a circular cylinder due to a source.

Using the Joukovskii transformation

$$\zeta = \frac{1}{2} \left(z + \frac{a^2}{z} \right),$$

map the cylinder onto an infinitely thin flat plate occupying the interval $[-a, a]$ on the real axis in the auxiliary ζ -plane. Find the position ζ_0 of the source in the ζ -plane.

Now, notice that an infinitely thin flat plate aligned with the source does not affect the flow from the source. Hence, write the complex potential in the auxiliary plane as

$$W(\zeta) = \frac{q}{2\pi i} \ln(\zeta - \zeta_0).$$

Finally, return to the physical z -plane, and show that the flow may be treated as being composed of the source situated at $z = b$, an additional source situated inside the cylinder at point $z = a^2/b$, and a sink at $z = 0$.

5. Consider the symmetrical flow past a parabola

$$y = \pm a\sqrt{x} \tag{3.7.15}$$

with the free-stream velocity V_∞ as shown in Figure 3.64.

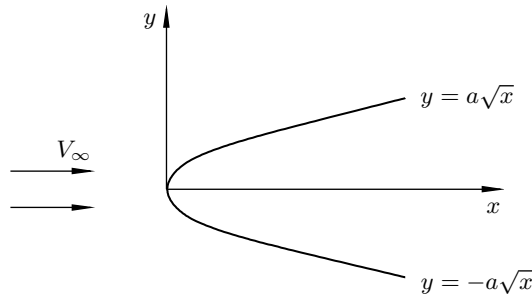


Fig. 3.64: Symmetrical flow past a parabola.

Use the conformal mapping $z = \zeta^2$ of the region $\Im\{\zeta\} > h$ in the auxiliary ζ -plane onto the exterior of the parabola in the physical z -plane, and find how h is related to the parabola ‘width’ parameter a .

Show further that the complex conjugate velocity \bar{V} on the surface of the parabola is given by

$$\bar{V} = V_\infty \frac{\xi}{\xi + ih},$$

where $\xi = y/2h$.

Finally, calculate the parabola drag

$$D = 2 \int_0^\infty (p - p_\infty) dy,$$

where p_∞ is the pressure in the oncoming flow.

6. Consider now a non-symmetric flow past the parabola (3.7.15). The degree of the non-symmetry may be characterised by the distance k from the stagnation point O to the x -axis (see Figure 3.65). Assume that the nose of the parabola has unit radius (in which case the factor a in (3.7.15) has to be set to $a = \sqrt{2}$) and demonstrate that the tangential velocity on the surface of the parabola surface may be written as

$$V = V_\infty \frac{y + k}{\sqrt{y^2 + 1}}.$$

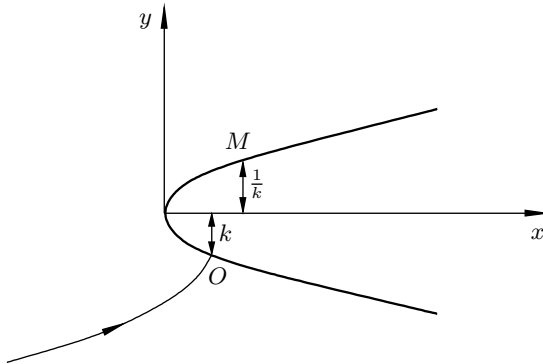


Fig. 3.65: Flow past a parabola at an incidence.

Show further that point M , where the velocity has a maximum, is situated at a distance $y = 1/k$ from the axis of the parabola, as shown in Figure 3.65.

What is the value of the maximum velocity?

7. Consider inviscid irrotational flow past a symmetric aerofoil that is made of two circular arcs as shown on the left-hand side of Figure 3.66. The modulus of the velocity in the free-stream far from the aerofoil is V_∞ , and the angle of attack is α .

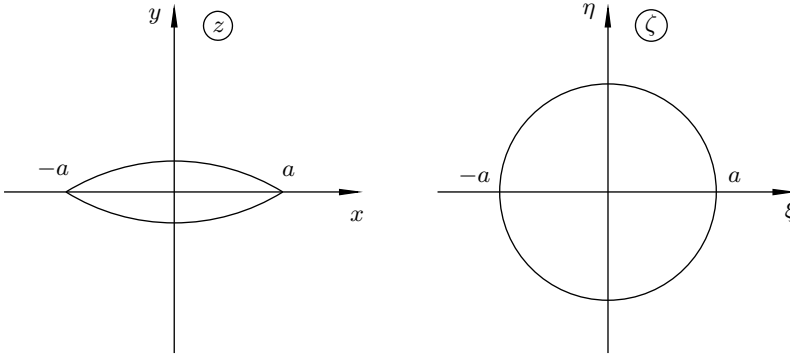


Fig. 3.66: Physical z -plane and auxiliary ζ -plane for the generalised Joukovskii transformation (3.7.16).

- (a) Demonstrate that the generalised Joukovskii transformation, written implicitly as

$$\frac{z - a}{z + a} = \left(\frac{\zeta - a}{\zeta + a} \right)^k, \quad (3.7.16)$$

maps the exterior of a circle of radius a in the auxiliary ζ -plane onto the exterior of the aerofoil. What should the parameter k in (3.7.16) be if the angle between the upper and lower sides of the aerofoil at its leading (trailing) edge is 2θ ?

Suggestion: In order to perform this task, introduce two additional planes

$$z_1 = \frac{z - a}{z + a} \quad \text{and} \quad \zeta_1 = \frac{\zeta - a}{\zeta + a},$$

and find the mapping between them in the form of the power function $z_1 = \zeta_1^k$.

- (b) Show that at large z and ζ , equation (3.7.16) reduces to

$$\zeta = kz + \dots \quad \text{as} \quad z \rightarrow \infty.$$

Hence, deduce that the free-stream velocity \tilde{V}_∞ in the auxiliary ζ -plane is

$$\tilde{V}_\infty = V_\infty/k.$$

- (c) Write the complex potential in the auxiliary plane in the form

$$W(\zeta) = \frac{V_\infty}{k} \left(\zeta e^{-i\alpha} + \frac{a^2}{\zeta e^{-i\alpha}} \right) + \frac{\Gamma}{2\pi i} \ln \zeta.$$

Argue that the Joukovskii-Kutta condition is satisfied if $dW/d\zeta$ is zero at the point $\zeta = a$ in the auxiliary ζ -plane, and deduce that

$$\Gamma = -4\pi a \frac{V_\infty}{k} \sin \alpha.$$

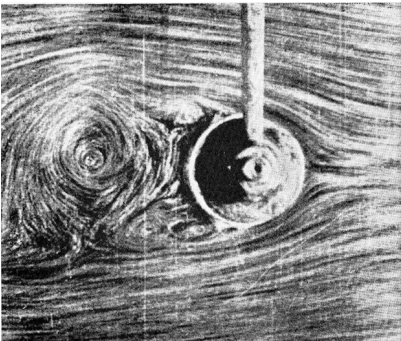
3.8 Free Streamline Theory

3.8.1 Kirchhoff model

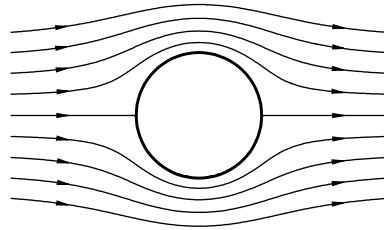
As has been mentioned previously, a major problem in inviscid flow theory is that for steady flows past finite bodies it predicts zero drag. This result is known as d'Alembert's paradox, and it is generally believed to be due to the fact that the theory fails to take into account flow separation. In particular, in Section 3.4.2, we analysed the flow past a circular cylinder. According to theoretical predictions, the flow proved to be symmetric not only with respect to the x -axis but also with respect to the y -axis; see Figure 3.27(a) on page 170, reproduced here as Figure 3.67(b). For this reason, the integral pressure force acting on the front side of the circle is fully compensated by the pressure force acting on its rear side. In contrast, in experiments, a large separation region is observed behind the cylinder (see Figure 3.67a). The separation leads to a redistribution of the pressure on the cylinder's surface and, as a result, a non-zero drag is produced.

Interestingly enough, experiments further show that the separation region does not become smaller when the fluid viscosity decreases. This suggests that, in addition to the 'attached solutions', the Euler equations should allow for solutions with separation regions. Kirchhoff (1869) was the first to demonstrate that this second family of solutions really exist. Following his original study, we shall consider here the inviscid incompressible fluid flow past a flat plate of width $2h$ placed perpendicular to the free-stream velocity vector as shown in Figure 3.68(b). We shall use a Cartesian coordinate system Oxy with the origin O at the stagnation point in the middle of the plate. The x - and y -axes are directed normal to and along the plate surface, respectively. The modulus of the velocity in the oncoming flow is denoted, as usual, by V_∞ and the pressure by p_∞ .

We start the flow analysis by considering the streamline that lies along the x -axis in front of the plate. If we start from point A in the unperturbed oncoming

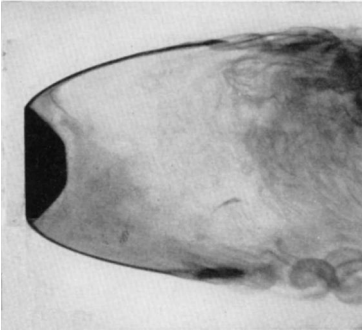


(a) Experimental observations by Prandtl and Tietjens (1934).

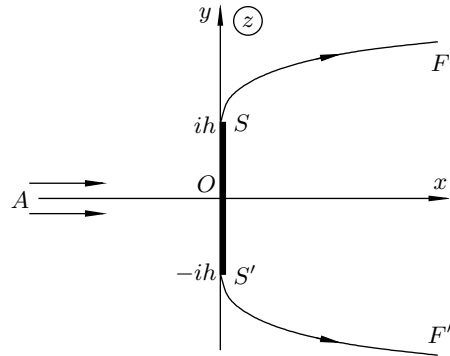


(b) Theoretical predictions.

Fig. 3.67: Comparison of experimental observations (see Figure 3.26 for details) with theoretical predictions for the flow past a non-rotating circular cylinder.



(a) Flow visualisation by Flachsbart (1935).
Copyright © 1935 WILEY-VCH Verlag
GmbH & Co. KGaA, Weinheim.



(b) Mathematical model.

Fig. 3.68: Helmholtz–Kirchhoff model for inviscid separated flows.

stream, and move towards the plate, then we can expect the velocity to decrease monotonically until the stagnation point O is reached; see Figure 3.68(b). At this point, the streamline considered splits into two branches. One branch turns upwards, and follows the plate surface until the upper edge S of the plate is reached. The second branch goes symmetrically downwards to the lower edge S' . At points S and S' , separation takes place. As a result, the so-called *free streamlines* SF and $S'F'$ are formed. Their positions in the flow field are not known in advance and need to be calculated as a part of the solution of our problem.

The Kirchhoff model is based on the following assumptions concerning the separation region that lies between the free streamlines SF and $S'F'$ behind the plate. It is assumed, first of all, that the fluid in the separation region is at rest, and therefore the pressure remains constant. It is, secondly, assumed that the value of the pressure in the separation region, p_s , coincides with that in the oncoming flow, i.e. $p_s = p_\infty$. We shall show that, under these assumptions, the separation region may be treated as semi-infinite, with the free streamlines SF and $S'F'$ extending from the plate edges to infinity.

Everywhere outside the separation region, the fluid motion obeys the laws of potential flow theory, and the only modification that has to be introduced into the formulation of Problem 3.2 (see page 165) concerns the boundary conditions on the free streamlines SF and $S'F'$. We note, first of all, that these lines are impermeable for the flow outside the separation region, and therefore we can write

$$\psi = \Im\{w(z)\} = \text{const} \quad \text{on} \quad SF \text{ and } S'F'. \quad (3.8.1)$$

Condition (3.8.1) is referred to as the *kinematic condition*. In addition to the kinematic condition, we also need to formulate the *dynamic condition*, which is a statement of the pressure balance at the boundary with the separation region:

$$p = p_\infty \quad \text{on} \quad SF \text{ and } S'F'.$$

Using the Bernoulli equation

$$\frac{p}{\rho} + \frac{V^2}{2} = \frac{p_\infty}{\rho} + \frac{V_\infty^2}{2},$$

this condition may be reformulated for the modulus of the velocity:

$$|\bar{V}| = V_\infty \quad \text{on } SF \text{ and } S'F'. \quad (3.8.2)$$

Our task is to solve Problem 3.2 with addition of conditions (3.8.1) and (3.8.2). To perform this task, we shall consider two analytic functions, namely the non-dimensional complex conjugate velocity

$$\zeta = \frac{\bar{V}}{V_\infty} = \frac{1}{V_\infty} \frac{dw}{dz}, \quad (3.8.3)$$

and the complex potential

$$w = \varphi + i\psi.$$

Through analysis of their complex planes, we will try to find the function $\zeta = \zeta(w)$ that performs the conformal mapping of the w -plane onto the ζ -plane. Once $\zeta(w)$ has been found, we will return to equation (3.8.3) and express it in the form

$$dz = \frac{1}{V_\infty} \frac{dw}{\zeta(w)},$$

which, being integrated,

$$z = \frac{1}{V_\infty} \int \frac{dw}{\zeta(w)}, \quad (3.8.4)$$

gives the inverse $z = z(w)$ of the complex potential function $w(z)$.

We start with the complex plane of the function (3.8.3), which is termed the *hodograph plane*; see Figure 3.69(a). Denoting, as before, the angle between the velocity vector \mathbf{V} and the x -axis by ϑ , we write (3.8.3) as

$$\zeta = \frac{|\bar{V}|}{V_\infty} e^{-i\vartheta}. \quad (3.8.5)$$

At any point in the z -plane (see Figure 3.68b) that is situated far upstream of the plate, and, in particular, at point A , we have $\vartheta = 0$ and $|\bar{V}| = V_\infty$. This means that in the ζ -plane (Figure 3.69a), the point A lies at $\zeta = 1$. If an observer moves in the physical z -plane from point A towards the plate along the x -axis (Figure 3.68b), then the angle ϑ will remain zero all the way to the stagnation point O . The modulus of the velocity $|\bar{V}|$ will decrease monotonically from V_∞ to zero, which means that the corresponding point in the ζ -plane (Figure 3.69a) will travel along the real axis from $\zeta = 1$ to the coordinate origin O .

As has already been mentioned, the streamline that lies along the axis of symmetry of the flow, AO , splits into two branches: an upper branch that follows the upper half of the plate, OS , and a lower branch that lies along the lower half, OS' ; see Figure 3.68(b). We shall follow, to begin with, the upper branch. As the velocity vector is tangent to

the plate everywhere on OS , the angle $\vartheta = \pi/2$, and therefore the argument of the function (3.8.5) is equal to $-\pi/2$. The modulus of ζ increases as the fluid accelerates towards the separation point S , where the condition (3.8.2) becomes applicable, and $\zeta = e^{-i\pi/2} = -i$. Thus, while the point in the physical z -plane moves along the plate from the front stagnation point O to the separation point S , its image in the ζ -plane (Figure 3.69a) moves along the imaginary axis from the coordinate origin O to the point $\zeta = -i$.

Continuing further downstream along the free streamline SF , we can use the condition (3.8.2), and we see that $|\zeta| = 1$ all the way from the separation point S to point F , which lies far downstream. As far as the velocity angle ϑ is concerned, it equals $\pi/2$ at point S , where the fluid leaves the plate surface tangentially, and decreases monotonically to zero as the fluid particles travel along the free streamline towards point F ; see Figure 3.68(b). Consequently, in the ζ -plane (Figure 3.69a) the free streamline SF is represented by a quarter-circle connecting the points $\zeta = -i$ and $\zeta = 1$.

Similarly, the lower half of the plate OS' in the z -plane maps onto a segment $[0, i]$ of the imaginary axis in the ζ -plane, and the second free streamline $S'F'$ is represented by a quarter-circle connecting the points $\zeta = i$ and $\zeta = 1$. We can conclude that the entire flow outside the separation region in the physical z -plane (Figure 3.68b) is represented by the interior of the semicircle in the ζ -plane (Figure 3.69a).

Let us now consider the plane of the complex potential $w = \varphi + i\psi$; see Figure 3.69(b). Since both the velocity potential φ and the stream function ψ are defined to within an arbitrary constant, we can choose w to be zero at the front stagnation point O . We know that the real negative semi-axis AO in the z -plane (Figure 3.68b) is a streamline with $\psi = 0$ along it. In order to predict the behaviour of the velocity

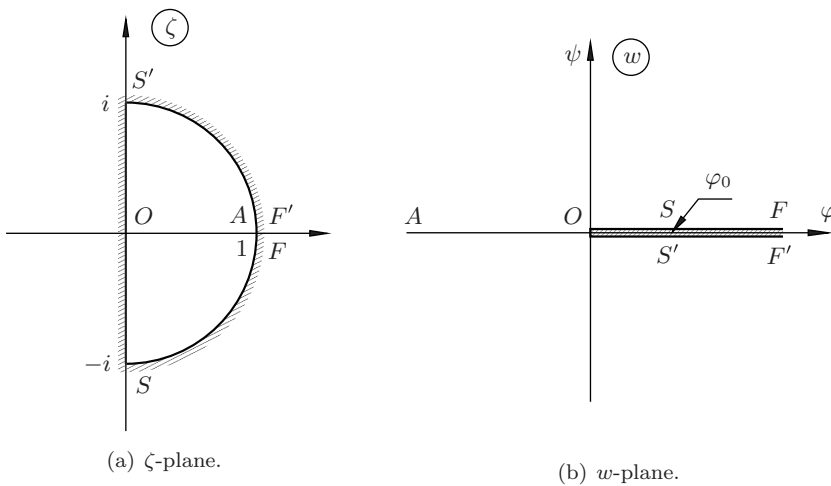


Fig. 3.69: Planes of the non-dimensional complex conjugate velocity ζ and of the complex potential w .

potential φ on this line, we use the equation

$$\frac{\partial\varphi}{\partial x} = u.$$

The velocity u is positive everywhere on AO (except at the front stagnation point O). This suggests that φ decreases from zero at point O to $\varphi = -\infty$ at point A far upstream of the plate surface. Consequently, the real negative semi-axis in the z -plane maps onto the real negative semi-axis in the w -plane (Figure 3.69b).

The branching of the streamline at the front stagnation point O in the z -plane (Figure 3.68b) requires a branch cut to be introduced in the w -plane (Figure 3.69b). The stream function ψ remains zero along the upper half OS of the plate and further downstream along the upper free streamline SF ; see Figure 3.68(b). It is also zero on the lower half OS' of the plate and the lower free streamline $S'F'$. Consequently, the cut in the w -plane should be made along the real positive semi-axis, as shown in Figure 3.69(b). In order to make clear which side of the cut corresponds to the upper half of the flow in the physical plane, and which to the lower, we shall use the equation

$$\frac{\partial\psi}{\partial y} = u.$$

Since u is expected to be positive everywhere except on the plate SS' , it follows from this equation that ψ is positive in the upper half of the flow and negative in the lower. Consequently, the image of the upper edge S of the plate should lie on the upper side of the branch cut, and the image of the lower edge S' of the plate should lie symmetrically on the lower side of the cut in the w -plane. The value φ_0 of the velocity potential φ at points S and S' is, of course, the same. It is not known in advance, but will be found as a result of the flow analysis.

Now we need to establish the conformal mapping between the ζ - and w -planes. We start by rotating the ζ -plane through an angle $\pi/2$ in the clockwise direction. This operation is performed by

$$\zeta_1 = -i\zeta. \tag{3.8.6}$$

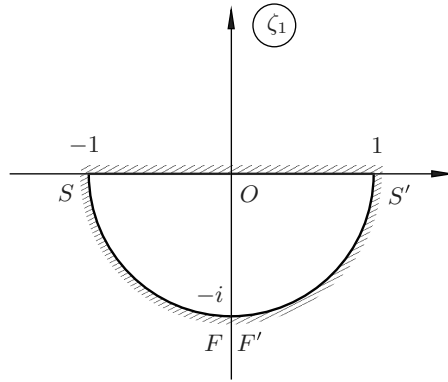
The resulting ζ_1 -plane is shown in Figure 3.70.

As the next step, we will apply the Joukovskii transformation to ζ_1 . Remember, in Section 3.5.6, it was expressed by equation (3.5.34),

$$z = \frac{1}{2} \left(\zeta + \frac{a^2}{\zeta} \right), \tag{3.8.7}$$

and it was shown that if in the ζ -plane we consider a circle of radius a centred at the coordinate origin,¹² then (3.8.7) maps the exterior of this circle onto the whole z -plane except for a branch cut along a segment $[-a, a]$ of the real axis. If we now consider two points, ζ' lying outside the circle of radius a and $\zeta'' = a^2/\zeta'$ lying inside the circle, then it is easily seen that (3.8.7) maps these into the same point in the z -plane. This means that, in addition to the exterior of the circle in the ζ -plane, the Joukovskii transformation (3.8.7) also maps its interior onto the entire z -plane except for a branch cut along a segment $[-a, a]$ of the real axis.

¹²This corresponds to $h = 0$ in Figure 3.53, page 195.

Fig. 3.70: Auxiliary ζ_1 -plane.

In the ζ_1 -plane (Figure 3.70), we are dealing with a semicircle of unit radius. Therefore we shall introduce a new auxiliary plane ζ_2 and write the Joukovskii transformation as

$$\zeta_2 = \frac{1}{2} \left(\zeta_1 + \frac{1}{\zeta_1} \right). \quad (3.8.8)$$

We expect the semicircle to be mapped by (3.8.8) onto a half-plane. Indeed, if we represent ζ_1 in the form $\zeta_1 = |\zeta_1|e^{i\vartheta}$ and substitute it into (3.8.8), then we will find

$$\zeta_2 = \frac{1}{2} \left(|\zeta_1| + \frac{1}{|\zeta_1|} \right) \cos \vartheta + \frac{i}{2} \left(|\zeta_1| - \frac{1}{|\zeta_1|} \right) \sin \vartheta. \quad (3.8.9)$$

The interior of the semicircle in the ζ_1 -plane corresponds to

$$|\zeta_1| < 1 \quad \text{and} \quad \vartheta \in (-\pi, 0).$$

Under these restrictions, the imaginary part of (3.8.9) is positive. Consequently, we can conclude that (3.8.9) maps the semicircle in the ζ_1 -plane onto the upper half of the ζ_2 -plane; see Figure 3.71(a).

It remains to identify the positions of points S , O , S' , F , and F' in the ζ_2 -plane. Let us consider, for example, the point S' . In the ζ_1 -plane (Figure 3.70), it is situated at $\zeta_1 = 1$, which on substitution into (3.8.8) gives the position of S' in the ζ_2 -plane to be $\zeta_2 = 1$. The other characteristic points are dealt with in a similar way, and their positions in the ζ_2 -plane are shown in Figure 3.71(a).

Now we need to return to the w -plane; see Figure 3.69(b). It may be mapped onto the upper half-plane by means of the transformation

$$w_1 = \sqrt{\frac{w}{\varphi_0}}. \quad (3.8.10)$$

The function $\sqrt{w/\varphi_0}$ has two roots. In what follows, we shall use the root that is

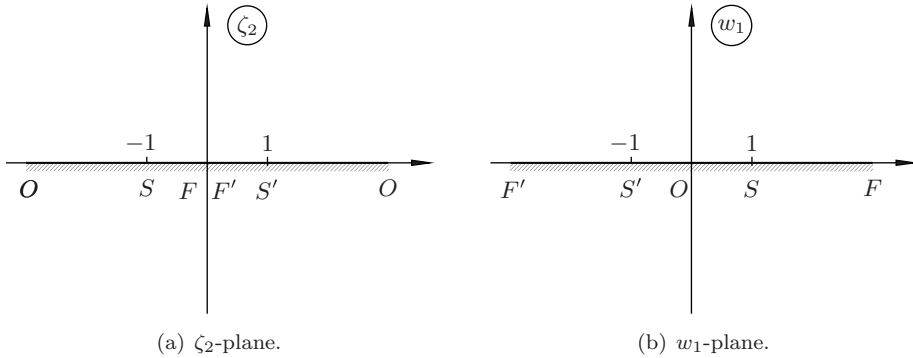


Fig. 3.71: Auxiliary ζ_2 - and w_1 -planes.

defined as follows. We write (see Figure 3.72)

$$w = |w|e^{i\vartheta},$$

and then we have

$$\sqrt{\frac{w}{\varphi_0}} = \sqrt{\frac{|w|}{\varphi_0}} e^{i\vartheta/2}. \tag{3.8.11}$$

Now we can easily see that point S ($|w| = \varphi_0, \vartheta = 0$) is mapped into $w_1 = 1$ and point S' ($|w| = \varphi_0, \vartheta = 2\pi$) into $w_1 = -1$; see Figure 3.71(b).

Finally, we need to relate the ζ_2 - and w_1 -planes. In both planes, the region we are interested in occupies the upper half-plane, but with different arrangement of points S, O, S', F , and F' on the real axis. Since the upper half-plane may be thought of as the interior of a circle of infinitely large radius, we shall seek the mapping in the form of a linear fractional transformation (see Section 3.5.4):

$$\zeta_2 = \frac{aw_1 + b}{cw_1 + d}. \tag{3.8.12}$$

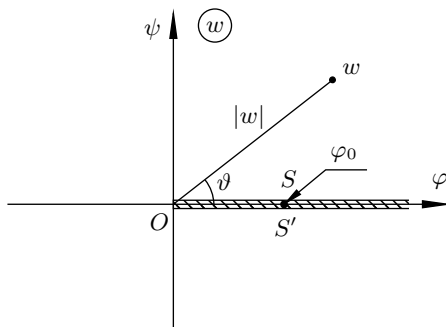


Fig. 3.72: The w -plane used in (3.8.11).

Here a , b , c , and d are complex constants, which have to be chosen in such a way that (3.8.12) performs the required mapping of the points S , O , S' , F , and F' . We start with the point O . In the w_1 -plane (see Figure 3.71b), it is situated at the coordinate origin $w_1 = 0$, which turns (3.8.12) into

$$\zeta_2 = \frac{b}{d}.$$

In the ζ_2 -plane (see Figure 3.71a), the point O is at $\zeta_2 = \infty$, which is only possible if $d = 0$. Taking this into account, we write (3.8.12) as

$$\zeta_2 = \alpha + \frac{\beta}{w_1}, \quad (3.8.13)$$

where $\alpha = a/c$ and $\beta = b/c$.

Let us now consider point F . The transformation (3.8.13) is supposed to map it from $w_1 = \infty$ to $\zeta_2 = 0$, which, obviously, only happens if $\alpha = 0$. It remains to find β , for which purpose either point S or point S' can be used. The correct mapping of both points is achieved by setting $\beta = -1$. Thus, we have

$$\zeta_2 = -\frac{1}{w_1}. \quad (3.8.14)$$

Substitution of (3.8.8), (3.8.6), and (3.8.10) into (3.8.14) yields

$$\frac{1}{2} \left(-i\zeta + \frac{1}{-i\zeta} \right) = -\sqrt{\frac{\varphi_0}{w}}.$$

In order to solve this equation for ζ , we express it in the form

$$\zeta^2 + 2i\sqrt{\frac{\varphi_0}{w}}\zeta - 1 = 0, \quad (3.8.15)$$

and we have

$$\zeta = -i\sqrt{\frac{\varphi_0}{w}} \pm i\sqrt{\frac{\varphi_0}{w} - 1}. \quad (3.8.16)$$

Since the inverse of Joukovskii transformation (3.8.8) is a double-valued function, it is not surprising that the mapping (3.8.16) is also double-valued. We need to choose the root that maps the w -plane (see Figure 3.69b) onto the interior of the semicircle in the ζ -plane (Figure 3.69a). We start by clarifying which root of the function

$$g(w) = \sqrt{\frac{\varphi_0}{w} - 1} = \sqrt{\frac{\varphi_0 - w}{w}} \quad (3.8.17)$$

we intend to use in (3.8.16). We make branch cuts in the w -plane as shown in Figure 3.73, and write

$$w - \varphi_0 = r_1 e^{i\vartheta_1}, \quad w = r_2 e^{i\vartheta_2}.$$

Since $\varphi_0 - w = -r_1 e^{i\vartheta_1} = r_1 e^{i(\pi + \vartheta_1)}$, we have

$$g(w) = \sqrt{\frac{r_1}{r_2}} e^{i(\pi + \vartheta_1 - \vartheta_2)/2}. \quad (3.8.18)$$

Now we are ready to identify the correct root in equation (3.8.16). Let us consider, for example, the point $w = -\varphi_0$, which lies on the real negative semi-axis between points A and O in Figure 3.69(b). Using the notation of Figure 3.72, we have for this point

$$|w| = \varphi_0, \quad \vartheta = \pi. \tag{3.8.19}$$

Substitution of (3.8.19) into (3.8.11) results in

$$\sqrt{\frac{w}{\varphi_0}} = i. \tag{3.8.20}$$

Similarly, in the notations of Figure 3.73, the point considered is represented by

$$r_1 = 2\varphi_0, \quad r_2 = \varphi_0, \quad \vartheta_1 = \vartheta_2 = \pi,$$

which, being substituted into (3.8.18), yields

$$\sqrt{\frac{\varphi_0}{w} - 1} = i\sqrt{2}. \tag{3.8.21}$$

It remains to substitute (3.8.20) and (3.8.21) into (3.8.16). We find

$$\zeta_1 = -1 - \sqrt{2}, \quad \zeta_2 = -1 + \sqrt{2}.$$

The first of these corresponds to the plus sign in (3.8.16) and the second to the minus. We have to choose the latter, since in the ζ -plane the point considered should find itself inside the semicircle of Figure 3.69(a). Consequently, we can conclude that

$$\zeta = -i\sqrt{\frac{\varphi_0}{w}} - i\sqrt{\frac{\varphi_0}{w} - 1}. \tag{3.8.22}$$

Let us now return to the physical z -plane (see Figure 3.68b on page 211) and remember that the non-dimensional complex conjugate velocity is defined as

$$\zeta = \frac{\bar{V}}{V_\infty} = \frac{1}{V_\infty} \frac{dw}{dz}. \tag{3.8.23}$$

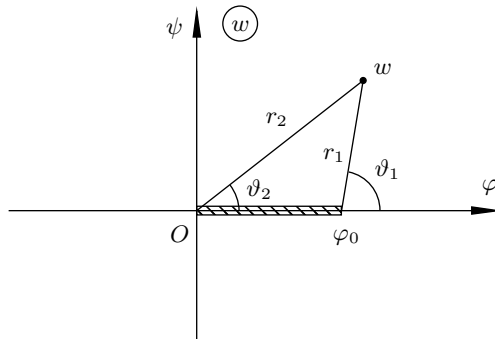


Fig. 3.73: The w -plane used in (3.8.18).

We know that, in the flow considered, ζ is related to the complex potential $w = \varphi + i\psi$ by the equation (3.8.22). If we rearrange (3.8.23) as

$$dz = \frac{1}{V_\infty} \frac{dw}{\zeta}, \tag{3.8.24}$$

and integrate (3.8.24), taking into account that both z and w are zero at the front stagnation point O ,¹³ then we will have

$$\begin{aligned} z &= \frac{1}{V_\infty} \int_0^w \frac{dw}{\zeta(w)} = \frac{i}{V_\infty} \int_0^w \frac{dw}{\sqrt{\varphi_0/w} + \sqrt{\varphi_0/w - 1}} \\ &= \frac{i}{V_\infty} \int_0^w \left(\sqrt{\frac{\varphi_0}{w}} - \sqrt{\frac{\varphi_0}{w} - 1} \right) dw. \end{aligned} \tag{3.8.25}$$

Our first task will be to find the value φ_0 of the velocity potential at the separation point S . We note that, at this point, $z = ih$ and $w = \varphi_0$, which reduces (3.8.25) to

$$h = \frac{1}{V_\infty} \int_0^{\varphi_0} \left(\sqrt{\frac{\varphi_0}{w}} - \sqrt{\frac{\varphi_0}{w} - 1} \right) dw. \tag{3.8.26}$$

Since the integrand in (3.8.26) is analytic, the integration can be performed along any contour C connecting points O and S in the w -plane; see Figure 3.74. We choose to integrate along a contour \tilde{C} that lies on the upper side of the branch cut. In order to select an appropriate branch of the first root in (3.8.26), we have to use Figure 3.72. It shows that, at any point immediately above the cut,

$$|w| = \varphi, \quad \vartheta = 0.$$

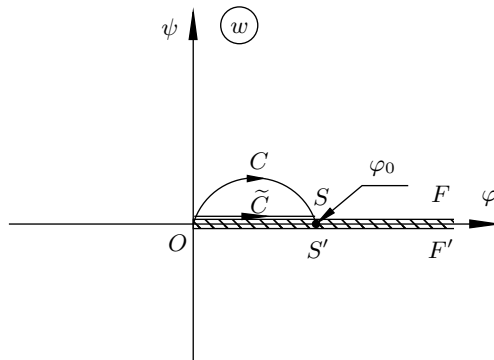


Fig. 3.74: Choice of integration contour in (3.8.26).

¹³See Figure 3.68(b) on page 211 and Figure 3.69(b) on page 213.

Substituting these into (3.8.11), we have

$$\sqrt{\frac{w}{\varphi_0}} = \sqrt{\frac{\varphi}{\varphi_0}}. \quad (3.8.27)$$

Similarly, Figure 3.73 shows that, at any point on the integration path,

$$r_1 = \varphi_0 - \varphi, \quad r_2 = \varphi, \quad \vartheta_1 = \pi, \quad \vartheta_2 = 0,$$

which, being substituted into (3.8.18), yields

$$\sqrt{\frac{\varphi_0}{w} - 1} = \sqrt{\frac{\varphi_0 - \varphi}{\varphi}} e^{i\pi} = -\sqrt{\frac{\varphi_0}{\varphi} - 1}. \quad (3.8.28)$$

Using (3.8.27) and (3.8.28) in (3.8.26), we have

$$h = \frac{1}{V_\infty} \int_0^{\varphi_0} \left(\sqrt{\frac{\varphi_0}{\varphi}} + \sqrt{\frac{\varphi_0}{\varphi} - 1} \right) d\varphi.$$

The integral on the right-hand side of this equation is easily calculated by changing the integration variable; $\varphi = \varphi_0 \sin^2 t$:

$$h = \frac{2\varphi_0}{V_\infty} \int_0^{\pi/2} (1 + \cos t) \cos t dt = \frac{2\varphi_0}{V_\infty} \int_0^{\pi/2} \left(\cos t + \frac{1 + \cos 2t}{2} \right) dt = \frac{2\varphi_0}{V_\infty} \left(1 + \frac{\pi}{4} \right).$$

Thus, the velocity potential at the separation point S is

$$\varphi_0 = \frac{2hV_\infty}{\pi + 4}. \quad (3.8.29)$$

Now we turn to the calculation of the plate drag D . Since the pressure behind the plate is p_∞ , the drag is given by

$$D = 2 \int_0^h (p - p_\infty) dy. \quad (3.8.30)$$

Here p denotes the pressure on the front face of the plate, and, owing to the symmetry of the flow, the integration is restricted to the upper half OS of the plate; see Figure 3.68(b) on page 211.

We note that, on OS , $z = iy$ and therefore

$$dz = i dy. \quad (3.8.31)$$

Combining (3.8.31) with (3.8.24), we can see that, on OS ,

$$dy = -\frac{i}{V_\infty} \frac{dw}{\zeta}. \quad (3.8.32)$$

Equation (3.8.32) allows us to convert the integration in the physical z -plane into integration in the w -plane. Substitution of (3.8.32) into (3.8.30) results in

$$D = -\frac{2i}{V_\infty} \int_0^{\varphi_0} (p - p_\infty) \frac{dw}{\zeta}. \quad (3.8.33)$$

Now we need to express the integrand in terms of the complex potential w . It follows from the Bernoulli equation that

$$p - p_\infty = \frac{1}{2}\rho(V_\infty^2 - V^2). \quad (3.8.34)$$

Substitution of (3.8.34) into (3.8.33) yields

$$D = -i\rho V_\infty \int_0^{\varphi_0} \left(1 - \frac{V^2}{V_\infty^2}\right) \frac{dw}{\zeta}. \quad (3.8.35)$$

On the plate surface, the longitudinal velocity component u is zero, which means that the complex conjugate velocity $\bar{V} = u - iv$ and the modulus of the velocity vector $V = \sqrt{u^2 + v^2}$ are given by

$$\bar{V} = -iv, \quad V = v,$$

respectively. Taking this into account, we can express the non-dimensional complex conjugate velocity as

$$\zeta = -i \frac{V}{V_\infty}. \quad (3.8.36)$$

Taking squares on both sides of (3.8.36) yields

$$\frac{V^2}{V_\infty^2} = -\zeta^2,$$

which, when substituted into (3.8.35), results in

$$D = -i\rho V_\infty \int_0^{\varphi_0} \left(\zeta + \frac{1}{\zeta}\right) dw.$$

It remains to make use of the equation (3.8.22) relating ζ and w . We see that

$$\frac{1}{\zeta} = \frac{i}{\sqrt{\varphi_0/w} + \sqrt{\varphi_0/w - 1}} = i \left(\sqrt{\frac{\varphi_0}{w}} - \sqrt{\frac{\varphi_0}{w} - 1} \right),$$

and therefore

$$\frac{1}{\zeta} + \zeta = -2i \sqrt{\frac{\varphi_0}{w} - 1}.$$

Consequently,

$$D = -2\rho V_\infty \int_0^{\varphi_0} \sqrt{\frac{\varphi_0}{w} - 1} dw.$$

On the integration path, a proper branch of $\sqrt{\varphi_0/w - 1}$ is given by (3.8.28). Hence,

$$D = 2\rho V_\infty \int_0^{\varphi_0} \sqrt{\frac{\varphi_0}{\varphi} - 1} d\varphi, \quad (3.8.37)$$

Now, all the quantities in (3.8.37) are real. Changing the integration variable, $\varphi = \varphi_0 \sin^2 t$, we find

$$D = \rho V_\infty \varphi_0 \pi = \rho V_\infty^2 2h \frac{\pi}{\pi + 4}. \quad (3.8.38)$$

Correspondingly, the drag coefficient

$$C_D = \frac{D}{\frac{1}{2}\rho V_\infty^2 2h} = \frac{2\pi}{\pi + 4}.$$

It should be noted that the Kirchhoff model underestimates the drag. The source of the discrepancy between the theoretical predictions and experimental observations lies in the simplifying assumptions upon which the theory is based. The first of these, that the pressure is constant in the separation region, proves to hold in real flows in the near wake. Experiments show that the fluid motion in the separation region immediately behind the plate is indeed relatively slow. However, further downstream, unsteadiness normally develops in the separation region, affecting the pressure distribution and the integral force acting on the plate.

The second assumption is that the pressure in the separation region, p_s , coincides with the free-stream pressure p_∞ . It was adopted in the Kirchhoff model, first, to simplify the theoretical description of the flow, and, second, to ensure that the plate drag is non-zero. With $p_s = p_\infty$, points F and F' , representing the 'ends' of the free streamlines in the z -plane (Figure 3.68b), have their images at the point $\zeta = 1$ in the non-dimensional complex velocity plane ζ ; see Figure 3.69(a). Because this point is also the image of the free-stream point A , the free streamlines SF and $S'F'$ extend to infinity in the z -plane, allowing the drag of the plate to become non-zero (see Problem 4 in Exercises 12). Experimental evidence clearly shows that the pressure in the separation region is always lower than in the free stream: $p_s < p_\infty$. Therefore, in reality, the drag coefficient appears to be larger than that predicted by formula (3.8.38).

Despite the Kirchhoff model being found to be insufficient to capture the full complexity of separated flows, it played an important role in the development of theoretical fluid dynamics. In particular, it demonstrated that for a wide class of body shapes, the Euler equations admit, in addition to smooth attached solutions, also discontinuous solutions that may be used to represent separated flow. Finally, it is interesting to note that while the Kirchhoff theory was originally intended for describing separated flows, it proved to be very useful in the analysis of cavitating flows, where the predictions of the theory were found to give surprisingly good accuracy (see e.g. Gurevich, 1966).

3.8.2 Two-dimensional inviscid jets

Let us consider a jet that forms when an incompressible inviscid fluid escapes from a large container through an orifice equipped with a mouthpiece as sketched in Figure 3.75. We shall assume that the mouthpiece is symmetric and composed of two flat plates AB and $A'B'$, which make an angle α with the axis of symmetry. The mouthpiece width, measured as the distance between the plates' edges B and B' , equals $2b$. After leaving the mouthpiece, the fluid comes in contact with the surrounding atmosphere of constant pressure. Keeping this in mind, we shall assume that, along the free streamlines BC and $B'C'$, the pressure and hence the modulus of the velocity remain constant; we shall denote the value of the latter as V_0 . Notice that at points B and B' the free streamlines are tangent to the walls of the mouthpiece. As a consequence, one has to expect a contraction of the jet, with its width decreasing from $2b$ at the mouthpiece edge BB' to a smaller value $2b'$ further downstream when the free streamlines ultimately become parallel to one another.

In order to describe this flow mathematically, we introduce Cartesian coordinates with x aligned with the axis of symmetry of the flow and y passing through the edge B of the upper plate. In what follows, the complex plane $z = x + iy$ will be referred to as the physical plane. In addition to the physical plane, we shall consider the complex plane of the function

$$\Omega = \ln \left(\frac{1}{V_0} \frac{dw}{dz} \right). \quad (3.8.39)$$

Denoting the modulus of the velocity vector \mathbf{V} by V and the angle that it makes with the x -axis by ϑ , we can write

$$\bar{V} = \frac{dw}{dz} = V e^{-i\vartheta},$$

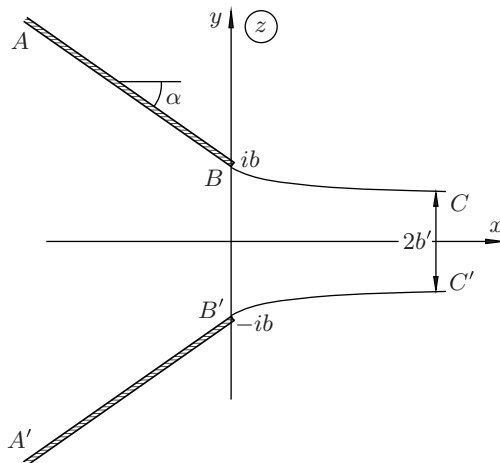


Fig. 3.75: Physical z -plane.

which, when substituted into (3.8.39), yields

$$\Omega = \ln \frac{V}{V_0} - i\vartheta. \tag{3.8.40}$$

Equation (3.8.40) allows us to see that in the Ω -plane the flow is represented by the semi-infinite strip shown in Figure 3.76. Indeed, at any point on the upper plate AB , the velocity vector angle $\vartheta = -\alpha$, which means that the imaginary part, $\Im\{\Omega\} = -\vartheta$, of Ω stays equal to α all along AB . At point B where the flow comes in contact with the atmosphere (see Figure 3.75), the modulus of the velocity, V , becomes equal to V_0 , making the real part, $\Re\{\Omega\} = \ln(V/V_0)$, of Ω zero. Upstream of B , the fluid velocity V is smaller than V_0 . In fact, V/V_0 decreases monotonically from unity at point B to zero at the ‘infinite point’ A . Correspondingly, the real part of Ω decreases from $\Re\{\Omega\} = 0$ at point B to $\Re\{\Omega\} = -\infty$ at point A . Thus, the upper side AB of the mouthpiece (Figure 3.75) is represented in the Ω -plane by the upper side of the semi-strip as shown in Figure 3.76.

Continuing further downstream of point B (see Figure 3.75), one can see that the modulus of the velocity, V , stays equal to V_0 all along the free streamline BC , while the velocity vector angle increases from $\vartheta = -\alpha$ at point B to $\vartheta = 0$ at the ‘infinite point’ C . This means that the free streamline BC is represented in the Ω -plane by the segment of the imaginary axis $\Im\{\Omega\} \in [0, \alpha]$.

The lower boundary of the flow, $A'B'C'$, is analysed in the same way, and it is easily seen that the second plate $A'B'$ is represented by the lower side of the semi-infinite strip in the Ω -plane, and the lower free streamline $B'C'$ maps onto the segment $\Im\{\Omega\} \in [-\alpha, 0]$ of the imaginary axis.

In addition to the Ω -plane, we shall also consider the plane of the complex potential $w = \varphi + i\psi$. We start again with the upper boundary ABC of the flow (Figure 3.75). Since it represents a streamline, we have

$$\psi = \text{const}$$

on ABC . Taking into account that the stream function ψ is defined to within an arbitrary constant, we choose ψ to be zero on ABC , and then in the w -plane this streamline will lie along the real axis (see Figure 3.77).

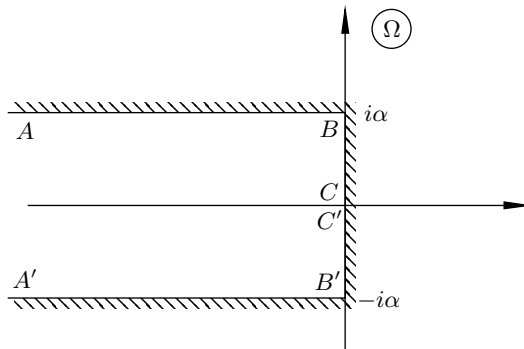


Fig. 3.76: Ω -plane.

If now we move from the upper plate down towards the lower plate (see Figure 3.75), then the stream function ψ becomes negative. Indeed, we know that

$$\frac{\partial\psi}{\partial y} = u.$$

Since, in the flow considered, u is positive, ψ decreases with decreasing y . In order to find the value of ψ on the lower plate, we apply equation (3.3.13) to the edges B and B' of the two plates. We have

$$\psi(B) - \psi(B') = Q.$$

Here Q is the fluid flux through the mouthpiece. Since $\psi(B) = 0$, we can conclude that $\psi(B') = -Q$, and, of course, the stream function remains constant on the lower boundary $A'B'C'$ of the flow as shown in Figure 3.77.

In order to explain why points A, B, C and A', B', C' are positioned in the w -plane as shown in Figure 3.77, we note, first of all, that the velocity potential φ is defined to within an arbitrary constant. This allows us to choose $\varphi = 0$ at the edge B of the upper plate (see Figure 3.75), which places the image of point B into the coordinate origin in the w -plane; see Figure 3.77. Now, it follows from the equation

$$\frac{\partial\varphi}{\partial x} = u$$

that φ increases when the observation point moves in the physical plane (Figure 3.75) along the upper boundary of the jet from point B towards point C . This means that the image of point C in the w -plane lies on the right-hand side of point B ; see Figure 3.77. Clearly, φ decreases as the observation point moves along the upper plate from point B towards point A . Hence, in the w -plane the image of point A should be placed on the left-hand side of point B . Owing to the symmetry of the flow considered, points A', B', C' should be placed opposite to points A, B, C on the lower boundary of the strip in the w -plane.

We are ready now to establish a relationship between the functions Ω and w , which is done through conformal mapping between the Ω -plane (Figure 3.76) and the

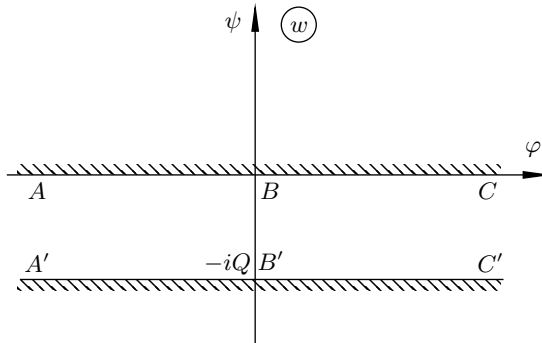


Fig. 3.77: w -plane.

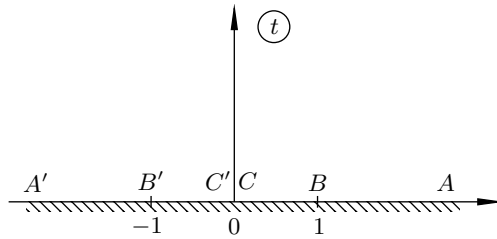


Fig. 3.78: Auxiliary t -plane.

w -plane (Figure 3.77). Since in both planes the flow is represented by polygons, it is convenient to introduce an auxiliary t -plane, shown in Figure 3.78, and use the Schwarz–Christoffel mapping.

A detailed discussion of the Schwarz–Christoffel theory may be found elsewhere (see e.g. Dettman, 1965). Here we shall restrict ourselves to stating the main result of the theory. It consists in the following. Suppose that in the z -plane we have a polygon with n vertices, A_1, A_2, \dots, A_n (see Figure 3.79a). The mapping of this polygon onto the upper half of the t -plane (Figure 3.79b) is given by the transformation

$$z = C_1 \int (t - t_1)^{\alpha_1/\pi-1} (t - t_2)^{\alpha_2/\pi-1} \dots (t - t_n)^{\alpha_n/\pi-1} dt + C_2, \quad (3.8.41)$$

where t_1, t_2, \dots, t_n , all lying on the real axis in the t -plane, are the images of the vertices, A_1, A_2, \dots, A_n , respectively, and $\alpha_1, \alpha_2, \dots, \alpha_n$ are the polygon angles; the complex constants C_1 and C_2 are not known in advance and have to be adjusted for each particular mapping. When using the Schwarz–Christoffel transformation, it is convenient to choose one of the boundary points in the t -plane, say t_1 , to be at infinity.

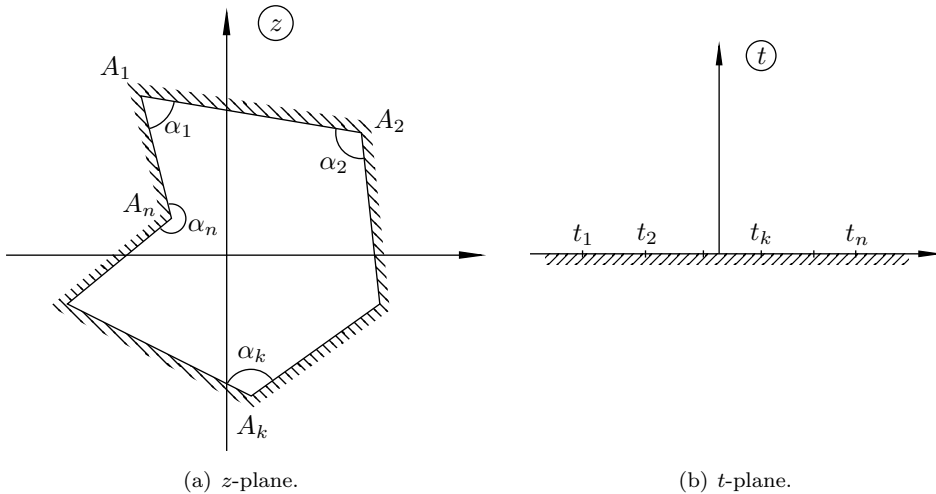


Fig. 3.79: Schwarz–Christoffel mapping.

Then the term $(t - t_1)^{\alpha_1/\pi-1}$ has to be omitted in (3.8.41), making the integration easier.

Let us now return to the particular problem we are dealing with here. Our task is to find the mapping of the Ω -plane (Figure 3.76) onto the auxiliary t -plane (Figure 3.78). In the Ω -plane, we have a triangle with one vertex situated at infinity. We have chosen its image in the t -plane to be also at infinity. We have placed the images of vertices B' and B into $t_1 = -1$ and $t_2 = 1$, respectively. The angles at B' and B are $\alpha_1 = \alpha_2 = \frac{1}{2}\pi$. Using these in (3.8.41), we have

$$\begin{aligned}\Omega &= C_1 \int (t+1)^{-1/2}(t-1)^{-1/2} dt + C_2 \\ &= -iC_1 \int \frac{dt}{\sqrt{1-t^2}} + C_2 = -iC_1 \arcsin t + C_2.\end{aligned}\quad (3.8.42)$$

The constants C_1 and C_2 are found by ensuring the correspondence of points B and B' in the Ω - and t -planes. In the Ω -plane (Figure 3.76), point B is situated at $\Omega = i\alpha$. It is mapped into the point $t = 1$ in the t -plane (Figure 3.78). Using these in (3.8.42), we have

$$i\alpha = -iC_1 \frac{\pi}{2} + C_2. \quad (3.8.43)$$

Similarly, the desired mapping of point B' is achieved if

$$-i\alpha = iC_1 \frac{\pi}{2} + C_2. \quad (3.8.44)$$

Solving (3.8.43) and (3.8.44) for C_1 and C_2 , we have

$$C_1 = -\frac{2}{\pi}\alpha, \quad C_2 = 0. \quad (3.8.45)$$

It remains to substitute (3.8.45) back into (3.8.42), and we can conclude that the mapping of the auxiliary t -plane onto the Ω -plane is given by

$$\Omega = i\frac{2\alpha}{\pi} \arcsin t. \quad (3.8.46)$$

Now we need to repeat this procedure for the w -plane (Figure 3.77). The polygon in the w -plane has only two vertices, $A(A')$ and $C(C')$. The first of these has its image at infinity in the t -plane (Figure 3.78) and does not need to be accounted for in the Schwartz-Christoffel integral (3.8.41). The second vertex, $C(C')$, is mapped into the point $t = 0$, and since this vertex angle $\alpha = 0$, we have

$$w = C_1 \int (t-0)^{-1} dt + C_2 = C_1 \ln t + C_2.$$

Let us first apply this mapping to point B . In the t -plane it is situated at point $t = 1$, and in the w -plane at point $w = 0$, whence $C_2 = 0$. In order to find C_1 , we consider the mapping of point B' . We have

$$-iQ = C_1 \ln(-1) = C_1 i\pi,$$

which gives $C_1 = -Q/\pi$, and we can conclude that

$$w = -\frac{Q}{\pi} \ln t. \tag{3.8.47}$$

We can now turn to the analysis of the geometry of the flow in Figure 3.75. For this purpose, we use equation (3.8.39). We write it in the form

$$\frac{1}{V_0} \frac{dw}{dz} = e^\Omega,$$

or, equivalently,

$$\frac{1}{V_0} \frac{dw}{dt} \frac{1}{dz/dt} = e^\Omega. \tag{3.8.48}$$

It follows from (3.8.47) that $dw/dt = -Q/(\pi t)$, which, being substituted into (3.8.48) together with (3.8.46), yields

$$\frac{dz}{dt} = -\frac{Q}{\pi V_0} \frac{e^{-i(2\alpha/\pi) \arcsin t}}{t}. \tag{3.8.49}$$

We can integrate equation (3.8.49) starting, for example, from point B . In the physical z -plane (Figure 3.75), it is situated at $z = ib$, and its image in the auxiliary t -plane (Figure 3.78) is at $t = 1$. Consequently,

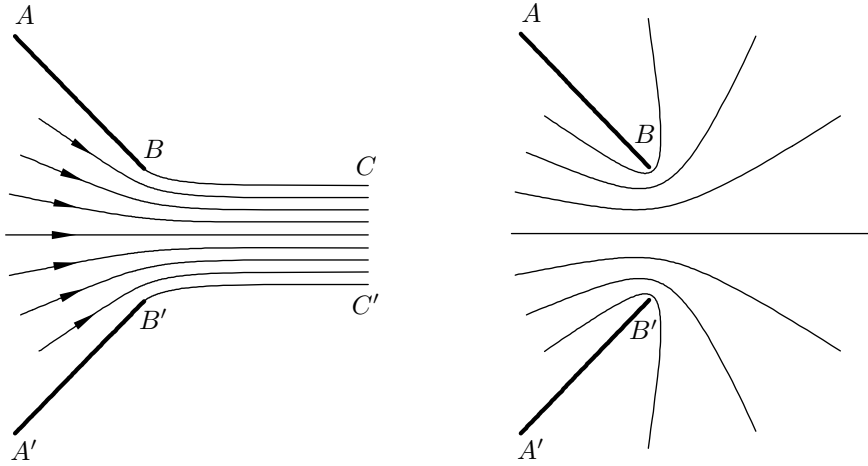
$$z = ib - \frac{Q}{\pi V_0} \int_1^t \frac{e^{-i(2\alpha/\pi) \arcsin t}}{t} dt. \tag{3.8.50}$$

Figure 3.80(a) shows the streamline pattern for the flow through the mouthpiece calculated for $\alpha = \frac{1}{4}\pi$. In order to explain the calculation procedure, it is convenient to express t in the exponential form $t = |t|e^{i\phi}$. Then it is easily deduced from (3.8.47) that the velocity potential φ and the stream function ψ are given by

$$\varphi = -\frac{Q}{\pi} \ln |t|, \quad \psi = -\frac{Q}{\pi} \phi.$$

We see that in the t -plane the streamlines are represented by rays emanating from the coordinate origin. We therefore distributed evenly nine rays in the upper half of the t -plane, two of these being along the positive real semi-axis and negative real semi-axis. We also introduced a semicircle of unit radius crossing the rays. We started from the point B where $t = 1$ (see Figure 3.78) and integrated equation (3.8.50) along the semicircle towards a chosen ray using the trapezoidal rule. Then we continued along the ray in both directions, towards the coordinate origin and away from it. The calculated values of $z = x + iy$ were then used to plot the corresponding streamlines in Figure 3.80(a).

For comparison, we show in Figure 3.80(b) the streamline pattern that would be observed if the fluid were able to go around the edges B and B' without separation. Interestingly enough, Figure 3.80(b) also shows the electrostatic field between two



(a) Flow with separation from the plates' edges B and B' (b) Flow without separation at the plates' edges.

Fig. 3.80: Comparison of separated and attached flows; $\alpha = \frac{1}{4}\pi$.

conductors having the form of semi-infinite plates AB and $A'B'$. Helmholtz (1868) was the first to point out this analogy.¹⁴ He also argued that it is the fluid viscosity that, despite being very small, always causes the flow to separate in situations like the one shown in Figure 3.80(a).

Exercises 12

1. Analyse the asymptotic behaviour of the free streamlines SF and $S'F'$ in the Kirchhoff flow past a flat plate (see Figure 3.81a). For this purpose, modify equa-

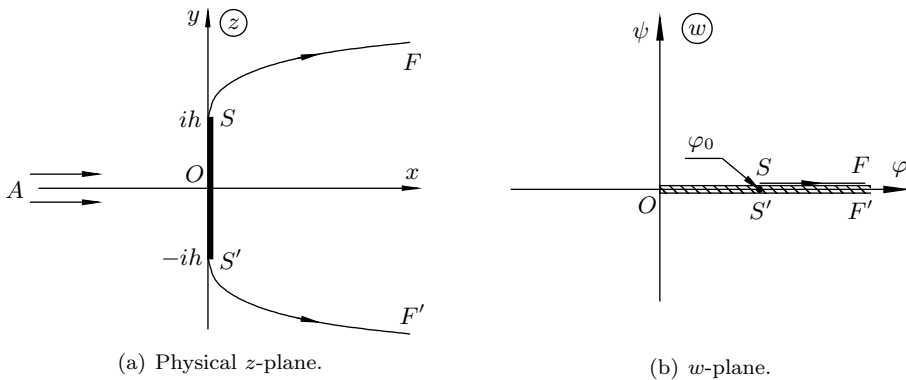


Fig. 3.81: The physical z -plane and the complex potential w .

¹⁴See the discussion in the Introduction.

tion (3.8.25) by writing it in the form

$$z = ih + \frac{i}{V_\infty} \int_{\varphi_0}^w \left(\sqrt{\frac{\varphi_0}{w}} - \sqrt{\frac{\varphi_0}{w} - 1} \right) dw. \quad (3.8.51)$$

Concentrate your attention on the upper free streamline SF , in which case the integration in (3.8.51) has to be performed along the upper side of the branch cut in the w -plane from point S toward point F ; see Figure 3.81(b).

Use Figures 3.72 and 3.73 to evaluate $\sqrt{\varphi_0/w}$ and $\sqrt{\varphi_0/w - 1}$ on the integration path, and show that, for any point that lies on the upper side of the branch cut on the right-hand side of point S , equation (3.8.51) may be written as

$$z = ih + \frac{i}{V_\infty} \int_{\varphi_0}^{\varphi} \sqrt{\frac{\varphi_0}{\varphi}} d\varphi + \frac{1}{V_\infty} \int_{\varphi_0}^{\varphi} \sqrt{1 - \frac{\varphi_0}{\varphi}} d\varphi. \quad (3.8.52)$$

Show further that, for large values of φ/φ_0 , equation (3.8.52) gives

$$z = \frac{\varphi}{V_\infty} + i \frac{2\sqrt{\varphi_0}}{V_\infty} \varphi^{1/2}. \quad (3.8.53)$$

Finally, separate the real and imaginary parts in (3.8.53) and deduce that at a large distance downstream of the plate, the equation for the upper free streamline SF is written as

$$y = 2\sqrt{\frac{\varphi_0}{V_\infty}} x^{1/2} = 2\sqrt{\frac{2h}{\pi + 4}} x^{1/2}. \quad (3.8.54)$$

2. Compare (3.8.54) with the parabola equation (3.7.15) in Problem 5, Exercises 11, and note that these can be reduced to one another by setting

$$a = 2\sqrt{\frac{2h}{\pi + 4}}. \quad (3.8.55)$$

Using (3.8.55) in (3.8.38), show that the plate drag in the Kirchhoff flow may be expressed in the form

$$D = \frac{1}{4}\rho V_\infty^2 a^2 \pi,$$

Compare it with the parabola drag calculated when solving Problem 5 in Exercises 11.

3. Sketch the region that the Kirchhoff flow (see Figure 3.81a) occupies in the complex plane of the function

$$\Omega = \ln\left(\frac{1}{V_\infty} \frac{dw}{dz}\right).$$

4. Assume that the separation region, forming downstream of the plate, is finite as shown in Figure 3.82.

Taking into account that the fluid in the separation region $SFF'S'$, whatever form of motion it assumes, is in a state of equilibrium, demonstrate that the plate cannot experience any drag as long as the flow remains steady.

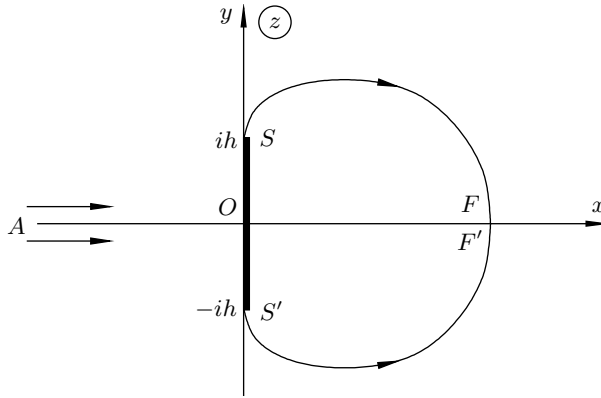


Fig. 3.82: Flow with finite separation region.

5. The *contraction coefficient* κ of the jet in Figure 3.75 is defined as the ratio of the jet width $2b'$ far downstream of the mouthpiece exit to the width $2b$ of the exit BB' itself.

You need to perform the following two tasks:

- (a) Show that

$$\kappa = \frac{b'}{b} = \frac{1}{1 + (2/\pi)I}, \quad \text{where} \quad I = \int_0^1 \sin\left(\frac{2\alpha}{\pi} \arcsin t\right) \frac{dt}{t}. \quad (3.8.56)$$

- (b) Calculate κ for $\alpha = \frac{1}{2}\pi$ and $\alpha = \pi$. The latter case is referred to as the *Borda mouthpiece*. Draw sketches of the two flows.

Suggestion: When the observation point moves in the physical plane (Figure 3.75) from point B along the upper boundary of the jet towards point C , the corresponding point in the t -plane (Figure 3.78) remains on the real axis, and lies in the interval $[0, 1]$. Keeping this in mind, separate the real and imaginary parts of equation (3.8.50), and concentrate your attention on the imaginary part. Notice that point C is situated in the auxiliary t -plane at $t = 0$. Also notice that the fluid flux Q may be calculated as $Q = 2b'V_0$.

6. Return once again to the problem of a jet that forms as an inviscid incompressible fluid escapes from a large container through an orifice equipped with a mouthpiece as shown in Figure 3.75. This time your task is to show that in a small neighbourhood of the separation point B , the pressure p on the upper plate AB may be written as

$$\frac{p - p_0}{\rho} = 2\alpha V_0 \sqrt{\frac{V_0}{\pi Q}} s^{1/2} + \dots,$$

where s is the distance measured from B along the lower side of AB .

You may perform this in the following steps:

- (a) Notice that, near point B , $t - 1$ is small and therefore

$$\arcsin t = \frac{1}{2}\pi \pm i\sqrt{2}(t - 1)^{1/2} + \dots \quad (3.8.57)$$

Substitute (3.8.57) into (3.8.46) and argue that, on AB ,

$$\Omega = i\alpha - \frac{2\alpha}{\pi}\sqrt{2}(t - 1)^{1/2} + \dots \quad (3.8.58)$$

- (b) Perform the corresponding simplifications in (3.8.47), and eliminate $t - 1$ from (3.8.58) to show that

$$\Omega = i\alpha - i2\alpha\sqrt{\frac{2}{\pi Q}}w^{1/2} + \dots$$

- (c) Use the definition (3.8.39) of the function Ω and the fact that $|w|$ is small near B to deduce the following equation for the complex potential $w(z)$:

$$\frac{dw}{dz} = V_0 e^{i\alpha} \left(1 - i2\alpha\sqrt{\frac{2}{\pi Q}}w^{1/2} + \dots \right). \quad (3.8.59)$$

- (d) The leading-order solution to (3.8.59) may be obtained by disregarding the $O(w^{1/2})$ term on the right-hand side of (3.8.59) and assuming that $w = 0$ at point B . Use this solution to evaluate $w^{1/2}$ in (3.8.59), and show that on the lower side of the upper plate, AB , where $z = ib + e^{-i(\pi+\alpha)}s$,

$$\bar{V} = \frac{dw}{dz} = V_0 e^{i\alpha} \left(1 - 2\alpha\sqrt{\frac{2V_0}{\pi Q}}s^{1/2} + \dots \right).$$

Finally, use the Bernoulli equation to determine the pressure distribution on AB .

4

Elements of Gasdynamics

4.1 General Properties of Compressible Flows

The influence of compressibility on the behaviour of gas flows depends on the flow regime considered. The non-dimensional parameter controlling this effect is the *Mach number*, defined as $M = V/a$, where V is the flow velocity and a the speed of sound. For sufficiently small flow speed, when $M \ll 1$, the pressure perturbations induced by gas motion prove to be small, and are capable of producing only $O(M^2)$ perturbations of the density (see Problem 4 in Exercises 4). Therefore, such flows may be treated as incompressible, enabling the theory discussed in Chapter 3 to be used. If, on the other hand, the Mach number is finite, $M = O(1)$, then Laplace's equation (3.2.7) is no longer valid. Instead, one has to use a set of equations (4.3.6), (4.3.8), and (4.3.9). We shall see that these equations are inherently nonlinear and more difficult to solve. However, for subsonic flow regimes, when $M < 1$, they still constitute an elliptic problem, and therefore the flow structure around a solid body remains similar to that for incompressible flows.

Fundamental changes take place when the Mach number increases to values larger than unity, $M > 1$, and the flow becomes supersonic. A major difference between supersonic and subsonic flows past a flying object is that in subsonic flow the perturbations are radiated in all directions such that the entire flow around the object appears to be perturbed. In contrast, in the supersonic case, the perturbations produced by the object are not capable of penetrating into the flow region upstream of the front shock (see Figure 4.1). All the perturbations are confined to a region between the shock and the body surface.

This may be explained as follows. Suppose that a flying object moves along a straight line AB through a motionless atmosphere, producing small-amplitude perturbations at each point of its trajectory (see Figure 4.2). Once created, these perturbations propagate in the atmosphere in all directions with the speed of sound, a . In particular, the perturbations radiated from the object when at point A form a sphere S . The radius of the sphere grows with time t as at . While this happens, the object moves to a new location B separated by a distance Vt from A . If the object speed V is supersonic, i.e. $M = V/a > 1$, then point B finds itself outside sphere S . The perturbations radiated from the intermediate points of the trajectory are produced by the object with a corresponding time delay. If, say, we consider the point situated midway between A and B , then it takes half the time for the object to reach this point, and consequently the radius of the corresponding perturbation sphere S' will be $\frac{1}{2}at$. Similar consideration may be given to other points of the trajectory AB ,

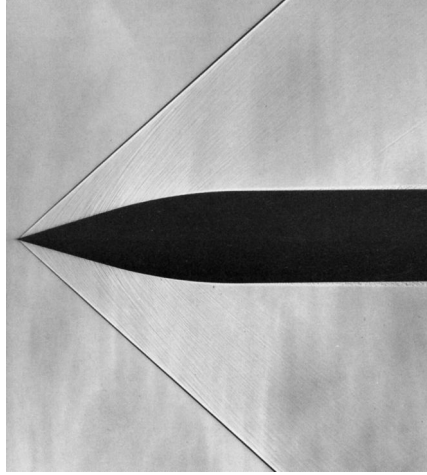


Fig. 4.1: Supersonic flow past an ogive cylinder. Photograph from Transonic Range, U.S. Army Ballistic Research Laboratory; reprinted from Van Dyke (1982), p. 161, Figure 261.

leading to the conclusion that all the perturbations are confined within a cone whose apex coincides with the current location of the object and whose semi-angle Θ is given by

$$\tan \Theta = \frac{at}{\sqrt{(Vt)^2 - (at)^2}} = \frac{1}{\sqrt{M^2 - 1}}. \quad (4.1.1)$$

This cone is called the *Mach cone*.

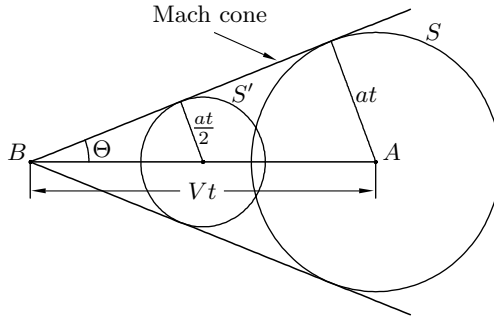


Fig. 4.2: Perturbations produced by an object that flies at a supersonic speed.

4.1.1 Euler equations for gas flows

The Euler equations governing the inviscid motion of compressible fluids may be obtained from the Navier–Stokes equations (1.7.21) by setting the viscosity μ to zero.

We have

$$\rho \left[\frac{\partial \mathbf{V}}{\partial t} + (\mathbf{V} \cdot \nabla) \mathbf{V} \right] = \rho \mathbf{f} - \nabla p \quad (\text{momentum equation}), \quad (4.1.2a)$$

$$\rho \left[\frac{\partial h}{\partial t} + (\mathbf{V} \cdot \nabla h) \right] = \frac{\partial p}{\partial t} + \mathbf{V} \cdot \nabla p \quad (\text{energy equation}), \quad (4.1.2b)$$

$$\frac{\partial \rho}{\partial t} + \text{div}(\rho \mathbf{V}) = 0 \quad (\text{continuity equation}), \quad (4.1.2c)$$

$$h = \frac{\gamma}{\gamma - 1} \frac{p}{\rho} \quad (\text{state equation}). \quad (4.1.2d)$$

4.1.2 Piston theory

Let us consider a perfect gas contained inside a long cylinder as shown in Figure 4.3. The gas is bounded from the left by a piston whose initial position is shown by the dashed line. We shall assume that initially the gas is in a state of rest, with pressure, density, and enthalpy being equal to p_0 , ρ_0 , and h_0 , respectively. We further assume that, at the instant $t = 0$, the piston is brought into motion, and its position at any time $t > 0$ is given by the equation

$$x = x_w(t),$$

where the x -axis is drawn parallel to the cylinder generator from the initial position of the piston surface.

As gases are light, the influence of gravity may be neglected under normal conditions, which enables us to treat the flow in the cylinder as one-dimensional. This means, first, that the velocity vector has only one non-zero component, $\mathbf{V} = (u, 0, 0)$, and, second, that all the fluid-dynamic quantities depend on x and t only. These simplifications allow us to reduce the Euler equations (4.1.2) to

$$\rho \left(\frac{\partial u}{\partial t} + u \frac{\partial u}{\partial x} \right) = - \frac{\partial p}{\partial x}, \quad (4.1.3a)$$

$$\rho \left(\frac{\partial h}{\partial t} + u \frac{\partial h}{\partial x} \right) = \frac{\partial p}{\partial t} + u \frac{\partial p}{\partial x}, \quad (4.1.3b)$$

$$\frac{\partial \rho}{\partial t} + \rho \frac{\partial u}{\partial x} + u \frac{\partial \rho}{\partial x} = 0, \quad (4.1.3c)$$

$$\rho h = \frac{\gamma}{\gamma - 1} p. \quad (4.1.3d)$$

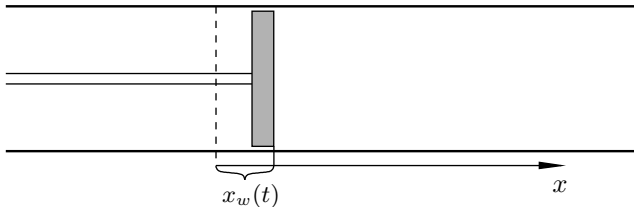


Fig. 4.3: Problem layout.

These are to be solved with the impermeability condition on the piston surface, which may be written as

$$u = \dot{x}_w(t) \quad \text{at} \quad x = x_w(t), \quad (4.1.4)$$

where the “upper dot” denotes the derivative of $x_w(t)$ with respect to time, t .

In order to simplify the analysis of equations (4.1.3) and (4.1.4), we shall assume that the piston displacement x_w and velocity \dot{x}_w are small.¹ In this case, one can expect the perturbations induced in the gas medium to be weak, which suggests that the solution may be sought in the form

$$\left. \begin{aligned} u(t, x) &= u'(t, x), & p(t, x) &= p_0 + p'(t, x), \\ \rho(t, x) &= \rho_0 + \rho'(t, x), & h(t, x) &= h_0 + h'(t, x). \end{aligned} \right\} \quad (4.1.5)$$

Here p_0 , ρ_0 , and h_0 are constants representing the unperturbed state of the gas. The ‘dashed quantities’ u' , p' , ρ' , and h' appear in (4.1.5) owing to the piston motion. We shall assume that they are small.

We need to substitute (4.1.5) into the Euler equations (4.1.3). To demonstrate how this is done, let us consider the first term on the left-hand side of the momentum equation (4.1.3a):

$$\rho \frac{\partial u}{\partial t} = (\rho_0 + \rho') \frac{\partial u'}{\partial t} = \rho_0 \frac{\partial u'}{\partial t} + \rho' \frac{\partial u'}{\partial t}.$$

Since both ρ' and $\partial u'/\partial t$ are small, the second term $\rho' \partial u'/\partial t$ represents a quantity referred to as ‘square of perturbations’. It is small compared with the first term $\rho_0 \partial u'/\partial t$ and can be neglected. We have

$$\rho \frac{\partial u}{\partial t} = \rho_0 \frac{\partial u'}{\partial t} + \dots.$$

The second term in (4.1.3a), $\rho u \partial u / \partial x$, is quadratic with respect to small perturbations, and should be disregarded. Finally, the pressure gradient on the right-hand side of (4.1.3a) may be written as

$$\frac{\partial p}{\partial x} = \frac{\partial p'}{\partial x},$$

and we see that the momentum equation (4.1.3a) turns into

$$\rho_0 \frac{\partial u'}{\partial t} = - \frac{\partial p'}{\partial x}. \quad (4.1.6a)$$

Applying the same treatment to the energy (4.1.3b), continuity (4.1.3c), and state (4.1.3d) equations, we have

$$\rho_0 \frac{\partial h'}{\partial t} = \frac{\partial p'}{\partial t}, \quad (4.1.6b)$$

$$\frac{\partial \rho'}{\partial t} + \rho_0 \frac{\partial u'}{\partial x} = 0, \quad (4.1.6c)$$

$$\rho_0 h' + h_0 \rho' = \frac{\gamma}{\gamma - 1} p'. \quad (4.1.6d)$$

¹More precisely, the velocity should be small compared with the speed of sound (see Problem 1 in Exercises 13).

With (4.1.5), the impermeability condition (4.1.4) may be written as

$$u'[t, x_w(t)] = \dot{x}_w(t). \quad (4.1.7)$$

We take into account that $x_w(t)$ is small and use the Taylor expansion of $u'[t, x_w(t)]$ with respect to the second argument,

$$u'[t, x_w(t)] = u'(t, 0) + x_w(t) \frac{\partial u'}{\partial x}(t, 0) + \dots$$

Since both x_w and $\partial u'/\partial x$ are small, $x_w \partial u'/\partial x$ represents a square of perturbations term. It may therefore be disregarded, which reduces (4.1.7) to

$$u' = \dot{x}_w(t) \quad \text{at} \quad x = 0. \quad (4.1.8)$$

It is interesting to note that, as a result of the approximation used, the impermeability condition has been *transferred* from the actual position $x = x_w(t)$ of the piston surface to $x = 0$.

Now our task will be to solve the linearised Euler equations (4.1.6) subject to the boundary condition (4.1.8). For this purpose, we shall try to eliminate from (4.1.6) all the unknown functions except for the pressure perturbation p' . We start with cross-differentiation of the momentum (4.1.6a) and continuity (4.1.6c) equations, which allows us to eliminate u' , leading to

$$\frac{\partial^2 \rho'}{\partial t^2} - \frac{\partial^2 p'}{\partial x^2} = 0. \quad (4.1.9)$$

Differentiating the state equation (4.1.6d) with respect to time t and using the resulting equation for eliminating h' from the energy equation (4.1.6b) yields

$$\frac{\partial \rho'}{\partial t} = \frac{1}{(\gamma - 1)h_0} \frac{\partial p'}{\partial t}. \quad (4.1.10)$$

Now we can use (4.1.10) to eliminate ρ' from equation (4.1.9). As a result, we arrive at the classical *wave equation* for p' :

$$\frac{\partial^2 p'}{\partial t^2} - a^2 \frac{\partial^2 p'}{\partial x^2} = 0, \quad (4.1.11)$$

where

$$a = \sqrt{(\gamma - 1)h_0}. \quad (4.1.12)$$

The solution of equation (4.1.11) may easily be found by introducing the *characteristic variables*

$$\xi = x - at, \quad \eta = x + at,$$

If we consider ξ and η as new independent variables, then equation (4.1.11) may be expressed in the form

$$\frac{\partial^2 p'}{\partial \xi \partial \eta} = 0,$$

with the general solution being

$$p'(t, x) = f(\xi) + g(\eta). \quad (4.1.13)$$

Here $f(\xi)$ and $g(\eta)$ are arbitrary functions of their respective arguments.

In order to determine these functions, it is helpful to clarify their physical content. It may easily be seen that the function $f(\xi) = f(x - at)$ represents a wave that propagates through the gas medium in the positive x -direction. It is produced by the motion of the cylinder surface, and then travels away from the cylinder with constant speed a , keeping the profile of perturbations unchanged. The function $g(\eta) = g(x + at)$ represents a similar wave travelling in the opposite direction. For such a wave to exist, there should be another source of perturbations situated at some position $x_0 > 0$. Therefore, if we assume that the piston shown in Figure 4.3 is the only source of perturbations in the cylinder, then we have to write (4.1.13) as

$$p'(t, x) = f(x - at). \quad (4.1.14)$$

To determine the function $f(x - at)$, the impermeability condition (4.1.8) should be used. It may be reformulated for p' by setting $x = 0$ in the momentum equation (4.1.6a) and using (4.1.8) for u' . We have

$$\left. \frac{\partial p'}{\partial x} \right|_{x=0} = -\rho_0 \ddot{x}_w(t). \quad (4.1.15)$$

Substitution of (4.1.14) into (4.1.15) yields

$$f'(-at) = -\rho_0 \ddot{x}_w(t),$$

which, being integrated, gives

$$f(-at) = a\rho_0 \dot{x}_w(t) + C.$$

Denoting the argument of the function f by s , we have

$$f(s) = a\rho_0 \dot{x}_w(-s/a) + C. \quad (4.1.16)$$

It remains to substitute (4.1.16) back into (4.1.14), and we find that the pressure perturbations propagating through the gas contained inside the cylinder are given by

$$p'(t, x) = a\rho_0 \dot{x}_w\left(t - \frac{x}{a}\right). \quad (4.1.17)$$

The constant of integration C has been disregarded in this formula for the simple reason that the gas medium should remain unperturbed ($p' = 0$) when the piston remains motionless ($\dot{x}_w = 0$).

Formula (4.1.17) may, in particular, be used to determine the pressure on the piston surface itself. Setting $x = 0$, we find

$$p' = a\rho_0 \dot{x}_w(t).$$

It is interesting to note that the solution of the piston problem could be expressed in a simple analytical form (4.1.17) without any particular restriction on the function $x_w(t)$, except that the piston speed $\dot{x}_w(t)$ was assumed to be small, such that only weak perturbations are induced in the gas medium. Piston theory has various applications.

It may be used, for instance, to describe the generation of sound, in which case the piston should be thought of as a membrane performing harmonic oscillations in the acoustic frequency range. The speed of acoustic waves, a , is, of course, the same as the speed of any other small perturbation, which is why the quantity given by equation (4.1.12) is referred to as the *speed of sound*.

In Section 4.5, we shall see that when the perturbations are not small, they can form shock waves. These are able to propagate through the gas medium with a speed that exceeds the speed of sound. This is illustrated in Figure 4.4, which shows a visualisation of supersonic flow past a sphere. A bow shock wave is clearly visible in front of the sphere. In the far field above and below the sphere, where the shock is weak, it degenerates into a sonic wave, and the slope angle Θ may be calculated using equation (4.1.1). However, closer to the sphere, the perturbations become stronger and the shock starts to bend, connecting smoothly the two extremes predicted by (4.1.1). Directly in front of the sphere, the shock is perpendicular to the oncoming flow, and moves in the same direction and with the same speed as the sphere itself; the latter may, obviously, be propelled through the gas with arbitrary velocity.

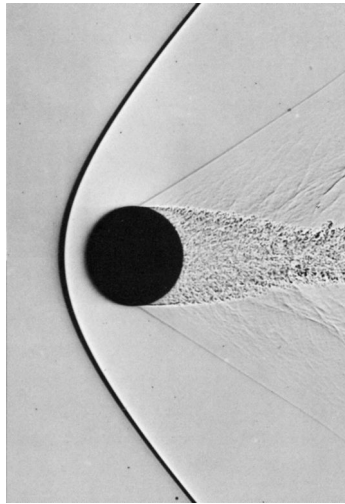


Fig. 4.4: Supersonic flow past a sphere. Photograph by A. C. Charters; reprinted from Van Dyke (1982), p. 164, Figure 266.

4.2 Integrals of Motion

Here we shall return to the nonlinear equations (4.1.2) and deduce a number of integrals of motion, starting with the compressible version of *Bernoulli's integral*.

4.2.1 Bernoulli's integral

Similar to the incompressible case (see Theorem 3.1, page 130) we shall assume that (i) the gas flow is steady and (ii) the body force has potential, $\mathbf{f} = -\nabla U$. Then the

momentum equation (4.1.2a) may be written as

$$(\mathbf{V} \cdot \nabla) \mathbf{V} = -\nabla U - \frac{1}{\rho} \nabla p, \quad (4.2.1)$$

and the energy equation (4.1.2b) takes the form

$$\mathbf{V} \cdot \nabla h = \frac{1}{\rho} (\mathbf{V} \cdot \nabla p). \quad (4.2.2)$$

Using the Lamb identity

$$(\mathbf{V} \cdot \nabla) \mathbf{V} = \nabla \left(\frac{V^2}{2} \right) + \boldsymbol{\omega} \times \mathbf{V}, \quad (4.2.3)$$

we can recast equation (4.2.1) in the form

$$\nabla \left(\frac{V^2}{2} \right) + \boldsymbol{\omega} \times \mathbf{V} = -\nabla U - \frac{1}{\rho} \nabla p. \quad (4.2.4)$$

Let us now consider the scalar product of (4.2.4) with the velocity vector \mathbf{V} . Taking into account that $\boldsymbol{\omega} \times \mathbf{V}$ is perpendicular to \mathbf{V} , we have

$$\mathbf{V} \cdot \nabla \left(\frac{V^2}{2} + U \right) = -\frac{1}{\rho} (\mathbf{V} \cdot \nabla p). \quad (4.2.5)$$

Combining (4.2.5) with the energy equation (4.2.2) yields

$$\mathbf{V} \cdot \nabla \left(h + \frac{V^2}{2} + U \right) = 0.$$

This proves that the following theorem is valid.

Theorem 4.1 *In a steady inviscid compressible fluid flow taking place in the field of the body force \mathbf{f} that has potential U , the **Bernoulli integral** holds; that is,*

$$h + \frac{V^2}{2} + U$$

remains constant along each streamline.

If the influence of the gravitational force \mathbf{f} on flow behaviour may be neglected, then Bernoulli's equation assumes the form

$$h + \frac{V^2}{2} = \text{const}, \quad (4.2.6)$$

which means that the function

$$H = h + \frac{V^2}{2}, \quad (4.2.7)$$

referred to as the *total enthalpy*, does not change along streamlines.

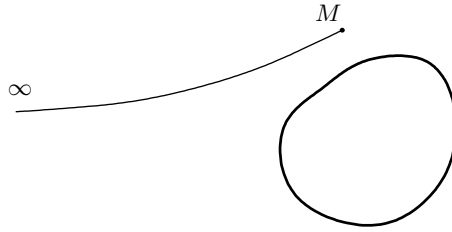


Fig. 4.5: Calculation of the constant in the Bernoulli equation (4.2.6).

In particular, when dealing with flow around a rigid body that is placed into a uniform stream, one can easily calculate the constant on the right-hand side of the Bernoulli equation (4.2.6) from the free-stream conditions. Indeed, for any point M in the flow field (see Figure 4.5) that may be ‘connected’ via a streamline with the oncoming unperturbed flow,² we have

$$h + \frac{V^2}{2} = h_\infty + \frac{V_\infty^2}{2}, \quad (4.2.8)$$

where h_∞ and V_∞ are undisturbed values of the enthalpy and velocity in the oncoming flow.

In Section 4.5 we will demonstrate that the total enthalpy H is also preserved across shock waves. This allows us to use the Bernoulli equation throughout the flow field even if there are multiple shock waves.

4.2.2 Entropy conservation law

This law may be easily deduced from the energy and state equations, for which purpose it is convenient to write the energy equation (4.1.2b) in terms of the full derivatives:

$$\rho \frac{Dh}{Dt} = \frac{Dp}{Dt}. \quad (4.2.9)$$

Differentiation of the state equation (4.1.2d) gives

$$\frac{Dh}{Dt} = \frac{\gamma}{\gamma - 1} \frac{1}{\rho} \frac{Dp}{Dt} - \frac{\gamma}{\gamma - 1} \frac{p}{\rho^2} \frac{D\rho}{Dt}.$$

When substituted into (4.2.9), this yields

$$\frac{1}{p} \frac{Dp}{Dt} - \gamma \frac{1}{\rho} \frac{D\rho}{Dt} = 0,$$

or, equivalently,

$$\frac{D}{Dt} \left(\ln \frac{p}{\rho^\gamma} \right) = 0.$$

We can conclude that the following theorem is valid.

²This apparently cannot be done for points in a recirculation region that might form if the flow separates from the body surface.

Theorem 4.2 *In an inviscid flow, the entropy*

$$S = \tilde{C} + \frac{R}{\gamma - 1} \ln \frac{p}{\rho^\gamma}$$

stays unchanged for any fluid particle as it travels through the flow field.

Unlike the Bernoulli integral (4.2.6), the entropy conservation law does not rely on the assumption of steady flow, nor does it require the body force \mathbf{f} to be potential. However, it should be noted that the entropy does not remain constant across shock waves. As will be shown in Section 4.5, it always increases when a fluid particle passes through a shock wave. Therefore, special care should be taken when using Theorem 4.2 in supersonic flows.

If we consider a flow free of shock waves (any subsonic flow belongs to this category), then we can write

$$\frac{p}{\rho^\gamma} = \frac{p_\infty}{\rho_\infty^\gamma} \quad (4.2.10)$$

for any fluid particle whose trajectory originates in the unperturbed flow, where the pressure and density are equal to p_∞ and ρ_∞ , respectively.

In a compressible flow, the Bernoulli equation (4.2.8) alone is not sufficient for converting the velocity field in a moving fluid into the pressure field. Using the state equation (4.1.2d), we can express (4.2.8) in the form

$$\frac{\gamma}{\gamma - 1} \frac{p}{\rho} + \frac{V^2}{2} = \frac{\gamma}{\gamma - 1} \frac{p_\infty}{\rho_\infty} + \frac{V_\infty^2}{2}. \quad (4.2.11)$$

Since the density ρ is also an unknown quantity, one has to consider equation (4.2.11) together with the entropy conservation law (4.2.10). These may be solved for pressure p and density ρ at any point in the flow field where the velocity V is known.

The entropy conservation law can also be used to extend Kelvin's Circulation Theorem (see page 132) to compressible flows.

4.2.3 Kelvin's Circulation Theorem

As in Section 3.1.2, we will be dealing here with a closed fluid contour C . Remember that a contour C is termed a *fluid contour* if it is composed of the same set of fluid particles. Obviously, the contour deforms with time as the fluid particles move in space. The circulation along such contour is given at any instant t by the integral (3.1.8):

$$\Gamma(t) = \oint_C \mathbf{V} \cdot d\mathbf{r}.$$

Manipulations with the derivative of this integral, leading to formula (3.1.12), do not rely on a particular form of the dynamic equations of fluid motion, and therefore may be used not only for a flow of incompressible fluid but also for any compressible flow. We have

$$\frac{d\Gamma}{dt} = \int_0^L \left(\frac{D\mathbf{V}}{Dt} \cdot \frac{\partial \mathbf{r}}{\partial s} \right) ds + \int_0^L \left(\mathbf{V} \cdot \frac{\partial^2 \mathbf{r}}{\partial s \partial t} \right) ds. \quad (4.2.12)$$

According to (3.1.13), the second integral in (4.2.12) may be reduced to

$$\int_0^L \left(\mathbf{V} \cdot \frac{\partial^2 \mathbf{r}}{\partial s \partial t} \right) ds = \frac{V^2}{2} \Big|_{s=L} - \frac{V^2}{2} \Big|_{s=0}.$$

It remains zero as long as the flow is free of shock waves and hence the velocity field is continuous.

In order to evaluate the first integral in (4.2.12), we use the momentum equation (4.1.2a). Assuming that the body force is potential, $\mathbf{f} = -\nabla U$, we have

$$\frac{D\mathbf{V}}{Dt} = -\frac{1}{\rho} \nabla p - \nabla U. \quad (4.2.13)$$

If the contour C does not intersect a shock wave, and all the fluid particles lying on C originate from a region where $p = p_\infty$ and $\rho = \rho_\infty$, then the entropy conservation law (4.2.10) can be used. If we take logarithms on both sides of (4.2.10) and differentiate the resulting equation, then we will have

$$\frac{1}{p} \nabla p - \frac{\gamma}{\rho} \nabla \rho = 0. \quad (4.2.14)$$

Similarly, it follows from the state equation (4.1.2d) that

$$\frac{1}{h} \nabla h = \frac{1}{p} \nabla p - \frac{1}{\rho} \nabla \rho. \quad (4.2.15)$$

Elimination of $\nabla \rho / \rho$ from (4.2.14) and (4.2.15) results in

$$\nabla h = h \frac{\gamma - 1}{\gamma} \frac{\nabla p}{p} = \frac{\nabla p}{\rho}. \quad (4.2.16)$$

This allows us to express equation (4.2.13) in the form

$$\frac{D\mathbf{V}}{Dt} = -\nabla(h + U),$$

which, being substituted into (4.2.12), yields

$$\frac{d\Gamma}{dt} = - \oint_C \nabla(h + U) \cdot d\mathbf{r}.$$

We see that

$$\frac{d\Gamma}{dt} = 0$$

for any fluid contour that does not intersect a shock wave. The Kelvin Circulation Theorem may be now rephrased as follows.

Theorem 4.3 *In an inviscid fluid flow, the circulation along any closed fluid contour C does not change with time, provided that (i) the body force \mathbf{f} is potential, (ii) all the fluid particles on C originate from a region where $p = p_\infty$ and $\rho = \rho_\infty$, and (iii) the contour C does not intersect a shock wave.*

In Section 3.1.2, we demonstrated how Kelvin's Circulation Theorem may be used to identify the physical situations where a fluid flow may be treated as potential. Now, having established that Kelvin's theorem also holds for perfect gas flows, we can see that the arguments of Section 3.1.2 are equally applicable to compressible flows. Another powerful tool, which allows us to distinguish between irrotational flows and flows with non-zero vorticity, is *Crocco's formula*.

4.2.4 Crocco's formula

Theorem 4.2 deals with the variation of the entropy S of a fluid particle as it travels through a flow field. Let us now instead consider the variation of S between neighbouring points in the flow field at a given time. For this purpose, we differentiate formula (1.3.37). We find that the gradient of the entropy

$$\nabla S = \frac{R}{\gamma - 1} \frac{\nabla p}{p} - R \frac{\gamma}{\gamma - 1} \frac{\nabla \rho}{\rho}. \quad (4.2.17)$$

With the help of the state equation (4.1.2d), formula (4.2.7) for the total enthalpy may be written as

$$H = \frac{\gamma}{\gamma - 1} \frac{p}{\rho} + \frac{V^2}{2}.$$

Differentiation of this formula yields

$$\nabla H = \frac{\gamma}{\gamma - 1} \frac{\nabla p}{\rho} - \frac{\gamma}{\gamma - 1} \frac{p}{\rho^2} \nabla \rho + \nabla \left(\frac{V^2}{2} \right),$$

which may be rearranged as

$$-\frac{\gamma}{\gamma - 1} \frac{\nabla \rho}{\rho} = \frac{\rho}{p} \nabla H - \frac{\gamma}{\gamma - 1} \frac{\nabla p}{p} - \frac{\rho}{p} \nabla \left(\frac{V^2}{2} \right). \quad (4.2.18)$$

Substitution of (4.2.18) into (4.2.17) leads to

$$\nabla S = \frac{R\rho}{p} \nabla H - R \frac{\nabla p}{p} - \frac{R\rho}{p} \nabla \left(\frac{V^2}{2} \right).$$

If we multiply both sides of this equation by the temperature T ,

$$T \nabla S = \frac{\rho RT}{p} \nabla H - RT \frac{\nabla p}{p} - \frac{\rho RT}{p} \nabla \left(\frac{V^2}{2} \right),$$

and recall that, for a perfect gas,

$$p = \rho RT,$$

then we will have

$$T \nabla S = \nabla H - \frac{1}{\rho} \nabla p - \nabla \left(\frac{V^2}{2} \right). \quad (4.2.19)$$

Let us now consider the momentum equation (4.1.2a). Using the identity (4.2.3),

we can write it in the Lamb form,

$$\frac{\partial \mathbf{V}}{\partial t} + \boldsymbol{\omega} \times \mathbf{V} + \nabla \left(\frac{V^2}{2} \right) = \mathbf{f} - \frac{1}{\rho} \nabla p. \quad (4.2.20)$$

Comparing (4.2.20) with (4.2.19), we can easily see that the equation

$$\boldsymbol{\omega} \times \mathbf{V} = T \nabla S - \nabla H - \frac{\partial \mathbf{V}}{\partial t} + \mathbf{f}, \quad (4.2.21)$$

termed *Crocco's formula*, is valid.

This formula shows that if we exclude from consideration a special class of so-called 'helical flows', for which $\boldsymbol{\omega}$ is parallel to \mathbf{V} , then the following theorem may be easily proven.

Theorem 4.4 *If a flow of a perfect gas is steady and free of shock waves, the body force is negligible, and the oncoming free-stream flow is uniform, then this flow is irrotational.*

Proof Under the conditions of the theorem, equations (4.2.8) and (4.2.10) hold throughout the flow field, and therefore $\nabla H = \nabla S = 0$. Since the flow is assumed to be steady, $\partial \mathbf{V} / \partial t = 0$, and the body force negligible, $\mathbf{f} = 0$, we can conclude that the right-hand side of equation (4.2.21) is zero. Thus, if the fluid is not at rest, i.e. $\mathbf{V} \neq 0$, and the vorticity $\boldsymbol{\omega}$ is not parallel to the velocity vector \mathbf{V} , then $\boldsymbol{\omega}$ should be zero. \square

It should be noted that Kelvin's Circulation Theorem allows us to arrive at the same conclusion without relying on the assumption of steady flow; the body force may be also included, provided it is potential, $\mathbf{f} = -\nabla U$. However, the importance of Crocco's formula becomes evident when analysing the influence of shock waves on the vorticity $\boldsymbol{\omega}$. Many flows of practical interest involve only weak shocks. To this category belong, for example, all transonic and supersonic flows past thin aerofoils (see Part 2 of this book series). The fact is that, in these flows, the velocity vector jump $\Delta \mathbf{V}$ across a weak shock is small, $|\Delta \mathbf{V}| \ll 1$, but the entropy jump is even smaller. It may be estimated (see Problem 3 in Exercises 15) as $\Delta S \sim |\Delta \mathbf{V}|^3$. Therefore, according to (4.2.21), the vorticity $\boldsymbol{\omega}$ may be treated as zero to the leading-order approximation.

4.2.5 D'Alembert's paradox

D'Alembert's paradox, which states that in an inviscid steady flow a rigid body cannot produce drag, was discussed in Section 3.2.1 in application to a sphere, and then in Section 3.4.3 in application to a general two-dimensional incompressible flow. Now our task will be to extend this result to include compressible flows. We shall deal here with three-dimensional flow of a perfect gas. Let us assume that a rigid body with surface S is placed into a uniform flow with free-stream velocity vector \mathbf{V}_∞ , pressure p_∞ , and density ρ_∞ ; see Figure 4.6(a).

Assuming that the flow is steady, we can write the governing Euler equations (4.1.2) in the form

$$\left. \begin{aligned} \rho(\mathbf{V} \cdot \nabla)\mathbf{V} &= \rho \mathbf{f} - \nabla p, & \rho(\mathbf{V} \cdot \nabla h) &= \mathbf{V} \cdot \nabla p, \\ \operatorname{div}(\rho \mathbf{V}) &= 0, & h &= \frac{\gamma}{\gamma - 1} \frac{p}{\rho}. \end{aligned} \right\} \quad (4.2.22)$$

They hold everywhere outside the body surface S , and should be solved subject to the impermeability condition

$$(\mathbf{V} \cdot \mathbf{n})\Big|_S = 0 \quad (4.2.23)$$

and the free-stream conditions

$$\left. \begin{aligned} \mathbf{V} &\rightarrow \mathbf{V}_\infty, \\ p &\rightarrow p_\infty, \\ \rho &\rightarrow \rho_\infty \end{aligned} \right\} \text{ as } |\mathbf{r}| \rightarrow \infty. \quad (4.2.24)$$

Let us assume that the solution of the boundary-value problem (4.2.22)–(4.2.24) has been found, such that the velocity vector \mathbf{V} , pressure p , density ρ , and enthalpy h are known throughout the flow field and, in particular, on the body surface. Then the resultant force acting upon the body may be calculated as

$$\mathbf{R} = - \iint_S p \mathbf{n} \, ds. \quad (4.2.25)$$

We shall now place the same body in the reversed flow; see Figure 4.6(b). In this case, the governing equations (4.2.22) and the impermeability condition (4.2.23) will remain unchanged. We only need to reformulate the free-stream conditions, which now assume the form

$$\left. \begin{aligned} \mathbf{V} &\rightarrow \check{\mathbf{V}}_\infty, \\ p &\rightarrow p_\infty, \\ \rho &\rightarrow \rho_\infty \end{aligned} \right\} \text{ as } |\mathbf{r}| \rightarrow \infty, \quad (4.2.26)$$

where $\check{\mathbf{V}}_\infty = -\mathbf{V}_\infty$.

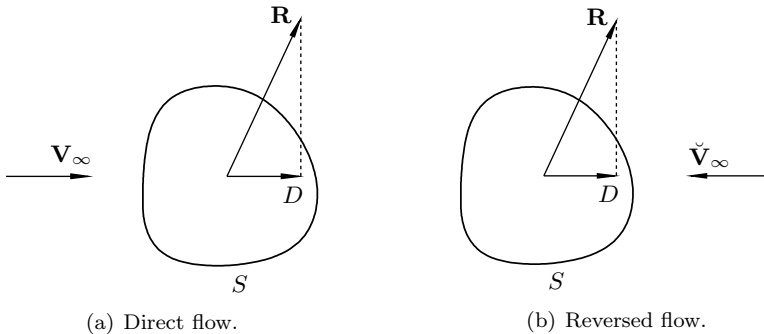


Fig. 4.6: Direct and reversed flows past a rigid body.

Of course, finding the solution of the boundary-value problem (4.2.22), (4.2.23), (4.2.26) for an arbitrary body shape is an impossible task. However, with a known solution \mathbf{V} , p , ρ , h for the direct flow, the velocity field $\check{\mathbf{V}}$, pressure \check{p} , density $\check{\rho}$, and enthalpy \check{h} in the reversed flow may easily be calculated by setting

$$\check{\mathbf{V}} = -\mathbf{V}, \quad \check{p} = p, \quad \check{\rho} = \rho, \quad \check{h} = h. \quad (4.2.27)$$

Indeed, taking into account that \mathbf{V} , p , ρ , and h satisfy equations (4.2.22)–(4.2.24), one can easily verify by direct substitution of (4.2.27) into equations (4.2.22), (4.2.23), and (4.2.26) that the latter reduce to identities.

The resultant force acting upon the body in the reversed flow is calculated as

$$\check{\mathbf{R}} = - \iint_S \check{p} \mathbf{n} \, ds = - \iint_S p \mathbf{n} \, ds,$$

and proves to coincide with the resultant force (4.2.25) in the direct flow. The drag D is the projection of the resultant force on the free-stream direction (see Figure 4.6). Hence, if, in the direct flow, the body drag is non-zero, presumed positive, then, in the reversed flow, it has to be negative. The latter, however, is impossible, since it would mean that each time when a body produces a drag, one could turn it over, and the body would be able to accelerate itself without consuming any energy. We have to conclude once again that the flow calculations based on the inviscid theory are bound to result in zero drag.

Exercises 13

- Using formula (4.1.17), demonstrate that for the pressure perturbations p' to be small compared with the initial pressure p_0 , the following condition should hold:

$$\dot{x}_w \ll a.$$

- Modify the analysis of pressure perturbations in Section 4.1.2 assuming this time that the cylinder has an end plate AA' situated at $x = x_0$ as shown in Figure 4.7.

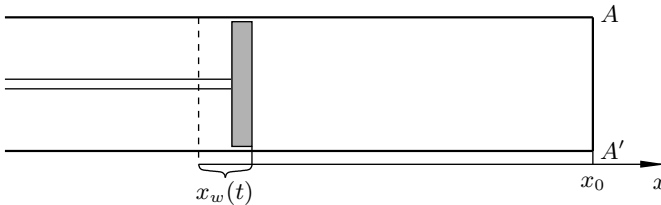


Fig. 4.7: A cylinder with a closed end.

- Argue that the solution (4.1.17) remains valid everywhere between the piston and the closing plate AA' during the time interval $t \in (0, x_0/a)$. Here $t = 0$ is the time when the piston starts to move. What is the significance of time $t = x_0/a$?

- (b) Notice that, after the perturbations start to reflect from the end plate AA' , the solution should be written as

$$p'(t, x) = a\rho_0\dot{x}_w\left(t - \frac{x}{a}\right) + g(x + at).$$

Find the function $g(x + at)$ by imposing the impermeability condition

$$v' = 0 \quad \text{at} \quad x = x_0$$

on the surface of the end plate AA' .

- (c) Show that the reflected wave increases the pressure on AA' twofold.
3. Consider an unsteady flow of a perfect gas in a region \mathcal{D} . Assume that
- (a) the flow is potential, i.e. $\mathbf{V} = \nabla\varphi$;
 - (b) the body force \mathbf{f} is also potential, i.e. $\mathbf{f} = -\nabla U$;
 - (c) all the fluid particles in region \mathcal{D} originate from a region \mathcal{D}_0 where $p = p_\infty$ and $\rho = \rho_\infty$, and the fluid particles do not cross shock waves as they travel from region \mathcal{D}_0 to region \mathcal{D} .

Show that, under these conditions, the *Cauchy-Lagrange integral*

$$\frac{\partial\varphi}{\partial t} + \frac{V^2}{2} + h + U = \mathcal{F}(t) \tag{4.2.28}$$

holds in region \mathcal{D} , where $\mathcal{F}(t)$ is a function of time t only.

Hint: Notice that, under conditions (a) and (b), the momentum equation (4.1.2a) may be written as

$$\nabla\left(\frac{\partial\varphi}{\partial t} + \frac{V^2}{2} + U\right) = -\frac{1}{\rho}\nabla p.$$

Then argue that, under condition (c), equation (4.2.16) may be used.

4. Consider a wind tunnel whose cross-sectional area A is known as a function of the longitudinal coordinate x , as shown in Figure 4.8. The flow in the tunnel is steady and may be assumed to be one-dimensional, i.e. the velocity vector has only one component, $\mathbf{V} = (u, 0, 0)$, and the fluid-dynamic functions u , p , and ρ depend on x only.

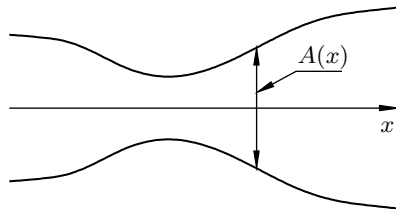


Fig. 4.8: Wind tunnel with a throat shaped in the form of a *Laval nozzle*.

Using the mass conservation law

$$\rho u A = \text{const}, \quad (4.2.29)$$

the Bernoulli equation

$$\frac{\gamma}{\gamma - 1} \frac{p}{\rho} + \frac{u^2}{2} = \text{const}, \quad (4.2.30)$$

and the entropy conservation law

$$\frac{p}{\rho^\gamma} = \text{const}, \quad (4.2.31)$$

deduce the following equation for the rate of change of the velocity along the tunnel:

$$\frac{1}{u} \frac{du}{dx} = \frac{1}{M^2 - 1} \frac{1}{A} \frac{dA}{dx}.$$

Here M is the local value of the Mach number.

Explain why the tunnel should be shaped as shown in Figure 4.8 to enable the flow to accelerate the flow from a subsonic to a supersonic speed?

5. Before entering a supersonic wind tunnel (see Figure 4.9), a gas is accumulated in a gas holder. Given that the speed of sound in the gas holder is a_0 , find
- the gas velocity V_* in the wind tunnel throat OO' , where the local Mach number $M = 1$;
 - the maximum possible gas speed that may be achieved by accelerating the flow to infinite Mach number. What happens with the gas temperature in this acceleration?

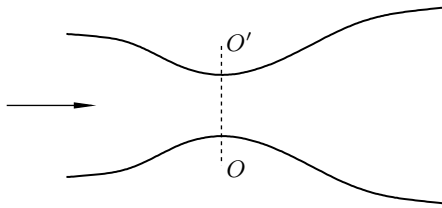


Fig. 4.9: Supersonic wind tunnel.

Suggestion: You may assume that the flow in the wind tunnel is one-dimensional.

6. Using the Bernoulli equation (4.2.30), prove that, along any streamline,

$$u \left(1 + \frac{2}{(\gamma - 1)M^2} \right)^{1/2} = \text{const}, \quad a \left(1 + \frac{\gamma - 1}{2} M^2 \right)^{1/2} = \text{const},$$

$$T \left(1 + \frac{\gamma - 1}{2} M^2 \right) = \text{const}.$$

Using further the entropy conservation law (4.2.31), prove that the following equa-

tions hold along streamlines:

$$\left[1 + \frac{1}{2}(\gamma - 1)M^2\right]^{\gamma/(\gamma-1)} p = \text{const}, \quad \left[1 + \frac{1}{2}(\gamma - 1)M^2\right]^{1/(\gamma-1)} \rho = \text{const}.$$

Consider now a wind tunnel. Assuming the flow in the wind tunnel to be one-dimensional, make use of the mass conservation law (4.2.29) and show that Mach number is related to the cross-sectional area A as

$$\frac{M}{\left[1 + \frac{1}{2}(\gamma - 1)M^2\right]^{\frac{1}{2}(\gamma+1)/(\gamma-1)}} A = \text{const}.$$

4.3 Steady Potential Flows

As was shown in Section 3.2, potential flows of incompressible fluids are governed by Laplace's equation (3.2.7) for the velocity potential φ . We shall now formulate an equivalent version of this equation for compressible flows. In order to simplify the analysis, we shall assume that the flow considered is steady and that there is no body force acting on the fluid, i.e. $\mathbf{f} = 0$. Then the Euler equations (4.1.2) may be written as

$$\boldsymbol{\omega} \times \mathbf{V} + \nabla \left(\frac{V^2}{2} \right) = -\frac{1}{\rho} \nabla p \quad (\text{momentum equation}), \quad (4.3.1a)$$

$$\rho (\mathbf{V} \cdot \nabla h) = \mathbf{V} \cdot \nabla p \quad (\text{energy equation}), \quad (4.3.1b)$$

$$\rho \operatorname{div} \mathbf{V} + \mathbf{V} \cdot \nabla \rho = 0 \quad (\text{continuity equation}), \quad (4.3.1c)$$

$$h = \frac{\gamma}{\gamma - 1} \frac{p}{\rho} \quad (\text{state equation}). \quad (4.3.1d)$$

Let us try to derive a single equation for the velocity \mathbf{V} by eliminating from equations (4.3.1) all other quantities. Substitution of the state equation (4.3.1d) into the energy equation (4.3.1b) yields

$$\rho \mathbf{V} \cdot \left(\frac{\gamma}{\gamma - 1} \frac{\nabla p}{\rho} - \frac{\gamma}{\gamma - 1} \frac{p}{\rho^2} \nabla \rho \right) = \mathbf{V} \cdot \nabla p,$$

which may easily be simplified to show that the gradient of the density, $\nabla \rho$, is related to the pressure gradient ∇p as

$$\gamma \frac{p}{\rho} (\mathbf{V} \cdot \nabla \rho) = \mathbf{V} \cdot \nabla p. \quad (4.3.2)$$

Combining equations (4.1.12) and (4.3.1d), we see that

$$\gamma \frac{p}{\rho} = (\gamma - 1)h = a^2, \quad (4.3.3)$$

where a is the local value of the speed of sound. Using (4.3.3) in (4.3.2), we find

$$\mathbf{V} \cdot \nabla \rho = \frac{1}{a^2} (\mathbf{V} \cdot \nabla p).$$

This equation allows us to eliminate the density gradient $\nabla\rho$ from the continuity equation (4.3.1c), leading to

$$a^2\rho\operatorname{div}\mathbf{V} + \mathbf{V} \cdot \nabla p = 0. \quad (4.3.4)$$

It remains to eliminate the pressure gradient ∇p from (4.3.4). For this purpose, we multiply the momentum equation (4.3.1a) by the velocity vector \mathbf{V} . We have

$$\mathbf{V} \cdot \nabla \left(\frac{V^2}{2} \right) = -\frac{1}{\rho} (\mathbf{V} \cdot \nabla p). \quad (4.3.5)$$

Comparing (4.3.5) with (4.3.4), we see that the sought equation for \mathbf{V} has the form

$$\mathbf{V} \cdot \nabla \left(\frac{V^2}{2} \right) = a^2 \operatorname{div}\mathbf{V}. \quad (4.3.6)$$

If the Mach number is small everywhere in the flow field, i.e. $V \ll a$, then equation (4.3.6) reduces to

$$\operatorname{div}\mathbf{V} = 0, \quad (4.3.7)$$

i.e. this is the same as the incompressible continuity equation (1.7.1). If, further, the flow is potential,

$$\mathbf{V} = \nabla\varphi, \quad (4.3.8)$$

then to describe the fluid motion, one needs to solve Laplace's equation

$$\nabla^2\varphi = 0,$$

which is obtained by substituting (4.3.8) into (4.3.7).

If, on the other hand, the gas velocity V is comparable to the speed of sound, a , then one has to deal with the entire equation (4.3.6). When solving this equation one needs to calculate the local value of the speed of sound, a , at each point in the flow. For this purpose, one uses the Bernoulli equation

$$\frac{a^2}{\gamma - 1} + \frac{V^2}{2} = \frac{a_\infty^2}{\gamma - 1} + \frac{V_\infty^2}{2}. \quad (4.3.9)$$

This form of the Bernoulli equation is obtained by substituting (4.3.3) into (4.2.11).

4.3.1 Two-dimensional flows

In the two-dimensional case, when the velocity vector is composed of two components $\mathbf{V} = (u, v)$, equation (4.3.6) is written as

$$u \frac{\partial}{\partial x} \left(\frac{u^2 + v^2}{2} \right) + v \frac{\partial}{\partial y} \left(\frac{u^2 + v^2}{2} \right) = a^2 \left(\frac{\partial u}{\partial x} + \frac{\partial v}{\partial y} \right),$$

and, after simple manipulations, it may be reduced to the form

$$(a^2 - u^2) \frac{\partial u}{\partial x} + (a^2 - v^2) \frac{\partial v}{\partial y} = uv \left(\frac{\partial v}{\partial x} + \frac{\partial u}{\partial y} \right). \quad (4.3.10)$$

If the flow is potential, then equation (4.3.8) may be used. Alternatively, we can state that the vorticity ω is zero. For two-dimensional flows, this condition is written as

$$\frac{\partial v}{\partial x} - \frac{\partial u}{\partial y} = 0. \quad (4.3.11)$$

In order to close the set of equations (4.3.10), (4.3.11), we finally need to use equation (4.3.9):

$$a^2 = a_\infty^2 + \frac{\gamma - 1}{2} [V_\infty^2 - (u^2 + v^2)]. \quad (4.3.12)$$

4.4 The Theory of Characteristics

Equations (4.3.10) and (4.3.11) represent a particular form of the quasi-linear set of partial differential equations

$$\left. \begin{aligned} a_{11} \frac{\partial u}{\partial x} + a_{12} \frac{\partial u}{\partial y} + b_{11} \frac{\partial v}{\partial x} + b_{12} \frac{\partial v}{\partial y} &= c_1, \\ a_{21} \frac{\partial u}{\partial x} + a_{22} \frac{\partial u}{\partial y} + b_{21} \frac{\partial v}{\partial x} + b_{22} \frac{\partial v}{\partial y} &= c_2, \end{aligned} \right\} \quad (4.4.1)$$

where the coefficients a_{ij} , b_{ij} , and c_i are function of x , y , u , and v .

We shall pose the following initial-value problem for (4.4.1). Let \mathcal{L} be a line in the (x, y) -plane given by the equation $y = y(x)$. We shall assume that along this line distributions of u and v are known, say, in the form of functions $u = \tilde{u}(x)$ and $v = \tilde{v}(x)$. Using these functions as initial data, our purpose will be to construct the solution $u(x, y)$, $v(x, y)$ of equations (4.4.1) in some neighbourhood of \mathcal{L} . This problem may be also formulated in the four-dimensional space (x, y, u, v) , where the initial conditions are represented by a line $\underline{\mathcal{L}}$, whose shape is defined by functions $y = y(x)$, $u = \tilde{u}(x)$, and $v = \tilde{v}(x)$. The task of finding the solution of equations (4.4.1) is equivalent to constructing an integral surface $\underline{\mathcal{S}}$ in the (x, y, u, v) -space passing through $\underline{\mathcal{L}}$.

Returning to the physical space (x, y) , we note that in order to extend the solution a small distance from the initial line \mathcal{L} , one needs to find the derivatives $\partial u/\partial x$, $\partial u/\partial y$, $\partial v/\partial x$, and $\partial v/\partial y$ at each point on \mathcal{L} . The functions $\tilde{u}(x)$, $\tilde{v}(x)$, representing the initial conditions, are related to the sought solution $u(x, y)$, $v(x, y)$ by the equations

$$\tilde{u}(x) = u[x, y(x)], \quad \tilde{v}(x) = v[x, y(x)]. \quad (4.4.2)$$

Differentiating (4.4.2), we have

$$\frac{d\tilde{u}}{dx} = \frac{\partial u}{\partial x} + \chi \frac{\partial u}{\partial y}, \quad \frac{d\tilde{v}}{dx} = \frac{\partial v}{\partial x} + \chi \frac{\partial v}{\partial y}, \quad (4.4.3)$$

where χ is the slope of line \mathcal{L} ,

$$\chi = \frac{dy}{dx}. \quad (4.4.4)$$

With equations (4.4.1) considered on line \mathcal{L} , we can use (4.4.3) to eliminate $\partial u/\partial x$

and $\partial v/\partial x$ in (4.4.1), leading to

$$\left. \begin{aligned} (a_{12} - \chi a_{11}) \frac{\partial u}{\partial y} + (b_{12} - \chi b_{11}) \frac{\partial v}{\partial y} &= c_1 - a_{11} \frac{d\tilde{u}}{dx} - b_{11} \frac{d\tilde{v}}{dx}, \\ (a_{22} - \chi a_{21}) \frac{\partial u}{\partial y} + (b_{22} - \chi b_{21}) \frac{\partial v}{\partial y} &= c_2 - a_{21} \frac{d\tilde{u}}{dx} - b_{21} \frac{d\tilde{v}}{dx}. \end{aligned} \right\} \quad (4.4.5)$$

The right-hand sides of equations (4.4.5) are known on \mathcal{L} , as are the coefficients of $\partial u/\partial y$ and $\partial v/\partial y$ on the left-hand sides. We need to find out if these equations can be resolved for $\partial u/\partial y$ and $\partial v/\partial y$. To answer this question, one has to consider the determinant of the matrix composed of the coefficient on the left-hand side of (4.4.5):

$$\Delta = \begin{vmatrix} a_{12} - \chi a_{11} & b_{12} - \chi b_{11} \\ a_{22} - \chi a_{21} & b_{22} - \chi b_{21} \end{vmatrix} = A\chi^2 + 2B\chi + C, \quad (4.4.6)$$

where

$$A = \begin{vmatrix} a_{11} & b_{11} \\ a_{21} & b_{21} \end{vmatrix}, \quad 2B = \begin{vmatrix} b_{11} & a_{12} \\ b_{21} & a_{22} \end{vmatrix} + \begin{vmatrix} b_{12} & a_{11} \\ b_{22} & a_{21} \end{vmatrix}, \quad C = \begin{vmatrix} a_{12} & b_{12} \\ a_{22} & b_{22} \end{vmatrix}.$$

If $\Delta \neq 0$, then the solution of equations (4.4.5) exists and is unique. With the condition $\Delta \neq 0$ holding everywhere along the initial line \mathcal{L} , one can calculate $\partial u/\partial y$ and $\partial v/\partial y$ at each point on \mathcal{L} . Then, using (4.4.3), $\partial u/\partial x$ and $\partial v/\partial x$ may also be found, and the solution of equations (4.4.1) may be extended into a small neighbourhood of the initial line \mathcal{L} . Choosing a neighbouring line \mathcal{L}' , one can repeat the above procedure and extend the solution further.

If, on the other hand,

$$\Delta = 0, \quad (4.4.7)$$

then, for a solution of (4.4.5) to exist, the initial functions $u = \tilde{u}(x)$ and $v = \tilde{v}(x)$ should satisfy a compatibility condition. In order to formulate this condition, one has to analyse the determinant of the matrix that is obtained by substituting the first column in (4.4.6) by the right-hand side of (4.4.5), i.e.³

$$\Delta_u = \begin{vmatrix} c_1 - a_{11} \frac{d\tilde{u}}{dx} - b_{11} \frac{d\tilde{v}}{dx} & b_{12} - \chi b_{11} \\ c_2 - a_{21} \frac{d\tilde{u}}{dx} - b_{21} \frac{d\tilde{v}}{dx} & b_{22} - \chi b_{21} \end{vmatrix} = (A\chi + E) \frac{d\tilde{u}}{dx} + D \frac{d\tilde{v}}{dx} + M + \chi N,$$

³Remember that, according to Cramer's rule, the solution of (4.4.5) may be written as

$$\frac{\partial u}{\partial y} = \frac{\Delta_u}{\Delta}, \quad \frac{\partial v}{\partial y} = \frac{\Delta_v}{\Delta}.$$

where Δ_v is obtained by substituting the second column in (4.4.6) by the right-hand side of (4.4.5),

$$\Delta_v = \begin{vmatrix} a_{12} - \chi a_{11} & c_1 - a_{11} \frac{d\tilde{u}}{dx} - b_{11} \frac{d\tilde{v}}{dx} \\ a_{22} - \chi a_{21} & c_2 - a_{21} \frac{d\tilde{u}}{dx} - b_{21} \frac{d\tilde{v}}{dx} \end{vmatrix}.$$

where

$$E = \begin{vmatrix} b_{12} & a_{11} \\ b_{22} & a_{21} \end{vmatrix}, \quad D = \begin{vmatrix} b_{12} & b_{11} \\ b_{22} & b_{21} \end{vmatrix}, \quad M = \begin{vmatrix} c_1 & b_{12} \\ c_2 & b_{22} \end{vmatrix}, \quad N = \begin{vmatrix} b_{11} & c_1 \\ b_{21} & c_2 \end{vmatrix}.$$

Under condition (4.4.7), which may be written as

$$A\chi^2 + 2B\chi + C = 0, \tag{4.4.8}$$

for a solution to exist, Δ_u should also be zero:⁴

$$(A\chi + E)\frac{d\tilde{u}}{dx} + D\frac{d\tilde{v}}{dx} + M + \chi N = 0. \tag{4.4.9}$$

In this case, equations (4.4.5) admit an infinite number of solutions; i.e., through the initial line $\underline{\mathcal{L}}$ in the four-dimensional space (x, y, u, v) , one can draw an infinite number of integral surfaces $\underline{\mathcal{S}}$.

Depending on the existence of real solutions of the quadratic equation (4.4.8), sets of partial differential equations (4.4.1) are classified as follows.

Definition 4.1 *If the coefficients of equations (4.4.1) are such that $B^2 - AC < 0$, then the set of equations (4.4.1) is called **elliptic**. If, on the other hand, $B^2 - AC > 0$, then it is called **hyperbolic**.*

No real solutions of equation (4.4.8) exist if equations (4.4.1) are elliptic, and there are two solutions

$$\chi_{1,2} = \frac{-B \pm \sqrt{B^2 - AC}}{A} \tag{4.4.10}$$

if they are hyperbolic. In the latter case, characteristics may be introduced according to the following definition.

Definition 4.2 *The line $\mathcal{L}^{(c)}$ whose slope $dy/dx = \chi$ at each point on $\mathcal{L}^{(c)}$ coincides with one of the solutions (4.4.10) of equation (4.4.8) is called a **characteristic** of the set of equations (4.4.1).*

The above discussion suggests that if the set of equations (4.4.1) is hyperbolic, then to ensure that the initial-value problem for (4.4.1) is well-posed, one has to choose the initial line \mathcal{L} in the (x, y) -plane in such a way that at no point on \mathcal{L} will its slope χ coincide with the slope (4.4.10) of a characteristic. This guarantees that $\Delta \neq 0$ on \mathcal{L} , and therefore a unique solution of (4.4.1) may be constructed at least in a small neighbourhood of \mathcal{L} .

Let us now suppose that the solution has been constructed in a region \mathcal{D} in the (x, y) -plane, and distributions of $u(x, y)$ and $v(x, y)$ over \mathcal{D} are therefore known. Using this solution, one can calculate the coefficients a_{ij} , b_{ij} , and c_i in equations (4.4.1) and then find distributions of the functions $\chi_1(x, y)$ and $\chi_2(x, y)$ in \mathcal{D} . With $\chi_1(x, y)$ and

⁴Note that if $\Delta = \Delta_u = 0$, then owing to the proportionality of the columns in Δ and Δ_u , the determinant Δ_v automatically turns out to be zero.

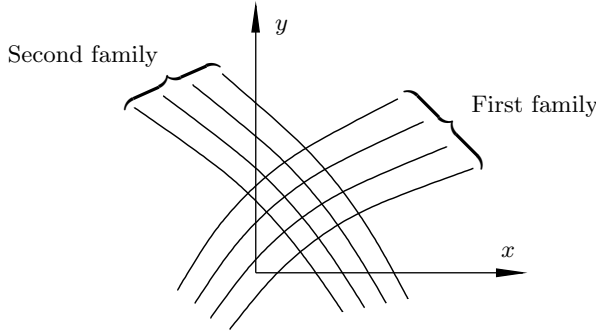


Fig. 4.10: Characteristics.

$\chi_2(x, y)$ known, one can draw through any point in \mathcal{D} two characteristics by integrating the equations

$$\frac{dy}{dx} = \chi_1, \quad \frac{dy}{dx} = \chi_2.$$

Considered together, they form two families of characteristics as shown in Figure 4.10.

Along each characteristic, $\Delta = 0$, and, since the characteristics have been constructed based on an existing solution, we can claim that Δ_u should also be zero. If, for example, we consider a characteristic of the first family, for which

$$\frac{dy}{dx} = \chi_1, \tag{4.4.11}$$

then, using χ_1 instead of χ in (4.4.9), we can write

$$(A\chi_1 + E)\frac{du}{dx} + D\frac{dv}{dx} + M + \chi_1 N = 0. \tag{4.4.12}$$

Here, instead of ‘initial functions’ \tilde{u} , \tilde{v} , we use functions u , v representing a solution of equations (4.4.1).

Equations (4.4.11) and (4.4.12) may be further written in the form

$$dy = \chi_1 dx, \tag{4.4.13a}$$

$$(A\chi_1 + E) du + D dv + M dx + N dy = 0. \tag{4.4.13b}$$

Similarly, for the characteristics of the second family, we have

$$dy = \chi_2 dx, \tag{4.4.14a}$$

$$(A\chi_2 + E) du + D dv + M dx + N dy = 0. \tag{4.4.14b}$$

If one thinks of a solution of equations (4.4.1) as being represented by a surface $\underline{\mathcal{S}}$ in the four-dimensional (x, y, u, v) -space, then through any point on this surface two characteristics may be drawn. Equations (4.4.13a) and (4.4.14a) represent their projections onto the physical (x, y) -plane. The projections onto the *hodograph* (u, v) -plane are given by equations (4.4.13b) and (4.4.14b), which, on integration, give the so-called *Riemann invariants* of the equations (4.4.1).

It should be noted that functions u and v do not remain independent when considered on a characteristic. Instead, they vary according to equations (4.4.13b) and (4.4.14b). This, first, confirms that if the initial line \mathcal{L} coincides with one of the characteristics, then the initial-value problem for equations (4.4.1) cannot be solved, at least for arbitrary initial functions $u = \tilde{u}(x)$ and $v = \tilde{v}(x)$. Second, it shows that the characteristics may be thought of as channels through which the information propagates in hyperbolic systems. To clarify this latter point, we shall now give a short description of the *method of characteristics*, one of the numerical techniques that may be used to calculate solutions to hyperbolic equations.

4.4.1 The method of characteristics

Suppose that the solution of equations (4.4.1) has to be found to the right of the initial line \mathcal{L} (see Figure 4.11). Suppose further that the initial conditions for u and v are given on an interval $[A, B]$ on this line. Then, in order to use the method of characteristics, one has to divide $[A, B]$ into N small subintervals

$$[M_{i-1}, M_i], \quad i = 1, \dots, N, \tag{4.4.15}$$

where M_0 is assumed to coincide with point A and M_N with point B .

Let us consider one of these subintervals, $[M_{i-1}, M_i]$. Using equations (4.4.13a) and (4.4.14a), we can draw two characteristics from each end of the subinterval. For this purpose, χ_1 and χ_2 are calculated using the values of u and v at points M_i and M_{i-1} , respectively. Provided that the slope $\chi = dy/dx$ of line \mathcal{L} does not coincide with χ_1 or χ_2 , we will have four characteristics lying to the right of line \mathcal{L} as shown in Figure 4.11. Two of them intersect at point M'_i . We shall denote the coordinates of this point by (x'_i, y'_i) . To find the values u'_i and v'_i of the functions u and v at M'_i , equations (4.4.13b) and (4.4.14b) should be used. To be definite, we shall assume that $M_{i-1}M'_i$ is a characteristic of the first family. Then writing (4.4.13b) in finite-difference form, we will have

$$(A\chi_1 + E)(u'_i - u_{i-1}) + D(v'_i - v_{i-1}) + M(x'_i - x_{i-1}) + N(y'_i - y_{i-1}) = 0. \tag{4.4.16}$$

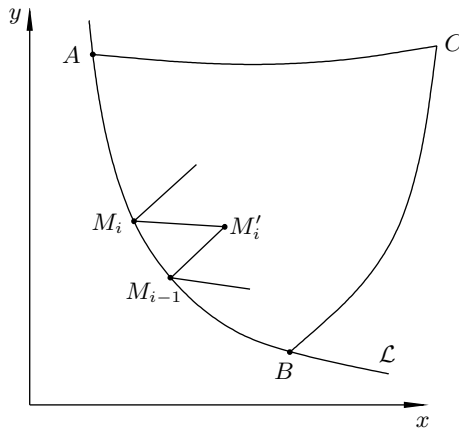


Fig. 4.11: The method of characteristics.

Here u_{i-1} and v_{i-1} are the values of u and v at point M_{i-1} and (x_{i-1}, y_{i-1}) are the coordinates of this point. Similarly, equation (4.4.14b) should be used on $M_i M'_i$. It gives

$$(A\chi_2 + E)(u'_i - u_i) + D(v'_i - v_i) + M(x'_i - x_i) + N(y'_i - y_i) = 0. \quad (4.4.17)$$

We have obtained two linear algebraic equations (4.4.16) and (4.4.17), which may easily be solved for u'_i and v'_i .

This procedure, being repeated for all subintervals (4.4.15), allows us to extend the solution one step into the triangular region ABC that is bounded by the characteristics AC and BC emerging from points A and B . The calculations may, of course, be continued until the solution is known in the entire region ABC .

4.4.2 Supersonic flows

Let us now return to the equations (4.3.10) and (4.3.11) governing two-dimensional steady potential gas flows. Comparing them with equations (4.4.1), we can see that

$$\begin{aligned} a_{11} &= a^2 - u^2, & a_{12} &= -uv, & b_{11} &= -uv, & b_{12} &= a^2 - v^2, & c_1 &= 0, \\ a_{21} &= 0, & a_{22} &= -1, & b_{21} &= 1, & b_{22} &= 0, & c_2 &= 0, \end{aligned}$$

and therefore

$$A = a^2 - u^2, \quad B = uv, \quad C = D = a^2 - v^2, \quad E = M = N = 0. \quad (4.4.18)$$

The type of the equations, i.e. elliptic or hyperbolic, is determined by the sign of $B^2 - AC$. Using (4.4.18), we find

$$\begin{aligned} B^2 - AC &= u^2 v^2 - (a^2 - u^2)(a^2 - v^2) \\ &= u^2 v^2 - a^4 + a^2 u^2 + a^2 v^2 - u^2 v^2 = a^2(u^2 + v^2) - a^4 = a^2(V^2 - a^2). \end{aligned}$$

Hence, equations (4.3.10) and (4.3.11) are elliptic if the flow is subsonic ($V < a$) and hyperbolic if it is supersonic ($V > a$). In the latter case, the characteristics may be introduced. Their slope in the (x, y) -plane is given by formula (4.4.10), which can now be written as

$$\chi_{1,2} = \frac{-uv \pm a\sqrt{V^2 - a^2}}{a^2 - u^2}. \quad (4.4.19)$$

With V being the velocity modulus and ϑ the angle made by the velocity vector with the x -axis, we can write (see Figure 4.12)

$$u = V \cos \vartheta, \quad v = V \sin \vartheta. \quad (4.4.20)$$

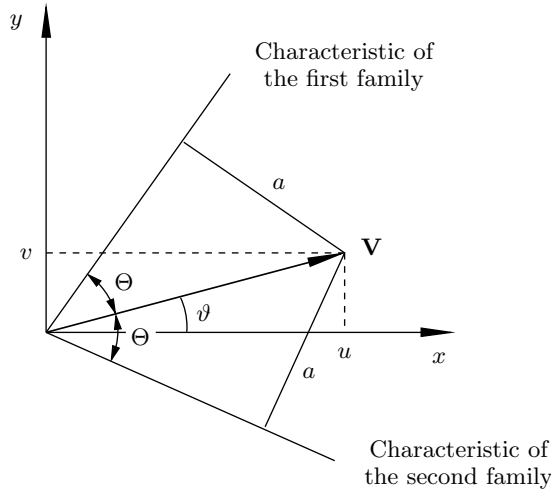


Fig. 4.12: Characteristics in the physical (x, y) -plane.

We can further see, by comparing Figure 4.12 with Figure 4.2, that

$$a = V \sin \Theta, \tag{4.4.21}$$

where Θ is the Mach angle. Substitution of (4.4.20) and (4.4.21) into (4.4.19) gives

$$\begin{aligned} \chi_{1,2} &= \frac{-V^2 \sin \vartheta \cos \vartheta \pm V^2 \sin \Theta \cos \Theta}{V^2 \sin^2 \Theta - V^2 \cos^2 \vartheta} = \frac{\sin \vartheta \cos \vartheta \mp \sin \Theta \cos \Theta}{\cos^2 \vartheta - \sin^2 \Theta} \\ &= \frac{\sin 2\vartheta \mp \sin 2\Theta}{\cos 2\vartheta + \cos 2\Theta} = \frac{\sin(\vartheta \mp \Theta) \cos(\vartheta \pm \Theta)}{\cos(\vartheta + \Theta) \cos(\vartheta - \Theta)} = \tan(\vartheta \mp \Theta). \end{aligned} \tag{4.4.22}$$

This proves that the projections of the characteristics onto the (x, y) -plane coincide with the Mach lines. The plus sign in $\tan(\vartheta \mp \Theta)$ is normally assigned to the characteristic of the first family, which is obtained by rotating the velocity vector in a counter-clockwise direction through an angle Θ , while the minus sign is assigned to the characteristic of the second family. Using this convention, we will write (4.4.19) as

$$\chi_{1,2} = \frac{-uv \mp a\sqrt{V^2 - a^2}}{a^2 - u^2}. \tag{4.4.23}$$

We shall now analyse the characteristics in the hodograph (u, v) -plane. Using (4.4.18) in equations (4.4.13b) and (4.4.14b), we find that, along a characteristic of either family,

$$(a^2 - u^2)\chi_{1,2} du + (a^2 - v^2) dv = 0. \tag{4.4.24}$$

Hence, the slope of the characteristic in the hodograph plane may be calculated as

$$\left. \frac{dv}{du} \right|_{1,2} = -\frac{a^2 - u^2}{a^2 - v^2} \chi_{1,2}. \tag{4.4.25}$$

Substitution of (4.4.23) into (4.4.25) yields

$$\left. \frac{dv}{du} \right|_{1,2} = \frac{uv \pm a\sqrt{V^2 - a^2}}{a^2 - v^2}. \quad (4.4.26)$$

Multiplying the numerator and denominator by $uv \mp a\sqrt{V^2 - a^2}$, we have

$$\begin{aligned} \left. \frac{dv}{du} \right|_{1,2} &= \frac{u^2v^2 - a^2V^2 + a^4}{(a^2 - v^2)(uv \mp a\sqrt{V^2 - a^2})} = \frac{u^2v^2 - a^2u^2 - a^2v^2 + a^4}{(a^2 - v^2)(uv \mp a\sqrt{V^2 - a^2})} \\ &= \frac{(u^2 - a^2)(v^2 - a^2)}{(a^2 - v^2)(uv \mp a\sqrt{V^2 - a^2})} = -\frac{a^2 - u^2}{-uv \pm a\sqrt{V^2 - a^2}}. \end{aligned} \quad (4.4.27)$$

Comparing (4.4.27) with (4.4.23), we can easily see that

$$\left. \frac{dv}{du} \right|_{1,2} = -\frac{1}{\chi_{2,1}}.$$

This proves that if two characteristics are drawn through a point on the surface \underline{S} representing the solution in the (x, y, u, v) -space, then the projection of the characteristic of the first family onto the hodograph (u, v) -plane appears to be perpendicular to the projection of the characteristic of the second family onto the physical (x, y) -plane, and vice versa.

Let us now return to equation (4.4.26) and write it in the form

$$(uv \pm a\sqrt{V^2 - a^2}) du = (a^2 - v^2) dv. \quad (4.4.28)$$

If we use for the velocity components u and v formulae (4.4.20), then their variations du and dv may be expressed as

$$du = -V \sin \vartheta d\vartheta + \cos \vartheta dV, \quad dv = V \cos \vartheta d\vartheta + \sin \vartheta dV. \quad (4.4.29)$$

Substitution of (4.4.20) and (4.4.29) into (4.4.28) yields

$$-aV(a \cos \vartheta \pm \sqrt{V^2 - a^2} \sin \vartheta) d\vartheta \pm \sqrt{V^2 - a^2}(a \cos \vartheta \pm \sqrt{V^2 - a^2} \sin \vartheta) dV = 0,$$

or, equivalently,

$$(a \cos \vartheta \pm \sqrt{V^2 - a^2} \sin \vartheta)(aV d\vartheta \mp \sqrt{V^2 - a^2} dV) = 0. \quad (4.4.30)$$

The first multiplier in this equation is not zero unless the angle ϑ made by the velocity vector \mathbf{V} with the x -axis is such that

$$\tan \vartheta = \mp \frac{a}{\sqrt{V^2 - a^2}} = \mp \frac{1}{\sqrt{M^2 - 1}},$$

which may easily be avoided by simple rotation of the coordinate system. Consequently, to study the variations of the velocity modulus V and its directional angle ϑ along the

characteristics, one has to set to zero the second multiplier in (4.4.30):

$$aV d\vartheta \mp \sqrt{V^2 - a^2} dV = 0.$$

We have

$$d\vartheta \mp \sqrt{M^2 - 1} \frac{dV}{V} = 0. \tag{4.4.31}$$

Here, as usual, the upper sign corresponds to the first family of characteristics and the lower to the second.

In order to integrate equation (4.4.31), one needs to find a relationship between the velocity V and the local Mach number M . For this purpose, the Bernoulli equation (4.3.9) is used:

$$\frac{a^2}{\gamma - 1} + \frac{V^2}{2} = \frac{a_\infty^2}{\gamma - 1} + \frac{V_\infty^2}{2}. \tag{4.4.32}$$

It may be rewritten in the form

$$\frac{V^2}{2} \left[1 + \frac{2}{(\gamma - 1)M^2} \right] = \frac{a_\infty^2}{\gamma - 1} + \frac{V_\infty^2}{2}. \tag{4.4.33}$$

Taking the logarithm of both sides of (4.4.33) and differentiating the resulting equation, we find

$$\frac{dV}{V} = \frac{1}{1 + \frac{1}{2}(\gamma - 1)M^2} \frac{dM}{M},$$

which, on substitution into (4.4.31), yields

$$d\vartheta \mp \frac{\sqrt{M^2 - 1}}{1 + \frac{1}{2}(\gamma - 1)M^2} \frac{dM}{M} = 0. \tag{4.4.34}$$

Integration of (4.4.34) leads to

$$\vartheta \mp \nu(M) = \text{const}, \tag{4.4.35}$$

where

$$\nu(M) = \sqrt{\frac{\gamma + 1}{\gamma - 1}} \arctan\left(\sqrt{\frac{\gamma - 1}{\gamma + 1}(M^2 - 1)}\right) - \arctan(\sqrt{M^2 - 1}) \tag{4.4.36}$$

is referred to as the *Prandtl–Meyer function*. Equation (4.4.35) holds along each characteristic in a supersonic flow, provided that the flow considered is potential. In the general case the constant of integration on the right hand side of (4.4.35) is different for different characteristics.

An alternative way to integrate equation (4.4.31) is to use the so-called *normalised velocity*

$$\lambda = \frac{V}{V_*}, \quad (4.4.37)$$

which is obtained by referring the velocity modulus V to the *critical velocity* V_* . The latter is defined as the velocity at a point in the flow field where the fluid speed coincides with the speed of sound. For this point, the Bernoulli equation (4.4.32) gives

$$\frac{V_*^2}{\gamma - 1} + \frac{V_*^2}{2} = \frac{a_\infty^2}{\gamma - 1} + \frac{V_\infty^2}{2}. \quad (4.4.38)$$

Of course, such a point might not physically exist in a particular flow considered. Still the Bernoulli equation (4.4.38) can be always used to formally define V_* .

Combining (4.4.38) with (4.4.33), we have

$$V^2 \left[\frac{1}{(\gamma - 1)M^2} + \frac{1}{2} \right] = \frac{V_*^2}{\gamma - 1} + \frac{V_*^2}{2} = \frac{\gamma + 1}{2(\gamma - 1)} V_*^2,$$

and we see that the normalised velocity λ is related to the Mach number M by

$$\left[\frac{1}{(\gamma - 1)M^2} + \frac{1}{2} \right] \lambda^2 = \frac{\gamma + 1}{2(\gamma - 1)}, \quad (4.4.39)$$

or

$$\lambda^2 = \frac{(\gamma + 1)M^2}{2 + (\gamma - 1)M^2}. \quad (4.4.40)$$

In subsonic flows ($M < 1$), the normalised velocity λ remains less than unity, while the supersonic speed range, $M \in (1, \infty)$, corresponds to

$$\lambda \in \left[1, \sqrt{\frac{\gamma + 1}{\gamma - 1}} \right].$$

We shall now return to equation (4.4.31) and write it in terms of the normalised velocity λ :

$$d\theta \mp \sqrt{M^2 - 1} \frac{d\lambda}{\lambda} = 0. \quad (4.4.41)$$

When integrating this equation, one can use the formula

$$M^2 - 1 = \frac{\lambda^2 - 1}{1 - \frac{\gamma - 1}{\gamma + 1} \lambda^2} \quad (4.4.42)$$

relating the Mach number M to λ ; it is easily deduced by solving equation (4.4.38) for M^2 .

Let λ_0 and ϑ_0 be the values of the normalised velocity λ and directional angle ϑ at an ‘initial point’ on a characteristic of either the first or the second family. Then, integrating equation (4.4.41), we have

$$\vartheta - \vartheta_0 \mp \int_{\lambda_0}^{\lambda} \sqrt{\frac{\lambda^2 - 1}{1 - \frac{\gamma-1}{\gamma+1}\lambda^2}} \frac{d\lambda}{\lambda} = 0,$$

or, equivalently,

$$\vartheta - \vartheta_0 \mp \left(\int_1^{\lambda} \sqrt{\frac{\lambda^2 - 1}{1 - \frac{\gamma-1}{\gamma+1}\lambda^2}} \frac{d\lambda}{\lambda} - \int_1^{\lambda_0} \sqrt{\frac{\lambda^2 - 1}{1 - \frac{\gamma-1}{\gamma+1}\lambda^2}} \frac{d\lambda}{\lambda} \right) = 0.$$

This proves that the following equation holds along any of the characteristics:

$$\vartheta \mp \sigma(\lambda) = \vartheta_0 \mp \sigma(\lambda_0), \tag{4.4.43}$$

where

$$\begin{aligned} \sigma(\lambda) &= \int_1^{\lambda} \sqrt{\frac{\lambda^2 - 1}{1 - \frac{\gamma-1}{\gamma+1}\lambda^2}} \frac{d\lambda}{\lambda} \\ &= \sqrt{\frac{\gamma + 1}{\gamma - 1}} \arctan \left(\sqrt{\frac{\gamma - 1}{\gamma + 1}} \sqrt{\frac{\lambda^2 - 1}{1 - \frac{\gamma-1}{\gamma+1}\lambda^2}} \right) - \arctan \left(\sqrt{\frac{\lambda^2 - 1}{1 - \frac{\gamma-1}{\gamma+1}\lambda^2}} \right) \end{aligned} \tag{4.4.44}$$

is the Prandtl–Meyer function (4.4.36) written in terms of the normalised velocity λ .

A graphical representation of equation (4.4.43) is given in Figure 4.13. Here two characteristics are drawn through an initial point (λ_0, ϑ_0) , one belonging to the first family of characteristics and the other to the second. It is interesting to note that, unlike in the physical (x, y) -plane, where the shape of the characteristics depends on the particular flow considered, in the hodograph (λ_x, λ_y) -plane all the characteristics have a universal shape defined by a single function $\sigma(\lambda)$ that is the same for characteristics of both families. Because of their shape, they are termed *epicycloids*. The reason is that they may be produced geometrically using the following procedure. Let us consider two circles in the (λ_x, λ_y) -plane, both having their centres at the coordinate origin. The radius of the inner circle is unity, and the radius of the outer circle is $\sqrt{(\gamma + 1)/(\gamma - 1)}$. Let us further introduce a third circle, whose radius is chosen in such a way that it fits precisely between the inner and outer circles. If we roll the third circle on the inner circle without slipping, then it may be shown that the points on the rolling circle will move along the characteristics in the hodograph plane.

In what follows, we shall denote the constant on the right-hand side of (4.4.43) by ξ for the characteristics of the first family and by η for the characteristics of the second family:

$$\vartheta - \sigma(\lambda) = \xi \quad (\text{first family}), \tag{4.4.45}$$

$$\vartheta + \sigma(\lambda) = \eta \quad (\text{second family}). \tag{4.4.46}$$

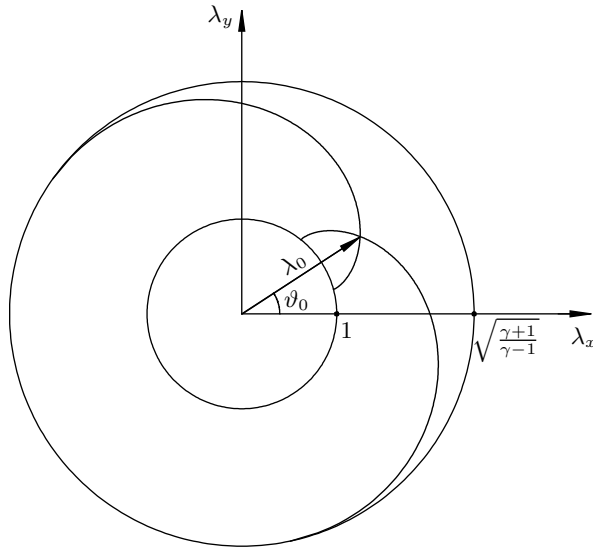


Fig. 4.13: Characteristics in the hodograph plane calculated for $\gamma = 1.4$. The non-dimensional velocity components λ_x and λ_y are defined as $\lambda_x = u/V_*$ and $\lambda_y = v/V_*$.

If we consider two characteristics of the first family with two different values of ξ on the right-hand side of (4.4.45),

$$\vartheta - \sigma(\lambda) = \xi_1, \quad \vartheta - \sigma(\lambda) = \xi_2,$$

then it may easily be seen that they may be obtained from one another by simple rotation through an angle $\Delta\vartheta = \xi_2 - \xi_1$. The same rule, of course, applies to the characteristics of the second family, (4.4.46).

4.4.3 Prandtl–Meyer flow

We shall now apply the theory of characteristics to the supersonic flow around a smooth bend of a rigid-body contour. We shall assume that the body surface is initially flat, with the flow above it being uniform. Then at point A the surface starts to bend as shown in Figure 4.14. To perform an analysis of the flow, it is convenient to choose the x -axis parallel to the initial flat part of the wall. The shape of the body contour may then be characterised by the angle $\theta(x)$ made by the tangent to the body contour with the x -axis.

The flow remains unperturbed everywhere upstream of the characteristic AA' of the first family originating from point A . Any point B on the bending part of the body contour may obviously be ‘connected’ to the unperturbed flow by the characteristic of the second family as shown in Figure 4.14. Along this characteristic, equation (4.4.46) holds. The parameter η on the right-hand side of this equation may be found taking into account that in the unperturbed flow upstream of AA' the velocity vector is parallel to the x -axis, i.e. $\vartheta = 0$. Denoting the value of the normalised velocity λ in

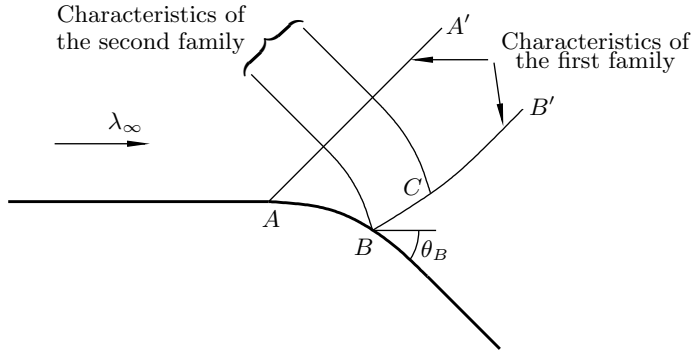


Fig. 4.14: Supersonic flow around a bend.

the undisturbed flow by λ_∞ , we have

$$\vartheta + \sigma(\lambda) = \sigma(\lambda_\infty). \tag{4.4.47}$$

The velocity vector, being tangent to the body contour, makes at point B an angle $\vartheta = -\theta_B$ with the x -axis. Consequently, the value λ_B of the normalised velocity λ at this point may be found from the equation

$$-\theta_B + \sigma(\lambda_B) = \sigma(\lambda_\infty).$$

The above discussion shows, interestingly enough, that the velocity variation along the body contour is completely described by equation (4.4.47). This equation is represented in the hodograph plane (see Figure 4.15) by the characteristic of the second family (epicycloid) that crosses the λ_x -axis at the point where $\lambda_x = \lambda_\infty$. The flow on the body surface between points A and B in the physical plane (see Figure 4.14) is represented by a segment of the epicycloid in the hodograph plane (Figure 4.15) between the initial point A , where $\lambda_x = \lambda_\infty$, and point B , where $\vartheta = -\theta_B$.

In order to analyse the flow behaviour above the body surface, let us consider the characteristic of the first family BB' originating from point B as shown in Figure 4.14. Along this characteristic, equation (4.4.45) holds. Any point C on the characteristic may be ‘connected’ to the unperturbed flow by the corresponding characteristic of the second family, and therefore, in addition to equation (4.4.45), we can use equation (4.4.47). Solving (4.4.45) and (4.4.47) for ϑ and $\sigma(\lambda)$, we find that, at point C ,

$$\vartheta = \frac{1}{2} [\sigma(\lambda_\infty) + \xi], \quad \sigma(\lambda) = \frac{1}{2} [\sigma(\lambda_\infty) - \xi].$$

Since the parameter ξ does not change as C moves along BB' , we can conclude that the normalised velocity λ and directional angle ϑ stay constant on BB' , and coincide with their values at point B on the body contour (see Figure 4.14).

The same conclusion may be made about the remaining fluid-dynamic functions. In particular, according to (4.4.42), with λ being constant, the Mach number M should also remain constant. Taking further into account that the critical velocity V_* is constant over the entire flow field, we can conclude that the dimensional velocity $V = \lambda V_*$

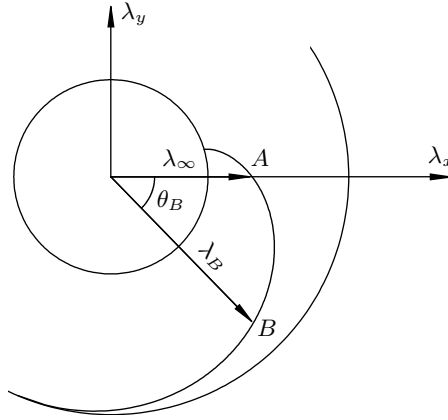


Fig. 4.15: Prandtl–Meyer flow in the hodograph plane.

does not change along BB' (see Figure 4.14). Then, using the entropy conservation law (4.2.10) and the Bernoulli equation (4.2.11), we can claim that the density ρ and pressure p are constant along BB' .

The shape of the characteristics in the physical (x, y) -plane is determined by equation (4.4.11), which, when combined with (4.4.22), shows that the slope of a characteristic of the first family is given by

$$\frac{dy}{dx} = \tan(\vartheta + \Theta). \quad (4.4.48)$$

Let us return to Figure 4.14 and consider characteristic BB' again. We already know that the velocity direction angle ϑ is constant on BB' . As far as the Mach angle Θ is concerned, it is determined by equation (4.4.21),

$$\Theta = \arcsin \frac{1}{M}, \quad (4.4.49)$$

and also proves to be constant. Hence, BB' is a straight line. Because of the arbitrariness of the characteristic considered, it is clear that in the Prandtl–Meyer flow all the characteristics of the first family are straight lines.

In the flow over a convex bend, these characteristics form an expansion fan, as shown in Figure 4.16. Indeed, using equation (4.4.48), one can see that the slope of the characteristics becomes smaller as an observer progresses downstream. This is due to the monotonic decrease of both the velocity vector directional angle ϑ and the Mach angle Θ . The former remains constant along each characteristic and coincides with the slope of the body contour at the foot of the characteristic. As far as the Mach angle Θ is concerned, it is given by equation (4.4.49), which clearly shows that Θ decreases with the flow acceleration round the bend.

The Prandtl–Meyer theory may in particular be used to describe expansion ramp flow.⁵ In this case, the entire bending section of the body contour is represented by

⁵For an alternative way to study this flow, see Problem 1 in Exercises 14.

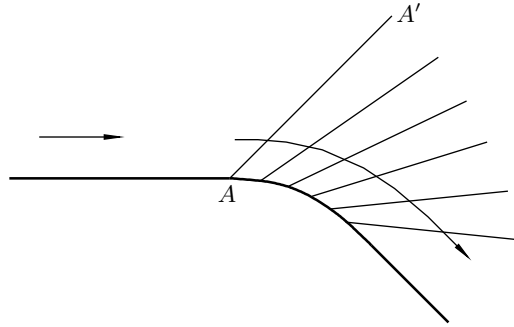


Fig. 4.16: Supersonic flow around a bend.

one point, the corner point A as shown in Figure 4.17. There are three distinct regions in the flow: (i) the undisturbed flow upstream of the first characteristic AA' of the expansion fan; (ii) the *expansion fan* $A'AA''$; and (iii) the region downstream of the last characteristic AA'' in the fan, where the flow again becomes uniform but with a higher value of the Mach number.

The above theory first appeared in the dissertation of Meyer (1908).

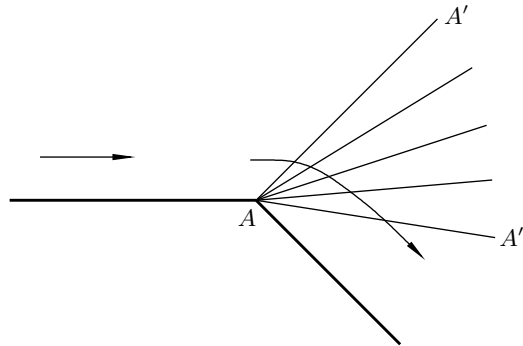


Fig. 4.17: Supersonic flow around an expansion ramp.

Exercises 14

1. In order to analyse the flow in the expansion fan $A'AA''$ in the Prandtl–Meyer flow in Figure 4.17, it is convenient to use cylindrical polar coordinates. When performing the analysis use the following suggestions:
 - (a) Take into account that the flow considered is two-dimensional and, using (1.8.9), (1.8.18), and (1.8.29), show that equation (4.3.6) is written in cylindrical polar coordinates (see Figure 4.18) as

$$(a^2 - V_r^2) \frac{\partial V_r}{\partial r} + (a^2 - V_\phi^2) \frac{1}{r} \frac{\partial V_\phi}{\partial \phi} = V_r V_\phi \left(\frac{\partial V_\phi}{\partial r} + \frac{1}{r} \frac{\partial V_r}{\partial \phi} \right) - a^2 \frac{V_r}{r}. \quad (4.4.50)$$

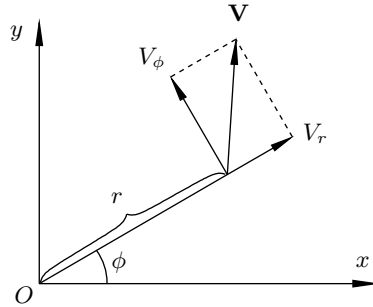


Fig. 4.18: Cylindrical polar coordinates.

The flow in the expansion fan is known to be irrotational. Therefore, using (1.8.38c), one can write

$$\frac{\partial V_\phi}{\partial r} - \frac{1}{r} \frac{\partial V_r}{\partial \phi} + \frac{V_\phi}{r} = 0. \quad (4.4.51)$$

- (b) Now take into account that inside the fan $A'AA''$ all the fluid-dynamic functions are independent of the radius r , which reduces equations (4.4.50) and (4.4.51) to

$$(a^2 - V_\phi^2) \frac{dV_\phi}{d\phi} = V_r V_\phi \frac{dV_r}{d\phi} - a^2 V_r, \quad (4.4.52a)$$

$$V_\phi = \frac{dV_r}{d\phi}. \quad (4.4.52b)$$

Combine equations (4.4.52a) and (4.4.52b) to show that

$$(a^2 - V_\phi^2) \left(\frac{dV_\phi}{d\phi} + V_r \right) = 0.$$

- (c) Assume first that

$$\frac{dV_\phi}{d\phi} + V_r = 0, \quad (4.4.53)$$

and show that the solution of equations (4.4.53) and (4.4.52b) represents a uniform flow. It may be used upstream or downstream of the expansion fan $A'AA''$.

- (d) In order to describe the flow inside the expansion fan, choose $V_\phi^2 = a^2$ and, using equation (4.3.12) for the speed of sound, a , deduce that

$$V_\phi^2 = \frac{\gamma - 1}{\gamma + 1} V_\infty^2 \left[1 + \frac{2}{(\gamma - 1) M_\infty^2} - \frac{V_r^2}{V_\infty^2} \right]. \quad (4.4.54)$$

Argue that, in the expansion fan, $V_\phi < 0$, and, combining (4.4.54) with

(4.4.52b), deduce that

$$\frac{dV_r}{V_\infty \sqrt{1 + \frac{2}{(\gamma - 1)M_\infty^2} - \frac{V_r^2}{V_\infty^2}}} = -\sqrt{\frac{\gamma - 1}{\gamma + 1}} d\phi. \quad (4.4.55)$$

Integrate (4.4.55) and conclude that, in the expansion fan,

$$V_r = V_\infty \sqrt{1 + \frac{2}{(\gamma - 1)M_\infty^2}} \sin \left[\sqrt{\frac{\gamma - 1}{\gamma + 1}} (\phi_0 - \phi) \right].$$

How can the constant of integration ϕ_0 be found?

2. This problem is designed to study the effect of compressibility in subsonic flows. Consider as an example the flow past a circular cylinder. Incompressible flow past a circular cylinder was studied in Section 3.4.2. If the circulation $\Gamma = 0$, then the complex potential for the flow is given by equation (3.4.28). Re-denoting the radius of the cylinder by r_0 , it may be written as

$$w(z) = V_\infty \left(z + \frac{r_0^2}{z} \right). \quad (4.4.56)$$

Your task here will be to investigate the effect of compressibility on the flow, for which purpose equation (4.4.50) may be used. The analysis is suggested to be conducted in the following steps:

- (a) Exclude the speed of sound, a , from (4.4.50) using the Bernoulli equation (4.3.9). Then introduce the non-dimensional variables

$$V_r = V_\infty \bar{V}_r, \quad V_\theta = V_\infty \bar{V}_\theta, \quad r = r_0 \bar{r},$$

and show that

$$\begin{aligned} \frac{\partial \bar{V}_r}{\partial \bar{r}} + \frac{1}{\bar{r}} \frac{\partial \bar{V}_\phi}{\partial \phi} + \frac{\bar{V}_r}{\bar{r}} = \frac{1}{2} M_\infty^2 \left[\left(\bar{V}_r \frac{\partial}{\partial \bar{r}} + \frac{\bar{V}_\phi}{\bar{r}} \frac{\partial}{\partial \phi} \right) (\bar{V}_r^2 + \bar{V}_\phi^2) \right. \\ \left. + (\gamma - 1) (\bar{V}_r^2 + \bar{V}_\phi^2 - 1) \left(\frac{\partial \bar{V}_r}{\partial \bar{r}} + \frac{1}{\bar{r}} \frac{\partial \bar{V}_\phi}{\partial \phi} + \frac{\bar{V}_r}{\bar{r}} \right) \right]. \end{aligned} \quad (4.4.57)$$

- (b) Introduce a velocity potential $\bar{\varphi}(r, \phi)$ such that

$$\bar{V}_r = \frac{\partial \bar{\varphi}}{\partial \bar{r}}, \quad \bar{V}_\phi = \frac{1}{\bar{r}} \frac{\partial \bar{\varphi}}{\partial \phi}, \quad (4.4.58)$$

and, assuming that the Mach number M_∞ is small, represent the solution in the form

$$\bar{\varphi} = \varphi_0(\bar{r}, \phi) + M_\infty^2 \varphi_1(\bar{r}, \phi) + \dots \quad (4.4.59)$$

Substitute (4.4.59) into (4.4.58) and then into (4.4.57). Disregard M_∞^4 terms

and, separating $O(1)$ and $O(M_\infty^2)$ terms, deduce that

$$O(1) : \frac{\partial^2 \varphi_0}{\partial \bar{r}^2} + \frac{1}{\bar{r}^2} \frac{\partial^2 \varphi_0}{\partial \phi^2} + \frac{1}{\bar{r}} \frac{\partial \varphi_0}{\partial \bar{r}} = 0, \quad (4.4.60)$$

$$\begin{aligned} O(M_\infty^2) : \quad & \frac{\partial^2 \varphi_1}{\partial \bar{r}^2} + \frac{1}{\bar{r}^2} \frac{\partial^2 \varphi_1}{\partial \phi^2} + \frac{1}{\bar{r}} \frac{\partial \varphi_1}{\partial \bar{r}} \\ & = \frac{1}{2} \frac{\partial \varphi_0}{\partial \bar{r}} \frac{\partial}{\partial \bar{r}} \left[\left(\frac{\partial \varphi_0}{\partial \bar{r}} \right)^2 + \frac{1}{\bar{r}^2} \left(\frac{\partial \varphi_0}{\partial \phi} \right)^2 \right] \\ & \quad + \frac{1}{2\bar{r}^2} \frac{\partial \varphi_0}{\partial \phi} \frac{\partial}{\partial \phi} \left[\left(\frac{\partial \varphi_0}{\partial \bar{r}} \right)^2 + \frac{1}{\bar{r}^2} \left(\frac{\partial \varphi_0}{\partial \phi} \right)^2 \right]. \end{aligned} \quad (4.4.61)$$

- (c) Formulate the boundary conditions for equations (4.4.60) and (4.4.61), for which purpose substitute (4.4.59) into the impermeability condition on the cylinder surface,

$$\left. \frac{\partial \bar{\varphi}}{\partial \bar{r}} \right|_{\bar{r}=1} = 0,$$

and the free-stream condition in the far field,

$$\bar{\varphi} = \bar{r} \cos \phi + \dots \quad \text{as } \bar{r} \rightarrow \infty.$$

- (d) Verify that the solution of the leading-order equation (4.4.60) is given by the real part of (4.4.56), which is written in non-dimensional variables as

$$\varphi_0 = \left(\bar{r} + \frac{1}{\bar{r}} \right) \cos \phi. \quad (4.4.62)$$

Using (4.4.62), demonstrate that the right-hand side of equation (4.4.61) may be written in the form⁶

$$\text{RHS} = \left(\frac{2}{\bar{r}^7} - \frac{4}{\bar{r}^5} \right) \cos \phi + \frac{2}{\bar{r}^3} \cos 3\phi.$$

Hence, seek the solution of equation (4.4.61) in the form

$$\varphi_1 = f(\bar{r}) \cos 3\phi + g(\bar{r}) \cos \phi.$$

3. Suppose that in the Prandtl–Meyer flow (see Figure 4.16), the wall slope angle $\theta(x)$ is small. Using equation (4.4.31), show that in the leading-order approximation, when $O(\theta^2)$ terms are disregarded, the velocity modulus V at any point along the bend may be calculated using the following simple formula:

$$V = V_\infty - V_\infty \frac{\theta}{\sqrt{M_\infty - 1}}.$$

Here θ is the value of the slope angle at the point where the velocity V is to be found and V_∞ denotes the unperturbed value of the fluid velocity before the characteristic AA' in Figure 4.16.

⁶You may use without proof the formula $\cos 3\vartheta = 4 \cos^3 \vartheta - 3 \cos \vartheta$.

Using further the entropy conservation law (4.2.10) and the Bernoulli equation (4.2.11), demonstrate that the pressure p on the body contour is given by the *Ackeret formula*

$$p = p_\infty + \rho_\infty V_\infty^2 \frac{\theta}{\sqrt{M_\infty^2 - 1}}.$$

4. Consider inviscid supersonic flow of a perfect gas around a corner (Figure 4.17) with the wall deflection angle θ_B ; see Figure 4.19.

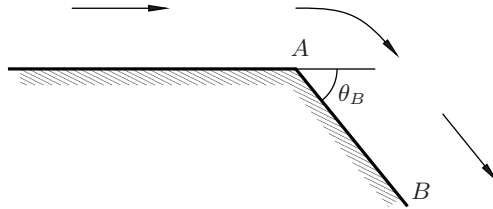


Fig. 4.19: Supersonic flow round corner.

Show that there exists a maximum value of the angle θ_B , given by

$$\theta_B \Big|_{\max} = \frac{\pi}{2} \left(\sqrt{\frac{\gamma+1}{\gamma-1}} - 1 \right) - \nu(M_\infty),$$

beyond which the flow downstream of the corner is no longer capable of remaining attached to the body surface AB . Here ν is the Prandtl–Meyer function (4.4.36),

$$\nu(M) = \sqrt{\frac{\gamma+1}{\gamma-1}} \arctan \left(\sqrt{\frac{\gamma-1}{\gamma+1}} (M^2 - 1) \right) - \arctan \left(\sqrt{M^2 - 1} \right),$$

and M_∞ is the Mach number before the corner point A .

How does the maximum value of θ_B depend on M_∞ ?

Suggestion: Remember that the flow expansion around the corner is described by equation (4.4.47). Using the Prandtl–Meyer function, this equation is written as

$$\vartheta + \nu(M) = \nu(M_\infty).$$

Set $M = \infty$, and take into account that, on the body surface AB , behind the corner, the velocity vector angle $\vartheta = -\theta_B$.

5. The theory of characteristics was presented in this section in application to irrotational flows when equations (4.3.10) and (4.3.11) may be used to describe the velocity field. However, most supersonic flows develop shock waves. The latter are known to be the sources of vorticity. In order to apply the theory of characteristics

to two-dimensional flows with non-zero vorticity, the following equations may be used:

$$u \frac{\partial u}{\partial x} + v \frac{\partial u}{\partial y} + \frac{1}{\rho} \frac{\partial p}{\partial x} = 0, \quad (4.4.63a)$$

$$u \frac{\partial v}{\partial x} + v \frac{\partial v}{\partial y} + \frac{1}{\rho} \frac{\partial p}{\partial y} = 0, \quad (4.4.63b)$$

$$\rho \frac{\partial u}{\partial x} + \rho \frac{\partial v}{\partial y} + \frac{u}{a^2} \frac{\partial p}{\partial x} + \frac{v}{a^2} \frac{\partial p}{\partial y} = 0. \quad (4.4.63c)$$

The first two of equations are the x - and y -components of the momentum equation (4.1.2a) with the unsteady term $\partial \mathbf{V} / \partial t$ and the body force \mathbf{f} disregarded. The third equation coincides with equation (4.3.4), which is used here instead of the continuity equation (4.1.2c). The reason for this choice is that equation (4.4.63c) relates the variations of the velocity components directly to the pressure variations. This enables us to exclude the density from the set of functions that are considered in the procedure leading to identification of the characteristics of the system considered. Of course, the density itself may be found at any stage of the calculations using the Bernoulli equation

$$\frac{\gamma}{\gamma - 1} \frac{p}{\rho} + \frac{1}{2}(u^2 + v^2) = \frac{\gamma}{\gamma - 1} \frac{p_\infty}{\rho_\infty} + \frac{1}{2}V_\infty^2.$$

In order to apply the theory of characteristics to equations (4.4.63) you may start, as before, by introducing an initial line \mathcal{L} that is defined by the equation $y = y(x)$. However, now three functions, $u = \tilde{u}(x)$, $v = \tilde{v}(x)$, and $p = \tilde{p}(x)$, should be assumed known along \mathcal{L} . Your task will be twofold:

- (a) First, you need to show that the system of equations (4.4.63) has three families of characteristics, with the slope $\chi = dy/dx$ given by

$$\chi_{1,2} = \frac{-uv \mp a\sqrt{V^2 - a^2}}{a^2 - u^2}, \quad \chi_3 = \frac{v}{u}.$$

Give a physical interpretation of these characteristics.

- (b) Second, you need to demonstrate that, along characteristics of the first two families, the following relation between the variations of u , v , and p holds:

$$v du - u dv + \left[(v - \chi_{1,2}u) \frac{u}{a^2} + \chi_{1,2} \right] \frac{1}{\rho} dp = 0,$$

while, along a characteristic of the third family,

$$u du + v dv + \frac{1}{\rho} dp = 0.$$

6. Generalise equation (4.3.10) for unsteady flow past an oscillating aerofoil. You may assume that (i) the flow far from the aerofoil is steady and uniform; (ii) the body force \mathbf{f} is negligible; and (iii) the flow is free of shock waves.

Argue that, under these conditions the flow is irrotational, and show that the velocity potential φ satisfies the equation

$$\begin{aligned} \left[a^2 - \left(\frac{\partial \varphi}{\partial x} \right)^2 \right] \frac{\partial^2 \varphi}{\partial x^2} + \left[a^2 - \left(\frac{\partial \varphi}{\partial y} \right)^2 \right] \frac{\partial^2 \varphi}{\partial y^2} \\ = 2 \frac{\partial \varphi}{\partial x} \frac{\partial \varphi}{\partial y} \frac{\partial^2 \varphi}{\partial x \partial y} + 2 \frac{\partial \varphi}{\partial x} \frac{\partial^2 \varphi}{\partial t \partial x} + 2 \frac{\partial \varphi}{\partial y} \frac{\partial^2 \varphi}{\partial t \partial y} + \frac{\partial^2 \varphi}{\partial t^2}, \end{aligned} \quad (4.4.64)$$

which is known as the *unsteady potential equation*.

Suggestion: In order to perform this task, proceed as follows:

- (a) Start with the entropy conservation law (4.2.10). Notice that it may be expressed in the form

$$\frac{a^2}{\rho^{\gamma-1}} = \gamma \frac{p_\infty}{\rho_\infty^\gamma}. \quad (4.4.65)$$

Take the logarithms of both sides of equation (4.4.65) and show that the full derivatives of a^2 and ρ are related to one another by

$$\frac{1}{a^2} \frac{D(a^2)}{Dt} = \frac{\gamma - 1}{\rho} \frac{D\rho}{Dt}. \quad (4.4.66)$$

- (b) Now write the continuity equation (4.1.2c) as

$$\frac{D\rho}{Dt} + \rho \operatorname{div} \mathbf{V} = 0, \quad (4.4.67)$$

and use (4.4.66) to eliminate $D\rho/Dt$ from (4.4.67). You should find that

$$\frac{\partial(a^2)}{\partial t} + \mathbf{V} \cdot \nabla(a^2) + (\gamma - 1)a^2 \operatorname{div} \mathbf{V} = 0. \quad (4.4.68)$$

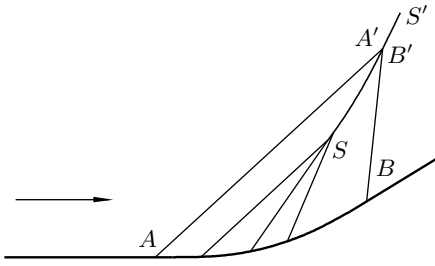
- (c) Finally, argue that, under conditions (i), (ii), and (iii), the Cauchy–Lagrange integral (4.2.28) may be written as

$$\frac{\partial \varphi}{\partial t} + \frac{V^2}{2} + \frac{a^2}{\gamma - 1} = \frac{V_\infty^2}{2} + \frac{a_\infty^2}{\gamma - 1}. \quad (4.4.69)$$

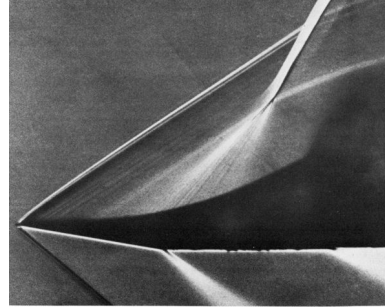
Solve equation (4.4.69) for a^2 and use it to calculate the time derivative and the gradient of a^2 in equation (4.4.68). Assuming, for simplicity, that the flow is two-dimensional, you will arrive at equation (4.4.64).

4.5 Shock Waves

Let us make a small modification to the problem depicted in Figure 4.16, and assume that, instead of bending down, the body contour bends up as shown in Figure 4.20(a). Obviously, the Prandtl–Meyer theory remains applicable to this flow. Moreover, one has to use the same epicycloid in the hodograph plane (see Figure 4.15), the one that crosses the λ_x -axis at point A, where λ_x coincides with the normalised velocity λ_∞ in the flow before the bend. However, the flow is now represented by the part of



(a) Prandtl-Meyer flow above a concave wall.



(b) Flow visualisation by Johannesen (1952). Reprinted by permission of Taylor & Francis Ltd.

Fig. 4.20: Formation of a shock wave in a steady supersonic flow.

the epicycloid that lies above point A . According to the Prandtl-Meyer theory, the characteristics of the first family will remain straight lines, but, instead of forming a divergent fan, they will start converging as soon as the body contour starts to bend up.

Assuming that the curvature of the body contour is finite, it may be demonstrated (see Problem 1 in Exercises 15) that the point of convergence of the characteristics, denoted by S in Figure 4.20(a), is situated at a finite distance from the body surface. Below this point, the flow field remains smooth, which ensures that the Prandtl-Meyer theory remains valid. However, in order to describe the flow above point S , a modification of the theory is needed. In this region, the characteristics of the first family begin to intersect. Two of these, AA' and BB' , are shown in Figure 4.20(a). They originate from different points on the body contour and 'bring' to the point of intersection different values of the velocity modulus V , directional angle ϑ , pressure p , density ρ , and other fluid-dynamic functions. The flow visualisation in Figure 4.20(b) shows that the convergence of the characteristics leads to the formation of a shock wave. In inviscid flow theory, it is represented as a surface across which the fluid-dynamic functions experience a discontinuity.

4.5.1 The shock relations

The differential equations of fluid motion (4.1.2) clearly cannot be used across discontinuities. Therefore, to deduce the shock equations, we have to return to first principles. In order to simplify our task, we shall assume that the flow considered is steady.⁷ We shall further assume that the surface representing the shock has a finite radius of curvature. In this case, a small element of the shock may be treated as a flat surface. The flow across such a element of the shock will now be analysed.

It is convenient to consider the fluid motion in the plane perpendicular to the shock and parallel to the velocity vector \mathbf{V}_1 immediately upstream of the shock. The shock wave is represented in this plane (see Figure 4.21) by a straight line SS' . We

⁷This assumption will be lifted in Section 4.7.2.

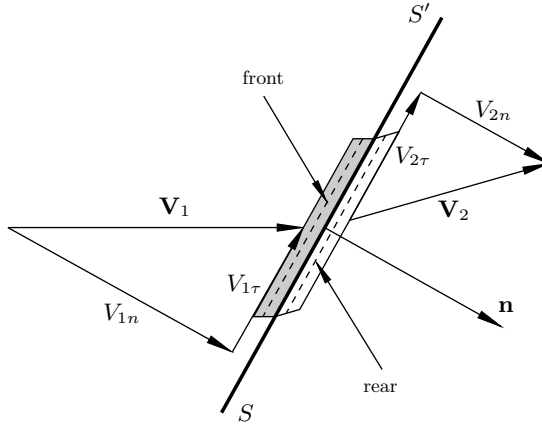


Fig. 4.21: Flow across a shock wave.

shall assume that the angle made by the shock with the velocity vector \mathbf{V}_1 is known together with the modulus of the velocity $|\mathbf{V}_1|$, pressure p_1 , density ρ_1 , and hence all other thermodynamic functions before the shock. The task is to find the corresponding quantities \mathbf{V}_2 , p_2 , ρ_2 , etc. behind the shock.

Let us choose a small area A on the surface of the shock and consider the fluid moving through A during a small time interval Δt . Before crossing the shock, the fluid is contained in the region that is shown in Figure 4.21 as a shaded parallelogram. The volume of this region is easily calculated to be $V_{1n}\Delta tA$, where V_{1n} is the component of the velocity vector \mathbf{V}_1 normal to the shock. Correspondingly, the mass of fluid in the parallelogram is $m_1 = \rho_1 V_{1n}\Delta tA$. When the fluid emerges on the other side of the shock, it occupies the region shown in Figure 4.21 as an unshaded parallelogram. The mass of the fluid may be now calculated as $m_2 = \rho_2 V_{2n}\Delta tA$. Hence, using the mass conservation law $m_2 = m_1$, we can write

$$\rho_2 V_{2n} = \rho_1 V_{1n}. \tag{4.5.1}$$

We now turn to the momentum equation (1.6.12). We shall write it in the form

$$\frac{\mathbf{K}_2 - \mathbf{K}_1}{\Delta t} = \mathbf{R}. \tag{4.5.2}$$

Here \mathbf{K}_2 is the momentum of the fluid behind the shock. It can be calculated as

$$\mathbf{K}_2 = m_2 \mathbf{V}_2 = \rho_2 A V_{2n} \Delta t \mathbf{V}_2. \tag{4.5.3}$$

Similarly, the momentum of the fluid before the shock is

$$\mathbf{K}_1 = \rho_1 A V_{1n} \Delta t \mathbf{V}_1. \tag{4.5.4}$$

The resultant force \mathbf{R} on the right-hand side of equation (4.5.2) is composed of the pressure forces \mathbf{F}_1 and \mathbf{F}_2 acting on the front and rear faces of the region containing

the fluid body as it makes its way across the shock:

$$\mathbf{R} = \mathbf{F}_1 + \mathbf{F}_2.$$

An intermediate position of the fluid body is shown in Figure 4.21 by the broken lines. Taking into account that the forces acting upon the fluid body should be used in (4.5.2), we write

$$\mathbf{F}_1 = p_1 A \mathbf{n}, \quad \mathbf{F}_2 = -p_2 A \mathbf{n}, \quad (4.5.5)$$

where the unit normal vector \mathbf{n} is directed as shown in Figure 4.21.

Substitution of (4.5.3)–(4.5.5) into the momentum equation (4.5.2) yields

$$\rho_2 V_{2n} \mathbf{V}_2 + p_2 \mathbf{n} = \rho_1 V_{1n} \mathbf{V}_1 + p_1 \mathbf{n}. \quad (4.5.6)$$

This is a vector equation. Its projection on the direction normal to the shock reads

$$\rho_2 V_{2n}^2 + p_2 = \rho_1 V_{1n}^2 + p_1. \quad (4.5.7)$$

The tangential projection of (4.5.6),

$$\rho_2 V_{2n} V_{2\tau} = \rho_1 V_{1n} V_{1\tau},$$

and the mass conservation law (4.5.1) allow us to conclude that the tangential velocity component does not change across the shock:

$$V_{2\tau} = V_{1\tau}. \quad (4.5.8)$$

It remains to consider the energy equation (1.6.28). Taking into account that in an inviscid fluid heat transfer is a negligible effect, $Q = 0$, we can write this equation in the form

$$\frac{E_2 - E_1}{\Delta t} = W. \quad (4.5.9)$$

The energy of the fluid body behind the shock is calculated as

$$E_2 = m_2 \left(e_2 + \frac{V_2^2}{2} \right) = \rho_2 A V_{2n} \Delta t \left(e_2 + \frac{V_2^2}{2} \right). \quad (4.5.10)$$

Similarly, before the shock,

$$E_1 = \rho_1 A V_{1n} \Delta t \left(e_1 + \frac{V_1^2}{2} \right). \quad (4.5.11)$$

The work W performed by the pressure forces \mathbf{F}_1 and \mathbf{F}_2 per unit time is

$$W = \mathbf{F}_1 \cdot \mathbf{V}_1 + \mathbf{F}_2 \cdot \mathbf{V}_2 = p_1 A V_{1n} - p_2 A V_{2n}. \quad (4.5.12)$$

Substituting (4.5.10)–(4.5.12) into the energy equation (4.5.9) and recalling that, according to (1.3.27), the enthalpy $h = e + p/\rho$, we find that

$$h_2 + \frac{V_2^2}{2} = h_1 + \frac{V_1^2}{2}. \quad (4.5.13)$$

This proves that the Bernoulli integral (4.2.6) holds not only in the flow before and after the shock wave but also across it. Hence, we can conclude that even if a flow

contains multiple shocks, the total enthalpy $H = h + \frac{1}{2}V^2$ will remain constant along all streamlines.

Summarising the results of the above analysis, we can write the shock relations (4.5.1), (4.5.7), (4.5.8) and (4.5.13), also termed the *jump conditions*, as

$$\rho_2 V_{2n}^2 + p_2 = \rho_1 V_{1n}^2 + p_1 \quad (\text{normal momentum equation}), \quad (4.5.14a)$$

$$V_{2\tau} = V_{1\tau} \quad (\text{tangential momentum equation}), \quad (4.5.14b)$$

$$h_2 + \frac{V_2^2}{2} = h_1 + \frac{V_1^2}{2} \quad (\text{energy equation}), \quad (4.5.14c)$$

$$\rho_2 V_{2n} = \rho_1 V_{1n} \quad (\text{continuity equation}). \quad (4.5.14d)$$

Together with the state equation

$$h_2 = \frac{\gamma}{\gamma - 1} \frac{p_2}{\rho_2}, \quad (4.5.15)$$

they form a set of five algebraic equations for five unknown quantities V_{2n} , $V_{2\tau}$, p_2 , ρ_2 , and h_2 , which fully describe the state of the flow immediately behind the shock.

In view of the fact that the early major contributions to understanding the behaviour of shock waves were due to Rankine (1870) and Hugoniot (1889), the shock jump conditions (4.5.14) are often referred to as the *Rankine–Hugoniot conditions*.

4.5.2 Normal shock

If the shock is normal to the direction of the flow, then the tangential velocity component is zero on both sides of the shock, $V_{1\tau} = V_{2\tau} = 0$, and the jump conditions (4.5.14) assume the form

$$\rho_2 V_2^2 + p_2 = \rho_1 V_1^2 + p_1 \quad (\text{momentum equation}), \quad (4.5.16a)$$

$$h_2 + \frac{V_2^2}{2} = h_1 + \frac{V_1^2}{2} \quad (\text{energy equation}), \quad (4.5.16b)$$

$$\rho_2 V_2 = \rho_1 V_1 \quad (\text{continuity equation}). \quad (4.5.16c)$$

Here V_1 and V_2 are the values of the velocity modulus upstream and downstream of the shock; see Figure 4.22.

We can note, first of all, that, according to the energy equation (4.5.16b), the critical velocity V_* , defined by the Bernoulli equation (4.4.38), remains unchanged across the shock. Using the state equation (4.5.15), we can express the left-hand side of the energy equation (4.5.16b) as follows:

$$\frac{\gamma}{\gamma - 1} \frac{p_2}{\rho_2} + \frac{V_2^2}{2} = \frac{V_*^2}{\gamma - 1} + \frac{V_*^2}{2} = \frac{\gamma + 1}{2(\gamma - 1)} V_*^2. \quad (4.5.17)$$

Hence, in the flow behind the shock,

$$\frac{p_2}{\rho_2} = \frac{\gamma + 1}{2\gamma} V_*^2 - \frac{\gamma - 1}{2\gamma} V_2^2. \quad (4.5.18)$$

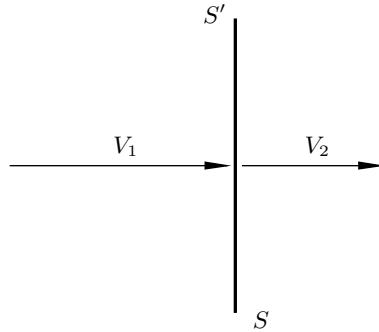


Fig. 4.22: Flow across a normal shock.

Similarly, in front of the shock,

$$\frac{p_1}{\rho_1} = \frac{\gamma + 1}{2\gamma} V_*^2 - \frac{\gamma - 1}{2\gamma} V_1^2. \quad (4.5.19)$$

We now turn to the momentum equation (4.5.16a). We divide its two sides respectively by $\rho_2 V_2$ and $\rho_1 V_1$, which are equal according to the continuity equation (4.5.16c). We have

$$V_2 + \frac{p_2}{\rho_2} \frac{1}{V_2} = V_1 + \frac{p_1}{\rho_1} \frac{1}{V_1}. \quad (4.5.20)$$

With the help of (4.5.18) and (4.5.19), p_2/ρ_2 and p_1/ρ_1 can be eliminated from (4.5.20), leading to

$$\frac{V_2}{V_*} + \frac{V_*}{V_2} = \frac{V_1}{V_*} + \frac{V_*}{V_1}. \quad (4.5.21)$$

Denoting the values of the normalised velocity (4.4.37) before and after the shock by λ_1 and λ_2 , respectively, we can express (4.5.21) in the form of a quadratic equation for λ_2 :

$$\lambda_2^2 - \left(\lambda_1 + \frac{1}{\lambda_1} \right) \lambda_2 + 1 = 0. \quad (4.5.22)$$

Its first root, $\lambda_2 = \lambda_1$, represents a trivial solution of equations (4.5.16):

$$V_2 = V_1, \quad \rho_2 = \rho_1, \quad p_2 = p_1, \quad h_2 = h_1,$$

which describes the flow without a shock wave.⁸

Since our interest here is in describing the shock properties, we have to consider the second root of (4.5.22),

$$\lambda_2 = \frac{1}{\lambda_1}. \quad (4.5.23)$$

This represents a basic law of shock theory, and is known as *Prandtl's relation*. According to (4.5.23), any supersonic flow ($\lambda_1 > 1$) passing through a normal shock becomes subsonic ($\lambda_2 < 1$).

⁸This solution automatically satisfies the momentum and energy equations as well as the mass conservation law, and therefore is always possible.

With the help of equation (4.5.23), one can easily calculate the ratio of the velocities across the shock:

$$\frac{V_2}{V_1} = \frac{V_2/V_*}{V_1/V_*} = \frac{\lambda_2}{\lambda_1} = \frac{1}{\lambda_1^2},$$

which may be expressed, using (4.4.40), in terms of the Mach number before the shock:

$$\frac{V_2}{V_1} = \frac{2 + (\gamma - 1)M_1^2}{(\gamma + 1)M_1^2}. \quad (4.5.24)$$

Using further the continuity equation (4.5.16c), we find the density ratio:

$$\frac{\rho_2}{\rho_1} = \frac{(\gamma + 1)M_1^2}{2 + (\gamma - 1)M_1^2}. \quad (4.5.25)$$

In order to determine the pressure ratio, we return to the momentum equation (4.5.16a). We have

$$p_2 = p_1 + \rho_1 V_1^2 - \rho_2 V_2^2 = p_1 + \rho_1 V_1^2 \left(1 - \frac{\rho_2}{\rho_1} \frac{V_2^2}{V_1^2} \right).$$

In view of the continuity equation (4.5.16c), this may be written as

$$p_2 = p_1 + \rho_1 V_1^2 \left(1 - \frac{V_2}{V_1} \right). \quad (4.5.26)$$

Substitution of (4.5.24) into (4.5.26) results in

$$p_2 = p_1 + \rho_1 V_1^2 \frac{2M_1^2 - 2}{(\gamma + 1)M_1^2}.$$

Dividing both sides of this equation by p_1 , and using formula (4.3.3) to calculate the speed of sound before the shock, we finally find

$$\frac{p_2}{p_1} = \frac{2\gamma M_1^2 - (\gamma - 1)}{\gamma + 1}. \quad (4.5.27)$$

Finally, in order to calculate the temperature ratio, we apply the Clapeyron equation (1.3.2) to the gas before and after the shock. We have

$$\frac{T_2}{T_1} = \frac{p_2}{p_1} \frac{\rho_1}{\rho_2}. \quad (4.5.28)$$

Substitution of (4.5.25) and (4.5.27) into (4.5.28) yields

$$\frac{T_2}{T_1} = \frac{[2\gamma M_1^2 - (\gamma - 1)] [(\gamma - 1)M_1^2 + 2]}{(\gamma + 1)^2 M_1^2}.$$

It should be noted that, while equation (4.5.23) does not preclude the possibility of an ‘expansion shock’ through which a subsonic flow with $\lambda_1 < 1$ accelerates to a

supersonic speed $\lambda_1 > 1$, such situations are never observed in real flows. To explain this, let us consider the entropy variation ΔS across the shock. Making use of (1.3.37), we can write

$$\Delta S = S_2 - S_1 = \frac{R}{\gamma - 1} \ln \left[\frac{p_2}{p_1} \left(\frac{\rho_1}{\rho_2} \right)^\gamma \right].$$

Using (4.5.25) and (4.5.27), we can further write

$$\Delta S = \frac{R}{\gamma - 1} \ln \left[\frac{2\gamma M_1^2 - (\gamma - 1)}{\gamma + 1} \right] + \frac{\gamma R}{\gamma - 1} \ln \left[\frac{2 + (\gamma - 1)M_1^2}{(\gamma + 1)M_1^2} \right]. \quad (4.5.29)$$

In particular, it follows from (4.5.29) that $\Delta S = 0$ at $M_1 = 1$. In order to predict the behaviour of the entropy in the shock wave for $M_1 \neq 1$, we differentiate (4.5.29) with respect to M_1 :

$$\frac{d(\Delta S)}{dM_1} = \frac{4\gamma R}{M_1} \frac{(M_1^2 - 1)^2}{[2\gamma M_1^2 - (\gamma - 1)][2 + (\gamma - 1)M_1^2]}. \quad (4.5.30)$$

Since the pressure should be positive both upstream and downstream of the shock, equation (4.5.27) suggests that we have to assume $2\gamma M_1^2 - (\gamma - 1) > 0$, and it then follows from (4.5.30) that the derivative $d(\Delta S)/dM_1$ is positive for all values of M_1 except $M_1 = 1$. This means that the entropy increases across the shock for all $M_1 > 1$, and is supposed to decrease for $M_1 < 1$. The latter, however, contradicts the Second Law of Thermodynamics, also known in the kinetic theory of gases as Boltzmann's *H*-theorem. This theorem states that, provided a body of gas is thermally isolated, its entropy can never decay. In fact, if a gas undergoes a transformation, remaining all the way in the state of thermodynamic equilibrium, then, according to (1.3.34), the entropy will remain unchanged. This is exactly what happens in the flow upstream and downstream of the shock. However, the transformation inside the shock is too fast for fluid particles to be able to adjust to the surrounding conditions promptly.⁹ As a result, the entropy has to rise in the shock wave, which is only possible if the Mach number before the shock $M_1 > 1$. It follows from (4.5.25) that $\rho_2/\rho_1 > 1$ for any $M_1 > 1$, which is why these shock waves are termed 'compression waves', in contrast to 'expansion waves' ($M_1 < 1$), which are possible mathematically, but cannot be observed in real flows.

4.5.3 Oblique shocks

Let us now return to the original problem of supersonic flow encountering an oblique shock wave (see Figure 4.21). In order to study the oblique shock, we can deal directly with equations (4.5.14). Alternatively, the results of the analysis for the normal shock may be adopted for our purposes. The fact is that the oblique shock problem, depicted in Figure 4.23(a), may easily be reduced to the corresponding problem for the normal shock. This is done by means of the following two-step procedure. First, we perform a rotation of the flow through an angle $\pi - \alpha$. The result of this operation is shown

⁹It is known from the kinetic theory of gases that, unless M_1 is close to unity, the thickness of the shock wave is comparable to the mean free path of molecules, and therefore the condition of equilibrium discussed in Problem 1 in Exercises 1 appears to be violated.

in Figure 4.23(b). Then we introduce a new coordinate frame that moves along the shock SS' with velocity $V_{1\tau}$. Thanks to equation (4.5.14b), in the new coordinates, the velocity vector appears to be normal to the shock on both sides of it, as shown in Figure 4.22.

It is obvious that the coordinate transformation leaves the thermodynamic quantities of the gas unchanged. The velocity component normal to the shock is also preserved. Therefore, when calculating the density ratio across the shock, we simply need to modify formula (4.5.25) as

$$\frac{\rho_2}{\rho_1} = \frac{(\gamma + 1)M_{1n}^2}{2 + (\gamma - 1)M_{1n}^2}. \tag{4.5.31}$$

Here M_{1n} is the normal component of the Mach number, defined as

$$M_{1n} = \frac{V_{1n}}{a_1}.$$

The speed of sound before the shock, a_1 , is calculated using equation (4.3.3),

$$a_1 = \sqrt{\gamma \frac{p_1}{\rho_1}},$$

and proves to be independent of the coordinate frame used. If we denote by α the angle of inclination of the shock to the velocity vector (see Figure 4.23), then

$$M_{1n} = \frac{V_{1n}}{a_1} = \frac{V_1 \sin \alpha}{a_1} = M_1 \sin \alpha,$$

which allows us to express equation (4.5.31) in the form

$$\frac{\rho_2}{\rho_1} = \frac{(\gamma + 1)M_1^2 \sin^2 \alpha}{2 + (\gamma - 1)M_1^2 \sin^2 \alpha}. \tag{4.5.32}$$

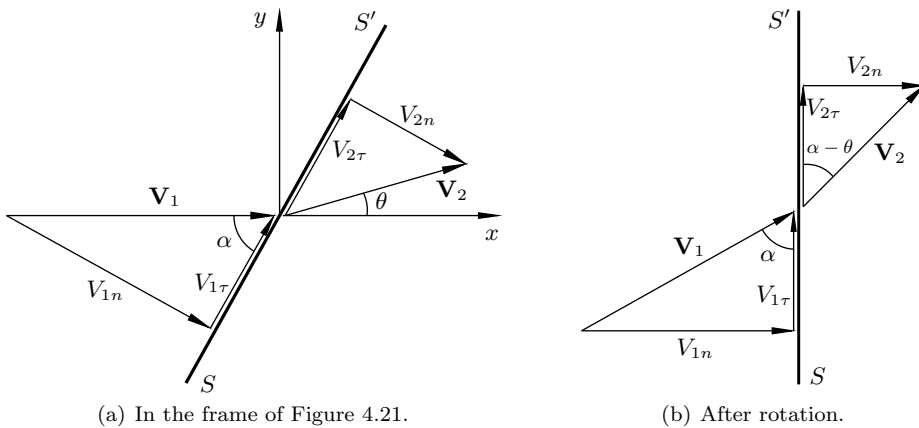


Fig. 4.23: Oblique shock wave.

Similarly, using (4.5.27) and (4.5.24), we find that

$$\frac{p_2}{p_1} = \frac{2\gamma M_1^2 \sin^2 \alpha - (\gamma - 1)}{\gamma + 1}, \quad (4.5.33)$$

$$\frac{V_{2n}}{V_{1n}} = \frac{\gamma - 1}{\gamma + 1} + \frac{2}{(\gamma + 1)M_1^2 \sin^2 \alpha}. \quad (4.5.34)$$

The oblique shock relations (4.5.32)–(4.5.34), supplemented by equation (4.5.14b), allow us to determine the two velocity components and the thermodynamic state of the gas behind the shock, provided that the shock angle α is given. However, in most cases, the orientation of the shock in the flow field is not known in advance. Instead, it should be found as part of the solution of the corresponding gas-dynamic problem. Taking this into account, it is useful to deduce a shock equation that does not involve α .

Since the shock always reduces the normal velocity component, leaving the tangential component unchanged, the velocity vector changes direction at the shock. With θ being the velocity vector deflection angle (see Figure 4.23), we can write

$$\begin{aligned} V_{2n} &= V_2 \sin(\alpha - \theta) \\ &= V_2(\sin \alpha \cos \theta - \cos \alpha \sin \theta). \end{aligned}$$

Let us now introduce a Cartesian coordinate system with x oriented parallel to the velocity vector in front of the shock and y in the normal direction, as shown in Figure 4.23(a). The velocity components with respect to these coordinates are calculated as

$$u_2 = V_2 \cos \theta, \quad v_2 = V_2 \sin \theta,$$

and therefore

$$V_{2n} = u_2 \sin \alpha - v_2 \cos \alpha. \quad (4.5.35)$$

Substituting (4.5.35) into (4.5.34) and taking into account that $V_{1n} = V_1 \sin \alpha$ yields

$$\frac{u_2}{V_1} - \frac{v_2}{V_1} \frac{1}{\tan \alpha} = \frac{\gamma - 1}{\gamma + 1} + \frac{2}{(\gamma + 1)M_1^2 \sin^2 \alpha}. \quad (4.5.36)$$

In order to eliminate α from (4.5.36), we use equation (4.5.14b), which may be written as

$$\begin{aligned} V_1 \cos \alpha &= V_2 \cos(\alpha - \theta) \\ &= V_2(\cos \alpha \cos \theta + \sin \alpha \sin \theta) = u_2 \cos \alpha + v_2 \sin \alpha, \end{aligned}$$

and it follows that

$$\tan \alpha = \frac{V_1 - u_2}{v_2}, \quad \sin^2 \alpha = \frac{(V_1 - u_2)^2}{(V_1 - u_2)^2 + v_2^2}. \quad (4.5.37)$$

Substitution of (4.5.37) into (4.5.36) leads to

$$\frac{u_2}{V_1} - \frac{v_2^2}{V_1(V_1 - u_2)} = \frac{\gamma - 1}{\gamma + 1} + \frac{2}{(\gamma + 1)M_1^2} \frac{(V_1 - u_2)^2 + v_2^2}{(V_1 - u_2)^2}. \quad (4.5.38)$$

Finally, it is convenient to express M_1 via the normalised velocity λ_1 . From equation (4.4.39),

$$\frac{1}{M_1^2} = \frac{\gamma + 1}{2} \frac{1}{\lambda_1^2} - \frac{\gamma - 1}{2} = \frac{\gamma + 1}{2} \frac{V_*^2}{V_1^2} - \frac{\gamma - 1}{2}. \quad (4.5.39)$$

Substituting (4.5.39) into (4.5.38) and solving the resulting equation for v_2^2 , we find

$$v_2^2 = \frac{(V_1 - u_2)^2 (V_1 u_2 - V_*^2)}{V_*^2 + \frac{2}{\gamma + 1} V_1^2 - V_1 u_2}. \quad (4.5.40)$$

A non-dimensional form of (4.5.40) may easily be obtained by dividing both sides by V_*^2 :

$$\lambda_{2y}^2 = \frac{(\lambda_1 - \lambda_{2x})^2 (\lambda_1 \lambda_{2x} - 1)}{1 + \frac{2}{\gamma + 1} \lambda_1^2 - \lambda_1 \lambda_{2x}}. \quad (4.5.41)$$

Here λ_{2x} and λ_{2y} are the two components of the normalised velocity behind the shock:

$$\lambda_{2x} = \frac{u_2}{V_*}, \quad \lambda_{2y} = \frac{v_2}{V_*}.$$

Figure 4.24 gives a graphical representation of equation (4.5.41) in the hodograph $(\lambda_{2x}, \lambda_{2y})$ -plane. Each point in this plane should be thought of as the tip of the normalised velocity vector drawn from the coordinate origin O . Given λ_1 , equation (4.5.41) allows us to calculate λ_{2y} for any λ_{2x} from the interval

$$\lambda_{2x} \in \left[\frac{1}{\lambda_1}, \frac{1}{\lambda_1} + \frac{2}{\gamma + 1} \lambda_1 \right]. \quad (4.5.42)$$

The restriction on the range of λ_{2x} arises from the observation that the right-hand side of equation (4.5.41) can never become negative. As λ_{2x} changes within the range

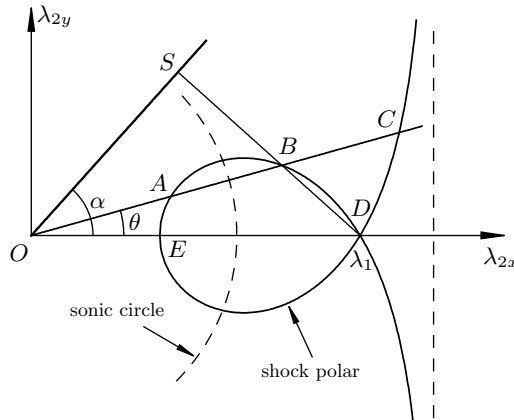


Fig. 4.24: Shock polar calculated for $\lambda_1 = 1.6$ and $\gamma = 1.4$.

(4.5.42), the point in the hodograph plane traces out a locus termed the *shock polar*; see Figure 4.24. It shows all possible positions of the tip of the normalised velocity vector behind the oblique shock for different possible orientations of the shock. Point D , where $\lambda_{2x} = \lambda_1$, represents the state of the flow in front of the shock. At this point, the numerator of the right-hand side of (4.5.41) becomes zero. The second zero of the numerator is attained at point E , which represents the normal shock wave with $\lambda_{2x} = 1/\lambda_1$. This point lies at the lower boundary of the interval (4.5.42). The upper boundary is given by the zero of the denominator in (4.5.41), which defines the asymptote of the shock polar, depicted in Figure 4.24 by the vertical dashed line.

Assuming that the velocity vector deflection angle θ is known, one can easily determine the state of the flow behind the shock. For this purpose, a ray from the origin O should be drawn at an angle θ to the λ_{2x} -axis. It intersects the shock polar at three points: A , B and C . At point C , the flow velocity is, obviously, larger than at point D , which means that point C represents an ‘expansion shock’, and therefore should be disregarded. Still, two solutions, namely those given by points A and B , are possible for each deflection angle θ unless it exceeds a maximum value θ_{\max} , the latter being dependent on λ_1 .

If we consider, for example, point B , then the position of this point in the hodograph plane determines not only the normalised velocity behind the shock but also the shock orientation. In order to find the shock angle α , the following procedure may be used. We draw a straight line through points D and B . Then, taking into account that the tangential velocity remains unchanged across the shock, we can conclude that the shock OS should be perpendicular to this line, as shown in Figure 4.24.

The same procedure may, of course, be used for point A . The main difference between the solutions represented by points A and B is that the latter has an oblique shock with a smaller angle α , which results in a smaller reduction in the flow speed. This is why this solution is said to have a *weak shock*. In contrast, the solution represented by point A shows a more significant reduction in the flow velocity, and is said to involve a *strong shock*.

By means of numerical analysis of the shock polar (4.5.41), it may be demonstrated that point A always lies inside the *sonic circle*, the latter being defined by the equation $\lambda = \sqrt{\lambda_{2x}^2 + \lambda_{2y}^2} = 1$. Hence, the strong shock acts similarly to the normal shock; i.e. it reduces the supersonic flow upstream of the shock to subsonic speed downstream of it. The situation with point B is slightly more complicated. It lies outside the sonic circle provided that the deflection angle θ is not very close to θ_{\max} . This suggests that despite the normal velocity component being smaller than the speed of sound behind the shock, the entire velocity appears to be supersonic. However, for any λ_1 , there exists a neighbourhood of θ_{\max} where both solutions, with the strong (point A) and weak (point B) shocks, reduce the flow speed to subsonic.

It should be noted that not only may both solutions described above be observed in real flows, but also they often appear together in the same flow. As an example, we can consider the flow past a sphere (see Figure 4.4). This flow is reproduced schematically in Figure 4.25. At point E situated directly in front of the sphere, the shock is normal to the oncoming flow, and the velocity deflection angle θ is zero. As the point of observation moves along the shock, say, upwards, the shock angle α decreases, causing

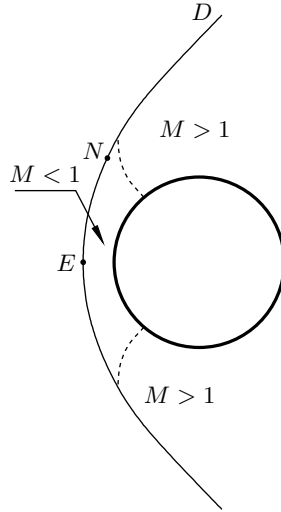


Fig. 4.25: Supersonic flow past a sphere.

the deflection angle θ to increase. However, as the shock becomes more and more oblique, it gradually weakens, making the jump in the normal velocity smaller. As a result, a point is reached (shown as point N in Figure 4.25) where the deflection angle θ reaches a maximum value θ_{\max} , and then θ decays monotonically, tending to zero as the distance from the sphere tends to infinity (point D in Figure 4.25), where the shock wave degenerates into a Mach line. Corresponding to this, the point in the hodograph plane (Figure 4.24) travels from the normal shock position E all the way to the weak shock point D , thus covering all the possible solutions on the upper branch of the shock polar. The lower branch, obviously, corresponds to the lower half of the shock in the physical plane (Figure 4.25).

An interesting feature of the flow past a sphere is that it represents a mixed type of flow containing both subsonic and supersonic flow regions. The subsonic region lies in front of the sphere. The flow then accelerates from the front stagnation point and becomes supersonic. *Sonic lines*, shown in Figure 4.25 as dashed lines, serve the role of the boundaries between subsonic and supersonic parts of the flow.

Finally, it should be noted that the presence of the shock makes the flow irreversible in the sense depicted in Figure 4.6. The entropy increases when the gas crosses the shock wave, and then remains constant along each streamline. As a result, a so-called *entropy wake* forms behind the body. When the distance from the body becomes large, the pressure in the wake returns to its free-stream value p_∞ . However, owing to the increased entropy, the density ρ remains smaller than ρ_∞ . It further follows from the Bernoulli equation

$$\frac{V^2}{2} + \frac{\gamma}{\gamma - 1} \frac{p}{\rho} = \frac{V_\infty^2}{2} + \frac{\gamma}{\gamma - 1} \frac{p_\infty}{\rho_\infty}$$

that the velocity V also stays below its free-stream value V_∞ . Consequently, a deficit of momentum is observed in the wake, which suggests that the body is bound to

experience a drag force. Taking into account that it originates from losses of mechanical energy in the shock wave, this is termed *wave drag*.

4.6 Supersonic Flows past a Wedge and a Cone

There are only a few known exact solutions of the compressible Euler equations. The first of these is the Prandtl–Meyer flow past a sharp expansion corner or a smooth bend of the body contour (see Section 4.4). Here we shall consider two more flows described by exact solutions of the Euler equations, this time involving shock waves.

4.6.1 Flow past a wedge

As soon as the shock polar is calculated for a given value of the normalised velocity λ_1 in the oncoming flow, it may be directly applied to describe the behaviour of a number of simple supersonic flows, including the flow past a wedge and the flow in a vicinity of a sharp corner in the body contour; see Figure 4.26. The latter is equivalent to a wedge installed on a flat wall.

In both flows, the impermeability condition on the wedge surface may be satisfied by assuming that the shock OS generated by the wedge is a straight line. In this case, the flow, which is unperturbed everywhere in front of the shock, appears to be uniform also behind the shock, and the problem reduces to finding the strength of the shock that would be sufficient to cause the flow to turn through an angle θ_w , making it parallel to the wedge surface. In the hodograph plane (Figure 4.24), the corresponding solution may be found by choosing $\theta = \theta_w$. Experimental observations show that in the flow past a wedge, the solution with a weak shock is usually realised. Therefore, the normalised velocity behind the shock is given by point B , and the shock angle α may be found by drawing a straight line through points B and D and recalling that the shock OS is perpendicular to this line. With known α , all the flow parameters in the region between the shock and the wedge surface are calculated using formulae (4.5.32)–(4.5.34) and (4.5.14b).

It is interesting to note that, as long as the shock is attached to the wedge tip O , as shown in Figure 4.26(a), the flow above the wedge is independent of that below it, and therefore cannot be influenced by a deformation of the lower surface of the wedge, say, its rotation around the tip O . However, when the wedge angle θ_w exceeds the

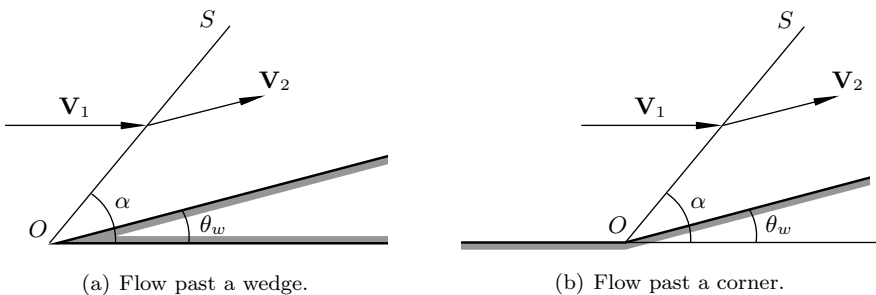


Fig. 4.26: Flow past a wedge and a corner with attached shock.

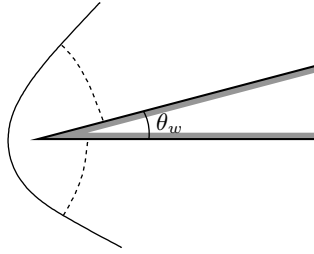


Fig. 4.27: Flow past a wedge with detached shock.

maximum value θ_{\max} , the solution with attached shock can no longer exist. Instead, flow with a detached shock is observed. It contains a subsonic region situated between the front bow shock and sonic lines, shown in Figure 4.27 as dashed lines. Within this region, perturbations are free to propagate in all directions.

4.6.2 Flow past a circular cone

Let a circular cone be placed in steady supersonic flow of a perfect gas as shown in Figure 4.28. To describe the flow, we shall use equation (4.3.6). If the cone is oriented in such a way that its axis is parallel to the free-stream velocity vector, then the flow may be expected to be axially symmetric. Keeping this in mind, we shall use cylindrical polar coordinates. In order to express equation (4.3.6) in these coordinates, one can follow the standard procedure described in Section 1.8. Alternatively, and in fact more easily, it can be done as follows.

We write equation (4.3.6) in Cartesian coordinates,

$$\begin{aligned}
 u \left(u \frac{\partial u}{\partial x} + v \frac{\partial v}{\partial x} + w \frac{\partial w}{\partial x} \right) + v \left(u \frac{\partial u}{\partial y} + v \frac{\partial v}{\partial y} + w \frac{\partial w}{\partial y} \right) \\
 + w \left(u \frac{\partial u}{\partial z} + v \frac{\partial v}{\partial z} + w \frac{\partial w}{\partial z} \right) = a^2 \left(\frac{\partial u}{\partial x} + \frac{\partial v}{\partial y} + \frac{\partial w}{\partial z} \right), \quad (4.6.1)
 \end{aligned}$$

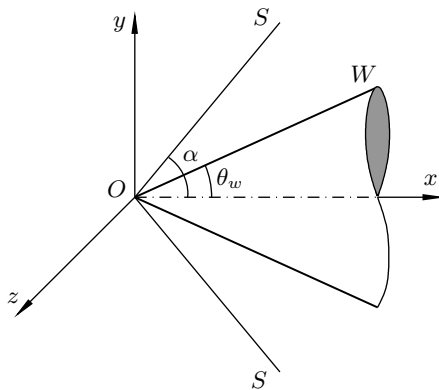


Fig. 4.28: Flow past a circular cone.

and choose the x -axis to coincide with the axis of the cone. Since the gas motion in each plane drawn through the cone axis should be the same, we can restrict our attention to one of these planes. We shall choose it to be the (x, y) -plane of our coordinate system. It is obvious that, at any point in this plane,

$$w = 0, \quad \frac{\partial w}{\partial x} = 0, \quad \frac{\partial w}{\partial y} = 0,$$

which reduces equation (4.6.1) to

$$u \left(u \frac{\partial u}{\partial x} + v \frac{\partial v}{\partial x} \right) + v \left(u \frac{\partial u}{\partial y} + v \frac{\partial v}{\partial y} \right) = a^2 \left(\frac{\partial u}{\partial x} + \frac{\partial v}{\partial y} + \frac{\partial w}{\partial z} \right). \quad (4.6.2)$$

It remains to clarify how the last term in this equation, $\partial w/\partial z$, has to be interpreted. For this purpose, a plane crossing the flow perpendicular to the cone axis will be used; see Figure 4.29. Let us consider two points in this plane. Point 1 is an arbitrary point lying on the y -axis. Point 2 has the same x - and y -coordinates, but is placed a small distance Δz off the (x, y) -plane. We have

$$\frac{\partial w}{\partial z} = \lim_{\Delta z \rightarrow 0} \frac{w_2 - w_1}{\Delta z},$$

where w_1 and w_2 are the values of w at points 1 and 2, respectively. Denoting by δ the angle between the y -axis and the ray drawn from the cone axis to point 2, we can write

$$w_1 = 0, \quad w_2 = v \sin \delta, \quad \Delta z = y \tan \delta,$$

and therefore

$$\frac{\partial w}{\partial z} = \frac{v}{y} \lim_{\delta \rightarrow 0} \frac{\sin \delta}{\tan \delta} = \frac{v}{y}. \quad (4.6.3)$$

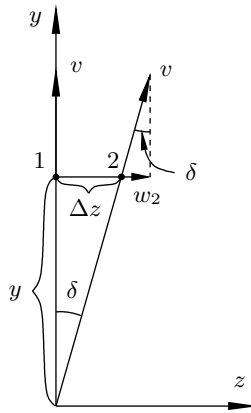


Fig. 4.29: Calculation of $\partial w/\partial z$.

Substituting (4.6.3) into equation (4.6.2) and dividing both of its sides by a^2 yields

$$\left(1 - \frac{u^2}{a^2}\right) \frac{\partial u}{\partial x} + \left(1 - \frac{v^2}{a^2}\right) \frac{\partial v}{\partial y} - \frac{uv}{a^2} \left(\frac{\partial u}{\partial y} + \frac{\partial v}{\partial x}\right) + \frac{v}{y} = 0. \quad (4.6.4)$$

The second equation relating the two velocity components u and v may be formulated based on the following observations. Taking into account the shape of the body, it is reasonable to expect that the front shock OS (see Figure 4.28) will have a conical form. In this case, the strength of the shock, being defined by the shock angle α , will to be the same for all streamlines crossing the shock. This means that, while the entropy will increase at the shock, it will increase by the same amount for all fluid particles crossing the shock, and therefore will be constant in the entire region between the shock and the body surface. Having established this fact, we can turn to Crocco's formula (4.2.21). Assuming, as usual, that the body force \mathbf{f} is negligible, we see that all the terms on the right-hand side of (4.2.21) are zero, i.e.

$$\boldsymbol{\omega} \times \mathbf{V} = 0.$$

Since in an axially symmetric flow the vorticity vector $\boldsymbol{\omega}$ has only one component, which is perpendicular to the velocity vector \mathbf{V} , we have to conclude that the flow behind the shock is irrotational, $\boldsymbol{\omega} = 0$. This is expressed by the equation

$$\frac{\partial u}{\partial y} - \frac{\partial v}{\partial x} = 0. \quad (4.6.5)$$

When solving equations (4.6.4) and (4.6.5) we will also need to use the Bernoulli equation, which relates the local speed of sound a to the flow velocity V . Combining (4.4.32) with (4.4.38), we have

$$\frac{a^2}{\gamma - 1} + \frac{V^2}{2} = \frac{\gamma + 1}{2(\gamma - 1)} V_*^2. \quad (4.6.6)$$

We shall now demonstrate that the solution of equations (4.6.4)–(4.6.6) may be found in a self-similar form, with the velocity components

$$u(x, y) = u(\xi), \quad v(x, y) = v(\xi),$$

being functions of a single variable ξ defined as

$$\xi = \frac{x}{y}. \quad (4.6.7)$$

Differentiation of (4.6.7) gives

$$\frac{d\xi}{dx} = \frac{1}{y}, \quad \frac{d\xi}{dy} = -\frac{x}{y^2} = -\frac{\xi}{y},$$

and we see that

$$\frac{\partial u}{\partial x} = \frac{1}{y} \frac{du}{d\xi}, \quad \frac{\partial u}{\partial y} = -\frac{\xi}{y} \frac{du}{d\xi}, \quad \frac{\partial v}{\partial x} = \frac{1}{y} \frac{dv}{d\xi}, \quad \frac{\partial v}{\partial y} = -\frac{\xi}{y} \frac{dv}{d\xi}. \quad (4.6.8)$$

Substitution of (4.6.8) into equations (4.6.4) and (4.6.5) reduces them to

$$\left(1 - \frac{u^2}{a^2}\right) \frac{du}{d\xi} - \xi \left(1 - \frac{v^2}{a^2}\right) \frac{dv}{d\xi} + 2\xi \frac{uv}{a^2} \frac{du}{d\xi} + v = 0, \quad (4.6.9)$$

$$\xi \frac{du}{d\xi} + \frac{dv}{d\xi} = 0. \quad (4.6.10)$$

Let us now use, instead of ξ , the longitudinal velocity component u as independent variable. Our task will be to find a function $v(u)$ that is related to function $v(\xi)$ by means of the equation

$$v(\xi) = v[u(\xi)].$$

Differentiating this equation, we have

$$\frac{dv}{d\xi} = \frac{dv}{du} \frac{du}{d\xi}. \quad (4.6.11)$$

Substitution of (4.6.11) into equations (4.6.9) and (4.6.10) yields

$$\left(1 - \frac{u^2}{a^2}\right) - \xi \left(1 - \frac{v^2}{a^2}\right) \frac{dv}{du} + 2\xi \frac{uv}{a^2} + v \frac{d\xi}{du} = 0, \quad (4.6.12)$$

$$\xi = -\frac{dv}{du}. \quad (4.6.13)$$

From (4.6.13), we find that

$$\frac{d\xi}{du} = -\frac{d^2v}{du^2}. \quad (4.6.14)$$

It remains to substitute (4.6.13) and (4.6.14) into (4.6.12), and we arrive at the following equation for the function $v(u)$:

$$v \frac{d^2v}{du^2} = 1 + \left(\frac{dv}{du}\right)^2 - \left(\frac{u}{a} + \frac{v}{a} \frac{dv}{du}\right)^2.$$

This may be more conveniently written using the normalised velocity components

$$\lambda_x = \frac{u}{V_*}, \quad \lambda_y = \frac{v}{V_*}.$$

We have

$$\lambda_y \frac{d^2\lambda_y}{d\lambda_x^2} = 1 + \left(\frac{d\lambda_y}{d\lambda_x}\right)^2 - \left(\frac{\lambda_x}{a/V_*} + \frac{\lambda_y}{a/V_*} \frac{d\lambda_y}{d\lambda_x}\right)^2. \quad (4.6.15)$$

Here a/V_* may be found using the Bernoulli equation (4.6.6):

$$\frac{a}{V_*} = \sqrt{\frac{\gamma+1}{2} - \frac{\gamma-1}{2}(\lambda_x^2 + \lambda_y^2)}.$$

From a physical point of view, it is natural to treat the cone angle θ_w as known and seek the shock angle α as part of the solution for the flow past the cone. However, mathematically, it is more convenient to consider the inverse problem, in which

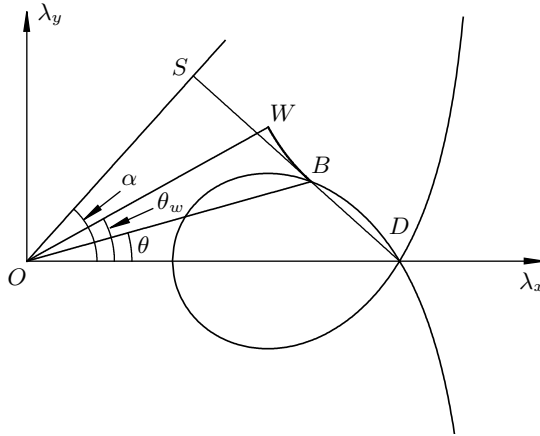


Fig. 4.30: The cone flow solution calculated for $\lambda_1 = 1.6$ and $\alpha = 50^\circ$.

equation (4.6.15) is calculated in the following way. We start with constructing the shock polar for a given normalised velocity λ_1 in the free stream; see Figure 4.30. Then, assuming the shock angle α to be known, we depict the shock position OS . A straight line DS , drawn perpendicular to the shock, intersects the shock polar at point B . The position of this point in the hodograph plane gives the values of both velocity components λ_x and λ_y immediately behind the shock, thus specifying the first initial condition for equation (4.6.15). Since (4.6.15) is a second-order differential equation, we also need to know the derivative $d\lambda_y/d\lambda_x$ at point B . This may be found from equation (4.6.13). Using the normalised velocity components, this equation may be written as

$$\frac{d\lambda_y}{d\lambda_x} = -\xi = -\frac{x}{y},$$

or, equivalently,

$$\mathbf{r} \cdot d\boldsymbol{\lambda} = 0, \tag{4.6.16}$$

which shows that, along the integral curve, the increment $d\boldsymbol{\lambda}$ of the normalised velocity vector $\boldsymbol{\lambda} = (\lambda_x, \lambda_y)$ is always perpendicular to the position vector $\mathbf{r} = (x, y)$. In particular, immediately behind the shock, the integral curve should be perpendicular to the shock or tangent to line DS ; see Figure 4.30.

Now we can start calculating equation (4.6.15) from the shock towards the cone surface. The impermeability condition suggests that the velocity vector should be parallel to the position vector on the cone surface. In view of (4.6.16), this may be written in the form

$$\boldsymbol{\lambda} \cdot d\boldsymbol{\lambda} = 0. \tag{4.6.17}$$

The calculations should stop as soon as condition (4.6.17) is met. The corresponding point in Figure 4.30 is denoted as point W . Its position in the hodograph plane determines both the cone angle θ_w and the value of the normalised velocity on the cone surface.

Exercises 15

1. Consider supersonic flow above a rigid-body surface that remains flat everywhere upstream of point O but then starts to bend up as shown in Figure 4.31. According to the Prandtl–Meyer theory, deceleration of the flow over a curved part of the wall should be observed, causing the characteristics of the first family to converge. Consider two of them, namely the characteristic emerging from point O and the neighbouring characteristic emerging from point O' situated a small distance Δx downstream of O . They intersect at point C ; see Figure 4.31. Using equations (4.4.48), (4.4.49), and (4.4.34), show that the distance d between points O and C may be calculated as

$$d = \frac{2(M^2 - 1)}{(\gamma + 1)M^3\theta'_w(0)}.$$

Here $\theta_w(x)$ is the angle made by the tangent to the body contour with the x -axis and M is the Mach number in the uniform flow upstream of OC . Assume that the derivative $\theta'(x)$ of the wall slope angle $\theta_x(x)$ is finite at point O .

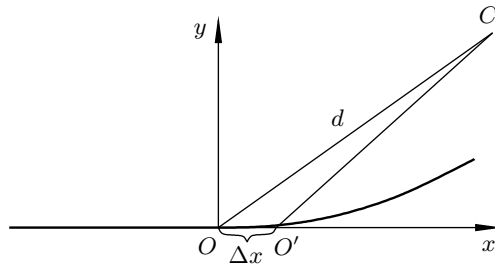


Fig. 4.31: Convergence of the characteristics.

2. Combining Prandtl's relation (4.5.23) with equation (4.4.40), demonstrate that the Mach number behind a normal shock may be calculated as

$$M_2 = \sqrt{\frac{1 + \frac{1}{2}(\gamma - 1)M_1^2}{\gamma M_1^2 - \frac{1}{2}(\gamma - 1)}}.$$

3. Using equation (4.5.30), show that if the Mach number before the shock, M_1 , is only slightly larger than unity, i.e. $M_1 - 1$ is small, then the entropy increment across the shock is proportional to the cube of $M_1 - 1$:

$$\Delta S = \frac{16\gamma R}{3(\gamma + 1)^2}(M_1 - 1)^3.$$

For comparison, also consider the pressure increment. Using equation (4.5.27), show that it is linear in $M_1 - 1$:

$$\frac{p_2 - p_1}{p_1} = \frac{4\gamma}{\gamma + 1}(M_1 - 1).$$

How are these formulae modified for an oblique shock?

4. It may be observed from Figure 4.23 that

$$\frac{V_{2n}}{V_{1n}} = \frac{\tan(\alpha - \theta)}{\tan \alpha}.$$

Using (4.5.34), show that the velocity vector deflection angle θ and the shock angle α are related by the equation

$$\tan \theta = \frac{(M_1^2 \sin^2 \alpha - 1) \cot \alpha}{1 + \left[\frac{1}{2}(\gamma + 1) - \sin^2 \alpha \right] M_1^2}. \quad (4.6.18)$$

Differentiating this equation with respect to α , demonstrate that the value α_{\max} of the shock angle corresponding to the maximum deflection angle θ_{\max} may be determined from the equation

$$\gamma M_1^2 \sin^2 \alpha_{\max} = -1 + \frac{\gamma + 1}{4} M_1^2 + (\gamma + 1)^{1/2} \sqrt{1 + \frac{\gamma - 1}{2} M_1^2 + \frac{\gamma + 1}{16} M_1^4}.$$

Hint: Use the relation

$$\tan(\alpha - \theta) = \frac{\tan \alpha - \tan \theta}{1 + \tan \alpha \tan \theta}.$$

5. It may easily be seen from (4.6.18) that when the velocity vector deflection angle θ is small, $M_1^2 \sin^2 \alpha - 1$ is also small, suggesting that the oblique shock generated by a thin wedge is indistinguishable from a Mach line with $\sin \alpha = 1/M_1$.

By solving (4.6.18) for $M_1^2 \sin^2 \alpha - 1$ and using the result in (4.5.33), demonstrate that the pressure on the wedge surface with small angle θ may be calculated with the help of the Ackeret formula

$$p_2 = p_1 + \rho_1 V_1^2 \frac{\theta}{\sqrt{M_1^2 - 1}}.$$

6. Show that the maximum possible compression ρ_2/ρ_1 in a shock wave is

$$\frac{\rho_2}{\rho_1} = \frac{\gamma + 1}{\gamma - 1}.$$

4.7 One-Dimensional Unsteady Flows

Here we shall return to the problem depicted in Figure 4.3. Remember that the task was to study the motion of a perfect gas in a cylinder caused by piston motion. It was assumed that initially the gas was motionless, with the pressure, density, and enthalpy being p_0 , ρ_0 , and h_0 , respectively. We further assumed that the piston was brought into motion at time $t = 0$, with its position at any $t > 0$ given by the equation $x = x_w(t)$. In Section 4.1, the flow analysis was conducted under the assumption that the perturbations produced in the gas are weak, which holds when the piston speed \dot{x} is much smaller than the speed of sound, $a_0 = \sqrt{\gamma p_0/\rho_0}$. We shall now lift this restriction.

4.7.1 Expansion wave

We shall consider first the case where the piston moves away from the gas as shown in Figure 4.32. If the piston speed $\dot{x}_w(t)$ is comparable to the speed of sound, a_0 , then the nonlinear equations (4.1.3) have to be used:

$$\rho \left(\frac{\partial u}{\partial t} + u \frac{\partial u}{\partial x} \right) = -\frac{\partial p}{\partial x}, \quad (4.7.1a)$$

$$\rho \left(\frac{\partial h}{\partial t} + u \frac{\partial h}{\partial x} \right) = \frac{\partial p}{\partial t} + u \frac{\partial p}{\partial x}, \quad (4.7.1b)$$

$$\frac{\partial \rho}{\partial t} + \rho \frac{\partial u}{\partial x} + u \frac{\partial \rho}{\partial x} = 0, \quad (4.7.1c)$$

$$h = \frac{\gamma}{\gamma - 1} \frac{p}{\rho}. \quad (4.7.1d)$$

In order to formulate the boundary conditions for these equations, we note, first of all, that as the piston starts to move it causes perturbations propagating through the gas with the speed of sound, a_0 . This means that for all $x > a_0 t$, the gas remains unperturbed. Since we are dealing with the process where the gas expands, no shock waves can form near $x = a_0 t$. Consequently, all the fluid dynamic-functions should remain continuous, and we can write

$$\left. \begin{array}{l} u = 0, \\ p = p_0, \\ \rho = \rho_0 \end{array} \right\} \text{ at } x = a_0 t. \quad (4.7.2)$$

The second boundary condition that we will be using is the the impermeability condition on the piston surface. It is written as

$$u = \dot{x}_w(t) \quad \text{at } x = x_w(t). \quad (4.7.3)$$

A simple analytic solution to the boundary-value problem (4.7.1)–(4.7.3) may be found if we assume that the piston moves with a constant speed, i.e.

$$x_w = \begin{cases} 0 & \text{if } t < 0, \\ -V_w t & \text{if } t \geq 0, \end{cases}$$

where V_w is a positive constant, then no characteristic length or time scale can be ascribed to the physical process considered, suggesting that the solution may be sought

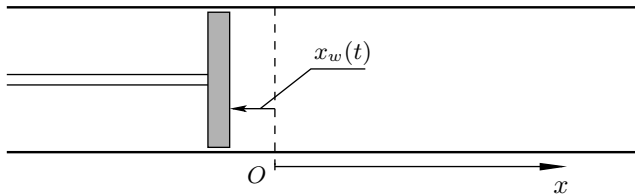


Fig. 4.32: Expansion flow in the cylinder.

in the self-similar form

$$\left. \begin{aligned} u(t, x) &= V_w U(\xi), & p(t, x) &= \rho_0 V_w^2 P(\xi), \\ \rho(t, x) &= \rho_0 R(\xi), & h(t, x) &= V_w^2 H(\xi), \end{aligned} \right\} \quad (4.7.4)$$

where

$$\xi = \frac{x}{V_w t}. \quad (4.7.5)$$

Substitution of (4.7.4) and (4.7.5) into the Euler equations (4.7.1) yields

$$R(U - \xi)U' = -P', \quad (4.7.6a)$$

$$RH' = P' \quad (4.7.6b)$$

$$(U - \xi)R' + RU' = 0, \quad (4.7.6c)$$

$$H = \frac{\gamma}{\gamma - 1} \frac{P}{R}, \quad (4.7.6d)$$

while the boundary conditions (4.7.2) and (4.7.3) become

$$\left. \begin{aligned} U &= 0, \\ P &= \frac{p_0}{\rho_0 V_w^2}, \\ R &= 1 \end{aligned} \right\} \text{ at } \xi = \frac{1}{M_w}, \quad (4.7.7a)$$

$$U = -1 \quad \text{at } \xi = -1, \quad (4.7.7b)$$

where $M_w = V_w/a_0$.

In order to simplify the set of equations (4.7.6), we differentiate (4.7.6d) and substitute the result into (4.7.6b). We find that

$$\frac{P'}{P} - \gamma \frac{R'}{R} = 0,$$

which, on integration, leads to the entropy conservation law

$$\frac{P}{R^\gamma} = C.$$

The constant of integration C is easily found from the conditions on P and R in (4.7.7a). We have

$$P = CR^\gamma, \quad C = \frac{p_0}{\rho_0 V_w^2}. \quad (4.7.8)$$

We now differentiate the first of equations (4.7.8) and use it on the right-hand side of equation (4.7.6a). This results in

$$(U - \xi)RU' = -C\gamma R^{\gamma-1}R'. \quad (4.7.9)$$

Eliminating U' from (4.7.9) and (4.7.6c), we find that the velocity U and density R

are related to one another as

$$(U - \xi)^2 = C\gamma R^{\gamma-1}. \quad (4.7.10)$$

If we take logarithms on both sides of equation (4.7.10) and perform differentiation, then we find that

$$2\frac{U' - 1}{U - \xi} = (\gamma - 1)\frac{R'}{R}. \quad (4.7.11)$$

It remains to eliminate R' from (4.7.6c) and (4.7.11), and we can conclude that the velocity U satisfies a rather simple equation, namely

$$U' = \frac{2}{\gamma + 1}.$$

The solution to this equation satisfying the boundary condition on U in (4.7.7a) has the form

$$U = \frac{2}{\gamma + 1}\left(\xi - \frac{1}{M_w}\right). \quad (4.7.12)$$

Clearly, in the general case, the solution (4.7.12) for the expansion wave cannot satisfy the boundary condition (4.7.7b) on the piston surface. In fact, if condition (4.7.7b) were satisfied, then it would follow from (4.7.10) that, on the piston surface, the gas density would become zero. What happens in reality is that the region between the front of the expansion wave ($x = a_0 t$) and the piston is subdivided into two subregions. The first (denoted as region 1 in Figure 4.33) is the expansion wave itself, where the gas accelerates from rest on the wave front to the velocity of the piston. In order to find the position of the rear of the wave where the piston velocity is attained, we have to set $U = -1$ in (4.7.12). This gives

$$\xi = \frac{1}{M_w} - \frac{\gamma + 1}{2}. \quad (4.7.13)$$

Combining (4.7.13) with (4.7.5), we see that the equation of the rear of the wave is written in dimensional variables as

$$x = \left(a_0 - \frac{\gamma + 1}{2}V_w\right)t.$$

The second region (denoted as region 2 in Figure 4.33) extends from the rear of the wave to the piston surface. In this region, the gas velocity remains constant and

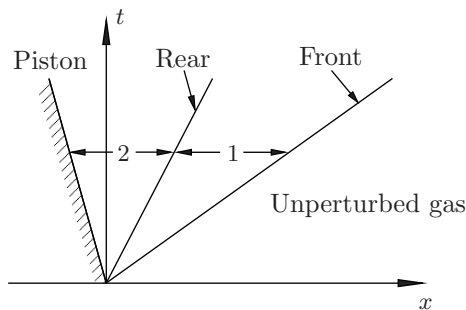


Fig. 4.33: Propagation of the perturbations in the cylinder with time.

coincides with the piston velocity.¹⁰ Since the density also stays constant, its value in region 2 can be found by applying equation (4.7.10) to the point situated at the boundary between regions 1 and 2. We know that, at the rear of the expansion wave, $U = -1$ and ξ is given by (4.7.13). Therefore, it follows from (4.7.10) that, at the boundary point,

$$R = \left(1 - \frac{\gamma - 1}{2} M_w\right)^{2/(\gamma - 1)}. \quad (4.7.14)$$

Returning to dimensional variables, we can conclude that in region 2 the density is given by

$$\rho_2 = \rho_0 \left(1 - \frac{\gamma - 1}{2} \frac{V_w}{a_0}\right)^{2/(\gamma - 1)}.$$

The pressure in region 2 is found by substituting (4.7.14) into (4.7.8). We have

$$p_2 = p_0 \left(1 - \frac{\gamma - 1}{2} \frac{V_w}{a_0}\right)^{2\gamma/(\gamma - 1)}. \quad (4.7.15)$$

4.7.2 Compression flow

Let us now suppose that the piston moves towards the gas, i.e. in the positive x -direction as shown in Figure 4.34. The piston motion causes a shock wave to form in the cylinder. It propagates through the gas with a speed larger than the speed of sound (see Problem 5 in Exercises 16). Before the shock, the gas remains at rest. As the shock passes, the gas immediately acquires a finite velocity $u > 0$; see Figure 4.35(a). The flow in the region between the shock and the piston is described by the Euler equations

$$\left. \begin{aligned} \rho \left(\frac{\partial u}{\partial t} + u \frac{\partial u}{\partial x} \right) &= - \frac{\partial p}{\partial x}, \\ \rho \left(\frac{\partial h}{\partial t} + u \frac{\partial h}{\partial x} \right) &= \frac{\partial p}{\partial t} + u \frac{\partial p}{\partial x}, \\ \frac{\partial \rho}{\partial t} + \rho \frac{\partial u}{\partial x} + u \frac{\partial \rho}{\partial x} &= 0, \\ h &= \frac{\gamma}{\gamma - 1} \frac{p}{\rho}. \end{aligned} \right\} \quad (4.7.16a)$$

In the problem considered, they have to be solved with the following conditions on the shock $x = x_s(t)$:

$$\left. \begin{aligned} \rho [\dot{x}_s(t) - u]^2 + p &= \rho_0 [\dot{x}_s(t)]^2 + p_0, \\ \frac{\gamma}{\gamma - 1} \frac{p}{\rho} + \frac{1}{2} [\dot{x}_s(t) - u]^2 &= \frac{\gamma}{\gamma - 1} \frac{p_0}{\rho_0} + \frac{1}{2} [\dot{x}_s(t)]^2, \\ \rho [\dot{x}_s(t) - u] &= \rho_0 \dot{x}_s(t), \end{aligned} \right\} \quad (4.7.16b)$$

¹⁰The situation is similar to steady flow past an expansion corner (see Figure 4.17). Recall that in this flow the gas acceleration process is confined to the Prandtl–Meyer fan $A'AA''$.

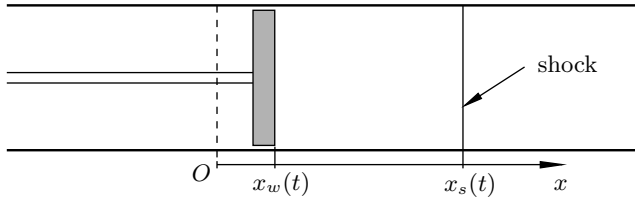


Fig. 4.34: Compression flow in the cylinder.

and the impermeability condition on the piston surface

$$u = \dot{x}_w(t) \quad \text{at} \quad x = x_w(t). \tag{4.7.16c}$$

Equations (4.7.16b) can be deduced by a simple reformulation of the normal-shock conditions (4.5.16) using a Galilean transformation. Recall that when deriving conditions (4.5.16) we assumed the flow to be steady and the shock motionless. Now we have to deal with the shock that propagates along the cylinder with speed $V_s = \dot{x}_s$; see Figure 4.35(a).

Let us call the coordinate frame used in Figures 4.34 and 4.35(a) the laboratory frame, and introduce a new frame that moves along the cylinder with the shock speed V_s ; see Figure 4.35(b). When an observer relocates from the laboratory frame to the moving frame, the Galilean transformation requires the gas velocity to be reduced by V_s . This means that the gas before the shock (region 1), which was stationary in the laboratory frame, should now have the velocity V_s directed towards the shock. The velocity behind the shock (region 2) becomes $V_s - u$. Since the thermodynamic functions are invariant with respect to the change of the coordinate frame, we can write

$$\left. \begin{array}{l} \text{region 1:} \quad V_1 = V_s, \quad \rho_1 = \rho_0, \quad p_1 = p_0, \quad h_1 = h_0, \\ \text{region 2:} \quad V_2 = V_s - u, \quad \rho_2 = \rho, \quad p_2 = p, \quad h_2 = h. \end{array} \right\} \tag{4.7.17}$$

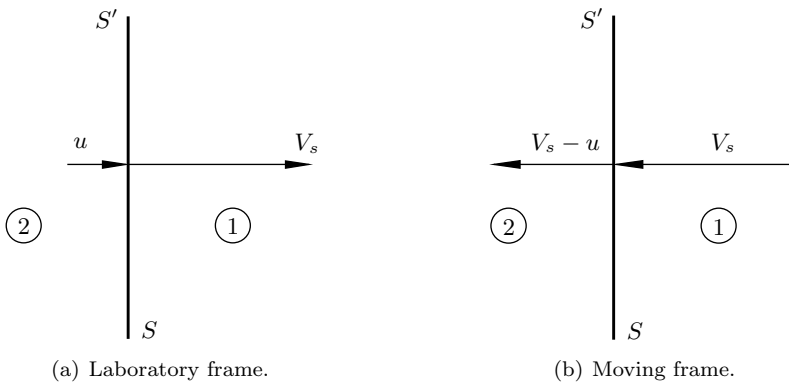


Fig. 4.35: Galilean transformation from the laboratory frame to a coordinate frame moving with the shock.

Substitution of (4.7.17) into (4.5.16) yields

$$\left. \begin{aligned} \rho(V_s - u)^2 + p &= \rho_0 V_s^2 + p_0, \\ h + \frac{(V_s - u)^2}{2} &= h_0 + \frac{V_s^2}{2}, \\ \rho(V_s - u) &= \rho_0 V_s. \end{aligned} \right\} \quad (4.7.18)$$

It remains to recall that

$$h = \frac{\gamma}{\gamma - 1} \frac{p}{\rho}, \quad h_0 = \frac{\gamma}{\gamma - 1} \frac{p_0}{\rho_0}, \quad V_s = \dot{x}_s(t),$$

and we can see that equations (4.7.16b) really hold for a shock wave propagating through an initially stagnant gas.

In the general case, the boundary-value problem (4.7.16) has to be solved numerically. However, if the piston velocity V_w is constant, then a simple analytical solution proves to be possible. Indeed, assuming the gas velocity u , pressure p , and density ρ to be constant between the piston and the shock allows the Euler equations (4.7.16a) to be satisfied. It then follows from the impermeability condition (4.7.16c) that

$$u = V_w. \quad (4.7.19)$$

In order to find the shock speed V_s and the values of the pressure and density in the region between the piston and the shock, we have to use the shock conditions (4.7.16b). Using (4.7.19) in (4.7.16b), we have

$$\rho(V_s - V_w)^2 + p = \rho_0 V_s^2 + p_0, \quad (4.7.20a)$$

$$\frac{\gamma}{\gamma - 1} \frac{p}{\rho} + \frac{(V_s - V_w)^2}{2} = \frac{\gamma}{\gamma - 1} \frac{p_0}{\rho_0} + \frac{V_s^2}{2}, \quad (4.7.20b)$$

$$\rho(V_s - V_w) = \rho_0 V_s. \quad (4.7.20c)$$

We write the continuity equation (4.7.20c) as

$$\rho = \frac{\rho_0 V_s}{V_s - V_w}, \quad (4.7.21)$$

and use it to eliminate ρ from the momentum (4.7.20a) and energy (4.7.20b) equations. We find

$$\rho_0 V_s V_w = p - p_0, \quad (4.7.22a)$$

$$\frac{\gamma}{\gamma - 1} \frac{p - p_0}{\rho_0} - \frac{\gamma}{\gamma - 1} \frac{V_w}{V_s} \frac{p}{\rho_0} - V_s V_w + \frac{1}{2} V_w^2 = 0. \quad (4.7.22b)$$

Elimination of the shock speed V_s from (4.7.22) leads to the following equation for the pressure jump $p - p_0$ across the shock:

$$(p - p_0)^2 - \frac{1}{2}(\gamma + 1)\rho_0 V_w^2 (p - p_0) - \gamma \rho_0 V_w^2 p_0 = 0.$$

This equation has two solutions:

$$(p - p_0)_{1,2} = \frac{\gamma + 1}{4} \rho_0 V_w^2 \pm \sqrt{\frac{(\gamma + 1)^2}{16} \rho_0^2 V_w^4 + \gamma \rho_0 V_w^2 p_0},$$

one with positive increment of the pressure across the shock $\Delta p = p - p_0$ and the other with negative Δp . Since ‘expansion shocks’ cannot be observed in real flows, we have to choose the first solution. It shows that the pressure behind the shock,

$$p = p_0 + \rho_0 V_w^2 \left(\frac{\gamma + 1}{4} + \sqrt{\frac{(\gamma + 1)^2}{16} + \frac{a_0^2}{V_w^2}} \right). \quad (4.7.23)$$

Now the shock speed V_s can be found from equation (4.7.22a) and the density ρ behind the shock from equation (4.7.21).

4.7.3 Shock-tube theory

A shock tube is a device designed for experimental studies of gases under the influence of shock waves. A shock tube is usually made of a long circular cylinder divided by a diaphragm into two chambers: a high-pressure chamber and a low-pressure chamber (see Figure 4.36a). The test gas is placed in the low-pressure chamber, while the high-pressure chamber is filled with a *driver gas*. To obtain a strong shock, the driver gas is compressed to a pressure significantly higher than atmospheric. When the pressure difference between the chambers reaches a desired level, the diaphragm is broken and the two gases come into contact with one another. The *contact surface* moves into the low-pressure chamber, leading to the formation of a shock wave propagating through the test gas. Simultaneously, an expansion wave forms in the high-pressure section (see Figure 4.36b).

Before the shock reaches the right-hand end of the tube or the expansion wave reaches its left-hand end, no characteristic length or time scales can be ascribed to the problem. This suggests that the solution has to have a self-similar form with the flow velocity u , pressure p , and gas density ρ being constant on each ray emanating from the coordinate origin in the (x, t) -plane (see Figure 4.36b). The contact surface has to have a constant speed in this solution; we shall denote it, as before, by V_w for the following reason. In the inviscid formulation, the perturbations produced in the gas medium by the moving contact surface are indistinguishable from the perturbations produced by the moving piston. This means that the solution for the expansion wave, presented above, is directly applicable to the flow on the left-hand side of the contact surface, and the solution for the compression flow is applicable in the region to the right of the surface. These solutions have to be adjusted to one another through the kinematic and dynamic conditions on the contact surface.

The kinematic condition states that the gas velocities on the two sides of the contact surface should be equal to one another and to the velocity V_w of the contact surface itself. If we denote the initial pressure, gas density, and speed of sound in the high-pressure chamber by p'_0 , ρ'_0 , and a'_0 , respectively, then, using (4.7.15), we can

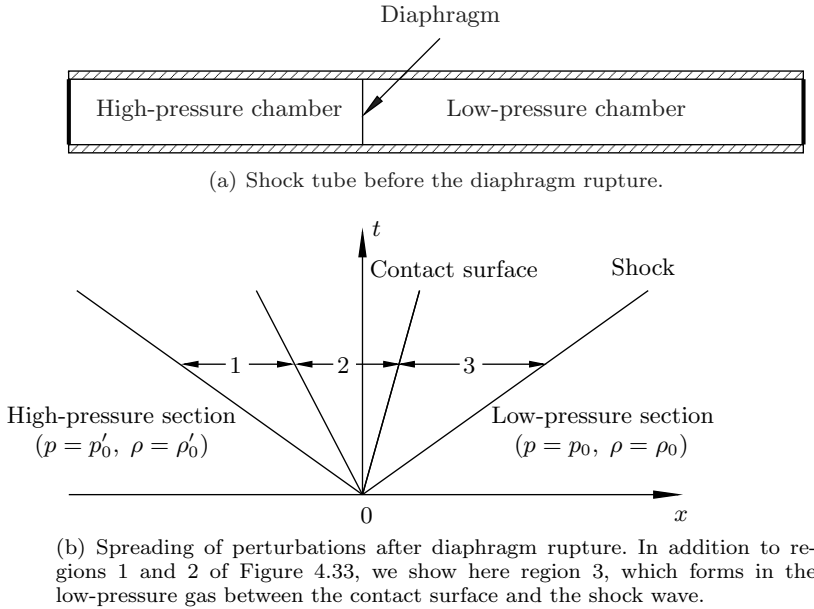


Fig. 4.36: Shock-tube analysis.

express the pressure in region 2 (see Figure 4.36) as

$$p_2 = p'_0 \left(1 - \frac{\gamma' - 1}{2} \frac{V_w}{a'_0} \right)^{2\gamma' / (\gamma' - 1)}, \quad (4.7.24)$$

where γ' is the specific-heat ratio of the driver gas. With p_0 , ρ_0 , a_0 , and γ denoting the initial pressure, density, speed of sound, and specific-heat ratio of the test gas, the pressure in region 3 is given by (4.7.23):

$$p_3 = p_0 + \rho_0 V_w^2 \left(\frac{\gamma + 1}{4} + \sqrt{\frac{(\gamma + 1)^2}{16} + \frac{a_0^2}{V_w^2}} \right). \quad (4.7.25)$$

The dynamic condition on the contact surface states that the pressure should be the same on the two sides of this surface, i.e.

$$p_2 = p_3. \quad (4.7.26)$$

Substitution of (4.7.24) and (4.7.25) into (4.7.26) leads to the following equation:

$$p'_0 \left(1 - \frac{\gamma' - 1}{2} \frac{V_w}{a'_0} \right)^{2\gamma' / (\gamma' - 1)} = p_0 + \rho_0 V_w^2 \left(\frac{\gamma + 1}{4} + \sqrt{\frac{(\gamma + 1)^2}{16} + \frac{a_0^2}{V_w^2}} \right), \quad (4.7.27)$$

which serves to determine the velocity of the contact surface, V_w . This task has to be performed numerically, except for limiting cases discussed in Problems 6 and 7 in Exercises 16.

Exercises 16

1. Extend the theory of characteristics (see Section 4.4) to one-dimensional unsteady flows. When performing this task, you may assume that you are dealing with a perfect gas that starts moving from rest, with the initial gas density and pressure being ρ_0 and p_0 , respectively. You may further assume that the flow is free of shock waves.

- (a) Argue that, under these conditions, the entropy conservation law holds and may be written as

$$\frac{p}{\rho^\gamma} = \frac{p_0}{\rho_0^\gamma}. \quad (4.7.28)$$

Use (4.7.28) to recast the momentum equation (4.7.1a) in the form

$$\rho \frac{\partial u}{\partial t} + \rho u \frac{\partial u}{\partial x} + a^2 \frac{\partial \rho}{\partial x} = 0, \quad (4.7.29)$$

where a is the local speed of sound.

- (b) Combine (4.7.29) with the continuity equation (4.7.1c), and, treating ρ as v and t as y , respectively, confirm that in the case considered the coefficients in equations (4.4.1) are

$$\begin{aligned} a_{11} &= \rho u, & a_{12} &= \rho, & b_{11} &= a^2, & b_{12} &= 0, & c_1 &= 0, \\ a_{21} &= \rho, & a_{22} &= 0, & b_{21} &= u, & b_{22} &= 1, & c_2 &= 0. \end{aligned}$$

Make use of this information to show that the set of equations (4.7.29), (4.7.1c) is hyperbolic.

- (c) Show further that equations (4.4.13) for the characteristics of the first family assume the form

$$dx + (a - u) dt = 0, \quad (4.7.30a)$$

$$du - \frac{a}{\rho} d\rho = 0, \quad (4.7.30b)$$

while equations (4.4.14) for the characteristics of the second family are written as

$$dx - (a + u) dt = 0, \quad (4.7.31a)$$

$$du + \frac{a}{\rho} d\rho = 0, \quad (4.7.31b)$$

- (d) Finally, use (4.7.28) to show that

$$\int \frac{a}{\rho} d\rho = \frac{2}{\gamma - 1} a.$$

Hence, conclude that the Riemann invariants on the characteristics of the first and second families are

$$u - \frac{2}{\gamma - 1} a = \xi \quad (\text{first family}), \quad (4.7.32)$$

$$u + \frac{2}{\gamma - 1} a = \eta \quad (\text{second family}). \quad (4.7.33)$$

2. Consider the expansion flow problem (depicted in Figure 4.32) again, but now allow the piston velocity $V_w(t)$ to vary with time. Using the theory of characteristics, demonstrate that formula (4.7.15) for the pressure on the piston surface remains valid.

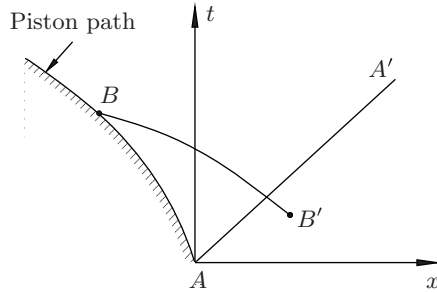


Fig. 4.37: Expansion flow: (x, t) diagram.

Suggestion: In order to perform this task, consider a point B in the (x, t) -plane (see Figure 4.37) that lies on the piston surface at given time t , and draw from B the characteristic of the first family to a point B' that lies to the right of the characteristic of the second family, AA' , emanating from the coordinate origin. Consider further the Riemann invariant (4.7.32) that holds along the characteristic BB' and find the value of the constant ξ , making use of the fact that point B' lies in the region where the gas remains unperturbed. Then take into account that at point B the impermeability condition holds, namely that the gas velocity coincides with the piston speed, $u = -V_w(t)$, and show that

$$a = a_0 - \frac{\gamma - 1}{2} V_w(t).$$

Finally, use the entropy conservation law (4.7.28) to show that the pressure on the piston surface

$$p = p_0 \left[1 - \frac{\gamma - 1}{2} \frac{V_w(t)}{a_0} \right]^{2\gamma/(\gamma-1)}.$$

3. Return to the (x, t) -diagram discussed in Problem 2 (Figure 4.37), and choose a point on the piston path; it is shown as point C in Figure 4.38. Draw the characteristic of the second family, CC' , from point C . Then choose a point on the characteristic CC' , say, point D and 'connect' this point with the unperturbed gas region with the characteristic of the first family, DB' .

Making use of the Riemann invariants (4.7.32) and (4.7.33) on the characteristics DD' and CC' , show that the gas velocity u and the speed of sound, a , remain constant along CC' . Hence, conclude that all characteristics of the second family are straight lines in the (x, t) -plane with slope

$$\frac{dt}{dx} = \frac{1}{a_0 - \frac{1}{2}(\gamma + 1)V_w},$$

where V_w is the value of the piston velocity at the foot of the characteristic. Discuss a possibility of a shock wave forming in the flow at some instance $t > 0$ after the piston starts to move.

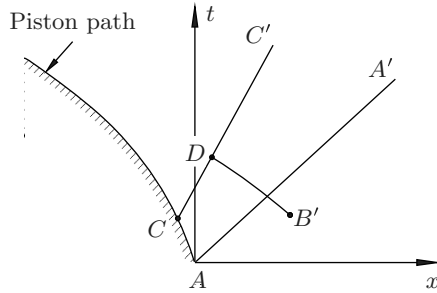
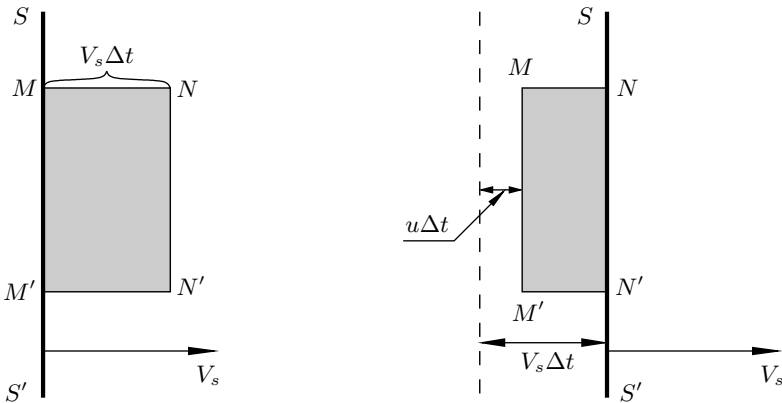


Fig. 4.38: Expansion flow: (x, t) diagram.

- Derive the shock conditions (4.7.18) from the first principles of mechanics, i.e. directly from the momentum equation (4.5.2), the energy equation (4.5.9), and the mass conservation law.

In order to perform this task, assume that the shock propagates with velocity V_s through a gas that is initially at rest, with the pressure, the density of the gas and internal energy being p_0 , ρ_0 , and e_0 , respectively. Consider the shock position at time t and select a fluid body that (at this time) is situated immediately in front of the shock and has a cylindrical shape $MNN'M'$ with the base lying in the shock plane (see Figure 4.39a). Denote the area of the cylinder base by A and choose its height to be $V_s \Delta t$. The latter ensures that after a time interval Δt , the fluid body appears to be immediately behind the shock as shown in Figure 4.39(b).



(a) The shock and fluid body at time t . (b) The shock and fluid body at time $t + \Delta t$. The dashed line shows the shock position at time t .

Fig. 4.39: Shock wave SS' passing through fluid body $MNN'M'$.

Show that the pressure p , density ρ , internal energy e , and gas velocity u behind the shock satisfy the following equations

$$\begin{aligned} \rho_0 V_s u &= p - p_0, \\ \rho_0 V_s \left(e + \frac{1}{2} u^2 - e_0 \right) &= pu, \\ \rho(V_s - u) &= \rho_0 V_s. \end{aligned}$$

Manipulate these equations and show that they may be reduced to equations (4.7.18).

5. Demonstrate that the speed V_s of a shock wave propagating through a perfect gas at rest is given by

$$V_s = a_0 \sqrt{\frac{\gamma - 1}{2\gamma} + \frac{\gamma + 1}{2\gamma} \frac{p}{p_0}}. \tag{4.7.34}$$

where a_0 and p_0 are the speed of sound and pressure in the gas before the shock and p is the pressure behind the shock.

Argue that for any $p/p_0 > 1$, the shock speed is greater than the speed of sound, a_0 , before the shock.

Also deduce that the speed of the gas behind the shock is

$$u = \frac{a_0}{\gamma} \frac{p/p_0 - 1}{\sqrt{\frac{\gamma - 1}{2\gamma} + \frac{\gamma + 1}{2\gamma} \frac{p}{p_0}}}.$$

Suggestion: Start with elimination of the gas density behind the shock, ρ , from the shock equations (4.7.18). Show that this leads to the following pair of equations:

$$\left. \begin{aligned} \rho_0 V_s u &= p - p_0, \\ \frac{\gamma}{\gamma - 1} \frac{p - p_0}{\rho_0} - \frac{\gamma}{\gamma - 1} \frac{u}{V_s} \frac{p}{\rho_0} - V_s u + \frac{u^2}{2} &= 0. \end{aligned} \right\} \tag{4.7.35}$$

Then eliminate the gas velocity behind the shock, u , from (4.7.35). You should find that the shock speed V_s is given by (4.7.34).

6. If the pressure in the two chambers of a shock tube is the same, $p' = p$, then one expects the contact surface to remain motionless after removal of the diaphragm, and, indeed, with $p' = p$, equation (4.7.27) is satisfied by setting $V_w = 0$. If $\Delta p = p' - p$ is small, then V_w is expected to be small.

Simplify both sides of equation (4.7.27), assuming that V_w is small compared with the speed of sound, and show that, for small Δp , the solution of (4.7.27) is given by

$$V_w = \frac{p'_0 - p_0}{\rho_0 a_0 + \rho'_0 a'_0}.$$

7. When running experiments with a shock tube, one normally wishes to increase the strength of the shock wave in the test gas. This can be achieved by increasing

the speed of the contact surface, V_w . Assume that the initial pressure p'_0 of the driver gas is very high such that

$$\frac{p'_0}{p_0} \gg 1, \quad \frac{p'_0}{\rho_0 V_w^2} \gg 1,$$

and deduce from the shock-tube equation (4.7.27) that the maximum attainable speed of the contact surface is

$$V_w = \frac{2}{\gamma' - 1} a'_0.$$

If you are given a choice between helium and air as the driver gas, which one would you choose?

Hint: When answering the last question, make use of the fact that the speed of sound,

$$a = \sqrt{\gamma \frac{R_u}{\mu_g} T},$$

where R_u is the universal gas constant and μ_g is the molecular weight of the gas.

4.8 Blast-Wave Theory

Here we shall study the shock wave that forms as a result of a massive explosion. As the shock expands in the radial direction, it brings the gas (which was stagnant before the shock) into motion. We shall study this motion from the viewpoint of an observer situated sufficiently far from the centre of the explosion. Then detailed analysis of various chemical processes taking place during the explosion becomes unnecessary. Instead, the explosion may simply be treated as an instantaneous release of energy in a region whose size is small compared with the observation distance.

The shock wave is expected to have a spherical shape, with the gas behind the shock moving in the radial direction away from the centre of explosion. Keeping this in mind, we shall express the Euler equations (4.1.2) in spherical polar coordinates (see Figure 1.31):

$$\rho \left(\frac{\partial V_r}{\partial t} + V_r \frac{\partial V_r}{\partial r} \right) = - \frac{\partial p}{\partial r}, \quad (4.8.1a)$$

$$\rho \left(\frac{\partial h}{\partial t} + V_r \frac{\partial h}{\partial r} \right) = \frac{\partial p}{\partial t} + V_r \frac{\partial p}{\partial r}, \quad (4.8.1b)$$

$$\frac{\partial \rho}{\partial t} + \frac{\partial(\rho V_r)}{\partial r} + \frac{2\rho V_r}{r} = 0, \quad (4.8.1c)$$

$$h = \frac{\gamma}{\gamma - 1} \frac{p}{\rho}. \quad (4.8.1d)$$

Here we choose the coordinate origin to coincide with the centre of the explosion, in which case the velocity vector has only one non-zero component, the radial velocity V_r .

Equations (4.8.1) describe the gas motion between the centre of the explosion and the shock wave. We now need to formulate the jump conditions across the shock. Writing the shock equation in the form

$$r = r_s(t),$$

and using V_r instead of u in (4.7.16b), we have

$$\rho[\dot{r}_s(t) - V_r]^2 + p = \rho_0[\dot{r}_s(t)]^2 + p_0, \quad (4.8.2a)$$

$$\frac{\gamma}{\gamma - 1} \frac{p}{\rho} + \frac{1}{2}[\dot{r}_s(t) - V_r]^2 = \frac{\gamma}{\gamma - 1} \frac{p_0}{\rho_0} + \frac{1}{2}[\dot{r}_s(t)]^2, \quad (4.8.2b)$$

$$\rho[\dot{r}_s(t) - V_r] = \rho_0\dot{r}_s(t). \quad (4.8.2c)$$

Our interest here is in a strong shock when the pressure p behind the shock is significantly larger than the pressure p_0 before the shock. We shall therefore disregard p_0 on the right-hand side of equation (4.8.2a). We further know that the density ratio ρ/ρ_0 is always finite (see Problem 6 in Exercises 15). This means that we can also disregard the term $\frac{\gamma}{\gamma - 1} \frac{p_0}{\rho_0}$ on the right-hand side of equation (4.8.2b). As a result, the shock equations (4.8.2) assume the form

$$\rho[\dot{r}_s(t) - V_r]^2 + p = \rho_0[\dot{r}_s(t)]^2, \quad (4.8.3a)$$

$$\frac{\gamma}{\gamma - 1} \frac{p}{\rho} + \frac{1}{2}[\dot{r}_s(t) - V_r]^2 = \frac{1}{2}[\dot{r}_s(t)]^2, \quad (4.8.3b)$$

$$\rho[\dot{r}_s(t) - V_r] = \rho_0\dot{r}_s(t). \quad (4.8.3c)$$

In order to complete the problem formulation, we need to establish a link between the explosion and the resulting gas motion. This can be done through making use of the energy conservation law. The kinetic energy of the gas behind the shock is $\frac{1}{2}V_r^2$ per unit mass. The shock also causes the internal energy $e = c_v T = \frac{1}{\gamma - 1} \frac{p}{\rho}$ of the gas to rise. Before the shock, the kinetic energy of the gas is zero and the internal energy $e = \frac{1}{\gamma - 1} \frac{p_0}{\rho_0}$ is much smaller than that after the shock. Consequently, the energy conservation law may be written as

$$\int_0^{r_s} \rho \left(\frac{V_r^2}{2} + \frac{1}{\gamma - 1} \frac{p}{\rho} \right) 4\pi r^2 dr = E. \quad (4.8.4)$$

Here the left-hand side is the total energy of the gas inside the spherical shock wave; the right-hand side is the energy released during the explosion.

Clearly, the problem at hand does not have any characteristic length or time scales.¹¹ Therefore we can expect the problem to admit a self-similar solution. The

¹¹The two dimensional parameters involved in the problem formulation are the energy of the explosion E and the initial gas density ρ_0 . These cannot be combined to produce a quantity with dimension of length or time.

form of this solution can be found using the method of affine transformations. We write

$$\left. \begin{aligned} V_r &= A\bar{V}_r, & p &= B\bar{p}, & h &= C\bar{h}, & \rho &= D\bar{\rho}, \\ t &= a\bar{t}, & r &= b\bar{r}, & r_s &= b\bar{r}_s, \end{aligned} \right\} \quad (4.8.5)$$

where A, B, C, D, a , and b are positive constants. Substitution of (4.8.5) into the Euler equations (4.8.1) yields

$$\begin{aligned} \frac{A}{a} \frac{\partial \bar{V}_r}{\partial \bar{t}} + \frac{A^2}{b} \bar{V}_r \frac{\partial \bar{V}_r}{\partial \bar{r}} &= -\frac{B}{Db} \frac{1}{\bar{\rho}} \frac{\partial \bar{p}}{\partial \bar{r}}, \\ \frac{DC}{a} \bar{\rho} \frac{\partial \bar{h}}{\partial \bar{t}} + \frac{DAC}{b} \bar{\rho} \bar{V}_r \frac{\partial \bar{h}}{\partial \bar{r}} &= \frac{B}{a} \frac{\partial \bar{p}}{\partial \bar{t}} + \frac{AB}{b} \bar{V}_r \frac{\partial \bar{p}}{\partial \bar{r}}, \\ \frac{D}{a} \frac{\partial \bar{\rho}}{\partial \bar{t}} + \frac{DA}{b} \frac{\partial (\bar{\rho} \bar{V}_r)}{\partial \bar{r}} + \frac{DA}{b} \frac{2\bar{\rho} \bar{V}_r}{\bar{r}} &= 0, \\ C\bar{h} &= \frac{B}{D} \frac{\gamma}{\gamma - 1} \frac{\bar{p}}{\bar{\rho}}. \end{aligned}$$

In order to ensure that the equations preserve their form, we have to set

$$\left. \begin{aligned} \frac{A}{a} &= \frac{A^2}{b} = \frac{B}{Db}, \\ \frac{DC}{a} &= \frac{DAC}{b} = \frac{B}{a} = \frac{AB}{b}, \\ \frac{D}{a} &= \frac{DA}{b}, \\ C &= \frac{B}{D}. \end{aligned} \right\} \quad (4.8.6)$$

In (4.8.6), only three equations are independent of others. They are

$$\frac{1}{a} = \frac{A}{b}, \quad A^2 = \frac{B}{D}, \quad C = \frac{B}{D}. \quad (4.8.7)$$

The shock conditions (4.8.3) are dealt with in the same way. We find that they preserve their form if, in addition to (4.8.7), the following equation holds:

$$D = 1. \quad (4.8.8)$$

Finally, from the energy conservation law (4.8.4), we have

$$DA^2b^3 = 1. \quad (4.8.9)$$

The set of algebraic equations (4.8.7)–(4.8.9) is easily solved to yield

$$A = a^{-3/5}, \quad B = a^{-6/5}, \quad C = a^{-6/5}, \quad D = 1, \quad b = a^{2/5}, \quad (4.8.10)$$

where a remains arbitrary.

Let us now assume that the original problem (4.8.1), (4.8.3), (4.8.4) admits a solution

$$V_r = V(t, r), \quad p = P(t, r), \quad h = H(t, r), \quad \rho = R(t, r),$$

with some functions U , P , H , and R . Then the solution of the transformed problem may be written as

$$\bar{V}_r = V(\bar{t}, \bar{r}), \quad \bar{p} = P(\bar{t}, \bar{r}), \quad \bar{h} = H(\bar{t}, \bar{r}), \quad \bar{\rho} = R(\bar{t}, \bar{r}). \quad (4.8.11)$$

Using (4.8.5), we can express equations (4.8.11) in terms of the original variables:

$$\frac{V_r}{A} = V\left(\frac{t}{a}, \frac{r}{b}\right), \quad \frac{p}{B} = P\left(\frac{t}{a}, \frac{r}{b}\right), \quad \frac{h}{C} = H\left(\frac{t}{a}, \frac{r}{b}\right), \quad \frac{\rho}{D} = R\left(\frac{t}{a}, \frac{r}{b}\right).$$

Finally, we make use of (4.8.10), which leads to

$$\left. \begin{aligned} V_r &= a^{-3/5} V\left(\frac{t}{a}, \frac{r}{a^{2/5}}\right), & p &= a^{-6/5} P\left(\frac{t}{a}, \frac{r}{a^{2/5}}\right), \\ h &= a^{-6/5} H\left(\frac{t}{a}, \frac{r}{a^{2/5}}\right), & \rho &= R\left(\frac{t}{a}, \frac{r}{a^{2/5}}\right). \end{aligned} \right\} \quad (4.8.12)$$

The parameter a in (4.8.12) may assume an arbitrary value, and therefore may be thought of as an additional independent variable. Keeping in mind that it was introduced artificially, we shall ‘hide’ it by choosing $a = t$. We have

$$\left. \begin{aligned} V_r &= t^{-3/5} V\left(1, \frac{r}{t^{2/5}}\right), & p &= t^{-6/5} P\left(1, \frac{r}{t^{2/5}}\right), \\ h &= t^{-6/5} H\left(1, \frac{r}{t^{2/5}}\right), & \rho &= R\left(1, \frac{r}{t^{2/5}}\right). \end{aligned} \right\} \quad (4.8.13)$$

This shows that the functions V , P , H , and R are, in fact, functions of one variable

$$\xi = \frac{r}{t^{2/5}}. \quad (4.8.14)$$

The functions V , P , H , and R , as defined by equations (4.8.13), are dimensional. If we wish to deal with non-dimensional variables, then we need to modify (4.8.13) and (4.8.14) slightly. We note that there are two dimensional parameters, namely the explosion energy E and the initial gas density ρ_0 , involved in the formulation of the problem (4.8.1), (4.8.3), (4.8.4). The dimension of the energy E may be expressed as

$$E = [\text{mass}] \cdot [\text{velocity}]^2. \quad (4.8.15)$$

Similarly, for the density ρ_0 , we have

$$\rho_0 = \frac{[\text{mass}]}{[\text{length}]^3}. \quad (4.8.16)$$

Keeping in mind that

$$[\text{length}] = [\text{velocity}] \cdot [\text{time}],$$

we can write (4.8.16) as

$$\rho_0 = \frac{[\text{mass}]}{[\text{velocity}]^3 \cdot [\text{time}]^3}. \quad (4.8.17)$$

and it follows from (4.8.15) and (4.8.17) that

$$\frac{E}{\rho_0} = [\text{velocity}]^5 \cdot [\text{time}]^3.$$

This suggests that, in order to make V dimensionless, we have to modify the first of equations (4.8.13) as

$$V_r = \left(\frac{E}{\rho_0}\right)^{1/5} t^{-3/5} V(\xi). \quad (4.8.18a)$$

Applying similar arguments to the rest of the sought functions, we shall write

$$p = \rho_0^{3/5} E^{2/5} t^{-6/5} P(\xi), \quad h = \left(\frac{E}{\rho_0}\right)^{2/5} t^{-6/5} H(\xi), \quad \rho = \rho_0 R(\xi), \quad (4.8.18b)$$

and

$$\xi = \left(\frac{\rho_0}{E}\right)^{1/5} \frac{r}{t^{2/5}}. \quad (4.8.19)$$

Also, corresponding to (4.8.19), we shall express the shock equation in the form

$$r_s(t) = \left(\frac{E}{\rho_0}\right)^{1/5} \xi_s t^{2/5}, \quad (4.8.20)$$

where the dimensionless constant ξ_s is to be found as a result of the solution of the problem.

The equations for the functions $V(\xi)$, $P(\xi)$, $R(\xi)$, and $H(\xi)$ are deduced by substituting (4.8.18) and (4.8.19) into equations (4.8.1). We start with differentiation of the similarity variable (4.8.19):

$$\frac{\partial \xi}{\partial t} = -\frac{2}{5} \left(\frac{\rho_0}{E}\right)^{1/5} \frac{r}{t^{7/5}} = -\frac{2}{5} \frac{\xi}{t}, \quad \frac{\partial \xi}{\partial r} = \left(\frac{\rho_0}{E}\right)^{1/5} \frac{1}{t^{2/5}}.$$

Now, we differentiate (4.8.18a), which yields

$$\begin{aligned} \frac{\partial V_r}{\partial t} &= \left(\frac{E}{\rho_0}\right)^{1/5} \left[-\frac{3}{5} t^{-8/5} V + t^{-3/5} V' \left(-\frac{2}{5} \frac{\xi}{t}\right) \right] = -\left(\frac{E}{\rho_0}\right)^{1/5} t^{-8/5} \left(\frac{3}{5} V + \frac{2}{5} \xi V'\right), \\ \frac{\partial V_r}{\partial r} &= \left(\frac{E}{\rho_0}\right)^{1/5} t^{-3/5} V' \left(\frac{\rho_0}{E}\right)^{1/5} \frac{1}{t^{2/5}} = \frac{1}{t} V'. \end{aligned}$$

Similarly, we find that

$$\begin{aligned}\frac{\partial p}{\partial t} &= -\rho_0^{3/5} E^{2/5} t^{-11/5} \left(\frac{6}{5} P + \frac{2}{5} \xi P' \right), & \frac{\partial p}{\partial r} &= \rho_0^{4/5} E^{1/5} t^{-8/5} P', \\ \frac{\partial h}{\partial t} &= -\left(\frac{E}{\rho_0} \right)^{2/5} t^{-11/5} \left(\frac{6}{5} H + \frac{2}{5} \xi H' \right), & \frac{\partial h}{\partial r} &= \left(\frac{E}{\rho_0} \right)^{1/5} t^{-8/5} H', \\ \frac{\partial \rho}{\partial t} &= -\frac{2}{5} \rho_0 \frac{\xi}{t} R', & \frac{\partial \rho}{\partial r} &= \rho_0^{6/5} E^{-1/5} t^{-2/5} R' .\end{aligned}$$

These reduce (4.8.1) to the following set of ordinary differential equations that are valid between the centre of the explosion and the shock wave:

$$R \left[\frac{3}{5} V - \left(V - \frac{2}{5} \xi \right) V' \right] = P', \quad (4.8.21a)$$

$$R \left[\frac{6}{5} H - \left(V - \frac{2}{5} \xi \right) H' \right] = \frac{6}{5} P - \left(V - \frac{2}{5} \xi \right) P', \quad (4.8.21b)$$

$$R V' + \left(V - \frac{2}{5} \xi \right) R' + \frac{2 R V}{\xi} = 0, \quad (4.8.21c)$$

$$H = \frac{\gamma}{\gamma - 1} \frac{P}{R}. \quad (4.8.21d)$$

Substituting (4.8.18)–(4.8.20) into the shock equations (4.8.3), we find that, at the shock,

$$\left. \begin{aligned} R \left(\frac{2}{5} \xi_s - V \right)^2 + P &= \frac{4}{25} \xi_s^2, \\ \frac{\gamma}{\gamma - 1} \frac{P}{R} + \frac{1}{2} \left(\frac{2}{5} \xi_s - V \right)^2 &= \frac{2}{25} \xi_s^2, \\ R \left(\frac{2}{5} \xi_s - V \right) &= \frac{2}{5} \xi_s \end{aligned} \right\} \text{ at } \xi = \xi_s. \quad (4.8.22)$$

Finally, substitution of (4.8.18)–(4.8.20) into the energy conservation law (4.8.4) reduces it to the form

$$4\pi \int_0^{\xi_s} R \left(\frac{V^2}{2} + \frac{1}{\gamma - 1} \frac{P}{R} \right) \xi^2 d\xi = 1. \quad (4.8.23)$$

The problem (4.8.21)–(4.8.23) has to be solved numerically. It is convenient to start with the shock $\xi = \xi_s$, where solution of equations (4.8.22) gives

$$V = \frac{4}{5(\gamma + 1)} \xi_s, \quad P = \frac{8}{25(\gamma + 1)} \xi_s^2, \quad R = \frac{\gamma + 1}{\gamma - 1} \text{ at } \xi = \xi_s. \quad (4.8.24)$$

In order to progress from the shock towards the centre of the explosion, we rearrange equations (4.8.21) as follows. Substitution of (4.8.21d) into (4.8.21b) allows us to

eliminate the enthalpy H and leads to the equation

$$\left(V - \frac{2}{5}\xi\right)\left(\frac{P'}{P} - \gamma\frac{R'}{R}\right) = \frac{6}{5}. \quad (4.8.25)$$

Solving the continuity equation (4.8.21c) for R' and substituting the result into (4.8.25), we find that

$$\left(V - \frac{2}{5}\xi\right)\frac{P'}{P} + \gamma V' + \frac{2\gamma V}{\xi} = \frac{6}{5}. \quad (4.8.26)$$

Finally, eliminating P' from (4.8.26) with the help of the momentum equation (4.8.21a), we have

$$V' = -\frac{3}{5} \frac{V(V - \frac{2}{5}\xi)R/P - 2 + \frac{10}{3}\gamma\xi^{-1}V}{\gamma - (V - \frac{2}{5}\xi)^2 R/P}. \quad (4.8.27)$$

With known V , P , and R at some location ξ , one can find the derivative V' of the radial velocity using (4.8.27). Then the derivative P' of the pressure is easily found from (4.8.26), and the derivative R' of the density from (4.8.25). These may then be used to make a step to a smaller value of ξ . Of course, the position of the shock, $\xi = \xi_s$, is not known in advance, and has to be determined through an iterative process to satisfy the energy conservation law (4.8.23). The results of the calculations are shown in Figure 4.40. Here the left-hand ordinate is used for V and P , and the right for R . We find the shock parameter to be $\xi_s = 1.0328$. Behind the shock, the density R experiences a sharp drop, and stays very low in the central region. This is due to the fact that the gas in this region has been exposed to a very strong shock, which has led to a significant increase of the entropy, $S = \frac{R}{\gamma - 1} \ln \frac{p}{\rho^\gamma}$. Since the pressure p remains finite in the centre of the explosion (see Figure 4.40), the density ρ has to become very low. This, in turn, means that the gas inertia is diminished, and explains why

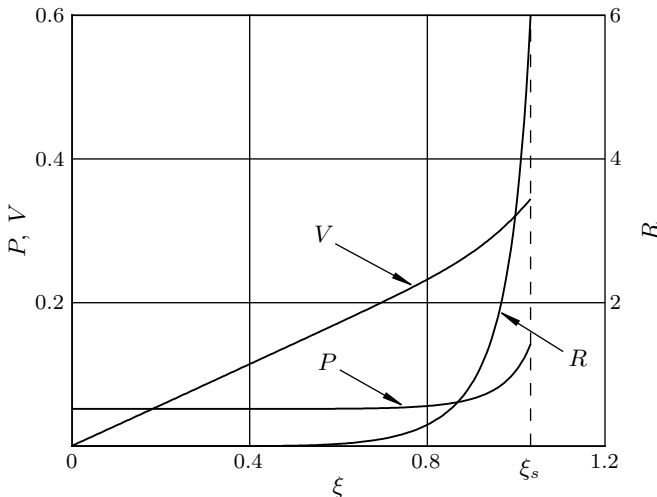


Fig. 4.40: Solution of the self-similar problem (4.8.21)–(4.8.23).

the pressure develops an extended 'plateau region'. Finally, it is interesting to notice that the radial velocity V is zero at the centre of the explosion ($\xi = 0$) and shows an almost linear rise with radius, except close to the shock.

In conclusion, we mention that the blast-wave theory described here was developed by Sedov (1946) and Taylor (1950).

References

- Blasius, P. R. H. (1910). Functiontheoretische methoden in der hydrodyamik. *Z. Math. Phys.*, **58**, 90–110.
- Chaplygin, S. A. (1910). On the pressure exerted by a plane-parallel flow on obstructing bodies. *Math. Collect. Moscow*, **28**, 120–166.
- Dettman, J. W. (1965). *Applied Complex Variables*. Macmillan (reprinted 1984 by Dover Publications).
- Euler, L. (1755). Principes généraux du mouvement des fluides. *Mém. Acad. R. Sci. Belles-Lettres Berl.*, **11**, 217–273 (printed 1757).
- Flachsbart, O. (1935). Der widerstand quer angeströmter rechteckplatten bei reynoldsschen zahlen 1000 bis 6000. *Z. Angew. Math. Mech.*, **15**, 32–37.
- Gurevich, M. I. (1966). *The Theory of Jets in an Ideal Fluid*. Pergamon Press.
- Hagen, G. (1839). Über die bewegung des wassers in engen zylindrischen Röhren. *Poggendorff's Ann. Phys. Chem.*, **46**, 423–442.
- Hamel, G. (1916). Spiralförmige bewegung zäher flüssigkeiten. *Jahresber. Dtsch. Math.-Vereinigung*, **25**, 34–60.
- Helmholtz, H. (1868). Über discontinuirliche flüssigkeits—bewegungen. *Monatsber. Akad. Wiss. Berlin*, **23**, 215–228.
- Hugoniot, H. (1889). Sur la propagation du mouvement dans les corps et spécialement dans les gaz parfaits. *J. École Polytech.*, **58**, 1–125.
- Johannesen, N. H. (1952). *Philos. Mag.*, **43**, 568–580.
- Joukovskii, N. E. (1906). On annexed vortices. *Trans. Phys. Sect. Imperial Soc. Friends Nat. Sci.*, **13**, 12–25.
- Joukovskii, N. E. (1910). Über die konturen der tragflächen der drachenflieger. *Z. Flugtech. Motorluftsch.*, **1**, 281–284.
- Kármán, Th. (1921). Über laminare und turbulente reibung. *Z. Angew. Math. Mech.*, **1**, 233–252.
- Kirchhoff, G. (1869). Zur theorie freier flüssigkeitsstrahlen. *J. Reine Angew. Math.*, **70**(4), 289–298.
- Kutta, M. W. (1910). Über eine mit den grundlagen des flugsproblems in beziehung stehende zweidimensionale strömung. *Sitzungsber. K. Bayer. Akad. Wiss.*, **40**, 1–58.
- Magnus, H. G. (1852). Über die abweichung der geschosse. *Abh. Berl. Akad. (Phys.)*, 1–24.
- Meyer, Th. (1908). Über zweidimensionale bewegungsvorgänge in einem gas, das mit überschallgeschwindigkeit strömt. Göttingen. *Forsch. Ver. Dtsch. Ing.*, **62**, 31–67.
- Navier, C. L. M. H. (1827). Mémoire sur les lois du mouvements des fluides. *Mém. Acad. R. Sci.*, **6**, 389–461.

314 REFERENCES

- Poiseuille, J. (1840). Recherches expérimentelles sur the mouvement des liquides dans les tubes de très petit diametres. *C. R. Acad. Sci.*, **11**, 961–967, 1041–1048.
- Poiseuille, J. (1841). Recherches expérimentelles sur the mouvement des liquides dans les tubes de très petit diametres. *C. R. Acad. Sci.*, **12**, 112–115.
- Poisson, S. D. (1831). Mémoire sur les equations générales de l'équilibre et du mouvement des corps solides elastique et des fluides. *J. École Polytech.*, **13**, 139–166.
- Prandtl, L. and Tietjens, O. G. (1934). *Applied Hydro- and Aeromechanics*. McGraw-Hill (reprinted 1957 by Dover Publications).
- Rankine, W. J. M. (1870). On the thermodynamic theory of waves of finite longitudinal disturbance. *Philos. Trans. R. Soc. Lond.*, **160**, 277–288.
- Saint-Venant, A. J. C. B. (1843). Note à joindre un mémoire sur la dynamique des fluides. *C. R. Acad. Sci.*, **17**, 1240–1244.
- Sedov, L. I. (1946). Propagation of strong shock waves. *Prikl. Mat. Mekh.*, **10**, 241–250.
- Stokes, G. G. (1845). On the theories of the internal friction of fluids in motion, and of the equilibrium and motion of elastic solids. *Trans. Cambridge Philos. Soc.*, **8**, 287–305.
- Stokes, G. G. (1851). On the effect of internal friction of fluids on the motion of pendulums. *Trans. Cambridge Philos. Soc.*, **9**, 8–106.
- Taylor, G. I. (1950). The formation of a blast wave by a very intense explosion. I. Theoretical discussion. *Proc. R. Soc. Lond. A*, **201**, 159–174.
- Thomson, W. (Lord Kelvin) (1869). On vortex motion. *Trans. R. Soc. Edin.*, **25**, 217–260.
- Van Dyke, M. (1982). *An Album of Fluid Motion*. Parabolic Press.

Index

- acceleration
 - in Eulerian variables
 - convective acceleration, 28
 - local acceleration, 28
 - in Lagrangian variables, 27
- Ackeret formula, 270, 292
- adiabatic process, 25

- Bernoulli integral
 - across shock wave, 275
 - compressible flow, 239
 - incompressible flow, 130
- Biot–Savart formula, 179
- Blasius–Chaplygin formula, 172
- blast-wave theory, 305
- body-fitted coordinates, 86
- Boltzmann distribution, 21
- Boltzmann equation, 4
- Boltzmann’s constant, 17
- Borda mouthpiece, 231
- boundary conditions
 - dynamic condition, 211
 - free-stream condition, 142
 - impermeability condition, 141
 - kinematic condition, 211
 - no-slip condition, 70, 97
 - thermally isolated wall, 70
- bow shock, 239, 286

- Cauchy–Lagrange integral
 - compressible flow, 248
 - incompressible flow, 134
- characteristic variables, 237
- characteristics, 252, 254, 270, 301
 - method of, 256
- circulation, 33
- Clapeyron equation, 15, 19
- complex conjugate velocity, 160
- complex potential, 160
 - potential vortex, 163
 - two-dimensional dipole, 163
 - two-dimensional source, 161
 - two-dimensional uniform flow, 161
- computational fluid dynamics, 3
- conformal mapping, 181, 184
 - bilinear transformation, 186
 - Joukovskii transformation, 197
 - generalised, 208
 - linear fractional transformation, 186
 - Schwartz–Christoffel, 226
 - with linear function, 181
 - with power function, 185
- conservation of entropy, 241
- constitutive equation, 41, 46, 49
- continuity equation
 - in Eulerian variables, 53
 - in Lagrangian variables, 27
- continuum hypothesis, 4
- Couette flow, 48, 95
- critical velocity, 261
- Crocco’s formula, 244
- curvilinear coordinates, 73
 - curl, 80
 - divergence, 78
 - gradient, 77
 - Lamé coefficients, 75
- cylindrical polar coordinates, 80

- d’Alembert’s paradox, 147, 174, 210, 245
- density, 5
- deviatoric stress tensor, 41
- differential equation type
 - elliptic, 254
 - hyperbolic, 254
 - parabolic, 106
- dipole
 - three-dimensional, 145
 - two-dimensional, 163
- drag
 - of infinite cylinder, 173
 - of sphere, 151
 - wave drag, 285

- energy equation, 60
 - for compressible flows, 65
 - for incompressible flows, 64
- enthalpy, 23
 - total enthalpy, 240
- entropy, 24
 - conservation of entropy, 241
- epicycloids, 262
- equation
 - continuity, 27, 53
 - of energy, 60
 - of momentum, 58
 - integral form, 67
 - of state, 15
- Euler equations
 - compressible, 234
 - incompressible, 129

- Eulerian description, 27
- exact solutions
 - of the compressible Euler equations, 285
 - of the Navier–Stokes equations, 95
- expansion ramp flow, 266

- First Law of Thermodynamics, 19
- flow past a circular cylinder
 - numerical solution, 123
 - potential theory, 165
- fluid, 13
- fluid particle, 7
- flux, 103
- forces acting on a fluid
 - body forces, 7
 - potential, 129
 - due to pressure, 9
 - electromagnetic, 8
 - inertial force, 8
 - surface forces, 8
 - volume forces, 7
- free streamline theory
 - Kirchhoff flow, 210
 - two-dimensional inviscid jets, 223
 - contraction coefficient, 231
- free streamlines, 211
- Froude number, 72
- full derivative, 28

- gas constant, 15
- Gromeko–Lamb form, 129

- Hagen–Poiseuille flow, 100
- heat conductivity coefficient, 59
- Helmholtz
 - first theorem, 34
 - second theorem, 38
- hodograph plane
 - in free streamline theory, 212
 - shock wave theory, 283
 - supersonic flow theory, 255, 262

- ideal gas law, 15
- incompressible flows, 15
- integral momentum equation, 67
- integrals of motion
 - compressible flows, 239
 - incompressible flows, 129
- internal energy, 19, 20
- inviscid incompressible flows
 - flat plate at an incidence, 197
 - flow past a circular arc, 205
 - flow past a parabola, 207
 - at an incidence, 208
 - flow past an ellipse, 205
 - past a circular cylinder, 165
 - past a corner, 191
 - past Joukovskii aerofoil, 201
 - rotating cylinder, 168
- irrotational flows, 133, 244, 245

- Joukovskii
 - aerofoils, 201
 - formula, 174
 - formula for lift, 169
 - transformation, 194, 197, 214
- Joukovskii–Kutta condition, 200
- jump conditions, 276

- Kármán flow, 113
- Kelvin’s Circulation Theorem
 - compressible flow, 242
 - incompressible flow, 130
- kinetic energy of molecules, 17
- kinetic theory of gases, 15
- Kirchhoff flow, 210
- Knudsen number, 4, 6

- Lagrangian description, 26
- Lamb formula, 73, 129
- Laval nozzle, 248
- lift force, 173

- Mach cone, 234
- Mach number, 72, 233
- macroscopic quantities, 6
- Magnus effect, 170
- material derivative, 28
- Maxwell distribution, 21
- mean free path, 6
- methods of characteristics, 256
- momentum equation, 58

- Navier–Stokes equations
 - compressible, 66
 - in body-fitted coordinates, 87
 - in cylindrical polar coordinates, 84
 - in spherical polar coordinates, 85
 - incompressible, 62
 - non-dimensional, 71
- Newtonian fluid, 50
- Newtonian model, 8
- Newtonian viscosity law, 48
- non-Newtonian fluid, 50
- normalised velocity, 261

- one-dimensional compressible flows
 - compression flow, 296
 - expansion wave, 293

- pathline, 29
 - equation of, 30
- perfect gas, 15
- piston theory, 235
- point source
 - three-dimensional, 142
 - two-dimensional, 161
- Poiseuille flow, 98
- potential flow equations, 251
 - compressible flow
 - steady, 251
 - unsteady, 272
 - incompressible flow, 141

- potential flow past a sphere
 - steady, 145
 - unsteady, 148
- potential flows
 - compressible, 250
 - incompressible, 139, 153
- potential vortex, 163
- Prandtl number, 59
- Prandtl's relation, 277
- Prandtl–Meyer flow, 263
 - expansion corner, 266
- Prandtl–Meyer function, 260
- pressure, 9, 14
- principle of superposition, 142

- Rankine body, 178
- Rankine–Hugoniot conditions, 276
- rate-of-strain tensor, 38
 - in curvilinear coordinates, 88
- ratio of specific heats, 23
- Reynolds number, 72
- Riemann invariants, 255

- Schwartz–Christoffel transformation, 226
- self-similar solution, 108
- separation point, 211
- shear stress, 9, 11
- shock polar, 283
- shock relations, 273
 - for normal shock, 276, 278, 279
 - for oblique shock, 276, 281
- shock tube, 299
- shock wave, 272
 - normal shock, 276
 - oblique shock, 279
- similarity of fluid flows, 69
 - dynamic, 72
 - geometric, 72
- specific heat
 - at constant pressure, 23
 - at constant volume, 20
- speed of sound, 239
- spherical polar coordinates, 84
- steady flows, 31
- Stokes layer, 110
- Stokes stream function, 159
- stream function, 155, 157
 - axisymmetric flow, 159
- streamline, 29
 - equation of, 29
- stress, 10, 11
 - normal stress, 11
 - tangential stress, 11
- stress tensor, 10, 19
 - deviatoric stress tensor, 41
 - in body-fitted coordinates, 92
 - in curvilinear coordinates, 92
 - in cylindrical polar coordinates, 92
 - in spherical polar coordinates, 92
- strong shock, 283
- Strouhal number, 72
- supersonic flow, 233
- supersonic flow past a circular cone, 286
- supersonic flow past a wedge, 285
- surface forces, 8

- temperature, 15, 17
- theory of characteristics
 - one-dimensional unsteady flows, 301
 - two-dimensional steady flows, 252, 270
- thrust, 137
- Torricelli formula, 136

- unsteady potential equation, 272

- velocity potential, 139, 153
- virtual mass, 152
- viscosity coefficient
 - dynamic, 48
 - first viscosity coefficient, 44
 - kinematic, 48
 - power law, 48
 - second viscosity coefficient, 44, 49
 - Sutherland law, 48
- viscous flows
 - above oscillating plate, 121
 - between two coaxial cylinders, 103, 121
 - Couette flow, 95
 - dissipation of potential vortex, 110
 - down a slope, 120
 - Hagen–Poiseuille flow, 100
 - impulsively started flat plate, 105
 - Kármán flow, 113
 - lid-driven cavity flow, 126
 - past a circular cylinder, 123
 - Poiseuille flow, 98
 - through elliptic tube, 119
- viscous forces, 13
- vortex line, 33
- vortex tube, 33
- vorticity, 31

- wave drag, 285
- weak shock, 283

